An investigation into the micromorphology and inorganic geochemistry of Prehistoric, Hellenistic and Roman graves

Helen Rachel Stokes Williams

Doctor of Philosophy

University of York

Archaeology

March 2015

Abstract

Burials are an important feature of archaeological investigations as they reveal information on the cultural and emotional significance of death and the dead by studying the placement of the body, pre-burial treatment of the body as well as grave goods (Parker-Pearson, 2003, Stutz, 2003). In addition to this a wealth of dietary, health and population information can also be obtained through the study of the skeleton (Müldner & Richards, 2007). However the majority of burial investigations focus on the macro remains and microanalytical studies are rarely undertaken, meaning that the soil in contact with the burial is currently underutilised and therefore any information contained in the soil is at present being lost.

This research takes a novel approach to the study of Prehistoric, Hellenistic and Roman burials by using microanalytical techniques, specifically micromorphology and complimentary inorganic geochemical analysis to unlock the hidden archive within the soils in contact with the inhumation. The aim of this research is to identify micromorphological and inorganic geochemical evidence that can be related to the degradation products of the body, grave goods and burial practices. This will be achieved by investigating 18 graves (two Prehistoric, two Hellenistic and twelve Roman), using micromorphological samples taken from the skull, pelvic and foot area as well as site and grave controls.

The micromorphological investigation identified distinct patterns of organic coarse materials and pedofeature formations in the burial plane, as well as features that were diagnostic of the post depositional burial environment. SEM-EDX inorganic geochemical analysis provided evidence of the body decomposition products (K, Fe and Ca) in the surrounding soils, which correlates well with earlier studies on body stains (Bethell & Carver, 2002, Keeley *et al.*, 1977, Macphail *et al.*, 2013). Further to this the micromorphological features and inorganic geochemical signatures were used as both direct and proxy evidence of burial practice and grave goods which were not visible in the macro scale.

Contents

List Tables

List of Figures

"Archaeological practice cannot divide the physical, social or individual body into discrete boxes since each is dependent on the other – they are different facets of the same phenomenon – and archaeologists must make living bodies out of those that are dead"

(Sofaer, 2006 p. 30)

Acknowledgements

I would first and foremost like to thank my supervisors Don Brothwell and Oliver Craig, at York University as well as Clare Wilson at Stirling University, for their unerring support, guidance and sense of humour through what was, at times, a difficult process. I would particularly like to thank Clare Wilson for her unending patience, hospitality, wealth of micromorphological knowledge and spelling expertise as well as her ability to coax images out of the scanning electron microscope!

I would like to thank York Archaeological Trust, especially Toby Kendall, for allowing our team to extensively sample the graves at Hungate. I would also like to thank Cath Neal for permitting sampling at Heslington East and Ian Hodder for agreeing for InterArChive to sample the burials at Çatalhöyük. I would also like to extend thanks to the Thessalonian team who agreed to InterArChive team members sampling at Thessaloniki. To the many technical staff who helped me, I owe a debt of gratitude as without their expertise this thesis would not have been possible, including David Broughton, Annika Burns and Harri Win Williams at the University of York and George McLeod at the University of Stirling for producing a seemingly countless number of thin sections. Endless thanks to Tom Fitton for resurrecting my computer and to Chris Mellor for his talents in the dark art of statistics. I would also like to thank all members of the InterArChive team for sampling sites and also for their valuable discussions on the intricacies of post deposition chemical and soil processes.

A very special thank you must go to my long suffering husband, Lee Williams, for his emotional and financial support during the years of this thesis. Thanks to my parents, for listening with keen enthusiasm to all of my ramblings in the name of science, especially my mother for babysitting. I would also like to thank my son, Arthur (20 months), for not only being the quietest most obliging baby and happily playing whilst I make my final corrections but also for sleeping through – most nights.

I would like to acknowledge and thank Dr Marie-Raimonda Usai of the Archaeology department and Dr Brendan Keely of the Chemistry department of the University of York for developing the InterArChive project and giving me the opportunity to contribute to it.

Last but not least I would like to thank my fellow PhD students and associates at the University of York; my co-conspirator Carol Lang for sharing in the dizzying highs and plummeting lows of the

PhD experience; Emily Hellewell, Suzanne Lilly, Kirsty High and Lisa Shillito I would also like to thank for their unswerving support and endless supply of tea and cake.

To all of the above I am thankful for their help and advice especially for those days when they showed me that the journey is more important than the destination. All the following mistakes and inaccuracies are consequently, and entirely, my own, but 'honi soit qui mal y pense!'

This study was funded by the European Research Council (ERC) under the European Communities Seventh Framework Programme (FP7/2007-2013)/ERC grant n°230193.

Authors Declaration

This is to certify that, to the best of my knowledge, the content of this thesis has not been submitted for any degree or other purpose and the information contained within is original. I certify that the intellectual content of this thesis is the product of my own work and that all the assistance received in preparing this thesis and sources have been acknowledged.

1 Introduction

Burials are important features of archaeological investigations that provoke a strong emotive response and are key to our understanding of past societies and social change. Parker-Pearson (2003 p.3) stated that 'the dead do not bury themselves', but burials are generally organised, sanctified and performed on a community level. The mode of the burial, the ceremony, the deceased appearance and the inclusions of grave goods are a reflection of how society perceives the individual and their place within the community (Parker-Pearson, 2003, Sofaer, 2006). Sofaer (2006) goes on to argue that human action and agency are also inextricably linked to the process of burial. Burial rituals are part of a transition between the world of the living and the world of the dead, the purpose of which is to facilitate a peaceful and safe transition between these two worlds and regulate the behaviours of both the bereaved and the deceased (Hope, 2007 p. 85, Parker-Pearson, 2003). The conceptualisation of personal and communal identity and ownership as well as any belief in the afterlife can be seen in the archaeological record, in the placement of the body within the landscape (Arnold, 2002, Fontijn, 1996, Whittle, 1996), the arrangement and pre-burial treatment of the body (Parker-Pearson, 2003, Pearson *et al.*, 2005) as well as the selection or absence of grave goods (Nilsson, 1998, Willis & Tayles, 2009). In addition to cultural knowledge, health and dietary data can be obtained from inhumations through osteological (Cole, 2013, Roberts, 2009) and isotopic (Müldner & Richards, 2007, Richards *et al.*, 2003) investigations of skeletal material. The majority of burial investigations focus on macro-scale examination. Microscale research is rarely undertaken and generally focuses on palynology or gut contents (Berg, 2002, Reinhard et al., 1992). The soil in contact with inhumations is underutilised and little research has been conducted into retrieving meaningful data from the grave fill. Therefore microscale cultural, health and dietary information, hidden in the grave fill, may be lost.

The InterArChive Project has been established to investigate the existence and extent of the 'hidden archive' of cultural, dietary and health information that may be present in the micro-scale, by analysing the soil in contact with human burials, using micromorphology, inorganic geochemistry and organic chemistry investigative techniques.

The overarching InterArChive project, which this research is part of, will be presented first (1.1). Then the more specific aims and objectives undertaken by the research presented in this thesis (1.2) followed by a review of factors affecting the process of human decomposition (1.3), the preservation of organic materials in burials (1.4), and previous microscale burial studies (1.5). This

will be followed by a series of conceptual models (1.6) that highlight the microscale cultural, health and dietary data that maybe recoverable from grave deposits.

1.1 InterArChive Project Summary and Research Aims

This study has been undertaken as part of the larger multidisciplinary InterArChive project, encompassing the Archaeological and Chemistry departments of York University and the Biological and Environmental sciences department at the University of Stirling. The InterArChive project has been established to investigate the possibility of recovering cultural and environmental information from human inhumations on the macro-, micro-, and nano observational scales, using soil micromorphology, inorganic geochemistry and trace organic chemical analysis. The evidence recovered from the InterArChive Project will then inform the interpretation of the physical remains of burials in relation to the morphology and chemical composition (both organic and inorganic) of the soil. To meet this objective, InterArChive has amassed burial material from multiple time periods, regions and soil types, using a well-documented, systematic sampling approach developed by the InterArChive team (see 2.1). The results from the InterArChive project will then be utilised to develop a sampling and analytical protocol that will be available for the archaeological and forensic communities to employ when investigating historic and modern burials, giving a new and richer suite of evidence from the 'unseen' cultural and biological record.

The work presented in this thesis had been undertaken as part of the InterArChive project, and specifically concentrates on the Prehistoric, Hellenistic and Roman periods in Europe. The purpose of the research was to take a novel approach to the study of Prehistoric, Hellenistic and Roman burials and systematically investigate the microscale structure and features of the grave fill using micromorphological techniques and the inorganic chemical composition of micromorphological features as well as the soil fine material using SEM-EDX analysis, a level of investigation that may be particularly significant for inhumations that are poorly preserved.

1.2 Aims and objectives of the research presented in this thesis

The aim of the research presented in this thesis is to attempt to recover decomposition products from Prehistoric, Hellenistic and Roman inhumations and associated cultural artefacts through the utilisation of novel microanalytical techniques: micromorphology and inorganic geochemistry. To the best of our knowledge, this approach has not previously been applied to Prehistoric, Hellenistic and Roman burials using such a unique set of systematic samples (see 2.1) and on such a wide scale. Micromorphological analysis was conducted to establish the morphology of the soil,

thus gaining understanding of the flow of soil water/chemicals within the grave, past soil changes and to investigate the presence of any micro artefacts in the grave. Inorganic geochemical analysis was conducted on soil thin sections to both provide a more secure identification of the microrphological features and to assess the presence of inorganic chemicals in the soil surrounding the burial. The investigative methods employed in this research (micromorphology and inorganic geochemistry) were employed due to a combination of the research goals and the constraints of the InterArChive project leading to these methods being forwarded and others such as XRD, particle size analysis and phytolith analysis being excluded. This work addressed the following research question and objectives;

Research question;

- Is it possible to identify body degradation products, burial practices, grave goods and preservation conditions in Prehistoric, Hellenistic and Roman burials using soil micromorphology and inorganic geochemistry?

Objectives

- Establish the presence of systematic soil micromorphological and inorganic geochemical variation in the soil at the following levels;
    - Inter site.
    - Inter grave, between the graves and site control samples.
    - Intra grave, between the burial plane and the grave control samples as well as laterally in the burial plane.
- Is there micromorphological and/or inorganic geochemical evidence of a body degradation products retained in the soil?
- Is there micromorphological and/or inorganic geochemical evidence of grave goods or burial practice retained in the soil?
- Is there micromorphological and/or inorganic geochemical evidence of preservation conditions retained in the soil?

The research presented in this thesis is original in its approach to inhumations, as it includes the use of a large number of Prehistoric, Hellenistic and Roman burials (18), across a range of burial environments that have been systematically sampled according to a strict sampling protocol. Micromorphological analysis and inorganic geochemical analysis has been applied for the first time to such a large Roman, Hellenistic and Prehistoric burial sample set, creating a unique

opportunity to assess the extent of the microscale inhumation archive as well as to test the validity of the methodology and sampling protocol to graves of this period. It is anticipated that the results from this thesis will be integrated with those of both the thin section and inorganic geochemical analysis from the post-Roman sites and also with trace organic chemical analysis of sites of all ages.

1.3 Degradation processes

As a human body decomposes in the soil, a series of stages and processes occur that produce a wide range of materials and morphological changes to the body that have the potential to effect the soil environment. This section will detail the stages and processes of human decomposition, identifying those that can potentially affect the immediate soil environment.

During degradation the body goes through three stages. The first stage occurs within a short time scale and centres on the process of autolysis (self digestion section 1.3.1) (Dent et al., 2004). The second stage is putrefaction of the soft tissue (1.3.2) and the third stage is chemical weathering of the remaining protein, mineral and organic components of the skeleton (1.3.3) (Dent et al., 2004). Although the stages occur in a well-researched and defined order, the interval between death and complete degradation is dependent on the environmental conditions (Fiedler & Graw, 2003).

1.3.1 First stage Autolysis

Autolysis begins approximately four minutes post-mortem (Vass, 2001). Immediately upon death the muscles relax, causing the jaw to open and eyelids to lose tension (Stutz, 2003) and bacteria and enzymes in the body begin to breakdown soft tissues (Dent et al., 2004), causing a rise in body temperature (Janaway, 2002), after which the body begins to cool until it reaches equilibrium with the surrounding environment know as algor mortis (Stutz, 2003, Vass, 2001). Livor mortis occurs shortly after, causing a loss of skin tone and a black/blue colour to the skin caused by the settling of bodily fluids (Stutz, 2003, Vass, 2001). The human body, which is primarily composed of water (64%), protein (20%), lipids (10%), carbohydrate (1%) and minerals (5%) (Dent et al., 2004), then begins to degrade into its component parts. Rigor mortis, the stiffening of the joints and muscles due to the release of actin and myosin in the muscles, occurs at approximately 2-4 hours post-mortem (Stutz, 2003). Rigor mortis is short lived and after 24 hours the body once again becomes flaccid (Stutz, 2003). It is therefore unlikely that rigor mortis is the cause of unusual burial positions, unless the body is buried within the 20 hour window in which it commonly occurs (Stutz, 2003). The three main substances which degrade during this early stage are protein, glycogen and lipids. The breakdown of the lining of the digestion tract

releases a flood of enzymes into the main part of the body (Janaway, 1987). Protein is broken down during a process known as proteolysis (Dent et al., 2004), which is highly dependent on moisture, pH and temperature, and is thus favoured by warm moist environments (Janaway, 1987). There is also some evidence to support that environments with a high pH increase the rate of proteolysis, particularly with regard to the decomposition of hair (Mathison, 1964). Proteolysis converts protein into proteoses, peptones, polypeptides and amino acids, which, are subsequently broken down into skatole, indole and CO_2, H_2S, CH^4 and NH_3 (Dent et al., 2004). Glycogen in the form of polysaccharides and carbohydrates are broken down by the action of micro-organisms into sugars (Dent et al., 2004). Adipocere, which is a type of waxy fat (Fiedler & Graw, 2003) can form around the body at this stage (Dent et al., 2004). The formation of adipocere occurs in specific circumstances, which currently are not well understood, but appear to be influenced by the age, sex, stature of the body, and the presence of any wounds and burial environment (Fiedler & Graw, 2003). Bodies which are interred within the ground generally degrade in fifteen to twenty years. However when adipocere is formed around the body the natural degradation process can be arrested and extended into a much longer period of time (Fiedler & Graw, 2003). As autolysis progresses, the tissues within the body experience oxygen depletion due to the large amounts of aerobic activity and a decrease in pH (Vass, 2001). In general the availability of oxygen around the body can be highly influenced by the soil type, depth and burial practice. For example, Janaway (1987) argues that bodies buried in shallow graves just below the ground surface have a greater degree of aeration than those which are deeply buried. However the amount of aeration decreases if the burial fill is compacted and pore space reduced. During autolysis sugar continues to be degraded through oxidisation by both anaerobic and aerobic bacteria, and fungi producing organic acids and alcohols, H^2O, CO^2 and other gasses (Dent et al., 2004).

1.3.2 Second stage Putrefaction

During putrefaction there is very little oxygen available around the body, as the rate of oxygen usage by microorganisms exceeds the rate of diffusion into the soil (Schlesinger, 1991), which has been observed by Janaway *et al*(2003). Janaway *et al*(2003) conducted an experimental study at Oxenhope on the burial and preservation of buried pigs, where the presence of decomposing pig carcases was found to create a reduced environment within the soil. Marbling, the appearance of reddish-green discolouration and blue and purple lines on the skin, then occurs and is caused by hemolysis as blood cells breakdown within the veins (Stutz, 2003). This is followed by the appearance of vescicles on the abdomen that eventually swell and burst to release a foul-smelling liquid (Stutz, 2003). Stutz (2003) argues that the body would now be unpleasant for the living

community if they were handling it, which may be a consideration when understanding unusual burial positions and the presence/timing of cultural practices. For example, if the body is only covered by a shroud, it is not unreasonable for there to be little physical contact with the body. Anaerobic organisms from both the gut and the surrounding soil and air begin putrefying the remaining bodily tissue (Dent et al., 2004). This causes the further release of gases CO^2, H^2O, CH_4, H, S^{2-}, NH_3, $C_5H_{14}N_2$ (cadaverine) and $NH_2(CH_2)_4NH_2$ (putrecine) (Dent et al., 2004). Wilson *et al*(2007) noted in experimental pig burials that areas where pig bodies were buried experienced an increase in acidity and hypothesised that this was due to the release of ammonia and nitrogen into the soil. With the production of internal gasses the body begins to bloat and in some cases the pressure increases to such an extent the contents of the stomach and rectum are expelled and on rare occasions unborn foetuses (Stutz, 2003). The physical effect of this was seen in experimental pig burials undertaken by Janaway *et al*(2009) in Peru, where adult pigs were buried in a large stone lined tomb 2mx2mx0.6m deep. Upon excavation the team discovered that the pig had bloated to fill the entire tomb, evidence of which was the presence of pig hair, decomposition products and pupal cases adhering to the sides of the tomb. The gasses released from the body permeate to the surface, preventing oxygen from percolating down into the soil (Dent et al., 2004). The soft tissues liquefy and are reduced to a putrescent mass. When bodies are buried in direct contact with the soil, a mucus membrane is formed by the fine silt fraction in the soil and the liquefied decomposition products from the body (Janaway, 1987). In coffined burials the liquefied products can pool in the coffin. In both cases the liquefied material eventually seeps into the surrounding soil forming 'leaches' that can be identified during geophysical surveys (Pringle et al., 2012, Schultz et al., 2006). The ligaments connecting the bones are one of the last soft tissues to degrade (Stutz, 2003). This has important implications for how the body lies within the grave as the bones tend to settle causing movement (Stutz, 2003). The more labile connections or articulations degrade in the first few weeks or months. The more substantial ligaments take months to years to degrade (Stutz, 2003). Stutz (2003) asserts that the sequence of ligament decomposition is predictable making it possible to identify if the body was surrounded by soil using the relative positions of the femur and the patella. Meaning that when bodies have degraded in cavities the femora will roll when the ligaments have degraded, causing the patella to slip from its position on the anterior face of the distal femoral epiphysis and the iliac blades will lie flat on the grave floor. The degradation of ligaments completes the tissue phase of decomposition (stages 1 and 2) and the body is now completely skeletonised.

1.3.3 Stage three: Bone Decomposition

Bone is composed of protein, in bone collagen, hydroxyapatite and an organic component (Dent et al., 2004). The protein is the first to degrade, by bacteria in the soil, into amino acids (Dent et al., 2004). This leaves behind an extremely brittle bone component which is attacked by inorganic mineral weathering. Bone decomposition is driven by bone morphology and soil conditions. Henderson (1987) identifies that the irregular shape of the skull and pelvis leave them susceptible to being crushed and fragmented by the weight of soil. Henderson (1987) also notes that the decay rates of bone are inversely proportional to the size of the bone i.e. that the larger surface area to volume ratio of larger bones leads them to have better survival rates. The maturity of bone can also play a significant part in the rate of decomposition with immature osseous material degrading much faster than the larger, denser mature specimens (Gordon & Buikstra, 1981). The rate and manner of bone degradation is highly dependent on the levels of moisture, temperature and oxygen in the environment (Henderson, 1987, Nielsen-Marsh et al., 2007, Smith et al., 2007).

1.4 Factors Effecting the Preservation of Materials in Burials

To understand the nature of material survival in funerary contexts the depositional matrix and environment should be considered. Soils are highly variable, but the most influential soil characteristics effecting preservation are pH, oxidation (redox conditions), aridity and temperature (Amendas *et al.*, 2012, Gordon & Buikstra, 1981, Klaassen, 2008a, Klaassen, 2008b, Nielsen-Marsh *et al.*, 2007, Smith *et al.*, 2007); and extremes of these conditions can result in exceptional preservation (Breuning-Madsen & Holst, 1998, Glob, 1973, Kutschera & Rom, 2000). This section will investigate the nature of the survival of the most common archaeological materials, wood, charcoal, bone and metal in soils. It will then go on to examine the preservation of soft tissue and organic material and conclude with how the survival rate of archaeological material can be influenced by the proximity of large amounts of organic material (the body) and burial practice.

1.4.1 Bone preservation

Bone taphonomy has been intensively studied (Gordon & Buikstra, 1981, Hanson & Cain, 2007, Nielsen-Marsh *et al.*, 2007, Smith *et al.*, 2007) and soil type can have a major effect on bone preservation (Henderson, 1987). It is commonly accepted that slightly alkaline or neutral soils preserve bone (Henderson, 1987) because it is the acid (H^+) in soils that attack the inorganic bone matrix (Henderson, 1987). However more recent studies can further refine this statement.

Smith *et al*(2007) and Nielsen-Marsh *et al*(2007) were part of a large scale study into the effects of burial environments on archaeological bone, to investigate the effect of environmental factors on bone stability in the soil in terms of its chemical and physical properties. 219 samples (98 animal and 121 human) and associated soil materials were included in the study and, through the use of PCA analysis, Smith *et al*(2007) was able to place the bone into four categories: well preserved, accelerated collagen hydrolysis, microbially attacked bone and catastrophic mineral dissolution. Further to this Nielsen-Marsh *et al*(2007) found that the preservation of bone relied primarily on soil pH, with early bone taphonomy also being a contributing factor. Cluster analysis revealed four major soil types that were grouped into those that were more acidic and those that were neutral or alkaline. The more acidic groups were typically soils found in Northern and Western Europe and primarily free draining, composed of sand and gravel with a lack of calcareous material. In these 'corrosive' soils, soil chemistry was highly influential in bone survival. The second set of soils had a neutral pH value, were organic rich anthropogic soils with high Ca^{2+} values. In these 'benign' soils there was no one major influence on bone preservation. Soil chemistry was not as influential in the second set of soils but taphonomic processes became a contributory factor with bones that were part of inhumations experiencing high levels of degradation due to microbial attack, dissolution and recrystalisation, whereas processed bone and discarded corpse had low levels of microbial attack. Nielsen-Marsh *et al*(2007) observed that these 'benign' soils were primarily the result of anthropogenic influences on the soil environment.

An example of this can be seen at the 7th to 10th century settlement site at Flixborough, Lincolnshire (Loveluck, 1998). Situated on a windblown spur, the site is highly stratified, consisting of layers of occupation material, dump deposits and repeated windblown sand deposits that also bury the settlement (Loveluck, 1998). Sand is generally considered to be a poor preservation medium for bone, due to its high acidity, however large volumes of bone survived at Flixborough (Loveluck, 1998), including several inhumations found in occupation layers. Loveluck, however, reports that the offsite burials did not survive well (1998), meaning that there were local site factors which aided in the preservation of bone. Another example of sand displaying differential preservation rates over short distances can be found at the experimental Earthwork Project at Wareham (Bell *et al*., 1996), where cooked and uncooked bone were placed in the mound to be excavated at predetermined intervals, to record the taphonomic processes occurring over time in the bank and ditch (Bell *et al*., 1996). The site was an acidic, sandy, well drained podzol (Bell *et al*., 1996) and the expectation was that all bone would degrade relatively quickly. During the nine, seventeen and thirty three year excavations all bone in these parts of the mound had completely degraded, as expected. However when the thirty three year section of the mound was excavated,

one piece of bone was recovered in a relatively well preserved state (Crowther, 2002). This was attributed by Crowther (2002) to have been caused by localised differences in soil micro-environment within the mound highlighting that small scale variation in the soil structure and environment can contribute to differential levels of bone preservation over short distances. In relation to this project it emphasises the potential for small pieces of bone to be well preserved in localised areas of the grave. Bone survival in the archaeological record is therefore due to the complex interaction of pre-burial treatment, taphonomy and soil conditions. This creates a high level of variation in bone survival at multiple scales of resolution, dependent on broad scale soil acidity and pre-burial treatment and in smaller scales on the properties of the soil morphology.

1.4.2 Wood and charcoal preservation in soil

Wood, composed of hemicellulose, lignin and cellulose (Janaway, 2002), is found in the archaeological record to a lesser extent than bone. There are several depositional pathways in which wood degrades; microbial degradation from bacterial degradation, soft rot, white rot and brown rot and physical/chemical weathering (Huisman & Klaassen, 2009, Huisman *et al.*, 2008). In most instances the survival of wood in the archaeological record relies on the moisture content of the soil prohibiting exposure to air and therefore preventing microbial degradation (Huisman & Klaassen, 2009 p. 29, Huisman *et al.*, 2008). Janaway *et al*(2003 p 57) also notes that, in an anoxic environment, the anaerobic micro-organisms can attack the cellulose in the cell walls of wood but leave the lignin intact. As with bone, the soil microenvironment can produce sporadic areas of localised wood preservation. Bell (1996) reported that in the Chalk bank Experimental Earthwork at Overton Down (the sister earthwork to Wareham) there was superior preservation of the oak recovered at the eight year excavation than that which was recovered in the four year excavation. Therefore not only are the macro (landscape and profile) scale soil properties important to wood preservation but, over smaller spatial scales, soil microenvironments have a key role in preservation. Charcoal is the result of pyrolysis (Scott & Damblon, 2010) and is considered to be relatively inert, however charcoal does degrade through photochemical and microbial attack and physical weathering (Czimczik *et al.*, 2003, Forbes *et al.*, 2006, Scott & Damblon, 2010, Scott *et al.*, 1986). Charcoal can be produced through natural means such as wildfires or through human agency by the burning of vegetable matter as fuel (Forbes *et al.*, 2006, Scott & Damblon, 2010). There are also several deposition pathways via which charcoal can enter the archaeological record inducing alluvia and aeolian deposition as well as in situ incorporation (Forbes et al., 2006).

1.4.3 Metal objects

Metal objects are often found in burials and in rare cases metal corrosion products have been a catalyst for organic preservation, particularly of textiles (Cameron, 1991, Janaway, 1987). The survival rate of metal objects is highly variable and is heavily influenced by burial interval as well as soil chemical conditions (Janaway, 2002 p.395). The composition of the metal is also pivotal, with metals such as gold being corrosion resistant, iron corroding rapidly and intermediate metals such as copper forming a surface layer of stable corrosion products (Janaway, 2002 p. 396). Soil condition can also influence corrosion rates with oxidising and acidic conditions contributing to corrosion whereas metals survive better in reduced and alkaline soils (Janaway, 2002 p 396). The preservation of organics by metals relies on the rate of metal corrosion being more rapid than the rate of organic degradation so that the metal can either act as a biocide (Cu), or form a cast of metal corrosion products which encompasses the organic material (Fe).

1.4.4 Soft tissue and organic preservation

The bodies soft tissue is unlikely to survive burial and does so only in rare cases, which can include extreme burial conditions: Bog Bodies and Mound People of North Western Europe (Glob, 1973), extreme environmental conditions such as the Franklin expedition (Notman et al., 1987), Ötzi (Kutschera & Rom, 2000, Oeggl *et al.*, 2007) and the St Lawrance Ice Mummy (Smith & Zimmerman, 1975). When the soft tissues do survive they give us a brief glimpse into the potential richness of the organic materials that could have been added to human burials.

Although not a burial as such, one of the most famous examples of organic preservation is Ötzi the ice man found in the Italian alps in September 1991 (Kutschera & Rom, 2000). At approximately 5200 years old Ötzi is the oldest prehistoric person to be recovered who was not deliberately buried (Kutschera & Rom, 2000) and provides an indication of the types of artefacts that were available in prehistory including; a bow made from yew, hay padded leather boots and an axe (Williams *et al.*, 1995). Ötzi's exceptional preservation is thought to have been caused by the body being wind dried and subsequently freezing (Kutschera & Rom, 2000), restricting the availability of water to microbes. The temperature decrease will also have significantly affected the functioning of microorganisms. Further examples of exceptional preservation can be found in the buried bodies of North Western Europe which range from the Neolithic to Medieval periods and consist of fully preserved bodies to skeletonised remains (Van der Sanden, 1996). The most famous examples of bog bodies, Tollund Man, Lindlow Man and Grauballe Man, however are the well preserved Iron Age examples. Human bodies are preserved in bogs due to a combination of

the anoxic and acidic environment as well as, crucially, due to the release of sphagnan from *sphagnum* moss (Van der Sanden, 1996 p.18). Through a series of complex reactions, sphagnan is converted into brown humic acid that binds to Ca and N from the body in such a way that it is unavailable for bacterial growth (Van der Sanden, 1996 p.18). Bacteria are therefore unable to flourish and the fleshy parts of the body become tanned and preserved. In addition to human remains, wool and leather textiles are also preserved including, but not exclusive to, wool and leather skirts, scarves, capes, stockings and shoes (Hald, 1980).

1.4.5 Modifying the burial environment

The modification of the burial environment by human agency such as the use of coffins, inclusion of lime and gypsum and embalming can affect preservation rates of organic material and decomposition.

When part of a burial, the coffin acts a medium to protect the body prior to burial and post burial. Coffins, whether composed of wood or lead, affect rates of inhumation decomposition. Both will, however, act as a form of water barrier (Janaway, 2002). Lead coffins, when well sealed, can create anoxic environments, the lead also acting as an antibacterial creating good conditions for soft tissue and body preservation (Vass, 2001). Wooden coffins however accelerate the rate of decay, and those with a thick layer of wood shavings experience temperature increases as the shavings degrade (Henderson, 1987). The type of wood may also have an impact, with spruce and pine allowing for more rapid decomposing than oak coffins (Fiedler & Graw, 2003). The presence of impenetrable surfaces around the body can produce pooling of bodily fluids and affect the environment of the burial with low redox conditions below liquid level and reducing conditions underneath the body (Janaway, 2002). In fact the presence of 'leachets' of bodily fluids leaking around the coffin and under the body are used during geophysical surveys to identify clandestine graves (Pringle et al., 2012, Schultz et al., 2006). Coffins also protect burials from soil collapse until the tensile strength of the coffin is compromised due to degradation and the weight of the soil overburden. McGowan and Prangnell (2015) conducted a study at a 19th century cemetery in the centre of Brisbane, Queensland, Australia, into the pressure of the soil overburden on coffins as they had identified several cases of highly compressed burials. During their investigation McGowan and Prangnell (2015) observed that wooden coffins experienced collapse of the coffin sides and that hexagonal shaped coffin lids collapsed at the widest point approximately level with the shoulders of the body. There is in general however little research conducted into the process of coffin collapse and infilling. In some instances human agency can intentionally or unintentionally increase the survival rate of archaeological material. The 'mound people' of north

Western Europe are an example of how burial practice modified the soil environment leading to exceptional wood and organic material preservation. The mound people as comprehensively documented by Glob (1973) are a population of Bronze-Age burials in Denmark, with similar burial types in North Eastern England. They are characterised by a series of inhumations where individuals were buried in log (often oak) coffins in peaty mounds, the most famous of which is Egtved girl discovered in 1921. These burials were often found complete with wooden coffins, clothing, wooden vessels and metal objects (Glob, 1973). Soon after burial the coffins were filled with water from the surrounding peat followed by surrounding soil becoming depleted in oxygen causing anoxic conditions and arresting the degradation of the wood and organic remains (Breuning-Madsen & Holst, 1998). In some cases distinct iron pans formed in the mounds that prevented water and oxygen circulation around the burial effectively preserving the wood and organic remains until a change in the environmental conditions (Breuning-Madsen & Holst, 1998, Klaassen, 2008a, Klaassen, 2008b). Although high acidity (arresting bacterial and fungal degradation) played a role in preserving the remains it is likely that the anoxic conditions initially preserved wood and components high in keratin such as hair and wool (Breuning-Madsen & Holst, 1998). The practice of adding lime or gypsum to create 'Plaster Burials' has been observed in Roman burials, which involved the pouring or sprinkling of plaster into stone, lead or wooden coffins (Philpott, 1991). The addition of plaster to the grave has been seen as an attempt to preserve the body as, due to its high absorbency, it would have reduced the amount of water in contact with the body. However it may have in fact stimulated the decomposition of the body and absorbed any resulting bodily fluids and odour, depending on the exact composition of the substance used (Philpott, 1991). Plaster burials have also been known to preserve impressions of textiles including linen and gold thread (Philpott, 1991).

1.4.6 Traces of the body

In some cases the body and associated grave goods degrade completely and the only evidence of a body being present is a dark soil pseudomorph. The process of body pseudomorph formation is not fully understood, however it is thought to relate to the reaction of the soil chemistry and the degradation of the body. Examples of body pseudomorphs were discovered at Sutton Hoo, Suffolk and Mucking in Essex. At Sutton Hoo, an Anglo-Saxon burial ground in Suffolk England, a series of body pseudomorphs were discovered surrounding the main burial mound (Bethell & Carver, 2002). Upon further analysis, these dark pseudomorphs appeared to be formed by phosphorus from the burial and manganese and copper from the surrounding soils (Bethell & Carver, 2002). Bethell and Carver (2002) hypothesised that pseudomorphs were caused by the acid sandy and gravel soils. In a study conducted by Keeley *et al*(1977) on an 5thC Anglo Saxon grave

pseudomorph from the multi-period site of Mucking, Essex samples were taken on three vertical transects within the grave fill/pseudomorphs, to investigate if there were concentrations of manganese and copper in the pseudomorph. The grave was located in the gravel sub-soil at an approximate depth of 60cm. The silhouette and some small pieces of bone centred on the skull and lower left leg was all that remained of the body and there were no visible grave goods. This investigation concluded that there was no relationship between copper accumulation and the body pseudomorph but that copper was being preserved by the relatively acid pH of the soil. Manganese however was accumulating in the body pseudomorph and had been drawn into the pseudomorph from the soil above and below the body. The accumulation of manganese in the pseudomorph was attributed to the tendency of biophile elements to accumulate in areas of high organic matter and microbial activity.

1.4.7 Summary

It has been established that the survival of archaeological material in inhumations is part of a complex interaction of degradation pathways. On a broad scale pH, temperature and moisture content of the soil influence the long term survival of archaeological material. However there are also local and microscale changes in the soil environment which influence the survival of archaeological material such as the connectivity of pore space that produce unexpected preservation such as that seen at the Wareham Experimental Earthwork. The burial environment can also be modified by human agency to produce conditions that are either detrimental or conducive to preservation. It has also been demonstrated that, even when bodies have been completely degraded, there are, in the cases of the bodily pseudomorphs, inorganic chemical signatures remaining in the soil that may be in detectable concentrations when using SEM-EDX analysis. Exceptional cases of preservation also highlight the wide range of organic material that may have been placed in burials but has subsequently been lost from the archaeological record.

1.5 Previous microscale burial studies

The majority of microscale analysis of graves have focused on palynology and gut contents (Berg, 2002, Reinhard *et al.*, 1992), although there has also been limited use of micromorphological and heavy residue analysis (Macphail *et al.*, 2013, Mays *et al.*, 2012, Usai *et al.*, 2010). Micromorphological studies of burials are still in their infancy, however much can be learnt from the wider established palynological and gut contents investigations, as they deal with similar issues of sample location, preservation potential and the influence of pre-internment processes.

Heavy residue analysis can also give an indication of what fragmentary remains can be retrieved from burial contexts.

Palynological and parasite egg studies have been periodically undertaken in burial contexts, yet a strong sampling regime has been developed. Reinhard *et al*(1992) first suggest the use of control samples and the most productive locations for palynological and parasite egg sampling, in an investigation of a single Anasazi burial excavated and sampled in 1983. The purpose of Reinhards *et al*(1992) study was to demonstrate that it was possible for macrobotanical remains, as well as pollen and parasite eggs, to be preserved and to ascertain if in supine burials the sacrum acted as a structural container for the contents of the lower digestive tract. Reinhard *et al*(1992) found that only the sacrum soil showed evidence of macrobotanical remains and pollen was present in higher levels in the sacrum soil than in the controls. Reinhard *et al*(1992) argued that the soil samples obtained from close to the sacrum bone were most productive, whereas soil from close to the pubic symphysis and the grave floor should be taken as controls. The importance of sampling the sacrum and the use of controls was confirmed by Berg (2002), in a study of 17 individuals from south central Arizona and Nordby Denmark. 12 of the 17 individuals sampled produced palynological evidence of digestive tract contents. Berg's study (2002) demonstrated that the sampling methodology could produce successful results in different ecozones with burial matrices consisting of compact silty-clays with calcium carbonate and gravel inclusions (Arizona) and loose sand with shell, gravel and limestone inclusions (Denmark). Both studies highlight the importance of sample location close to the sacrum bone and the extensive use of controls.

Sieving of the basal grave soils can successfully retrieve bone fragments that would otherwise have been missed. Mays *et al*(2012) conducted an experimental heavy residue study to assess the amount of fragmented bone that could be recovered from burials after all of the visible material had been collected. Mays *et al*(2012) examined material from seventy adult internments from 7^{th}-9^{th} century AD cemetery site at Whitby using 8mm, 4mm and 2mm sieves. This study showed that sieving the basal grave deposits increased the weight of human remains by 53%, establishing that a large quantity of fragmented bone was present in the grave fill. The soil matrix at Whitby was boulder clay that had contributed to the generally poorly preserved and fragmentary nature of the skeletal material (Mays *et al*., 2012). Although none were found in Mays' *et al*(2012) study, Mays highlights that at sites with better rates of preservation, sieving may aid in the recovery of calcified soft tissue or bladder stones. Unfortunately Mays *et al*(2012) study did not attempt to separate the basal burial fill by zones therefore does not give an

indication as to whether the fragmented bone was concentrated in any particular area of the grave and no control samples were taken.

An initial micromorphological sampling strategy was developed for clandestine samples by Goldberg and Macphail (2006 p.291) that suggested sampling adjacent to and beneath the body, in the grave fill using a column and a control soil profile from outside of the burial. However few micromorphological studies have been conducted on burials and those that have were undertaken on an ad-hoc basis. Macphail *et al*(2013) conducted a micromorphological study on the Gokstad ship mound burial in Norway. The burial consisted of a wooden Viking long ship (C AD 900) with associated grave goods including an iron encrusted sword which was the presumed location of the body (Macphail *et al.*, 2013). Micromorphology samples were taken through the base of the grave and one along the burial plane in the pelvic area. Macphail *et al*(2013) found that both micromorphological samples contained poorly sorted sandy fill with pellet humus that was phosphate rich. The burial plane sample was also rich in woody remains, presumably from the degradation of the boat. An amorphous yellow material with embedded microfossils was also observed and found to be rich in calcium and phosphorous under SEM-EDX examination (15.2-16.9% P; 12.6-23.0% Ca). Macphail *et al*(2013) interpreted this to be either the remains of human faecal material or part of an amorphous Fe-P-Ca 'body stain'. Although there are some strong conclusions drawn from the micromorphological investigation of the Gokstad Viking Ship burial, this was very much part of a wider study of the environmental context of the mound which included an extensive reconstruction of the mound construction and marine inundation. It therefore would have benefited from a more systematic approach with a greater degree of sampling in the burial plane as suggested by Goldberg and Macphail (2006). The Macphail *et al*(2013) study does however highlight that micromorphological and SEM-EDX analysis of inhumations can be productive and the value of such studies where no macroscopic traces of human remains exist.

Microscale studies of burials can be productive and have produced palynological, heavy residue, micromorphological and inorganic geochemical data of culture, health and diet. Gut contents investigations highlighted the sacrum as a particularly productive sample location. What is also clear is that evidence must be supported by the use of carefully placed control samples. Micromorphological sampling of burials should therefore include strong controls as well as a sample from the pelvic area. The Macphail *et al*(2013) study has shown that it would be possible to observe wood and 'body stains' whereas the Reinhard *et al*(1992), Berg (2002) and Mays

(2012) studies suggest that bone fragments, parasite eggs, macro botanical remains as well as pollen may be visible and partially concentrated in the pelvis.

1.6 Conceptual models

A series of conceptual models, developed from the preceding sections (1.31.5) will now be presented (Figure 1). The conceptual models detailed in Figure 1 comprise three scenarios: (a) is a single supine uncoffined burial, (b) a single supine coffined burial, (c) is a more complex burial scenario in a dense cemetery where there has been truncation of earlier graves and the inclusion of an empty grave, (e) and (d) presents a model for the collapse of the coffin around the body. The purpose of the conceptual model in Figure 1 (a) and (b) is to explore the possible movement of fluids around the body and soil collapse as well as to hypothesise how these two processes will be effected with the use of a coffin or other barrier. Fluid movement and soil collapse will be assessed using micromorphological examination of key features such as coatings and peds, and chemical movement will be further investigated using the inorganic chemical signatures in different locations in the burial environment, using SEM-EDX analysis of the fine material and pedofeatures. Figure 1 (c) is a consideration of how the presence of multiple graves in cemetery settings may affect the movement of chemicals and development of soil features. Figure 1 (d) shows the possible process of coffin collapse and the impact of collapse on body degradation and associated material. Although the sampling strategy has been defined by the InterArChive project (see method 2.1 and InterArChive (Unpublished)) sample placement and what may be visible in each sample will also be discussed. In the first conceptual model (Figure 1 (a)) there is a single uncoffined inhumation. The conceptual model shows the physical compaction of the soil, which would be visible in the micromorphological analysis, and proposed movement of soil water in both vertical and horizontal planes above and below the body, waterlogging and inorganic chemical movement around the body. The soil around inhumations has undergone excavation and backfill creating a vertical column of disturbed soil, normally surrounded by undisturbed soil. This creates a column of soil immediately above the burial, which extends to the surface that has a greater volume of pore space than the soil around it (Dent, 2002), this will be assessed using image analysis of the thin sections. This has two repercussions for the soil structure and water movement; firstly, in the short term, the column of soil creates a ‘sponge’ for soil water (Dent, 2002) and secondly, in the longer term the soil becomes more compact due to the soil settling and a loss of pore space (McGowan & Prangnell, 2015). MaGowan and Parngnell (2015) demonstrated that in adult graves there will be significant downward pressure from the soil that could result in the eventual compression of the body. The weight of the soil onto the burial may

also cause the deformation of the skull and pelvic bones (Henderson, 1987). Evidence of compression in soils can be expressed by the formation of platy peds, which may therefore form in the grave fill (Kooistra & Tovey, 1994) and be seen during micromorphological analysis. The compaction and settling of the soil may also result in a dip being created on the surface, which may act as an area for water to pool (Dent, 2002). In Figure 1 a), water is moving in a downward direction due to gravity, however there is also an upward movement due to water logging and capillary action (Schaetzl & Anderson, 2005). Water also moves in a horizontal direction which is exaggerated due to lenticular ped development in the compaction zone above the burial plane. Soil water may also become trapped in the grave backfill due to a higher number of macro-pores present in the backfill (Dent, 2002, McGowan & Prangnell, 2015) which in turn add to the weight of the soil pressing down on the grave. As the body liquefies and comes into contact with the surrounding soil a mucus film forms (Janaway, 1987). The liquefied decomposition products will then disperse in the soil carried by the soil water through the soil structure. This can be seen in some geophysical surveys as 'leachets' (Pringle et al., 2012, Schultz et al., 2006), and may also be responsible for the formation of body pseudomorphs as seen at Sutton Hoo (Bethell & Carver, 2002), Mucking (Keeley et al., 1977) and Gokstad (Macphail et al., 2013). Differences in the directionality of chemical movement around the body caused by the local variation in soil structure will be assessed using a combination of inorganic geochemical analysis and the identification of micromorphological features such as redoximorphic nodules and impregnations. Upon total body degradation the soil will collapse further into the resulting void. However this will be regulated by the soil texture with sand soils collapsing quickly whereas those high in clay will maintain their shape for longer (Buckman & Brady, 1969). In coffined or chambered graves, (Figure 1 (b)) there would be similar processes occurring in regards to the backfill 'sponge effect' and compression of the soil: however the presence of a coffin will have some specific implications. Body decomposition products may be more evenly distributed along the burial plane due to bloating (Janaway *et* al., 2009) and the coffin acting as a 'bucket' (Dent, 2002) retaining water as it moves down the soil profile. This may cause the formation of a 'soup' of degradation products retained by the coffin which become evenly spread along the burial plane and may be expressed by little inorganic geochemical variation in the burial plane. There have been few studies conducted on the sequence and factors effecting how wooden coffins collapse and degraded. MaGowan and Parngnell (2015) presented evidence for collapse occurring, as the sides of the coffin lose structural strength and the coffin lids collapsing at the widest point. MaGowan and Parngnell (2015) hypothesised that the collapse of the coffin lid was exacerbated not only by the weight of the soil overburden but also by soil water contributing through the hydrolysis of hemicelluloses contained in the wood. The coffin may also act as a physical barrier to soil

organisms and prevent them from accessing the body something which may be apparent in the micromorphological analysis by a lack of excremental and soil organism features in the samples from inside the coffin. The movement of degradation products around the grave soil will become more complicated where cemeteries are denser as in Figure 1 (c) to the point where degradation signatures become widespread. Figure 1 (d) presents a model of the proposed collapse of a coffin around the body as described in McGowan and Prangnell (2015), with the side of the coffin collapsing outwards and the lid deteriorating until it falls into the grave.

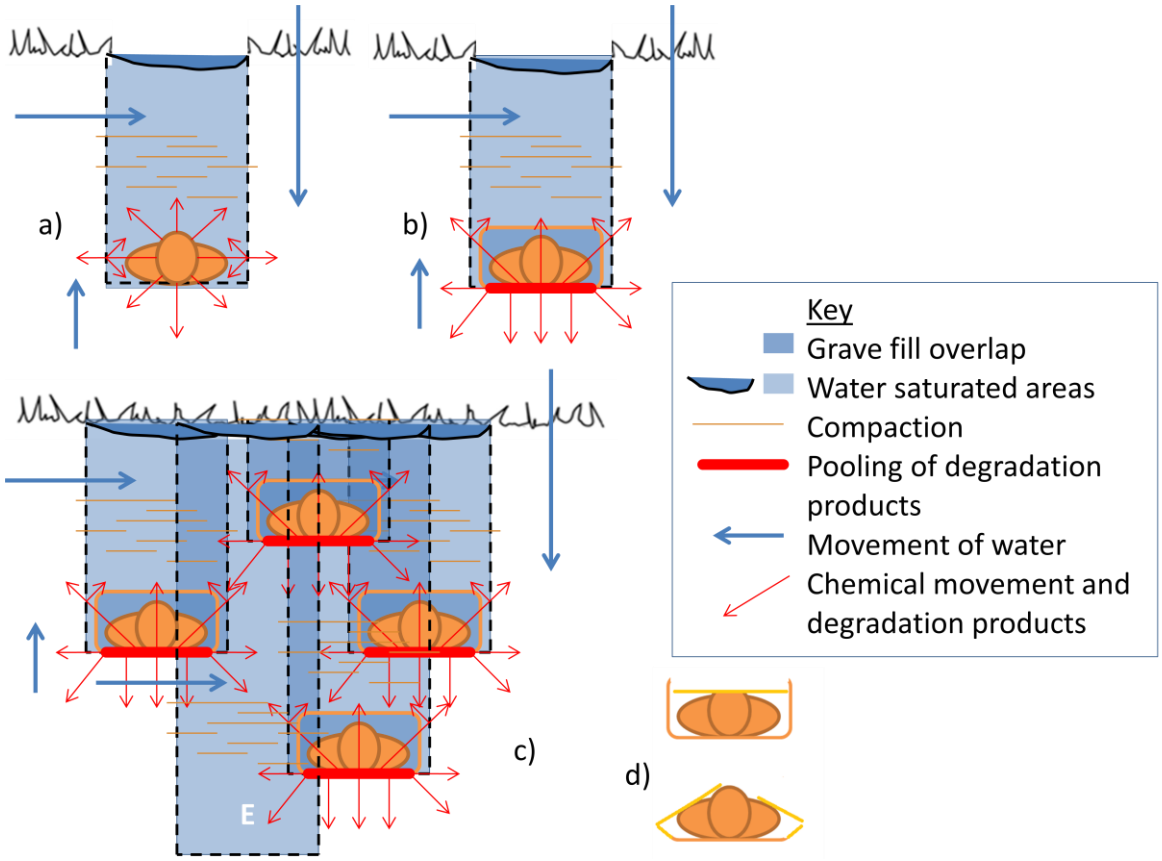

Figure 1: Conceptual module a) of a single supine inhumation with some compaction occurring due to the settling of the soil in the mid burial fill b) as left but coffined c) example of what may occur in a high density cemetery with an example of an empty grave d) collapse of the coffin.

The InterArChive sampling protocol is detailed in the section 2.1. However from the above it may be possible to hypothesise what types of micromorphological and inorganic geochemical signatures may be present in the grave and ascertain if these are location specific. Generally we may expect the grave backfill to contain compaction features such as lecticular platy peds and planes (Adderley *et al.*, 2010, Pagliai *et al.*, 2003, Pagliai *et al.*, 2004), which could be seen upon micromorphological examination. Collapse features, such as fragmented coatings (Kühn *et al.*, 2010), may also be present due to the backfilling, settling of the grave and/or the collapse of the

soil into the body/coffin void. It would not be unreasonable to observe a larger degree of bioturbation in the burial plane thin sections caused by decomposers being attracted to the higher organic content of the soil around the body, provided there was no barrier to their ingress such as a coffin. The development of a crumb microstructure (Davidson & Grieve, 2006, Pagliai *et al.*, 2003, Russell, 1971), mixing of microfabric types, passage features in filled with bow-like structures (Kooistra & Pulleman, 2010) and a larger degree of soil faunal excrement may therefore be present in the thin sections from the burial plane. The inorganic geochemical signatures may also change with higher levels of P, Fe, S and Ca in the fine material of burials compared to the controls (Bethell & Carver, 2002, Keeley *et al.*, 1977, Macphail *et al.*, 2013), possibly accompanied by discolouration of the soil as in the case of the body pseudomorphs (Bethell & Carver, 2002, Keeley *et al.*, 1977). There may be higher concentrations of wood or lead present in the soils if internments were placed in coffins. Spatial differences in inorganic geochemical signatures may be more pronounced in uncoffined graves due to the pooling of bodily fluids in coffined internments (Janaway et al., 2009). Spatial differences along the burial plane may be difficult to detect. However the pelvic area has been highlighted by Reinhard *et al*(1992) as an area where the gut contents may collect. This would also be the area where anything which was expelled from the lower abdomen, such as excrement and foetus tissue, would be present (Reinhard et al., 1992, Stutz, 2003), and if present, it may be possible to observe features during the micromorphological analysis that could be related to these processes. Reinhard *et al*(1992) however emphasises the need for the careful placement of the pelvic samples as concentrations of archaeologically interesting materials are present in the soil closest to the sacrum, with samples more generally in the pelvic area acting as controls. Other more specific materials, generally culturally generated, that may be present in the graves, will be discussed further in the methods section (Table 1, Table 2 and Table 3).

1.7 Prehistoric, Hellenistic and Roman burial practices

From the above we can make a reasonable assumption that there may be scope for the identification of hereto unknown evidence for burial practice and decomposition in inhumations. However, to effectively study the effects of Prehistoric, Hellenistic and Roman burials on soil development and to have a comprehension of what micromorphological and inorganic geochemical elements might be found in Prehistoric, Hellenistic and Roman graves it is necessary to have a broad understanding of the funeral practices in each period. The specifics of burial practices at each site investigated will be discussed in the method (sections 2.2.2.2, 2.2.3.2 and 2.2.5) however a brief chronological overview will be given here.

1.7.1 Prehistoric

A detailed description of all prehistoric burial practices is beyond the scope of this thesis however a brief synopsis of temporal change and regional variability as well as an outline of the different styles of burials that were practiced can be given. This synopsis will focus mainly on European Prehistoric burials as this is the region where the majority of the samples have originated. In early prehistory burials were uncommon and only a few isolated incidents, many positioned in caves, have been discovered which include Gough's Cave in the British Upper Palaeolithic (Hunter & Ralston, 1999 p.22) where five, skinned and dismembered, individuals were found. Moving into the European Mesolithic cave burials are still found which include isolated burials as at Theopetra Cave in the Thessalonikian plane as well as group burials as at Grotta dell'Uzzo, Sicily and Franchthi Cave burials which were found in association with shell, bone and antler grave goods (Whittle, 1996). Human bone fragments in the Mesolithic are rare but found at Aveline's Hole in the Mendip Hills, in association with beads made from pig and deer incisors and red ochre, however it is more common to find disarticulated fragments of human skeletons in shell middens (Hunter & Ralston, 1999 p. 43), meaning that burials were not the standard form of burial rite. Burials in the Mesolithic may therefore warrant more extensive investigation to ascertain the rationale behind an interment as opposed to midden disposal of the body. In central Europe during the mid Holocene (7000-6500BC) burials are sporadic but visible in contexts associated with structures and generally placed in settlements, creating close links between the living and the dead, as well as found on their own (Whittle, 1996). At this time inhumations, with sparse grave goods, predominate. However secondary burials and cremations are also found (Whittle, 1996). In the mid Holocene Europe is dominated by regional trends in burials with styles varying from individuals buried in large cemeteries with elaborate grave goods divided on gender lines (limestone beads, copper rings and bracelets) such as at Tiszapolgar-Basatanya, Hungary, to more modest cemeteries that were commonly associated with Linearbandkeramik (LBK) settlements in central Europe and to some extent with the Ertobølla (Whittle, 1996). In these areas individuals were selectively buried in simple earth cut graves with increasingly rare grave goods comprised of pots, bone, flint and ochre. There is a suggestion that coffins may also have been used but this is tentative. The investment in cemeteries created a closer link between people and place and a stronger emotional investment around settlements and group allegiances. Old traditions however still continue with human bones present in the community (Whittle, 1996). In the later Neolithic there are changes in burials with some areas becoming more formal in the placement of bodies which coincides with more formal inclusion of animals in burials. Collective burials also begin to be more prominent with the construction of large burial monuments in Western and North

Western Europe such as Avebury and the West Kennet Long Barrow (Parker-Pearson, 2003), mounds, platform and cairns where also constructed for the disposal and burial of the dead (Whittle, 1996). Individual burials were however still occurring with flexed burials in ditches and pits of causewayed enclosures in Britain (Hunter & Ralston, 1999) and the internment of Corded Ware and Globular Amphora burials in Europe (Whittle, 1996). Grave goods in the latter included pots, flint axes, amber, the remains of funeral feasts and animals (Whittle, 1996). In the Bronze Age single inhumations once again became common in Britain, having increased in number from the Neolithic, there were also regional influences apparent with the introduction of the Beaker burials. Grave goods had again increased to include arrowheads, daggers, flint and stone axes and amber buttons for men as well as awls and antler picks for women (Hunter & Ralston, 1999). In Bronze-Age Denmark and North Eastern England log (often oak) coffin mound burials of the type described above (see Egtved girl 1.4.5) have been found with extensive organic grave goods (Glob, 1973). Cremations became popular in the British Middle to Late Bronze age meaning that there is very little in the way of burial evidence for this period. In the Iron Age burial practices in Britain moved towards regional areas of cremations, mostly in the South with inhumation being common in the rest of Britain (Cunliffe, 1991). Inhumations in the Iron Age generally consisted of either single burials in earth pits, cists or sporadic deposition of bodies in storage pits within settlements. Grave goods were rich and varied and gender and/or social differences could be demarked with carts, mirrors and weapons (Cunliffe, 1991). There were some exceptions with strong regional preferences for coffined supine burials in the Arras culture in the Humberside and North Yorkshire regions (Cunliffe, 1991).

1.7.2 Hellenistic Burials

Traditional Hellenistic burial practices were strongly regulated by strict laws that limited the more ostentatious burials although these tended to be relaxed with distance from Athens and for individuals of high status (Garland, 1971 p.163, Mee, 2011 p.249). The initial focus was on creating a profound set of 'last words' and a belief that the dying were closer to the spirit world and could prophesise future events (Garland, 1971). After death the body was then washed, anointed, garlanded and dressed to be laid out in the home (Mee, 2011 p.245). Following the funeral procession the body was placed in a hearse and taken to the cemetery for inhumation (Garland, 1971 p.162). Hellenistic inhumations involved the placement of the body, which was generally shrouded, in simple earth or stone cut pits (Garland, 1971 p.164). At times the body was placed in a wooden coffin although examples of sarcophagi are frequent and tile lined tombs were also popular (Garland, 1971 p.164). Hellenistic cemeteries were often divided into plots with separating stone walls or enclosures and rituals at the graveside were complex including the

burning of individual or communal offering pyres which encompassed among other goods, food which was incorporated into the grave (Garland, 1971 p.205). Hellenistic graves were generally poorly furnished but could include oil, strigils, mirrors, toys, jewellery, coins and funeral clothing (Garland, 1971).

1.7.3 Roman burials

There is a high degree of both spatial and temporal variation in burial practice within the Roman period. Spatially burial practice varies between the core area of Rome and its Mediterranean provinces which can be considered more 'Romanised', and the outlying areas where there is a higher degree of influence from native and pagan burial traditions (Hope, 2007 p. 129, Philpott, 1991). This section will first consider Roman burial practices on mainland Europe followed by an overview of how Roman burial practices were adopted in Britain.

1.7.3.1 Mainland Europe

Traditional Roman burial practice followed a prescribed sequence of events designed to regulate the behaviour of the bereaved and the transition of the deceased from the world of the living into that of the dead (Hope, 2007 p. 93). The initial focus in Roman traditions was on creating a 'good death' that involved the presence of the family around the dying individual, whose key role was to portray violent and dramatic expressions of grief (Hope, 2007 p. 96). As in Hellenistic practices the body was then washed, anointed and dressed in the finest clothes and garlanded (Hope, 2007 p. 97, Mee, 2011 p.245) to be laid out on a funeral couch with perfumes and flowers scattered around the body (Hope, 2007 p. 98). Following the funeral procession the body was placed on a bier or sandapila, depending on wealth and status (Hope, 2007, Mee, 2011).

Cremation and burial went in and out of fashion with cremation becoming more popular in Rome by the 1st C BC, followed by a shift back to inhumation in the 2nd C AD (Hope, 2007). Roman inhumations encompassed a wide variety of burial practices including; shrouded, wooden and lead coffin burials (Morris, 1986); plaster burials (Norman, 2002) and stone sarcophagi. The plaster burial package involved the incorporation of plaster or gypsum into the burial. In some cases this involved placing the body in wet plaster (Norman, 2002) or packing plaster/gypsum around the body during burial. Recently there have been suggestions that plaster burials may be related to Christian burial rites (Philpott, 1991), however in some sites they have also been linked to the age of the individual (Norman, 2002). In Roman beliefs a post funeral meal and offerings of food to the dead would have signalled the beginning of nine days of rest and mourning, after

which there would have been a second phase of cleansing rituals, sacrifices and a feast near the tomb completing the transition of both the living and the dead (Hope, 2007 p 115-6).

1.7.3.2 Roman Britain

In outlying areas, like Britain, there are local spatial variations in burial practice that are highly dependent on the strength of Roman influence and the level of immigration of Roman citizens into an area (Cunliffe, 1991, Philpott, 1991). Temporally there was change in the fundamental burial rituals with a dynamic change from a preference for cremation in the early part of the Roman Empire to inhumation in the later stages (Hope, 2007). With Roman colonisation cremation became prevalent, particularly in the urban centres were there was a strong Roman influence. In the mid 2nd Century AD changing fashions in Rome meant that inhumations once again became popular among the Romano-British population, beginning with isolated examples in cremation cemeteries in urban areas, perhaps relating to the burial of Roman immigrants. The influence of the new preference for inhumations meant that in urban areas inhumations became the norm and that in more rural areas where crouched inhumations were still practiced the position of the body and the rituals around the burial became more 'Romanised' (Philpott, 1991). Pre burial treatment of the body consisted of embalming and in some instance wrapping the body in a shroud (Philpott, 1991 p.53). There is evidence however for clothing in the form of metal fastenings and hobnails from shoes which are reasonably common (Philpott, 1991 p.53).

From the 2nd Century AD onwards it became common for bodies to be buried in wooden coffins, however stone and lead coffins were symbols of status and tended to be reserved for more wealthy individuals. Bodies were placed in grave pits lined with slabs/tiles and stone sarcophaguses or more commonly placed directly into the earth. Further burial treatments applied to the body consisted of the inclusion of gypsum or lime plaster into the burial which consisted of pouring the plaster into the casket and covering the body (Philpott, 1991 p.90), a practice which has Christian undertones (Philpott, 1991). Other funeral objects included pottery, glass and metal vessels, pendants, amulets and gems, knifes, combs, coins, and lamps. The tradition of including food and offerings for the deceased was practiced in Roman Britain and animal and food remains, including nuts, poppy seeds and carbonised cereals (Philpott, 1991 p.195) have been recovered. Although there are examples of ostentatious and wealthy burials in Roman Britain the majority were composed of low status individuals with minimal funeral furniture (Philpott, 1991).

Although the above is only a brief glimpse into the fascinating world of Prehistoric, Hellenistic and Roman body disposal what is clear is that it is important to recognise differences and similarities between burial practices and appreciate that there is potentially a large and important part of the burial record missing due to the degradation of organic remains. For example coffins have been tentatively identified in some early burials and in some Bronze Age inhumations however it is not known how widespread this practice may have been. There is also a wide breadth of perishable artefacts such as clothing, wooden object, flowers, skins and food which may have had important cultural and ritual significance in seemingly 'low status' graves that we are not able, at present, to access due to the destructive nature of time. Not to mention any number of pre-burial treatments, such as embalming, mummification and anointing the body which are not currently visible in the archaeological record.

2 Methodology

The method is presented in three sections. The first details the InterArChive sampling protocol which was utilised to collect the samples for this research (2.1). The second focuses on sites employed in this research (2.2), giving contextual information for the burials, period and samples taken at each site. The final section will explore the methods used in this research and their development during the course of this project (2.3).

2.1 Field Methods: InterArChive Micromorphology Protocol

Graves were sampled using the InterArChive micromorphology sampling protocol (Usai *et al*., 2014). Ideally three sampling points in contact with, or near to, the body were collected at; 1) the skull, 2) pelvis and 3) feet (Figure 2). The skull, pelvis and feet were selected to give a wide lateral spatial representation of the grave and to detect any remains from the scalp, hair and adornments, ectoparasites, gut contents, faecal remains, endoparasites, coffin, skin, footwear and possible soil inclusions (InterArChive, Unpublished). The successful identification of such features would enable the reconstruction of dietary information (gut contents and faecal remains), burial practices through the identification of coffins as well as grave goods and personal information such as the presence of hair. Additional sampling occurred at the left and right hand (4 and 5), and any other areas of interest. Through the use of the burial plane samples it may also be possible to establish the presence of collapse features or an indication of high soil saturation levels around the body as hypothesised in the conceptual models (section 1.5). This would enable the reconstruction of the soil conditions inside the burial and begin to elucidate upon post depositional taphonomic processes. Site control samples (C1) were collected, to provide a comparison for the burial plane samples, from similar local soils that did not contain inhumations. In practice this meant sampling from an area of the site that was free of any known inhumations but often containing other archaeological material that may have effected soil development. The purpose of the C1 sample was to establish the nature of the soil at the site to compare with the soil from the burial plane, therefore separating grave specific micromorphological and inorganic geochemical features from those already present in the soil. Addition control samples were taken from the upper grave fill (C2) and the lower grave fill (C3). The purpose of these samples was to gain an understanding of the soils in the immediate location of the burial and of the grave fill. In retrospect that would have perhaps been better thought of as ‘burial fill’ samples rather than ‘controls’. In addition to the micromorphological block samples, small bulk samples were collected where possible, for macroscale soil description (Appendix 1.1.1). A recording sheet was

designed by the InterArChive project to collect sampling and contextual information for each inhumation (Appendix 1.1.2).

Sites were sampled by members of the InterArChive team on an availability basis. This meant that although a high number of sites could be sampled by InterArChive there were some issues with standardisation of the placement and coverage of the samples. There were also problems because the person who eventually analysed the samples did not have first-hand experience of the sites being studied: this was partly because analysts were not assigned to sites/burials till much later in the project. The repercussions of which are discussed in section 9.3.

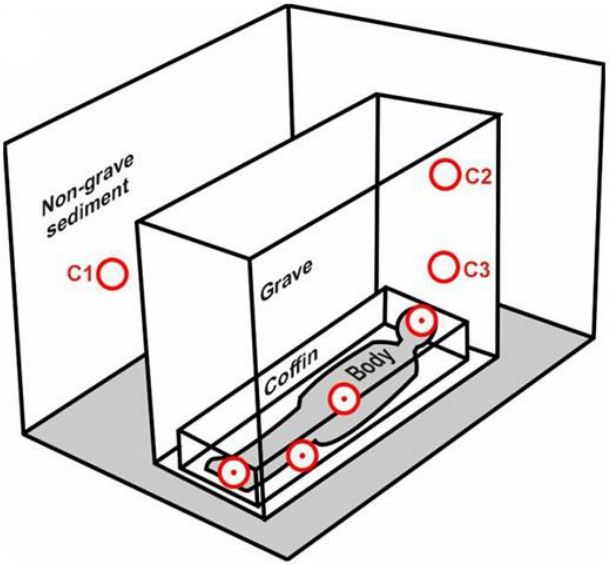

Figure 2: Location of sampling positions around the body (Usai et al., 2014 fig. 1).

2.2 Sites

2.2.1 Rationale for inclusion

The InterArChive project relied heavily on the co-operation of archaeological excavations to allow access to burials, this therefore influenced the environment, period and location of sites (Usai *et al*., 2014). The sites analysed in this research; Çatalhöyük (Turkey), Thessaloniki (Greece), Heslington East (UK) and Hungate (UK), were therefore sub-sampled from the 31 sites investigated by the wider InterArChive project (Usai *et al*., 2014). Sites were selected for inclusion in this thesis by the InterArChive team at the management level. However the selection criteria for sites was broadly based on time period, therefore, those from and prior to the Roman period were included in this work. The method of site selection did present some challenges when it came to interpreting the results across sites, especially at less well documented sites

(Thessaloniki), and when making more wide scale comparisons, which will be discussed below and reviewed in the discussion (Chapter 9).

Thessaloniki and Heslington East were included in this thesis as they were prioritised to meet the overarching needs of the InterArChive project, and were particularly relevant to the organic chemistry investigations (conducted by the chemistry department). Thessaloniki provides a continental example of Roman burial practice to compare to the Romano-British inhumations at Hungate and Heslington East. Three of the five graves at Thessaloniki had good sample coverage, however samples were taken early in the InterArChive project therefore bulk soil samples and archaeological documentation were not obtained. A lack of documentation proved problematic as much of the wider contextual and site information for the graves was lost.

Heslington East was a single Romano-British burial with good sample coverage (C1 soil profile, C2, C3, Skull and foot samples) from York. Unfortunately the pelvic sample from Heslington East was omitted by the onsite sampling team. Fortunately the site was excavated by York University therefore documentation and wider site information was freely available. Heslington East also complimented the burials sampled at Hungate as they were from similar time periods and had similar burial practices.

Hungate was selected for inclusion by the wider InterArChive project. As Hungate was extensively sampled by the InterArChive team, grave selection was conducted by the author. Hungate is a Romano-British site with good sample coverage that provided a large number of samples that had minimal variation in geographic location, soil type, burial practice and period. The large number of graves that could be analysed at Hungate meant that direct comparisons between graves could be made and there was the potential of highlighting common features that are grave or burial practice specific, thus answering the main part of the research question. Graves were to include both coffined and uncoffined burials as well as adult and juveniles.

The archaeological context of Çatalhöyük provided a contrasting environment as well as a high level of time depth to the overall InterArChive project. Micromorphological techniques at Çatalhöyük have also previously shown a high level of success in other research areas (Matthews, 1996, Matthews, 2006, Stokes, Unpublished BSc Dissertation). The burial practice at Çatalhöyük presents a contrast to the supine inhumations found at the later sites in the study and will allow testing of the applicability of the InterArChive protocol to non supine burials. The calcareous nature of the sediment at Çatalhöyük also provided a good comparison for the burials at

Thessaloniki, which also had a calcareous element, meaning that features that are specific to burials in calcareous soils maybe established. Çatalhöyük was sourced and sampled by the author.

On reflection the sites that contained multiple graves were preferred as they allowed intra site comparisons to be made which aided in the identification of soils formations that may be directly related to burials. Those with accessible site documentation (site and grave plans, contexts recording sheets, InterArChive recording sheets and background information), such as Çatalhöyük, Heslington East and Hungate were also useful as this meant commonalities that were not immediately obvious from site photographs could be identified such as comparisons between locations and burial type (coffin/uncoffined).

Each site included in this study as well as the burials sampled, archaeological and environmental context will now be discussed in more detail.

2.2.2 Çatalhöyük

2.2.2.1 Location.

Çatalhöyük is a Neolithic site located in the Konya Basin in Central Turkey (Figure 3 (a)), inhabited between 7400cal BC and 6000 cal BC (Cessford, 2001) and reused during the Chalcolithic, Roman and Byzantine periods. The site consists of two contemporary mounds North and South (Figure 3 (b)), both of which were sampled for this study.

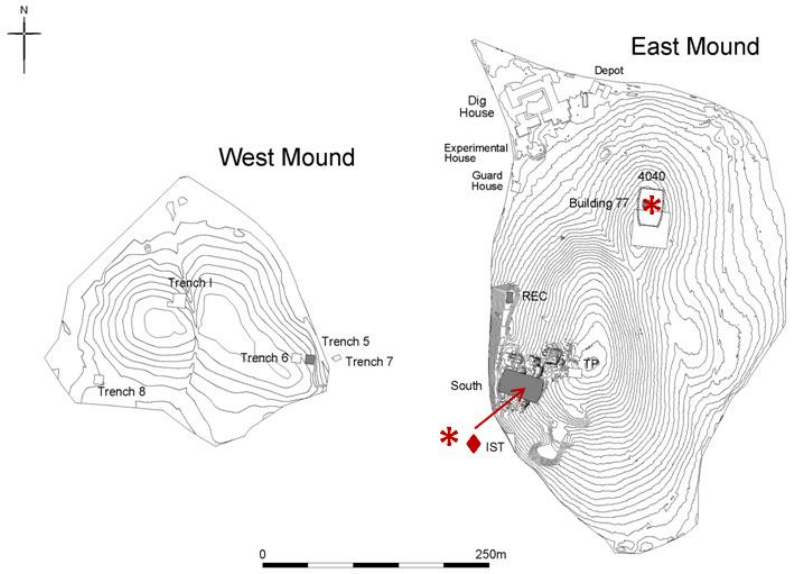

Figure 3: Plan of Çatalhöyük showing the North and South areas of the East mound with burial locations '✶' and C1 location '♦' from Hodder (2005 fig 1.2).

2.2.2.2 Burial practice

Internments at Çatalhöyük are located in buildings under floors in raised platform areas and consist of articulated skeletons or disarticulated primary and secondary burials. Although both types of burial occur at Çatalhöyük, the majority of burials are fully articulated, fleshed individuals and are buried without preference for direction or orientation (Hodder, 2006). Burial contexts at Çatalhöyük have produced high levels of artefacts and ecofacts (Table 1), including evidence of matting, cordage (binding flexed skeletons (Figure 4)) and coiled infant or neonate baskets (Ryan, 2011, Wendrich, 1995). Rosen (2005) has shown that wild panicoid grass was used to construct neonate funeral baskets and that the majority of the matting was produced using Cyperaceae (sedge). Large numbers of beads composed of bone, shell, clay, mineral and rock fragments (Hamilton, 1997, Hodder, 2006, Wright, 2010) have been found with burials, as has obsidian in the form of mirrors, daggers and pointers (During, 2003). Shells containing pigments, bone, flint and wooden objects as well as cloth (During, 2003, Hamilton, 1997, Wright, 2010) and faecal/scat remains (Jenkins, 2012) have been recorded in burial contexts. Despite the rich archive of grave goods, the deposition of goods in burials is not ubiquitous (Nakamura & Maskell, 2005).

Figure 4: Cordage on tibia of skeleton SK12875, Building 56, scale incremented in centremeters. Photographed by Jason Quinlan. Photograph from Ryan (2011 fig 1.)

Table 1: Known burial practices at Çatalhöyük and potential field, micromorphological and inorganic geochemical evidence (During, 2003, Hamilton, 1997, Jenkins, 2012, Nakamura & Maskell, 2005, Rosen, 2005, Ryan, 2011, Wendrich, 1995, Wright, 2010).

Burial practice.	Field evidence.	Potential micromorphological/inorganic geochemical evidence.
The inclusion of matting, binding or basketry.	Impressions of matting or basketry in plaster.	Phytoliths.
Beads composed of shell, bone, clay, minerals and rocks.	Beads.	Concentrations of unusual mineral deposits, with internal voids if in cross section.
Shells.	Complete shells or fragments present.	Evidence of shell/aragonite material. High levels of $CaCO^3$.
Colouring (ochre).	Red staining.	Concentrations of Iron oxides.
Obsidian objects (mirrors, daggers and pointers).	Objects themselves and/or fragments of glass.	Obsidian fragments.
Bone objects.	Bone object or bone fragments.	Bone fragments or high levels of Ca or P.
Wooden vessels.	Wooden objects or fragments.	Wood fragments.
Cloth.	Impressions of cloth in plaster.	Evidence of animal hair/keratin.
Faecal material/scats.	Scats or coprolites and yellow/orange soil discolouration.	Coprolitic material present.
Pottery	Pottery fragments or whole objects	Pottery fragments

2.2.2.3 Soil conditions

The alluvial soils around Çatalhöyük and the building material used to construct the mound have been extensively studied, making a reconstruction of the alluvial soils and origins of the building materials possible (Boyer *et al.*, 2006, Doherty, 2013, Matthews *et al.*, 2013, Rosen & Roberts, 2005, Stokes, Unpublished BSc Dissertation, Tung, 2005). Thin dark layers of organic clay overlying the original Pleistocene lake marl signify the beginning of the flooding regime prior to the occupation of the mound (Boyer *et al*., 2006), dark grey back-swamp clay was then formed during the mounds occupation. Sharp contrasts between a later reddish brown upper alluvium and the lower alluvial layer suggest the occurrence of dry periods (Boyer *et al*., 2006). Matthews (1996, 2013) and Stokes (Unpublished BSc Dissertation) presented evidence arguing that the building materials at Çatalhöyük were sourced from the surrounding sediments, supported by XRD analysis of alluvial sediment of the Konya basin and the plaster building material which are both high in calcite and quartz with some gypsum present. From this, we can surmise the burial soils at

Çatalhöyük are high in calcite and originated from the manufacturing of building material from mostly local sources including alluvial clays.

2.2.2.4 Sampling

Two Neolithic burials were sampled at Çatalhöyük, 18666 and 19295. 18666 was a flexed adult burial, positioned on their back in a west east orientation, located under the north west platform of building 97, in space 365 (Figure 5). The knees were bent by the chin with legs resting on the chest. The bones were discoloured and in poor condition having been partially baked. Samples were taken from under the skull, feet and pelvis as well as a C3. The C1 sample was taken from a platform that did not contain inhumations opposite 18666 (Figure 5). The second inhumation, 19295, was a double burial of two adult disarticulated skulls (19500 and 19501) located in building 77, space 336 (Figure 5). At least one skull was fleshed when buried. The fleshed skull contained a large amount of dark carbonised material and a stone artefact was found directly underneath. Two samples were taken, one under each skull, as well as a C3. Sampling was conducted by the author.

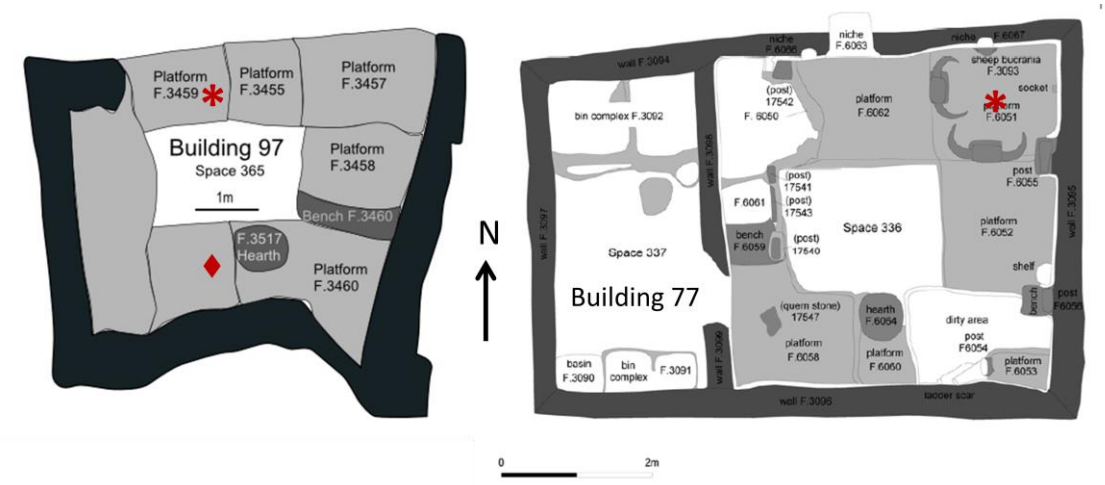

Figure 5: Location of burials at Çatalhöyük, burial locations '✶' and C1 location '♦'. Left building 97 and right building 77. Modified from (House, 2010 fig 23 & fig 26).

2.2.3 Thessaloniki

2.2.3.1 Location

Thessaloniki is located in North Eastern Greece, along its Southern Coast (Figure 6). Thessaloniki was founded in 315BC and became an important Mediterranean port during the Roman era (Kourkoutidou-Nicolaidou, 1997). The site is located in the centre of the city and was investigated as part of a survey project to install a new system of public services (Acheilara, 2010).

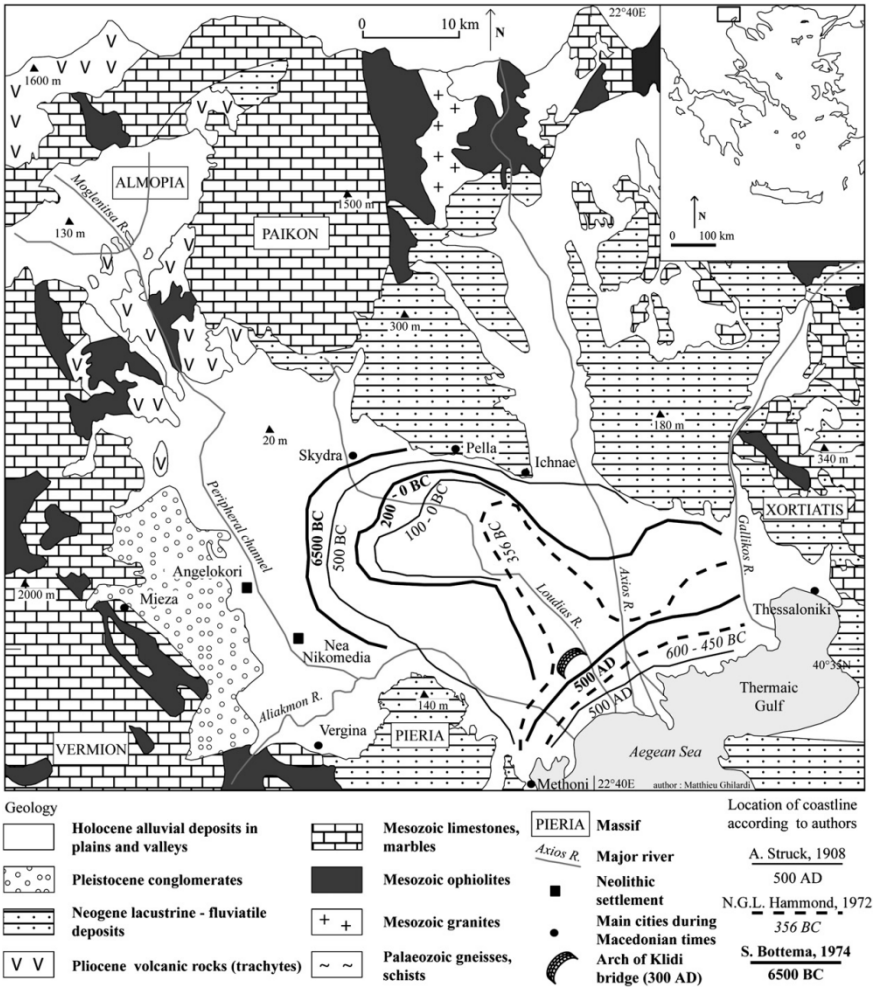

Figure 6: Location and geological and sedimentary context for Thessaloniki (Ghilardi *et al.*, 2008a fig 1).

2.2.3.2 Burial practice

At Thessaloniki the graves dated from the Hellenistic to Roman period (3rd Century BC – 3rd Century AD) and contained burials and funeral gardens (Acheilara, 2010). A variety of objects were found in the graves including glass and ceramic vessels, copper and silver coins, jewellery (copper and gold), golden danakes, metal artefacts and bone objects (Acheilara, 2010, Kourkoutidou-Nicolaidou, 1997). Four wells and a square tank were also identified (Acheilara, 2010). Hellenistic and Roman burial practices and their possible micromorphological and inorganic geochemical evidence are given in Table 2.

Table 2: Known burial practices at Roman and Hellenistic cemeteries and potential field, micromorphological and inorganic geochemical evidence (Acheilara, 2010, Devreker *et al.*, 2003, Garland, 1971, Pemberton, 1985, Rife *et al.*, 2007).

Field evidence	Burial practice	Potential micromorphological/inorganic geochemical evidence
Visible at macroscale	Tiles/slabs	Unusual stone fragments or ceramic fragments in the section.
	Cist graves	NA
	Chambered tombs	NA
	Sarcophagi.	Collapse of soil into the grave (peds and microstratigraphy). Lack of variation in inorganic geochemical signal due to pooling of biological fluids.
	Lead coffins (Roman only).	Fragments of lead embedded in the soil as well as high levels of lead in the fine material (SEM-EDX). Collapse or infilling of soil into the grave (peds and microstratigraphy). Lack of variation in inorganic geochemical signal due to pooling of biological fluids.
May be visible at macroscale but present as fragmented remains.	Eggs and chicken bones	Egg shell fragments and/or bone fragments.
	Sea shells	Shell fragments.
	Faïence and rock-crystal beads	Fragments of glass.
	Jewellery.	High levels of Cu, Fe, Au or Ag. Fragments of unusual inclusions such as jet.
	Coins	Increase in metallic elemental composition Ca, Au, and Ag.
	Lamps	Fragments of ceramic.
	Glass vessels	Fragments of glass.
	Inclusion of pottery	Fragments of ceramics.
	Iron or bronze objects	Fragments of Iron or Bronze in the soil. High levels of Fe, Cu and Sn.
	Shoes.	Fragments of leather, hobnails, and high levels of Fe, S, Mn or P.
	Cremations.	Burnt fragmented bone and/or ashes.
	Nourishment of the dead through the inclusion of liquid and food offerings.	Fragments of burnt and unburnt bone, ceramics and/or wood.
	Feasting at and after the time of burial.	Fragments of burnt and unburnt bone, ceramics and/or

		wood/charcoal.
	Use of wooden coffins.	Fragmented wood and Fe nails. Collapse of soil into the grave as coffin degrades (peds and microstratigraphy). Lack of variation in inorganic geochemical signal due to pooling of biological fluids.
	Inclusion of large amounts of lime or gypsum plaster.	Highly calcareous fine material. Presence of large amounts of Gypsum or $CaCO_3$
	Carved bone	Fragments of bone.
Not visible at macroscale	Clothing.	Presence of fabric or fibres in thin section.
	Inclusion of oils and other biological products.	NA

2.2.3.3 The soil conditions

Thessaloniki is located at the edge of a complex alluvial system that has formed the Thessaloniki plain (Figure 6) (Ghilardi *et al.*, 2008a). The city is situated on a young soil developed from alluvial deposits and contains secondary calcium carbonate Neogene lacustrine fluviatile deposits (Ghilardi *et al.*, 2008a).

2.2.3.4 Sampling

Five graves were sampled at Thessaloniki TF157 and TF182 from the Early and Late Hellenistic respectively, and TF177 and TF178 from the Roman period. TF162 was also tentatively dated to the Roman period. The graves where sampled by the InterArChive team prior to the commencement of this thesis and grave selection was made by the on site team, before the author joined the project. The cemetery also contained a series of small walls which were probably the remains of dividing features or funeral gardens, although this is yet to be confirmed by the excavators.

TF157 was an adult supine burial of undetermined age and sex. The skeleton was positioned with the head to the west, one hand over the iliac blades and feet apart. Samples were taken by the skull, pelvis, hand and feet. The burial was not located close to any other features (Figure 7).

TF182 was a supine adult burial with feet together in an upright position and hands placed by the side of body. Grave goods included two ceramic vessels and two bottles in the left of the grave. The edges of the grave appeared to have been reinforced with sediment. C2 and C3 samples were

taken as were samples from the skull, pelvis, hand and foot areas. The grave was adjacent to a wall and in close proximity to other graves (Figure 7).

TF177 was a supine burial of an adult, located in the centre of a walled structured, with the head towards the north (Figure 7). Grave goods included a coin placed on the chest and a bone hair pin under the skull. The sides of the grave were partially tiled in the area of the knees. A C3 sample and samples from the skull, pelvis, hand and foot areas were taken.

TF178 was a double burial of an adult with an infant by their right shoulder. The adult was a supine burial with its head to the north west. The appearance of the adult burial would be consistent with a body that had decomposed in an open chamber or tomb, as the iliac blades had fallen laterally and the femora had rotated (Stutz, 2003). The grave was tiled with a red ceramic that formed a 'pillow' under the head of the adult burial and a bead was found at the right hand side of the child's skull. The infant burial was covered with plaster. Only the adult was sampled for micromorphological analysis in the skull and pelvic area. TF178 was located at the intersection of two walls, close to other graves (Figure 7).

TF162 was a supine adult burial of indeterminate age and sex, positioned in a north east to south west orientation. The burial was in a large grave that had been lined with sediment and contained a ceramic vessel. Samples were taken from the skull, pelvis and foot areas. TF162 was located in a central area close to other graves (Figure 7). Samples were taken by Brendan Keely and Raimonda Usai prior to the author commencing the project.

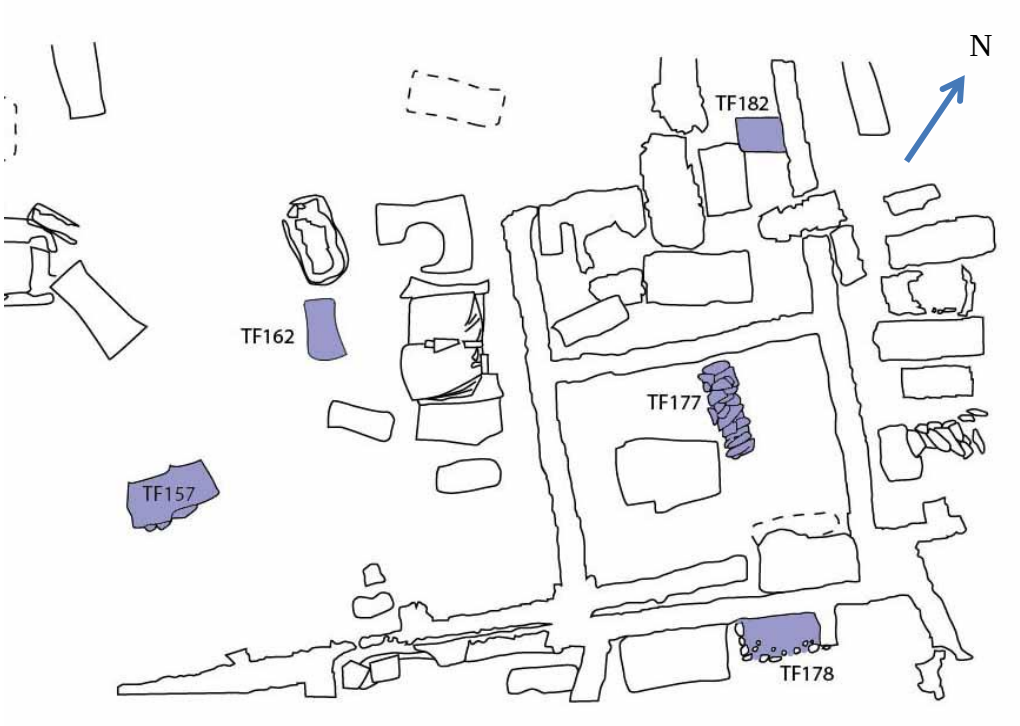

Figure 7: Location of graves at Thessaloniki. A scale was not provided with the site records.

2.2.4 Heslington East

2.2.4.1 Location

Heslington East was excavated by York Archaeological Trust and a team from York University (O'Connor *et al*., 2011). The excavation, conducted between 2003 and 2011, focused on Bronze Age to Roman period deposits across a gentle southward facing slope situated along a spring line (Figure 8) (O'Connor *et al*., 2011). The site is situated on pre-existing agricultural land (O'Connor *et al*., 2011) with a deep, free draining soil, that is highly permeable with a high water storage capacity (National Soil Resources Institute, 2011a). The soil parent material is a heterogeneous mixture of sand, silts and gravels of glacial fluvial origin (O'Connor *et al*., 2011).

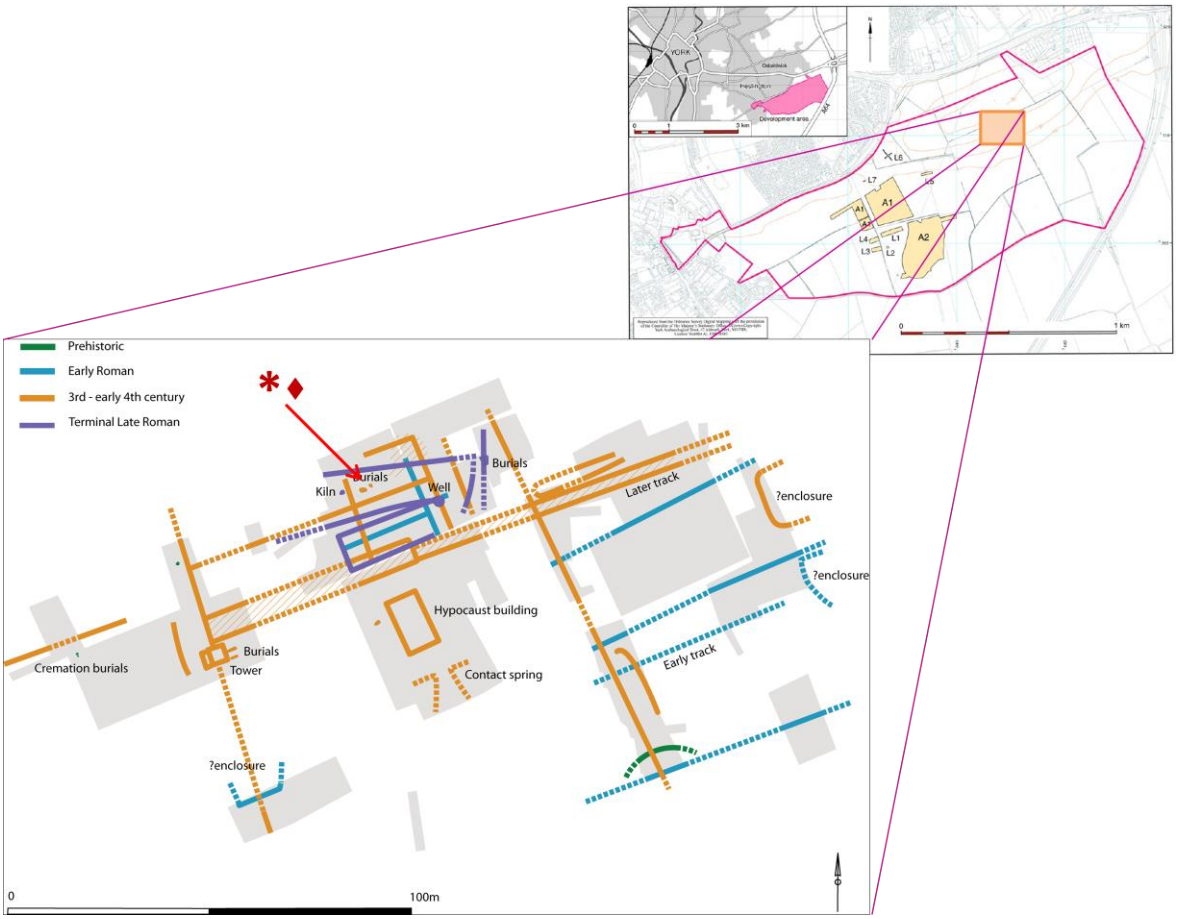

Figure 8: Map of Heslington East showing the location of the excavations (yellow square) (modified from O'Connor *et al*., 2011 Fig 1a p1642) and insert with burial '✶' and C1 location '♦' (site plan kindly provided by Cath Neal, University of York).

2.2.5 Burial practice

The burial from Heslington East was one of a small number that were found at the site, dated to the Late Roman period. The skeletons were generally poorly preserved. Practices specific to the Roman-British period and their possible micromorphological and inorganic geochemical signatures are detailed in Table 3.

Table 3: Known burial practices at Roman–British and potential field, micromorphological and inorganic geochemical evidence (Boylston *et al.*, 2000, Going *et al.*, 1997, Morris, 1986) .

Burial Practice	Field Evidence	Micromorphological/inorganic geochemical evidence
Wooden coffins	Coffin stain and/or Fe nails	Fragmented wood and Fe nail fragments. The collapse of soil into the grave as the coffin degrades visible as peds and microstratigraphy. Lack of variation in inorganic geochemical signal due to pooling of biological fluids.
Cremation	Burnt fragmented bone and/or ashes	Burnt fragmented bone and/or ashes.
Decapitation	Visible on the macroscale	NA
Lead coffins	Lead coffin present or fragments of lead.	Fragments of lead embedded in the soil as well as high levels of lead in the fine material (SEM-EDX). Collapse or infilling of soil into the grave (peds and microstratigraphy). Lack of variation in inorganic geochemical signal due to pooling of biological fluids.
Nourishment of the dead through the inclusion of liquid and food offerings.	Fragments of burnt and unburnt bone, ceramics and/or wood.	Fragments of burnt and unburnt bone, ceramics and/or wood.
Feasting at and after the time of burial.	Fragments of burnt and unburnt bone, ceramics and/or wood.	Fragments of burnt and unburnt bone, ceramics and/or wood.
Shoes	Fragments of leather and/or hobnails.	Fragments of leather, hobnails, and high levels of Fe, S, Mn or P.
Jewellery	Whole pieces of jewellery, fragments of unusual inclusions such as jet.	High levels of Cu, Fe, Au or Ag. Fragments of unusual inclusions such as jet.
Pottery	Whole pieces of pottery or fragments.	Fragments of ceramics.
Lime or gypsum plaster.	Visible in the macroscale	Highly calcareous fine material. Presence of large amounts of Gypsum or $CaCO_3$
Coins	Visible in the macroscale	Increase in metallic elemental composition Ca, Au, and Ag.
Cist graves	Visible in the macroscale	NA
Chambered tombs	Visible in the macroscale	NA
Carved bone	Complete bone carvings or bone fragments	Fragments of bone.

2.2.5.1 Sampling

The inhumation (713) dated to the Late Roman Period (1704 ± 30BP) and was a supine burial of a mature adult female (46yr+). The grave was partially surrounded by large stones lining the sides. The skeleton had a north to south orientation, with hands placed over the pelvis and feet together (Holst, 2010). The bones were generally in poor condition (60% complete) (Holst, 2010) and had possible brucellosis lesions on both hips (Holst, 2010). A C1 soil profile, C2 and C3

samples were taken as well as samples from the skull, hand and foot areas. Sampling was conducted by Brendan Keeley, Mat Pickering and David Broughton prior to the Author joining the project.

2.2.6 Hungate

2.2.6.1 The site

Hungate is a large archaeological excavation within the city of York undertaken by York Archaeological Trust (Figure 9). The first known occupation of Hungate dates from the Roman period, when it was settled by Roman legionaries to regulate the local population (York Archaeological Trust for Excavation and Research Limited). During the Roman period Hungate was located just outside of the legionary fortress, adjacent to the main road into and out of the settlement and is now located in the centre of York having been urbanised (Evans, 2007a). Although the presence of a Roman cemetery in this area has been well documented there had been few prior opportunities, to excavate and study the site.

2.2.6.2 Soil conditions

The soil at Hungate has formed through sedimentation from the nearby River Foss creating a loam with a high clay content that is slowly permeable to seasonally waterlogged (National Soil Resources Institute, 2011b). Hungate has a drift geology, composed mainly of boulder clay with complex layers of alluvium, sand and gravel with several possible phases of water inundation due to flooding of the River Foss (Evans, 2007b).

2.2.6.3 Burial practice

The burials from Hungate dated to the Roman-British period. Practices specific to the Roman-British period and their possible micromorphological and inorganic geochemical signatures are detailed in Table 3.

Figure 9: Location of the Hungate site in York showing proximity to the River Foss, (street map modified from Evans (2007a fig 1) and grave locations with the C1 '♦'.

2.2.6.4 Samples

Hungate was extensively sampled, therefore a sub-sample of graves were chosen for inclusion in this research on the basis of burial practice and age of burial. The graves selected consist of three infant graves and seven adults, with one lead, six wooden coffins and three burials with no coffin evidence. The infant burials were chosen as they would provide a good comparison for one another and also to determine if there was a 'critical mass' which needed to be reached for the degradation of the body to effect the soil. The mix of coffined and 'uncoffined' adult burials was chosen to ascertain if the presence of a coffin could be determined using soil micromorphology and inorganic geochemistry. The details of the graves included follow below with the grave

positions shown in Figure 9. Sampling was conducted by the majority of the InterArChive team, including the author.

The lead coffined burial, SK54898, was a badly preserved, supine infant, of indeterminate sex. The pelvic area and lower limbs were visible only as stains in the sediment. The coffin had been infiltrated with fine, blue grey coloured partially stratified sediment. A jet hair pin was found in the coffin and jet beads and bracelets were found in the backfill. A C2 sample was taken from the upper grave fill and a C3 sample was taken from inside the lead coffin. Samples were taken from the skull, pelvis and shoulder areas.

SK51326 was a supine coffined burial with an east west orientation and the head facing north west, with arms folded over the chest. A C2 sample was taken ~30 cm above the body and a C3 was taken adjacent to the body in the area of the coffin stain. In addition a skull, pelvic and foot area sample were also taken.

SK51387 was an adult burial lying on its right side and oriented east to west. Preservation was generally good, however there had been some degradation of the left pelvis and femur. From the appearance and body position this individual was most likely shrouded. A C3 sample was taken above the feet in addition to skull, pelvic and foot area samples.

SK51351 was a waterlogged inhumation that was contaminated with diesel, located under the soil profile C1 samples. The grave contained a degraded adult skeleton with jet and copper grave goods, as well as a collection of material at the foot of the grave. Samples were taken from below the skull, pelvic and foot area. An additional sample was taken from the collection of materials at the foot of the grave.

SK54090 was an uncoffined child/juvenile situated across a Roman ditch. The burial was placed on its right side with an east west orientation and was well preserved. A C3 sample was taken in the burial plane and a skull and pelvic area sample were also obtained.

SK54085 was a supine adult inhumation, on a north west to south east orientation, with the hands placed over the pelvis and feet close together. The ribs, spine and shoulder blades were degraded and a ceramic vessel was placed over the area of the feet with a second ceramic vessel near the head, adjacent to a bowl. An iron object was found adjacent to the feet. A coffin stain was observed as were 13 iron nails. A C2 and C3 sample were taken as were a skull and pelvic area sample.

SK54341 was a supine adult burial with hands crossed over the pelvis and the head turned to the left. The C3 sample was taken just above the skull (fill No. 54053). The skull, pelvis and feet areas were also sampled. The feet were not present in the burial, therefore this sample was taken from where the feet would have been. In addition to the skeleton there were the remains of a shoe and a possible coffin stain present, which were both sampled for micromorphological examination.

SK54342 was a supine, adult burial of indeterminate sex and age. The body was orientated in a north west to south easterly direction with the head facing east. The preservation of the skeleton's long bones was good, however the ribs and spine were degraded and the left arm was missing due to being truncated by a later feature. Grave goods included a copper coin found in the left hand and eight coffin nails. The C3 sample was taken level with the body in line with the skull. The skull and foot area samples were taken adjacent to the body with the pelvic area sample taken below the pelvis.

SK54908 was a well preserved supine infant inhumation with a north west to south east orientation with the head facing south. The burial was placed with feet together and hands by their side. Coffin nails were identified as was a wide range of grave goods including two glass bottles, probably containing ointment, within the coffin by the skull were, a ceramic container containing chicken bones and three small vessels. A C2 sample was taken as were samples adjacent to the skull, pelvis and feet.

SK51350 was a supine adult burial in a north east to south west orientation. The bones were generally in moderate to poor condition as a later cess pit truncation located close to the right side of the body had resulted in the degradation of the right forearm, hand and the iliac blades. The left forearm and hand were missing but a finger bone from the right hand was found over the pelvis. The rib cage and shoulder bones on the right hand side of the skeleton were also degraded. In addition to the skeleton there were coffin nails and a coffin stain. The C2 sample was taken ~15cm below surface level with the C3 sample being taken ~48cm below the surface level parallel to the skull. A skull, pelvis and foot area sample were also taken.

2.3 Laboratory methods

Soil micromorphology and slide, based image and inorganic geochemical analysis were utilised. This section will detail the methods used, highlighting how they were developed during the research period and justify why each method was selected in relation to the research questions and objectives. A summary of the samples taken at each site and the methods applied to each sample is given in Table 6 at the end of this chapter (see page 56).

2.3.1 Micromorphological analysis

Soil micromorphology has been successfully applied to a variety of archaeological applications including the impact of ancient agriculture on soils (Carter & Davidson, 1998, Davidson & Carter, 1998, Macphail, 1998, Macphail *et al.*, 1990, Usai, 2001), investigation of floors and stabling deposits (Banerjea *et al.*, 2015, Macphail *et al.*, 2004), marine sediment deposits (Macphail *et al.*, 2013) and soil formation in archaeological contexts (Slager & van de Wetering, 1977).

Soil micromorphology was selected as it can be used to investigate the presence of micro-artefacts in the burial, such as the remains of grave goods that have degraded beyond the visible scale, thus enabling the reconstruction of burial practices from the microscale evidence and answering the third research objective. Micromorphology also has the added advantage in that it preserves the physical effects of soil processes in the internal structure of the soil and relationships between soil features. Interpretation of the soil structure and pedofeatures could then be used to reconstruct grave formation and taphonomic processes such as the presence of waterlogged soils as well as traces of iron in the fine material and pedofeatures. This would enabling the reconstruction of soil preservation conditions as well as body degradation products by analysing frequencies of iron pedofeatures, answering the second and fourth research objectives. The sample also acts as a permanent record of the soil structure for future analysis.

2.3.1.1 Thin section preparation

Blocks were processed by David Broughton, Annika Burns and Harri Win Williams at the University of York. In brief after being dried using acetone replacement, blocks were impregnated with 17449 Crystic resin, under vacuum. The blocks were cut along two axis, where possible, one perpendicular and one parallel to the body. The cut blocks were bonded to glass slides, using epoxy 301 resin and ground to a thickness of ~30 µm. The slides were left uncoverslipped to allow the use of SEM-EDX analysis. Micromorphological description was conducted using standard methods published in Bullock *et al*(1985), Stoops (2003) and MacKenzie and Adams (2005). Usai (1996) protocol was modified by the InterArChive team and used as the basis for micromorphological description (see section 2.3.1.2). Analysis was conducted using a Zeiss AxioLab A1 petrographic microscope and an AxioScope A1 *x*/*y* motorised stage microscope in plane polarised light (PPL) and cross polarised light (XPL). Photomicrographs were taken using the AxioCam ERc 5c and mosaic images were taken using AxioVision Rel. 4. 8 software. Micromorphological descriptions were conducted using the standard 10x magnification within the binoculars and optic magnification at x2.5, x5, x10, x20 and x40.

2.3.1.2 Micromorphology protocol development

The micromorphological protocol was developed as part of the InterArChive project by Carol Lang, Raimonda Usai and Helen Williams. The protocol was adapted from Bullock *et al*(1985), Stoops (2003) and Usai (1996), with the majority of the terminology originating from Stoops (2003). Each slide was photographed using the mosaic imaging AxioVision software. Once under the microscope preliminary separation and identification of microfabric types was undertaken then each microfabric was described in detail. The photo mosaics of each slide were extensively annotated to assess the distribution and orientation of each feature observed in thin section (Appendix 1.1.3). This facilitated the investigation of the spatial arrangement of the features, both in relation to each other and to the body and ground surface. A detailed description of all seven protocol categories (fine material, inorganic coarse material, organic coarse material, coarse fine relationship and ratio, pedality, voids and pedofeatures) and their sun-categories will now follow. The protocol developed for the InterArChive project was standardised between all participating micromorphologists, however the protocol has been adapted for this thesis, and detailed where appropriate.

2.3.1.2.1 Fine material

The fine material is closely related to pedogenic processes due to its large surface area and it's physico-chemical properties (Bullock *et al.*, 1985 p. 65, Stoops, 2003 p.85). Fine material was defined as all the material that was below 50µm, which is within the range suggested by Bullock *et al*(1985 p. 18) and Stoops (2003 p. 46). The percentage of fine material was estimated using percentage charts given in Stoops (2003 p. 48). The percentage of fine material is shown as the overall amount of solid soil material that is fine, giving a C:F related distribution that equals 100% (percentage of fine material + percentage of coarse material). In this instance the coarse material only included the mineral element and did not include bone, shell and charcoal. The colour, limpidity, interference colour and birefringence fabric of the fine material were recorded using plane polarised and cross polarized light at x5 magnification and the terminology outlined in (Stoops, 2003). In the grave environment the quantification and classification of the fine material will give an indication of shrinking and swelling by the classification of the orientation and translocation of particles (Courty *et al.*, 1989 p. 151), the presence of inorganic geochemicals in the sediment from absorption and staining of the fine material (Bullock *et al.*, 1985 p. 66) and an indication of the history and evolution of the soil (Stoops, 2003 p 85).

2.3.1.2.2 Coarse components

Coarse components were defined as all the material above 50µm. Coarse components were further sub-divided into mineral and rock fragments and organic coarse components.

2.3.1.2.2.1 Mineral and Rock fragments

Inorganic components are defined as those identified as discreet units above 50µm and are not organic or of organic origin. In practice this encompassed the single and compound mineral grains and rock fragments. The abundance of mineral and rock fragments were estimated using the percentage charts given in Stoops (2003 p.48) and were given as the percentage area of the solid soil material (not including bone, shell and charcoal) composed of each mineral and rock fragment type. The optical properties of each inorganic component were recorded: colour, interference colour, the presence or absence of weathering, size category, abundance and angularity using plane polarised and cross polarized light, at x2.5, x5, x10, x20 and x40 magnification and the terminology outlined in (Stoops, 2003). This facilitated the reconstruction of the grave soil parent material and mode of transport (Schaetzl & Anderson, 2005, White, 1997), post depositional pedogenic processes (Stoops, 2003 p. 78, Weiner, 2010, White, 1997) and post depositional chemical change (Weiner, 2010).

2.3.1.2.2.2 Organic coarse components

Organic coarse components were defined as all those materials that were organic or of biological origin, which could be identified as discreet units above 50µm. The abundance of organic coarse components were estimated using the percentage charts given in Stoops (2003 p.48) and were given as a percentage of the solid soil material composed of each organic coarse component type. Basic optical properties were recorded: weathering, size category, abundance, angularity, colour and interference colour, using plane polarised and cross polarized light, at x2.5, x5, x10, x20 and x40 magnification using the terminology outlined in (Stoops, 2003). The identification of organic material within thin section was problematic as most organic material had degraded significantly, a problem that is exacerbated with the age of the sites considered in this study. This created some ambiguity in the identification of organic matter, meaning that organic matter could only be tentatively identified, particularly when in its amorphous form (Stoops, 2003). Other organic coarse components that could be more securely identified included bone, charcoal, shell, fungal sclerotia, phytoliths and roots. These organic coarse components were identified using well established diagnostic features. A ‘ropey’ internal appearance as well as high inference colours in XPL and pale yellow colour in PPL was used to establish the presence of bone (Macphail &

Goldberg, 2010, Stoops, 2003) whereas shell was distinquished by a fibriouse internal fabric coupled with high inference colours (Stoops, 2003). The overall external shape of shell fragments was also considered. Inclusions that were dark black in PPL and XPL with sharp boundaries were identified as charcoal (Bullock *et al.*, 1985, Courty *et al.*, 1989, FitzPatrick, 1993, Stoops, 2003). Fungal sclerotia were identified by their spherical shape, a dark red/brown colour in PPL and their cellular internal structure (Fitzpatrick, 1993). Phytoliths were identified as both linear and clustered features and distinguished due to their external and internal structure as well as being translucent in PPL (Piperno, 2006). In the grave environment the quantification and classification of organic coarse components will give an indication of whether organic artefacts were included with the burial, such as food offerings and what subsequent formation processes have occurred such as the chemical and physical weathering of bone fragments or the in situ fragmentation of shells.

2.3.1.2.3 Coarse fine relationship and ratio

The description of the coarse fine related distribution identifies how the coarse material relates to the fine material present within a soil which is important for understanding basic soil hydrological properties (Stoops, 2003 p. 44). The coarse fine relationship and ratio of the soil material is described using the coarse fine related distribution charts and descriptions from Stoops (2003) in polarised light at x5 magnification. In a grave environment the quantification and classification of the coarse fine relationship will give an indication of the shrink and swell capacity of the soil (Stoops, 2003 p. 44) which may be important when interpreting the presence of peds and pedofeatures in the fine material.

2.3.1.2.4 Pedality

Pedality was defined as the degree and extent of ped formation. Peds were formed by voids developing along planes of weakness when the soil had been influenced by stress factors such as compaction or water loss (Brewer, 1964, White, 1997 p58-59). Soil horizon, organic matter and clay content may also influence ped development (Birkeland, 1984 p15-17). In a grave environment the quantification and classification of peds maybe diagnostic of soil formation processes such as compaction and the presence of large amounts of organic matter (Table 4) (Birkeland, 1984, Bullock *et al.*, 1985, FitzPatrick, 1993, Stoops, 2003).

Peds were classified using the terminology in both Bullock (1985) and Stoops (2003) in plane polarised light in hand specimen and at x2.5, and x5 magnification. Ped development as opposed to separateness was recorded, as development is an indication of how developed the peds had

been in the past, even if inter pedal voids had subsequently been in filled or aggregated. Ped abundance was estimated using the percentage charts given in Stoops (2003 p. 48) and taken as a percentage of the sample area, peds were also recorded as primary, secondary and tertiary according to Stoops' classification (2003 p.60). The size of peds was measured across the widest width of the ped. The distribution of the peds was given as the basic distribution and referred distribution as outlined in Stoops (2003 p.38-42). The referred distribution was given in reference to either the body or the ground surface.

Table 4: Ped types and their formation processes (Birkeland, 1984, Bullock *et al.*, 1985, FitzPatrick, 1993, Hussein & Adey, 1998, Stoops, 2003).

Type	Description	Effects	Formation processes
Platy	Flat plate like formations which are normally oriented horizontally. There are three main types which are recognised; 1) straight, 2) wavy and 3) lecticular (thin at the edges and thick in the middle.	Particle size orientation	Cyclic wetting and drying Frost action Pre-existing layering Compaction
Prismatic (including columns)	Prisms are vertical structures within the soil which have accommodated surfaces. A sub category of prisms are columns which are prismatic structures with rounded ends.		Wetting and drying of soils and are most common in the middle and lower horizons. Columns can be formed when prisms experience higher degrees of erosion or greater amounts of upward swelling in column centres.
Blocky	Blocky peds come in two subtypes, angular blocky which just have straight edges and subangular blocky which consist of both straight and round edges.		Wetting and drying Freeze/thaw processes. Fine blocky peds may be produced by faunal activity especially when loosely packed.

Table 4 continued

Type	Description	Effects	Formation processes
Spheroidal peds	Bullock recognised two types of spheroidal peds; Crumbs (porous) Granules (non-porous) These are generally peds with the same height as length which have rounded sides.		Faecal pellets of some organisms, Reworking of the soil by organisms Wetting and drying processes.
Apedal	Absence of peds.		Destruction of aggregates by cultivation or compaction Water logging inhibiting ped formation. Lack of time for ped development. Soil composition.

2.3.1.2.5 Void space

The soil pore structure is highly influential in the movement of soil water and therefore micro-organisms and nutrients within the soil matrix (Table 5) (Nunan *et al.*, 2001a, Nunan *et al.*, 2001b, Pagliai & De Nobili, 1993, Van Veen & Kuikman, 1990). Pagliai and Kutilek (2008b) argued that the size, morphology and connectivity of soil pores is a highly significant factor in the movement of both soil water and organisms within the soil. This was further supported by Bundt *et al*(2001) who found that preferential flow rates of water through a soil profile, caused by the pore morphology, affected the distribution of microbial biomass within soil creating 'hot spots' of biological activity. Any increases in pore space have also been linked to wetting and drying cycles (Hussein & Adey, 1998, Pires *et al.*, 2008). In a grave environment the quantification and classification of voids have the potential to retain information about soil formation, biological activity, taphonomic changes and the movement of fluids.

Voids were classified using the terminology in Stoops (2003). The following void attributes were recorded; type, diameter, abundance in percent, orientation and distribution in plane polarised light and at x2.5, and x5 magnification. Abundance was estimated as a percentage area of the sample using the percentage charts provided in Stoops (2003 p.48). The type of void was established using the void description criteria given in Stoops (2003 p.64), whereas the orientation and distribution of the voids were recorded according to the criteria for referred and related distribution patterns also given in Stoops (2003). The distribution patterns were recorded

in reference to either the body or the ground surface. The size of the void was measured along the widest part of the width of the void.

Table 5: Pore space types with functional properties and formation processes (Brewer, 1964, Kooistra & Pulleman, 2010, Ringrose-Voase & Bullock, 1984, Stoops, 2003).

Pore type	Functional properties	Formation processes
Packing voids	Rapid infiltration of liquids, easily worked by roots, low water storage capacity.	Loose packing of soil materials, fauna excreta and shrinking and swelling processes.
Vughs	Mainly seen as water storage pores. However their role in water movement and root penetration is not well understood and highly dependent on the connectivity of voids, which can only be understood fully in three dimensional analysis.	Dissolution of components, aggregation, flocculation and soil fauna.
Channels	Form easy conduits for roots and water movement. However most are too large to form a significant part of the water storage system.	Roots or biogalleries formed by soil fauna. May also be caused in rare cases by escaping gasses.
Planes	Fulfils a similar role to channels and depending on orientation, can assist in the vertical drainage of saturated soils.	Result from shrinking and swelling during wetting and drying or slipping.
Vesicles		Air bubbles which become trapped in the soil matrix, caused by raindrop impact in soils.
Chambers		Produced by soil organisms for the purposes of reproduction, retreat or for the deposition of material such as seeds or eggs.

2.3.1.2.6 Pedofeatures

Pedofeatures are units in the soil that are recognised by differences in their concentration or internal fabrics which separate them from the coarse and fine material (Stoops, 2003). In a grave environment pedofeatures could identify soil formation and development processes including, but not exclusive to, periods of saturation (Kemp *et al.*, 1998, Lindbo *et al.*, 2010, Veneman *et al.*, 1976), bioturbation and the presence of soil organisms (Davidson *et al.*, 2004, Jongmans *et al.*, 2001, Kooistra & Pulleman, 2010) and particle movement (Courty *et al.*, 1989, Gunal & Ransom, 2006, Kemp *et al.*, 1998, Macphail *et al.*, 1990). As at the initial stages it was unclear which pedofeatures were to be of particular importance all pedofeatures were recorded and treated equally.

The optical properties recorded for each pedofeature were; colour, interference colour, size, type, sub-type, attribute, abundance, size and basic and referred orientation and distribution, using plane polarised and cross polarized light, at x2.5, x5, x10, x20 and x40 magnification and the

terminology outlined in (Stoops, 2003). The abundance of the pedofeatures was estimated using the percentage charts given in Stoops (2003 p.48) and given as an area percentage of the whole samples. The size of the pedofeatures was given as the width of the feature at the widest point. The basic and referred orientation and distribution pattern was categorised according to Stoops (2003 p.38-42) and was given in reference to either the ground surface or the body.

2.3.2 Relational Access Database

A relational database was produced to store and manage the data collected during micromorphological description. The database was designed to group and retrieve information quickly, through the use of queries, store information using a small amount of space and to standardise data. The design of the database had three levels of information (Figure 10); site level (A), grave level (B) and slide level (C) which were used as the primary means of organising the data. This section will outline the tables used in the database with all tables presented in Appendix 1.1.4.

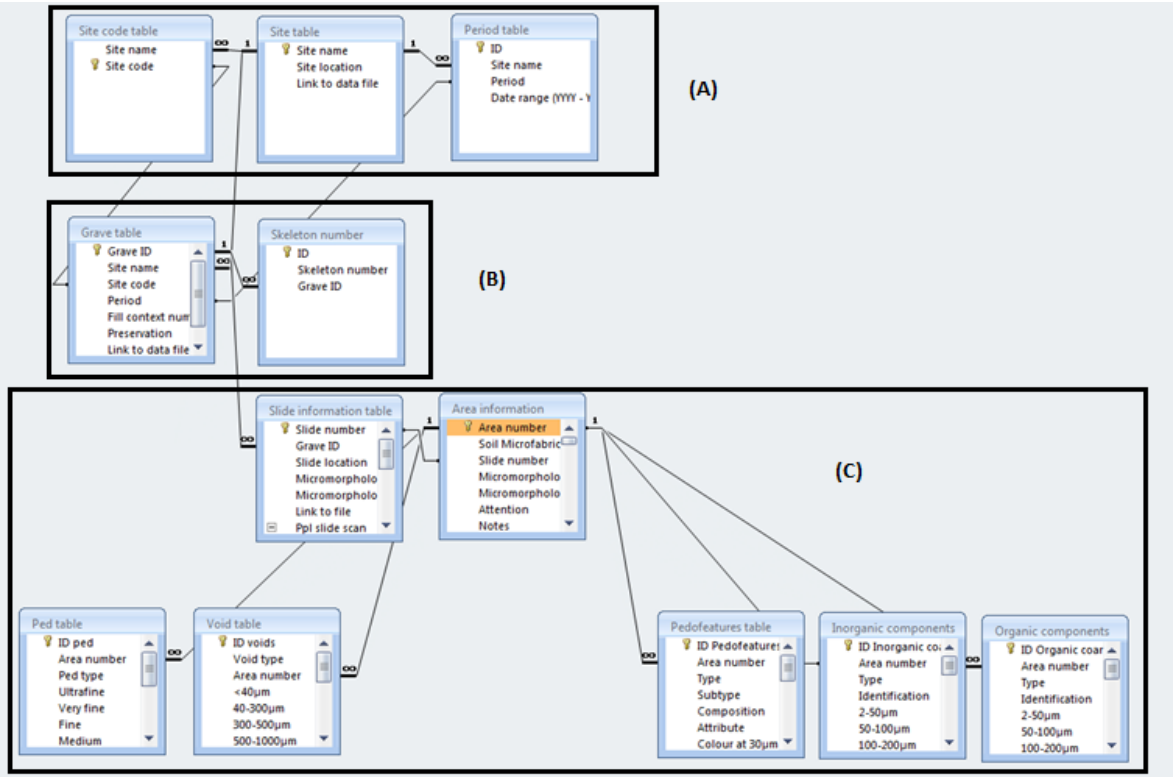

Figure 10: Structure of relational database showing site related information (A), grave related information (B) and sample related information (C).

2.3.2.1 Site level data

Site level data was defined as all data that related to multiple graves across a site. This consisted of three tables; the Site table, Period table and Site Code table. The Site table encompassed all information which related to the entire site. Two additional tables were created for aspects of the site that may differ between graves such as site codes that relate to different areas or different excavation seasons.

2.3.2.2 Grave level data

Grave level data was all data that was specific to graves but could be applied to multiple samples. These included the Grave table that contained all information that related to a single grave and a second table, Skeleton Number, which was introduced to cater for situations where more than one skeleton was present in a grave. These two tables also contained information to link each sample to the onsite record kept by the excavators.

2.3.2.3 Slide level data

Slide level data was defined as all information that related to a specific slide spread across seven tables. The Slide Information table recorded all data that related to a slide, including its position and orientation. The Area Information table was used to identify and record microfabrics types and linked to five subsequent tables; Inorganic Components, Organic Components, Peds, Voids and Pedofeatures. In addition to the relational database there was extensive image recording for each slide, composed of a whole slide PPL and XPL mosaic images that were annotated. Each pedofeature and organic component was photographed in PPL and XPL creating a comprehensive archive of each slide for reference during subsequent analysis and interpretation.

2.3.3 Image analysis of void space

In a grave environment the accurate quantification of void space through image analysis has the potential to highlight areas of unusually high or low void volume giving a better understanding of the spatial variation in void space around the grave. Photo mosaics were taken of each slide using the AxioCam ERc 5c at x5 magnification and using AxioVision Rel. 4. 8 software. To isolate the void space three images were taken, one in plane polarised light and two in cross polarised light, the second cross polarised light image was taken after the slide had been turned 45°. The threshold function was then used to create binary images with the void space in white. The three images were then combined creating a single image with all void space in white. The amount of white

space was then measured by area using the AxioVision Rel. 4. 8 software (for further information on protocol development see Appendix 1.1.5).

2.3.4 Inorganic geochemical analysis using a scanning electron microscopy energy dispersive x-ray spectrometry (SEM-EDX).

SEM-EDX is an analytical technique used to ascertain the elemental composition of materials at the microscale. In archaeological micromorphology studies SEM-EDX analysis has been used to recognise materials that have optical properties which are insufficient for a secure identification with micromorphological description alone (Macphail *et al.*, 2013, Shillito *et al.*, 2009, Shillito *et al.*, 2011b). A targeted approach is usually adopted with sites of interest identified during micromorphological description and then analysed with the SEM-EDX. In a limited number of cases inorganic geochemical analysis has been used to identify the chemical composition of microfabrics or larger areas in thin section (Macphail *et al*., 2004), although an accepted sampling framework is yet to be established.

Part of the overall research objectives presented in this thesis was to understand if the presence of a human burial affects the inorganic geochemical signature of the soil. In order to ascertain this, the inorganic geochemical signature of the non burial soils and the soils in contact with the body needed to be identified, thus, establishing the presence of body decomposition products and answering research objective two. It was important that the inorganic geochemical signature was obtained for the fine material as it was anticipated that this is where changes in the inorganic geochemical signature caused by the presence of a body would occur. For this reason the SEM-EDX was chosen, as this method could specifically target areas of the soil and therefore just analyse the fine material. Using SEM-EDX analysis also meant that changes in the geochemical signature moving away from the body could be investigated by taking observation points in a transect away from the body. The SEM-EDX was also used to establish the inorganic geochemical composition of pedofeatures in the soil by targeting them specifically. This meant that Mn and Fe pedofeatures could be accurately identified and those elements that were more difficult to detect using micromorphology alone and maybe the result of the decomposition of the body, such as P, could be established, again answering the second research objective.

SEM-EDX analysis was conducted using a Zeiss variable pressure (~60pa) EVO MA15 scanning electron microscope with a motorised 5 axis stage, large *xy* and *z* travel, Backscatter and VP-SE detectors and Oxford Instruments 80 mm^2 silicon drift X-ray detector. 20kV accelerating voltage was used with a target size of 2.6-2.7A (11cpm), a count time of 75 seconds and working distance

of 8.5mm. Dolomite and Spinal externally certified mineral standards were used to check the accuracy of non-normalised data and a cobalt standard was used every two hours to calibrate the beam and correct for drift.

2.3.4.1 SEM-EDX protocol

2.3.4.1.1 Fine material characterisation.

To characterise the inorganic geochemical composition of the fine material, and assess if it had been affected by the presence of a body, a sampling strategy was developed using the SEM-EDX. A 5 x 5mm grid was laid over the slide and ten grid squares from each microfabric type were selected at random. In each grid square five SEM-EDX analyses were taken in the fine material, making a maximum total of 50 point count values for each microfabric in each slide. Where the microfabric area was less than 250mm^2 the maximum number of available grid squares were used. For further information on the SEM-EDX protocol development see Appendix 1.1.6.

2.3.4.1.2 Assessing variation in inorganic geochemical signatures across the slide

To assess if there was variation in the inorganic geochemical signatures with distance from the body, a transect was made across slides cut perpendicular to the body using the grid system. Five observations were taken from each grid square and then the means and standard errors compared for each element.

2.3.4.1.3 Identification of materials.

The recognition of elements in thin section relies heavily on the identification of the elements optical properties but unfortunately, the identification of such is not always conclusive. For example Fe and Mn pedofeatures can both be opaque in PPL and isotropic in XPL (Lindbo *et al.*, 2010 p. 132). It is therefore reasonable to adopt multiple microanalytical techniques when the secure identification of materials is vital to the interpretation of the overall soil forming factors. In addition to this elements such as P, that can be difficult to identify in thin section, could be recognised. The SEM-EDX was therefore used to provide additional elemental information where needed to achieve this. Five observations were taken from the material being identified and also from the surrounding fine material. The average of the material elemental analysis was then compared to the average of the elemental analysis of the surrounding fine material.

Further to this SEM-EDX analysis was used to establish the elemental composition of the impregnations in the burial and control soils as these were seen to be of particular interest.

Elements of interest were those that had been previously found in body pseudomorphs and those that were related to the decomposition of organic matter especially P, Ca, Mg, Cu and Fe (Bethell & Carver, 2002, Keeley *et al*1977). In soils with available P, P may be bound by iron and aluminium oxides thus co-precipitating into iron and iron and manganese pedofeatures (Schlesinger 1997 p. 98). The ratio of P:Fe can therefore be calculated and be compared between the fine material and the impregnations to determine firstly where there is high availability of P in the grave and secondly if the P is precipitating into pedofeatures with Fe or remaining in the fine material. This is a modified application of the method outline by Lang (2014).

2.3.4.1.4 Sample selection

Graves were chosen based on the completeness of the sample set (C1, C2, C3 samples and skull, pelvis and foot area samples) and the quality of micromorphological information. The physical condition of the slides and amount of contextual information was also a consideration and those with a high standard of contextual information as well as a lack of manufacturing errors were preferred. Hungate was extensively studied as it was also an opportunity to compare the inorganic geochemical signatures of several graves which had minimal variation in burial practice, time period and environmental context in the hope that, if there were common inorganic geochemical signatures associated with burials, they would be more readily detectable when there were fewer external variables.

2.3.5 Data Analysis

A key aim of this research was to establish if there was spatial variation in micromorphological features that related to degradation or grave specific soil formation, which required that the data for each sampling location: control, skull, pelvis, hand and feet, was comparable. Where there was more than one slide or microfabric type per sampling point the data was combined giving an overall value for the sampling location. To facilitate this, the percentage abundance for each microfabric type was added by converting into decimals and using the following equation:

(Area of slide covered by microfabric type x area of microfabric type covered by feature)

The result was then converted back into a percentage and the percentages for the whole slide were added together. Where there were multiple slides present in a sample location an average was produced.

2.3.6 Statistical analysis

Basic statistics were conducted on the majority of micromorphological data so that micromorphological characteristics could be compared across sites, graves and sample locations in the burial plane. A more in-depth statistical interrogation of the micromorphological data proved ineffective due to the low number of observations in each sample location. Principle component analysis (PCA) was successfully utilised for the SEM-EDX data using SPSS 21. In basic terms, PCA is a statistical method that can be used as a foundation to investigate the structure of the data and highlight causal connections. Given the complexity of the SEM-EDX data and the large number of data points, it was anticipated that PCA would assist in the visualisation of the structure of the data. The selection of elements to be included in PCA analysis was based on either the Kaiser-Meyer-Olkin (KMO) measure of sample accuracy (≥.5) (Hutchenson & Sofroniou, 1999), a correlation coefficient with one or more elements ≥ .1, or an element being identified as of interest due to its release during human decomposition processes. In all cases oblique rotation (varimax) was chosen to optimally identify patterns in the chemical variability of the soil which could then be assessed for their relationship to decomposition process. O and C were omitted from the analyses as they were present in high levels in the resin, to the extent that they may have obscured more subtle chemical patterns. Ni, F, Cr, Zr, As, Cu, Ac, Ba and Zn were also omitted as they were only sporadically identified. In addition, Cu was found to be a contaminant from the Cu tape applied to samples to generate a three point spatial referencing system for the mosaic images as well as the SEM-EDX analysis.

2.4 Presentation of results

The results are presented in six thematic chapters (Microfabrics, SEM-EDX of the fine material, inorganic coarse material, organic coarse material, soil structure and pedofeatures) where the characteristics of the soil are fully explored to gain a better understanding of the effect of burial. 'Microfabrics', Chapter 3, describes, interprets and assesses the relevance of each microfabric to grave contexts. In the microfabrics chapter the soil development processes that are occurring in each microfabric are introduced, however they are then discussed in full in the following results chapters. Each thematic chapter includes the presentation of the results (SEM-EDX, inorganic coarse material, organic coarse material, soil structure and pedofeatures) analysed first by sample location and then by microfabric type as well as a detailed discussion about each micromorphological and inorganic-geochemical feature and any possible links to the presence of the grave or the burial environment, so answering the first research objective.

Table 6: Samples and techniques used. 'MM' = micromorphology, 'IA' = image analysis, 'SEM' = SEM-EDX analysis, 'OR' = slide orientation, 'Perp' = slide cut perpendicular to body, 'Para' = slide cut parallel to body, '✓' = analysis conducted, 'U' = Unknown.

Burial number	Period	Control samples									Body samples														Additional			
		C1			C2			C3			Skull				Pelvis				Hand				Feet							
		MM	IA	SEM	MM	IA	SEM	MM	IA	SEM	OR	MM	IA	SEM	OR	MM	IA	SEM	OR	MM	IA	SEM	OR	MM	IA	SEM	OR	MM	IA	SEM
Thessaloniki																														
TF157	Early Hellenistic										Para	✓	✓		Para	✓	✓						Para	✓	✓					
																			Perp	✓	✓									
TF182	Late Hellenistic				✓	✓		✓	✓		Para	✓	✓		Para	✓	✓		Para	✓	✓		Para	✓	✓					
											Perp	✓	✓		Perp	✓	✓		Perp	✓	✓									
TF177	Roman							✓	✓	✓	Para	✓	✓	✓	Para	✓	✓	✓					Para	✓	✓	✓				
											Perp	✓	✓	✓	Perp	✓	✓	✓	Perp	✓	✓		Perp	✓	✓	✓				
TF178	Roman										Para	✓	✓		Para	✓	✓													
TF162	Unknown										Parap	✓	✓		Parap	✓	✓						Para	✓	✓					
Heslington East																														
713	Late Roman	✓	✓		✓	✓		✓	✓		U	✓	✓						U	✓	✓		U	✓	✓					
Çatalhöyük																														
18666	Neolithic							✓	✓	✓	Para	✓	✓	✓	Para	✓	✓	✓					Para	✓	✓	✓				
											Perp	✓	✓	✓	Perp	✓	✓	✓					Perp	✓	✓	✓				
19295	Neolithic	✓	✓	✓				✓	✓	✓	Para	✓	✓		Not present in burial															
												✓	✓																	
											Perp	✓	✓																	
												✓	✓																	
Hungate																														
54898	Roman				✓	✓	✓	✓	✓	✓	Para	✓	✓	✓	Para	✓	✓	✓													
											Perp	✓	✓	✓	Perp	✓	✓	✓									Perp	✓	✓	✓
51326	Roman				✓	✓	✓	✓	✓	✓					Para	✓	✓	✓					Para	✓	✓	✓				
											Perp	✓	✓	✓	Perp	✓	✓	✓					Perp	✓	✓	✓				
51387	Roman							✓	✓	✓					Para	✓	✓	✓					Para	✓	✓	✓				
											Perp	✓	✓	✓	Perp	✓	✓	✓					Perp	✓	✓	✓				
51351	Roman										Para	✓	✓	✓	Para	✓	✓	✓					Para	✓	✓	✓	Para	✓	✓	✓
											Perp	✓	✓	✓	Perp	✓	✓	✓					Perp	✓	✓	✓	Perp	✓	✓	✓

Table 6 continued.

Burial number	Period	Control samples									Body samples																Additional			
		C1			C2			C3			Skull				Pelvis				Hand				Feet							
		MM	IA	SEM	MM	IA	SEM	MM	IA	SEM	OR	MM	IA	SEM	OR	MM	IA	SEM	OR	MM	IA	SEM	OR	MM	IA	SEM	OR	MM	IA	SEM
54090	Roman							✓	✓	✓	Para	✓	✓	✓	Para	✓	✓	✓												
											Perp	✓	✓	✓	Perp	✓	✓	✓												
54085	Roman							✓	✓	✓	Para	✓	✓	✓	Para	✓	✓	✓												
											Perp	✓	✓	✓	Perp	✓	✓	✓												
54341	Roman							✓	✓	✓	Para	✓	✓	✓	Para	✓	✓	✓					Para	✓	✓	✓	Para	✓	✓	✓
											Perp	✓	✓	✓	Perp	✓	✓	✓					Perp	✓	✓	✓	Perp	✓	✓	✓
54342	Roman	✓	✓	✓				✓	✓		Para	✓	✓		Para	✓	✓						Para	✓	✓					
											Perp	✓	✓		Perp	✓	✓						Perp	✓	✓					
54908	Roman				✓	✓	✓								Para	✓	✓	✓					Para	✓	✓	✓				
											Perp	✓	✓	✓	Perp	✓	✓	✓					Perp	✓	✓	✓				
51350	Roman				✓	✓		✓	✓		Para	✓	✓		U	✓	✓						U	✓	✓					

3 Soil microfabrics

Microfabrics were defined as the texture and appearance of soil in thin section at x5 magnification, related to a functional, configurational and/or genetic aspect of the soil. This chapter presents a description and interpretation of each microfabric as well as an evaluation of the arrangement and diversity of microfabrics using the following scales;

- Inter site (Çatalhöyük, Thessaloniki, Heslington East and Hungate).
- Intra site (Çatalhöyük, Thessaloniki and Hungate).
- Inter grave (Çatalhöyük, Thessaloniki, Heslington East and Hungate).

In the microfabric interpretation, the formation processes and origin of the microfabrics will be evaluated. However a more detailed discussion of formation processes and soil features is given in the following chapters for each of the soil characteristics (SEM-EDX of the Fine Material Chapter 4, Inorganic Coarse Material Chapter 5, Organic Coarse Material Chapter 6, Soil Structure Chapter 7 and Pedofeatures Chapter 8).

3.1 Microfabric description and interpretation

The microfabric descriptions are presented in full in Appendix 2.1. A summary of the defining microfabric characteristics, their number and arrangement as well as their initial interpretations are presented here, on a site by site basis.

3.2 Çatalhöyük

3.2.1 Çatalhöyük Microfabric Description

Six microfabrics were identified at Çatalhöyük (CH1-6). CH1 was primarily composed of pale grey white to pale yellow grey well sorted silt with sporadic angular to sub-angular coarse grains. Void space was low (5-10%) and consisted of planes and channels. Curvilinear pseudomorphic plant voids were present in CH1 as well as in CH2, CH3 and CH4. Post depositional pedofeatures (typic hypocoatings on inter and intra pedal voids, typic coatings, impregnations and nodules) were present. CH2 was a moderately sorted pale white grey, fine textured microfabric with sporadic angular to sub-angular coarse grains. The structure of CH2 was apedal with high levels of packing voids (40% of total slide area). CH2 had sporadic inter pedal infillings, impregnations and nodules. CH3 was a fine textured, perfectly sorted, homogeneous microfabric that was mid yellow to orange in PPL. CH3 had a monic C:F related distribution with low levels of coarse material and sporadic planar voids that related to the intrapedal void structure. Pedofeatures were rare and consisted of intrapedal opaque impregnations, nodules (potentially iron or manganese), and coatings. CH4 was a coarse textured, heterogeneous unsorted microfabric. Coarse material abundance ranged from 10-30% of total slide area, and was composed primarily of poorly sorted quartz. Packing voids composed the majority of pore space (10% to 80% abundance). Pedofeatures were infrequent and consisted of typic/external hypocoatings and coatings, strong opaque, red and orange impregnations and nodules, and sporadic intercalations and infillings. Coprolitic material was observed in CH4 as isolated embedded aggregates but not identified to species. CH5 was a moderately to poorly sorted, heterogeneous microfabric that was mid yellow to brown in PPL, due to large amounts of charred plant material (10-30%). The structure was variable and consisted of strongly developed sub-angular blocky and granular peds and variable abundances of packing voids, vughs channels and planes. Pedofeatures consisted of sporadic dusty clay coatings. The finial microfabric, CH6, was a moderately sorted, homogeneous, black opaque microfabric. The internal structure of CH6 was apedal with low abundances of vughs and channels reflecting high aggregation and stress fractures. CH1, CH2, CH3 and CH6 were present as embedded granular and angular to sub-angular blocky aggregates with sharp boundaries in CH4. CH1 was also present as sporadic examples of embedded micro laminated angular blocky aggregates. In contrast diffuse boundaries existed between CH2, CH5 and CH4.

3.2.2 Çatalhöyük Intra-site Microfabric Variation

The C1 sample contained CH1, CH2, CH3 and CH5 (Table 7), whereas grave 18666 contained all six microfabrics, whilst CH6 was absent from grave 19295. The C1 was dominated by heterogeneous microfabric arrangements, as was grave 18666, with only one example of homogenous microfabric, whereas grave 19295 contained both heterogeneous and microstratigraphic layers.

3.2.3 Çatalhöyük Inter-grave Microfabric Variation

CH4 dominated the microfabric assemblage in the C1 sample and graves 18666 and 19295 (Table 7). CH1 and CH2 were common whereas CH3, CH5, and CH6 were sporadic. There was no systematic correlation between the arrangement of microfabrics and their sample location and orientation (Table 7); however there were higher abundances of CH4 in the parallel samples compared to the corresponding perpendicular samples in grave 19295. With a small sample set, however, this may be coincidental.

Table 7: Distribution and arrangement of microfabric types in the C1 and graves 18666 and 19295 at Çatalhöyük. Values are the percentage of slide area covered by each microfabric. * = heterogeneous samples, ♦ = homogeneous and ● = microstratigraphic layers.

				CH1	CH2	CH3	CH4	CH5	CH6
C1*				5%		2%	86%		2%
18666	C3*			15%			80%	5%	
	Skull		Perp*	5%	2%	5%	84%	2%	2%
			Para*	5%	5%	5%	85%		
	Pelvis		Perp*		10%	2%	86%		2%
			Para*	5%	10%	5%	70%		
	Feet		Perp♦				100%		
19295	C3●			5%			85%	10%	
	Skull	19500	Perp*	15%		2%	83%		
			Para*	5%			95%		
		19501	Perp●	10%	25%		65%		
			Para*	10%	5%		85%		

3.2.4 Çatalhöyük Microfabric Interpretation

An initial interpretation will now be presented for the origin and formation processes of the Çatalhöyük microfabrics. Depositional pathways will be explored in light of the morphology and arrangement of the microfabrics in the graves with reference to supporting literature.

CH1, CH2 and CH3 were primarily composed of well sorted silt and clay suggesting a low energy depositional environment (Brown, 1997 p. 327). This would be consistent with sourcing the sediments from the nearby marl and back swamp areas close to Çatalhöyük (Matthews *et al*., 2013, Stokes, Unpublished BSc Dissertation). The colour of CH1, CH2 and CH3 (pale grey white to pale yellow grey, pale white grey and mid yellow to orange respectively) would also be consistent with the water laid marl, oxidised lake marl and water laid deposits (clear, pale gray, pale orange brown and dark red orange respectively) (Matthews, 1996, Roberts *et al.*, 1996, Stokes, Unpublished BSc Dissertation). CH5 was distinguished by high levels of randomly orientated charcoal (10-30%). Charcoal deposits were present at Çatalhöyük in midden areas (Shillito *et al.*, 2011b) and in thin lenses of charred plant material and ashes in proximity to oven installations within the buildings (Matthews, 2006). There are, however, no specific examples from the literature of charcoal being deliberately added to burials at Çatalhöyük meaning that the charcoal in this instance was either accidently included or part of a burial practice specific to 18666. CH6 was composed of opaque black material in PPL that was undifferentiated black in XPL, suggestive of a burnt aggregate (Courty *et al.*, 1989 p.107). Pseudomorphic plant voids visible in CH1, CH2, CH3 and CH4 were suggestive of the inclusion of plant stabilisers (Matthews, 1996, Matthews, 2006, Tung, 2013 p.74). CH4 was the most extensive microfabric from Çatalhöyük in which the other five microfabrics were embedded. The primarily sharp external boundaries between CH4 and CH1, CH3 and CH6 would support that there was little chemical or physical interaction between these microfabrics (Brewer, 1964). In contrast, CH2 and CH5 had diffuse boundaries with CH4 suggesting that there was chemical or physical interaction occurring in this instance. The types, arrangements and abundances of microfabrics present in the C1 and the grave samples are similar, suggesting that distinctions were not made in the placement and abundance of microfabrics between burial and non burial contexts. Although there are some differences in sporadic microfabrics (CH5 and CH6) this may be a sample size issue.

CH1, CH2 and CH3 are likely to have originally been used as building materials that have subsequently been dismantled and incorporated into the burial platform packing material. Matthews *et al*(1996) states that packing material used under platforms can include aggregates from the building materials of previous structures that appear as embedded aggregates with sharp boundaries. The fine texture and light colour of CH1 coupled with low levels of coarse grains are similar to Matthews' (2006) descriptions of white plaster floor and wall surfaces at

Çatalhöyük. The finest plasters were applied to walls creating finely laminated layers (Matthews, 2005, Matthews, 2006), which would be consistent with those observed in aggregates of CH1 (Figure 11). There are also visual parallels between CH2 and the thick white floor plasters described by Matthews (2006), with both showing an open structure. Orange building materials have also been recorded at Çatalhöyük as mud bricks, thick plaster wall coverings, foundation deposits for platform construction (Matthews, 2005) and burnt orange clay (Shillito *et al.*, 2011b). CH5 may have been charred plant material that was dumped into the platform fill during construction as similar practices occurred in midden areas where frequent dumping of oven rake out occurred (Shillito *et al.*, 2011b), suggesting the presence of CH5 in the skull sample may be incidental rather than deliberate.

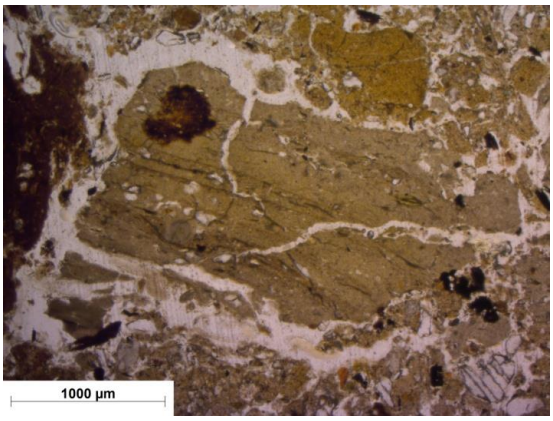

Figure 11: Microlaminated example of CH1 from the pelvic sample of 18666 in PPL

3.3 Thessaloniki

3.3.1 Thessaloniki Microfabric Description

Two microfabrics were identified at Thessaloniki. Ti1 was an unsorted to poorly sorted heterogeneous microfabric that was dark yellow to pale orange brown in PPL. Coarse material abundance varied (10-40% of total slide area) and was mainly composed of weathered quartz. Organic coarse components included weathered bone, some of which demonstrated a low birefringence, shell and charcoal fragments. Peds varied with apedal soils, strongly to moderately developed crumbs, moderately developed plates and weakly to strongly developed sub-angular blocky peds (further explored in soil structure Chapter 7). C:F related distribution was predominantly porphyric, with minor areas of chitonic, gefuric and enaulic areas and compound

packing voids (2-30% of total slide area). Voids consisted of channels, planes and vughs (2-20%), creating, in places, an open structure. Coatings on voids walls and mineral grains were composed of carbonates, Mn/Fe, silt and clay, as well as relict coatings with carbonate hypercoatings present on inter-pedal channels. Mn/Fe intrapedal impregnations and anorthic, disorthic and aggregated nodules (1-2%) were also present.

Ti2 was present as embedded sub-angular blocky peds in Ti1 with sharp boundaries (Figure 12 (a) and (b)) and areas of apedal material with sharp to diffuse boundaries with Ti1 (Figure 13 (a), (b) and (c)). Ti2 was unsorted to moderately sorted, heterogeneous sediment. Fine material of Ti2 had a pale grey white colour in PPL (Figure 12 (a)) and crystalline b-fabric caused by high levels of carbonate (Figure 12 (b)). Ti2 had similar inorganic coarse components to Ti1 but a more closed structure with apedal soils and high vugh abundance (2-20% of total slide area). Pedofeatures in Ti2 consisted of dusty and impure clay typic coatings on intrapedal void walls (c1%) and intrapedal Mn/Fe coatings (<1%), anorthic and disorthic nodules (<1%).

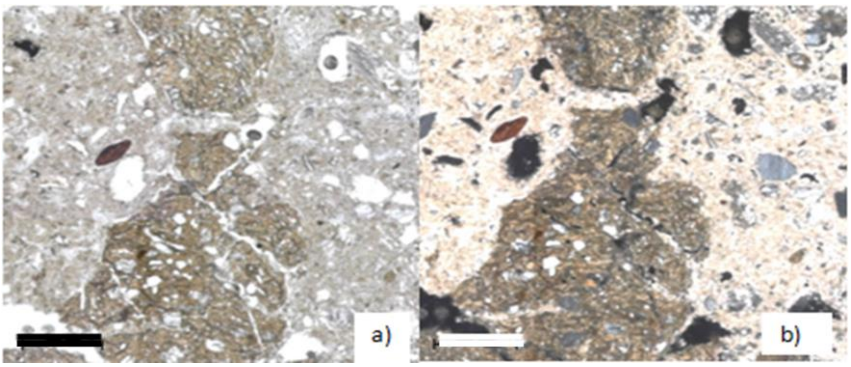

Figure 12: Ti1 (centre of image) and Ti2 (Left and right of image) from the pelvic sample in TF182 showing a clear boundary between Ti1 (in the centre of both images) and Ti2 (to the left and right of both images), scale = 500µm; (a) shown in PPL and (b) shown in XPL.

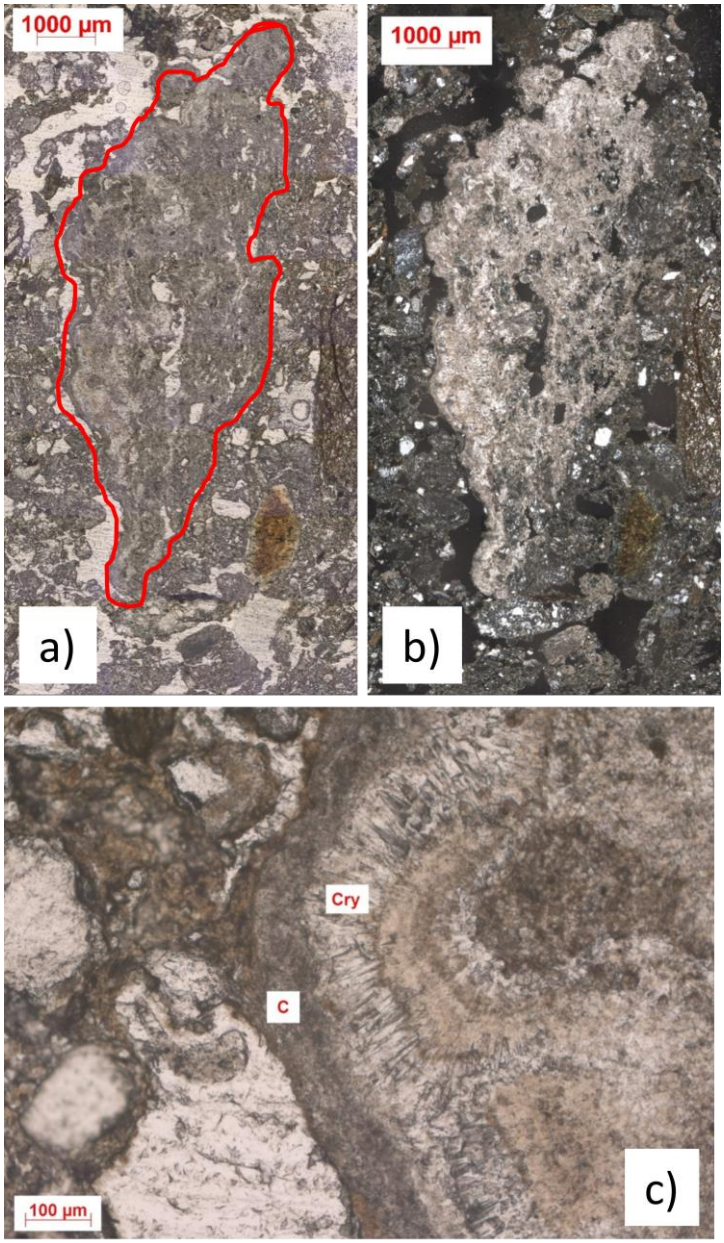

Figure 13: Ti2 (outlined in red). a) Left = PPL and b) right = XPL. c) Photomicrograph showing Ti2 with fanlike crystalline coatings (Cry) and typic coatings (C) in PPL. Note the fanlike crystal pedofeatures are concentrated on the left boundary of Ti2.

3.3.2 Thessaloniki Intra-site Microfabric Variation

Ti1 was ubiquitous in the Thessaloniki samples, whereas Ti2 was sporadic and present only in graves TF182 and TF177 (Table 8). Homogenous microfabric arrangements dominated at Thessaloniki and were present in all graves (Table 8); this was inevitably due to the low number of microfabrics and the scarcity of Ti2.

Table 8: Distribution of microfabrics and their arrangement in graves TF157, TF182, TF177, TF187 and TF162 from Thessaloniki. Shown in as the percentage of slide covered by each microfabric. * = heterogeneous samples, ♦ = homogeneous and ● = microstratigraphic layers

Grave	Location	Orientation	Microfabric types	
			Ti1	TI2
TF157	Skull	Para♦	100%	
	Pelvis	Para♦	100%	
	Hand	Perp♦	100%	
	Foot	Para♦	100%	
TF182	C2♦		100%	
	C3♦		100%	
	Skull	Para*	90%	10%
	Pelvis	Perp*	90%	10%
		Para♦	100%	
	Hand	Perp♦	100%	
		Para♦	100%	
	Foot	Para*	70%	30%
TF177	C3♦		100%	
	Skull	Perp♦	100%	
		Para♦	100%	
	Pelvis	Perp♦	100%	
		Para♦	100%	
	Hand	Para♦	100%	
	Foot	Perp*	90%	10%
		Para♦	100%	
TF178	Skull	Para♦	100%	
	Pelvis	Para♦	100%	
TF162	Skull	Para♦	100%	
	Pelvis	Para♦	100%	
	Hand	Para♦	100%	
	Foot	Para♦	100%	

3.3.3 Thessaloniki Inter-grave Variation

There is no relationship between sample location and orientation and the presence of microfabrics or their arrangement (Table 8). Table 8 confirmed the majority of samples from Thessaloniki are homogenous (contain only Ti1).

3.3.4 Thessaloniki Microfabric Interpretation

An initial interpretation will now be presented for the origin and formation processes occurring in the Thessaloniki microfabrics. Depositional pathways will also be explored in light of the morphology and arrangement of the microfabrics in the graves.

Ti1 and Ti2 were composed of minerals and rock fragments that were consistent with the geology of the area surrounding Thessaloniki (see Inorganic Coarse Material Chapter 5.2). Dusty clay and impure coatings, signifying particle movement (Macphail *et al.*, 1990, Thompson *et al.*, 1990, Usai, 2001) were present in Ti1 and Ti2. Further to this there were fragmented coatings in Ti1 meaning that once coatings had formed on surfaces there had been subsequent disturbance of the soil (Kühn *et al.*, 2010). Channels were present and may have formed through the action of roots or as biogalleries (Brewer, 1964, Kooistra & Pulleman, 2010, Ringrose-Voase & Bullock, 1984, Stoops, 2003), creating a high porosity to the soil structure and further disaggregation. Intrapedal Mn and Fe pedofeatures suggest that there was redoximorphic conditions which could have exacerbated the dissolution of chemical bonds between soil particles furthering soil movement (Barbiero *et al.*, 2010, Brinkman, 1970, Brinkman *et al.*, 1973, Lindbo *et al.*, 2010). Apedal soils sub-angular blocky/platy peds suggests that there was physical stress on the soil (Birkeland, 1984, Bullock *et al.*, 1985, FitzPatrick, 1993, Lindbo *et al.*, 2010, Stoops, 2003). Moist conditions could also have impacted the placidity of the soil (Kooistra & Tovey, 1994). Carbonate hypercoatings around the inter-pedal channel voids indicated carbonate rich water was flowing through voids (for further discussion see Pedofeature Chapter 8). In some instances chemical diffusion had occurred between Ti1 and Ti2; in the foot sample from TF177 and was expressed as a diffuse boundary and fanlike crystallisations with overlying typic dusty clay coatings (Figure 13). The majority of the backfill soil was composed of Ti1 with only sporadic instances of Ti2 confined to TF177 and TF182, which would imply that Ti1 was the backfill whereas the rarer Ti2 was an inclusion, which had, in some instances, continued to develop in-situ forming diffuse boundaries and neofoemed

crystalline coatings. What was not clear was if Ti2 was intentionally incorporated as part of the Hellenistic/Roman burial practice or if the inclusion of Ti2 was non-deliberate.

3.4 Heslington East

3.4.1 Microfabric description

One microfabric was identified at Heslington East (HE1). HE1 was heterogeneous and moderately sorted with high levels of coarse material (60-80%), which were primarily composed of angular quartz. Organic coarse material consisted of sporadic fragments of bone and charcoal. Poro and grano striations were present in the b-fabric. Microstructure included apedal, moderately to strongly developed plates and weakly to strongly developed sub-angular blocks. HE1 had an open soil microstructure reflected in the presence of chitonic, gefuric and enaulic C:F related distributions, as well as packing voids. The C:F related distribution was, however, dominated by porphyric material. Void space consists of planes, vughs (2-30%) and channels. Roots and sporadic excremental pedofeatures were also present. Typic coatings on void walls, ped surfaces and mineral grains (5%) were composed of limpid and dusty clay. Mn/Fe coatings (<1%), moderate to strong intrapedal impregnations (5%) and intrapedal anorthic and disorthic nodules (6%) were also present.

3.4.2 Heslington East Microfabric Interpretation

The inorganic coarse material assemblage was consistent with the local parent material described by O'Connor *et al*(2011) (see Coarse Material Chapter 5 for more information). Weathered root fragments in HE1 suggested channels were formed, at least in part, by roots, with sporadic excremental pedofeatures indicating the presence of soil fauna. Vughs were also common (2-30%) and suggest soil aggregation and compaction (Brewer, 1964, Kooistra & Pulleman, 2010, Ringrose-Voase & Bullock, 1984, Stoops, 2003). Platy and sub-angular blocky peds indicated cyclic wetting and drying or pressure causing fractures along planes of weakness and poro and grano striations in the b-fabric (Birkeland, 1984, Bullock *et al.*, 1985, Dalrymple & Jim, 1984, FitzPatrick, 1993, Stoops, 2003). Dusty and limpid clay coatings indicate movement of soil particles (Birkeland, 1984, Bullock *et al.*, 1985, FitzPatrick, 1993, Stoops, 2003), possibly due to surface disturbance or from internal disturbance from bioturbation (Kühn *et al.*, 2010, Macphail *et al.*, 1990, Usai, 2001). Intrapedal Mn and Fe pedofeatures suggest redoximorphic conditions, possibly intensifying the

dissolution of chemical bonds between soil particles (Barbiero *et al.*, 2010, Brinkman, 1970, Brinkman *et al.*, 1973, Lindbo *et al.*, 2010).

3.5 Hungate

3.5.1 Hungate Microfabric Description

Thirty microfabrics were originally identified at Hungate; however these were consolidated into thirteen microfabrics as some were amalgamated upon comparisons made between graves. The combining of microfabrics was based on key features that could be related to the soil history such as the C:F related distribution, abundance and type of voids and pedofeatures and ped types. The genesis of the microfabric was also taken into consideration for example those that were water laid were grouped together. The mineral and rock assemblages in all microfabrics at Hungate were consistent with the parent material found at the site (see Chapter 5 for more details). The abundance of inorganic coarse material varied widely between and within microfabrics. Those with particularly wide variations in inorganic coarse material abundance were HU13 (30-90%), HU5 and HU8 (20-70%), and HU9 and HU10 (60-70%). Microfabrics HU2 and HU7 both contained high abundances of inorganic coarse material (above 50%), whereas HU6 had none. The remaining microfabrics contained ≤50% inorganic coarse material. HU8 was of note as quartz grains were arranged in clusters embedded in fine material. The majority of microfabrics had formed as embedded aggregates in HU13 with diffuse (HU5, HU8, HU9, HU12 and HU13) or sharp (HU3 and HU4) boundaries whereas HU1 and HU10 exhibited sharp and diffuse boundaries. Layered microfabrics were present, the most notable being HU6 that had formed a series of laminated clays with sharp boundaries. HU1, HU2, HU5 and HU13 were also layered in places but exhibited diffuse boundaries. The degree of sorting varied between microfabrics, HU2, HU3 and HU6 were perfectly to well sorted. HU7 was moderately to poorly sorted and HU5, HU8 and HU9 demonstrated very little to no sorting. The remaining microfabrics had a broader range of sorting with HU1 and HU12 poorly to well sorted, HU13 and HU10, well to unsorted and HU1 and HU4 perfectly to unsorted.

Biologically derived coarse material was common at Hungate with microcharcoal and charcoal present at low levels (1-10%) in all microfabrics apart from HU6 and HU9. HU6 had no organic coarse components, whereas HU9 contained high levels of charcoal (30-40%). There was also a

charcoal peak in HU12 at 40% in the perpendicular pelvic sample of SK54898, the lead coffin, but this was unusually high for HU12. In addition bone was present in HU5, HU10 and HU13, fungal sclerotia in HU8, HU12 and HU13 and spherulites in HU10 and HU13, all at low levels (<10%). In HU7 the microfabric itself was composed of large fragments (>2000µm) of bone that comprised 40% of the microfabric.

Individual microfabrics varied in soil microstrucutre with HU1, HU2, HU3, HU4, HU6, HU8, HU9, HU11 and HU12 exhibiting a fairly closed structure with low void abundance (<20%). Of these HU6 contained no visible void space. The remaining microfabrics were high in void abundance and have an open microstructure. Those with particularly high void space were HU7 and HU10 with 40% vughs and some instances of HU13 with high levels of vughs (40%) and packing voids (80%) and HU5 (60% vughs). Apedal areas in microfabrics were common and were present in HU1, HU2, HU3, HU6, HU8, HU9, HU10, HU11, HU12 and HU13. Crumbs peds were less frequent, but present in HU1, HU3, HU4, HU5, HU8, HU10, HU12 and HU13. Angular to sub-angular blocky peds were common and present in HU1, HU3, HU4, HU5, HU8, HU9, HU10, HU12 and HU13 and were mostly strongly to well developed. Strongly developed platy peds were expressed in HU3, HU4, HU6 and HU11. HU13 was the most complex microfabric with the greatest degree of variation in microstrucutre, with predominantly apedal soil (47% of total slide area), with strongly developed crumb peds (3%), strongly to moderately developed granules (<1%), weakly to strongly developed platy (11%) and sub-angular blocky peds (32%). C:F related distribution was porphyric, and undifferentiated, stipple, mosaic speckled, grano-, poro- and random striations had developed. HU13 contained high abundances of voids (up to 80%) composed of channels, packing voids, planes and vughs. Common types of pedofeatures in the Hungate microfabrics were those that had resulted from Mn/Fe precipitation and clay translocation. Typically these took the form of typic clay, impure clay and dusty coatings (<6%) on void surfaces and sporadic infillings, and intrapedal Mn/Fe impregnations, anorthic and typic nodules at approximately 1-2% abundance. Some microfabrics, however, contained unusual types or abundances of pedofeatures.

Excremental and passage pedofeatures were rare, but were present in HU1, HU4, HU5, HU8, HU12 and HU13. In HU8 the passage features composed up to 80% of the microfabric. Microlaminated coatings were present in HU13 and pendant/fragmented impure clay coatings were present in HU7. Coatings were absent from HU2. HU1 and HU12 were the only microfabric

to contain depletion pedofeatures. HU6 was composed of fine clay layers and included hypocoatings on the ped surfaces. HU4 contained low levels (1-20% of total slide area) of coarse material and alternating layers of fine to coarse material which coincided with a fine material colour alteration, from dark to light red in PPL (fabric pedofeature). The fabric pedofeatures in HU4 were present in vertical or horizontal orientations to the ground surface depending on the orientation of the aggregate. The colour and birefringence of the fine material was generally consistent between microfabrics, HU5, however, showed some variation. HU5 was dark orange to black in PPL and had an undifferentiated brown/orange b-fabric in XPL.

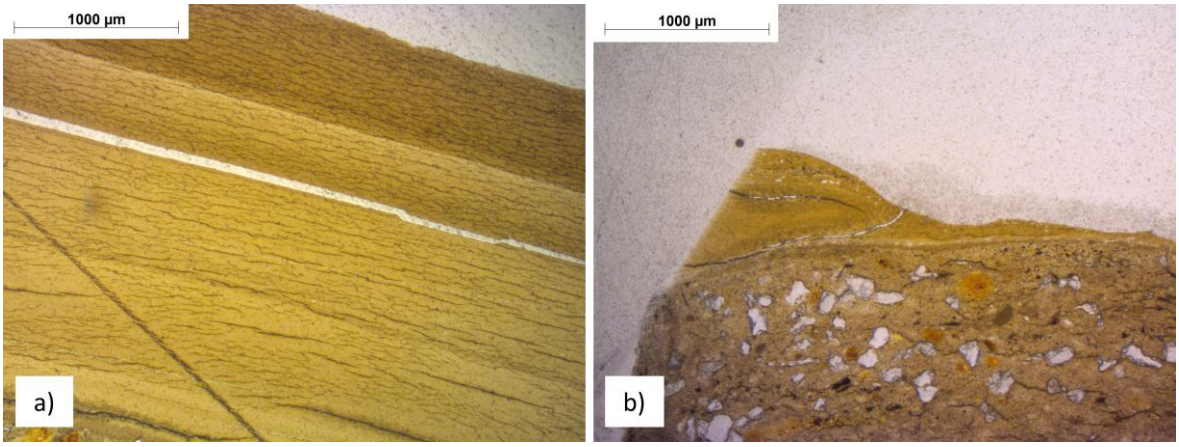

Figure 14: HU6 a) Shoulder area sample from SK54898 and b) C3 sample from same grave.

3.5.2 Intra-site microfabric variation – Hungate

Microfabrics were inconsistently distributed (Table 9), with HU13 being ubiquitous in the C1 samples and every grave. The C1 samples contained a limited number of microfabrics HU8, HU12 and HU13, whereas collectively the graves contained all 13 microfabrics. HU1, HU2, HU6, HU7, HU9 and HU11 were sporadic. HU2, HU5, HU6, HU7, HU9 and HU11 were grave specific with grave SK54898, the lead coffin, containing the highest number of grave specific microfabrics and incidentally the highest overall number of microfabrics (7). Microfabric arrangements varied between graves (Table 9) with heterogeneous being the most common. Graves SK51326, SK54085 and SK51350 contained more homogenous samples than heterogeneous or microstratigraphic layers. However these graves had low total numbers of microfabrics demonstrating, as at Thessaloniki, a link between high numbers of homogeneous samples and low numbers of

microfabrics. Microstratigraphic layering was present in graves SK54898, SK54341, SK54342 and SK54908. The last three were all situated in the northern part of the cemetery (see Figure 15).

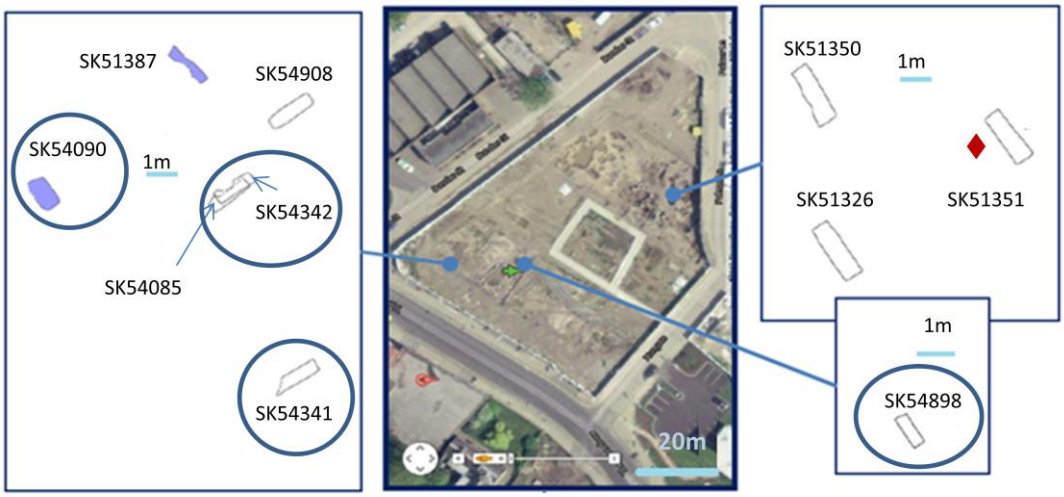

Figure 15: Locations of Hungate graves with microstratigraphic layering (circled).

Table 9: Presence of microfabrics and their arrangement at Hungate in the C1 sample and all graves. Grave SK51326 contains one microfabric type but one sample is heterogeneous due to the microfabrics being deposited in two depositional events. * = heterogeneous samples, ♦ = homogeneous and ● = microstratigraphic layers. The percentage of slides in each grave with each arrangement is in brackets

		Microfabric arrangement			Microfabric type												
		♦	●	*	HU1	HU2	HU3	HU4	HU5	HU6	HU7	HU8	HU9	HU10	HU11	HU12	HU13
C1 (n=3)		1 (33%)	0 (0%)	2 (66%)								✓				✓	✓
Graves	SK54898 (n=7)	0 (0%)	4 (57%)	3 (43%)	✓	✓	✓			✓			✓			✓	✓
	SK51326(n=8)	7 (87%)	0 (0%)	1 (13%)													✓
	SK51387 (n=6)	3 (50%)	0 (0%)	3 (50%)				✓	✓							✓	✓
	SK51351 (n=7)	3 (43%)	0 (0%)	4 (57%)										✓		✓	✓
	SK54090(n=5)	2 (40%)	0 (0%)	3 (60%)				✓								✓	✓
	SK54085(n=5)	3 (60%)	0 (0%)	2 (40%)	✓											✓	✓
	SK54341(n=9)	2 (22%)	1 (11%)	6 (66%)				✓							✓	✓	✓
	SK54342(n=7)	0 (0%)	1 (14%)	6 (86%)	✓		✓	✓				✓		✓			✓
	SK54908 (n=6)	1 (16%)	1 (16%)	4 (68%)								✓		✓		✓	✓
	SK51350 (n=5)	4 (80%)	0 (0%)	1 (20%)							✓					✓	✓

3.5.3 Hungate Inter site microfabric variation

There was a greater number of microfabric types in the lower two C1 samples compared to the upper C1 sample, which were both heterogeneous (Table 9). However, as the C1 was a small sample set, it is difficult to establish if this was a true trend or circumstantial. HU13 was the most abundant microfabric type and dominated all slides in graves SK51387 (50-100%), SK54085 (85-100%), SK54341 (60-100%) and SK51350 (70-100%) (Table 13, Table 16, Table 17 and Table 20). In grave SK51351, HU13 dominated the foot and 'other' samples, and in grave SK54090 HU13 dominated the C3, skull and pelvic samples (90-100%) (Table 14) The significance of this is discussed further in 3.5.4. Most slides had heterogeneous microfabric arrangements, which coincided with the presence of multiple microfabric types. Graves SK54908, SK54342 and SK54898, were not dominated by HU13. Grave SK54908 contained HU8 (40-100%) in all but the C3 sample (Table 19). HU10 and HU12 presented pockets of finer and coarser material (respectively). The parallel foot sample contained microstratigraphic layering indicating episodic deposition or bioturbation, creating passage features. The presence of HU8 would also support bioturbation. In grave SK54342, HU4 was present at between 20-60% abundance, and in the perpendicular pelvic sample was interleaved with HU13 forming microstratigraphic layering suggesting in-situ formation of HU4 and HU13. Grave SK54898, the lead coffin, had the greatest microfabric variation. HU13 was only present in the C2 sample taken from outside of the coffin whereas HU1, HU2, HU3, HU6 and HU9 were found inside the lead coffin (Table 11). There were differences in the distribution of microfabric types laterally across the grave with HU1, HU2, HU3 and HU6 found near the skull and HU12 near to the pelvis. Microstratigraphic layers formed in the C2, C3, perpendicular pelvic and shoulder area samples, which when combined with the fine grained nature of the microfabrics indicated episodic deposition as well as a degree of sorting. The nature of the microstratigraphy varied between the samples from inside and outside of the coffin, with the C2 sample containing a layer of fine material (HU12) that extended across two thirds of the slide. The layering within the coffin extended across the whole of the slide and generally consisted of easily differentiated microfabrics.

Table 10: Microfabric distribution and arrangement in each slide at Hungate for C1 soil profile. * = heterogeneous samples, ♦ = homogeneous and ● = microstratigraphic layers

	HU8	HU12	HU13
C1 7-16cm♦			100%
C1 27-36cm*	90%	10%	
C1 49-58cm*		10%	90%

Table 11: Microfabric distribution and arrangement in each slide at Hungate for grave SK54898. * = heterogeneous samples, ♦ = homogeneous and ● = microstratigraphic layers

		HU1	HU2	HU3	HU6	HU9	HU12	HU13
C2●							10%	90%
C3●		70%			2%	30%		
Skull	Perp*	85%	2%	13%				
	Para*	60%	5%	35%				
Pelvis	Perp●	90%					10%	
	Para*	85%				15%		
Other	Perp●	85%			15%			

Table 12: Microfabric distribution and arrangement in each slide at Hungate for grave SK51326. * = heterogeneous samples, ♦ = homogeneous and ● = microstratigraphic layers

		HU13
C3♦		100%
Skull	Para♦	100%
Pelvis	Perp*	100%
	Para♦	100%
Foot	Perp♦	100%
	Para♦	100%

Table 13: Microfabric distribution and arrangement in each slide at Hungate for grave SK51387. * = heterogeneous samples, ♦ = homogeneous and ● = microstratigraphic layers

		HU4	HU5	HU12	HU13
C3*		10%	40%		50%
Skull	Perp*		10%	20%	70%
Pelvis	Perp♦				100%
	Para♦				100%
Foot	Perp♦		10%		90%
	Para*				100%

Table 14: Microfabric distribution and arrangement in each slide at Hungate for grave SK51351. * = heterogeneous samples, ♦ = homogeneous and ● = microstratigraphic layers

		HU10	HU12	HU13
Skull	Perp♦	100%		
	Para*	70%		30%
Pelvis	U♦	100%		
Foot	Perp*		10%	90%
	Para♦			100%
Other	Perp*		5%	95%
	Para*		20%	80%

Table 15: Microfabric distribution and arrangement in each slide at Hungate for grave SK54090. * = heterogeneous samples, ♦ = homogeneous and ● = microstratigraphic layers

		HU4	HU12	HU13
C3♦				100%
Skull	Perp♦			100%
	Para*		10%	90%
Pelvis	Perp*	10%		90%
	Para*		10%	90%

Table 16: Microfabric distribution and arrangement in each slide at Hungate grave SK54085. * = heterogeneous samples, ♦ = homogeneous and ● = microstratigraphic layers

		HU1	HU12	HU13
C3*			10%	90%
Skull	Perp♦			100%
	Para♦			100%
Pelvis	Perp♦			100%
	Para*	5%	10%	85%

Table 17: Microfabric distribution and arrangement in each slide at Hungate for grave SK54341. * = heterogeneous samples, ♦ = homogeneous and ● = microstratigraphic layers

		HU11	HU12	HU13
C3*			30%	70%
Skull	Perp●	30%		70%
	Para*		30%	70%
Pelvis	Perp*	30%		70%
	Para*		10%	90%
Foot	Perp♦			100%
	Para♦			100%
Other	Perp*		40%	60%
	Para*		15%	85%

Table 18: Microfabric distribution and arrangement in each slide at Hungate for grave SK54342. * = heterogeneous samples, ♦ = homogeneous and ● = microstratigraphic layers

		HU1	HU3	HU4	HU8	HU10	HU13
C3*				40%	60%		
Skull	Perp*	20%	10%				70%
	Para*	20%				80%	
Pelvis	Perp●			50%			50%
	Para*			20%			80%
Foot	Perp*			60%			40%
	Para*	60%					40%

Table 19: Microfabric distribution and arrangement in each slide at Hungate for grave SK54908. * = heterogeneous samples, ♦ = homogeneous and ● = microstratigraphic layers

		HU8	HU10	HU12	HU13
C2*			45%	10%	45%
Skull	Perp♦	100%			
	Para				
Pelvis	Perp♦	90%		10%	
	Para♦	50%		50%	
Foot	Perp*	90%		10%	
	Para●	40%			60%

Table 20: Microfabric distribution and arrangement in each slide at Hungate for grave SK51350. * = heterogeneous samples, ♦ = homogeneous and ● = microstratigraphic layers

		HU7	HU12	HU13
C2♦				100%
C3*			10%	90%
Skull	Perp			
	Para♦			100%
Pelvis				
	U♦			100%
Foot				
	U*	30%		70%

3.5.4 Hungate Microfabric Interpretation

An initial interpretation will now be presented for the origin and formation processes occurring in the Hungate microfabrics. Depositional pathways will also be explored in light of the morphology and arrangement of the microfabrics in the graves.

The microfabrics were unevenly distributed through Hungate. Out of thirteen microfabrics only three were present in the C1 sample, HU8, HU12 and HU13, suggesting that they were produced through formation processes that were not necessarily associated with the act of burial or related to decomposition. An alternative implication is that the C1 samples were not extensive enough to encompass all of the local soil conditions that were not related to human burials. SK54898 was also of interest as it contained the highest number of microfabrics (7) and also had a high frequency of microstratigraphic layers.

The coarse inorganic material observed in the microfabrics at Hungate was consistent with the surrounding geology (see Inorganic Coarse Material Chapter 5 for more information). Abundance of coarse material varied between microfabrics meaning, there had been multiple depositional environments occurring at Hungate. HU6 contained no coarse material and was deposited as a series of layers in the C3 sample and the perpendicular shoulder sample of SK54898 (Table 11) in the last phase of deposition (Figure 14). HU6 was homogeneous, perfectly sorted and composed of 100% fine material, which is consistent with a low energy depositional environment (Brown, 1997). HU1, HU3, HU6, the majority of HU4 and HU11 also have low levels of inorganic coarse material (<30%) indicating a high degree of sorting at source or during deposition (Brown, 1997) especially in the homogenous fine textured microfabrics (HU6). Fine textured microfabrics were present in SK54898, SK51387, SK54090, SK54085, SK54341, SK54342 and SK54908, but were most extensive in SK54898. HU2, HU7, HU8, HU9, HU10 and HU12 however, were particularly rich in coarse material indicating the microfabrics were deposited in a higher energy environment (Brown, 1997). Microfabrics of particular note were HU2 and HU8. HU2 was a well sorted, coarse, microfabric forming linear bands in both skull samples from SK54898 (Table 11) meaning formation by either high energy deposition in the grave environment (Brown, 1997) or the removal of fine material leaving behind the coarse fraction as a linear band. HU8 was a poorly sorted, heterogeneous, microfabric with 20-70% coarse material arranged in clusters. The presence of channels in HU8, crumb and sub-angular blocky microstructures suggest soil organism

activity (Brewer, 1964, Pagliai *et al.*, 2003, Ringrose-Voase & Bullock, 1984, Russell, 1971), while vughs indicate aggregation or dissolution of soil components (Kooistra & Pulleman, 2010). Loose discontinuous and continuous infillings composed of clusters of quartz surrounded by fine material (Figure 16) and dusty clay coatings were common. Similar quartz clusters were described by Fitzpatrick (1993) and Jongmans (2001) as occurring in soils that had experienced long periods of earthworm activity (Figure 16). HU8 was common in grave SK54908 suggesting that there was a high degree of bioturbation occurring in this inhumation. The C3 sample from SK54342 was taken in the burial plane close to the skull, suggesting that this area too was high in biological activity.

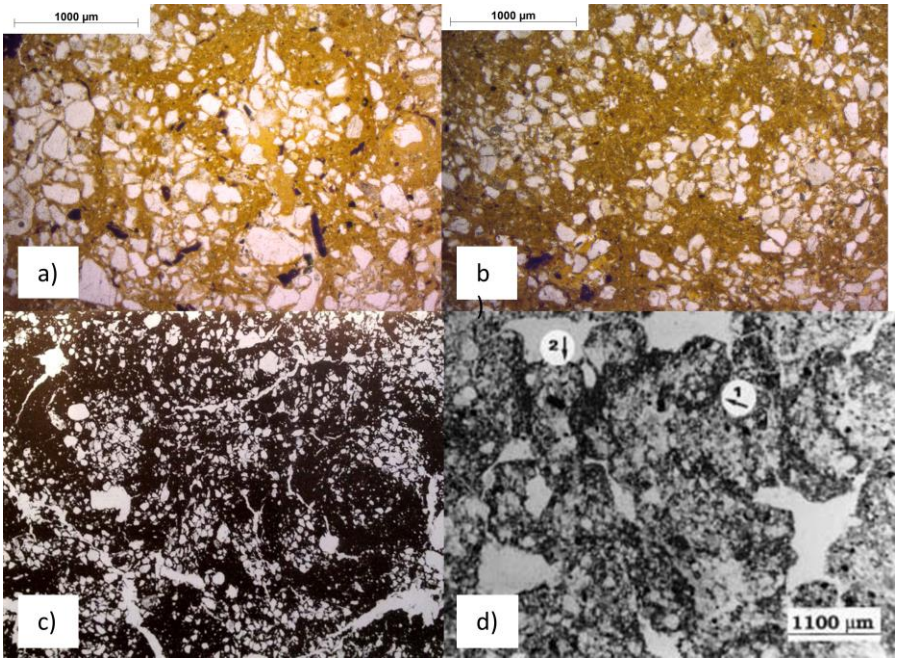

Figure 16: HU8 heavily bioturbated microfabric; a) SK54908 pelvic sample and b) SK54908 skull sample. Examples of earthworm bioturbation in c) topsoil creating clusters of sand grains from Fitzpatrick (1993 fig 7.10) scale = 4mm and d) a heavily earthworm bioturbated soil showing at 1 and 2 the presence of worm casts. From Jongmans *et al*(2001 fig 3b).

Organic coarse material was low with the exception of bone in HU7 present only in the foot sample of SK51350. HU7 was composed of large pieces (>2000µm) of bone (40%) with chemical weathering, which obscured the histological features and reduced the bone's birefringence (Figure 17). Due to the obscured histology the origin of the bone (animal or human) was not established. The rest of the microfabric had formed as infillings or coatings in and around the bone fragments (Figure 17). This combined with the weathered bone, suggests that there had been a high level of post depositional soil movement and chemical or biological weathering.

Sporadic examples of bone fragments, fungal sclerotia and spherulites were observed, however these were generally rare and will be discussed further in the (SEM-EDX Fine Material Chapter 4 and Coarse Material Chapter 5).

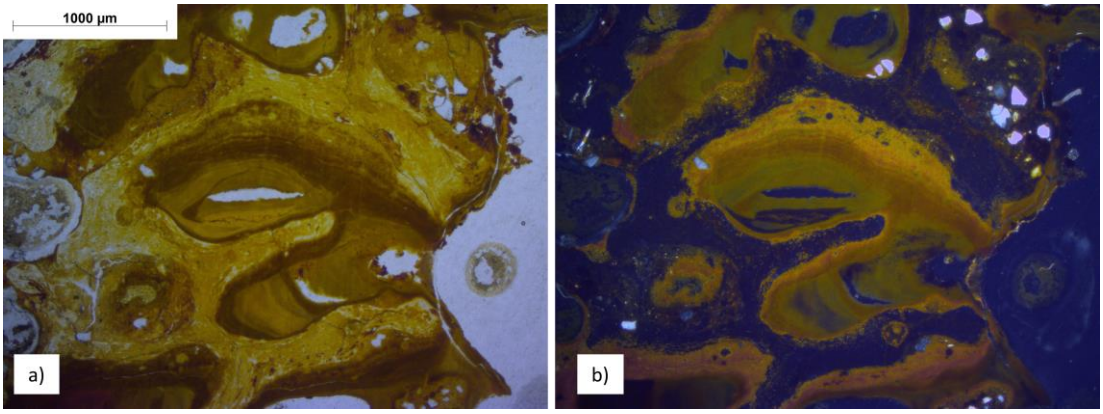

Figure 17: HU7 from the foot sample SK51350. a) in PPL and b) in XPL.

Microstructure varied considerably between microfabrics. Those exhibiting a fairly closed microstructure (HU1, HU2, HU3, HU4, HU6, HU8, HU9, HU11 and HU12) had low abundances of voids (<20%). Of these HU6 contained no visible voids. HU1, HU3, HU4, HU8, HU9, HU11 and HU12 all contained low levels of channels, planes and vughs. Channel voids relate to the formation of biogalleries or the ingress of roots (Kooistra & Pulleman, 2010, Ringrose-Voase & Bullock, 1984), whereas planes are indicative of shrinking and swelling (Kovda *et al.*, 2008), or compaction in the soil (Kooistra & Tovey, 1994), supporting moist conditions as well as soil organisms and vughs relate to aggregation or the dissolution of soil components (Ringrose-Voase & Bullock, 1984), both processes that can be linked to pressure in the soil, bioturbation or high soil water levels (Brewer, 1964, Kooistra & Pulleman, 2010, Ringrose-Voase & Bullock, 1984, Stoops, 2003). HU9 contained only planes, whereas vughs and planes were present in HU3. HU2, which contained only packing voids, could be the result of faunal excreta and the loose packing of materials, or shrinking and swelling (Brewer, 1964, Kooistra & Pulleman, 2010, Ringrose-Voase & Bullock, 1984, Stoops, 2003). Crucially a lack of void space in these microfabrics indicates that there is minimal air and water space for chemical and physical translocation of soil components and low levels of void connectivity. HU10 had particularly high void space abundance with 10-40% packing voids and vughs. The remaining microfabrics HU5, HU7 and HU13 had high void abundance and an open microstructure. HU13 contained channels, planes and vughs relating to

shrinking and swelling, the presence of soil organisms and formation of biogalleries as well as the presence of roots, and dissolution of soil components (Brewer, 1964, Kooistra & Pulleman, 2010, Ringrose-Voase & Bullock, 1984, Stoops, 2003). Whereas HU5 and HU7 only contained planes and vughs HU13 also contained packing voids. Again the implication of high levels of voids, particularly planes and channels, is that movement of soil particles, water and air was less restricted in these microfabrics (Pagliai & Kutilek, 2008a). The exterior of the microfabrics formed embedded aggregates in HU13 with either sharp (HU3) or diffuse boundaries (HU5, HU8, HU9 and HU12). In some instances microfabrics (HU1, HU4 and HU10) had both sharp and diffuse boundaries. The nature of the boundaries can give an indication of the level of physical and chemical interaction occurring between microfabrics. A sharp boundary indicates little interaction, whereas a diffuse boundary indicates some in-situ interaction between microfabrics. HU13 was the most abundant microfabric and formed the majority of the grave backfill in many of the graves analysed and dominated the C1 samples, implying that HU13 was the unmodified local soil. As most microfabrics were embedded crumb, angular and sub-angular blocky shaped aggregates with sharp boundaries, this would indicate that these microfabrics were included as part of the backfill process and there was little physical interaction with the 'local' soil. This scenario would apply to microfabrics such as HU4. Layered microfabrics (for example HU2, HU5, HU6 and HU13) with diffuse boundaries (all but HU6 which had a sharp boundary) are likely to have been formed by either episodic deposition or, as in the case of HU8 in the C1 sample, through the ingress of bioturbators. There is a large quantity of microstratigraphic layering present in SK54898, which is also the only lead coffined grave analysed from Hungate, implying that the microfabrics may have been sheltered from bioturbation and collapse by the coffin preserving their arrangement (for a further discussion see Pedofeatures Chapter 8).

The internal microstructure varied between microfabrics. HU6 had an apedal internal structure with platy peds supporting the occurrence of wetting and drying, pre-existing layers and/or compaction (Birkeland, 1984, Bullock *et al.*, 1985, FitzPatrick, 1993, Hussein & Adey, 1998, Kooistra & Tovey, 1994, Kovda *et al.*, 2008, Stoops, 2003). Platy peds were also present in HU3, HU11, HU12 and HU13. Pre-existing layering is unlikely, as none were visible in the control samples, whereas compaction from the soil overburden (Dent, 2002) or wetting and drying may have occurred. Spheroidal peds (crumbs and granules) were present in HU1, HU3, HU4, HU5, HU8, HU10, HU12 and HU13. These can be caused by wetting and drying and soil organisms (Birkeland,

1984, Bullock *et al.*, 1985, Davidson & Grieve, 2006, FitzPatrick, 1993, Hussein & Adey, 1998, Pagliai *et al.*, 2003, Russell, 1971, Stoops, 2003). The crumb peds in HU13, formed in the shoe sample from SK54341 (Table 17 and Figure 18), however, HU13 appeared to have been formed on the exposed surface of the excavation and was visible on site photographs (Figure 19). As InterArChive samples are taken through the exposed soil surface this feature has been recorded as a distinct layer on the upper edge of the slide. It is proposed that the formation of this material is due to the soil consistency and the act of 'trowelling back' over surfaces as well as through the drying of the exposed soil to form a crumb structure (Hussein & Adey, 1998, Kovda & Mermut, 2010). If this is the case future samples should be taken from freshly exposed surfaces to reduce the occurrence of misleading soil formations that relate to the present day. Apedal soils are present in HU1, HU2, HU3, HU4, HU6, HU7, HU8, HU9, HU10, HU11, HU12 and HU13 and are caused by an absence or destruction of peds through cultivation, compaction or waterlogging (Birkeland, 1984, Bullock *et al*., 1985, FitzPatrick, 1993, Stoops, 2003). There is no evidence for cultivation at Hungate, however waterlogging may have occurred as the soils are seasonally saturated (onsite observation). Compaction may also have occurred due to the soil overburden (McGowan & Prangnell, 2015). Angular and sub-angular blocky peds were frequently observed and present in HU1, HU3, HU4, HU5, HU8, HU9, HU10, HU12 and HU13. Blocky peds are usually caused by wetting and drying (Kovda & Mermut, 2010, Kovda *et al.*, 2008), freeze thaw (Bockheim & Tarnocai, 1998, Van Vliet-Lanoë, 1998) and when they are fine in appearance, by soil organisms (Birkeland, 1984, Bullock *et al.*, 1985, FitzPatrick, 1993, Stoops, 2003).

Figure 18: ‘Other’ sample (shoe) from SK54341 showing HU13 outlined in blue.

Figure 19: Photograph of SK54341 showing crumb peds (circled in blue) that have formed on the surface of the soil and to a lesser extent over the skeleton.

Translocation of soil particles was widespread at Hungate, resulting in typic clay, impure clay, dusty clay, unsorted coatings and sporadic channel infillings in most microfabrics and pendant/fragmented impure clay coatings in HU7. Episodic depositional events are suggested in HU5 with the formation of microlaminated coatings and depletion pedofeatures in HU1 suggesting physical or chemical movement in the fine material (Payton, 1993, Vepraskas, 2001). Almost all microfabrics contained intrapedal Mn/Fe pedofeatures indicating that there were redoximorphic conditions which probably occurred due to periodic waterlogging (Lindbo et al., 2010). Further evidence of chemical or physical movement was observed in HU12 where the fine material contained both depletion and impregnation pedofeatures where there had been chemical movement of Mn/Fe, whereas extensive hypocoatings, caused by the impregnation of black speckles, were present on ped surfaces in HU6, suggesting chemical or physical movement into the microfabric.

HU4 contained alternating layers of fine to coarse material, which coincided with fine material colour alterations that were recorded as fabric pedofeatures (Figure 20 (a), (b) and (c)). HU4 was present in the C3 sample from SK51387, pelvic and perpendicular foot sample from SK54342, perpendicular pelvis sample from SK54090 and C3 sample from SK54342 (Table 13, Table 18 and Table 15). HU4 formed as aggregates embedded in more extensive microfabrics, with in the majority of cases sharp boundaries. In HU4 from SK54342 the bedding was not parallel to the ground surface suggesting that HU4 may have been incorporated into the burial upon backfill or as later disturbance. In the perpendicular pelvic sample from SK54342, HU4 composed a large part of the slide and is interleaved with HU13 suggesting in-situ formation. As this sample was taken under the pelvis, it is possible that it formed prior to the burial. Layering of the nature observed in HU4 has been previously documented by Goldberg *et al*(2001) and Courty (1989) as the result of standing or flowing water (Figure 20 (d) and (e)). Previous studies have identified periods of inundation from the River Foss at Hungate forming complex layers of alluvium, sand and gravel (Evans, 2007b). A possible origin for HU4 is that they formed at Hungate during flooding events of the River Foss and were subsequently incorporated into the grave backfill. Excremental and passage pedofeatures were rare (present in HU8, HU10, HU12 and HU13) and indicate that, apart from in HU8, there has been limited biological activity.

The colour and birefringence of the fine material was generally consistent between microfabrics, however HU5 showed some variation. The colour of HU5 in PPL was dark orange to black and undifferentiated brown/orange b-fabric in XPL, and was suggestive of abundant amorphous organic material obscuring the b-fabric. HU5 had formed vertical layers in the C3 sample from SK51378 with diffuse boundaries, and embedded aggregates in the skull and foot sample. The vertical orientation and high organic content of HU5 suggests that HU5 may have formed through bioturbation with soil organisms moving up and down the soil profile (Canti, 2003).

In summary there are a large number of microfabrics identified at Hungate, however the microfabric assemblage is dominated by HU13, in which other microfabrics had become embedded. The soil environment at Hungate appears to have been dynamic with widespread pedogenic evidence for: the translocation of soil particles to form coatings, chemical movement of Mn/Fe, and the presence of bioturbators seen in the formation of channels, vughs, packing voids, spheroidal and blocky peds and in the presence of HU8. A high degree of sediment mixing during backfill is evident and had introduced microfabrics into HU13, in places there has been subsequent soil development and chemical interaction occurring producing diffused boundaries.

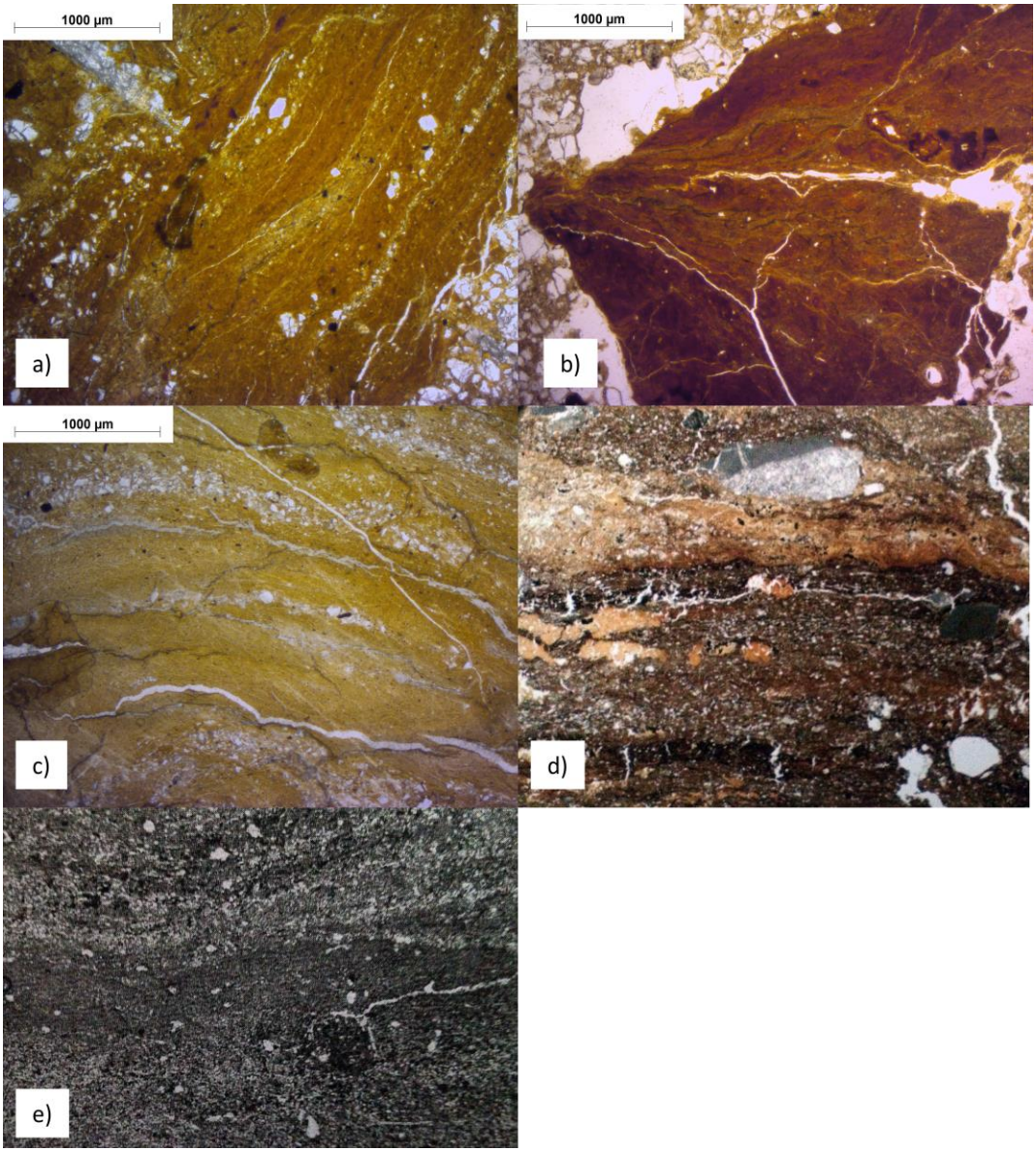

Figure 20: HU4 water laid sediment a) pelvic sample from SK54342, b) pelvic sample from SK54090 and c) pelvis sample from SK54342. Examples of water laid sediments from d) Zhoukoudian Cave China from Goldberg and Macphail (2006 plate 8.2 b) for case study see (Goldberg et al., 2001) and e) graded bedding in Late Pleistocene flood-plain sediments of the River Seine France (Courty et al., 1989)

3.6 Inter site microfabric variation

The four sites varied in the number and arrangement of microfabrics. Heslington East had the lowest number of microfabrics at 1 and Hungate the highest at 13. Whilst Çatalhöyük was dominated by heterogeneous material (75% of the samples), Thessaloniki and Heslington East had mainly homogenous material (100% and 84% of the samples). Hungate contained all three

microfabric arrangements, although heterogeneous material dominated (51%), closely followed by homogenous (38%).

Table 21: Number of different microfabric types and their arrangements; homogenous, microstratigraphic layers and heterogeneous, at each site. The percentage of slides in each grave with each arrangement is in brackets. Sample sizes; Çatalhöyük n=12, Thessaloniki n=25, Heslington East n=8 and Hungate n=68.

	Number of microfabrics	Microfabric arrangement		
		Homogenous	Microstratigraphic layers	Heterogeneous
Çatalhöyük	6	1 (8%)	2 (17%)	9 (75%)
Thessaloniki	2	21 (84%)	0 (0%)	4 (16%)
Hes East	1	8 (100%)	0	0
Hungate	13	26 (38%)	7 (10%)	35 (51%)

3.7 Summary and discussion

3.7.1 Inter site variation

Inter site variation was explored in terms of the number of microfabric types, their arrangements and nature. The nature of the microfabrics reflected the contextual and environmental difference between the four sites analysed in this study, whereas the inter site examination highlighted that sites with multiple microfabrics had a greater number of heterogeneous and microstratigraphicly layered samples. The inter site data illustrated that as sample size increased so did the number or microfabric types. Both relationships were positively correlated suggesting that sample size was important.

Çatalhöyük was a deeply stratified environment at the time of burial and therefore the arrangement, morphology and distribution of the microfabrics and any post depositional microfabric changes have been heavily influenced by their environmental context. At Çatalhöyük the microfabrics were derived from fragmented building material, sourced from the surrounding environment (Matthews et al., 2013) and used to fill the burial platforms (Matthews et al., 1996). This produced a series of granular and blocky microfabric aggregates embedded in CH4. There was also evidenced for material being 'dumped' into the platforms (CH5) possibly during their construction. Further to this there was a limited amount of post depositional activity with rare examples of coatings and bioturbation. This has probably been influenced by the environmental context of the burials, within buildings, as the graves would have been sheltered from the ingress of water and surface disturbance as well as access by bioturbators being problematic due to the

successive reuse of the site for building construction. The distribution of microfabrics at Çatalhöyük was also striking, as there was an even distribution of CH1, CH2, CH3 and CH4 between the C1, burial 18666 and burial 19295. Crucially, this suggests that the microfabrics from Çatalhöyük were not heavily influenced by the grave environment and that they were not 'special' sediments reserved for the act of burial.

Hungate also contained a high number of microfabrics (13), which were dominated by HU13 in both the C1 and the majority of graves. The majority of microfabrics, however, were not visible in the C1 meaning that either the burials were affecting the surrounding sediment or the C1 sample was not representative of all non-burial related sediments. This is partially apparent in the development of HU4 which is likely to have originated from the inundation of the River Foss (Evans, 2007b) and had been interleaved with HU13, suggesting that both microfabrics had formed *in situ*. In some instances the arrangement of the microfabrics at Hungate also appeared to be influenced by burial conditions. This was particularly apparent in SK54898, the lead coffin, where microfabrics had become stratified indicating that there had been minimal bioturbation or disturbance of the soils (Canti, 2003), possibly due to the protection of the lead coffin isolating the sediments from the surrounding environment.

In contrast to Hungate and Çatalhöyük, Thessaloniki and Heslington East contained few microfabrics (two and one respectively). Their nature, distribution and morphology however had been influenced by their wider context. At Thessaloniki the site was dominated by Ti1 which, although there was no C1 sample from Thessaloniki, was likely to be the back fill soil common at Thessaloniki. Coatings, fragmented coatings as well as channels and root fragments, suggest that the soil was disturbed (Brewer, 1964, Carter & Davidson, 1998, Macphail, 1998, Macphail *et al.*, 1990, Usai, 2001), (these aspects will be explored further in Pedofeatures Chapter 8), and there was also evidence of chemical changes in the soil including iron and manganese pedofeatures suggesting redoximorphic conditions (Barbiero *et al.*, 2010, Brinkman, 1970, Brinkman *et al.*, 1973, Lindbo *et al.*, 2010) as well as $CaCO_3$ percolation forming impregnations and hypocoatings on void surfaces. $CaCO_3$ was also found in Ti2 which had, in places, chemical interaction with Ti1, creating diffuse boundaries. The origin of the $CaCO_3$ at Thessaloniki is unclear. 'Plaster burials' where 'plaster' was deliberately incorporated into the burial matrix are known in the Roman period (Philpott, 1991, Sparey-Green & STRUCK, 1993). However other sources of $CaCO_3$ do exist including the surrounding geology and the proximity to buildings at the site (Ghilardi *et al.*, 2008a).

Heslington East was an Iron Age site which had been reused by the Romans and later turned over to agricultural land (O'Connor *et al.*, 2011). The abundance of dusty clay coatings would be consistent with an area that had been disturbed by, among other processes, bioturbation and agriculture (Macphail *et al.*, 1990, Thompson *et al.*, 1990, Usai, 2001). There are C1 samples from Heslington East which makes it possible to establish that the soil in contact with the grave was either not significantly influenced by it or that other site influences exerted a heavier influence on the soil. There is also no evidence of layering of heterogeneity in the arrangement of the microfabrics at Heslington East implying that after backfill the soils had been well mixed and there was no evidence for the burial being sheltered from surrounding soil formation processes. The wider site influences of the natural spring and slow permeability of the soil (National Soil Resources Institute, 2011a) can also be seen in the development of iron and manganese pedofeatures (Lindbo *et al.*, 2010) (see Pedofeatures Chapter 8).

Çatalhöyük, Thessaloniki and Hungate all contained multiple microfabrics and slides that were heterogeneous. Heslington East contained one microfabric and only had homogeneous material. Although microfabrics can form a layered deposit without needing a second type of microfabric (HU6 Hungate), multiple microfabrics increases the likelihood of microstratigraphic layering and heterogeneous deposits forming. This likelihood also increases as the number of microfabrics increases. The second issue of sample size is more problematic, as it is not clear to what extent sample size has affected the number of microfabrics observed and therefore the security and depth of interpretation. Heslington East, Çatalhöyük, Thessaloniki and Hungate contained one, six, two and thirteen microfabrics respectively and the samples sizes were one, two, five and ten respectively. When plotted as a simple line graph (Figure 21) there is a positive correlation (R^2 = 0.6687) between number of graves and the number of microfabrics, meaning that there may be a sample size element to the discovery of microfabric types. However, some graves such as SK54898 contained high numbers of grave specific microfabrics. If SK54898 had not been sampled Hungate would have ten microfabrics, whereas if only SK54898 (the lead coffined grave) had been sampled the overall number of microfabrics would have been eight, (seven from the grave and one unique microfabric from the C1). It is therefore difficult to correct for sample size bias in this case using statistical methods, without clouding the data, although it is an issue that should be taken into account during interpretation of the results.

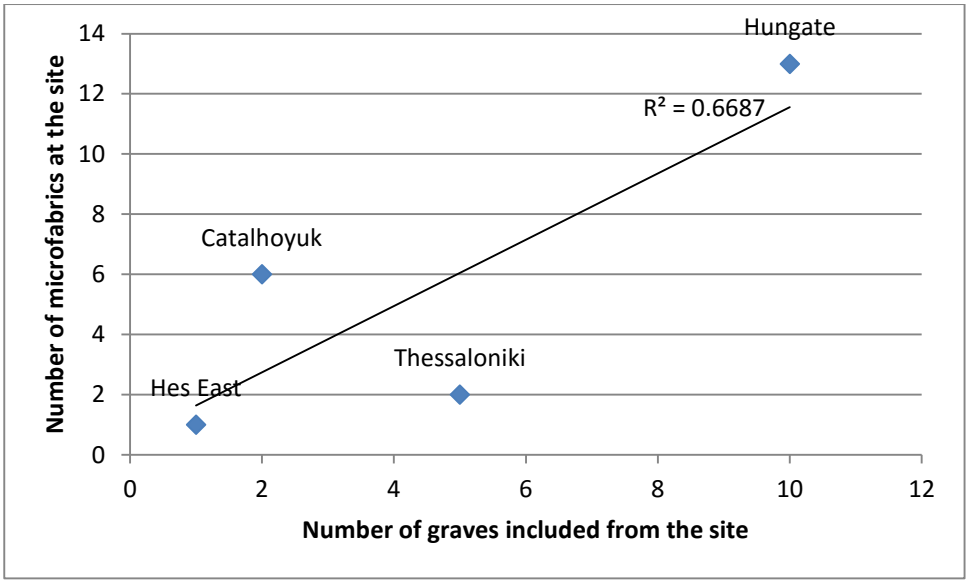

Figure 21 Graph showing the number of graves vs the number of microfabrics at each site.

3.7.2 Intra site variation: control samples vs samples from the burial plane and distinguishing between graves.

Intra site variation between control samples and the burial samples as well as between graves was assessed at Çatalhöyük, Thessaloniki and Hungate. Thessaloniki had two microfabrics, one ubiquitous (Ti1) and one sporadically distributed (Ti2), and minimal variation in microfabric arrangements. Although there was variation in microfabric type and arrangement between graves this did not appear to be linked to any form of burial practice. Therefore only Çatalhöyük and Hungate will be discussed here.

The microfabrics present at Çatalhöyük were formed from sediments used to construct the buildings in which the burials were located. There are four microfabrics in the C1, six in 18666 and five in 19295, meaning that the majority of microfabrics from Çatalhöyük were present in burial and non burial contexts. The microfabrics that were only present in the burial, CH2 and CH5, were rare and only observed sporadically in the burials, meaning that their omission from the C1 may be due more to their limited abundance and small C1 sample size compared to the graves, rather than their actual absence. In terms of microfabric arrangement, the C1 sample is heterogeneous, as are the majority of the grave samples. Homogeneous material was present in 18666 and microstratigraphic layering in two samples from 19295. However, it would be difficult to establish that these differences from the C1 were caused by the graves, as both homogenous and

microstratigraphic layering have previously been observed in non-burial contexts (Matthews, 2006).

Hungate contained thirteen microfabrics, most of which were absent from the C1 suggesting that the majority of microfabrics relate to grave formation processes or that the C1 sampling was not sufficient to identify all non-grave related microfabrics, for example HU4. In reality, a combination of these two factors is probably responsible for the distribution of microfabrics at Hungate. HU13 was present in all graves and the C1 soil profile, suggesting that HU13 probably represents the 'natural' soil at Hungate. There were also several microfabrics that can be related to general site formation processes (HU4) and have been incorporated into graves during backfill and not specifically related to grave formation processes. Nevertheless the presence of these 'non-specific' and 'natural' microfabrics can reveal some information about the burial environment. For example SK51326 contained only HU13, suggesting that the micromorphology of the soil has-not been significantly influenced by the burial. What perhaps is more interesting to this study are those microfabrics that have been caused specifically by the presence of an inhumation. These, however, are difficult to identify. SK54898 was unusual in that it contained seven microfabrics, most of which were grave specific and had a high incidence of microfabric layering, which set SK54898 apart from the other graves at Hungate. SK54898 was the only lead coffined grave to be analysed from Hungate and it is likely, though difficult to prove, that the environment created by the lead lined coffin was influential in distinguishing the microfabrics in SK54898 from those in other graves.

In summary the C1 sample and grave sample comparison at Çatalhöyük and Hungate demonstrate different distribution patterns at a site level, with the Çatalhöyük C1 being very similar to the graves samples and the Hungate C1 being very different. In both cases the C1 samples may not be sufficient to identify all 'natural' sediments present at a site. Meaning that careful consideration must be given to microfabrics that are exclusively present in graves to establish that they have been influenced by the burial and are not 'natural' microfabrics that have been 'missed' by the C1 sampling. At Çatalhöyük the similarities between the C1 sample and the grave samples, as well as the microfabric interpretations, indicates that the sediments around the burials are not burial specific nor had they been drastically modified by the presence of the burial. At Hungate the majority of microfabrics are not present in the C1 sample, meaning that the microfabrics observed in the graves are either due to grave specific formation processes or, as in the case of HU4, the C1 sample did not encompass all 'natural' soils present on site.

3.7.3 Differences between sample locations/orientations in the burial

There was no systematic variation detected at any of the levels or sites analysed in the microfabric type or arrangements, illustrating that a grave by grave analysis is important. There is also the issue of the orientation of the samples and whether this changes the visibility of microfabric types and arrangements. As always in micromorphology anything that is present in small quantities may not necessarily be visible in all samples or both orientations. However, standardisation is needed to give a better understanding as to what orientations the samples were cut in. For example, in this study samples were cut parallel or perpendicular to the body. As samples could have been taken adjacent to, above or below body parts this, meant that perpendicular to the body may be either parallel or perpendicular to the ground surface. Where samples are small and only the perpendicular sample is taken, microstratigraphic layering information could be lost.

3.8 Conclusions

Studying the nature of microfabrics, their frequency and arrangements can give an understanding of grave soil formation processes. As well as interpreting the microfabrics micromorphological features, key areas for consideration are comparisons with the C1 samples, the nature of the microfabrics, microstatigraphic relationships and microfabric distribution.

The evidence from Çatalhöyük and Hungate suggests that C1 samples are fundamental to understanding microfabric dynamics. The C1 sample doesn't represent all microfabric types and distributions that may be recoverable from none grave contexts, meaning that if a microfabric is only present in the grave, it must then be fully interpreted to understand if its formation is part of the grave taphonomy or if it is a non grave microfabric that has been 'missed' from the C1 sampling. More extensive C1 sampling to minimise this occurrence is recommended. The distributions of microfabrics between the C1 and graves samples can give an indication as to the type of site is being analysed. At Çatalhöyük the majority of microfabrics were ubiquitous, and those that were not were present in small quantities. Crucially, this suggests that the microfabrics from Çatalhöyük were not heavily influenced by the grave environment and that they were not 'special' sediments reserved for the act of burial. Çatalhöyük is an urban site where inhumations are located in buildings and thus the non-grave deposits are likely to be diverse. The microfabric at Heslington East would also suggest that the soil has not been heavily influenced by the burial or that other none burial processes had a greater influence on soil formation because specific 'burial'

microfabrics have either failed to form or been subsequently destroyed. At Hungate microfabrics that were not observed in the C1 samples were sporadic and in some cases grave specific. This would indicate that in contrast to Çatalhöyük the burials were affecting the surrounding sediment. This is particularly apparent in SK54898, the lead coffin grave, where detailed examination of microfabrics and their arrangements has produced a more complete grave history. This understanding of the formation of the grave fill may not have been possible using traditional excavation techniques or bulk analysis, indicating that, in some circumstances it is worth conducting in-depth micromorphological analysis. What remains to be developed is a robust protocol to identify which graves and sites would benefit from such an in-depth micromorphological grave analysis and also to determine which aspects of micromorphological analysis are most diagnostic for establishing the presence of a grave and identifying burial practice. The following results chapters will explore the soil composition, structure and pedofeatures in detail, to gain a better understanding of the effect of burials on the soil, in order to help identify which sites and graves would most benefit from intensive micromorphological examination and which features are most diagnostic of burial practices and body decomposition.

4 SEM-EDX Fine Material Analysis

SEM-EDX analysis was used to determine if there were any inorganic geochemical changes in the fine material that could be related to the decomposition of the body, burial taphonomy or associated burial practices. Previous studies have investigated examples of dark body pseudomorphs in burial contexts, and identified that they have higher concentrations of P, Mn and Cu than the surrounding soils (Bethell & Smith, 1989, Keeley *et al.*, 1977). Janaway *et al*argued that the presence of the body will modify the chemistry of the immediate soil environment creating a reducing environment encouraging the solubilisation of Fe and Mn (2003), which then precipitates in oxidised conditions. Further to this, concentrations of Ca were found in the pelvic area of the Gokstad ship burial (Macphail *et al*., 2013). With the employment of SEM-EDX analysis, it is hoped that changes in the concentration of P, Mn, Cu and Fe in the fine material can be detected in the grave samples making them chemically distinct from the controls. It is the aim of the SEM-EDX investigation to identify which chemicals vary between sites, graves and samples and then relate these changes to either the degradation of the body, associated taphonomic changes or burial practices. SEM-EDX analysis was conducted on ten graves; 18666 from Çatalhöyük, TF177 from Thessaloniki and SK54898, SK51331, SK51387, SK51351, SK54090, SK54085, SK54341 and SK54908 from Hungate. These graves were chosen as they had the most complete sample sets, the slides were in good condition and there was a high quality of contextual information available. The approach used during the SEM-EDX analysis is outlined in 2.3.6. Principle component analysis (PCA) is a statistical approach used as a foundation to explore the structure of data and provide insight into causal connections. PCA analysis was conducted on three levels;

- Inter site (Çatalhöyük, Thessaloniki and Hungate).
- Intra site (Hungate).
- Intra grave (Çatalhöyük, Thessaloniki and Hungate).

Intra sample changes in the inorganic geochemical signature were assessed by establishing the presence of changes in Fe, P, S and Mn along transects moving away from the body. Fine red spherulites were identified as part of the fine fraction at Hungate. These were investigated further using SEM-EDX analysis the results of which are presented here with the PAC for Hungate.

4.1 Inter site inorganic geochemical variation – Çatalhöyük, Thessaloniki and Hungate

All samples from the burial plane, as well as control samples, were utilised in the inter site PCA analysis. PCA was conducted using seven elements (Si, P, S, Cl, Ca, Mn and Fe). The Kaiser-Meyer-Olkin (KMO) measure verified the sampling adequacy for the analysis (KMO = .503) and varied between .471 to .536 for individual elements. Three components had eigenvalues over Kaiser's criterion of 1 (Table 22). Combined, the three components explained 59.4% of the variance. Table 22 shows the factor loadings after rotation. Components 2 (P and Ca) and 3 (Fe) were chosen as this combination best resolved the individual sites and P, Ca and Fe are known derivatives of body degradation (Bethell & Carver, 2002, Bethell & Smith, 1989, Janaway *et al.*, 2003, Macphail *et al.*, 2013). The components where colour coded by site and presented in Figure 22.

Table 22: Rotated component matrix for Hungate. Items with factor loadings higher than 0.4 are highlighted in green.

Element	Component		
	1	2	3
S	.873		
Mn	.818	-.112	
Cl	.362	.159	-.158
Si		-.812	
P		.668	.338
Ca		.552	-.535
Fe		.138	.820
Eigenvalues	1.662	1.398	1.099
% variance	23.74%	19.98%	15.70%

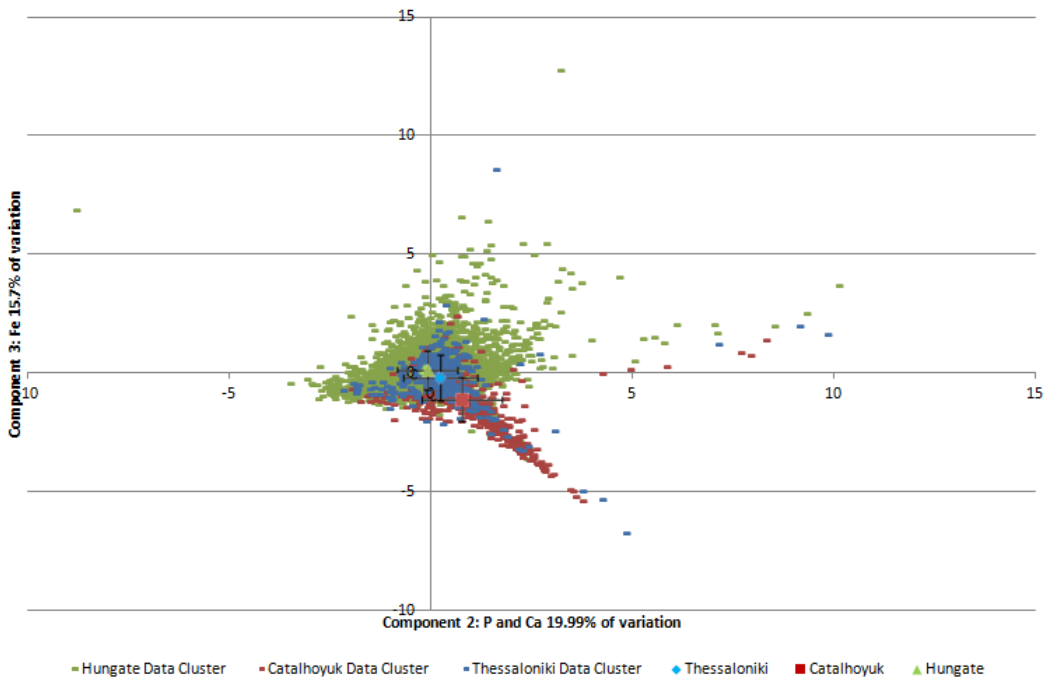

Figure 22: PCA loading for component 1 and component 3 from Table 22 for Çatalhöyük, Thessaloniki and Hungate. The centre point shows the mean value with error bars of one standard deviation.

Çatalhöyük and Thessaloniki have similar shaped data distributions in terms of component two (P and Ca) and three (Fe) (Figure 22). Çatalhöyük and Thessaloniki have a negative variation along component three (Fe), whereas Hungate does not. There is some horizontal distribution along component two, the extremes of which are confined to a small group of outliers. Hungate has a different distribution, with vertical and horizontal variation forming a circular cluster of points with sporadic vertical outliers. When the means of the data clouds are considered, all three sites are located within one standard deviation of each other. Thessaloniki and Hungate plot closely together with Çatalhöyük plotting slightly further along component two and slightly more negatively on component three, meaning that Çatalhöyük is higher in P and Ca but lower in Fe than Thessaloniki and Hungate. This may be a reflection of the calcium carbonate rich sediments used in the construction of Çatalhöyük (Matthews, 1996). The extreme outliers, those that plot on the negative for component three and high positives for component two, include the highly calcareous microfabric Ti2. However there does not appear to be any other sample position preference for results to plot in this area for Thessaloniki. The outliers that plot high on component two were also investigated but were not a systematically biased to sample location or microfabric type. With high loadings of P and Ca, component two appears to either represent Ca and P residues from the burial or the retention of P by the calcareous parent materials (Alvarez *et*

al., 2004). Component three is high in Fe and has probably been derived from either the local parent material or through the precipitation of Fe into the soil due to redoximorphic conditions, which are pH dependent (Schlesinger, 1991) and may therefore have been partly inhibited at Çatalhöyük.

4.2 Intra site inorganic geochemical variation - Hungate

All control samples and those from the burial plane at Hungate were used for the intra site inorganic geochemical analysis. Mg, Al, Si, P, K, Ca, Ti and Fe were used in the PCA. The overall KMO value was .590 and all individual elements were over .5. Bartlett's test of sphericity x^2 (253) = 7915.969 $p < .001$ indicated that correlations between elements were large enough to conduct PCA analysis. Two components have eigenvalues over 1 and account for 51.1% of the total variance. The scree plot showed an inflection at the third component, justifying retaining two components. Table 23 shows factor loadings after rotation. Component 1 and 2 were plotted and colour coded by grave (Figure 23), microfabric type (Figure 24) and sample location (Figure 25).

Table 23: Rotated component matrix for Hungate. Items with factor loadings higher than 0.4 are highlighted in green.

Element	Component	
	1	2
P	.857	
Ca	.803	
Si	-.643	
Al	-.263	.814
K	-.249	.751
Fe	.220	.662
Mg	.293	.546
Ti		.210
Eigenvalues	2.27	1.82
% Variation	28.32	22.74

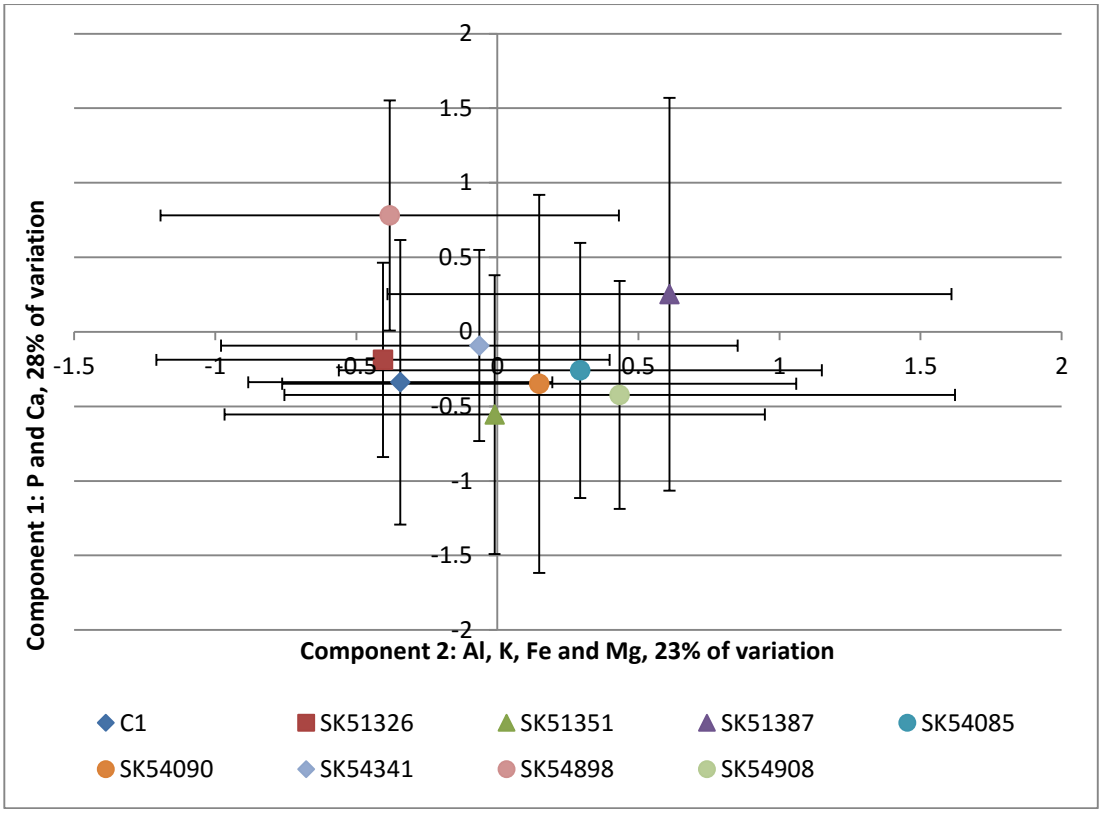

Figure 23: Component 1 and component 2 PCA results for Hungate colour coded by grave and C1 sample. The centre point shows the mean value with error bars of one standard deviation

In terms of component one and two all graves and the C1 samples have a similar distribution across both axis (Figure 23). SK54898 (lead coffin grave) is somewhat distinct as its distribution is shifted slightly more towards the negative of component two and along the positive axis of the component one than the majority of graves and the C1, meaning that SK54898 contains a higher concentration of P and Ca and a lower concentration of Al, K, Fe and Mg compared to the majority of graves. However, the mean points for SK54898 and the other graves were within one standard deviation of one another.

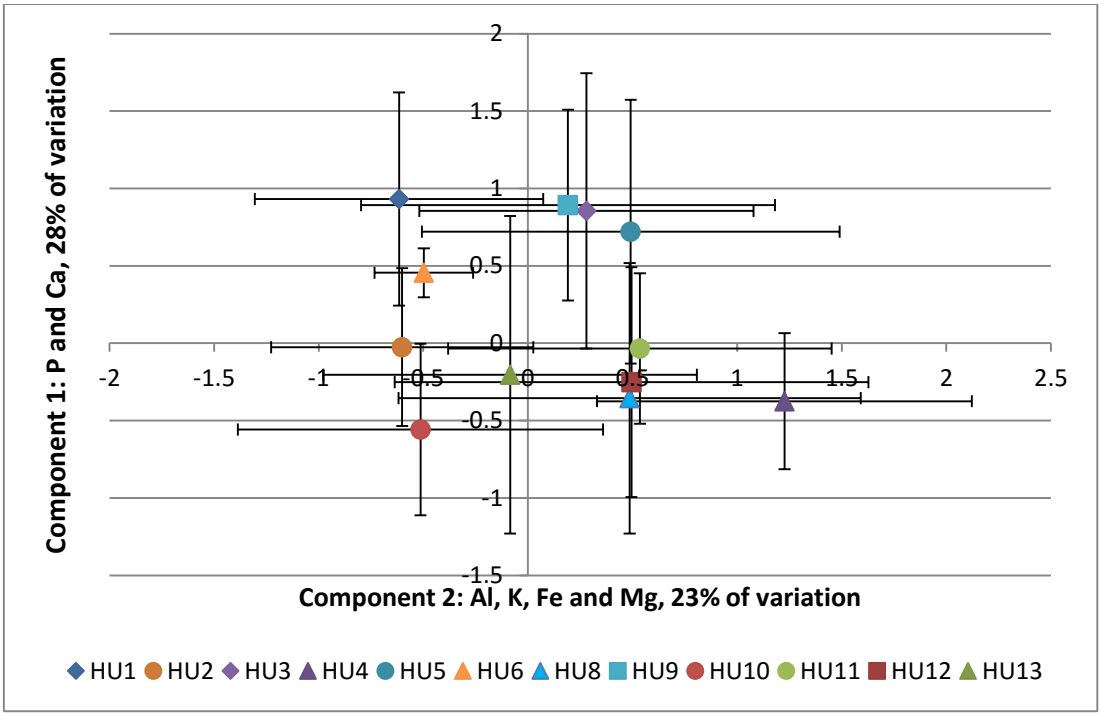

Figure 24: Component 1 and component 2 PCA results for Hungate coded by microfabric type. The centre point shows the mean value with error bars of one standard deviation

The microfabrics at Hungate are distributed widely along component two (Al, K, Fe and MG) and component one (P and Ca) (Figure 24). Those microfabrics that were present in the C1 samples HU8, HU12 and HU13 as well as HU4, the water laid deposit from the River Foss, plot negatively for component one, meaning that they are low in P and Ca. A large number of microfabrics (HU1, HU3, HU5, HU6 and HU9,) plot positively for component one, meaning that they contain elevated levels of Ca and P compared to the remaining microfabrics. HU8 and HU12 plot close together, indicating that they have a similar inorganic geochemical signature. HU6 was also a microfabric of interest and has a narrow distribution across both components compared to the other microfabrics. HU6 plots positively for component one and negatively for component two.

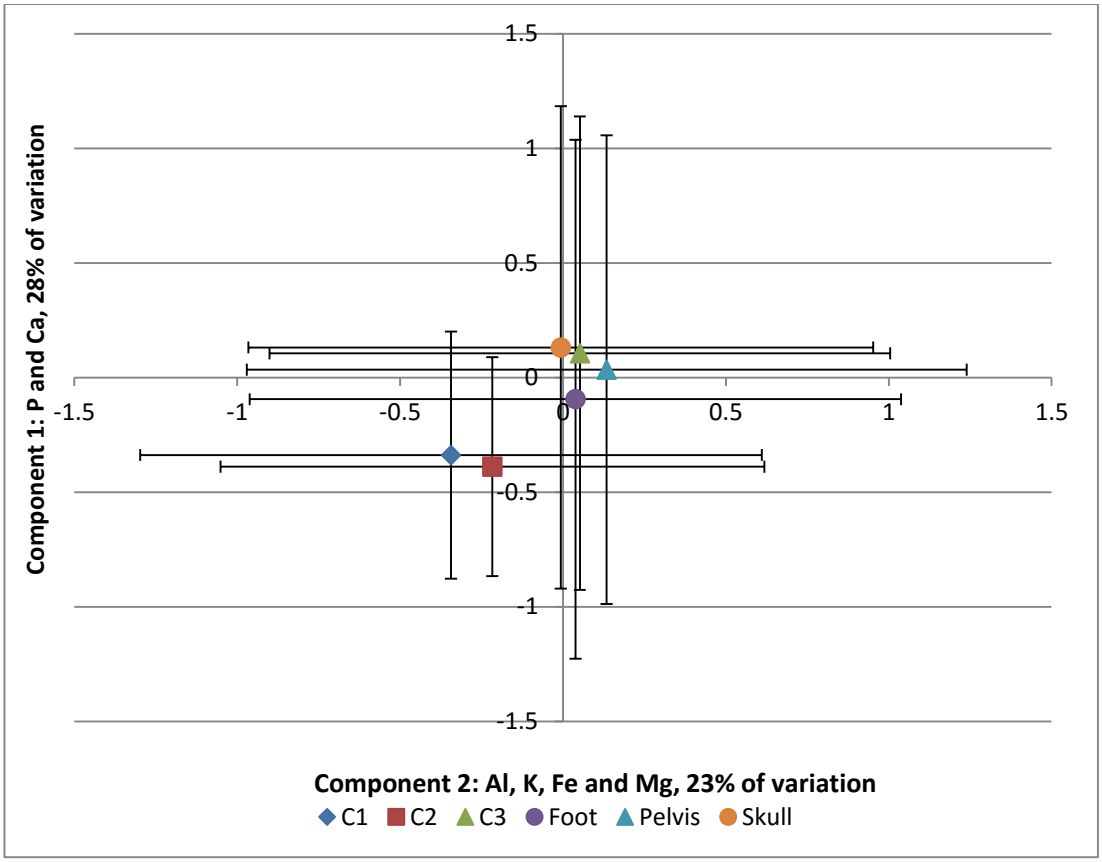

Figure 25: Component 1 and component 2 PCA results for Hungate coded by sample location. The centre point shows the mean value with error bars of one standard deviation

C1 and C2 have a negative distribution along component one (Ca and P) and component two (Al, K, Fe and Mg) (Figure 25). In terms of component one and two, differences between the sample locations in the burial plane were not discerned. The C3 sample and burial plane samples all cluster in a similar location with foot area samples being slightly more negative on component one. The position and clustering of the samples suggest that the C1 contained less Al, K, Fe, Mg, Ca and P than the samples from the burial plane, as did the C2 sample. The suite of elements that cluster on component two suggests that it relates to minerogenic and pedogenic processes, the presence of Fe may also be influenced by body degradation products. Component one may relate to the presence of Ca rich parent material and the retention of Ca and P from the decomposed body meaning that component two may be a broad grave signal.

4.2.1 Spherulites.

4.2.1.1 Description and presence

Spherulites were present in the fine material at Hungate and to further their interpretation the inorganic geochemical composition of the spherulites were investigated using SEM-EDX analysis. Spherulites are spherical mineral formations that have characteristic pseudo-uniaxial negative extinction crosses (Canti, 1998b). Small (c 5µm) reddish spherulites (Figure 26) were observed in the fine material and as part of pedofeatures (coatings, hypocoatings and impregnations) in five of the Hungate graves (Table 24 and Figure 27).

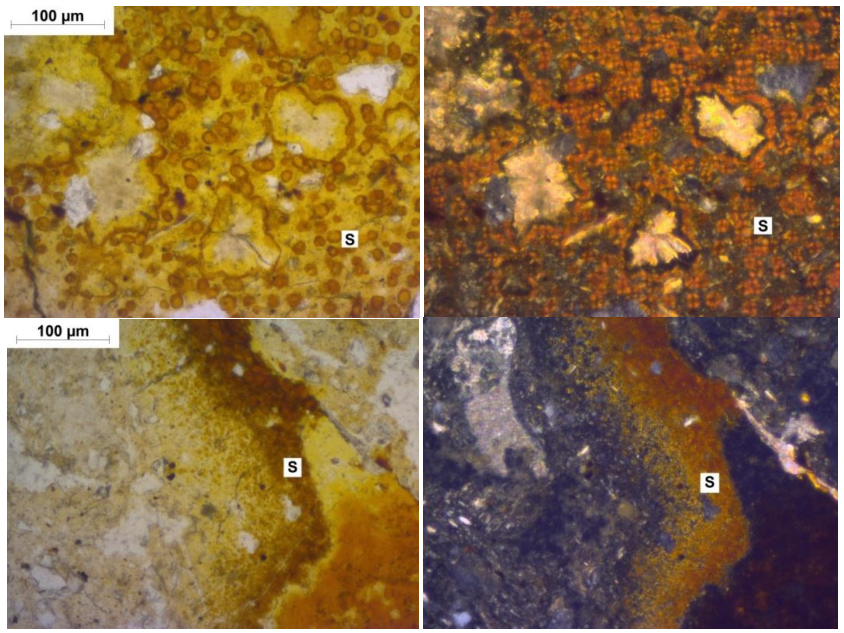

Figure 26: Examples of spherulites within the burials from Hungate. Top images are Fe spherulite impregnation with large $CaCO_3$ spherulites from the pelvic sample of SK54342 in PPL (left) and XPL image (right). Bottom image are Fe spherulites forming a hypocoating in the pelvic sample from SK54342 in PPL (left) and XPL (right).

Table 24: Location of spherulites in the graves analysed at Hungate. '*' = red spherulites, blue cells indicate where there was no sample available.

Grave number	Age	Burial type	C2	C3	Skull		Pelvis		Foot		Additional samples
					Perp	Para	Perp	Para	Perp	Para	
SK54898	Infant	Lead coffin									
SK51326	Adult	Coffin		*			*		*		
SK51387	Adult	-									
SK51351	Adult	Coffin			*	*	*		*	*	*
SK54090	Infant	-									
SK54085	Adult	Coffin									
SK54341	Adult	Coffin		*							
SK54342	Adult	Coffin					*	*			
SK51350	Adult	Coffin		*			*		*		
SK54908	Infant	Coffin									

Figure 27: Location of graves containing spherulites at Hungate

The spherulites were investigated using SEM-EDX analysis to determine their inorganic chemistry (Figure 28 and Table 25). The red spherulites contain high levels of Fe (18.48%) and Si (11.98%) with lower levels of P (1.03%), Ca (4.23%) and Mn (4.11%).

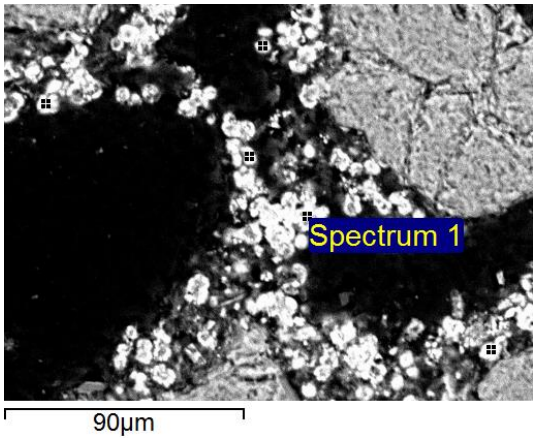

Figure 28: SEM-BSE image of spherulites in the foot sample from SK51326. With an example of where observation points were taken (spectrum 1)

Table 25: SEM-EDX inorganic chemistry results presented as atomic % for red spherulite features in the perpendicular foot sample from SK51326, Hungate.

	C	O	Na	Mg	Al	Si	P	Cl	K	Ca	Mn	Fe
Mean (wt %)	50.52	60.15	0.45	0.18	1.61	11.98	1.03	0.24	0.46	4.23	4.11	18.48
Standard deviation (wt %)	4.18	13.39	0.09	0.02	0.18	1.71	0.18	0.04	0.07	1.35	2.15	1.98
Max (wt %)	54.14	69.65	0.53	0.21	1.84	14.87	1.3	0.27	0.57	6.06	7.03	20.46
Min (wt %)	43.54	37.65	0.3	0.16	1.43	10.47	0.84	0.17	0.38	2.5	1.33	15.97

4.2.1.2 Spherulite variation

Table 24 shows that the Fe (red) spherulites were present in five graves (SK51326, SK51351, SK54341, SK54342 and SK51350). There was no relationship between the age at death of the individual and the presence of spherulites. Spherulites were, however, confined to samples from around coffined bodies and associated C3 samples; they did not occur in the C1 or the C2 samples, suggesting that the spherulites had formed in the burial plane (discussed further in section 4.5.3).

4.3 Intra grave inorganic geochemical variation – Çatalhöyük, Thessaloniki and Hungate.

4.3.1 Çatalhöyük

The C1 sample and all samples from burial 18666 were used for the intra grave inorganic geochemical variation at Çatalhöyük. Burial 18666 was included in the SEM-EDX analysis as it was the only grave from Çatalhöyük that had an almost complete sample set (C1, C3, skull, pelvis and foot). Mg, Al, Si, P, S, K, Ca, Ti and Fe were used in the PCA. Overall KMO measure was calculated at .701 and all KMO values for individual elements were over .5. Bartlett's test of sphericity x^2 (253) = 1367.736 $p < .001$ indicated that correlations between elements were large enough to conduct PCA analysis. Three components had eigenvalues over 1 and account for 60.2% of the variance. The scree plot (not shown) was ambiguous therefore three components were used, as indicated by the eigenvalues. Table 26 shows factor loadings after rotation. Component 2 and 3 were plotted for Çatalhöyük as they best resolved the individual samples. The resulting plots were coded for microfabric type (Figure 31) and sample location (Figure 32).

Table 26: Rotated component matrix for 18666. Items with factor loadings higher than 0.4 are highlighted in green.

Elements	Component		
	1	2	3
Ca	-.802	.211	
Si	.764	-.128	-.146
Al	.746	.420	-.103
K	.690	.301	
Ti	.194		
Mg		.875	
Fe	.514	.661	
S			.819
P			.792
Eigenvalues	2.892	1.305	1.258
% variance	32.136	14.500	13.982

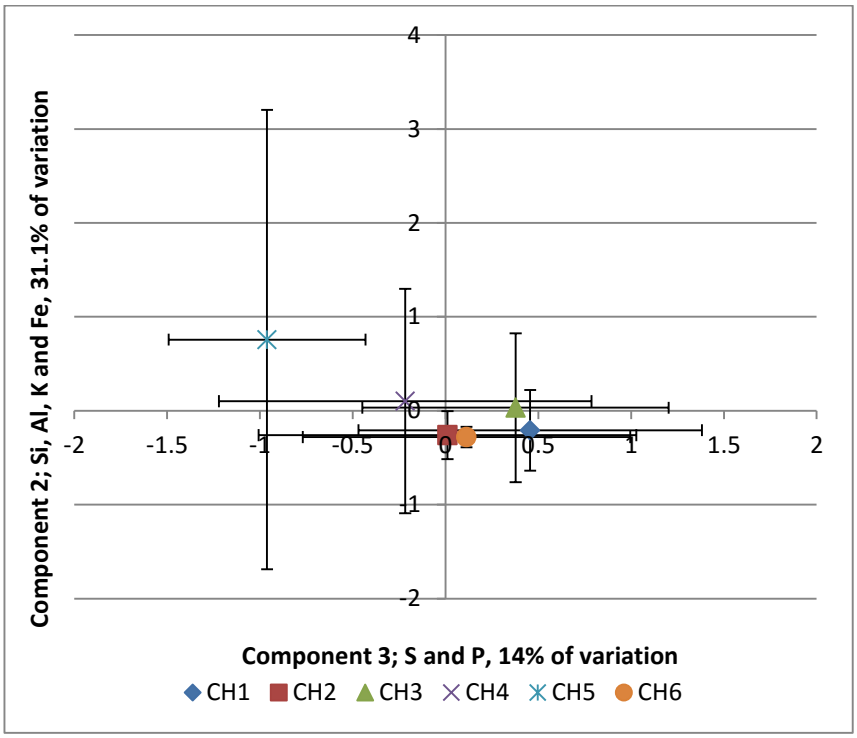

Figure 29: Component 1 and component 3 PCA results for 18666 Çatalhöyük coded by microfabric type. The centre point shows the mean value with error bars of one standard deviation

Microfabrics CH1, CH2, CH3, CH4 and CH6 cluster together near to zero on both component axis (Figure 29). Microfabric CH5, however, is more negatively distributed along the component three and positively distributed along the component two than the other microfabrics, meaning that CH5 contains more Si, Al, K and Fe than the other microfabrics and less S and P. All the microfabrics, particularly those that have formed near to zero, have overlapping error bars indicating that they had a similar inorganic geochemical distribution in terms of component two and three.

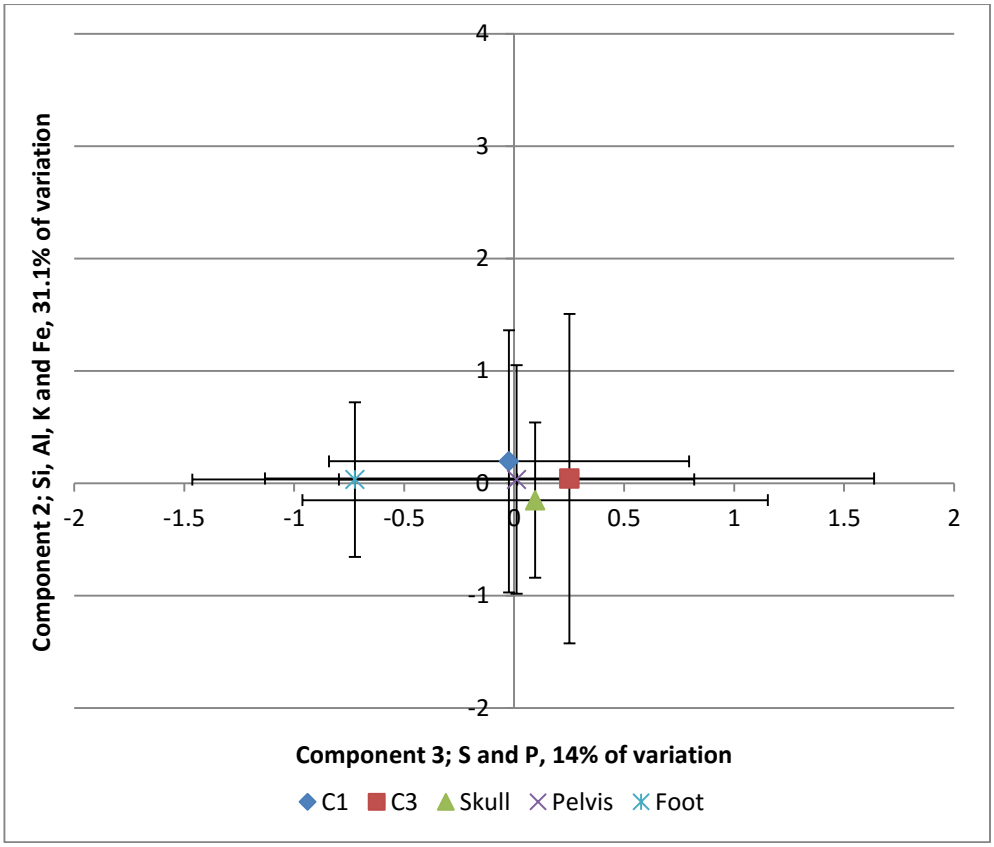

Figure 30: Component 1 and component 3 PCA results for 18666 Çatalhöyük colour coded by sample location. The centre point shows the mean value with error bars of one standard deviation.

The samples from the burial plane and control samples were all similarly distributed with larger variations along the component three axis than on component two (Figure 30). The foot area data has a narrower error for component two and three than other sample locations and was more negative along component three, meaning that the foot area sample was depleted in S and P compared to the others. Component two has high loadings for Mg, Al and Fe and likely relates to pedogenic Fe in the soil as well as the presence of high abundances of clay minerals in the soil. Component 3 may relate to elements that were associated with organic decomposition (S and P). The implications of which are discussed further in 4.5.3.2.

4.3.2 Thessaloniki

All control samples (C2 and C3) and burial plane samples from TF177 were used. P, Ca, Mn and Fe were assessed in the PCA, Si was excluded as it had a KMO value of <.5 and brought the overall KMO value to <.5. The overall KMO measure for P, Ca, Mn and Fe was .549 and values for individual elements were >.5, except Mn which was .494. Bartlett's test of sphericity x^2 (253) =

1032.306 p < .001 indicated that correlations between elements were large enough to conduct PCA. Two components have eigenvalues over 1 and account for 62.4% of the variance. The scree plot showed a slight inflection at the third component justifying retaining two components. Table 27 shows factor loadings after rotation. Components 1 and 2 were plotted for Thessaloniki and coded for microfabric type (Figure 31) and sample location (Figure 32).

Table 27: Rotated component matrix for TF177. Items with factor loadings higher than 0.4 are highlighted in green.

Element	Component	
	1	2
P	.757	.202
Ca	.752	-.187
Mn	.142	.855
Fe	-.462	.564
Eigenvalues	1.426	1.071
% of variance	35.659	26.768

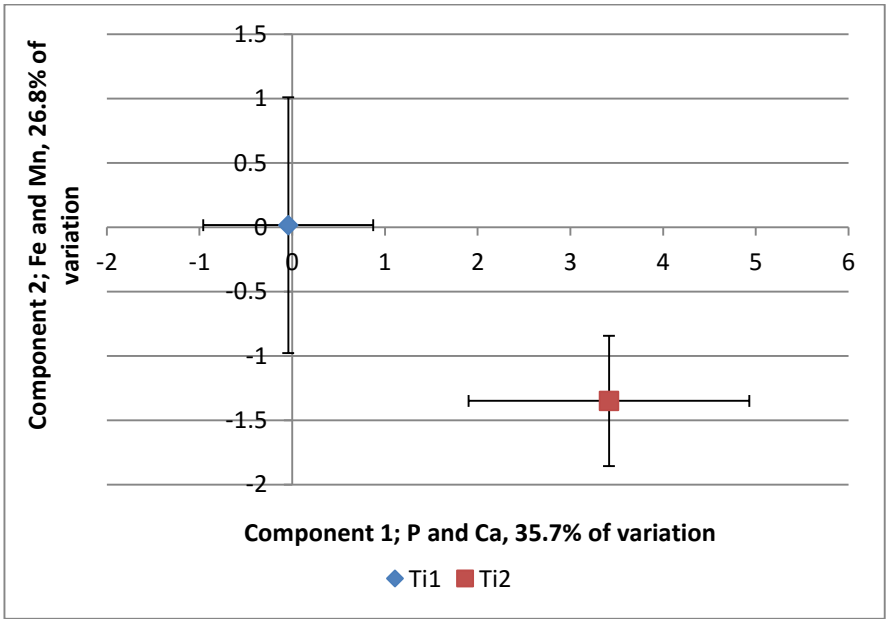

Figure 31: Component 1 and component 2 PCA results for TF177 Thessaloniki coded by microfabric type. The centre point shows the mean value with error bars of one standard deviation

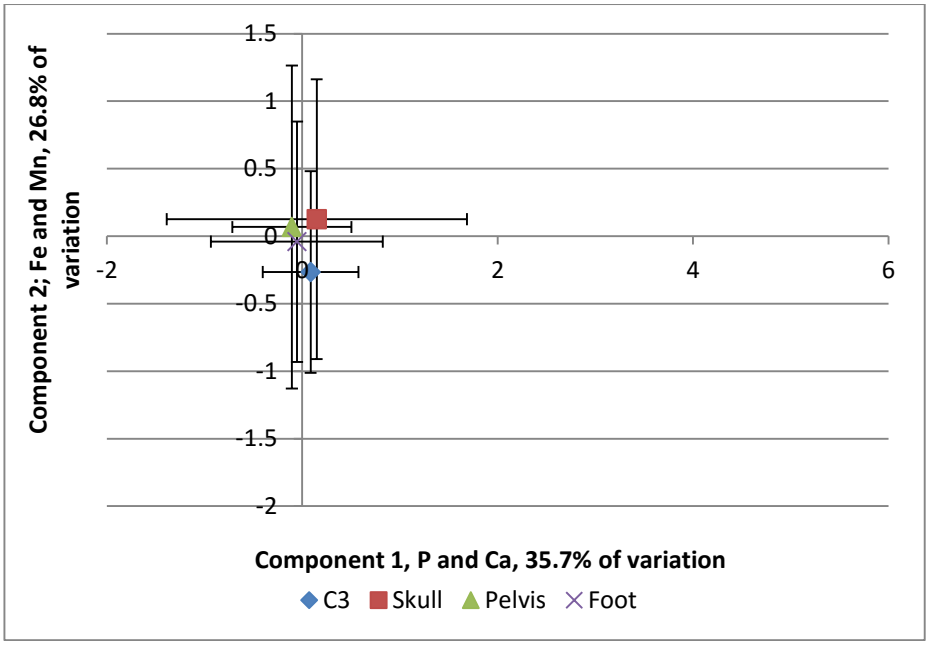

Figure 32: Component 1 and component 2 PCA results for TF177 Thessaloniki coded by sample location. The centre point shows the mean value with error bars of one standard deviation

When considering the microfabrics (Figure 31) Ti1 and Ti2 have a clear separation, with Ti2 loading positively on component one (P and Ca) and negatively on component two (Fe and Mn), meaning that Ti2 is richer in P and Ca than Ti1 but contains less Fe and Mn. The C3 (blue Figure 32) and burial plane samples showed little separation. When coded by sample location the samples cluster in a similar distribution to Ti1, meaning that the influence of Ti2 is lost. This probably reflects the low number of points taken in Ti2 compared to Ti1. Component one has high loadings for P and Ca and may relate to the parent material or the retention of P and Ca in the soil. Component two likely relates to pedogenic Mn and Fe present within the soil or possibly to the presence of redoximorphic conditions encouraging Mn and Fe precipitation (Hseu & Chen, 2001).

4.3.3 Hungate – C1, SK54898, SK51331, SK51387, SK51351, SK54090, SK54085, SK54341 and SK54908

For the intra grave analysis at Hungate, the C1 sample and all control and burial plane samples from the respective graves were utilised.

4.3.3.1 Grave SK54898

Na, Al, Si, P, K, Ca, Fe and Pb were used in the PCA. The overall KMO was .741. Bartlett's test of sphericity x^2 (253) = 4372.308 p < .001 indicated that correlations between elements were large enough to conduct PCA analysis. Two components had eigenvalues over 1 and accounted for 61.37% of the variance. Table 28 shows factor loadings after rotation. Component 1 and 2 were plotted for Hungate SK54898 and colour coded for microfabric type (Figure 33) and sample location (Figure 34).

Table 28: Rotated component matrix for Hungate SK54898. Items with factor loadings > 0.4 are in green.

Elements	Component	
	1	2
P	.936	-.132
Ca	.856	
Pb	.839	-.179
Si	-.624	.319
Al	-.328	.823
K	-.286	.756
Fe	.217	.633
Na	-.146	.383
Eigenvalues	3.49	1.42
% Variation	43.6	17.77

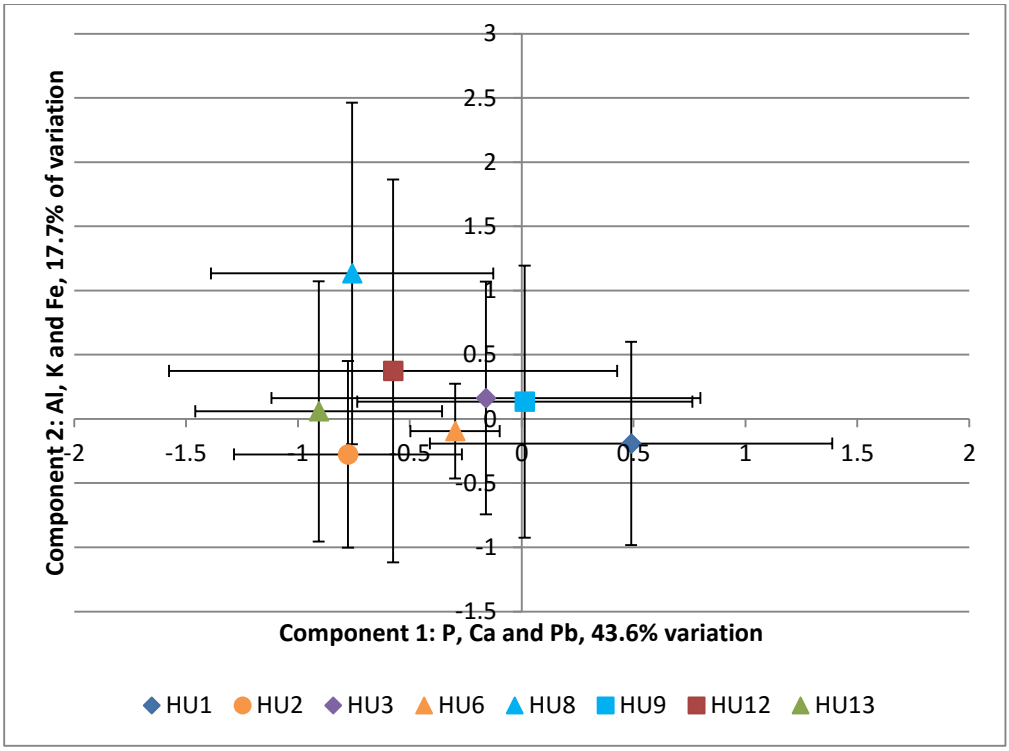

Figure 33: Component 1 and Component 2 PCA results for Hungate SK54898 coded by microfabric type. The centre point shows the mean value with error bars of one standard deviation.

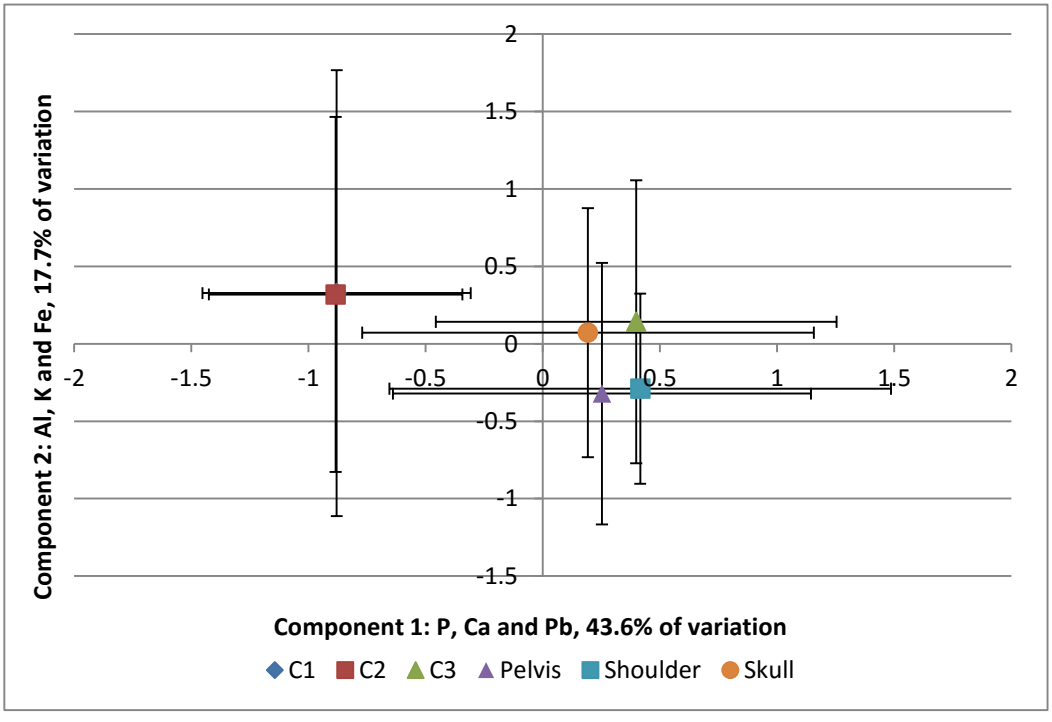

Figure 34: Component 1 and component 2 PCA results for Hungate SK54898 coded by location. The centre point shows the mean value with error bars of one standard deviation.

The results grouped by microfabric type show that those from the C1 (HU8, HU12 and HU13) samples are grouped more negatively on component one than the other microfabrics from the burial plane, meaning that the C1 microfabrics contain less P, Ca and Pb than those from the burial plane (Figure 33). HU2 also groups towards the control microfabrics despite it being only visible in the grave. This would indicate that it was more similar to the control microfabrics in terms of component one and two than the grave microfabrics. In Figure 34 the C1 and C2 samples plot lower on component one than the samples from the burial plane, reflecting the trend seen in Figure 33, whilst the C3 sample (taken from inside the lead coffin) has a similar distribution to those from the burial plane with higher levels of Ca, P and Pb. P, Ca and Pb have high loadings on component one suggesting that it relates to taphonomic processes, such as the degradation of organic material and the presence of a lead coffin. Component two likely relates to minerogenic weathering or the presence of clays with some possible influence of organic degradation (Fe). Fe also loads positively for component one suggesting a possible link to degradation processes.

Inorganic geochemical changes in HU6 were investigated further to ascertain if the optical differences in the layers observed in HU6 was reflected in the inorganic geochemical composition of the layers (Figure 14 and Figure 35). Minor fluctuations in Al, Si and minimal variation in the remaining inorganic geochemicals indicated that differences between clay lamina were more optically, rather than chemically, expressed (Figure 35). This would suggest that the clay had a common origin but was deposited in distinct events. Lead concentrations were also enhanced in the fine material from grave SK54898 (Table 29).

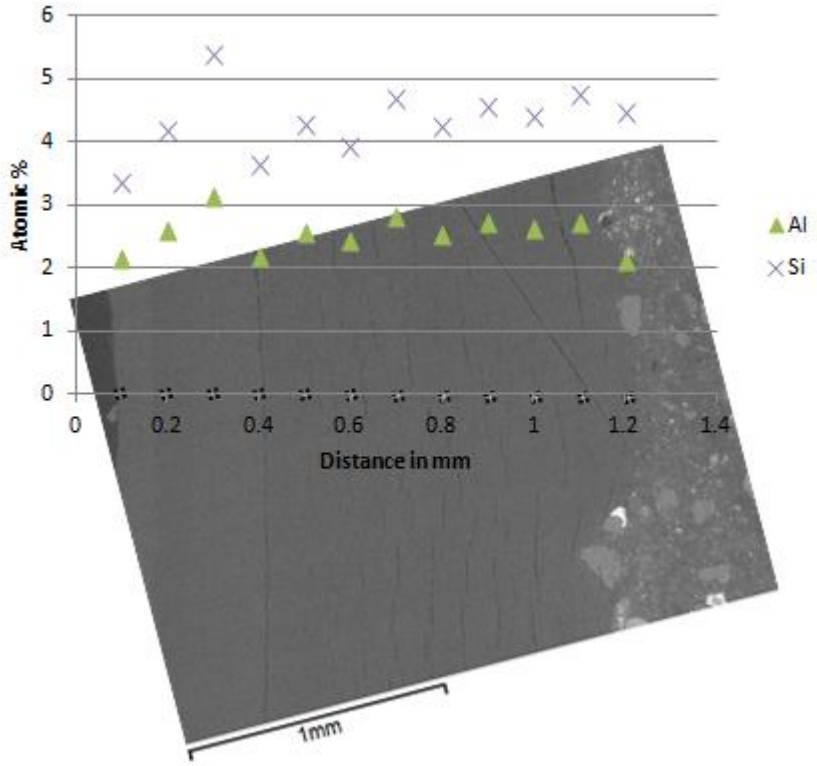

Figure 35: Al and Si inorganic geochemical vitiation in HU6 in the shoulder sample from SK54898 in atomic %.

Table 29: Weight % of lead within the fine material at Hungate between the C1, none lead coffined burials and lead coffined burials as determined using SEM-EDX.

	C1	Non lead coffin graves	Lead coffin
Mean (wt %)	0	0	1
Standard Deviation (wt %)	0	0	2
Minimum (wt %)	0	0	0
Maximum (wt %)	0	2	26
Count	195	3322	871

4.3.3.2 SK51326

Al, Mg, K, Fe, Ca, P, Mn, Si and S were used in the PCA analysis. The overall KMO was .600. Bartlett's test of sphericity x^2 (253) = 2548.090 $p < .001$ indicating that correlations between elements were large enough to conduct PCA analysis. Three components had eigenvalues over 1 and account for 69.7% of the variance. Table 30 showed factor loadings after rotation. Components 1 and 2 were plotted for Hungate SK51331 as they best resolved the variation in the samples and colour coded for microfabric type (Figure 36) and sample location (Figure 37).

Table 30: Rotated component matrix for Hungate SK51326. Items with factor loadings higher than 0.4 are highlighted in green.

Element	Component		
	1	2	3
Mg	.813		
Al	.809	-.141	
K	.730	-.134	
Fe	.638	.545	-.111
P		.887	
Ca		.843	.141
Si	.126	-.460	
S			.978
Mn			.977
Eigenvalues	2.325	2.067	1.883
% variation	25.8	23.0	20.9

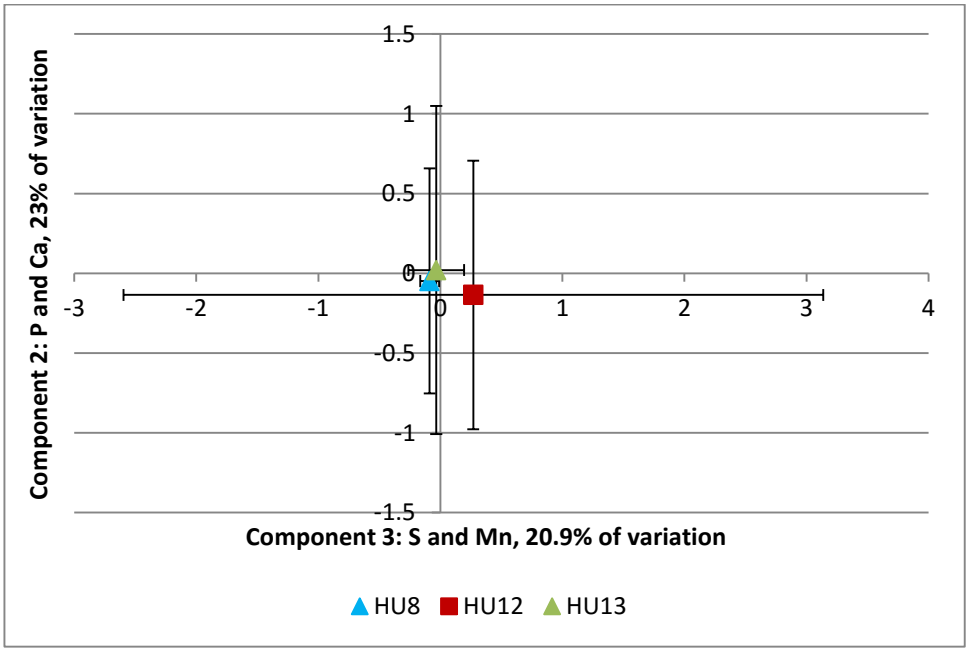

Figure 36: Component 1 and component 2 PCA results for Hungate SK51326 coded by microfabric type. The centre point shows the mean value with error bars of one standard deviation

The microfabrics in SK51326 are all chemically similar clustering near to zero on component two and a wider distribution of points along component three (Figure 36). HU8 is the most negatively placed on component two meaning that it contains less P and Ca than HU12 and HU13.

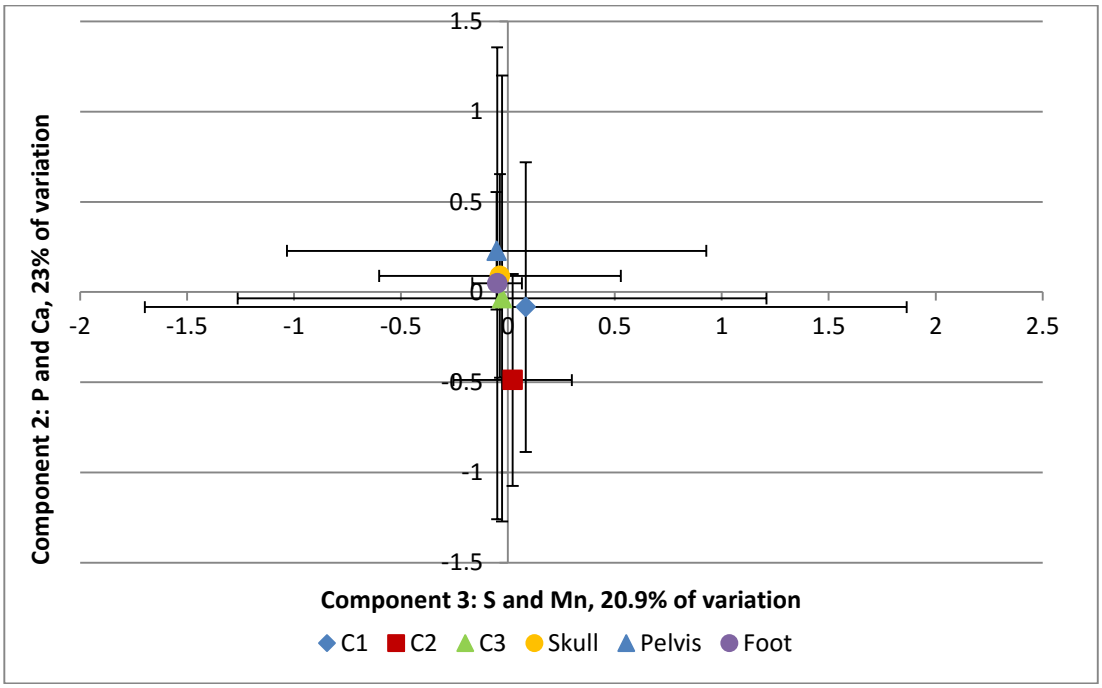

Figure 37: Component 1 and component 2 PCA results for Hungate SK51326 coded by location. The centre point shows the mean value with error bars of one standard deviation.

All sample locations cluster close to zero on component three and all but the C2 cluster close to zero on component 2, meaning that the C2 contains less P and Ca than those from the burial plane and the C1 (Figure 37). That being said when the sample locations are considered in more detail the skull, pelvis and foot samples have a negative value for component 3 and a positive distribution for component two whilst the control samples have the opposite pattern, meaning that the samples from the burial plane contained more P and Ca, but less S and Mn than the controls. However the samples are all within one standard deviation of each other indicating that this effect is only very slight. S and Mn dominate loadings along component three suggesting that component one relates to pedogenic and minerogenic processes, including redoximorphic conditions or possibly decomposition with the presence of Mn. Component two contains P and Ca and is less concentrated in the C1 samples than in the burial plane therefore component two may relate to the presence of post depositional pedogenic processes and organic decomposition.

4.3.3.3 SK51387

Na, Mg, Al, Si, P, S, Cl, K, Ca, Ti, Mn and Fe were used in the PCA analysis. The overall KMO was .532. Bartlett's test of sphericity x^2 (253) = 2737.842 p < .001 indicated that correlations between elements were large enough to conduct PCA analysis. Five components had eigenvalues over 1 and accounted for 68.71% of the variance. Table 31 shows factor loadings after rotation. Components 2 and 3 were plotted for Hungate SK51387, and colour coded for microfabric type (Figure 38) and sample location (Figure 39), as these two components best resolved the data.

Table 31: Rotated component matrix for Hungate SK51387. Items with factor loadings higher than 0.4 are highlighted in green.

Elements	Component				
	1	2	3	4	5
Al	.865			.145	
K	.772				
Fe	.671	-.116	.212	-.353	.148
Mn		.973			
S		.960			
Ca			.880	.142	
P			.698		.194
Mg	.490		.601		-.203
Na	.195			.714	.161
Ti	.102	.231		-.531	
Cl		.129		.240	.798
Si			-.390	.390	-.590
Eigenvalues	2.286	2.029	1.710	1.163	1.058
% variation	19.0	16.9	14.2	9.7	8.8

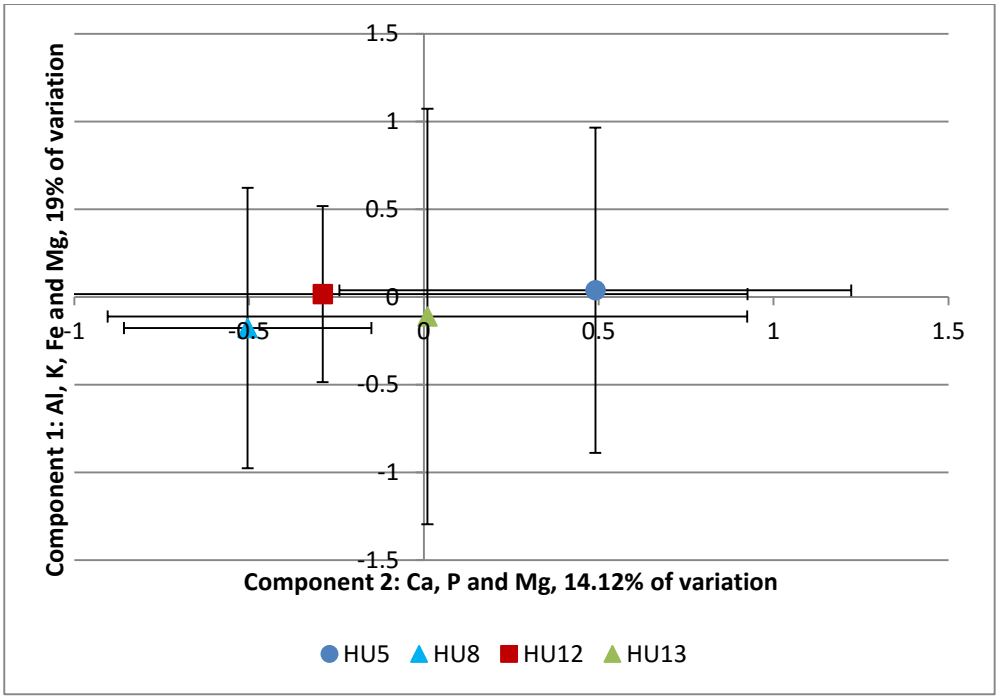

Figure 38: Component 1 and component 2 PCA results for Hungate SK51387 coded by microfabric type. The centre point shows the mean value with error bars of one standard deviation

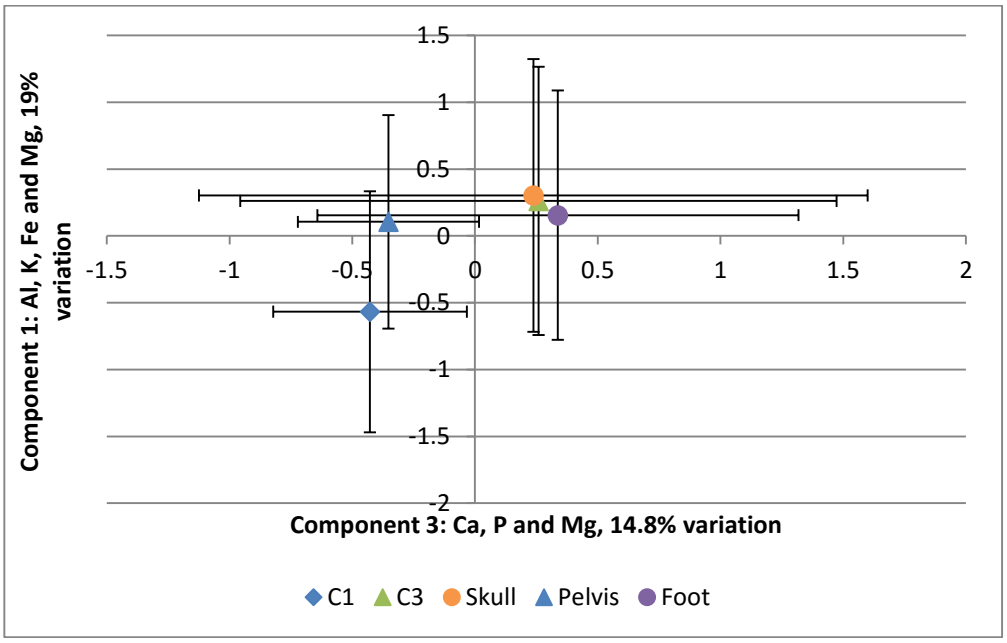

Figure 39: Component 1 and component 2 PCA results for Hungate SK51387 coded by location. The centre point shows the mean value with error bars of one standard deviation.

HU5, HU8, HU12 and HU13 are closely clustered near to zero for component one but more widely distributed for component three (Figure 38). HU5, which is the only microfabric not found in the C1 samples, is positioned positively for component three meaning that it contains elevated levels of Ca, P and Mg, compared to the other microfabrics. All microfabrics are however positioned within one standard deviation of one another.

The C1 sample is the only sample that plots negatively on component 1 (Figure 39). The C3, skull and foot sample cluster close together and positively for both component one and three meaning that they are higher in Ca, P, Mg, Al, K, Fe and Mg than the control and higher in Ca, P and Mg than the pelvic sample. Component one and three contains Ca, P, Fe and Mg which may relate to organic degradation products. Whereas the Al and K elements in component one may relate to the presence of clays in the soil.

4.3.3.4 SK51351

Mg, Al, Si, Cl, K and Fe were used in the PCA analysis. The overall KMO was .595. Bartlett's test of sphericity x^2 (253) = 2438.169 p < .001 indicated that correlations between elements were large enough to conduct PCA analysis. Three components had eigenvalues over 1 and accounted for 70.13% of the variance. Table 32 shows factor loadings after rotation. Components 1 and 2 were plotted for Hungate SK51351 and coded for microfabric type (Figure 38) and sample location (Figure 39).

Table 32: Rotated component matrix for Hungate SK51351. Items with factor loadings higher than 0.4 are highlighted in green.

Elements	Component		
	1	2	3
Al	.854		
Mg	.836		.105
K	.748		-.143
Fe	.674	.113	.346
P		.971	
Ca		.962	
Cl			.756
Si		-.212	-.690
Eigenvalues	2.490	2.014	1.107
% variance	31.12	25.17	13.82

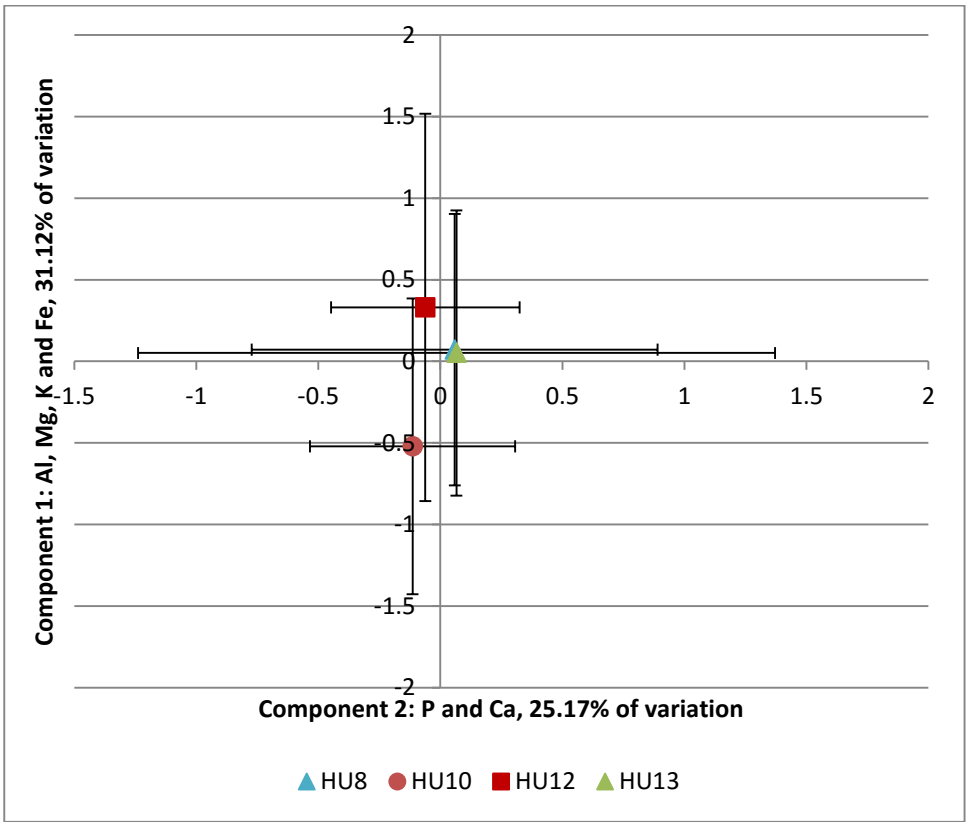

Figure 40: Component 1 and component 2 PCA results for Hungate SK51351 coded by microfabric type. The centre point shows the mean value with error bars of one standard deviation

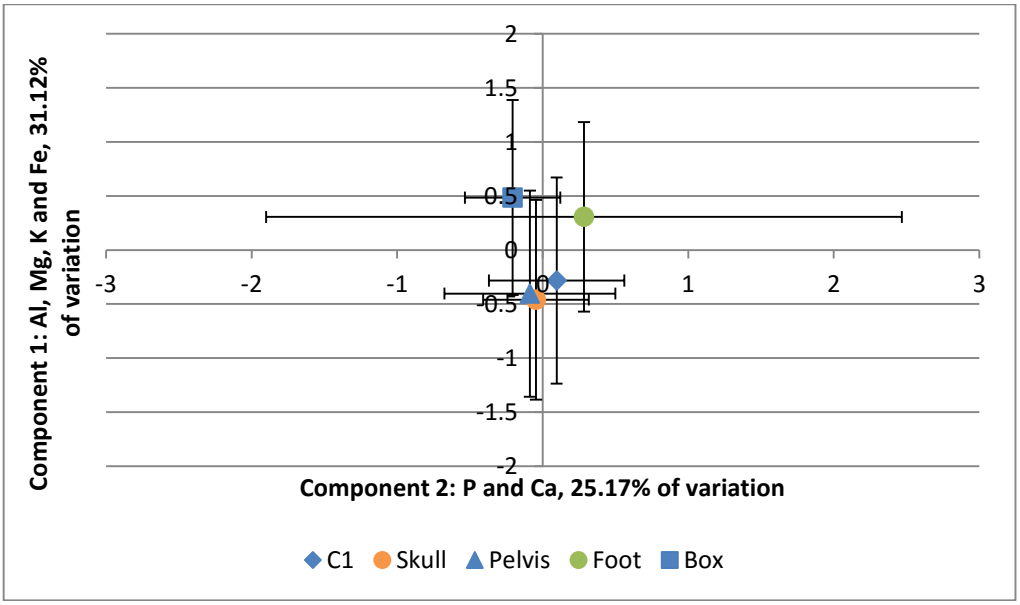

Figure 41: Component 1 and component 2 PCA results for Hungate SK51351 coded by location. The centre point shows the mean value with error bars of one standard deviation.

Microfabrics HU8, HU10 HU12 and HU13 cluster close to zero on the component two axis meaning that they contain similar quantities of P and Ca (Figure 40). HU10 is the only microfabric that is present in the burial plane and not the C1 samples and is also the only microfabric that plots negatively for component one meaning that HU10 contains less Al, Mg, K and Fe than the other microfabrics.

All sample locations plot close to zero in terms of component two indicating that levels of P and Ca are similar in all samples (Figure 41). Samples are slightly wider distributed along component one with the foot and Box sample containing more Al, Mg, K and Fe than the skull, pelvis and C1 sample. Al, Mg, K and Fe in component one may relate to pedogenic and minerogenic processes, including the presence of clays and the decomposition of organic matter, whilst component two probably relates to the presence of P and Ca in the soil possibly from digenesis.

4.3.3.5 SK54090

Mg, Al, Si, K, Mn and Fe were used in the PCA. The overall KMO was .693. Bartlett's test of sphericity x^2 (253) = 921.927 $p < .001$ indicated that correlations between elements were large enough to conduct PCA analysis. Three components have eigenvalues over 1 and accounted for 79.2% of the variance. Table 33 shows factor loadings after rotation. Components 1 and 3 were plotted for Hungate SK54090 and colour coded for microfabric type (Figure 42) and sample location (Figure 43).

Table 33: Rotated component matrix for Hungate SK54090. Items with factor loadings higher than 0.4 are highlighted in green.

Element	Component		
	1	2	3
Al	.902		
Mg	.877	-.132	
K	.788	.139	
Fe	.612	-.508	-.160
Si		.920	
Mn			.992
Eigenvalues	2.62	1.11	1.02
% of variation	43.47	18.50	17.04

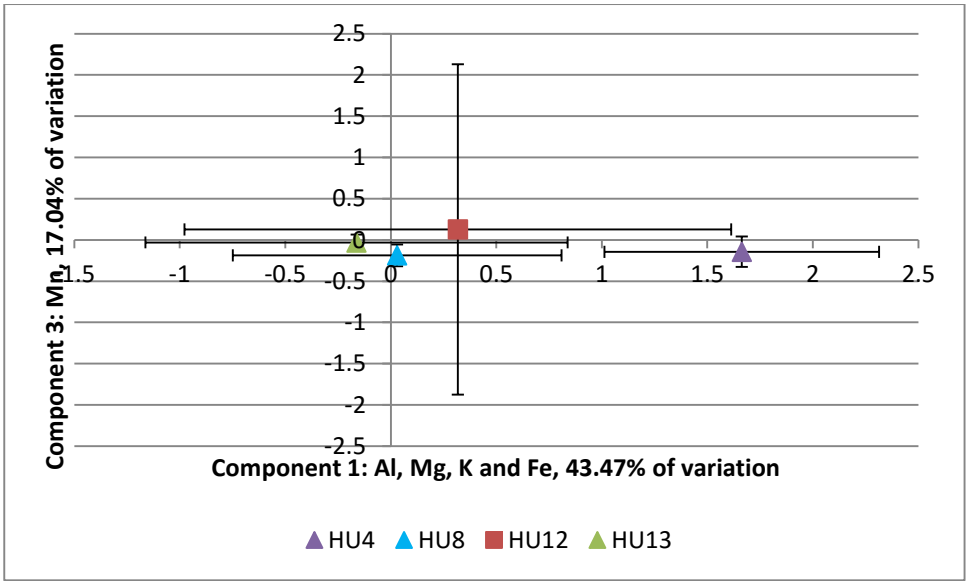

Figure 42: Component 1 and component 2 PCA results for Hungate SK54090 coded by microfabric type. The centre point shows the mean value with error bars of one standard deviation

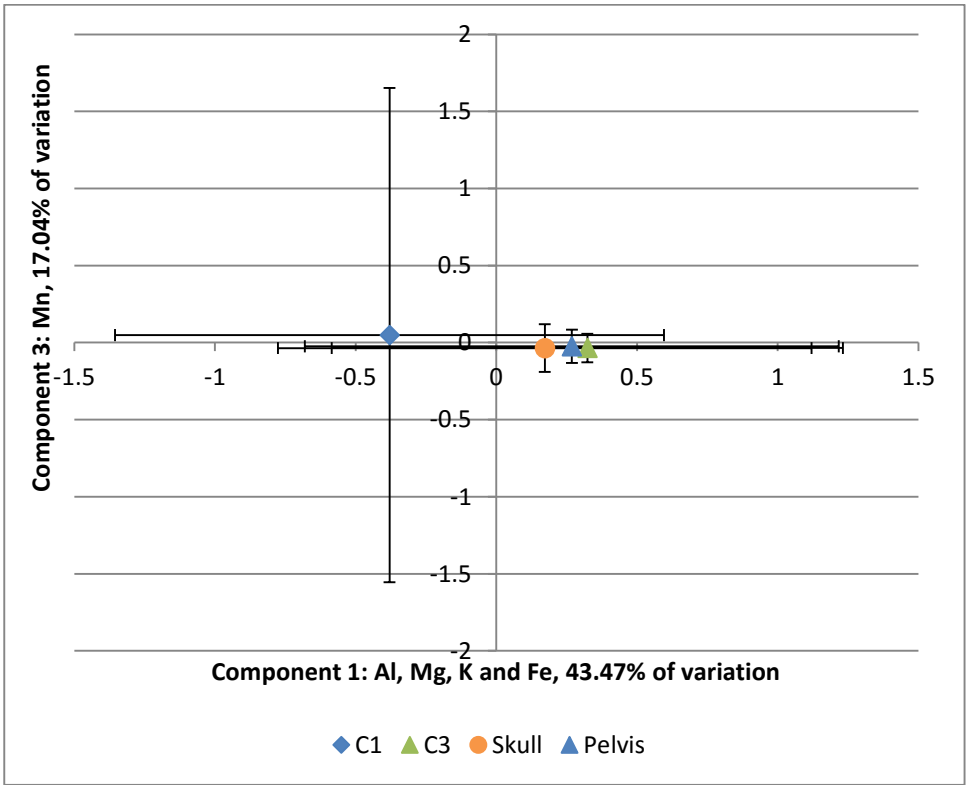

Figure 43: Component 1 and component 2 PCA results for Hungate SK54090 coded by location. The centre point shows the mean value with error bars of one standard deviation.

The microfabrics in SK54090 were narrowly distributed near to zero on component three, and widely distributed on component one (Figure 42). There was some separation of the microfabrics

with those in the C1 (HU8, HU12 and HU13) generally distributed in the low negatives and positives for component one and those just present in the burial plane (HU4, although this is thought to be formed through deposition of river sediments) situated more positively along component 1.

Figure 43 illustrated a distinction between the C1 and all other samples. The samples from the C3, skull and pelvis area were chemically similar. All samples from the burial plane and the C3 are positively distributed along component one and therefore richer in Fe, Mg, Al and K. The elements on component one appeared to relate to pedogenic and minerogenic processes, including the presence of clays and redoximorphic processes. Component three may relate to the presence of possible post depositional pedogenic processes.

4.3.3.6 SK54085

Mg, Al, Si, P, K, Ca and Fe were used in the PCA. The overall KMO was .623. Bartlett's test of sphericity x^2 (253) = .1572.167 p < .001 indicated that correlations between elements were large enough to conduct PCA analysis. Two components had eigenvalues over 1 and accounted for 78.53% of the variance. The scree plot had a slight inflection on the third component, confirming the use of the first two components. Table 34 shows factor loadings after rotation. Components 1 and 2 were plotted for Hungate SK54085 and colour coded for microfabric type (Figure 44) and sample location (Figure 45)

Table 34: Rotated component matrix for Hungate SK54085. Items with factor loadings higher than 0.4 are highlighted in green.

Elements	Component	
	1	2
Al	.907	
Mg	.875	.107
K	.756	-.126
P		.910
Ca		.845
Fe	.461	.642
Si	.157	-.502
Eigenvalues	2.45	2.20
% of variables	34.93	31.37

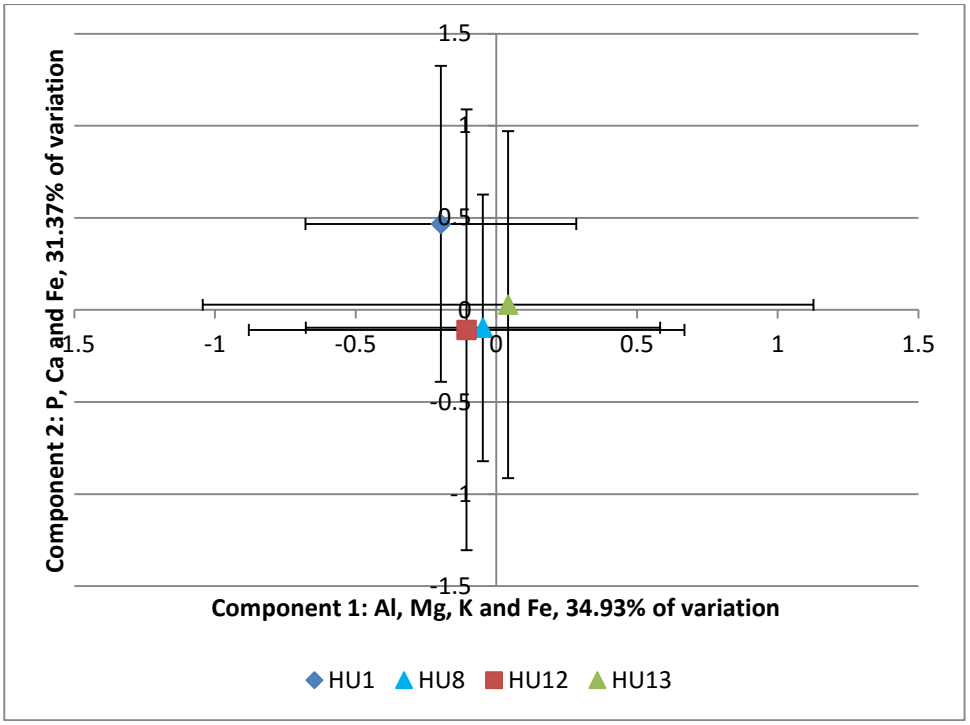

Figure 44: Component 1 and component 2 PCA results for Hungate SK54085 coded by microfabric type. The centre point shows the mean value with error bars of one standard deviation

The microfabrics in SK54085 are chemically similar in terms of component one (Figure 44). HU8, HU12 and HU13, present in the C1 samples, also plotted at near to zero for component two. HU1, which was the only microfabric that was only present in the burial plane plotted more positively on component two meaning that it contained more P, Ca and Fe than HU8, HU12 and HU13. HU13 dominated the data cloud and was fairly central because this microfabric was widespread across the grave and C1 samples.

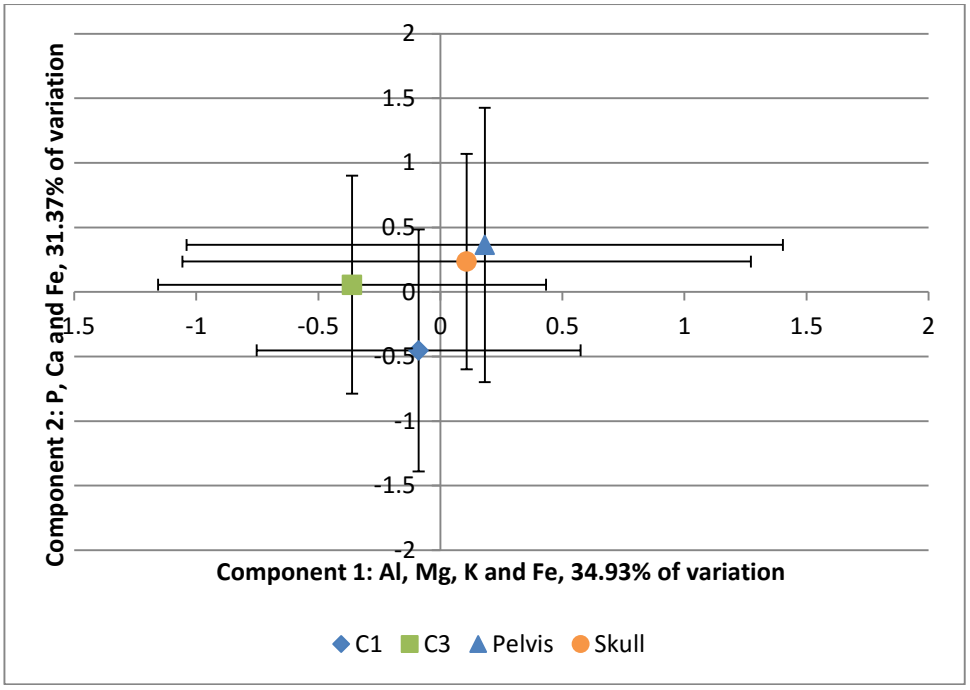

Figure 45: Component 1 and component 2 PCA results for Hungate SK54085 coded by location. The centre point shows the mean value with error bars of one standard deviation.

The C1 sample clustered on the low negatives of both component one and component two (Figure 45), meaning that it was lower in Al, Mg, K, Fe, P and Ca than the skull and pelvic area samples. The C3 was similarly distributed along component two to those of the burial plane but more negative along component one. Component one contains elements that may relate to the weathering of minerals and the presence of high levels of clay. The presence of Fe in both components suggests that Fe was prevalent in the fine material of the grave either due to redoximorphic processes or the Fe being inherited from parent material. Component two appears to relate to a broader organic signal with high Ca and P as well as Fe present.

4.3.3.7 SK54341

Mg, Fe, Al, K, Cl, Ca, P and Mn were used in the PCA. The overall KMO was .655. Bartlett's test of sphericity x^2 (253) = 1332.753 $p < .001$ indicated that correlations between elements were large enough to conduct PCA analysis. Three components had eigenvalues over 1 and account for 51.290% of the variance. Table 35 shows factor loadings after rotation. Components 1 and 2 were plotted for Hungate SK54341 and coded for microfabric type (Figure 46) and sample location (Figure 47).

Table 35: Rotated component matrix for Hungate SK51342. Items with factor loadings higher than 0.4 are highlighted in green.

Elements	Component		
	1	2	3
Al	.819		
Mg	.803	.183	
K	.743	-.210	
Fe	.692	.433	
P		.817	
Ca		.755	
Mn			.798
Cl			.653
Eigenvalues	2.44	1.44	1.09
% of variation	30.47	18.02	13.59

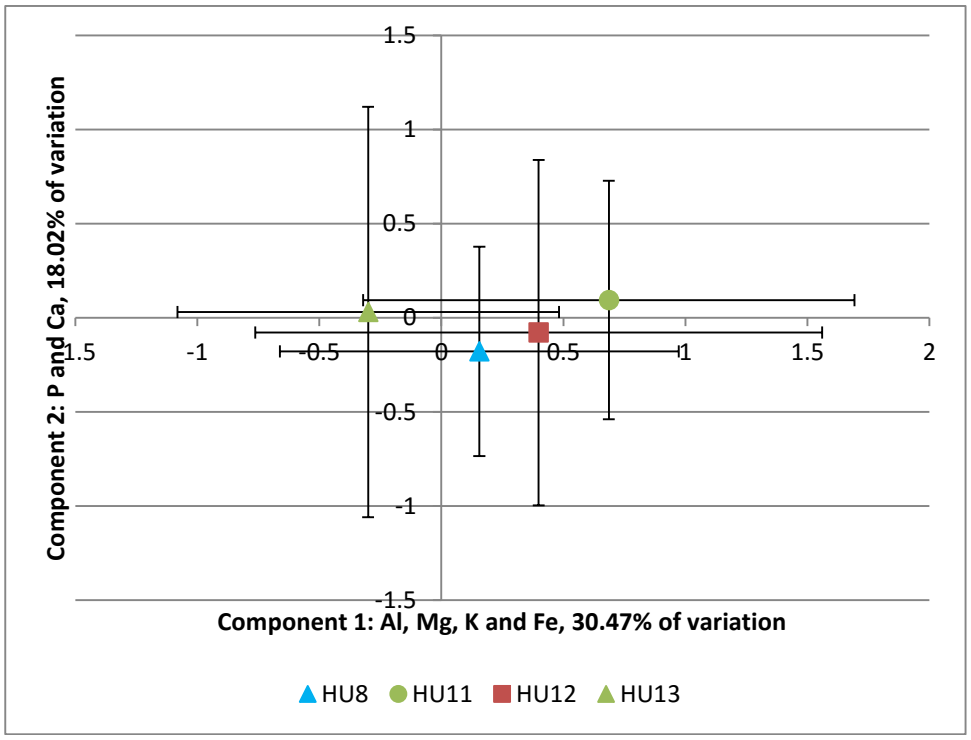

Figure 46: Component 1 and component 2 PCA results for Hungate SK54341 coded by microfabric type. The centre point shows the mean value with error bars of one standard deviation

Microfabrics in SK54341 are chemically similar in terms of components two (Figure 46) where the microfabrics cluster at approximately zero. The microfabrics have a wider distribution along the component one axis, with HU11 showing the highest positive value meaning that it contained

more Al, Mg, K and Fe than the remaining microfabrics which, unlike HU11, can also be found in the C1 samples.

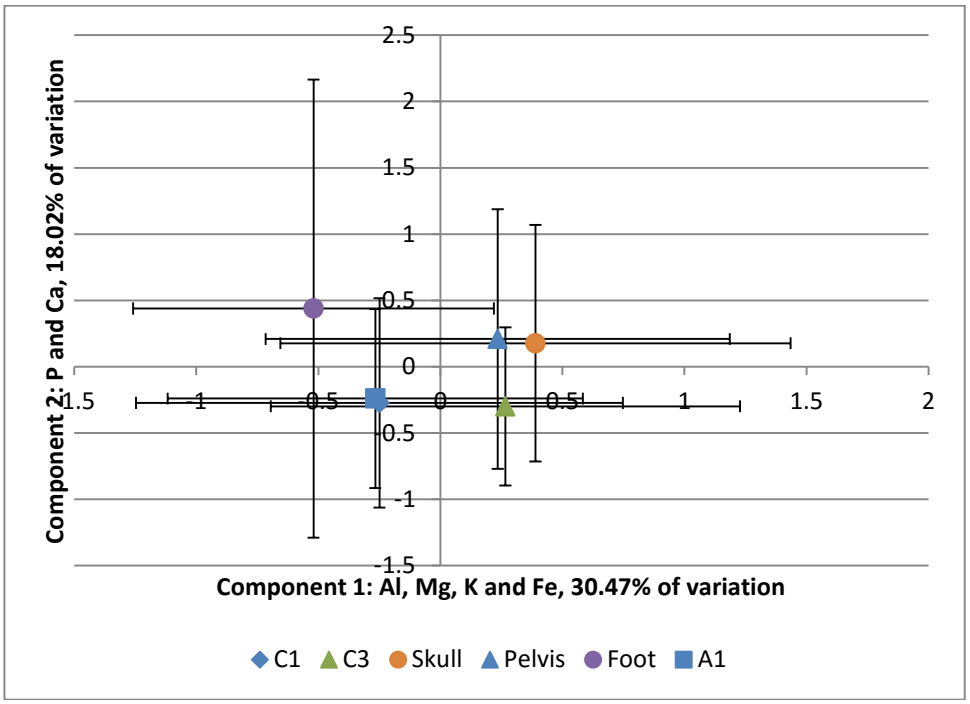

Figure 47: Component 1 and component 2 PCA results for Hungate SK54341 coded by location. The centre point shows the mean value with error bars of one standard deviation.

The C1 and A1 sample is distributed in the low negatives of component one and component two (Figure 47). There is some cross over between the control samples; however the C3 sample has a greater distribution in the positive values of component one. The C1, C3 and A1 sample are all plotting negatively on component two, meaning that they are deficient in P and Ca compared to the samples from the burial plane, which are all positively distributed for component two. The elements that cluster on the same component suggest that component one relates to pedogenic and minerogenic processes including the presence of clays. Component two may relate to the presence of post depositional processes such as organic decomposition.

4.3.3.8 SK54908

Al, Mg, K, Fe, Mn, Si and Ti were used in the PCA. The overall KMO was .667. Bartlett's test of sphericity x^2 (253) = 1024.718 $p < .001$ indicated that correlations between elements were large enough to conduct PCA analysis. Three components had eigenvalues over 1 and accounted for 67.23% of the variance. Table 36 showed factor loadings after rotation. Component 1 and 3 were

plotted for Hungate SK54908 and colour coded for microfabric type (Figure 48) and sample location (Figure 49).

Table 36: Rotated component matrix for Hungate SK54908. Items with values higher than 0.4 are highlighted in green.

Elements	Component		
	1	2	3
Mg	.855		
Al	.803	.360	
Fe	.774	-.285	
K	.570	.490	
Si		.848	
Mn		.105	.793
Ti	.135	-.146	.725
Eigenvalues	2.45	1.19	1.07
% of variation	34.97	17.00	15.25

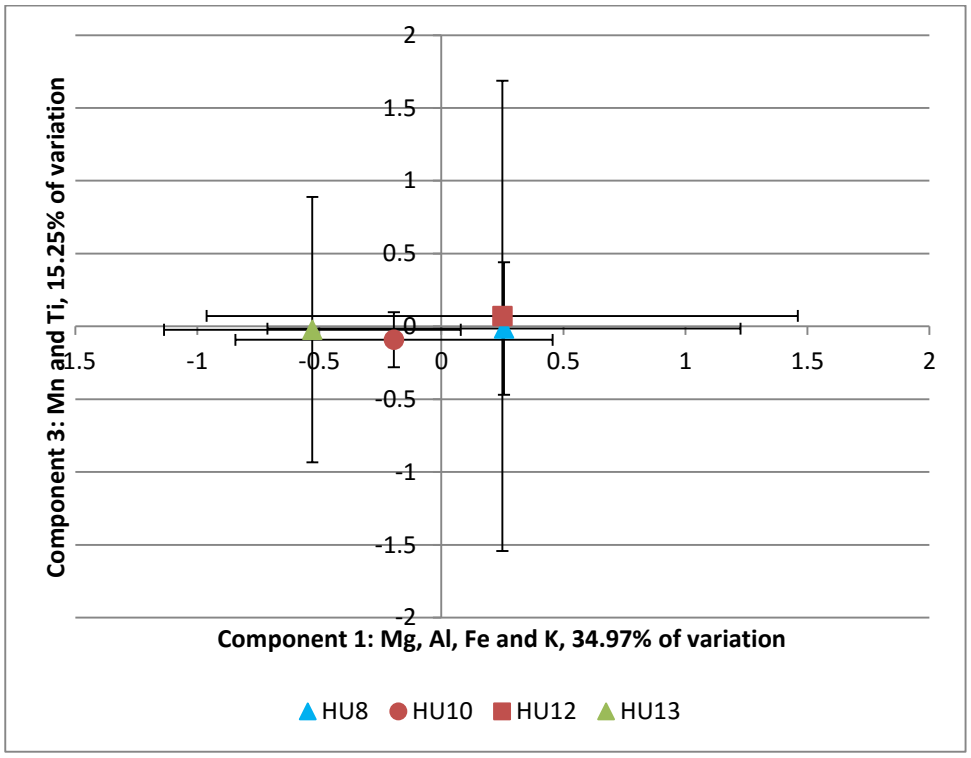

Figure 48: Component 1 and component 2 PCA results for Hungate SK54908 coded by microfabric type. The centre point shows the mean value with error bars of one standard deviation.

All microfabrics are similar in terms of component three and plotted near to zero (Figure 48). HU8 and HU10 plot more positive for component one meaning that they have the highest

concentrations of Al, Mg, K and Fe. The remaining microfabrics plot negatively for component one with HU13 being at the furthest extreme.

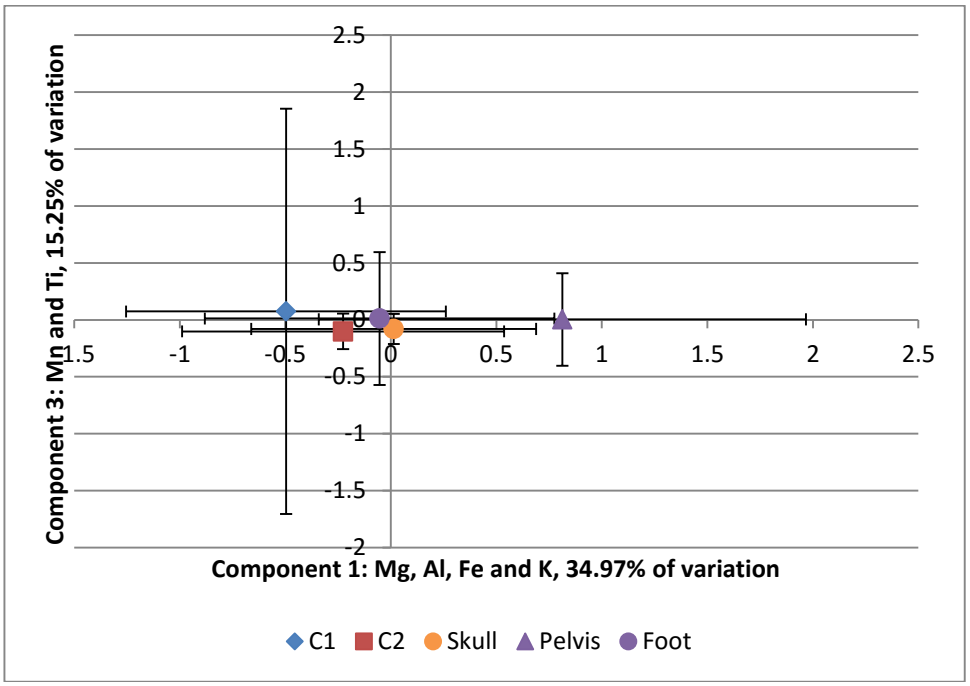

Figure 49: Component 1 and component 2 PCA results for Hungate SK54908 coded by location. The centre point shows the mean value with error bars of one standard deviation.

All of the samples clustered close together on the component three axis meaning that they contained similar levels of Mn and Ti (Figure 49). There was a greater degree of chemical separation of samples along the component one axis. However the samples were still within one standard deviation of one another. That being said the C1 and C2 samples pot at the most negative extreme for component one meaning that they have the lowest concentrations of Mg, Al, Fe and K, whereas the pelvic sample plots at the most positive and away from the other burial plane samples indication that it has more concentrated abundances of Al, Mg, Fe and K. Component one contains Al which is likely to represent the clay fraction of the fine material. The presence of Fe in component one may relate to Fe concentrations in the fine material either caused by redoximorphic processes or due to the inheritance of Fe rich material from the parent material. Component two also contains an element which is precipitated in redoximorphic reactions (Mn).

4.4 Inorganic chemical changes away from the body

P, Fe, Mn and S concentrations were mapped with distance away from the body. In previous studies, both P and Mn were found to concentrate in body silhouettes (Bethell & Carver, 2002, Keeley *et al.*, 1977), and Fe and S have also been identified in enhanced concentrations in human burials (Bethell & Carver, 2002, Bethell & Smith, 1989). Fe and P were present at detectable concentrations in all transects (Table 37), however, S and Mn distributions were more sporadic.

Table 37: Table showing the presence of P, Fe, Mn and S in transects away from the body across the slide. The direction of change in P and Fe concentration is also given moving away from the body as indicated by trend lines. Dark shading indicates missing samples.

Sample		P			Fe			Mn	S
		Level	Rise	Lower	Level	Rise	Lower		
SK54898	Skull			*			*		
	Pelvis			*		*			*
	Foot								
	Other	*					*		
SK54085	Skull			*		*			
	Pelvis	*					*		
	Foot								
SK54341	Skull		*			*			
	Pelvis	*				*			*
	Foot			*			*		
	Other		*				*		
SK54908	Skull								
	Pelvis	*				*			
	Foot	*				*		*	
SK54090	Skull	*			*				
	Pelvis	*				*			
	Foot								
SK51331	Skull		*			*			*
	Pelvis	*				*			*
	Foot	*					*		
SK51387	Skull			*				*	*
	Pelvis	*				*			*
	Foot	*					*		*
SK51351	Skull			*			*		*
	Pelvis								
	Foot		*			*			

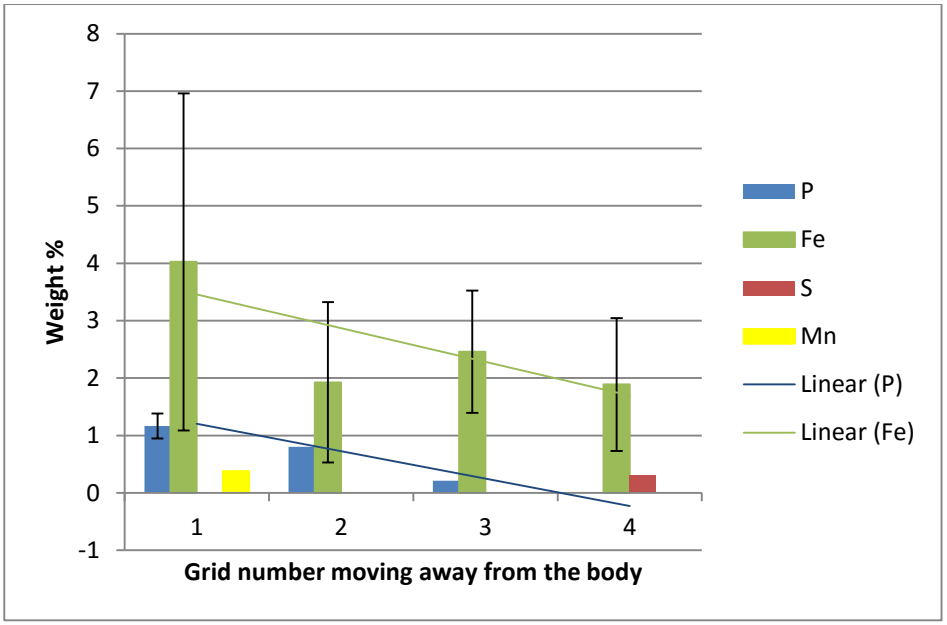

Figure 50: SK51351 Transect moving away from the Skull with P and Fe trendlines showing an overall reduction in both elements as you move away from the body. Grids were taken at 5mm intervals.

Overall there were no universal trends in the nature of the change in concentrations of Fe, P, Mn and S moving away from the body. When considering the direction of elemental trend lines (Table 37 and Figure 50) there were no observable patterns in the skull area, foot area or 'other' samples. In all, but one of the pelvic area samples (SK54085), however, the amount of Fe increases with distance away from the body. The amount of P around the pelvis remains level or, in the case of SK54898, lowers slightly, this will be discussed further in 4.5.5. Other patterns observed, are a tendency for S to be present in the pelvic area samples and for some graves (SK51387) to contain detectable concentrations of S in all of the samples analysed.

4.5 Summary and Discussion

The aim of the SEM-EDX analysis of the fine material was to identify the nature and extent of inorganic geochemical variation that can be attributed to the presence of a human inhumation. The initial part of this process was to understand where variation exists and then to assess to what extent the variation is due to the presence of an inhumation and associated artefacts. To achieve this, the variation in the inorganic geochemical signatures between; sites; graves; control samples and samples from the burial plan; samples in the burial plane; and moving away from the body were ascertained.

4.5.1 Distinguishing different sites (Inter site variation)

The inter site variation in inorganic geochemical signatures is most likely related to broad differences in parent material. Figure 22 illustrated that in terms of principle component two (P and Ca) and three (Fe), Çatalhöyük and Thessaloniki had a similar linear data distribution and Hungate has a more circular pattern. Çatalhöyük however plotted more negatively for component three and positively for component two than either Hungate or Thessaloniki. P and Fe are associated with the decomposition of organic material (Holliday & Gartner, 2007, Janaway *et al.*, 2003) and P is relatively stable in the soil (Alvarez *et al.*, 2004). Ca is an abundant element in most soils originating from the weathering of minerals in the parent material. Ca and P also form Ca-P compounds in the soil (Alvarez *et al.*, 2004), which was possibly why they have been grouped together in the PCA. The patterns in Figure 22 showed that Çatalhöyük, and to a much smaller extent Thessaloniki and Hungate, were plotting positively for Ca and P but negatively for Fe. Çatalhöyük had a highly calcareous element to their parent material, being derived from the calcareous marl sediment from the Konya Basin and surrounding area (Matthews, 1996, Stokes, Unpublished BSc Dissertation), which was one reason why Çatalhöyük has a positive response to component two (P and Ca). Thessaloniki and Hungate had a more positive response to component three compared to Çatalhöyük meaning that they contained more Fe. This may be due to two reasons. Firstly Çatalhöyük may have a parent material that contains less Fe than Thessaloniki or Hungate meaning that the soil fine material also has less Fe present. Secondly Fe can impregnate the fine material during redoximorphic processes (Hseu & Chen, 2001, Kemp *et al.*, 1998, Lindbo *et al.*, 2010, Veneman *et al.*, 1976). These processes can be limited by high pH levels and the availability of oxygen and water (Schlesinger, 1991), meaning that the soil environment at Çatalhöyük may have limited Fe precipitation into the fine material.

4.5.2 Distinguishing different graves (Intra site variation)

The inorganic geochemistry from the intra grave analysis has produced mixed results. Although a large number of the graves are chemically similar at Hungate, it is possible to distinguish grave SK54898 from the other Hungate graves due to the high values of SK54898 along component one (P and Ca). SK54898 had a very different burial context than the other graves, as it was a lead coffin burial. The environmental and anthropogenic factors in this grave may have contributed to greater retention of these elements. This may be due to differences in hydrological regime, with the lead coffin acting as a barrier, or to P and Ca being retained by some other means, possibly

adsorption (Alvarez *et al.*, 2004). Lead was also concentrated in the fine material of SK54898, although the PCA analysis did not highlight Pb as one of the factors loading on the components. There is some variation in the inorganic geochemistry of the graves. However, this variation is only strongly expressed in cases where there are clear differences between burial processes.

Investigation of the neoformed spherulites at Hungate suggested that there may be a relationship between their presence, coffined graves and increased abundances of Fe. Spherulites are spherical mineral formations that have characteristic pseudo-uniaxial negative extinction crosses (Canti, 1997, Canti, 1998b, Canti, 1999). When composed of $CaCO_3$ these biomineral features are associated with faecal material in archaeological deposits (Canti, 1997), but may also be caused by the presence of calcium oxalate, avian uric acid and coccoliths (Canti, 1998b). Canti states that spherulites are formed commonly when there is slow diffusion of reactants caused by the presence of a viscous media or saturated solutions that are slowly percolating (Canti, 1997, Canti, 1999). Spherulites are formed in two ways, firstly by a single branching fibre that first forms a leaf, then spherulite structure (Kelly *et al.*, 2007). The second is through radial growth from a single nucleation site (Kelly *et al.*, 2007). Similar Fe rich spheralitic features have been observed by Leguédois *et al*(2004) during her thin section examination of agricultural land that had been heavily polluted by metallurgical point-source pollution. During their investigation, Leguédois *et al*(2004) found large quantities of very fine (c. 1-30µm) yellowish to red spherulites present as impregnated features that were in contact with crucible fragments within the fine material, and lower down the soil profile they were preferentially located around voids (channels and vughs). SEM-EDX examination of the spherulites (Leguédois *et al.*, 2004) showed they were primarily composed of Fe, P, Mn, Ca, Zn and minor amounts of Pb for the yellow spherulites, and Fe, Zn, P, Ca and Mn for the red spherulites. Leguédois *et al*(2004) concluded that the spherulites were a neoformed metalliferous species, caused by a reaction between heavy metal weathering products from industrial waste and chemical fertilisers that had been applied to the soils. The formation process was promoted by the slowly permeable soil horizons at the site. Similar features have also been observed by Lund and Fobian (1991) during a study conducted in Denmark on As, Cr and Cu pollutants in soil in Denmark. In this case the spherulites measured 20-100 µm and were composed of malachite ($Cu_2(OH)_2CO_3$). Lund and Fobian (1991) hypothesised that the malachite spherulites had been produced by the slowly permeable soils and the concentration of Cu in the soil solution. The spherulites at Hungate were red in colour and contained Si, Fe, Ca, Mn, Al, and P, and trace amounts of Cl, K and Mg (Table 25). They were also solely located in coffined graves and in the samples from or immediately above the burial plane (Table 27). As in Leguédois *et*

al(2004) study, the red colour of the spherulites is probably related to the presence of Fe in the samples. Interestingly, unlike the Leguédois *et al*(2004) study, the spherulites were only found in the burial plane and lower grave fill and not throughout the soil profile. This would suggest that, if the spherulites at Hungate have been caused by metals such as Fe, then this material has not percolated into the graves from a source higher up the soil profile. Looking at the spatial distribution of the graves, SK51351, SK51350 and SK51326 are clustered close together to the north of the site with SK51327, SK54908, SK54085, SK54342 and SK54090 in the south of the site. The graves in the north all contain spherulites and are coffined. Of the graves in the southern cluster, only one of the graves contained spherulites SK54342, which was also a coffined grave. As only coffined graves contained red spherulites, it may be possible that there is a relationship between the presence of coffin nails or other Fe objects within the grave and the occurrence of spherulites. They do not, however, appear in all coffined graves indicating that there may also be wider environmental conditions affecting their formation, such as water percolation rates. Further investigation at Hungate would be needed to confirm this, as data on differences in hydrology across the site is not currently available. The coffin may, in some cases, also act as a barrier to the percolation of water (Dent, 2002). The spherulites at Hungate, are therefore, probably caused by the presence of high concentrations of Fe in the burial plane. The source of the Fe, however, is yet to be confirmed. There may also be a relationship to the presence of a coffin, however, it is clear from the literary evidence that environmental factors such as slow percolation of water are also key to *in situ* spherulite development (Canti, 1997, Canti, 1999, Leguédois *et al.*, 2004, Lund & Fobian, 1991).

4.5.3 Control samples vs samples from the burial plane and variations in the burial plane (intra grave variation).

4.5.3.1 Control samples vs samples from the burial plane

The intra site analysis demonstrates that there are clear inorganic geochemical differences between the C1 and C2 samples and the samples taken from the burial environment at Hungate, but not at Çatalhöyük (a comparison could not be made at Thessaloniki).

At Hungate, Figure 25 demonstrates a well defined separation between the C1 and C2 samples that are negatively distributed along the component one and two. The C3 samples have a distribution and similar to the samples from the burial plane. At Çatalhöyük there is no noticeable difference between the C1 and C3 samples and burial plane samples (Figure 30). In several graves

(18666, TF177, SK54898, SK51326, SK51387 and SK54090) the C3 samples are chemically similar to the samples from the burial plane.

When all graves are considered on an intra site level at Hungate the C1 and C2 sample is depleted in Al, K and Fe compared to the samples from the burial plane (Figure 25). Al is commonly found in clays (Birkeland, 1984), whereas K and Fe are common elements found in the human body and readily available in soils and organic matter (Abdel-Wahab *et al.*, 1992, He *et al.*, 2015, Lindbo *et al.*, 2010). When each grave is considered SK51387, SK54090 and SK54908 maintain a depilation in Al, K and Fe in the C1 sample compared to those from the burial plane, interestingly these graves are all located in the northern part of the cemetery and are furthest away from the C1 sample (Figure 51). This may be caused by differences in the weathering rates of minerals, with more weathering occurring in the burial plane or the environment in the burial plane being favourable to the retention or precipitation of K and Fe. It may also simply be due to the C1 sample not covering a wide enough area to encompass all of the inorganic geochemical variations in none grave soils. In grave SK54898, the lead coffin grave, the fine material in the C1 contains a slightly higher amount of Al, K and Fe compared to the grave soils. This may be due to the further complication of Pb in the soil influencing the retention or weathering of inorganic chemicals within the burial. In graves SK54085, SK51387 and SK54898 the C1 sample is depleted in Ca and P compared to the samples from the burial plane. Ca and P are products produced during decomposition and therefore may have been retained in the soil from bodily decomposition (Bethell & Carver, 2002, Bethnell & Smith, 1989, Janaway *et al*2003, Macphail *et al*2013).

Figure 51: Distribution of the inorganic chemical differences between the C1 and burial samples at Hungate. Green = samples with elevated levels of Al, K and Fe in the burial plane compared to the C1 samples. Red = graves with elevated

levels of Ca and P compared to the C1 samples. Blue = graves where there is no chemical distinction between the burial plane or C1 samples.

At Çatalhöyük 18666 and Hungate SK51326, SK51351 and SK54341, however, the controls and samples from the burial plane are not chemically distinct. This would suggest that the presence of the burial was having little effect on the overall inorganic geochemical signatures of the samples or that the effect of the burial was diminished by other influences such as the influence of the soil parent material.

4.5.3.2 Variations in the burial plane

The analysis of inorganic geochemical differences in the samples from the burial plane produced mixed results. Most of the graves had burial plane samples with very similar inorganic geochemical signatures, regardless of the location of the sample around the burial. The exception was SK51351, SK54908 and SK54341. SK51351 was a waterlogged Roman inhumation containing several artefacts including jade bracelets, shoes, Fe objects and Cu bracelets. The burial was also heavily contaminated with diesel from a nearby petrol station. SK54908 was a well preserved supine infant inhumation with a north west to south east orientation with the head facing south. SK54341 was a supine adult burial with hands crossed over the pelvis and the head turned to the left. These graves hinted at the possibility of lateral changes across the burial with an increase in Al, Mg, K and Fe towards the foot and box area samples (Figure 41). Generally however, there were no inorganic geochemical differences between samples in the burial plane this may be because of several reasons. Firstly the manner of burial may be influencing the inorganic geochemical signatures. Experimental studies on decomposing adult pigs have shown that bodies that decompose in a vaulted chamber expand after burial to fill the chamber and then rupture, spreading decomposed matter evenly in the burial plane (Janaway *et al*., 2009). It is also possible that upon decomposing, liquid from the body forms a pool in the coffin or chamber (Dent, 2002) (see conceptual module 1.6), again distributing the inorganic geochemical signature widely across the burial plane. However, the burials that showed no evidence of a coffin or vaulted chamber (Çatalhöyük 18666 and Hungate SK51387 and SK54090) also failed to show a strong inorganic chemical distinction based on sample location in the burial plane. This may be because either the same processes occurred as in the coffin and vaulted burials (Janaway, 1987) or that post depositional processes such as bioturbation have resulted in the mixing or alteration of the inorganic geochemical signatures. Further to this, elements such as Ca, P and S can be fairly

widely and commonly distributed in the body (Heymsfield, 2005, White & Hannus, 1983) and therefore they may not be varying in the burial plane.

4.5.4 Microfabric types

The inorganic geochemical signatures of the microfabric types at each site were investigated. This was to understand two aspects: their role in influencing the overall inorganic geochemical signature of the sample, and to gain information about the origin of the grave fill. The inorganic geochemical nature of the microfabrics in the case of Çatalhöyük has a dramatic effect on the overall chemical signature of the burial soil. At Thessaloniki and Hungate the inorganic geochemical analysis shows that differences in microfabrics are due to either differences in origin or are chemically similar but visually distinct.

At Çatalhöyük there are several different microfabrics that are ubiquitous in the samples, and these have formed due to the use of different building materials during building construction (see Microfabric Chapter Section 3.2) (Matthews, 1996, Matthews, 2006, Stokes, Unpublished BSc Dissertation). Figure 29 and Figure 30 show that, despite this, the microfabrics are not particularly chemically distinct, apart from CH5 the oven rake out material. However, the microfabrics show a wider degree of variation than when the samples are plotted by sample location. This would suggest that the microfabric type has the overriding influence on the inorganic geochemistry above that of location in the grave.

At Thessaloniki the microfabrics are chemically distinct with Ti2 containing more P and Ca than Ti1 (Figure 31). However, when the samples are plotted in terms of sample positions (Figure 32), the signal from Ti2 disappears. Ti2 covers a small area in the samples from TF177 therefore it is most likely that the signal from Ti2 has been overwhelmed by the results from Ti1.

Hungate has 13 different microfabric types, which are discussed in detail in the microfabric chapter (see section 3.5). Two microfabrics of note are HU2, which plotted with the control samples for SK54898 (Figure 33), and HU6. HU2 is visible in SK54898 as thin slivers of coarse material surrounded by a pale orange fine material in the skull sample. As it shares a similar inorganic geochemical signature to the microfabrics from the C1 samples in terms of component 1 (Ca, P and Pb), it is possible that HU2 has formed by later in-wash into the grave, infilling voids in the fine silt of the grave fill. HU6 was also a microfabric that was suspected in-wash forming laminated clay on top of the sediment that composed the main grave fill. However, the inorganic

chemistry of this microfabric was more similar to the samples from around the burial plane than to the C1 samples, indicating that either the infill of this grave is all from the same origin or HU6 is very early in-wash, but had been *in situ* long enough for it to adsorb the chemical signature of the surrounding soil.

4.5.5 Inorganic geochemical changes moving away from the body

There are no consistent trends in the concentrations of Fe, Mn and S with distance away from the body. P did vary with the concentration of P increasing with the distance away from the pelvic area. The reason for this is not however clear. There may be several reasons for a lack of variation in Fe, Mn and S with distance away from the body. Firstly, the scale that has been used is quite small, the longest transect within this study is 55 mm. The distances represented in the samples may actually be too small to show any real variation in Fe, P, S and Mn. It may therefore be beneficial for future sampling strategies to include bulk samples moving away from the body to increase this distance. Secondly, the soil geochemistry is extremely variable and natural differences in the concentrations of Fe, P, S and Mn may be obscuring any trends produced by body degradation. Thirdly, the sample position may be affecting the results. Although there were standard points for sampling at the skull, pelvis and feet, there was little standardisation in the sample distance or orientation in relation to the body. Standardising sample orientation and placement in future sampling protocols may therefore help produce more consistent results. Fourthly, in this analysis, the samples were taken across a straight line, whereas soil porosity works in three dimensions and can have a very high tortuosity (Allaire-Leung *et al.*, 2000, Pagliai & Kutilek, 2008a), meaning that, in this particular analysis, the directionality of preferential soil water through macro and meso channels (vertical movement) or by capillary action through microspores and void surfaces (all directions) (Schaetzl & Anderson, 2005) has not been accounted for and may be influencing the inorganic chemical signatures moving away from the body.

4.6 Conclusions

Overall the inorganic geochemical analysis gave mixed results. On a broadly site based level, the influence of parent material is dominating the inorganic geochemical results, meaning that sites with similar parent material have very similar inorganic geochemical distributions.

There does seem to be grounds to tentatively be able to distinguish C1 samples from those from the burial plane especially on an intra site scale with the C1 sample plotting away from the burial plane with low concentrations of Al, K, Fe, Mg, P and Ca. There is also evidence to suggest that it would be possible to chemically identify atypical burial practices, such as the inclusion of artefacts like the lead coffin, the main criteria being that differences in burial practices must be able to be expressed chemically, e.g. by the inclusion of different metals. It was not possible, however, to distinguish between coffined and non-coffined burials.

In all but three of the burials, sample location in the burial plane does not leave a distinct inorganic geochemical trace. The reason for this is not clear but may be due to either the small distances between samples, slight differences in sample locations, or the post depositional changes to corpses affecting the distribution of degradation products within the grave.

One of the issues with the PCA analysis conducted here is that many of the data points largely overlap at one sigma precision. This seems to be due to the large number of data points taken and to the variable nature of the soil. It must be noted that when the standard error is applied to the data the degree of overlap is much smaller, the standard deviation was given in this instance to present the 'worst case scenario' in order not to present data that perhaps showed a stronger relationship than was really present. What must be remembered about PCA analysis is that it is a starting point to highlight where the data maybe showing relationships so that more specific statistical data analysis can be conducted. It is recommended that linear regression be conducted on this data (or a sub-set of the data presented here), to ascertain if the variation in Al, K, Fe, P and Ca between the control and burial plane and the lateral changes in Ca and P in some graves can be further resolved and produce stronger relationships.

The spherulites seem to be produced by a combination of burial practice and soil conditions. Fe needs to be available to form the spherulites in the grave; in the form of either Fe nails, Fe objects or generally higher concentrations of Fe in the soil. However, there also needs to be specific environmental conditions in order for them to precipitate. The link between Fe spherulite formation and coffins is however currently circumstantial and would require further investigation to confirm a causational relationship.

Further insight into the post depositional grave environment can be gained by investigating the inorganic geochemical signature of the different microfabrics. This allows the identification of

those materials that may have moved into the burial environment at a later date (HU2), giving a temporal dimension to our understanding of the grave environment.

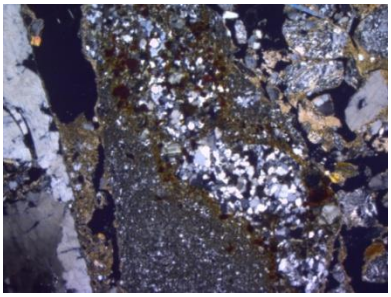

5 Coarse Components: Mineral and Rock Fragments and the C:F Related Distribution.

Coarse components were defined as all material above 50µm and further sub-divided into mineral and rock fragments and organic/organically derived coarse components. This chapter examines the mineral and rock fragment fraction of the coarse components, as well as the relationship between the coarse and fine fraction (C:F related distribution). Mineral and rock fragments are important as they contain information pertaining to the soil parent material and pedogenic processes (Bullock *et al*., 1985 p. 50). Establishing the parent material of the grave backfill and the 'not grave' soils can be useful in identifying grave fill modification through anthropogenic intervention or from the decomposition of the body. The identification of neoformed minerals can also be diagnostic of past and present pedogenic processes (Bullock *et al*., 1985 p. 50). The C:F related distribution is also an important diagnostic tool as it can give further information as to the water holding capacity of the soil, as well as to the occurrence of pedogenic process such as shrink/swell (Dalrymple & Jim, 1984, Stoops, 2003 p. 44). This chapter details the mineral and rock fragments as well as the C:F related distributions present at each site. Variation will be assessed at three levels;

- Inter site variation (Çatalhöyük, Thessaloniki, Heslington East and Hungate)
- Intra site (Çatalhöyük, Thessaloniki and Hungate)
- Intra grave (Çatalhöyük, Thessaloniki, Heslington East and Hungate)

Lead fragments and secondary phosphate minerals will be investigated further, as they could relate to burial practice and anthropogenically induced pedogenic processes. In this chapter abundances are given as average percentages of slide area.

5.1 Mineral, Rock Fragments, Coarse material abundance and C:F related distribution

5.1.1 Inter site variation

Overall abundance of mineral and rock fragments varied with the lowest levels at Çatalhöyük at 16% followed by Thessaloniki at 32% and Hungate and Heslington East at 53% and 75% respectively (Table 38). Hungate and Heslington were dominated by quartz grains at 47% and 64% respectively (Table 38), whilst they also contained high levels of phyllosilicates, with tectosilicates, carbonates, vivianite and unknown minerals also present (Table 38). Quartz was less abundant at Çatalhöyük and Thessaloniki (8% and 11%). Sulphates were unique to Çatalhöyük, which also had the lowest level of phyllosilicates, whereas Thessaloniki had high levels of an unidentified coarse mineral, carbonates and phyllosilicates compared to Çatalhöyük, Heslington East and Hungate. There were also minimal differences in C:F related distributions between the sites (Table 38). The mineral, rock fragments, coarse material abundance and C:F related distribution for each site will now be examined in terms of the intra site and intra grave variation.

Table 38: The average percentage of slide area composed of different and total mineral and rock fragments by site as well as the C:F related distributions present at each site. Percentages are rounded to whole numbers and '*' indicates trace amounts (<0.5%).

	Çatalhöyük	Thessaloniki	Heslington East	Hungate
Quartz	8	11	64	47
Silicate	2	12	8	3
Phyllosilicate	1	2	1	2
Tectosilicates	1	0	1	1
Nesosilicates	0	0	0	0
Carbonates	0	3	0	0
Secondary phosphate minerals	0	0	*	*
Sulphates	2	0	0	0
Inosilica based rock fragments	0	0	0	0
Unknown	2	4	1	0
Lead	0	0	0	*
Total coarse material	16	32	75	53
C:F related distribution				
Enaulic	✓	✓	✓	✓
Monic	✓			✓
Chitonic	✓	✓	✓	✓
Gefuric		✓	✓	✓
Porphyric	✓	✓	✓	✓

5.1.2 Çatalhöyük

5.1.2.1 Çatalhöyük Intra Site Comparison of Mineral, Rock Fragments, Coarse Material abundance and C:F Related Distribution

The control samples and those from the burial plane contained similar inorganic coarse material assemblages, although there was slightly less quartz present in the controls which was partly reflected in the overall inorganic coarse material abundance (Table 39). The control samples, although limited in number, (C1 n=1 and C3 n=2), suggest that the observed variation may be circumstantial. Graves 19295 and 18666 were similar in the coarse material assemblage, although higher levels of carbonates were observed in 19295 (Table 39). The C:F related distributions were similar between the control samples and the burial plane samples.

Table 39: The percentage of sample area composed of mineral and rock fragments by sample location as well as the C:F related distributions present in each slide and overall coarse material abundance. Percentages are rounded to whole numbers.

Grave	Location	Orientation	Quartz	Silicate	Phyllosilicate	Tectosilicates	Carbonates	Sulphates	Inosilica based rock fragments	Unknown	Total	C:F related distribution	Enaulic	Monic	Chitonic	Gefuric	Porphyric
C1		NA	2	4	2	1	0	2	0	1	12		✓	✓			✓
18666	C3	NA	6	1	1	1	0	2	0	0	11		✓	✓			✓
	Skull	Para	9	4	1	1	0	0	0	0	15		✓	✓			✓
		Perp	9	2	0	1	0	1	1	0	14		✓	✓			✓
	Pelvis	Para	15	1	0	1	0	1	0	1	19		✓				✓
		Perp	5	1	1	1	0	0	0	0	8						✓
	Feet	Perp	20	2	0	2	0	1	1	1	27						✓
19295	C3	NA	2	0	0	0	0	4	0	15	21		✓				✓
	Skull 19501	Para	15	1	1	1	1	2	0	0	21		✓	✓			✓
		Perp	4	1	1	1	0	2	0	0	9		✓				✓
	Skull 19500	Para	5	1	1	0	1	2	0	0	10		✓	✓			✓
		Perp	5	0	1	1	0	4	0	0	11		✓	✓	✓		✓

5.1.2.2 Çatalhöyük Intra Grave Comparison of Mineral, Rock Fragments, Coarse Material abundance and C:F Related Distribution

There was variation in the inorganic coarse material assemblage across 19295. The C3 sample had a lower diversity of mineral and rock types compared to the burial plane samples. This is based on a low sample size however, and may not be representative (C3 n=1, burial plane n=4). There were peaks in quartz abundance in the perpendicular foot and parallel pelvic samples from 18666, as well as in the parallel skull sample from 19501 (19295) compared to the rest of the samples. There were, however, no major differences in the C:F related distributions based on sample location in either grave 18666 or 19295.

5.1.2.3 Çatalhöyük Microfabric Comparison of Mineral, Rock Fragments and Coarse Material abundance

To establish whether there was a common origin for the six microfabrics from Çatalhöyük (Chapter 3), the inorganic coarse material assemblages were compared. CH1, CH2, CH3 and CH6 contained only trace amounts of inorganic coarse materials (Table 40). Coarse quartz, however,

dominated the assemblage in CH4 at 8%, and CH4 had the highest level of coarse material overall at 13%.

Table 40: The average percentage area of microfabric composed of mineral and rock fragments. Percentages are rounded to whole numbers and '*' indicates trace amounts (<0.5%).

Microfabric type	CH1	CH2	CH3	CH4	CH5	CH6
Quartz	*	*	*	8	1	*
Silicate	*	*	0	2	*	0
Unknown	*	*	*	*	2	*
Phyllosilicates	*	*	0	1	0	0
Tectosilicates	*	*	0	1	0	0
Carbonates	*	*	0	*	*	*
Sulphates	*	*	*	1	*	0
Inosilica based rock fragments	*	0	0	*	0	0
Total	*	*	*	13	3	*

5.1.3 Thessaloniki

5.1.3.1 Thessaloniki Intra Site Comparison of Mineral, Rock Fragments, Coarse Material abundance and C:F Related Distribution

Inorganic coarse material at Thessaloniki was dominated by quartz (≤20%) and silicate based rock fragments (≤24%, Table 41). The remaining coarse material was composed of minor amounts (≤7%) of phyllosilicates (muscavite, glauconite), tectosilicates (microcline and simple twinned feldspar), nesosilicates (garnet), carbonates (calcite) and a small amount (≤10%) of unidentified mineral and rock fragments (Table 41). There was no systematic variation in the abundance of mineral, rock fragments or overall coarse material abundances between graves. All C:F related distribution types were present in the samples from the burial plane. However, the control samples contained only enaulic, chitonic and porphyric types. The individual graves contained three groupings of C:F distributions: those with just porphyric material (TF178); those that contained only porphyric and enaulic material (TF157 and TF182); and those that contained multiple different types of distributions (TF177 and TF162).

Table 41: The percentage of sample area composed of different mineral and rock fragments, and overall coarse material abundance, by sample location, as well as the C:F related distributions present in each slide. Percentages are rounded to whole numbers. '*' indicate trace abundances (<0.5%).

Grave	Location	Orientation	Quartz	Silicate	Phyllosilicate	Tectosilicates	Nesosilicates	Carbonates	Unknown	Total	C:F related distribution	Chitonic	Gefuric	Porphyric	Enaulic
TF157	Skull	Para	20	20	2	0	0	2	5	49				✓	✓
	Pelvis	Para	10	10	2	0	0	2	5	29				✓	
	Hand	Perp	10	10	2	0	0	2	5	29				✓	
	Feet	Para	20	20	2	0	0	5	4	51				✓	
TF162	Skull	Para	10	20	2	2	0	5	2	41		✓		✓	✓
	Pelvis	Para	10	5	2	0	0	2	5	24				✓	✓
	Feel	Para	10	10	2	0	0	2	5	29		✓		✓	✓
TF177	C3	NA	5	12	2	0	0	2	5	26		✓		✓	✓
	Skull	Para	20	20	2	0	0	2	7	51				✓	✓
		Perp	20	10	0	0	0	5	5	40				✓	
	Pelvis	Para	10	20	2	0	0	2	5	39		✓		✓	
		Perp	20	0	5	0	0	5	12	42				✓	
	Hand	Para	20	5	3	2	0	2	3	35				✓	
	Feet	Para	10	10	2	0	2	2	5	31		✓		✓	
		Perp	1	18	2	0	0	5	1	27			✓	✓	
TF178	Head	Para	10	24	2	0	0	2	2	40				✓	
	Pelvis	Para	5	7	2	2	2	7	2	27				✓	
TF182	C2	NA	10	7	2	0	0	2	2	23				✓	✓
	C3	NA	20	10	2	0	0	2	2	36				✓	✓
	Skull	Para	10	7	*	2	0	2	2	23				✓	
	Pelvis	Para	5	5	2	0	0	2	2	16				✓	✓
		Perp	6	3	2	0	0	2	0	12				✓	
	Hand	Para	5	12	2	0	2	2	2	25				✓	
		Perp	10	5	2	0	0	2	0	19				✓	
	Feet	Para	11	21	2	1	0	3	7	45				✓	✓

5.1.3.2 Thessaloniki Intra Grave Comparison of Mineral, Rock Fragments, Coarse Material abundance and C:F Related Distribution

There was no systematic trend in the C:F related distribution according to sample location or orientation (Table 41). There were no significant differences in the inorganic coarse material assemblage or overall abundance of coarse material in graves TF177, TF178 and TF162. However,

the abundance of quartz in TF182 increased between the C2 sample at 10% and the C3 sample at 20% (Table 41). There were spatial differences in quartz abundances in TF182 and TF157, with lower quartz abundances in the central part of the burials (pelvis and hand). This pattern was partly reflected in the overall coarse material abundance (Table 41).

5.1.3.3 Thessaloniki Microfabric Comparison of Mineral, Rock Fragments and Coarse Material abundance.

To establish if there was a common origin for the two microfabrics from Thessaloniki (see Microfabrics Chapter 3), the inorganic coarse material assemblages were compared. Ti1 and Ti2 had similar coarse material assemblages with quartz, silicate rock fragments, carbonates and phyllosilicates common to both (Table 42). The relative abundance of quartz and silicate rock fragments was, however, elevated in Ti1 compared to Ti2.

Table 42: The average percentage area of microfabric composed of mineral and rock fragments at Thessaloniki. Percentages are rounded to whole numbers and '*' indicates trace amounts (<0.5%).

	Ti1	Ti2
Quartz	11	3
Silicate	12	1
Unknown	4	0
Carbonates	3	1
Phyllosilicates	2	1
Tectosilicates	2	0
Nesosilicates	2	0
Total	36	5

5.1.4 Heslington East

5.1.4.1 Heslington East Intra Grave Comparison of Mineral, Rock Fragments, Coarse Material abundance and C:F Related Distribution

The coarse material fraction at Heslington East was dominated by quartz 50-70% (Table 43) and silicate based rock fragments at ≤10%. The remaining coarse material was composed of minor amounts (≤4%) of phyllosilicates (muscavite, glauconite, biotite), tectosilicates (microcline and plagioclase), secondary phosphate minerals (vivianite), calcium carbonate, and a small amount (≤7%) of unidentified mineral and rock fragments. Quartz abundance varied with high abundances

in the C1 and C2 samples compared to the C3 sample and samples from the skull and pelvic areas. This was reflected in the overall coarse material abundances. The material in the burial plane was generally richer in coarse material and also had a higher degree of variation in the C:F related distribution compared to the control samples.

Table 43: The percentage of sample area composed of mineral and rock fragments by sample location as well as the C:F related distributions present in each slide and overall coarse material abundance. Percentages are rounded to whole numbers.

Location	C1			C2	C3	Burial plane		
	22-28cm	46-52cm	74-80cm			Skull	Hand	Foot
Quartz	70	70	70	70	50	50	60	70
Silicate	5	5	2	10	20	10	5	5
Phyllosilicate	0	2	2	0	0	0	4	2
Tectosilicates	0	4	0	0	0	0	2	0
Nesosilicates	0	0	0	0	0	0	0	0
Carbonates	0	0	0	0	0	0	0	2
Secondary phosphate minerals	0	0	0	0	0	2	0	0
Unknown	0	0	7	1	0	0	0	0
Total	75	81	81	81	70	62	71	79
C:F Related Distribution								
Enaulic						✓	✓	✓
Monic								
Chitonic		✓					✓	✓
Gefuric				✓	✓			
Porphyric	✓	✓	✓	✓	✓	✓	✓	✓

5.1.5 Hungate

5.1.5.1 Hungate Intra Site Comparison of Mineral, Rock Fragments, Coarse Material abundance and C:F Related Distribution

The C1 and grave samples all contained similar inorganic coarse material assemblages (see appendix 3.1), which were dominated by quartz (≤90%) with lower abundances of silicate based rock fragments (≤50%). The remaining coarse material was composed of minor amounts (≥12%) of phyllosilicates (muscovite, glauconite, biotite), tectosilicates (microcline, feldspar, plagioclase) that were present in all graves, nesosilicates (garnet, olivine) and carbonates (calcite), as well as fragments of lead and sporadic neoformed secondary phosphate minerals. There were two grave specific inorganic coarse materials; lead fragments in SK54898 and neosilicates in grave SK54090. The abundance of quartz was variable with low abundances in SK54898 (18%) and SK51387 (25%).

Compared to the C1 samples, the majority of graves contained lower abundances of quartz and overall inorganic coarse material, the exception being grave SK51326 (80%). The C:F related distribution in the C1 sample was porphyric, however the samples from the graves were more varied with all graves containing two or more C:F related distribution types.

5.1.5.2 Hungate Intra Grave Comparison of Mineral, Rock Fragments, Coarse Material abundance and C:F Related Distribution.

There were no noteworthy differences in the type or abundance of inorganic coarse materials in SK51351, SK51326, SK51387, SK54090, SK54342, SK54085 or SK54908. In the remaining graves (SK54898, SK54341 and SK51350) there was some variation in the nature and abundance of inorganic coarse material, mainly variations in quartz abundance (see appendix 3.1). SK54341 and SK51350 showed an increase in quartz abundance in the burial plane compared to the grave control samples (C2 and C3). SK54898, however had the most dramatic change in quartz levels with abundance dropping from 64% in the C2 to ≤23% in the burial plane samples (including the C3). There was further lateral variation with a drop in quartz abundance from the skull into the pelvic area. There was a high abundance of lead fragments in the C3 (taken from within the coffin) and pelvic area samples. These changes were also reflected in the overall abundance of coarse material in SK54898. The distribution of vivianite and lead will be explored further below in section 5.1.5.3. As stated above, the C1 samples were exclusively porphyric, yet, the C2 and C3 samples contained similar C:F related distribution types to samples from the burial plane. Porphyric was the most frequent C:F related distribution present in the C2 and C3 samples as well as all samples from the burial plane, with the exception of the skull and pelvic area samples from SK51351 (see section 2.2.6.4). Monic, chitonic and gefuric C:F related distribution types were present at low levels and enaulic C:F related distributions were only present in the C3 sample from SK51387.

5.1.5.3 Hungate Microfabric Comparison of Mineral, Rock Fragments and Coarse Material abundance.

To establish if there was a common origin for the microfabrics from Hungate identified in the microfabrics chapter, the inorganic coarse material assemblages were compared. A secondary objective was to understand if the low level of coarse material in SK54898 was due to high abundances of grave specific microfabric types that were low in coarse material meaning that the microfabrics may have been influenced by the burial.

Quartz was present in all of the microfabric types at Hungate, except HU6 (Table 44), HU1, HU3, HU4, HU6 and HU7 contained the lowest levels of quartz (≤10%) three of which were found in SK54898 (the lead coffined infant). Silicate based rock fragments were present in smaller quantities than quartz with all abundances <5%. Other inorganic coarse materials and lead fragments were present sporadically throughout HU1 (<10% of slide area) (Table 44). HU1 was found in SK54898 and the lead probably originated from the lead coffin. Phyllosilicates and tectosilicates were present in low abundances and were not evenly distributed among the microfabrics. Vivianite was sporadic and visible in four microfabrics including HU13, the most common microfabric at Hungate (Chapter 3).

Table 44: The average percentage area of microfabric composed of different mineral and rock fragments at Hungate. Percentages are rounded to whole numbers and '*' indicates trace amounts (<0.5%).

Microfabrics	Quartz	Silicate	Lead	Phyllosilicate	Secondary Phosphate Mineral	Tectosillicate	Total
HU1	8	1	3	0	0	0	13
HU2	57	0	0	0	0	0	57
HU3	1	0	0	*	0	0	1
HU4	4	1	0	0	0	0	5
HU5	37	1	0	0	0	0	38
HU6	0	0	0	0	0	0	0
HU7	10	0	0	0	0	1	11
HU8	54	2	0	1	*	1	57
HU9	16	0	0	0	0	0	16
HU10	62	2	0	*	*	0	64
HU11	20	1	0	0	0	0	21
HU12	14	*	0	*	*	*	14
HU13	60	4	0	1	*	*	64

5.2 Inorganic coarse material of interest

5.2.1 Secondary Phosphate Mineral Formation (Vivianite)

5.2.1.1 Vivianite description and presence

Vivianite ($Fe_3(PO_4)_2 \cdot 8H_2O$) (Figure 52) was present in both Heslington East and Hungate. At Hungate vivianite formation was sporadic as detailed in Table 45. At Heslington East vivianite was tentatively identified in the skull area sample.

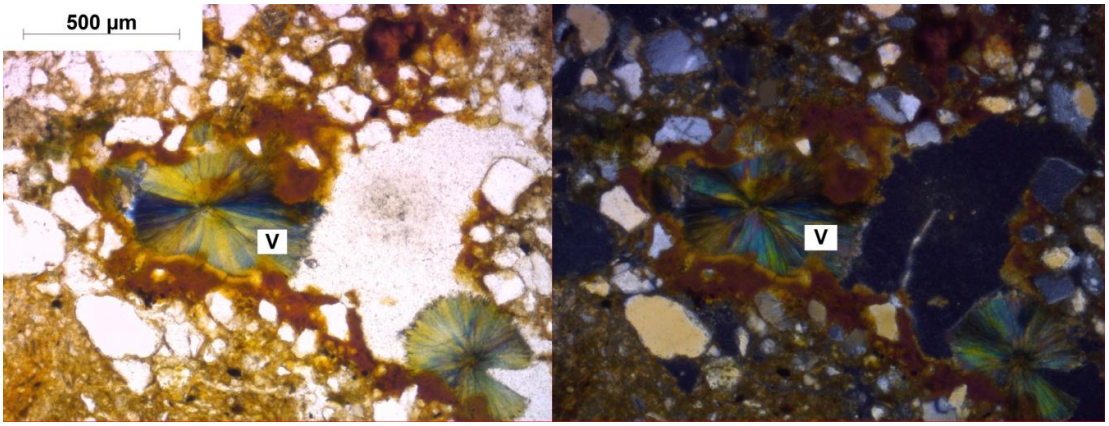

Figure 52: Radially formed Vivianite (V) from the C1 samples, Hungate. Left = PPL and right = XPL.

Table 45: Location of vivianite in the graves analysed at Hungate. '*' = the presence of vivianite, greyed out cells indicate where there was no sample available. A = adult, I = infant, LC = lead coffin, C = coffin and UC = uncoffined

Grave number		SK54898	SK51326	SK51387	SK51351	SK54090	SK54085	SK54341	SK54342	SK51350	SK54908
Age		I	A	A	A	I	A	A	A	A	I
Burial type		LC	C	UC	C	UC	C	C	C	C	C
C2											
C3		*						*			
Skull	Perp		*								
	Para										
Pelvis	Perp				*						*
	Para	*									
Foot	Perp				*						
	Para				*						
Other					*						
C1		1-16cm				27-36cm			49-58cm	*	

5.2.1.2 Vivianite variation

There was no relationship between the presence of vivianite and the age of the individual at death. At Hungate vivianite was only present in coffined graves (Table 45) and the C1 sample.

5.2.2 Lead

5.2.2.1 Lead description and occurrence

Lead fragments (Figure 53) were observed in the C3 and pelvic samples of grave SK54898 at Hungate.

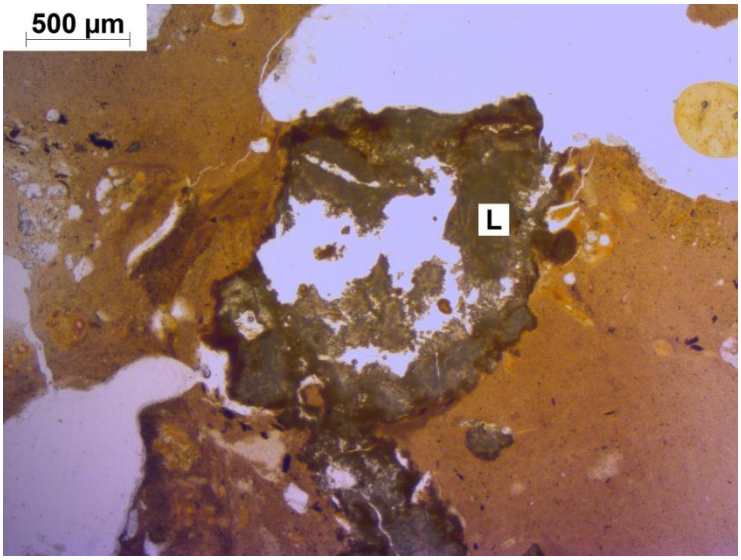

Figure 53: Lead fragment (L) from SK54898 shown in PPL.

5.2.2.2 Lead variation

The inorganic coarse material from SK54898 had a higher lead content than the C1 and other graves from Hungate. It is highly likely that the lead originated from the lead coffin in SK54898.

5.3 Summary and Discussion

The aim of the inorganic coarse material analysis was to identify patterns in the occurrence and abundance of inorganic coarse material that relate to either burial practice or the presence of a body. The variation was assessed at three levels; inter site; intra site and intra grave.

5.3.1 Inter site variation

The inter site variation of inorganic coarse material appears to be primarily caused by differences in parent material and transportation / deposition processes. The overall mineral and rock fragment assemblages at Thessaloniki, Heslington East and Hungate are consistent with the local parent materials. However, at Çatalhöyük more complex depositional pathways were apparent.

The soils at Thessaloniki are composed of small amounts of quartz and other silicate based rock fragments (Table 38), along with phyllosilicates (muscavite, glauconite), tectosilicas (microcline and simple twinned feldspar) nesosilicas (garnet) and carbonates (calcite) minerals. The area around Thessaloniki is rich in limestone, marble, and alluvial deposits containing secondary calcium carbonate (Ghilardi *et al.*, 2008a, National Soil Resources Institute, 2011b). Granites and shists are present in the river catchments that feed into the Thermaic Gulf and Aegean sea (Ghilardi *et al.*, 2008a). This may account for the presence of the other types of minerals at the site (Brady, 1969). Heslington East and Hungate are similar in their abundances of quartz and silicate rock fragments (Table 38), but differed in their assemblages of less abundant inorganic coarse material. Similarities in the levels of quartz and silicate rock fragments between Hungate and Heslington East are unsurprising, as they have similar parent materials and are located within close proximity to one another. Heslington East's parent material is composed of a heterogeneous mix of sand, silts and gravels of glaciofluvial origin (O'Connor et al., 2011), whereas soils in Hungate were formed by alluvial deposition, most likely from the River Foss (National Soil Resources Institute, 2011b). Differences in parent material transportation and the large catchment area of the River Foss may have resulted in slight differences in coarse material assemblages at Hungate and Heslington East.

Çatalhöyük was an unusual site, as all of the sediments present have been introduced through human agency (Tung, 2013). Çatalhöyük is situated on an alluvial basin and sediments may have been obtained from a relatively large catchment area (Matthews *et al.*, 2013, Rosen & Roberts, 2005, Stokes, Unpublished BSc Dissertation). In addition to this, the original sediments may then have been modified through processes such as sieving and the addition of temper to the clay to produce suitable building materials (Tung, 2005). Of the four sites studied, Çatalhöyük contained the lowest amounts of quartz and silicate based rock fragments (Table 38). This would be consistent with the fine textured fluvial nature of the sediments in proximity to the site and with the sieving of sediments to create fine plasters for use within buildings (Matthews *et al.,* 2013, Tung, 2013). The inorganic coarse materials found at Çatalhöyük were consistent with soils from both the site and the environmental catchment area of the Konya basin (Matthews, 1996, Matthews *et al.*, 1996). Çatalhöyük also contained secondary minerals in the form of sulphates. Sulphates such as gypsum can form in multiple ways, including from the combination of sulphate from organic degradation with base cations (Weiner, 2010) and evaporation.

At Thessaloniki, Heslington East and Hungate the inorganic coarse material assemblages are consistent with the local geology indicating that, in terms of their inorganic coarse components, the sediment used for backfill of the graves or that in contact with the remains has not been imported to the site or been significantly modified by either decomposition or human agency. At Çatalhöyük, however, all sediments have been primarily introduced through human agency and possibly modified before being incorporated into the grave fill. As with the previous sites, at Çatalhöyük the inorganic coarse components that are present would be consistent with the local geology, meaning that the grave sediments were sourced from the area already used for the Çatalhöyük building material.

5.3.2 Distinguishing different graves (intra site variation)

The inorganic coarse material assemblages and abundance are fairly consistent between graves at Çatalhöyük and Thessaloniki (Heslington East was exempt from the intra site variation analysis). Hungate also has a large degree of consistency between graves with the exception of SK54898, the infant lead coffined grave. SK54898 can be defined based on the inorganic coarse material as it contains low level of quartz at 18.4% (next lowest value is 34%) and the overall coarse material abundance was low compared to the other Hungate graves. SK54898 was also the only grave that contained lead fragments (Table 44). It is highly likely that the presence of a lead coffin in the burial at SK54898 is responsible for the abundances of lead fragments. The low overall coarse material abundance may relate to transportation processes as the presence of the lead coffin would have created a different depositional microenvironment compared to the wooden coffins and shrouded burials at Hungate. The lead coffin may also have restricted the ingress of larger particle sizes into the coffin, this only being possible when large enough gaps opened into the coffin space.

Overall the inorganic coarse material assemblages and abundances are only grave specific in exceptional circumstances, such as the infant coffin grave at Hungate. This overall lack of variation may be because there is no variation to be found due to low levels of natural variation in the soils or uniform distribution of inorganic coarse material due to mixing of the soil through back fill or bioturbation (Canti, 2003). Hungate had the largest samples size available for analysis, it may be possible, that other sites would also show variation related to burial practice or neoformed minerals if more graves were sampled to create a larger comparison set.

5.3.3 Controls vs. burial plane samples and variations in the burial plane (Intra grave variation).

5.3.3.1 Control vs burial plane

At Thessaloniki and Çatalhöyük there were no systematic differences in the inorganic coarse material between control samples and those from the burial plane. Hungate SK54898 and to some extent Heslington East, however, showed a decrease in abundance of coarse material down through the soil profile that continued into the burial plane that may be due to natural differences in the distribution of coarse material in the soil such as the influence of worm sorting. There is also a possibility, however, that it has been influenced by the presence of large amounts of organic matter present in the burial plane. At Heslington East and Hungate there was also an increase in the diversity of the C:F related distributions with depth from the C1 samples at both sites, which only contained porphyric material at Hungate and primarily porphyric material with some chitonic C:F related distribution at Heslington East, to a greater diversity of C:F related distribution present in the burial plane. The C:F related distribution of the soil gives an indication of the spatial relationships between the amount of coarse material and the amount of fine material, which can elucidate upon the degree of shrink swell capacity in the soil as well as formation processes (Stoops & Jongerius, 1975, Stoops *et al.*, 2010). Therefore an increase in C:F related distribution diversity may be due to natural variation in the soil with depth or an artefact of sample size. However it may also be indicating that there was a wider variety of depositional and pedogenic processes occurring in the burial plane creating a more diverse range of C:F related distributions.

5.3.3.2 Variations in the burial plane

In general there was no systematic variation in the intra grave abundances of inorganic coarse material across the burial plane. Where there was variation, it was not systematic across graves suggesting that it may have been due to natural variation rather than related to the burials.

5.3.4 Microfabric types.

Microfabrics have been identified and described for all four sites in this study (see Microfabrics Chapter 3). The microfabric identification and description, however, highlighted key questions relating to the inorganic coarse material types and overall abundance of coarse material at each site. This mainly centred on establishing whether microfabrics were consistent with the local

parent material, asking specific questions related to the microfabrics at Çatalhöyük and whether they could be linked to building material, and at Hungate to establish if differences in coarse material abundances were related to graves and/or to the presence of specific microfabrics.

Previous studies have argued that to distinguish the parent material of soils, or indeed microfabrics, the minerals present must be the same as the original sediments (Tung, 2005). When this method is adopted for micromorphological analysis, identical mineral assemblages are only present at Hungate (seven out of twenty). This approach, however, may be problematic as it does not take into account minerals that are present in low abundances in the environment. The low abundant minerals may therefore be absent from microfabrics due to their scarcity and because micromorphological techniques only examine a small section of the soil, meaning that inorganic coarse component in low abundances may be missed. In addition, the presence of neoformed minerals may also skew the results as these may be created *in situ*, and therefore be unrelated to the parent material. It could be argued that only minerals present in high abundances should be considered when determining sediment origins. This, however, has its own problems, as those minerals and rock fragments present in high abundances are likely to be present in most soils regardless of parent material (such as quartz). That being said, there are some tentative conclusions that can be made by examining the inorganic coarse material assemblages.

At Çatalhöyük, microfabric CH4 showed clear differences in mineralogy compared to the other microfabrics present, with elevated abundances of quartz and a higher diversity of minerals. The other five microfabrics all contained similar inorganic coarse material assemblages. This would normally indicate that CH4 originated from a different area to the other five microfabric types. However, as all of the materials within the site were anthropogenically produced, it may have been possible that some other process(es) caused the differences in the inorganic coarse material. For example, once the sediment was collected there may have been modifications made to it such as the inclusion of temper or the removal of materials (Tung, 2013). The question remains, therefore; Was there a process that was specific to either the grave environment or the location of the sample? CH4 is found in all of the samples apart from the C3 from 19295, indicating that this was not a microfabric type that was specific to the grave and that this was more likely a building material. At Thessaloniki there were two microfabric types, Ti1 and Ti2. Although micromorphologically very distinct (3.3.1), the samples are similar in their inorganic coarse material, with relatively few differences in abundance of mineral types.

Hungate had the largest number of different microfabrics (13). There were two particularly distinctive microfabrics present HU6 that contained no inorganic coarse material, and HU1 that contained lead fragments. Otherwise there were only small differences in mineralogy and abundance. Again it would be difficult to rule out a common origin for these samples, as there are only small variations present. It is also possible that differences in transportation and deposition may have caused some of the variation seen in the abundance of inorganic coarse material. For example, HU6 consists of a series of fine layers of clay situated on the top of the stratagraphic matrix (3.5.1). HU6 may have had a common origin to other microfabrics at Hungate however as HU6 appears to be clay inwash depositional sorting may have occurred removing the coarse material. A further question at Hungate was is the low abundances of inorganic coarse material in SK54898 caused by the presence of 'grave specific' microfabrics that were low in inorganic coarse material or due to low abundances of inorganic coarse material in microfabrics that were common amongst the Hungate graves. Although there were specific microfabrics in SK54898 that were low in inorganic coarse material, such as HU6, the majority of microfabrics were found in other graves. Therefore, it can be concluded that microfabrics found in SK54898 were low in inorganic coarse material compared to similar microfabrics in other graves and the C1 sample.

5.3.5 Vivianite as an indicator of burials.

Vivianite typically occurs in areas that have been rich in phosphate and experienced reducing conditions (Macphail *et al*., 2013). In archaeological contexts, vivianite is generally associated with the presence of human remains and waste in association with iron rich soils (McGowan & Prangnell, 2006) and, as such, it is not specific to burials. Vivianite was present at two sites in this study, Heslington East and Hungate. Hungate was periodically waterlogged (Evans, 2007b, National Soil Resources Institute, 2011a), creating the necessary anaerobic conditions needed for vivianite formation (McGowan & Prangnell, 2006). The presence of vivianite in the lower C1 sample at Hungate would indicate that this is not a burial specific phenomena and it may have originated from alternative sources. As Hungate was reused up until the present day it would be difficult to rule out non-burial phosphate sources. Heslington East was, until quite recently, used as agricultural land, which would have necessitated the addition of phosphate into the soil through the use of fertilisers or animal waste if the land was grazed, which maybe the source of phosphate needed for vivianite formation in this instance. It is, therefore, possible that at both sites there may have been alternate possibilities for the inclusion of phosphate driving vivianite development in the soils.

5.4 Conclusions

At the broadest scale, inter-site variation seems to be driven by local factors such as parent material and site location. Unusual burial practice, however, does seem to be distinguished in grave SK54898, Hungate, which shows distinctions in the inorganic coarse material type and abundance caused by the presence of the lead coffin.

There were two inorganic coarse materials of particular interest: vivianite and lead. The vivianite appears to relate to particular environmental conditions occurring at Heslington East and Hungate, and were not grave specific. The lead present at Hungate, as both coarse aggregates and in the fine material (4.2) is related to the presence of a lead coffin, as evidenced by its general absence in all other soils.

What is clear is that, in a broad scale, the inorganic coarse material assemblages are consistent with the local parent material and what we might expect at each site, meaning that the soil at the sites had a similar origin and that the soil coarse component was not radically changed by either burial practice or the degradation of the body. There are examples of anthropogenically induced changes in the assemblages, either deliberately as at Çatalhöyük or indirectly as in the lead coffin at Hungate. There are also instances of the effect of decomposition of the body and associated grave goods influencing the presence of some inorganic coarse material fragments (lead).

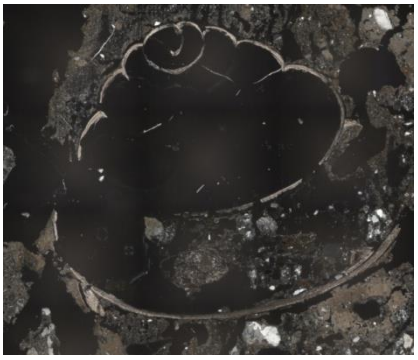

6 Coarse Components; Bone, Charcoal, Shell, Fungal Sclerotia, Phytoliths and Roots.

Coarse components were defined as material above 50µm, then further subdivided into mineral and rock fragments and organic/organically derived coarse components. This section examines the organic/organically derived coarse components, which were dealt with as two groups, those which were commonly occurring (bone, charcoal and shell) and those that were sporadic (fungal sclerotia, phytoliths and roots). All sizes of phytoliths and microcharcoal were included in the coarse component category to facilitate a holistic approach to the data.

Commonly occurring, organically derived coarse components (bone, charcoal and shell) and their taphonomy have been the subject of extensive research both in archaeology and the natural sciences (Bobrowsky, 1984, Claassen, 1998, Forbes *et al.*, 2006, Nielsen-Marsh *et al.*, 2007, Scott & Damblon, 2010, Smith *et al.*, 2007). In terms of inhumations, the inclusion of fragmented bone, charcoal and shell may be the result of the decomposition of grave goods, grave furniture, offerings and feasting associated with inhumation rites. In the case of bone fragments, these may also be the result of the decomposition of the skeleton. Bone, charcoal and shell fragments may, however, occur naturally in the soil. If the presence of organically derived coarse components were caused by intentional or unintentional human agency, they should be present at higher levels in the burial plane than in the control samples and possibly concentrated in specific areas of the burial plane for example high levels of shell and bone where grave goods have decayed.

Phytoliths are formed as intracellular or extracellular silica deposits in higher plants and remain in soils and sediments after the organic plant material has decomposed (Piperno, 2006). Phytoliths can, therefore, be useful indicators of past vegetation coverage and anthropogenic use of plant

materials (Piperno, 2006). In a grave context, concentrations of phytoliths in burials may relate to the inclusion of higher plants as grave goods, furnishings or food offerings. Organic coarse components such as roots and fungal sclerotia are potentially important as they may concentrate in inhumations due to the presence of large amounts of organic material.

The coarse organic material was assessed for all of the samples analysed in this study, according to the methods outlined in 2.3.1.2. The variation in bone, charcoal and shell abundance will be assessed on three levels;

- Inter site (Çatalhöyük, Thessaloniki, Heslington East and Hungate).
- Intra site (Çatalhöyük, Thessaloniki and Hungate).
- Intra grave (Çatalhöyük, Thessaloniki, Heslington East and Hungate).

The less common organic and organically derived coarse material (fungal sclerotia, phytoliths and roots) are presented separately as they were often sporadic (for example only one instance of phytolith concentrations were observed in this study) and therefore broad scale analysis was not appropriate for these components.

6.1 Bone

6.1.1 Inter site bone variation

Bone was identified by its low interference colours (first order grey in XPL) as well as by the 'ropey' appearance of the internal structure and its yellowish/yellowish brown colour in PPL (Macphail & Goldberg, 2010, Stoops, 2003). Bone was observed as both small (<1000 µm) (Figure 54) and larger (>1000 µm) fragments (Figure 55). Although the structure of the haversian canals was visible in some fragments, they were not large enough to distinguish between human and animal bone (Henderson 1987).

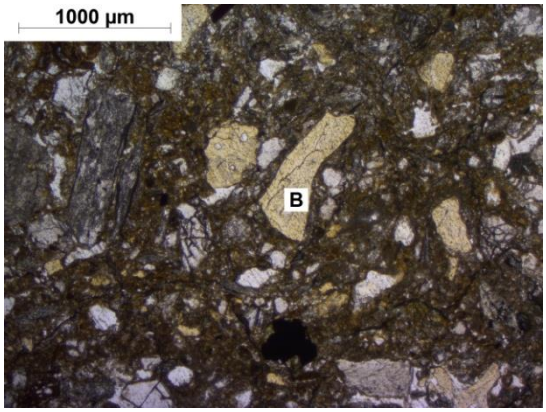

Figure 54: Fragmented bone (B) from TF182 hand sample shown in PPL.

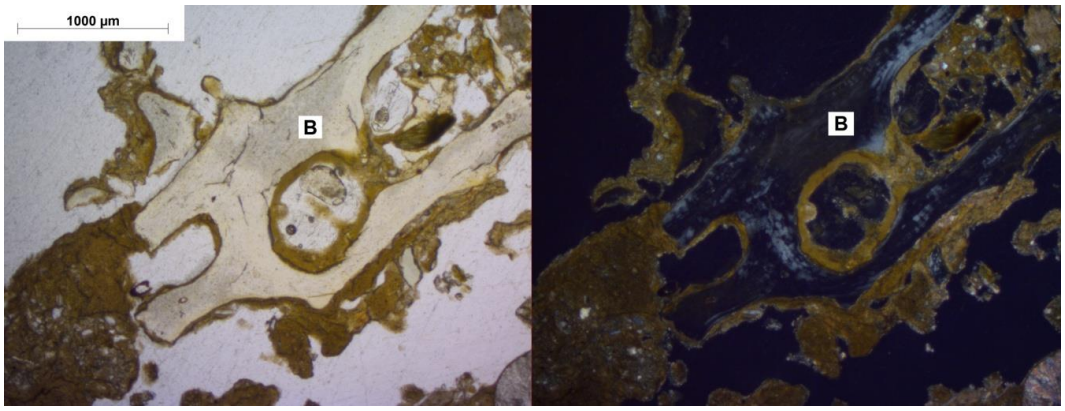

Figure 55: Larger pieces of fragmented bone in TF177, parallel pelvis sample. Show in PPL left and XPL right.

Çatalhöyük contained the narrowest distribution of bone abundances, with a median of 0.9%, and maximum values at 3%. The widest distribution of bone fragments was at Thessaloniki with a median at 2% and maximum at 20%. Heslington East and Hungate had similar overall fragmented bone abundances illustrated by the shape of the data (Figure 56).

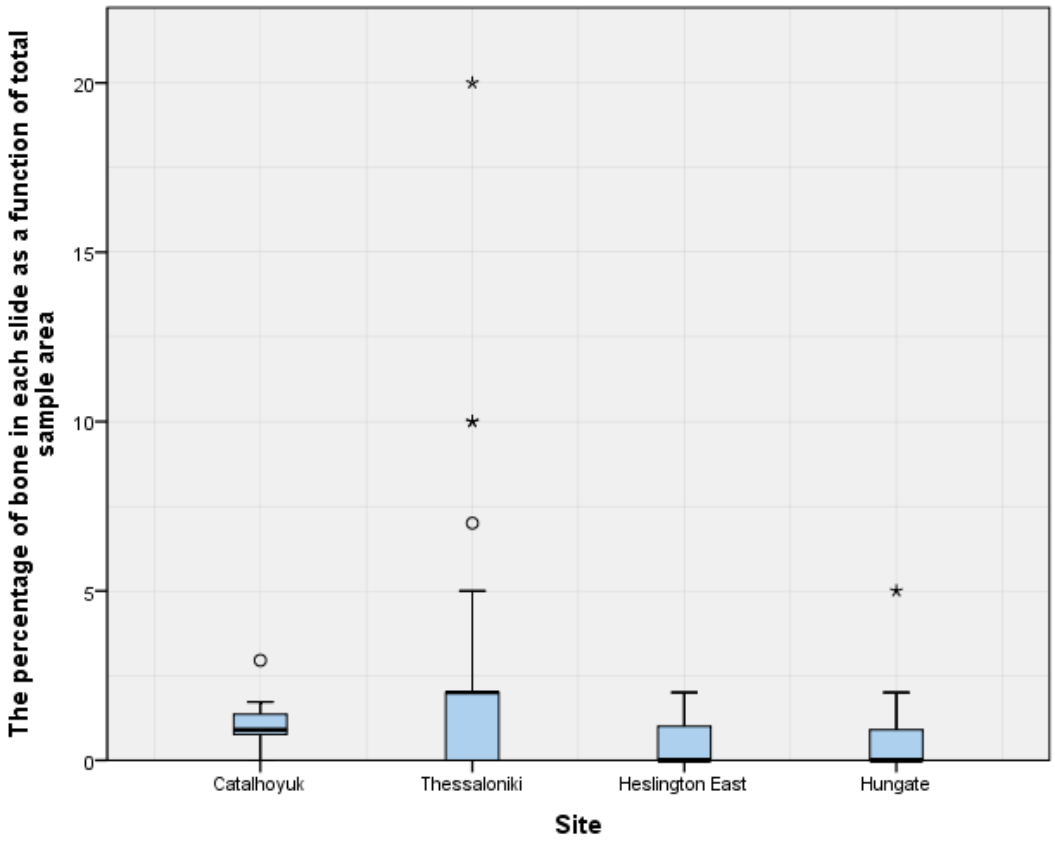

Figure 56: Box and whisker plot showing the abundance of bone as a function of percentage of slide area covered per slide at each site. Number of slides at each site are as follows; Çatalhöyük n=12, Thessaloniki n=26, Heslington East n=7 and Hungate n=64. Whiskers extend to x1.5 the height of the box or highest/lowest value. '*' indicate extreme outliers more than three times higher than the extent of the box and 'o' illustrate values between x1.5 and x3 the height of the box.

6.1.2 Intra site bone variation

6.1.2.1 Çatalhöyük

Both graves at Çatalhöyük had a similar bone fragment distribution (Figure 57), although the distribution was slightly wider in grave 18666 compared to grave 19295. The C1 consisted of a single sample that contained a higher median bone abundance than grave 19295 and 18666, but was within the range of both graves.

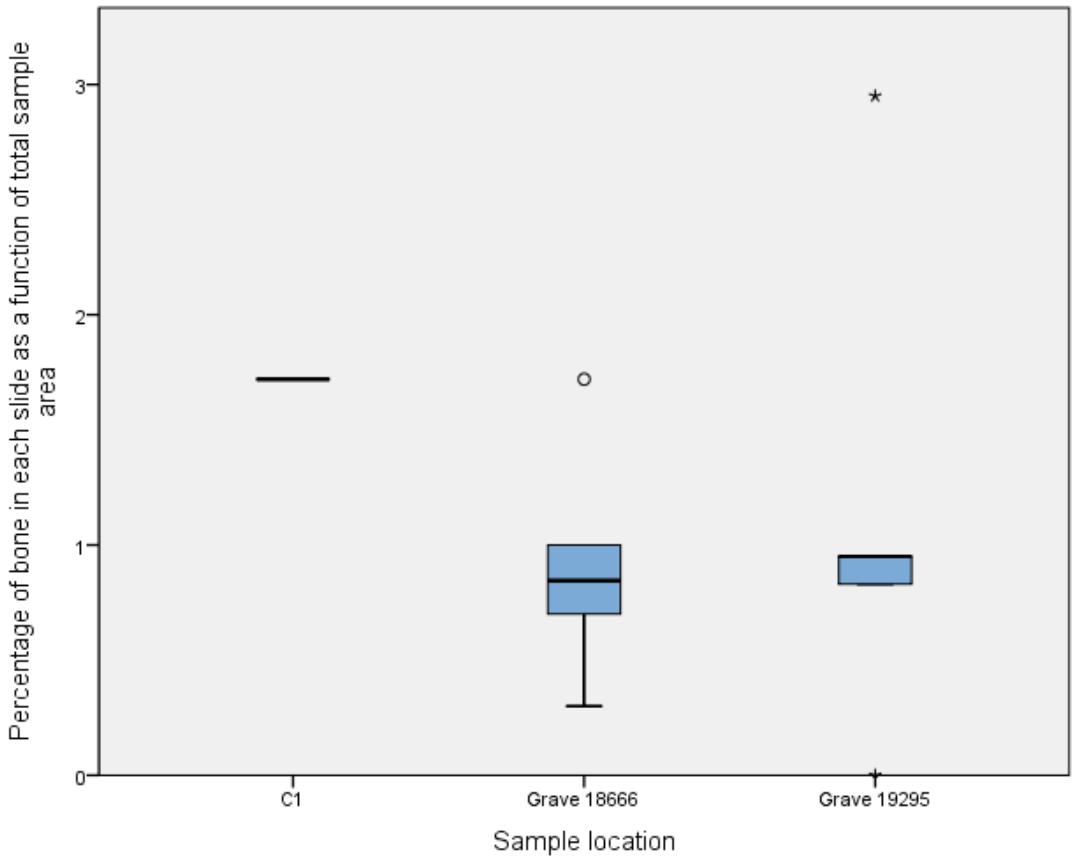

Figure 57: Box and whisker plot of bone fragment abundances given in percent at Çatalhöyük by grave. Sample sizes are as follows C1 n=1, 18666 n=6, 19295 n=5. 'O' illustrates values between x1.5 and x3 the height of the box

6.1.2.2 Thessaloniki

At Thessaloniki graves could be divided into two groups based on the range of fragmented bone abundances (Figure 58). TF159, TF178 and TF162 had narrow distributions of bone abundance, whilst TF177 and especially TF182 had wider distributions. TF177 and TF182 were located within structures (Figure 59). Those with narrow distributions also had a low number of samples (n = 5, 2 and 3 respectively), compared to those with wider distributions (both n=8). Thus sample size may be a factor.

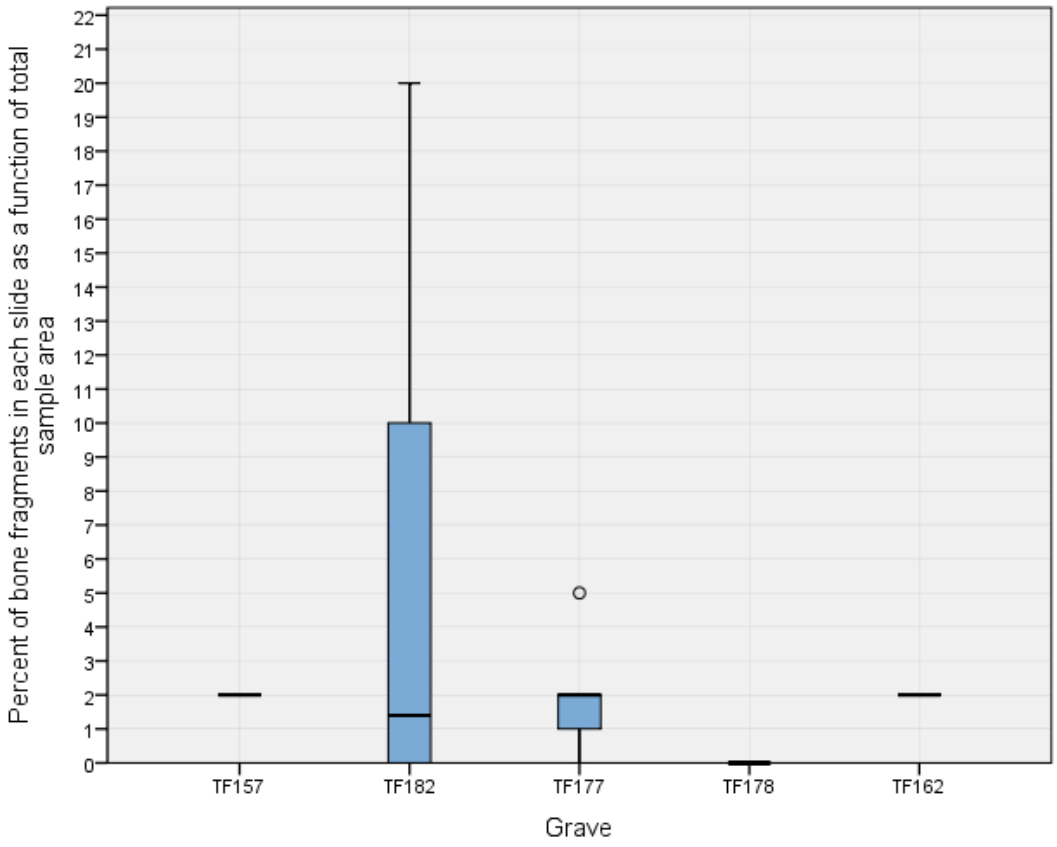

Figure 58: Box and whisker plot of bone percentages at Thessaloniki by grave. Sample sizes are as follows; TF159 n= 5, TF182 n=8, TF177 n=8, TF178 n=2 and TF162 n=3. 'O' illustrate values between x1.5 and x3 the height of the box

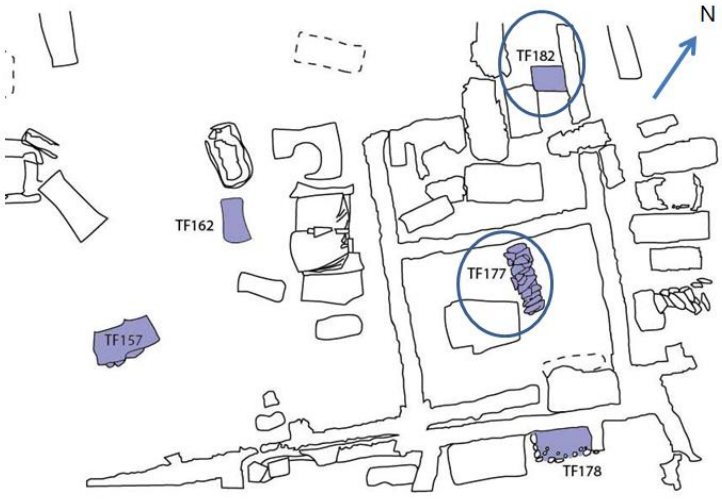

Figure 59: Location of burials with wide bone distributions (circled)

6.1.2.3 Heslington East

The C1 and grave samples from Heslington East both had median values of 0% (Figure 60). Grave 713, however, had a higher maximum value and range both at 2%, with fragments of bone only present in the skull area and C2 sample.

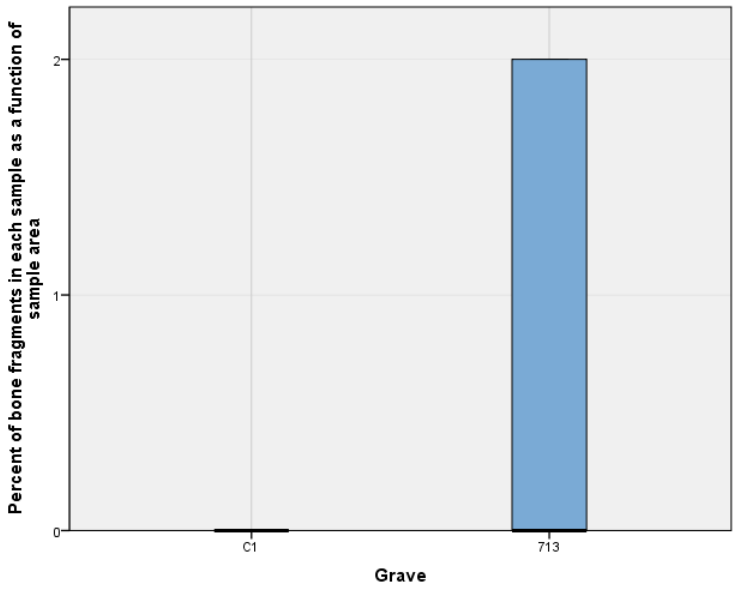

Figure 60: Box and whisker plot of bone percentages at Heslington East by grave. Sample sizes are as follows; C1 n=3 and 713 n=5.

6.1.2.4 Hungate

SK54908, SK54898, SK54341 and SK54085, as well as the C1 control, contained no or very few bone fragments (Figure 61 and Figure 62). In this instance the location of the grave seems to be a leading factor in bone preservation. Of the remaining samples two patterns emerged; those with median abundances close to zero and with upper quartile values and extremes of approximately 1% (SK51350, SK51351, SK54090 and SK54342), and those that had higher bone abundance medians at approximately 3% (SK51326 and SK51387).

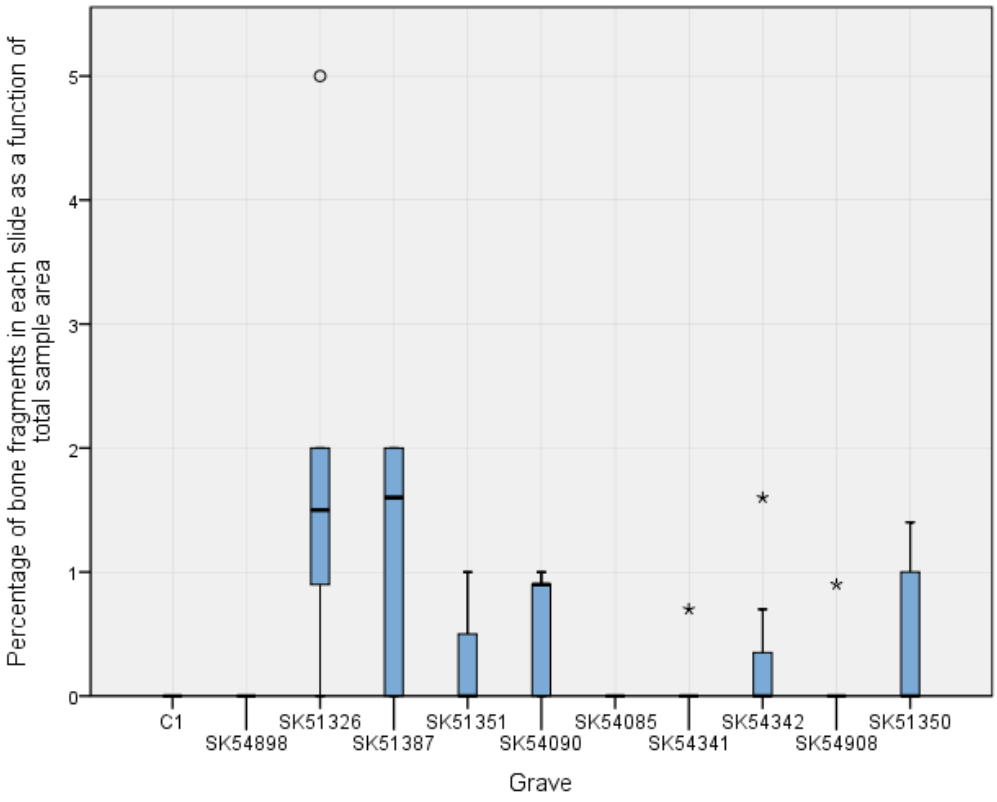

Figure 61: Box and whisker plot of bone abundances in percentages at Hungate by grave. Sample sizes are as follows; C1 n=3, 51326 n= 8, 51350 n= 5, 51351 n= 7, 51387 n= 6, 54085 n= 5, 54090 n= 5, 54341 n= 9, 54342 n= 7, 54898 n= 6 and 54908 n= 7. '*' indicate extreme outliers more than three times higher than the extent of the box and 'o' illustrate values between x1.5 and x3 the height of the box.

Figure 62: Location of burials with no or very little bone present (circled).

6.1.3 Intra gave bone variation

6.1.3.1 Variation in bone distribution within all graves

Bone was sporadic in the grave controls at all sites appearing in the C2 sample from Heslington East (2%) and grave SK54908 (1%), Hungate. Bone was slightly more common in the C3 samples appearing in 19295 and 18666 at Çatalhöyük (<1%), SK54090 (1%) and SK51326 (2%) at Hungate as well as 2% in the C3 from TF177 Thessaloniki. There was, however, no systematic variation in bone abundance between the C1, C2, C3 and samples from the burial plane. A comparison was made between the skull, pelvis and foot samples for all graves (Figure 63). The skull, pelvis and foot were used as these were the three main sampling points which had been consistently sampled in all of the graves.

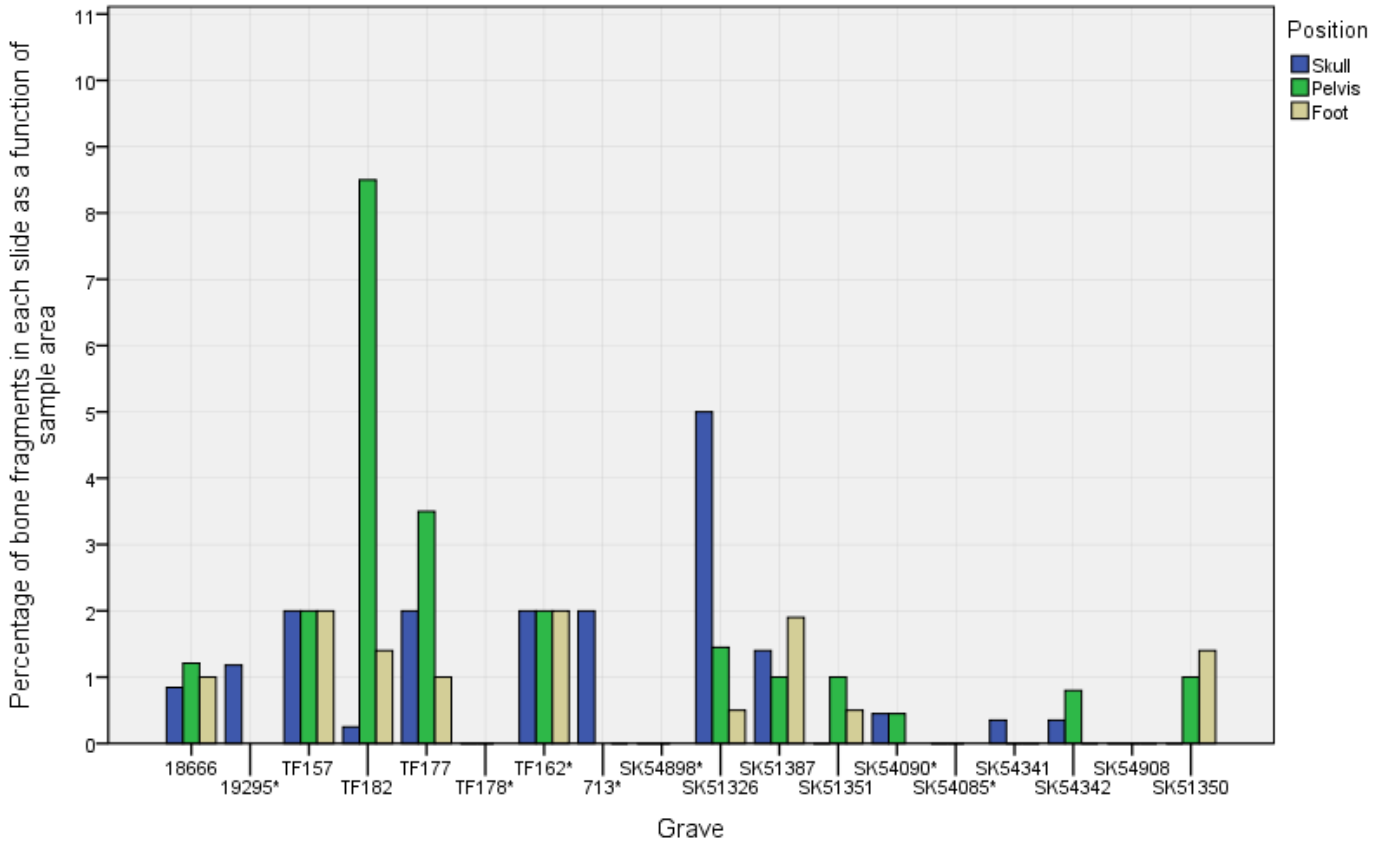

Figure 63: Abundance of bone in the skull, pelvic and foot samples shown in percent for all graves in the study. Those graves that do not have all three sample points (skull, pelvis and foot) are identified by '*'. Where there is more than one sample available the average bone percent is given.

TF177, TF182, 18666, SK51351 and SK54342 had elevated abundances of bone fragments in the pelvic area sample compared to the skull and foot area samples (Figure 63 and Figure 64). 42% of all the complete graves had raised abundances of bone in the pelvis area compared to 17% that had raised abundances in the skull or foot area samples. At Thessaloniki, Çatalhöyük and Hungate, 50%, 100% and 28% respectively, of complete graves had high levels of bone in the pelvic area compared to the skull and foot area, implications of which will be discussed more fully in section 6.6.3, however this may relate to the degree of weathering occurring in the pelvic bones.

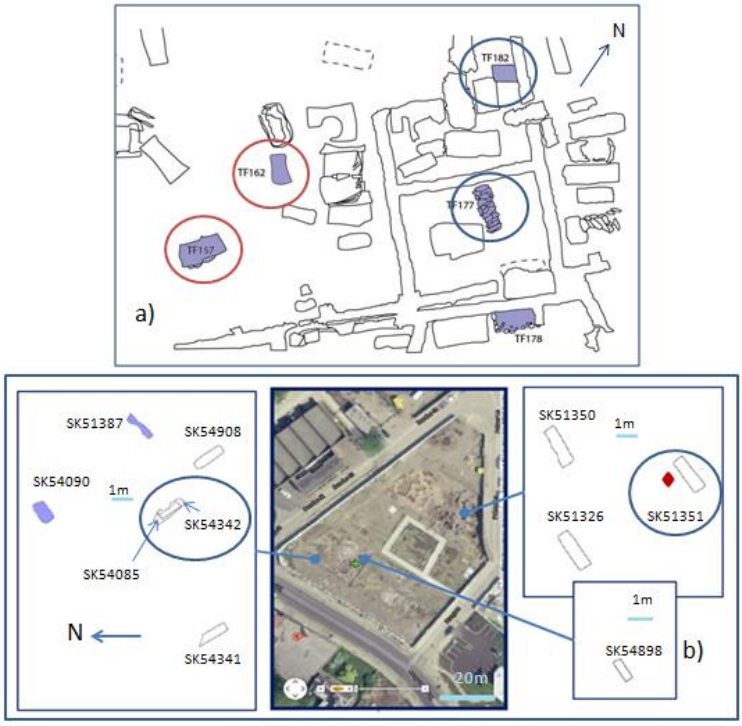

Figure 64: Location of graves with high raised abundances of bone fragments in the pelvic area (blue) and with even distributions of bone in the skull, pelvis and foot samples (red) at a) Thessaloniki and b) Hungate.

6.1.4 Variation in bone distributions moving away from the body.

There was no observable difference in the distribution of fragmented bone moving away from the body in the perpendicular slides at Thessaloniki, Heslington East and Hungate. However, in the perpendicular skull area sample from 19295, Çatalhöyük, there was a fine horizontal layer of bone in the soil that was in direct contact with the skull (Figure 65). This

has shown that, in some cases, it is possible for small abundances of fine fragmented bone to be deposited presumably from the skeleton.

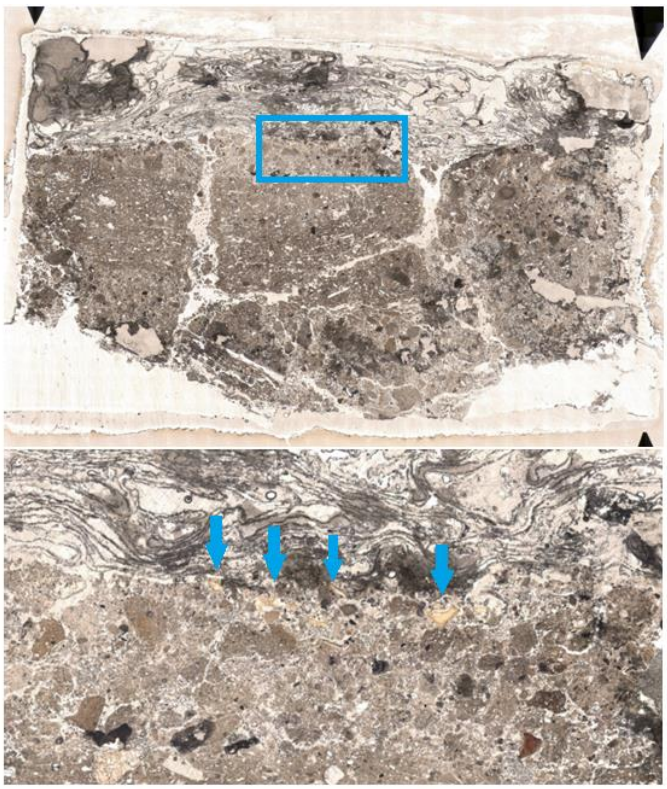

Figure 65: Upper image is a large scale photomicrograph mosaic image for the perpendicular skull sample from 19295 skull 19501 Çatalhöyük in PPL, fov is 6cm. The blue rectangle denotes the location of lower image. Lower image is a photomoricrograph showing a line of bone. Blue arrows are pointing to bone fragments, fov is 1.5cm.

6.2 Charcoal

Charcoal was identified by its very dark brown to black colour in PPL along with its sharp boundaries that distinguished charcoal from other organic materials (Bullock *et al.*, 1985, Courty *et al.*, 1989, FitzPatrick, 1993, Stoops, 2003). No fragments of charcoal could be identified to species level. Charcoal was present as both weathered and unweathered fragmented coarse material (>50 µm) and as flakes of microcharcoal (<50 µm) (Figure 66).

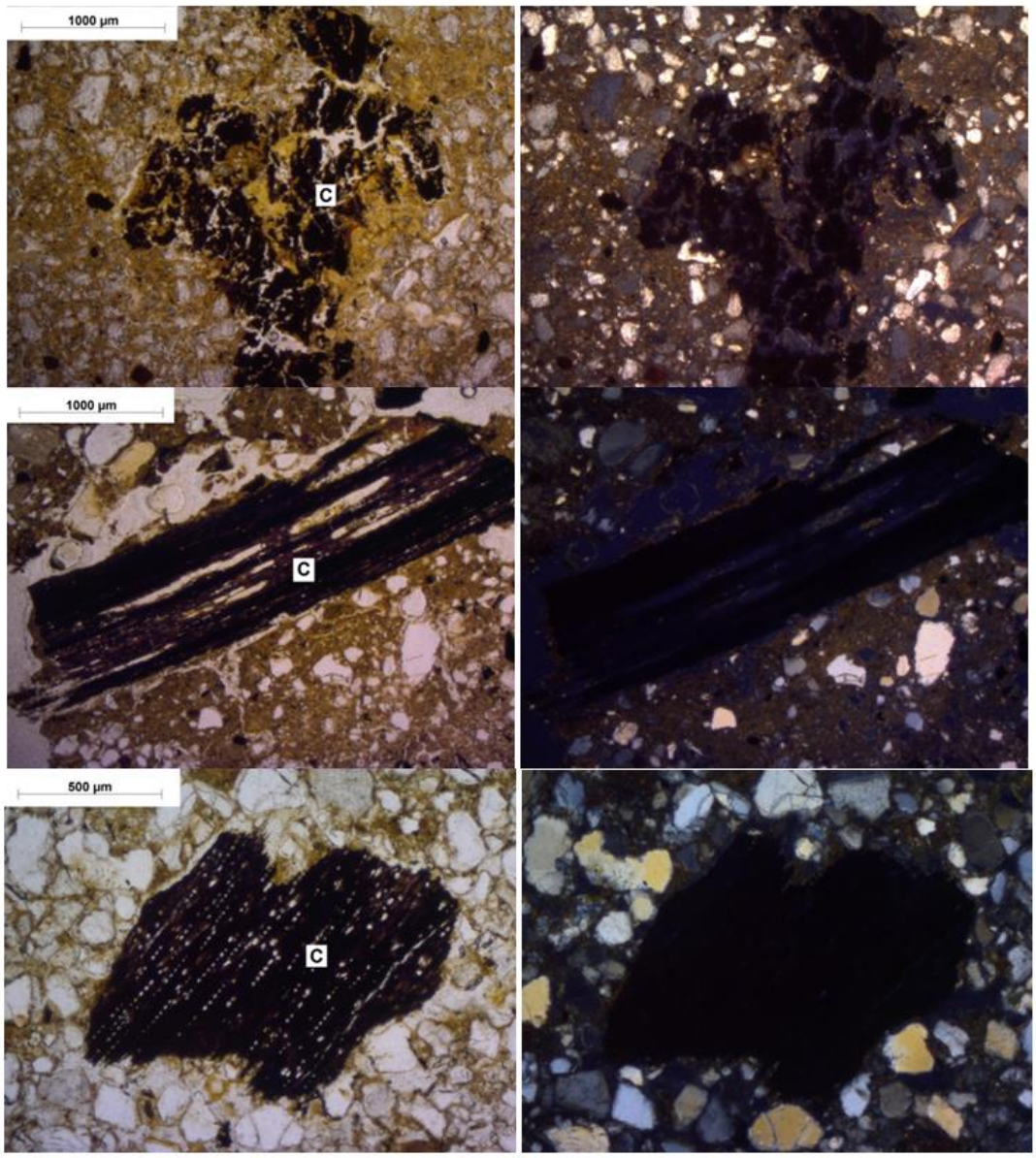

Figure 66: Charcoal fragments (C). Top degraded charcoal from SK54341 in PPL (left) and XPL (right). Middle charcoal fragment from SK51387 in PPL (left) and XPL (right) and bottom images from SK51367 in PPL (left) and XPL (right).

Çatalhöyük and Hungate had similar inter site charcoal abundance distributions with medians at 2.5% and 2%, 0% minimums, and maximums of 9% and 10% respectively (Figure 67). Thessaloniki had the lowest charcoal abundance with a median of 0% and maximum value at 2%. Heslington East contained charcoal in all of the samples analysed, with a minimum and median value at 2%. The highest charcoal abundance at Heslington East was 3% and also demonstrated low variability.

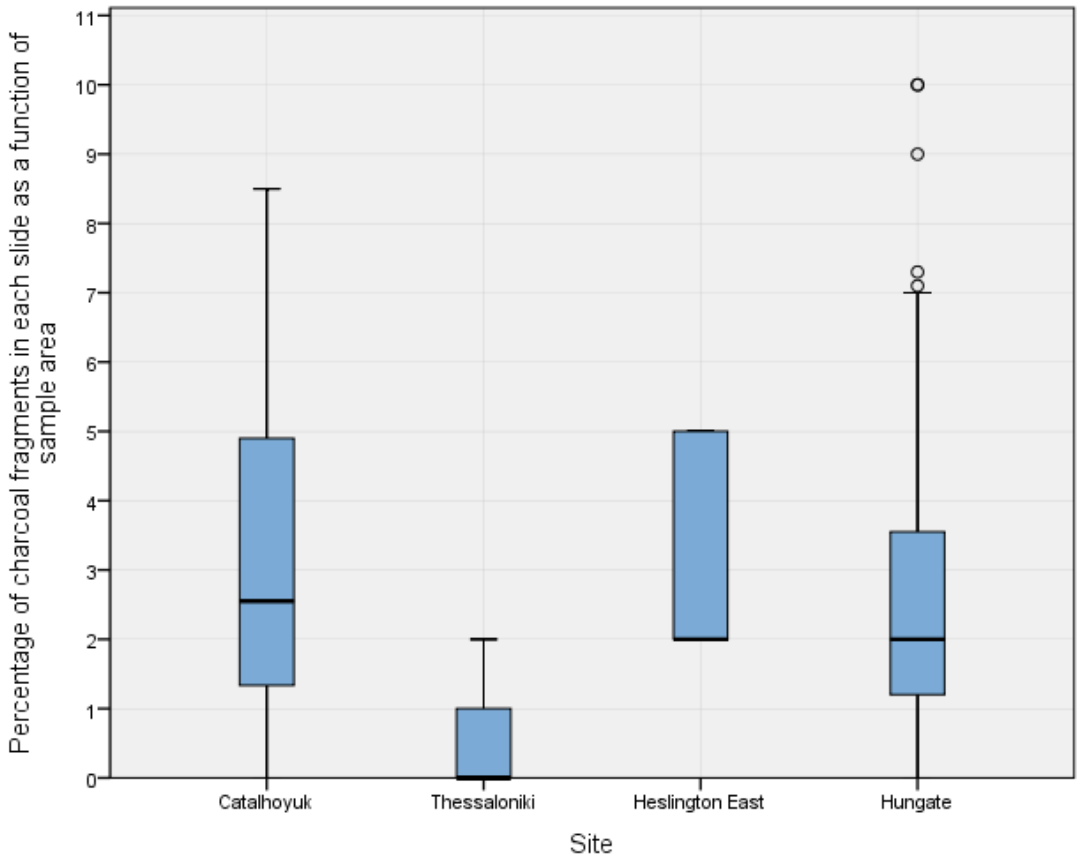

Figure 67: Box and whisker plot of the abundance of charcoal in percent, present at each site. Number of slides at each site are as follows; Çatalhöyük n=12, Thessaloniki n=26, Heslington East n=7 and Hungate n=64. 'O' illustrate values between x1.5 and x3 the height of the box

6.2.1 Intra site charcoal variation

6.2.1.1 Çatalhöyük

18666 contained a wider distribution and higher abundance of charcoal than 19295 (Figure 68). 18666 contained a median charcoal abundance of 5%, and minimum and maximum values of 2% and 9% respectively. 19295 in contrast had a median charcoal abundance of 0.95%, a minimum value of 0%, maximum and outlier of 4.5%.

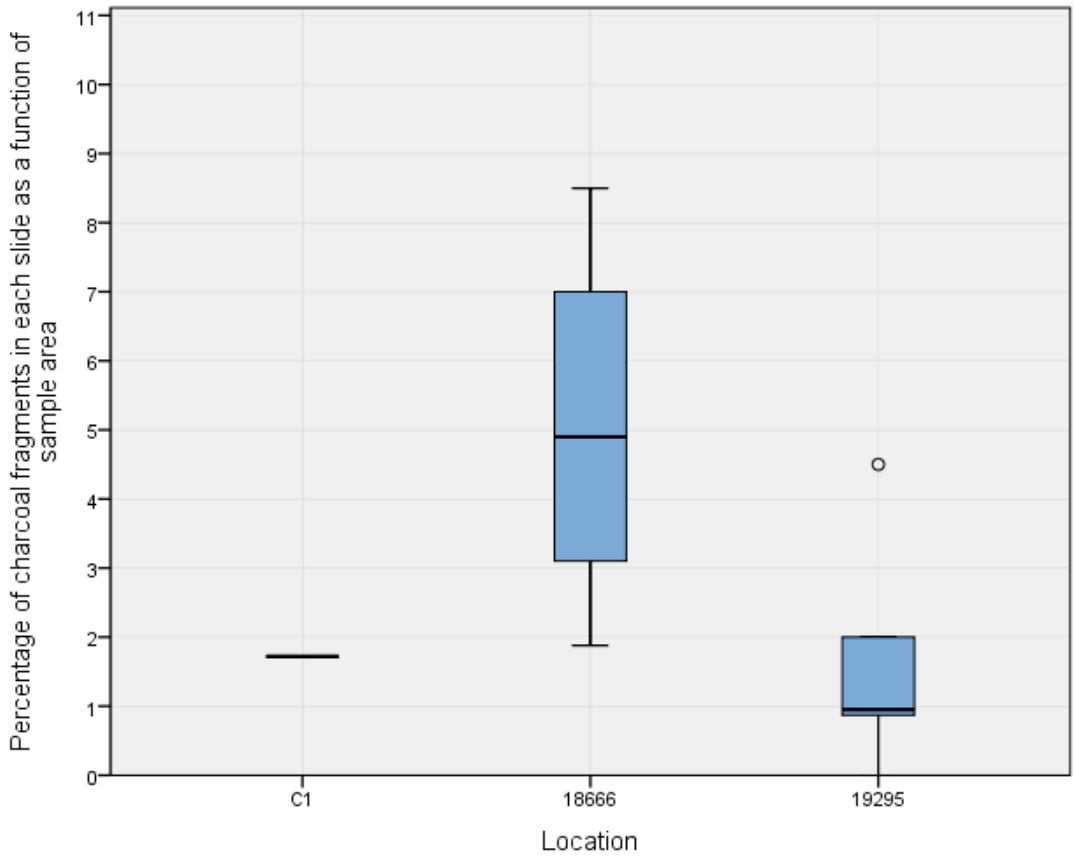

Figure 68: Box and whisker plot of charcoal abundance in percentage at Çatalhöyük by grave. Sample sizes are as follows C1 n=1, 18666 n=6, 19295 n=5. '*' indicate extreme outliers more than three times higher than the extent of the box and 'o' illustrate values between x1.5 and x3 the height of the box

6.2.1.2 Thessaloniki

Charcoal abundance in TF157, TF182 and TF162 were the same, with a median at 0%, upper interquartile at 0.5% and maximum value at 1% (Figure 69). TF177 contained slightly more charcoal, with an upper interquartile range at 1% and maximum value at 2%. TF178 contained two samples that both contain 1% charcoal.

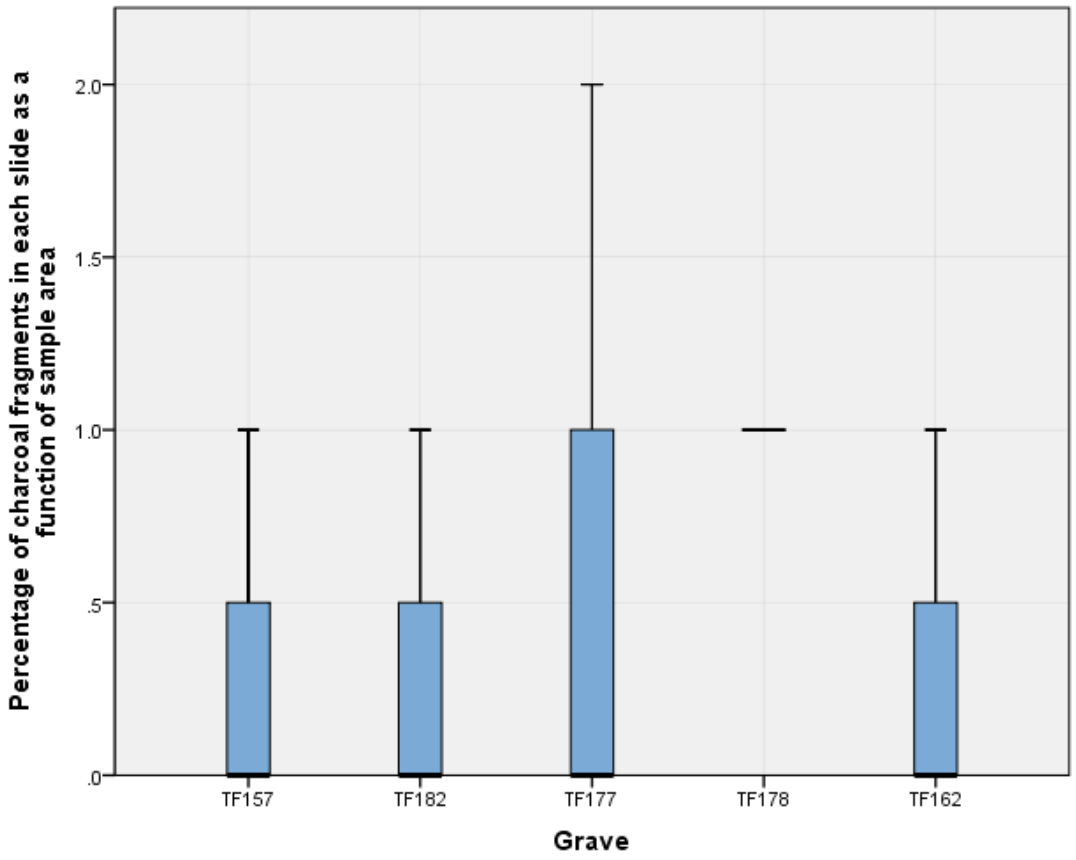

Figure 69: Box and whisker plot of charcoal abundances in percentage at Thessaloniki by grave. Sample sizes are as follows; TF157 n= 5, TF182 n=8, TF177 n=8, TF178 n=2 and TF162 n=3.

6.2.1.3 Heslington East

The abundance of charcoal in the C1 and grave samples from Heslington East were similar with median values at 2% and ranges of 3% (Figure 70).

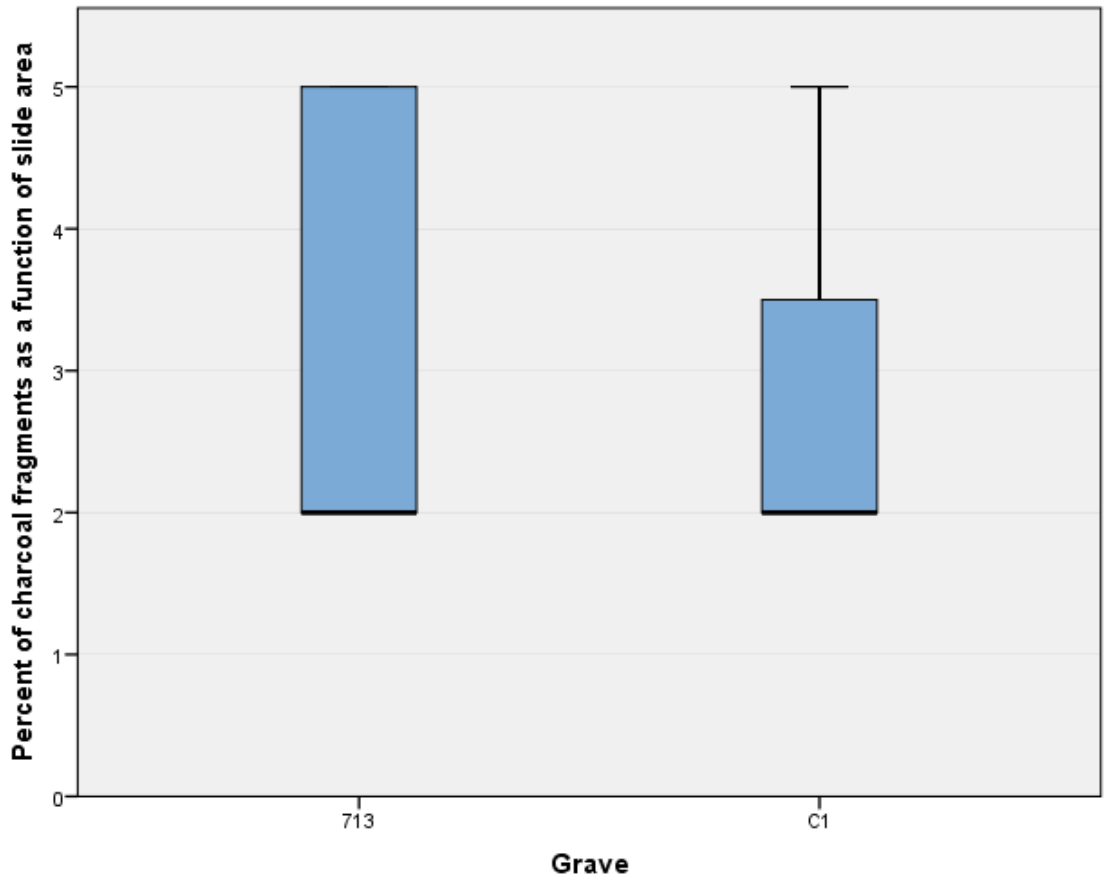

Figure 70: Box and whisker plot of charcoal abundances in percentage at Heslington East by grave. Sample sizes are as follows; C1 n=3 and 713 n=5. '*' indicate extreme outliers more than three times higher than the extent of the box and 'o' illustrate values between x1.5 and x3 the height of the box.

6.2.1.4 Hungate

There were small intra site differences in the charcoal distribution at Hungate (Figure 71). SK54898 had an elevated charcoal median abundance compared to the other graves and C1 sample. All other samples had similar means and charcoal distributions.

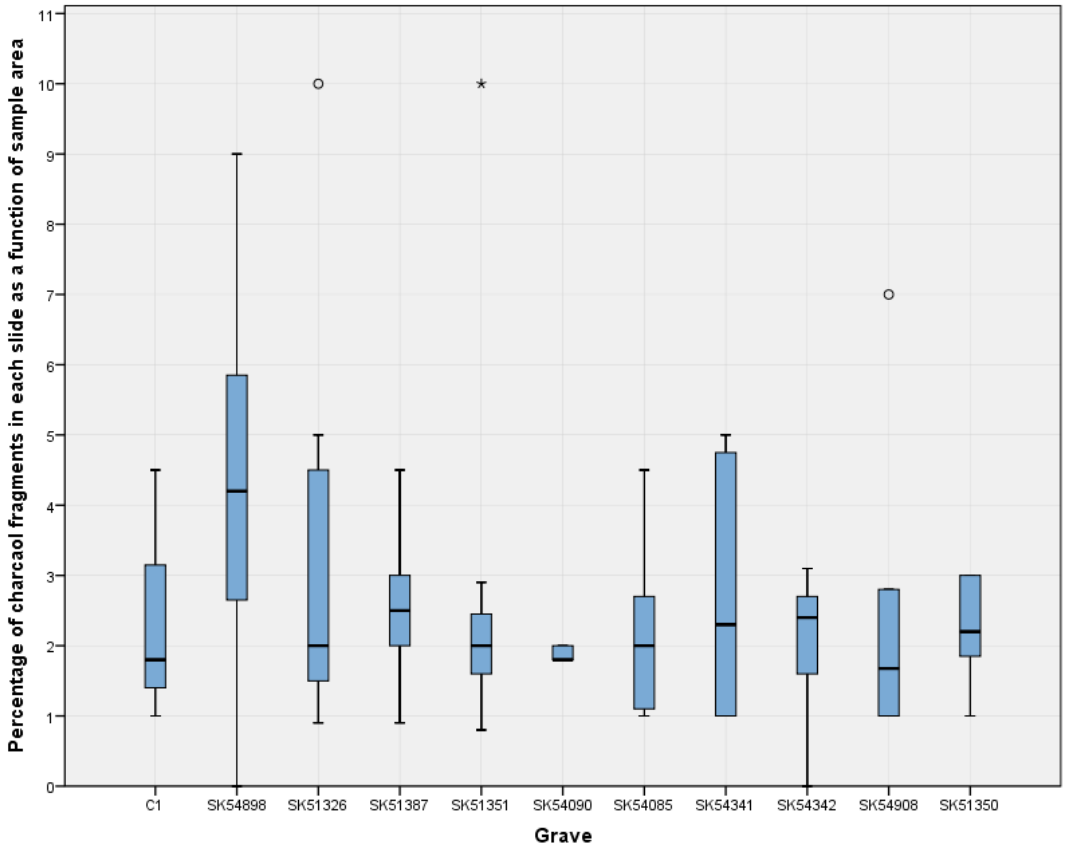

Figure 71: Box and whisker plot of charcoal abundance in percentage at Hungate by grave. Sample sizes are as follows; Control n=3, 51326 n= 8, 51350 n= 5, 51351 n= 7, 51387 n= 6, 54085 n= 5, 54090 n= 5, 54341 n= 9, 54342 n= 7, 54898 n= 6 and 54908 n= 7. '*' indicate extreme outliers more than three times higher than the extent of the box and 'o' illustrate values between x1.5 and x3 the height of the box.

6.2.2 Intra grave charcoal variation

Charcoal was common in the grave control samples and was present at 2% in the C2 and C3 samples from Heslington East, 3% in the C3 from 18666 Çatalhöyük and 1% in the C3 sample from TF177 Thessaloniki. At Hungate there was charcoal in the C2 sample from SK51350 and SK51326 (2%), as well as the C3 samples from SK54085 (5%), SK54898, SK51326 (4%), SK51387, SK51350 (3%), SK54342, SK54090, (2%) and SK54341 (1%). There was no systematic variation in charcoal abundance between the C1, C2, C3 and samples from the burial plane. A comparison was made between charcoal abundance in the skull, pelvis and foot area samples for all graves (Figure 73 and Figure 72). TF157, TF182 and TF162 from Thessaloniki and SK54898, SK51326, SK51387, SK51351, SK54090, SK54342, SK54908 and SK51350 from Hungate had elevated levels of charcoal in the skull areas compared to the pelvis and foot area samples (Figure 73). High levels of charcoal in the

skull may relate to the general taphonomic processes occurring within the grave however this will be discussed fully in section 6.6.3. Overall, 66% of all graves sampled and 80% of all completely sampled graves had elevated levels of charcoal in the skull area sample compared to the pelvic and foot area samples. At Çatalhöyük the one complete grave did not contain elevated amounts of charcoal in the skull area sample. At Thessaloniki and Hungate, 66% and 60% of complete graves respectively, had elevated amounts of charcoal in the skull area sample.

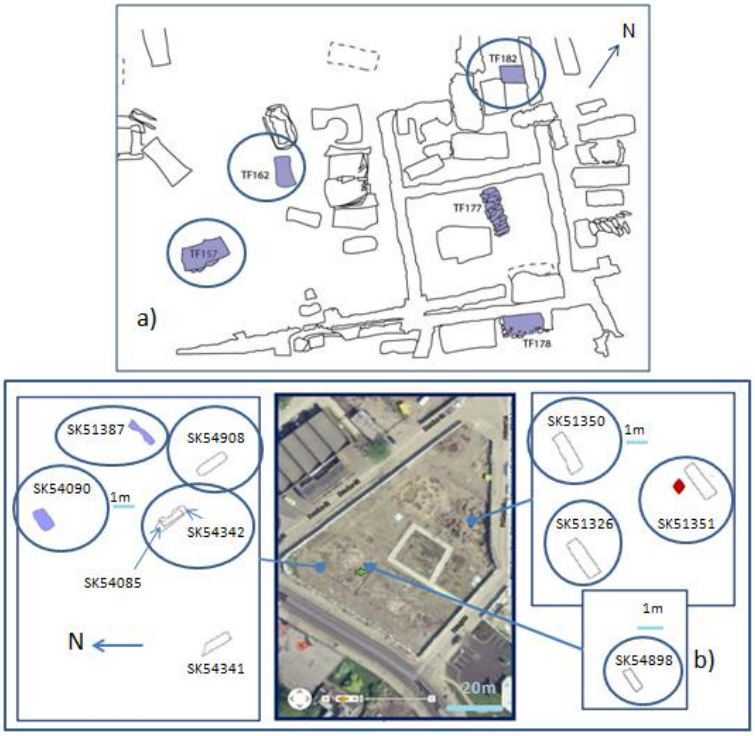

Figure 72: Location of graves with peaks of charcoal abundance in the skull at a) Thessaloniki and b) Hungate.

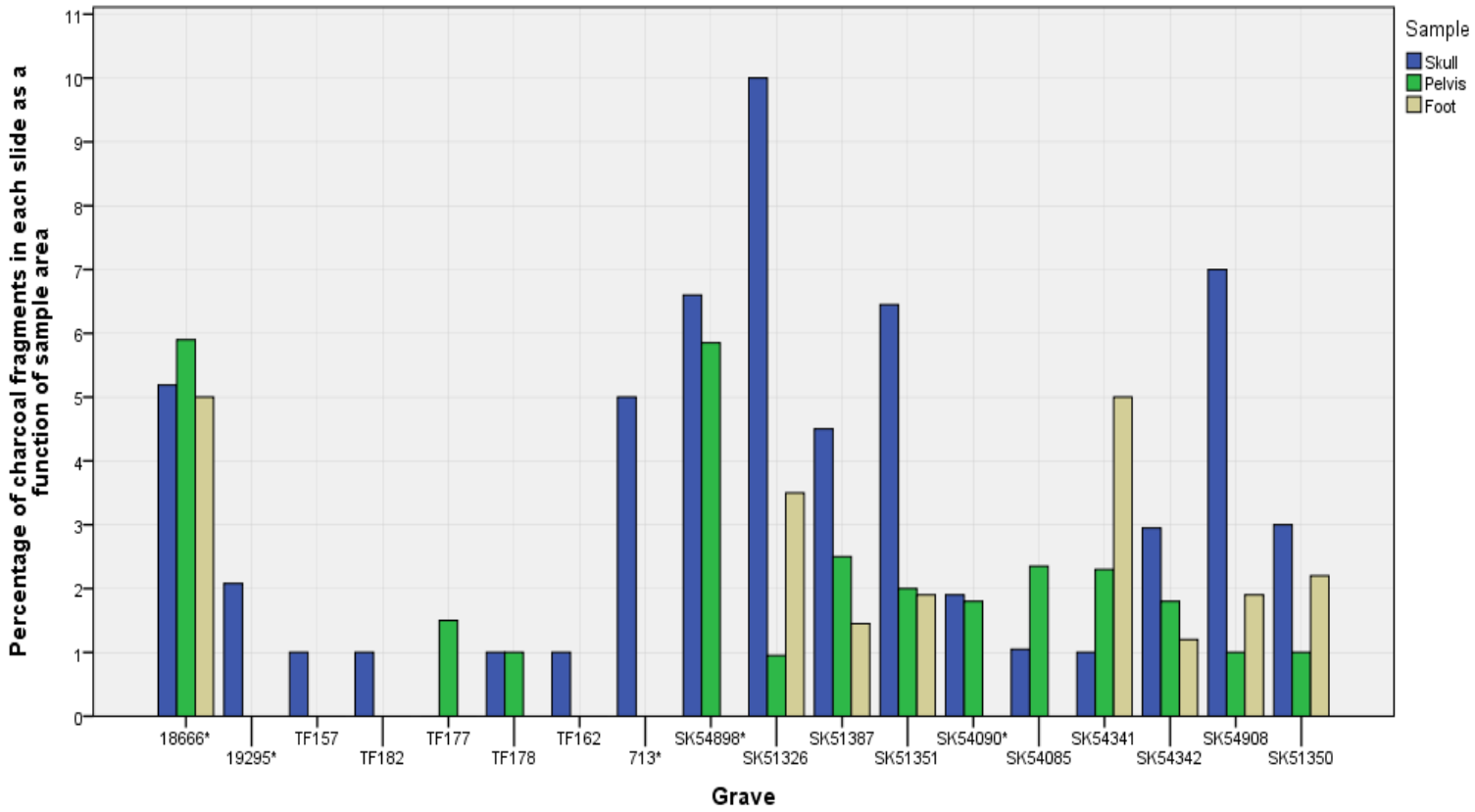

Figure 73: Percentage abundance of charcoal in the skull, pelvic and foot samples for all graves in the study. Those graves that do not have all three sample points (Skull, Pelvis and foot) are identified by '*'. Where there is more than one sample available for a point in a grave the average charcoal percent is given.

6.3 Shell

Shell was identified by its high birefringence colours, fibrous internal fabric as well as their external shape (Stoops, 2003). Shell was visible as both weathered and unweathered fragments (Figure 74) and as whole gastropod cross sections (Figure 75).

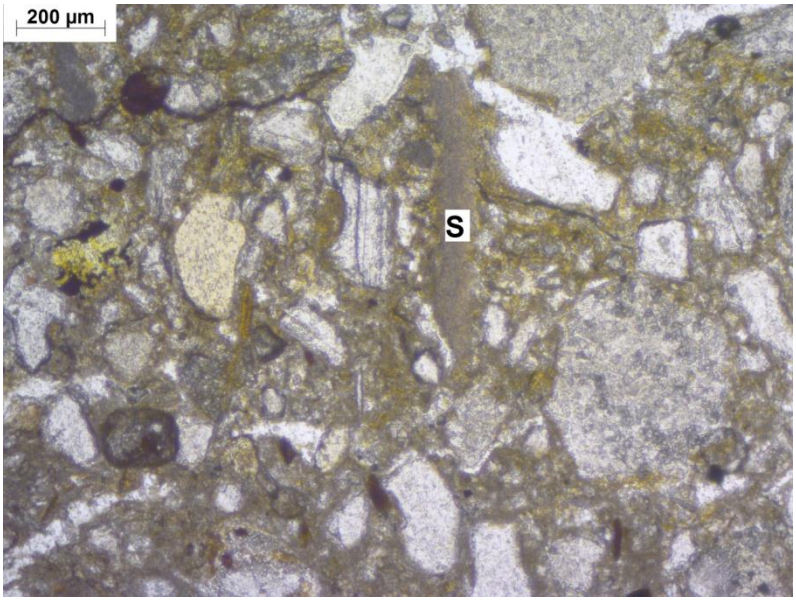

Figure 74: Shell (S) within the hand sample of TF182 in PPL.

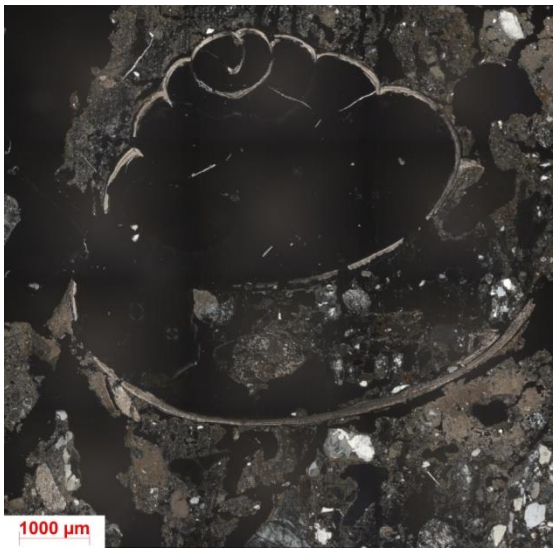

Figure 75: Snail shell from TF178 in XPL.

6.3.1 Inter site shell variation

Shell was absent from Heslington East and only present in the C3 from SK51387 Hungate. Çatalhöyük contained low levels of shell with a median value of 0% (Figure 76), whereas Thessaloniki had a higher median value at 2%. The implications of which are discussed in section 6.6.1

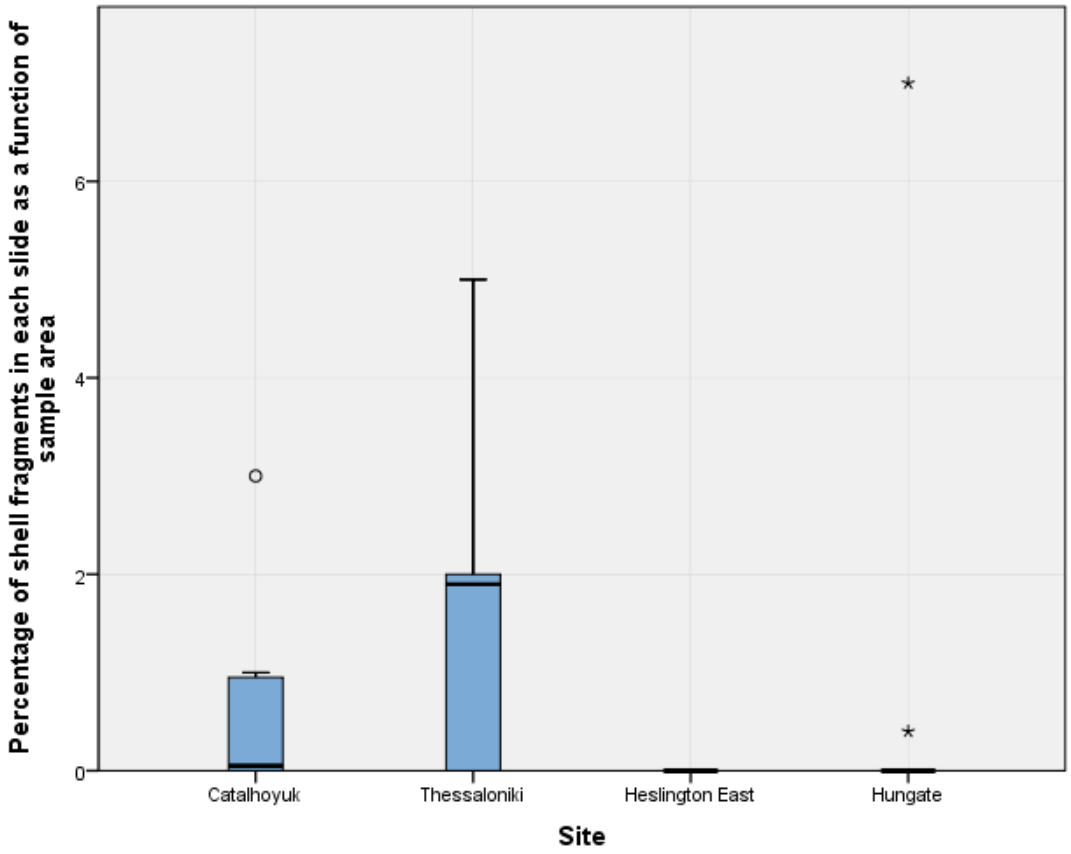

Figure 76: Box and whisker plot of shell abundance in percentages by site. Sample sizes are as follows; Çatalhöyük n=12, Thessaloniki n=26, Heslington East n=7 and Hungate n=64. '*' indicate extreme outliers more than three times higher than the extent of the box and 'o' illustrate values between x1.5 and x3 the height of the box.

6.3.2 Intra site shell variation

The intra site variation in shell abundance at Thessaloniki and Çatalhöyük was investigated further. An investigation into the shell at Hungate and Heslington East is not presented here as shell abundances were so low at both sites.

6.3.2.1 Çatalhöyük

Shell presence at Çatalhöyük was sporadic and fragmented. Grave 18666 and 19295 had median values of 0.5% and 0% respectively, and grave 18666 had a wider shell abundance range than 19295 (Figure 77).

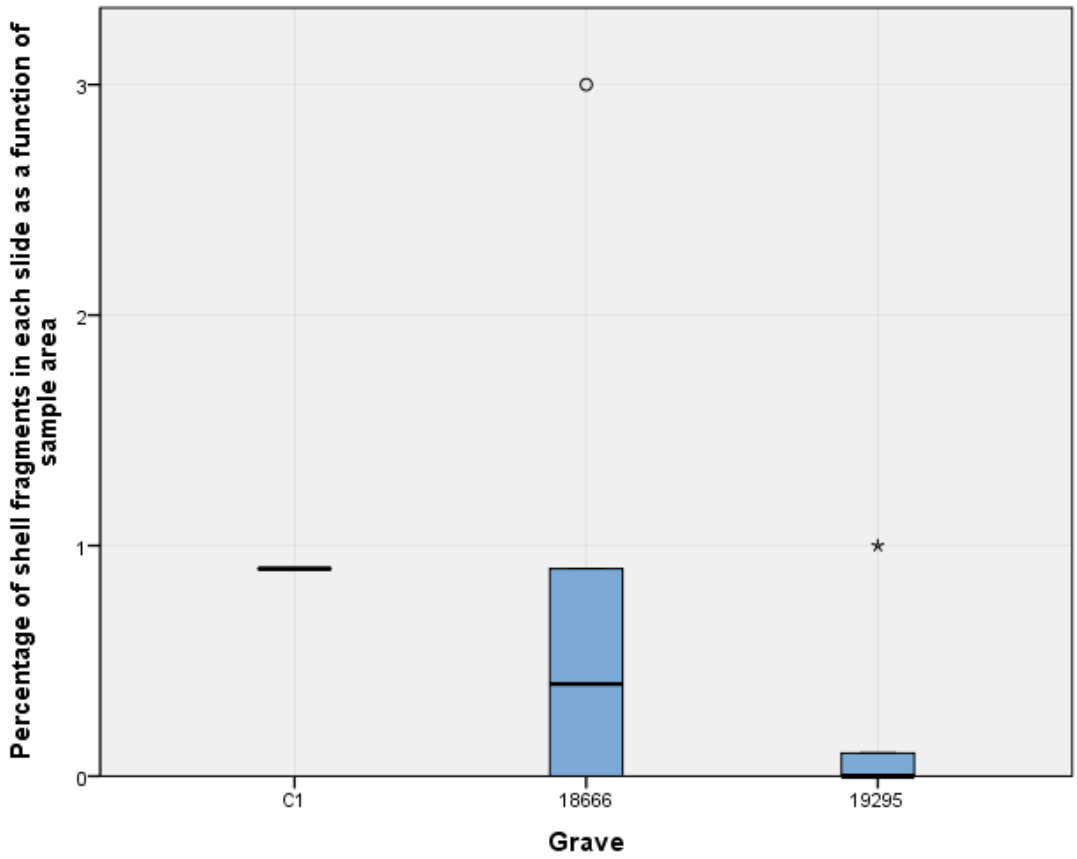

Figure 77: Box and whisker plot of shell abundances in percentage at Çatalhöyük by grave. Sample sizes are C1 n=1, 18666 n=6, 19295 n=5. '*' indicate extreme outliers more than three times higher than the extent of the box and 'o' illustrate values between x1.5 and x3 the height of the box.

6.3.2.2 Thessaloniki

Graves TF157 and TF182 had low median values of shell at 0%, however their overall ranges were similar to TF177 and TF178 at 2-3% (Figure 78). TF178 had a high median value compared to all other graves at Thessaloniki at 3.5% and TF162 the narrowest range at 0%.

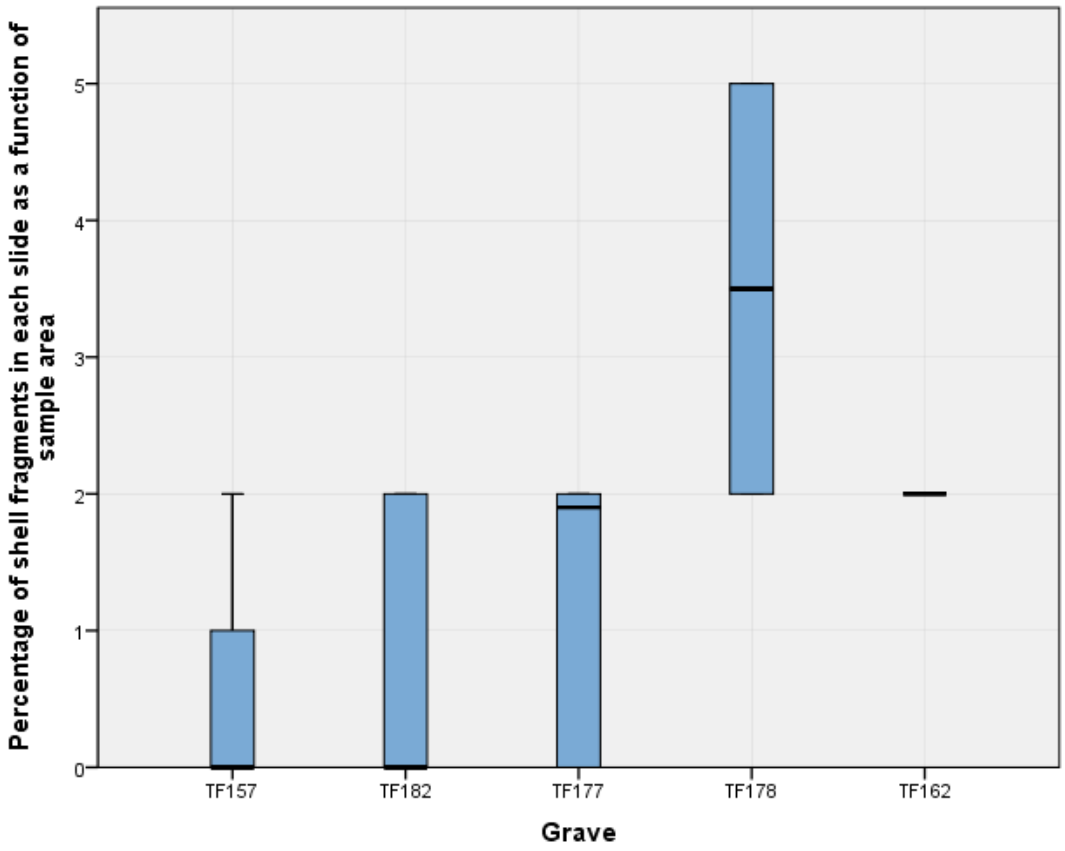

Figure 78: Box and whisker plot of shell percentages at Thessaloniki by grave. Sample sizes are as follows; TF159 n= 5, TF182 n=8, TF177 n=8, TF178 n=2 and TF162 n=3.

Shell preservation at Thessaloniki was variable, with highly weathered and fragmented shell present in all graves except TF178 (Figure 74). Evidence of gastropods was found in the pelvic sample from TF177 and the skull sample from TF178 (Figure 75). Intact snail shells were recovered from the grave bulk samples from Thessaloniki and were tentatively identified by Eva Laurie, University of York, as Pomatias elegans, a species of snail which prefers loose soils that are damp and high in calcium (Kerney, 1999).

6.3.3 Intra grave shell distribution at Çatalhöyük and Thessaloniki

Shell was sporadic in the grave controls but present in low abundances in the C2 and C3 sample from TF182 (2%), and the C3 sample from TF177 (2%). There was no systematic variation between shell abundance between the C1, C2, C3 and samples from the burial plane. There was no pattern in the distribution or abundance of shell between the skull, pelvis and foot area sample positions at either Çatalhöyük or Thessaloniki.

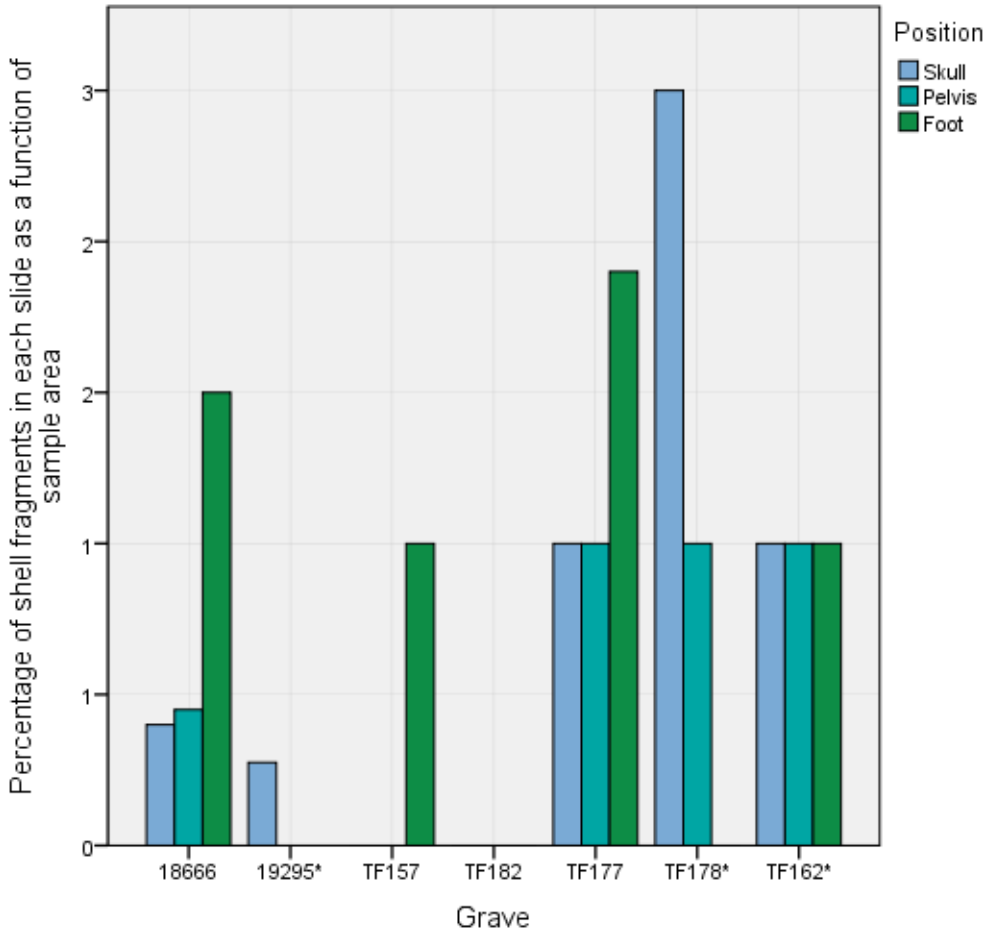

Figure 79: Percentage of shell in the skull, pelvic and foot samples at Çatalhöyük and Thessaloniki by grave. Those graves that do not have all three sample points (Skull, Pelvis and Foot) are identified by '*'. Where there is more than one sample available for a point in a grave the mean value is given.

6.4 Other organic remains

6.4.1 Fungal Sclerotia

Fungal sclerotia are a phase in the life cycle of some fungal bodies that can be observed within soils (Fitzpatrick, 1993). Fungal sclerotia were only identified at Hungate (Table 46) and were visible as single bodies and fungal clusters in the soil (Figure 80). There was no systematic variation in the presence of fungal sclerotia in relation to grave or sample position.

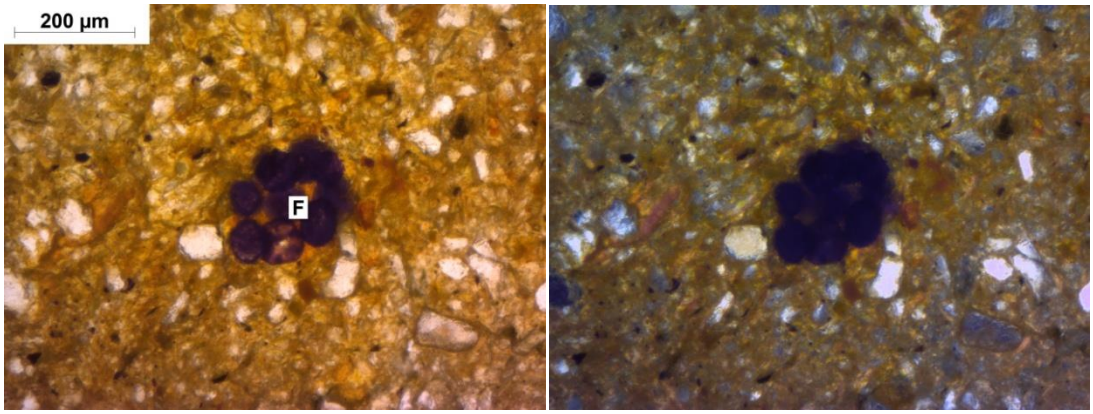

Figure 80: Clusters and single bodies of fungal sclerotia present at Hungate (F) from SK54341 in PPL (right) and XPL (left)

Table 46: Location of fungal sclerotia in the graves analysed at Hungate. '*' = the presence of fungal sclerotia, greyed out cells indicate where there was no sample available. A = adult, I = infant, LC = lead coffin, C = coffin and UC = uncoffined.

Grave number		SK54898	SK51326	SK51387	SK51351	SK54090	SK54085	SK54341	SK54342	SK51350	SK54908
Age		I	A	A	A	I	A	A	A	A	I
Burial type		LC	C	UC	C	UC	C	C	C	C	C
C2											
C3				*							
Skull	Perp			*							
	Para					*			*		
Pelvis	Perp								*	*	
	Para										
Foot	Perp										*
	Para										
Other								*			
C1		1-16cm				27-36cm			49-58cm	*	

6.4.2 Phytoliths

Phytoliths were present in the foot sample from 18666, Çatalhöyük and were distributed in clusters and linear formations (Figure 81). The cluster phytolith formation was tentatively identified by Lisa Shillito, University of Edinburgh, as a cereal husk.

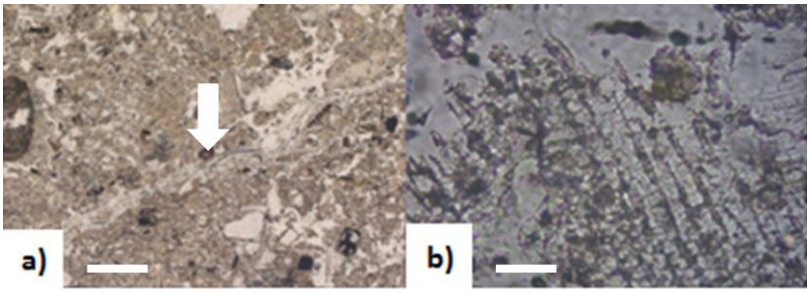

Figure 81: a) linear phytoliths from the foot sample from 18666 in PPL scale = 300µm, b) clustered phytoliths in the foot sample from 18666 in PPL. Scale = 100µm.

6.4.3 Roots

Roots were only present at Heslington East and then in low quantities (2%), in the hand area, C3 and the upper soil profile samples. All of the root fragments were partially decomposed, except in the hand area sample where the roots appeared less degraded (Figure 82), although the reason for this is unclear it may be due to natural variation.

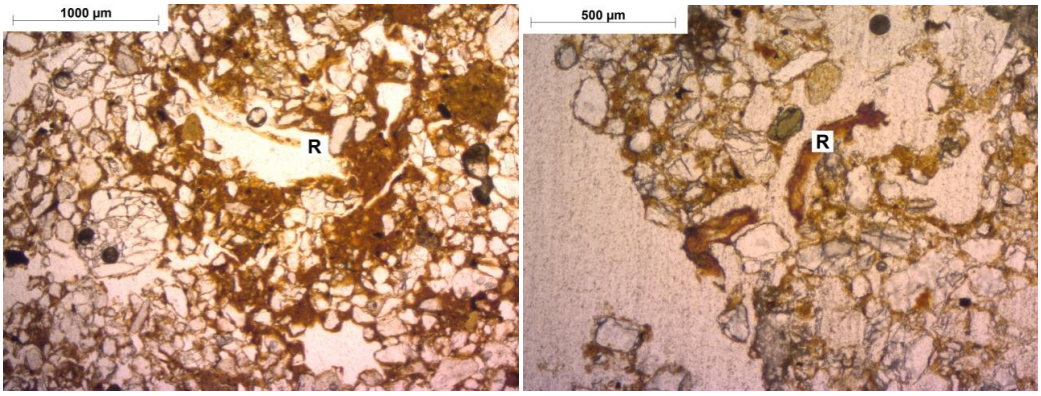

Figure 82: Roots (R) in thin section shown in PPL. Left = root from the hand sample and right = root from the 46-52 cm soil profile.

6.5 Organic coarse components by microfabric type

The distribution of organic coarse component across microfabrics was calculated (Table 47) to ascertain if any of the microfabrics were contributing to high concentrations of organic coarse components in the grave. Bone was present in nine microfabrics at low levels (≤2%). Charcoal, however, was present in all microfabrics except HU6 and Ti2 and in high concentrations in CH5 and HU9. CH5 was composed of high abundances of randomly orientated charcoal and possibly related to oven rake out of dump deposits at Çatalhöyük (3.2.4). HU9 was a grave specific microfabric to SK54898. Shell was absent from the Heslington East microfabric and from the majority of the microfabrics at Hungate only appearing in HU5. Shell was however present in the most common microfabrics at Çatalhöyük (CH4) and Thessaloniki (Ti1), but otherwise scarce. Phytoliths, roots and fungal sclerotia were sporadic throughout all microfabrics.

Table 47: Organic coarse components by microfabric type, shown as percentage of each microfabric area. The calculation for bone fragments in HU7 excludes the large piece of bone that composes the majority of the microfabric.

Site	Microfabrics	Shell	Charcoal	Bone	Phytoliths	Roots	Fungal sclerotia
Çatalhöyük	CH1	0.20	0.20	0.50			
	CH2		1.33	0.33			
	CH3		0.33				
	CH4	0.42	3.75	1.17	0.58		
	CH5		13.33				
	CH6		6.67				
Thessaloniki	Ti1	1.24	0.84	3.00		0.08	
	Ti2			2.50			
Hes East	HE1		3.44	1.11		2.00	
Hungate	HU1		3.88				
	HU2		3.33				
	HU3		3.40				
	HU4		0.50				
	HU5	0.33	5.00	0.33			
	HU6						
	HU7		2.00				
	HU8		2.57				0.14
	HU9		20.50				
	HU10		4.00	0.60		0.20	
	HU11		1.00				
	HU12		2.68				0.18
	HU13		2.38	0.54			0.07

6.6 Summary and discussion of the organic material data

The aim of the analysis was to identify the composition, abundance and distribution of the organic coarse material and any systematic patterns in its distribution that might relate to the presence of the grave. The variation was assessed on three levels; inter site, intra site and intra grave. Bone, charcoal and shell were the most abundant organic coarse material classes and were present at multiple sites. Phytoliths, fungal sclerotia and roots were only identified sporadically; therefore they will be investigated only briefly, with the final section of the discussion focused on the distribution of all organic coarse components in the microfabrics.

6.6.1 Inter site variation

The inter site variation in organic material was primarily caused by differences in the depositional pathways of bone, charcoal and shell as well as being influenced by burial practice, soil composition and microenvironment. Bone and charcoal were widespread at Çatalhöyük, Thessaloniki, Heslington East and Hungate, and shell was common at Çatalhöyük and Thessaloniki. Bone, charcoal and shell have different depositional processes and survival rates in the archaeological record, which has influenced their inter site distribution patterns.

The preservation of bone and shell is influenced by soil pH (Behrensmeyer, 1978, Gordon & Buikstra, 1981, Weiner, 2010), age of skeleton/shell (Gordon & Buikstra, 1981), broad regional climate, burial conditions, vegetation (Behrensmeyer, 1978, Claassen, 1998), soil temperature and soil microorganisms (Behrensmeyer, 1978, Claassen, 1998, Piepenbrink, 1986). The soil microenvironment can also contribute to localised instances of unusual preservation and decomposition (Bell *et al*., 1996). Bone was present in all sites and in most of the samples analysed. Bone survival relies primarily on soil pH and early bone taphonomy (Nielsen-Marsh et al., 2007). The shape, size and maturity of bone are also a factor (Gordon & Buikstra, 1981, Henderson, 1987), particularly over smaller scales where soil conditions and pre-burial treatments are similar. The bone abundance distributions (Figure 56) for Heslington East and Hungate had a similar shape although their sample sizes were very different (Heslington East n=7 and Hungate n=64). pH showed a small amount of variation with Hungate giving a pH of 7.2-8.3 and Heslington East slightly lower with a value of 6.2-7.2 (see Appendix 1.1.1), suggesting that pH did not vary significantly enough to create large differences in the bone assemblage. Similar burial practices occurred at Heslington East and Hungate suggesting that similarities in pre-burial treatment may also have influenced the pattern seen in the bone assemblages at Hungate and Heslington East. They were, however, both located in similar soil types (see 2.2), which may help account for their overall similarities. Çatalhöyük and Thessaloniki are older sites and situated on calcareous soils or contain high levels of calcareous material (Ghilardi *et al.*, 2008a, Matthews *et al.*, 2013), conditions favourable to bone preservation, which may account for the higher abundance of bone at the two sites compared to Hungate and Heslington East.

Gastropod shell is generally composed of aragonite (Weiner, 2010) and is considered less stable in the archaeological environment than either bone or calcite based shells (mollusc and egg shells) (Weiner, 2010). The survival of gastropod shell at Thessaloniki and shell at Çatalhöyük implies that the soil pH hasn't dropped below seven for a significant period of time, since the shells were deposited otherwise they would have dissolved (Weiner, 2010 p.160). Calcareous microfabrics were identified at Thessaloniki (see section 3.3 for Thessaloniki and 3.2 for Çatalhöyük) which was situated on a soil developed from secondary calcium carbonate and alluvial deposits (Ghilardi *et al.*, 2008a) and Çatalhöyük which was located on an alluvial basin (Rosen & Roberts, 2005). Several depositional pathways for shell can, therefore, be proposed for Thessaloniki and Çatalhöyük 1) shell was present in the environment and unrelated to human agency, 2) the intentional introduction of shell as part of a burial rite and 3) the un-intentional introduction of shell into the burial by human agency. Pomatias elegans, a species of snail which prefers loose soils that are damp and high in calcium (Kerney, 1999), was recovered from the grave bulk samples from Thessaloniki as intact shells. Its presence is generally taken to indicate some form of soil disturbance, as Pomatias elegans preferred soil in which it is able to burrow (Evans, 1972) and would support the presence of loose highly calcareous bare soils at Thessaloniki. Shell was not detected in Ti2, the highly calcareous microfabric from Thessaloniki (Table 47), ruling Ti2 out as a possible source. The sediment used to construct the Çatalhöyük mound was calcareous (Matthews *et al.*, 2013) and sourced from the local alluvial environment (Matthews, 1996, Stokes, Unpublished BSc Dissertation). Instances of fragmented shell have been observed in the sediments surrounding Çatalhöyük, as well as being common in the building material at the site (Matthews, 2006, Stokes, Unpublished BSc Dissertation), suggesting that shell may have been present in the sediments before burial occurred. The absence of any shell at Heslington East and Hungate may be a product of local soil environments or the material may not have been deposited on site. In order to distinguish between these two hypothesis one would need to establish if shell had been recovered from any of the contexts excavated at the two sites, this would then give an indication as to whether shell was being deposited more generally and if it was surviving on site. Inter site comparisons between the control and graves sample shell abundances will be discussed in section 6.6.2.1 to investigate this further.

The charcoal data demonstrates a scarcity of charcoal at Thessaloniki compared to the other three sites. The differences between the sites have been caused by either 1) different

rates of charcoal degradation through microbial attack, 2) different charcoal production and deposition rates or 3) differences in the net loss of charcoal from the soil through alluviation. Examining the pattern of charcoal abundance at an inter and intra site level will help distinguish between different charcoal depositional pathways. Charcoal can be produced through natural means such as wildfires or through human agency by the burning of vegetable matter as fuel (Scott & Damblon, 2010). It is likely that the rates of charcoal production and deposition at each site will vary depending on the proximity of the site to sources of anthropogenically produced charcoal as well as the frequency of wildfires in the area. At Çatalhöyük charcoal was being regularly produced on site through the burning of fuel for cooking (Matthews, 2006, Shillito *et al.*, 2011b). Charcoal is also ubiquitous at Çatalhöyük due to its incorporation into the source sediments for building materials (Matthews, 2006). Charcoal may also have been incorporated into the alluvial deposits used to build Çatalhöyük from further afield, as the Konya basin has a large catchment area (Forbes *et al.*, 2006, Rosen & Roberts, 2005). Heslington East and Hungate were both Roman in date (see sections 2.2.4 and 2.2.6). Hungate was situated close to a Roman fort where there is likely to have been burning occurring, either from domestic fires for cooking and warmth or industrial activity in the area. In addition to this Hungate is located close to the River Foss and some sediments at the site have been identified as alluvial (section 3.5.4), indicating that charcoal may have been transported to the site from the rivers catchment area (Forbes *et al.*, 2006). Heslington East is more difficult to resolve as it is located on the outskirts of York on what is now agricultural land. It was, however, part of a Prehistoric to Roman settlement and the charcoal may have originated from settlement activity. Thessaloniki had much lower levels of charcoal compared to the other sites. Roman and Hellenistic burial practices included cremation and the burning of ritual food offerings (Garland, 1971, Hope, 2007) practices that would have necessitated onsite burning. If these practices were occurring at Thessaloniki and with the proximity of the cemetery to the settlement it is reasonable to assume that there would have been charcoal present at the site. Whether charcoal was effectively incorporated into the soil, however, is not known. It is also possible that, once buried, the charcoal didn't survive well either because there was more microbial activity here than in other sites or that combustion was occurring at lower temperatures resulting in a more degradable charcoal product (Baldock & Smernik, 2002, Scott *et al.*, 1986).

6.6.2 Control vs, burial plane samples and distinguishing different graves (intra site variation).

6.6.2.1 Control vs burial plane samples

There are multiple depositional pathways by which bone may have entered the archaeological record; 1) bone fragments may originate from skeletal decomposition, 2) from the decomposition of grave goods, 3) offerings or ritual feasting or 4) fragmented bone may have accidently become incorporated into the grave due to bone fragments being present in the soil. At Çatalhöyük fragmented bone had been deposited under one of the skulls from 19295, suggesting that bone may have been deposited *in situ* from the fragmenting skeleton. Bone was sporadic in the C1 samples and only present in Çatalhöyük at abundances comparable to the grave contexts, supporting the fact that bone at Çatalhöyük had a site wide distribution and was not specific to grave context. Bone objects were also included in burials as part of the ritual practice at Çatalhöyük (Hamilton, 1997) and fragmented bone is routinely found in non burial contexts where it had become incorporated into building material and floor deposits (Matthews, 2006), which may also account for the high abundance of bone in the Çatalhöyük C1 sample (Figure 57). Hungate bone was absent from the C1 samples, indicating that either the C1 samples taken were not representative of the underlying soil conditions or that bone was concentrated in the burial. Bone was generally sporadic at Heslington East with the only examples present in the C2 and skull area samples. There was no C1 sample from Thessaloniki therefore abundances in the grave controls must be considered; bone was absent from the C2 and C3 from TF182 but present in the C3 from TF177. The C3 sample is taken near to or in some cases in the burial plane, therefore the presence of bone in the C3 sample of TF177 may not be a good indicator of general bone abundance on site, but the absence of bone from the C2 and C3 samples from TF182 would imply that bone was sporadic, if present, in the general grave back fill. As a comparison the C2 and C3 samples from the other site will be considered. Bone is present at similar levels to the C1 in the C2 and C3 samples from Çatalhöyük, again reinforcing that bone was not burial specific, whereas at Hungate bone remains sporadic in the C2 and C3 samples suggesting that bone maybe localised in burial contexts. Graveside feasting as well as food offerings to the dead was a feature of Hellenistic and Roman burial practice (Garland, 1971, Hope, 2007), and are both possible mechanisms for bone fragments to become incorporated into the grave soil at Thessaloniki,

Heslington East and Hungate. Charcoal was common in the C1, C2 and C3 samples at all sites, again supporting that charcoal is present in non-burial contexts meaning that charcoal is likely to be an incidental inclusion in grave formation.

Shell was present in the C1 Çatalhöyük sample implying that the shell found in the burials at Çatalhöyük was accidently incorporated into the backfill. Shell however has been observed as part of the burial practice at Çatalhöyük, therefore a ritual origin can not be completely discounted (Hamilton, 1997). There was no C1 sample from Thessaloniki, however all three available grave controls contained shell fragments indicating that shell may have been present in Ti1 and therefore incorporated into the burial unintentionally.

6.6.2.2 Distinguishing different graves

Although, at some sites, bone, charcoal and shell was not specific to burial context, there were several examples of organic coarse materials concentrating in specific graves. Bone concentrated in SK51326 and SK51387 at Hungate as well as some graves with no bone fragments; SK54908, SK54898, SK54341 and SK54085 (Figure 61). At Hungate there may be a spatial effect on the abundance of bone, as SK54898 was located centrally and the other three graves where bone fragments were absent where located in the northern area of the cemetery (Figure 9). Bone also varied at Thessaloniki where TF177 had a wider distribution of bone abundance between samples compared to the other graves.

18666 at Çatalhöyük had a higher mean charcoal abundance and broader range than 19295 and the C1 (Figure 68). The two Çatalhöyük graves had differences in burial practice with 18666 being an articulated crouched burial and 19295 being two disarticulated skulls. Interestingly 19295 had a lower abundance of charcoal but contained what was identified as carbonised material in the cavity of one of the skulls. With such a low sample size it would be difficult to argue that the difference observed in the charcoal abundance between 19295 and 18666 was anything more than circumstantial. There were also a limited number of C1 comparisons at Çatalhöyük, again making any firm conclusions on the origins of large amounts of charcoal in 18666 difficult. Charcoal was also particularly high in SK54898 the lead coffined grave at Hungate compared to the C1 sample and the other nine graves (see Figure 71). The remaining nine graves have median charcoal abundances similar to the C1 suggesting that the high abundance of charcoal in SK54898 is a 'real' concentration. SK54898 is located in the centre of the cemetery (Figure 9) away from all of

the other graves meaning that the high concentration in charcoal may be due to its location. Cremations, feasting at the grave side are some of the Romano-British burial practices that may have contributed to high concentrations of charcoal (Boylston *et al.,* 2000. Going *et al.,* 1997, Morris, 1986). High concentrations of charcoal may also be related to environmental or taphonomic causes. The environment inside the lead lined coffin was very sheltered compared to other graves, with the lead coffin acting as a barrier. It is possible that the lead coffin allowed charcoal to enter but not to exit through the bottom preventing charcoal from being washed out of the coffin, causing it to concentrate. However this hypothesis is only based on circumstantial evidence. TF178 had high median shell abundances compared to the other graves at Thessaloniki. TF178 was the double burial of an infant with an adult. Upon excavation there was calcium carbonate plaster identified on the infant skeleton. The inclusion of the calcium carbonate plaster on this burial may have influenced the preservation of shell by increasing the pH. If the plaster material used to coat the graves came from the same origin as Ti2 it is unlikely that shell was introduced into the burial in the plaster material as shell was absent from Ti2.

6.6.3 Variations in the burial plane (intra grave variation).

When the samples from the burial plane are considered there were clear differences in the distribution of bone and charcoal, with peak abundances in the pelvic area and skull areas respectively. These differences may be caused by taphonomic process in the burial environment induced by the presence of a grave or burial pit. Shell, although common at Thessaloniki and Çatalhöyük, did not demonstrate any variation in abundance along the burial plane.

The bone data showed that 42% of all complete graves have elevated abundances of bone fragments in the pelvic area. This rise, however, is site specific with Thessaloniki containing 50% of complete graves with elevated levels of bone in the pelvic area, Hungate 28% and Çatalhöyük 100% (Heslington East did not contain a complete grave). High levels of bone in the pelvic area sample also appears to correlate with the presence of large bone fragments (>1000µm). An aspect that requires clarification is whether the bone fragments originate from the presence of the skeleton, were already present in the soil, or where part of grave goods and funerary offerings. The bone fragments were not large enough to identify to species, therefore, it is not possible to confirm if the fragments originated from the

skeleton. As mentioned above, the comparison between the controls and grave samples at Thessaloniki and Hungate suggests that the bone is related to the burials. At Heslington East, however, the presence of bone in the graves is likely to be circumstantial and a product of natural variation in the abundance of organic coarse material rather than an artefact of human agency. Bone, however, is ubiquitous at Çatalhöyük, therefore suggesting that the abundances of bone in the burial plane in 18666 and 19295 were circumstantial. The pelvic bone, where the bone peaks were observed, was identified by Henderson (1987) as susceptible to crushing and fragmentation due to the weight of the soil overburden and their large irregular shape. Henderson (1987) also noted that surface area to volume ratio has an impact on the survival rate of bone. The location of peaks in the bone abundance in the pelvic area samples at all sites suggest that it is either a product of skeletal degradation due to the structure of the pelvis or due to a common burial rite. The former is more likely however, as the bone peaks appear in vastly different geographic locations, periods and burial traditions. The visibility of bone peaks in the pelvic area was also modified by the location of the burial in the cemetery. At Thessaloniki two graves TF177 and TF182 contained peaks of fragmented bone in the pelvis and were located close to walls or within structures. Those graves that were in more open areas, TF157 and TF162, however similar bone abundances in the skull, pelvic and foot samples. At Hungate the abundances of bone was also spatially modified with fragmented bone peaks in the pelvic area in those graves in the northern part of the cemetery.

The charcoal data showed that when all graves are considered, 80% of complete graves had elevated levels of charcoal in the skull area. Once again these results were site specific with Thessaloniki and Hungate showing charcoal peaks in the skull at 66% and 85%, respectively, of complete graves. The only complete grave at Çatalhöyük, however, did not have a charcoal peak in the skull. Heslington East contained one incomplete grave. The skull and foot area samples, however, showed a peak in charcoal abundance in the skull. The peak in charcoal at the head of the burial may be caused by 1) naturally high levels in the soil (i.e. circumstantial), 2) the inclusion of charcoal in the head end of the grave as part of a burial rite, or 3) due to common taphonomic processes that will now be discussed further. The graves were located in different parts of the cemetery and in different orientations at Hungate and Thessaloniki making a circumstantial cause of high concentrations of charcoal in the skull area unlikely. Some Hellenistic and Roman burial practices involved the burning of offering pyres at the graveside (Garland, 1971, Hope, 2007), however there was no

mention of the remains being included with the burial. A further possibility is a taphonomic origin of the distribution of charcoal in the burial. Coffins act as a barrier to liquids effectively moving into the surrounding soil, trapping liquids in the burial void (otherwise known as the 'bucket effect' Dent 2002). Charcoal is low density and floats. Therefore, if present in the coffin, charcoal fragments would have been able to circulate in the decomposition liquids. This scenario also does not account for how charcoal became distributed in the non-coffined graves. The mechanism for charcoal becoming preferentially located in the skull area, however, is at this point unknown.

6.6.4 Rare organic coarse materials; phytoliths, fungal sclerotia and roots

The phytoliths observed in the foot area sample from 18666 were probably related to burial practices; specifically the inclusion of plant material such as basketry within which the body was placed (Wendrich, 1995) or from binding the body before it was buried (Nakamura *et al.* 2005). Similar linear phytolith formations have previously been interpreted as the remains of matting (Matthews, 2006). However, the phytoliths were only found in the foot sample from 18666, and not in the samples from the rest of the grave or 19295. The foot sample itself was damaged during processing creating a slide that was less than 30µm in places. This may have made the phytoliths more visible in the slide as the clustered phytoliths appeared within areas of damage. It is, therefore, perhaps not a true representation of the phytolith distribution within the grave. Fungal sclerotia and roots were site specific and of limited use as they did not show a systematic relationship between their presence and either burial practice or sample location.

6.6.5 Organic coarse components by microfabric type

Bone, shell, phytoliths, roots and fungal sclerotia were not concentrated in any of the microfabrics identified at Çatalhöyük, Thessaloniki, Heslington East or Hungate. Charcoal however was concentrated in two microfabrics CH5 and HU9. CH5 was evenly distributed between the graves at Çatalhöyük; it was therefore not responsible for the high abundance of charcoal in 18666. HU9 had a charcoal abundance of 20.5% (Table 47) and was exclusive to SK54898 (Table 9) which had a high median charcoal abundance (4.5% Figure 71) compared to the other graves and C1 at Hungate. The other microfabrics present in SK54898 (HU1, HU2, HU3, HU6, HU12 and HU13 see microfabrics chapter) had charcoal abundances ≤ 4.5%, and of those, HU2 and HU6 were exclusive to SK54898 and ranged in

charcoal abundance from 0-3.33%; meaning that it was the microfabrics themselves (HU9) that were high in charcoal which in turn raised the overall charcoal abundance of SK54898.

6.7 Conclusions

Bone and charcoal were the most abundant coarse organic material and were present in a large number of the samples. These two materials also appear to have the strongest relationship to burial practices and, on a broad scale, to on site depositional and taphonomic processes. Bone fragments appear to have originated from the burials at Hungate and Thessaloniki due to a lack of bone in the control samples, whereas charcoal and shell look to be circumstantial and a product of natural variation in the abundance of organic coarse material rather than an artefact of human agency. Bone and charcoal however were good potential indicators of grave orientation with clear relationships between the skull area and charcoal abundance in a majority of the graves and a less dramatic, but equally important relationship between the pelvic area and elevated levels of fragmented bone. The causes of this relationship appear to be taphonomic process within the graves and are not strongly related to burial practice or to soil conditions. However in sites such as Çatalhöyük the on-site soil conditions may be obscuring any patterns present. More sporadic organic coarse components (phytoliths, roots and fungal sclerotia) were only diagnostic of burial practices in specific cases such as the phytoliths at Çatalhöyük.

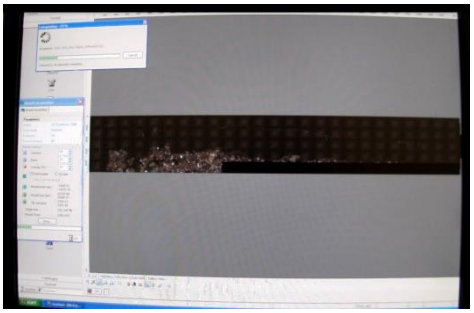

7 Soil Structure

Two interrelated aspects of soil structure will be considered in this chapter, pedality and void space. Pedality and void space are relevant to the interpretation of the grave environment, as they are key diagnostic features for soil formation processes such as compaction, wetting and drying and freeze thaw, as well as evidence for biological activity (Birkeland, 1984, Bottinelli *et al.*, 2010, Brewer, 1964, Bullock *et al.*, 1985, FitzPatrick, 1993, Fortun *et al.*, 1990, Stoops, 2003, VandenBygaart *et al.*, 2000). In addition, void morphology and abundance are also crucial for ascertaining the directionality and availability of soil water, as well as the mobility of materials in solution and bacteria within soils (Pagliai & De Nobili, 1993, Pagliai & Kutilek, 2008a, Van Veen & Kuikman, 1990). In grave environments, studying the soil structure and the location of peds in the burial plane and control samples may give an indication as to the rate and extent of any soil collapse through the identification of compaction features. The investigation of the void space will allude to the available surface area for cation exchange, as well as indicate the connectivity of pore space and, therefore, the ease with which chemicals can move from the body into the surrounding soil structures. To this end, the shape and abundance of peds and voids will be considered. Where possible and appropriate, the structure will be assessed on three levels;

- Inter site (Çatalhöyük, Thessaloniki, Heslington East and Hungate).
- Intra site (Çatalhöyük, Thessaloniki and Hungate).
- Intra grave (Çatalhöyük, Thessaloniki, Heslington East and Hungate).

7.1 Peds

7.1.1 Inter site variation

Sub-angular blocky peds and apedal soils were present at all sites. Hungate and Çatalhöyük contained the highest degree of ped variation with six ped types, angular and sub-angular blocky, crumbs, granules, plates and apedal soils. Thessaloniki contained four ped types; sub-angular blocks, crumbs, apedal soils and platy peds. Heslington East showed the least amount of variation with sub-angular blocky and platy peds as well as apedal soil. Differences in ped types generally relate to differences in the soil texture and stress factors in the soil. What may have caused ped differences between sites will be discussed further in section 7.3.1.

7.1.2 Çatalhöyük

7.1.2.1 Intra site variation in peds at Çatalhöyük

The C1 at Çatalhöyük contained sub-angular blocky peds, granules and apedal soils, all of which were also present in graves 18666 and 19295 (Table 48). In addition, 18666 contained angular blocky peds and 19295 contained crumbs, angular blocky peds and plates.

7.1.2.2 Intra grave variation in peds at Çatalhöyük

Sub-angular blocky peds and granules were abundant in the C1 and throughout graves 18666 and 19295 (Table 48). The sub-angular blocky peds however were more developed in the burial plane samples than in the C1. The size of peds varied slightly with the C1 containing very fine to medium sized primary granular peds whereas the granular peds in the graves were limited to fine and below. The sub-angular blocks in the C1 and grave 19295 were also sized between ultra fine and medium where as in grave 18666 they only ranged between ultra fine and fine. Meaning that, in general, the peds were smaller in the graves than in the C1 samples. Apedal soils were abundant in grave 18666 and were at high abundances in the perpendicular samples in both graves. In 19295 the granular peds where the primary peds that had developed with sub-angular blocky peds being secondary, apart from the samples from skull 19501 where sub-angular blocky peds were the only peds present in the perpendicular sample and angular blocky peds and crumbs were primary in

the parallel sample. The samples from grave 18666 however contained sub-angular blocky and crumb primary peds.

Table 48: The percentage of peds present in each slide in 18666 Çatalhöyük and the C1 sample, as a percentage of sample area. Red indicates weak ped development, yellow moderate ped development and green strong ped development. Numbers in brackets indicate primary ped (1), secondary peds (2) and so on where applicable according to Stoops (2003 p. 60). Size range key; UF = ultra fine, VF = very fine, F = fine, M = medium, C = coarse and VC = very coarse according to Bullock *et al*(1985 pp 42).

Location	Orientation	Apedal	Sub-angular blocky	Angular blocks	Granules	Plates	Crumbs
C1		2%	76% (2) UF-M		95% (1) VF-M		
18666							
C3		85%	15% (1) UF-VF				
Skull	Perp	90%	19% (1) UF-VF		9% (1) UF-F		
	Para	22%	43% (1) F	10% (1) UF	26% (1) F		
Pelvis	Perp	96%	12% (1) UF-VF		4% (1) UF-F		
	Para	10%	80% (2) VF-C		12% (1) VF-F		
Foot	Perp	100%					
19295							
C3			44% (2) UF-VF		9% (1) UF	43% (2) F-C	
Skull 19500	Perp		67% (2) VF-F		33% (1) UF-F		
	Para	5%	95% (2) VF-F		15% (1) UF		
Skull 19501	Perp	79%	21% (1) UF-VF				
	Para		35% (2) UF-M	12% (1) UF			75% (1) UF-M

7.1.3 Thessaloniki

7.1.3.1 Intra site variation in peds at Thessaloniki

Sub-angular blocky peds were present in all five Thessaloniki graves (Table 49). In addition to this, crumb peds were present in all but TF157 and apedal soils in all but TF162. Plates were sporadic and only visible in TF177.

7.1.3.2 Intra grave variation in peds at Thessaloniki

There was no C1 sample taken from Thessaloniki, however two of the graves TF177 and TF182 contained controls from the burial fill (Table 49). The C3 sample from TF177 contained sub-angular blocky peds in similar abundances and sizes to the grave samples. They were however moderately developed in the C3 but weakly developed in the grave (Table 49). The C3 sample also contained platy peds, as did the perpendicular skull sample.

In TF182 (Table 49) the C2 and C3 samples both contained sub-angular blocky peds which were poorly developed in the C2 but moderately developed in the C3. Compared to the sample from the burial plane the control samples from TF182 had more ped development, the grave soils mostly contained apedal material, with the exception of well-developed crumb peds in the foot at 24% abundance, which may indicate the presence of bioturbation in the foot area however this will be further explored in the discussion. The size of the peds however did not show a distinct variation between the control samples and those from the burial plane.

Sub-angular blocky peds and apedal soils were common in the graves from Thessaloniki and were present in most of the samples. TF162 was a slight exception to this as although sub-angular blocky peds were abundant there were also moderately to strong developed crumbs in all of the samples. In addition to this TF178 contained strongly developed sub-angular blocky peds. The platy peds present in the perpendicular skull sample from TF177 were coarse therefore quite large compared to the other peds in that grave; otherwise there was no systematic distinction in ped size in the Thessaloniki graves. There was, however, no systematic pattern, which occurred in every grave at Thessaloniki, in the spatial distribution, the abundance or occurrence of peds, or their development. In TF157 sub-angular blocky peds were the primary ped type, however in TF162, TF177, TF178 and TF182 where other peds types were present they were primary and the sub-angular blocky peds become secondary peds.

Table 49: The percentage of peds present in each slide in Thessaloniki, as a percentage of sample area, showing ped development. Red indicates weak ped development, yellow indicated moderate ped development and green indicates strong ped development. Numbers in brackets indicate primary ped (1), secondary peds (2) and so on where applicable according to Stoops (2003 p. 60). Size range key; UF = ultra fine, VF = very fine, F = fine, M = medium, C = coarse and VC = very coarse according to Bullock *et al*(1985 pp 42).

Location	Orientation	Apedal	Sub-angular Blocky	Crumbs	Plates
TF157					
Skull	Para	30%	60% (1) UF-F		
Pelvis	Para	30%	100% (1) M-C		
Foot	Para	0%	100% (1) M-C		
Hand	Perp	80%	20% (1) VF-M		
TF162					
Skull	Para		60% (2) VF-F	30% (1) UF-F	
Pelvis	Para		90% (2) VF-F	10% (1) VF-M	
Foot	Para		90% (2) UF-F	10% (1) UF-VF	
TF177					
C3			80% (1) F-M		20% (2) VF-M
Skull	Perp	40%	30% (2) UF-VF		30% (1) M-C
	Para		90% (2) F	10% (1) UF-VF	
Pelvis	Perp	30%	100% (2)UF-VF	60% (1) UF-VF	
	Para	10%	90% (1) UF-F		
Foot	Perp	10%	90% (1) UF-M		
	Para		100% (1) VF-F		
Hand	Perp	30%	70% (1) F-M		
TF178					
Skull	Para	30%	100% (1) F-M		
Pelvis	Para		80% (2) VF-M	20% (1) UF-VF	
TF182					
C2			100% (1) F-M		
C3			100% (1) F-C		
Skull	Para	37%	63% (1) VF-C		
Pelvis	Perp	100%			
Foot	Para	90%	86% (2)UF-F	24% (1) M-C	
Hand	Perp	100%			
	Para	100%			

7.1.4 Heslington East

7.1.4.1 Intra grave variation in peds at Heslington East

The C1 soil profile from Heslington East showed an increase in apedal soil with depth, from 30% in the 22-28 cm sample to 100% in the 46-52 cm sample (Table 50). The abundance of apedal material then decreased into the grave, with 80% in the C2 and 50% in the skull, indicating that there had been more ped development in the burial plane. Sub-angluar blocky peds were the primary ped type in all of the grave samples at Heslington East apart from the C2. Moderately developed sub-angular blocky peds increase from 70% in the 22-28 cm sample to 100% in the 74-80cm sample, but were absent from the 46-52cm C1 sample, and decreased in the skull (50%) and foot samples (40%). In the upper (C2) and lower (C3) samples there was a marked increase in the abundance of plates from 20% to 70%. The hand sample, which was taken directly over the pelvic area, contained 100% moderately developed coarse platy peds and the foot sample 60% strongly developed coarse platy peds, which are possibly the result of compaction (Kooistra & Tovey, 1994). The size of the sub-angular blocky peds were generally very coarse in the control and the grave samples, however there were finer sub-angular blocky peds present in the burial plane.

Table 50: The percentage of peds present in each slide in 713 Heslington East and the C1 sample, as a percentage of sample area, showing ped development. Red indicates weak ped development, yellow indicated moderate ped development and green indicates strong ped development. Numbers in brackets indicate primary ped (1), secondary peds (2) and so on where applicable according to Stoops (2003 p. 60). Size range key; UF = ultra fine, VF = very fine, F = fine, M = medium, C = coarse and VC = very coarse according to Bullock *et al*(1985 pp 42)

	Apedal	Sub-angular blocky	Plates
C1 22-28cm	30%	70% (1) C	
C1 46-52cm	100%		
C1 74-80cm		100% (1) M-C	
C2	80%		20% (1) VC
C3		30% (1) F-M	70% (2) VC
Skull (para)	50%	50% (1) UF-C	
Foot (para)		40% (1) F-M	60% (2) C
Hand (para)			100% (1) C

7.1.5 Hungate

7.1.5.1 Intra site variation in peds at Hungate

All three C1 samples from Hungate were 100% apedal (Table 51). All graves also contained apedal material along with sub-angular blocky peds. In addition to apedal soils and sub-angular blocky peds, SK54898 and SK54342 contained angular blocky peds. SK51326, SK54341, SK54908 and SK51350 contained plates and SK51387, SK54342, SK54908 and SK54085 contained crumb peds. Granules were rare and confined to SK54341. The implications of which will be discussed in section 7.3.

7.1.5.2 Intra grave variation in peds at Hungate

As stated above, the C1 samples from Hungate were 100% apedal. The majority of control samples from the burial fill also contained a high abundance of apedal soil, as well as other ped types (Table 51). The C2 and C3 samples from SK51326 were unusual as they, like the C1 samples, contained 100% apedal material. However, the grave samples from SK51326 contain a greater diversity of ped types with sub-angular blocky peds and platy peds present, although apedal material was still in high abundance in the pelvic and perpendicular foot area samples (70-90%). The majority of grave controls had a ped profile similar to the grave samples especially the C3 samples, which is probably a reflection of some C3 samples being taken from the burial plane. Apedal soils and sub-angular blocky peds were common in the Hungate graves (Table 51). Sub-angular blocky peds ranged from weakly to strongly developed, were ultra fine to coarse in size, and were generally present at above 50% when observed in a sample. However, SK54090 and SK54085 went against this general trend. Although sub-angular blocky peds were common in SK54085, there was a lack of apedal material in the C3 and grave deposits. In addition to sub-angular blocky peds, well-developed crumbs were present in SK54085 but at low abundances (9%). SK54090 contained apedal sediments as well as low abundances (9-18%) of sub-angular blocky peds. However the grave was dominated by medium sized secondary platy peds which were common in the pelvic area sample. SK54090 also contained frequent, well developed angular blocky peds and crumbs. SK54898 was also unusual as it contained a high abundance of ultra fine to very fine sub-angular blocky peds meaning that there was only a small distance between interpedal voids. Sub-angular blocky peds were present as primary peds in most samples however where there was more than one ped type present,

sub-angular blocky peds were formed as secondary peds. This was the case in SK51387 in the C3 and perpendicular skull sample as well as samples from SK54898, SK51326, SK54090, SK54085, SK54341, SK54342 and SK54908. The pelvic area sample of SK54341 contained high levels of moderately developed coarse primary platy peds (97%) as well as fine primary and secondary platy peds in the 'other' sample from SK54341. Platy peds were common in SK51350, where they were generally found in high abundances (100%), although moderately developed in the C3 and skull area samples, and in lower abundances (40%) in the pelvic area sample. The platy peds in SK51350 were also unusual as they were predominantly very coarse in size, meaning that intrapedal voids were well spaced. Crumb, angular blocky peds and granules were infrequent at Hungate and there was no systematic pattern to their distribution within the graves. They were also generally present at low abundances (<50%), although there were some examples of angular blocky and crumb peds present as high as 60%. Crumb peds were generally found as ultra fine to medium primary ped developments, however there was a concentration of coarse to very coarse crumb peds in SK54342 and SK54908. SK51351 was an unusual grave as there was a distinct lack of ped development in the grave, with the samples from the burial plane containing high abundances of apedal soils and sporadic sub-angular blocky peds that were confined to low abundances in the skull, pelvis and perpendicular foot area samples.

Table 51: The percentage of peds present in each slide in the C1 soil profile and graves from Hungate, as a percentage of sample area, showing ped development. Red indicates weak ped development, yellow indicated moderate ped development and green indicates strong ped development. Numbers in brackets indicate primary ped (1), secondary peds (2) and so on where applicable according to Stoops (2003 p. 60). Size range key; UF = ultra fine, VF = very fine, F = fine, M = medium, C = coarse and VC = very coarse according to Bullock *et al*(1985 pp 42).

Location		Apedal	Sub-angular blocky	Plates	Prisms	Angular blocks	Crumbs	Granules
C1	7-16cm	100%						
	27-36cm	100%						
	49-58cm	100%						
SK54898								
C2		54%	10% (1) VF-C	18% (2) M	18% (2) F			
C3		50%	41% (1) UF-VF					
Skull	Perp	85%	50% (1) UF	8% (1) UF				
	Para	44%	41.5% (2) UF			50% (1) UF		
Pelvis	Perp		100% (1) UF-F					
	Para		100% (1) UF-VF					
Other	Perp	82%	53.5% (1) UF	5% (1) UF				
SK51326								
C2		100%						
C3		100%						
Skull	Perp		90% (2) F	10% (1) C				
Pelvis	Perp	73%		27% (1) M-C				
	Para	90%	10% (1) F-M					
Foot	Perp	70%	30% (1) M					
	Para		80% F	20% F				
SK51387								
C3		10%	58% (2) UF-F				32% (1) UF-M	
Skull	Perp	20%	73% (2) VF-F				7% (1) F-M	
Pelvis	Perp	70%	30% (1) F					
	Para	90%					10% (1) F	
Foot	Perp		100% (1) VF-M					
	Para		100% (1) VF-M					
SK51351								
Skull	Para	43%	37% (1)UF-F					
Pelvis	NA	90%	10% (1) VF					
Foot	Perp	46%	54% (1) F					
	Para	100%						
Other	Perp	100%						
	Para	100%						

Table 51 cont.

Location		Apedal	Sub-angular blocky	Plates	Prisms	Angular blocks	Crumbs	Granules
SK54090								
C3	NA	10%		80% (2) M			10% (1) F	
Skull	Perp	90%					10% (1) VF	
	Para	81%	10% (1) VF				9% (1) M	
Pelvis	Perp		18% (1) VF	72% (2) M		10% (1) VF		
	Para	27%	9% (2) F	54% (2) M		27% (1) VF		
SK54085								
C3	NA		100% (1) VF-C					
Skull	Perp		100% (1) VF-M					
	Para		81% (2) VF-F				9% (1) F-M	
Pelvis	Perp		100% (1) UF-C					
	Para	5%	95% (1) UF-F					
SK54341								
C3		86%	14% (1) UF-VF					7% (1) M
Skull	Perp	58%	63% (1) M					
	Para	20%	81% (2) UF-M					7% (1) M
Pelvis	Perp	21%		97% (1) C				
	Para	10%	90% (2) F				10% (1) M	
Foot	Perp	100%						
	Para	80%	20% (1) M					
Other	Perp	40%	56% (2) VF-M	4% (1) F			40% (1) VF-M	
	Para	42.50%	46% (2) VF-F	25.5% (2) F				3% (1) M
SK54342								
C3	NA	60%	64% (2) VF-F				40% (1) M-C	
Skull	Perp		90% (2) UF-F				10% (1) UF-VF	
	Para	76%	52% (1) UF-VF					
Pelvis	Perp	50%	50% (1) UF-VF					
	Para	90%	19% UF-VF					
Foot	Perp	40%	54% (2) VF-F			42% (1) UF-VF	6% (1) M	
	Para	40%				60% (1) UF-M	60% (1) M-VC	
SK54908								
C2		95.50%	10% (1) VF				4.5% (1) VF	
Skull	Perp		100% (2) VF-M				10% (1) C	
Pelvis	Perp	100%						
	Para	100%					50% (1) C-VC	
Foot	Perp	10%	90% (2) F				10% (1) C	
	Para	36%	4% (1) UF	60% (2) M-C				
SK51350								
C2		50%	50% F-C					
C3				100% (1) C-VC				
Skull				100% (1) M-VC				
Pelvis		40%	30% (1) VF-M	40% (1) VF-VC				
Foot			100% (1) VF-F					

7.1.6 Variation in peds by microfabric type

The distribution of ped types across microfabrics was calculated (Table 52). At Çatalhöyük the microfabrics were dominated by apedal material, sub-angular blocky and granular peds. The high predominance of granules at Çatalhöyük compared to other microfabrics is likely to be a reflection of the microfabrics themselves forming into spherical deposits embedded in CH4 (see section 3.2). The size of the peds at Çatalhöyük range between ultra fine and fine in all microfabrics, apart from CH4 and CH6. In CH6 granules range from ultra fine to medium, the medium sized peds are likely to be from the aggregates of CH6 themselves. CH4 however contains coarse sub-angular blocky peds and coarse plates, this is likely to be a true reflection of the ped development within the microfabric. As with previous micromorphological features, Ti1 contained higher abundances and a more diverse ped profile than Ti2. Again, sample size is likely to be partly responsible for this trend. Ti1 was characterised by sub-angular blocky peds, whereas Ti2 had a predominance of apedal sediments. The size of peds also varied between Ti1 and Ti2, with Ti2 containing ultra fine to fine peds and Ti1 containing coarser peds. Apedal and sub-angular blocky sediments also dominated the microfabrics at Hungate. However there were some microfabrics that had peaks in angular blocky peds (HU1, HU3, HU4 and HU12), plates (HU3, HU6, HU11, HU12 and HU13) as well as crumb peds (HU1, HU3, HU4, HU5, HU8, HU10, HU12 and HU13). The size of peds were generally between ultra fine and medium, however there are coarse sub-angular blocky peds in HU12 and HU13, as well as coarse crumb peds in HU1, HU4, HU8 and HU12, and coarse platy peds in HU11, HU12 and HU13. The presence of coarse peds in HU12 and HU13 is likely due to these being the most dominant peds therefore they have a larger surface area for large peds to develop, particularly sub-angular blocky peds. Coarse crumb peds in HU1 and HU4 are probably due to the shape of the aggregates of the microfabrics themselves embedded in larger microfabrics. For all sites the high abundances of ped types in the microfabrics do not correspond to high abundances of the same in graves or sample locations around the body (Chapter 3).

Table 52: Total ped abundance shown as a percentage of the average area of the microfabric composed of ped types. In some instances the total percentage of ped types for one microfabric equates to more than 100% This is due to the presence of primary, secondary and tertiary peds. However it has not been possible to denote the order of ped types as, particularly in the larger microfabrics ped, order changes between slides. Size range key; UF = ultra fine, VF = very fine, F = fine, M = medium, C = coarse and VC = very coarse according to Bullock *et al*(1985 pp 42).

Microfabrics	Apedal	Sub-angular blocky	Angular blocks	Granules	Crumbs	Plates
CH1	19%	52% (UF-F)	19% (UF)	22% (UF-F)		
CH2	47%	18% (UF)	10% (UF)		17% (VF)	
CH3	33%	83% (UF-F)	17% (UF)	50% (UF-F)		
CH4	43%	38% (VF-C)		17% (UF-F)	6% (UF)	4% (F-C)
CH5	67%	50% (UF-VF)		30% (UF)		
CH6	100%	33% (VF)		67% (UF-M)		
Ti1	28%	65% (UF-C)			7% (UF-C)	2% (VF-C)
Ti2	75%	25% (UF-F)				
HE1	33%	61% (UF-C)				31% (C-VC)
HU1	31%	76% (UF-F)	18% (UF-M)		6% (M-VC)	
HU2	33%					
HU3	24%	26% (UF)	20% (UF)		20% (UF-VF)	20% (UF)
HU4	25%	50% (UF-F)	21% (UF-VF)		14% (M-C)	
HU5		73% (UF-VF)			27% (UF-M)	
HU6	33%					33% (UF)
HU7	100%					
HU8	70%	36% (UF-M)			1% (C)	
HU9	50%	50% (UF)				
HU10	64%	18% (UF-F)			2% (VF)	
HU11	50%					50% (C)
HU12	66%	40%(UF-C)	5% (VF)	1% (M)	14% (M-VC)	5% (C-VC)
HU13	47%	35% (UF-C)			3% (VF-M)	14% (VF-VC)

7.2 Void space

The aspects of void space which will be explored are the total abundance of void space measured using image analysis (see method 2.3.3 and Appendix 1.1.5 for more details) and the distribution and abundance of void types, as recorded using standard micromorphological methods (see 2.3.1.2.5).

7.2.1 Total void space abundance

7.2.1.1 Inter site total void space

Çatalhöyük had the lowest mean void space at 8.38% compared to 12.63% at Hungate, 17.82% at Heslington East and 15.29% at Thessaloniki. Çatalhöyük had the narrowest range of void space of the four sites, with a difference of 15.7% between the highest and lowest values, compared to 20.71% at Thessaloniki, 24.5% at Heslington East and 52.81% at Hungate (Figure 83). Hungate had the highest range of values and also a large number of extreme outliers compared to the other sites (Figure 83). The outliers at Hungate, however, do not relate to a specific grave, sample location or sample orientation. The shape of the data from the box plot suggests that there are differences in the distribution of void space between Çatalhöyük and Thessaloniki and Heslington East and between Hungate, Thessaloniki and Heslington East.

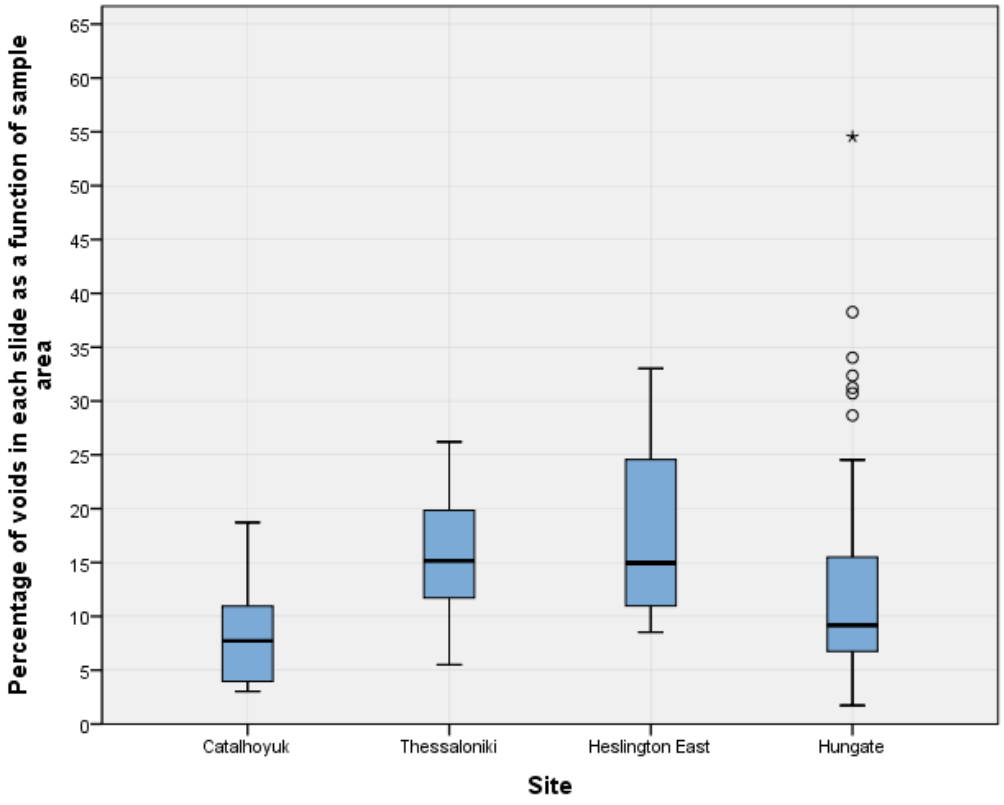

Figure 83: Box and whisker plot of void abundance per slide by site shown as a total percentage of slide area. Number of slides at each site are; Çatalhöyük n=12, Thessaloniki n=26, Heslington East n=7 and Hungate n=64. The centre line of the box plot indicates the median values for each sample set. Whiskers extend to x1.5 the height of the box or highest/lowest value. '*' indicate extreme outliers more than three times higher than the extent of the box and 'o' illustrate values between x1.5 and x3 the height of the box,

7.2.1.2 Intra site void percentage distributions

7.2.1.2.1 Çatalhöyük

The C1 and grave 19295 had similar total void space means (10.74% and 12.51% respectively), grave 18666, however, had a lower mean value, 4.55%. The void space ranges in the two graves also differed at 5.19% in 19295 and 11.5% in 18666. A range was not calculated for the C1 due to the low sample size; however the C1 void space value plotted within the range of that for 19295.

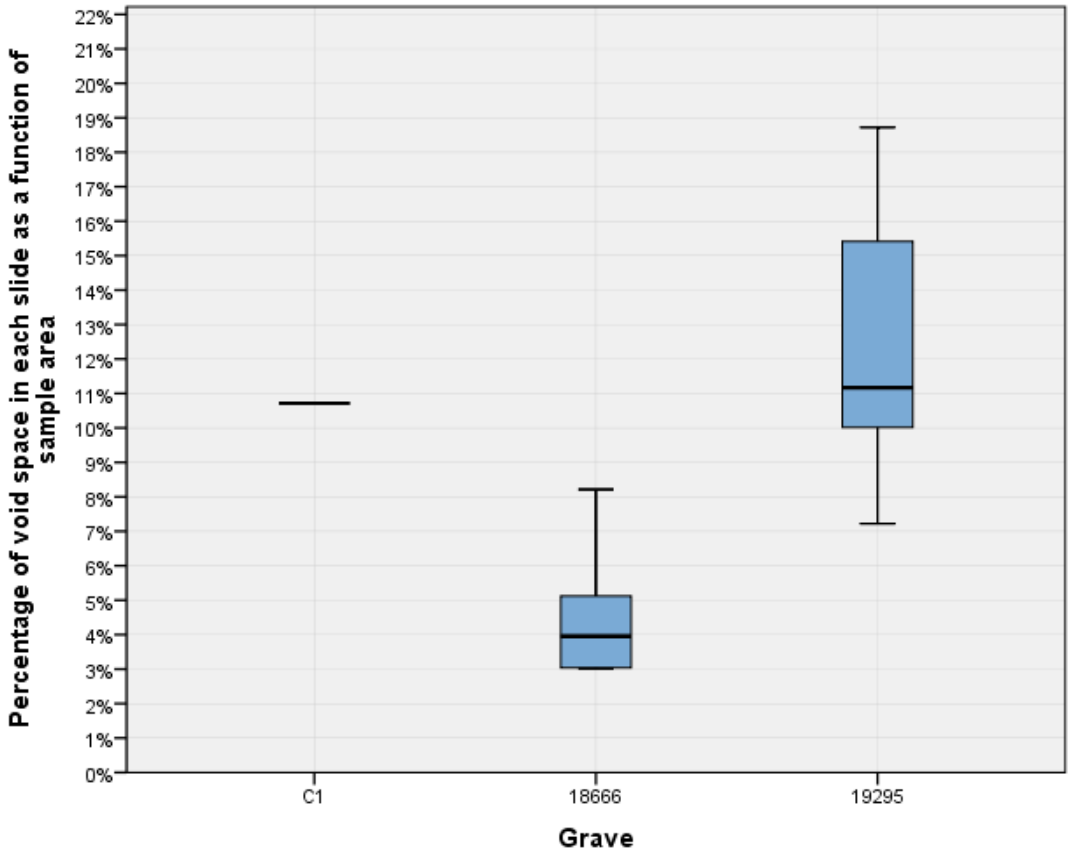

Figure 84: Box and whisker plot of void abundances in percent at Çatalhöyük by grave. Sample sizes are C1 n=1, 18666 n=6, 19295 n=5. The centre line of the box plot indicates the median values for each sample set. Whiskers extend to x1.5 the height of the box or highest/lowest value if there are no values outside of that range.

7.2.1.2.2 Thessaloniki

The graves at Thessaloniki split into two groups based on their mean total void space: TF157, TF182 and TF177 in the first group, with mean abundances between 9-15%, and

TF178 and TF162 in the second group, with mean abundances between 22-23%. The same pattern is also clearly demonstrated in the median values for the data (Figure 85). Ranges typically varying between 1.86% in TF187 and 8.69% in TF177, although TF182 had a much larger range at 17.28%. The location of the grave does not seem to be a contributory factor to high void abundance (Figure 86).

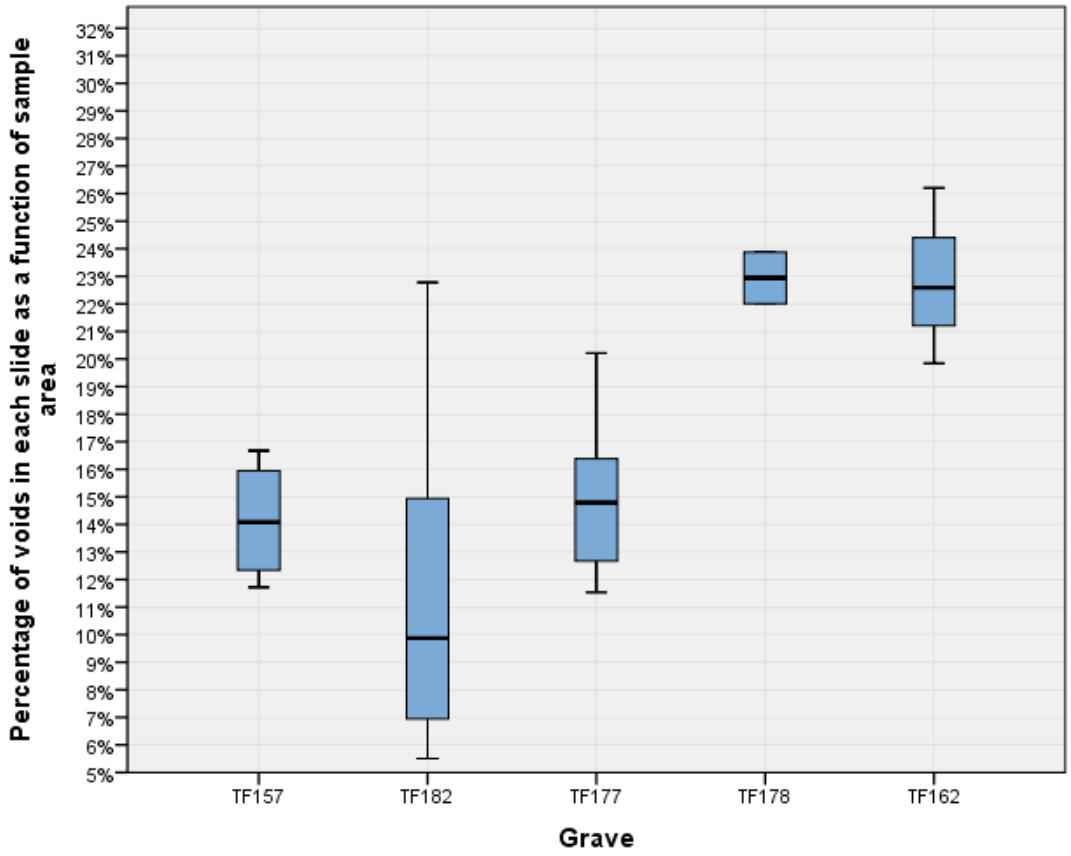

Figure 85: Box and whisker plot of void abundance at Thessaloniki by grave. Sample sizes are as follows; TF159 n= 5, TF182 n=8, TF177 n=8, TF178 n=2 and TF162 n=3. The centre line of the box plot indicates the median values for each sample set. Whiskers extend to x1.5 the height of the box or highest/lowest value if there are no values outside of that range.

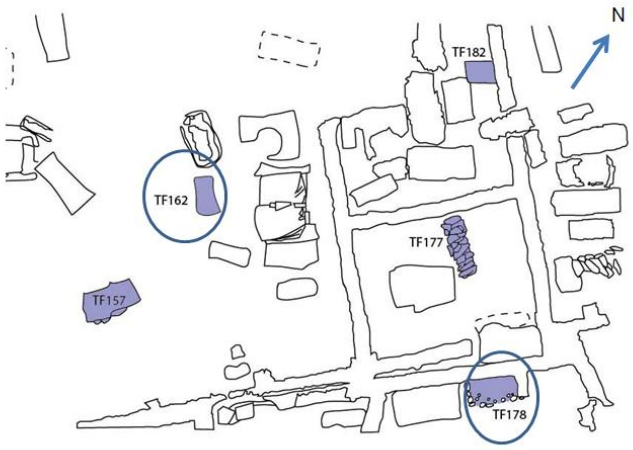

Figure 86: Location of graves at Thessaloniki with high total void space (circled)

7.2.1.2.3 Heslington East

The C1 samples at Heslington East had a slightly lower mean abundance of voids than the samples from the grave at 12.79% of the total slide area and 20.84% respectively. The C1 samples also had a narrower range than the grave samples. This may be due, however, to sample size, rather than a true reflection of the nature of the soil.

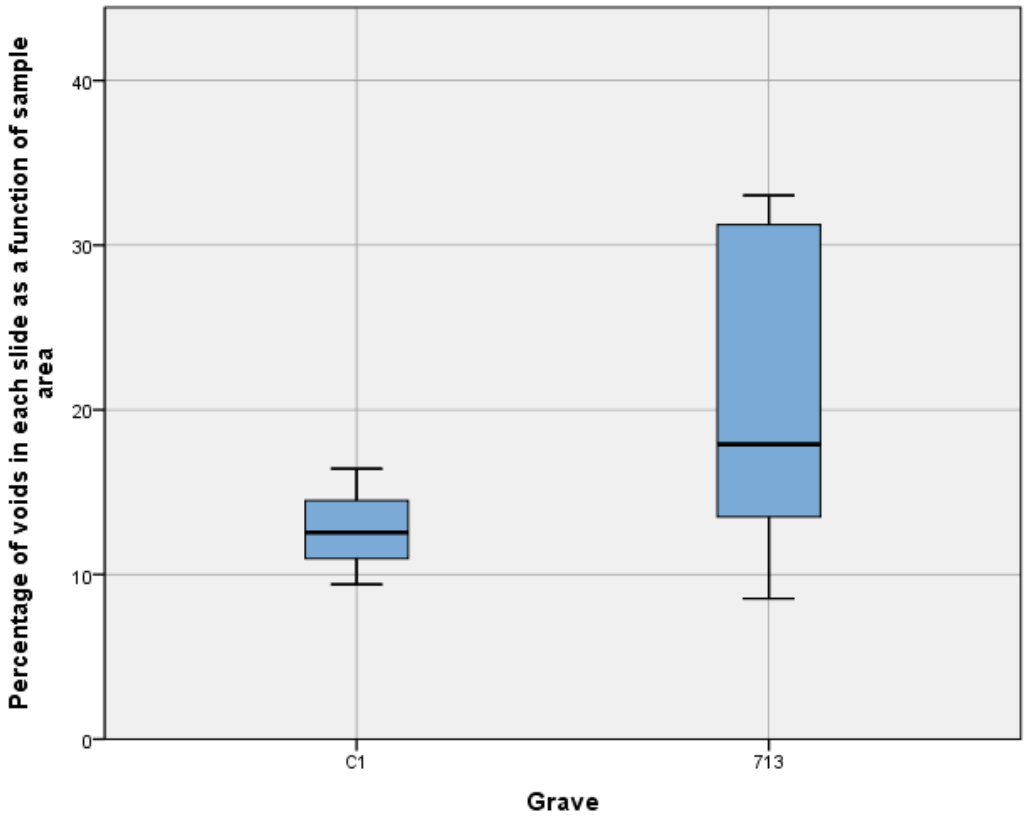

Figure 87: Box and whisker plot of void abundances in percentages at Heslington East. Sample size C1 n=3 and 713 n=5. The centre line of the box plot indicates the median values for each sample set. Whiskers extend to x1.5 the height of the box or highest/lowest value if there are no values outside of that range. '*' indicate extreme outliers more than three times higher than the extent of the box and 'o' illustrate values between x1.5 and x3 the height of the box.

7.2.1.2.4 Hungate

The total void space at Hungate varied in both mean abundance and range (Figure 88). The C1 sample had a low mean void space (5.08%) compared to the grave samples that varied between 6.45-22.22%. The range of void space in the C1 samples (n=3) was also narrow (2.26%) compared to the grave samples (5.15% in SK51351 (n=7) to 52.81% in SK51326 (n=8)). Mean void abundances separate the Hungate graves into two groups. SK54898, SK51326, SK51387, SK51351, SK54341, SK54342 and SK54908, with low median void abundances between 6.45-16.93% and low upper quartiles between 8.22-16.13% with SK51387 at 29.59% (Figure 89). The second group consisted of SK54090, SK54085 and SK51350 with higher median void abundances between 17.89-24.16% and high upper quartile ranges between 20.04-30.97%.

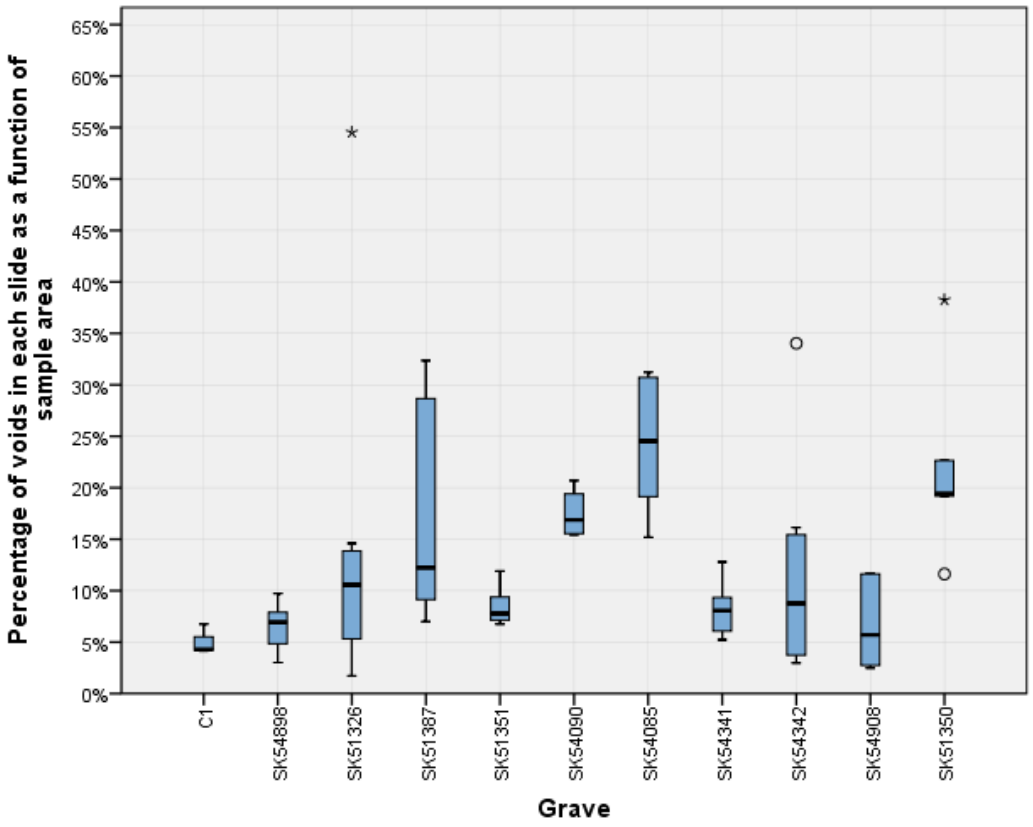

Figure 88: Box and whisker plot of void abundances in percentages at Hungate by grave. Sample sizes are; Control n=3, 51326 n= 8, 51350 n= 5, 51351 n= 7, 51387 n= 6, 54085 n= 5, 54090 n= 5, 54341 n= 9, 54342 n= 7, 54898 n= 6 and 54908 n= 7. The centre line of the box plot indicates the median values for each sample set. Whiskers extend to x1.5 the height of the box or highest/lowest value if there are no values outside of that range. '*' indicate extreme outliers more than three times higher than the extent of the box and 'o' illustrate values between x1.5 and x3 the height of the box.

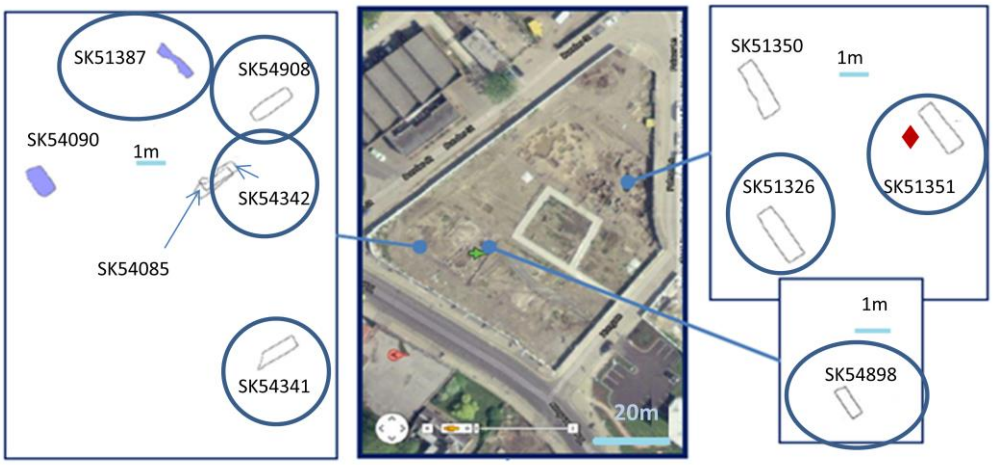

Figure 89: Location of Hungate graves with low porosity (circled), group one in text.

7.2.1.3 Variation in total void space within graves

When the C1, C2 and C3 samples from the graves were compared with the burial samples, there was no systematic variation in the abundance of void space. A comparison was also made between the skull, pelvis and foot area samples from all graves (Figure 90) as these were the three most consistently sampled locations.

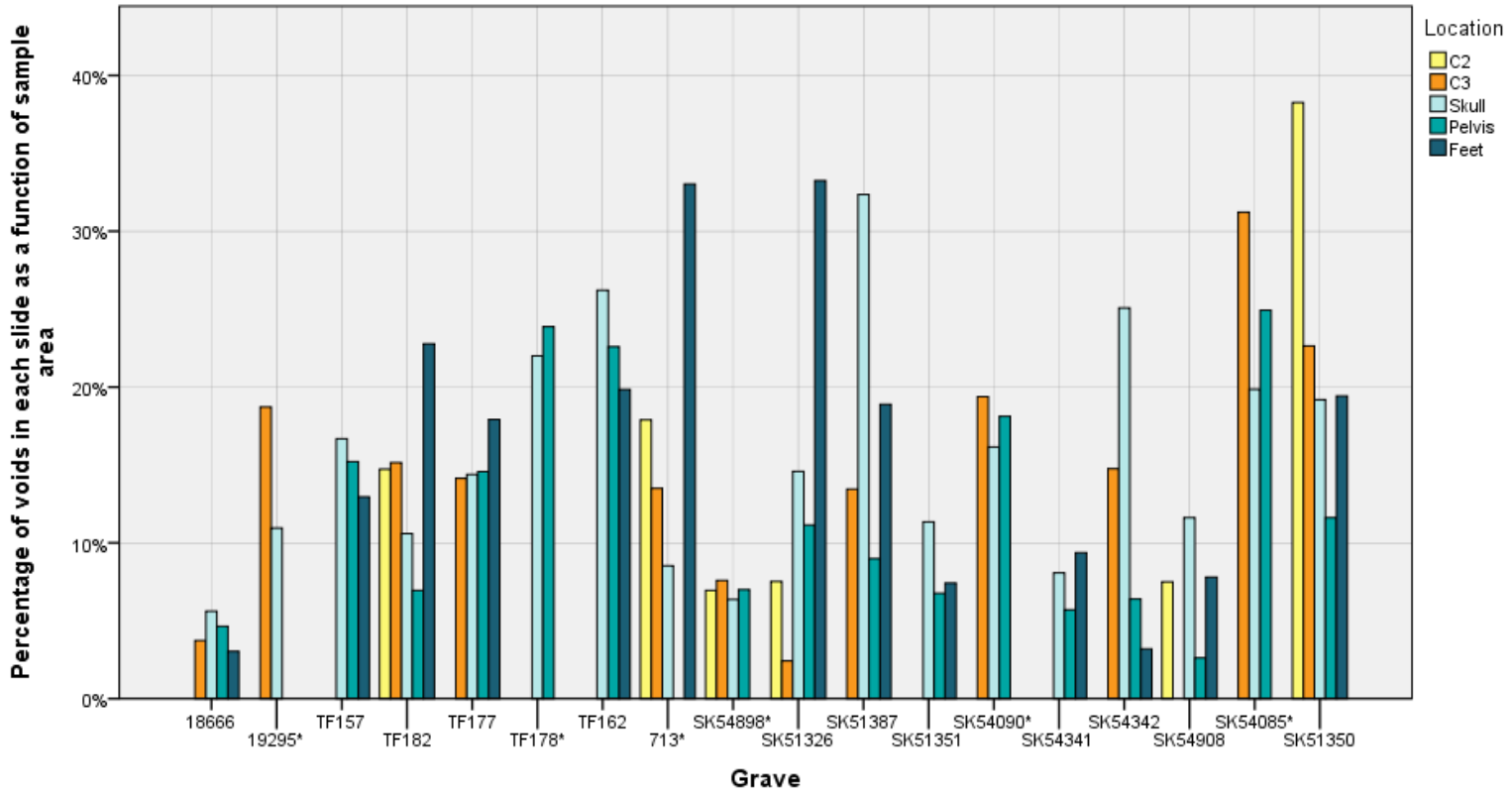

Figure 90: Abundance of void space in the C2, C3, skull, pelvic and foot area samples shown in percent for all graves in the study. Those graves that do not have all three sample points (skull, pelvis and foot) are identified by '*'. Where there is more than one sample available for a point the average void abundance is given.

TF182, SK51326, SK51387, SK51351, SK54341, SK54908 and SK51350 all had low void abundance in the pelvic areas (Figure 91); meaning that 58% of complete graves had lower void abundance in the pelvic samples compared to the skull and foot areas, which may relate to compaction or aggregation occurring in the pelvis but will be discussed further in section 7.3.3.2. However, there was considerable variation in this pattern between sites. At Çatalhöyük, none of the graves fit this pattern, at Thessaloniki 25% of complete graves did, Heslington East is missing a pelvic sample, and at Hungate 62.5% of complete graves had low abundances of voids in the pelvic samples.

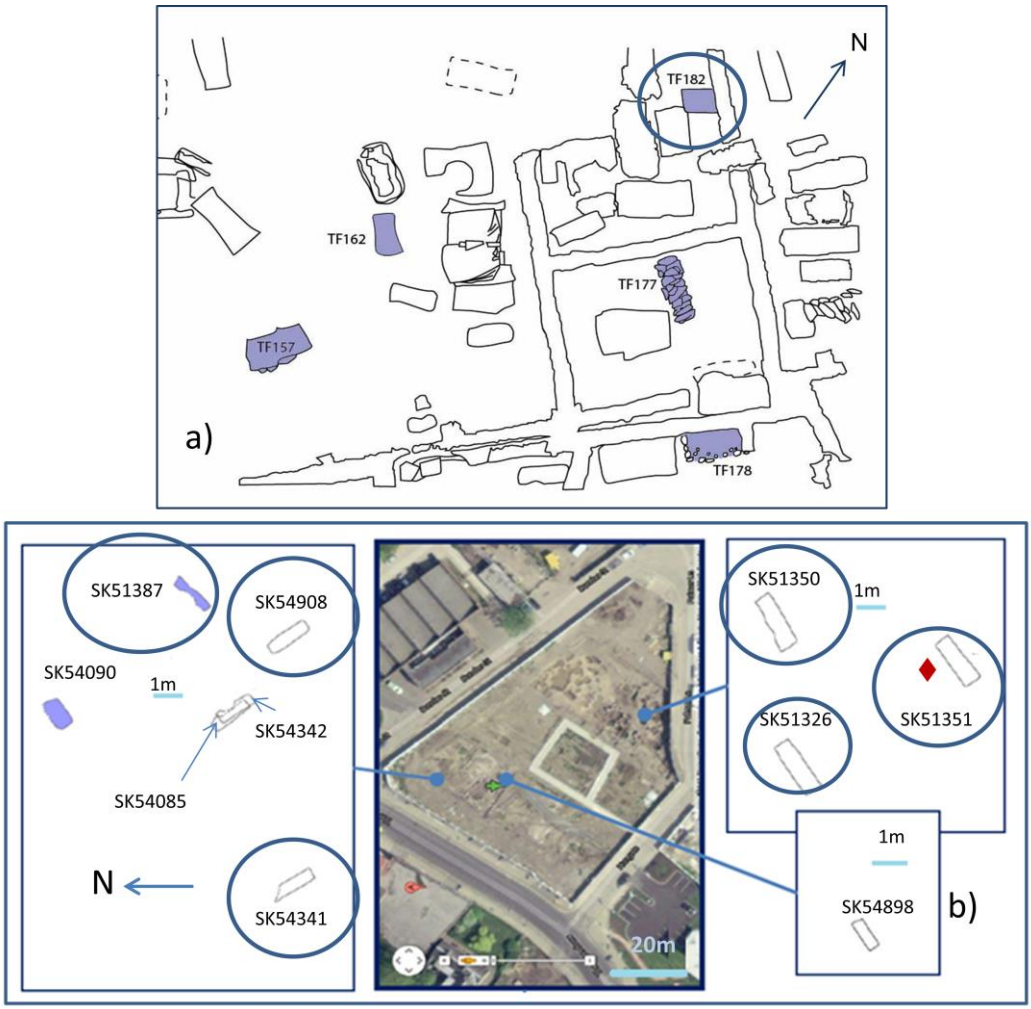

Figure 91: Spatial distribution of graves with low porosity in the pelvic area.

7.2.2 Variation in void types

The four most common void types in this study were considered: channels, packing voids, planes and vughs. Simple, compound and complex types of packing voids were included in the 'packing void' category as they are similar in terms of their interconnectivity and functional properties (Brewer, 1964 p.187). Their genesis can be slightly more varied with all types of packing voids being formed through the loose packing of soil material and all but simple packing voids through biological excreta and shrinking and swelling processes (Brewer, 1964). Although the genesis of simple packing voids is slightly different to either compound or complex types they were generally rare in terms of both frequency and abundance (Brewer, 1964).

7.2.2.1 Inter site void type variation

All sites contained channels, packing voids, planes and vughs in assorted abundances and distributions (Figure 92), creating different void profiles at each site. Çatalhöyük was dominated by a high abundance of packing voids (median 30% of total slide area) compared with 1.23% for channels, 3.35% for planes and 1.40% for vughs. Median abundances of packing voids at Çatalhöyük were also higher than median packing void abundances at Thessaloniki (10%), Heslington East (2.5%) or Hungate (0%). As at Çatalhöyük, Thessaloniki also had high abundances of packing voids compared to the other void types at the site and both sites had wide packing void distributions (Figure 90). Hungate contained high median abundances of vughs compared to all other void types with vugh abundances at 9.5% of total slide area compared to 1% for channels, 1.8% for planes and packing voids at 0%. Vughs were also higher in abundance at Hungate than at Çatalhöyük, which was particularly low at 1.4%, Thessaloniki at 6% and Heslington East at 5%. Heslington East was unique in that all of the void abundances were quite low for all void types with no one void category dominating the profile, meaning that there probably was not a dominating soil process; however the implications of this will be discussed in section 7.3.1.

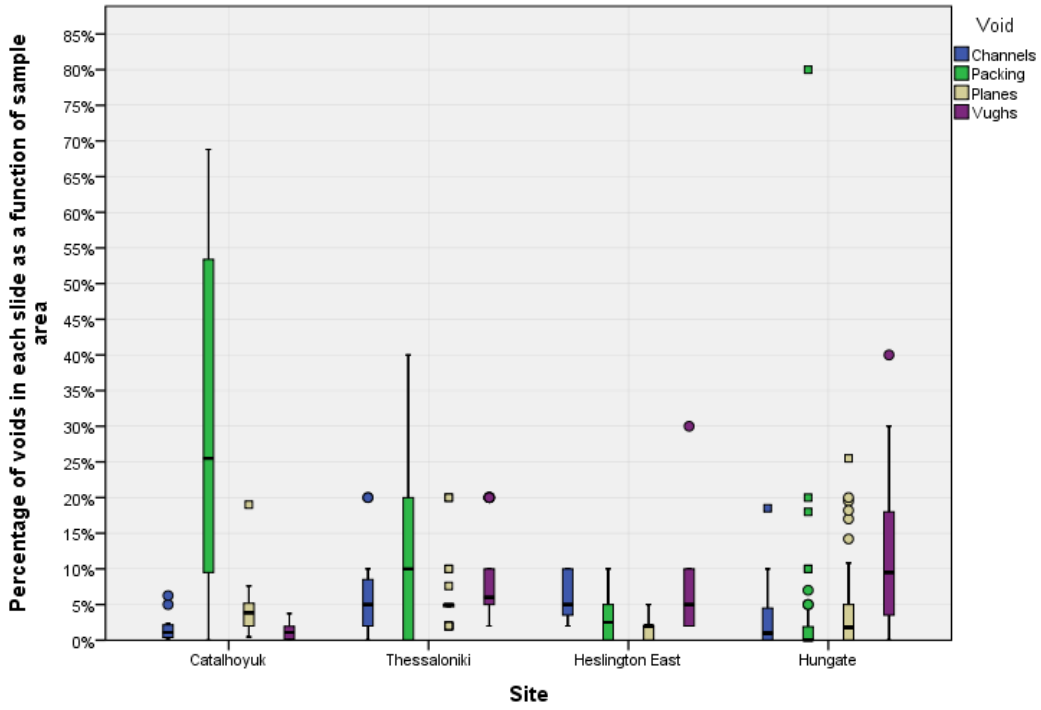

Figure 92: Inter site void abundance distribution for channels, packing voids, planes and vughs given as percentage of slide area. Number of slide in each site are; Çatalhöyük n=12, Thessaloniki n=26, Heslington East n=7 and Hungate n=64. The centre line of the box plot indicates the median values for each sample set. Whiskers extend to x1.5 the height of the box or highest/lowest value if there are no values outside of that range. '□' indicate extreme outliers more than three times higher than the extent of the box and 'o' illustrate values between x1.5 and x3 the height of the box.

7.2.2.2 Intra site void variation – Çatalhöyük, Thessaloniki and Hungate

7.2.2.2.1 Çatalhöyük

Channel and planar voids were present in the C1 at median abundances of 0.2% and 0.25% of total slide area respectively, lower than median abundances in either grave 18666 or 19295 (Figure 93). The C1 sample also lacked vughs, which were present in low abundances in the graves. Packing voids, however, were present in the C1 sample at much higher median abundances (68.8%) compared to the graves at 25.35% in 18666 and 49.8% in 19295.

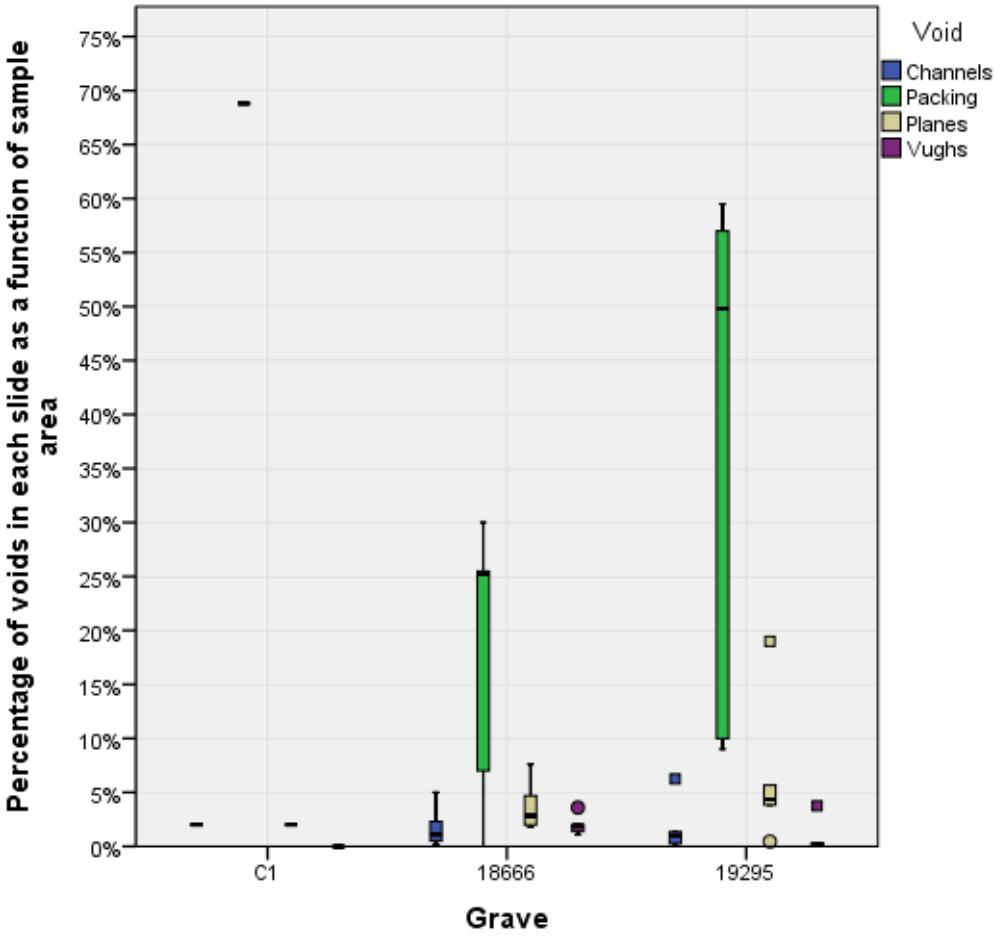

Figure 93: Void abundance at Çatalhöyük for channels, packing voids, planes and vughs given as percentage of slide area composed of each void type. Sample sizes are C1 n=1, 18666 n=6, 19295 n=5. The centre line of the box plot indicates the median values for each sample set. Whiskers extend to x1.5 the height of the box or highest/lowest value if there are no values outside of that range. '□' indicate extreme outliers more than three times higher than the extent of the box and 'o' illustrate values between x1.5 and x3 the height of the box.

7.2.2.2.2 Thessaloniki

Channels, planes and vughs were present in all graves at Thessaloniki (Figure 94), whereas packing voids were present in TF157, TF182, TF177 and TF162. Void types were present in assorted abundances and distributions creating a void profile for each grave. Their variation was not systematic between graves. There were some noteworthy trends however. TF162 was distinct, as channels, planes and vughs were present at a median of 5% of total slide area. Packing voids however dominated the grave at 30%, which was the highest abundance of packing voids in the Thessaloniki graves. In TF157 and TF182, the two Hellenistic graves, the median abundance was similar for all void types, although the range

varied between void types in TF182. TF177 was characterised by low abundances of channels and planes compared to packing voids and vughs which dominated the grave. Vugh median abundance and range differentiated the graves at Thessaloniki into two groups; those with low abundances and narrow ranges, TF178 and TF162 (median abundances of 3.5% and 5% respectively and ranges of 3%), and those with elevated median abundances and wider ranges, TF157, TF182 and TF177 (median abundances of 7.5%-14.75% and ranges of 8-15%).

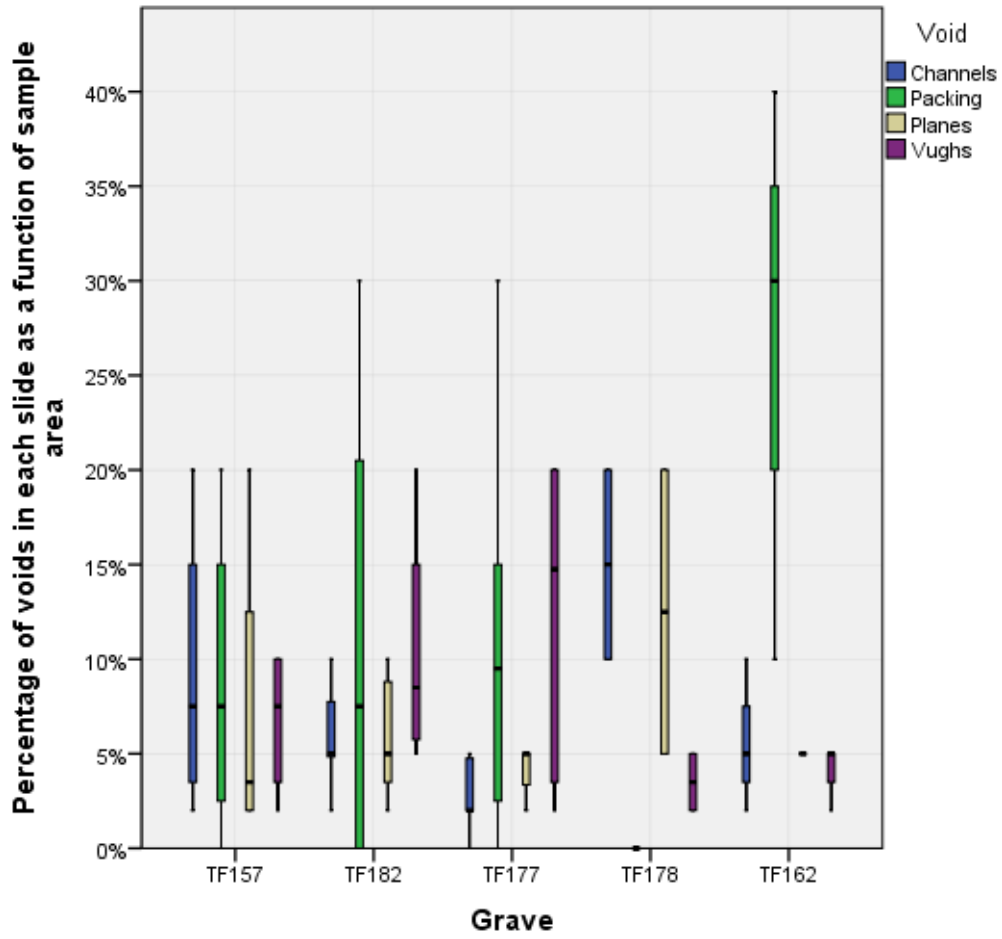

Figure 94: Box and whisker plot of void abundance at Thessaloniki by grave and void type. Sample sizes are; TF159 n= 5, TF182 n=8, TF177 n=8, TF178 n=2 and TF162 n=3. The centre line of the box plot indicates the median values for each sample set. Whiskers extend to x1.5 the height of the box or highest/lowest value if there are no values outside of that range.

7.2.2.2.3 Heslington East

The abundance of vughs was similar in the C1 samples and in the grave samples with medians of 5%. Planes were also low in both contexts at 0% in the C1 samples and 2% in

the grave. There was a greater abundance of packing voids in the C1 samples at a median value of 5% of total void space compared to 0% in the grave, channels however were lower in the C1 samples at 2% compared to 5% in the grave.

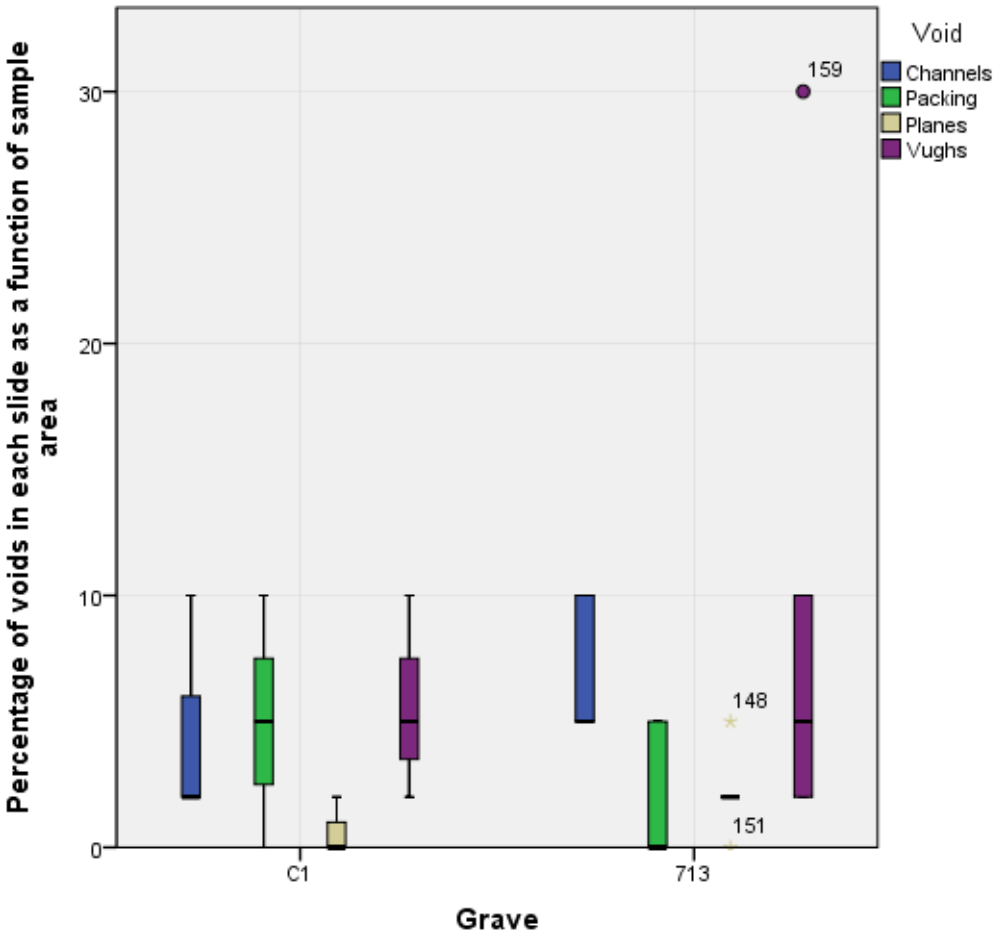

Figure 95: Inter site void abundance distribution for channels, packing voids, planes and vughs given as percentage of slide area. Number of slide in each sample are; C1 n=3 and 713 n=5. The centre line of the box plot indicates the median values for each sample set. Whiskers extend to x1.5 the height of the box or highest/lowest value if there are no values outside of that range. '□' indicate extreme outliers more than three times higher than the extent of the box and 'o' illustrate values between x1.5 and x3 the height of the box.

7.2.2.2.4 Hungate

Channel, packing, planar voids and vughs were present in the C1 samples and all graves at Hungate (Figure 97). The C1 samples at Hungate contained a high abundance of vughs at a median of 18.5% of total slide area compared to the channels, packing voids and planes (0%). Vughs were also generally the most abundant voids within graves and varied between

the graves splitting them into two groups. The first group (C1, SK51351, SK54090, SK54342, SK54908 and SK51326) contained those with high median abundances (9.7-18.5%) and wide ranges (11-32.4%) (Figure 97). The second group (SK51387, SK54341, SK54898, SK54085 and SK51350) consisted of those with low median abundances (1-10%) and narrow ranges (7.7-18.2%). The distribution of these graves however does not seem to related to their spatial distribution (Figure 96).Whilst there was variation in the median abundance of channels and packing voids between graves at Hungate (as calculated using the method outlined in 2.3.5), it was not systematic (i.e. related to location, age or burial practice) (Figure 97). Planes at Hungate all had low median abundances compared to the other void types at the site, with all median values at less than 11%. SK54898 was unusual as it had the highest median abundance of planes and the widest distribution.

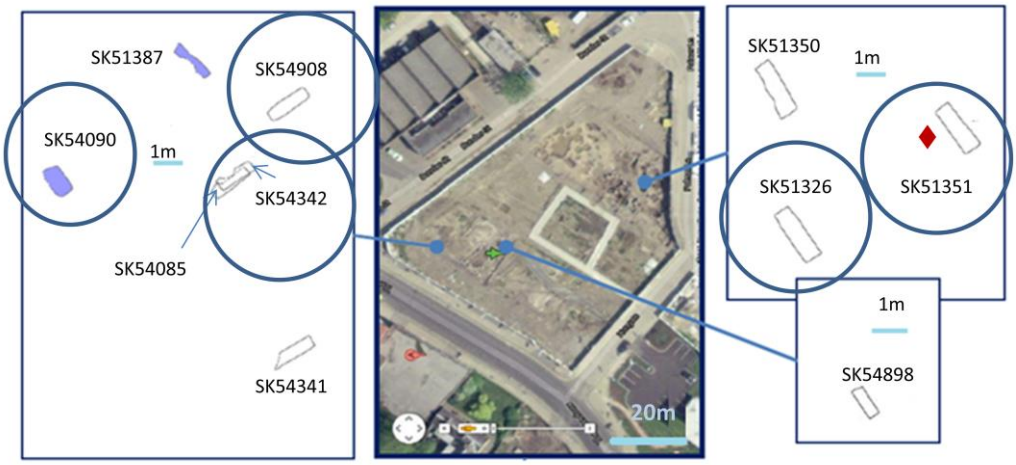

Figure 96: Distribution of the abundance of vughs at Hungate split into groups one (circled), high median abundances and wide ranges and two (uncircled) those with low median abundances and narrow ranges.

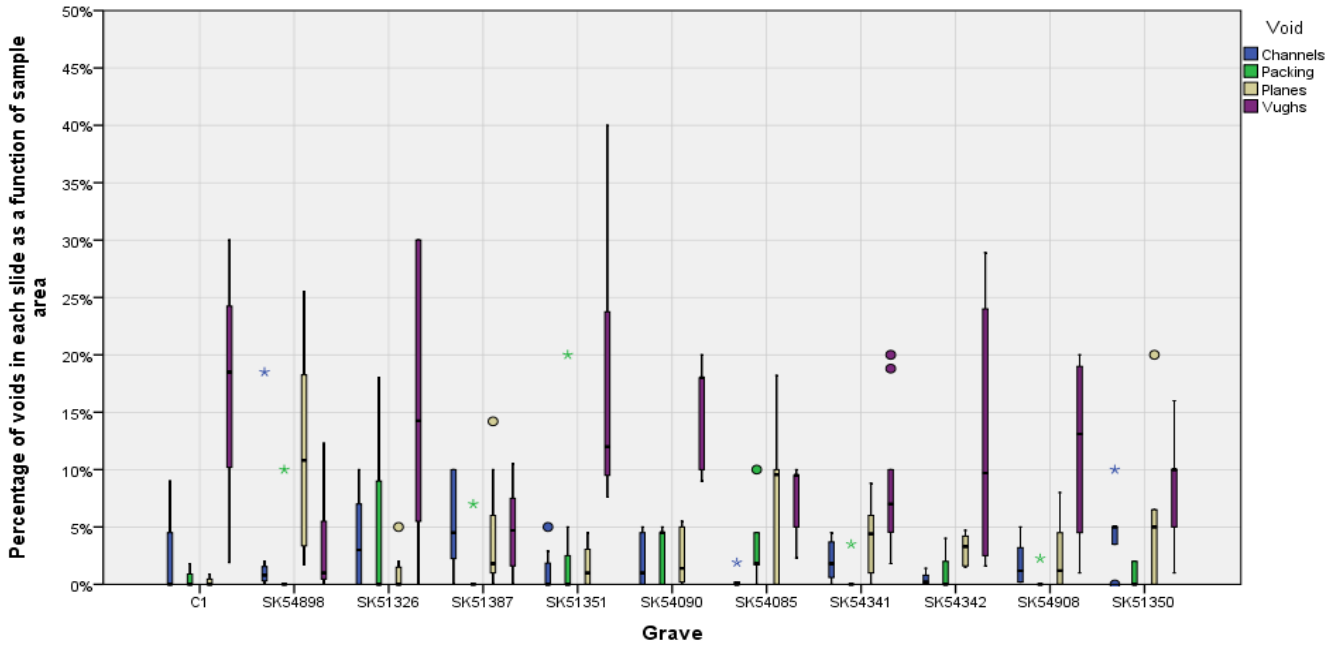

Figure 97: Box and whisker plot of void abundances in percentages at Hungate by grave and void type. Additional outlier in C2 sample from SK51326 for packing voids at 80% (not shown on graph). Sample sizes are as follows; Control n=3, 51326 n= 8, 51350 n= 5, 51351 n= 7, 51387 n= 6, 54085 n= 5, 54090 n= 5, 54341 n= 9, 54342 n= 7, 54898 n= 6 and 54908 n= 7. The centre line of the box plot indicates the median values for each sample set. Whiskers extend to x1.5 the height of the box or highest/lowest value if there are no values outside of that range. '□' indicate extreme outliers more than three times higher than the extend of the box and 'o' illustrate values between x1.5 and x3 the height of the box.

7.2.2.3 Variation in total void space within graves by void type

There was no systematic variation in channel void abundance between the C1, C2, C3 and samples from the burial plane. However, of the eleven complete graves in the study, 77% had low levels of channels in the skull compared to the pelvis and foot (Figure 98), but this varied by site. At Çatalhöyük no complete grave contained low levels of channel voids in the skull area, whilst at Thessaloniki 75% of complete graves did and 50% did at Hungate. These patterns will be discussed further in 7.3.3.2

There was no systematic variation in packing void abundance between the C1, C2, C3 and samples from the burial plane (Figure 99). 40% of complete graves had elevated abundances of packing voids in the skull compared to the pelvis and foot at 10% and 20% respectively and 30% (SK54341, SK54342 and SK54908) did not show a concentration of packing voids in any of the three sample areas, skull, pelvis and foot. At the site level, Çatalhöyük and Heslington East had 0% of complete graves with elevated levels of packing voids in the skull, Thessaloniki had 50%, and Hungate had 33%. It was, therefore, not a strong correlation. Reduced levels of packing voids existed in the pelvic sample in 50% of complete graves, compared to 30% with reduced levels in the skull, 20% in the feet and 20% no preference. Some graves also had low values in both the pelvic and the foot samples and were therefore counted twice. On a site by site basis this value changes to 100% at Çatalhöyük, 0% at Heslington East, 60% at Thessaloniki and 40% at Hungate. These patterns will be discussed further in 7.3.3.2

There was no one sample location in the complete graves that was consistently high in plane abundance (Figure 100). There was also no systematic variation between plane void abundance between the C1, C2, C3 and samples from the burial plane. When complete and incomplete graves were considered, 33% of graves had elevated abundances of planes in the skull, 38% in the pelvis and 16% in the feet. This may be slightly distorted due to the tendency for foot samples to be missing due to block lifting of feet at some sites (Hungate). 100% of complete graves at Çatalhöyük had elevated levels of planes in the pelvis, 50% at Thessaloniki, 0% at Heslington East (no complete graves at Heslington East) and 20% at Hungate.

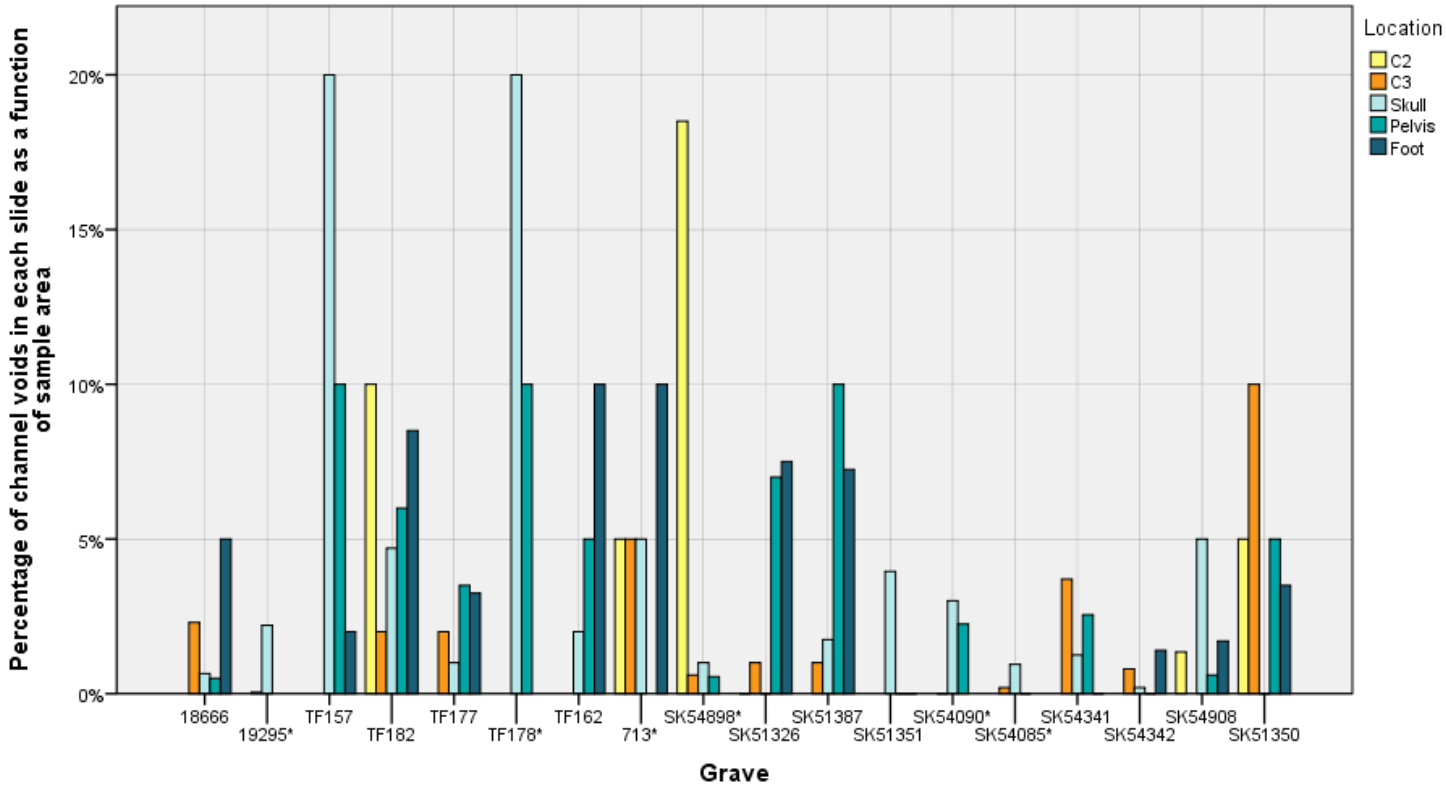

Figure 98: Abundance of channel void space in the C2, C3, skull, pelvic and foot samples shown in percent for all graves in the study. Those graves that do not have all three sample locations (skull, pelvis and foot) are identified by '*'. Where there is more than one sample available for a location the average void abundance is given.

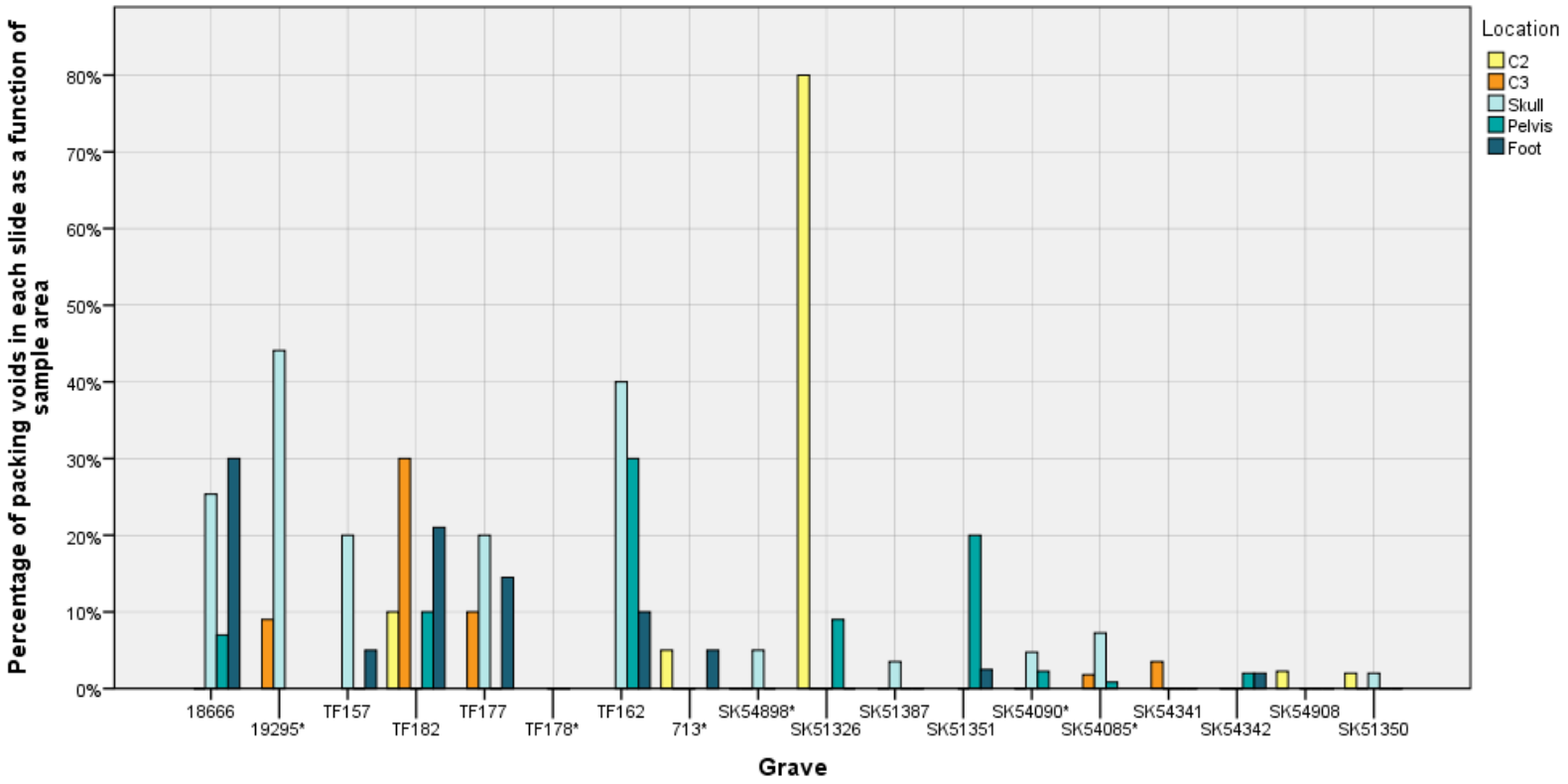

Figure 99: Abundance of packing void space in the C2, C3, skull, pelvic and foot samples shown in percent for all graves in the study. Those graves that do not have all three sample locations (skull, pelvis and foot) are identified by '*'. Where there is more than one sample available for a point the average void abundance is given.

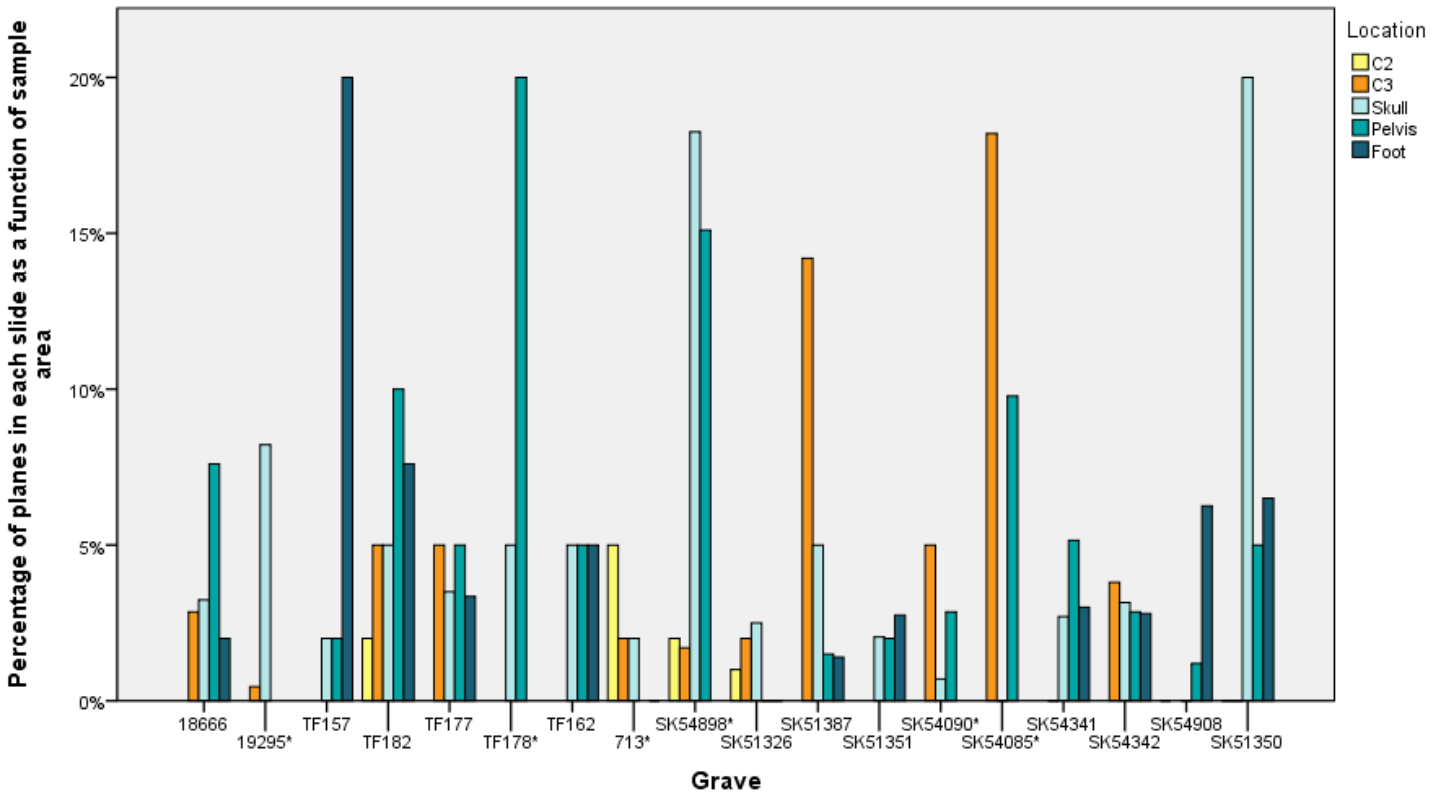

Figure 100: Abundance of plane void space in the C2, C3, skull, pelvic and foot samples shown in percent for all graves in the study. Those graves that do not have all three sample locations (skull, pelvis and foot) are identified by '*'. Where there is more than one sample available for a point the average void abundance is given.

Although there was no systematic variation in vugh void abundance between the C1, C2, C3 and samples from the burial plane, there was systematic lateral variation across the burial plane (Figure 101). Of the complete graves, 50% had elevated abundances of vughs in the pelvic samples compared to 30% in the skull and 40% in the foot (Figure 101). However, there was no increase in vugh abundance in the pelvic region of complete graves from Çatalhöyük and Heslington East, compared to 66% at Thessaloniki and 42% at Hungate. The lowest levels of vughs were present in the skull samples in 60% of complete graves, the pelvic samples in 20% and 30% in the foot samples. On a site basis, the complete graves with low levels in the skull varied from 0% at Çatalhöyük and Heslington East, 66% at Thessaloniki and 57% at Hungate. This indicates that overall there tend to be high levels of vughs in the pelvic area samples and low levels in the skull area.

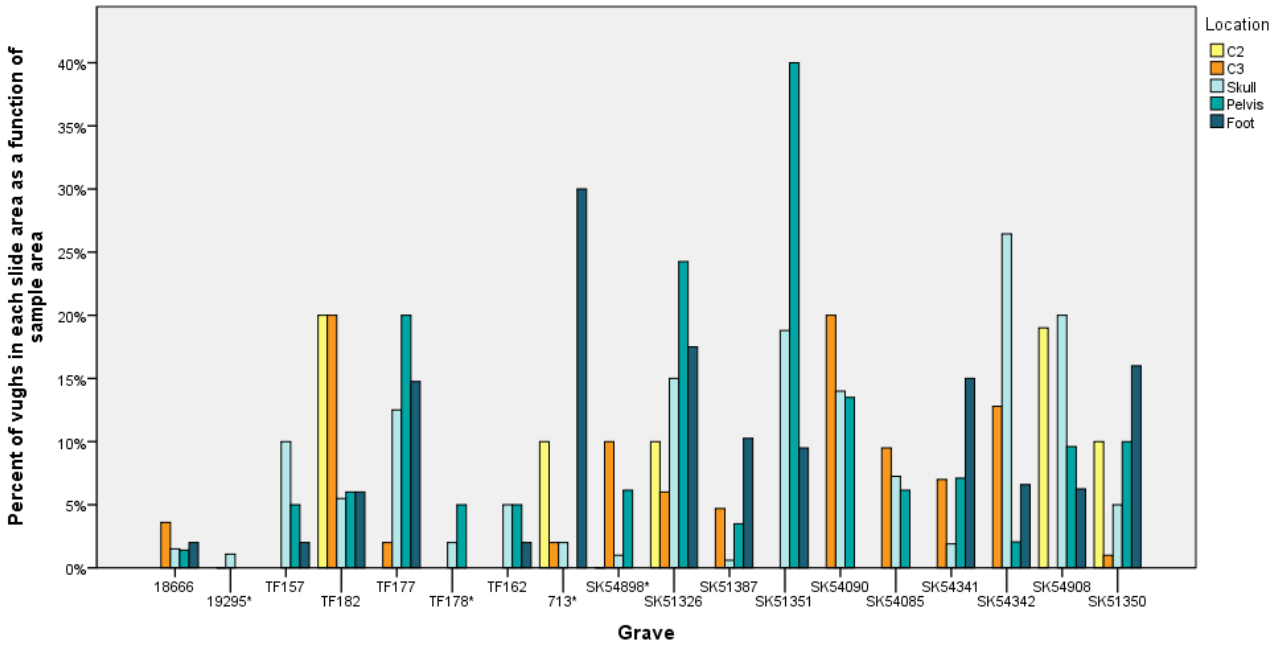

Figure 101: Abundance of vugh void space in the C2, C3, skull, pelvic and foot samples shown in percent for all graves in the study. Those graves that do not have all three sample locations (skull, pelvis and foot) are identified by '*'. Where there is more than one sample available for a point the average void abundance is given.

7.2.3 Void abundance and type by microfabric

The distribution of total void abundance and void types across microfabrics was calculated (Table 53) to ascertain if any of the microfabrics were contributing to high concentrations of void abundance in the graves or sample locations. The total void abundance was calculated as a sum of the abundance of void types, as there was no image analysis data that related specifically to microfabric types. At Çatalhöyük, CH4 and CH5 had peaks in the abundance of packing voids compared to CH1, CH2, CH3 and CH6. In CH5 this also coincided with a peak in vugh abundance. At Thessaloniki, Ti1 contained higher abundances of channels, planes and packing voids compared to Ti2 which, overall, had a much lower void abundance. The disparity between the abundance and formation of void types at Çatalhöyük and Thessaloniki, however, did not appear to affect the overall results.

Total void abundance at Hungate was high (>20%) in HU5, HU7, HU10 and HU13. Peaks in plane and vugh abundances coincided in HU5 and HU7. Vughs were also high in HU10 and HU13. HU13 was widespread therefore the influence of the high abundance of void space in this microfabric on high levels of voids in each grave would have been minimal, HU5, HU7 and HU10 where however more sporadic. HU7 was present in small quantities (30%) in the foot sample from SK51350, which had a high total void space abundance, however HU7 was present in such low abundances it is unlikely to be the causes of high level of overall voids in SK51350. Similarly a link could not be made between high abundance of HU7 and HU10 and high abundance of total void space in any grave. There were several microfabrics at Hungate where there were corresponding peaks in planes and vughs in HU5, HU7 and HU10, however these could not be linked to corresponding high levels of plane or vughs in any of the Hungate graves (for microfabric locations see chapter 3), probably due to the limited abundance of HU5, HU7 and HU10.

Table 53: Total void abundance (calculated as a sum of void type abundance) and void type abundance, shown as a percentage of the average area of the microfabric composed of void space.

	Channels	Planes	Vughs	Packing	Total
CH1	5.00	3.70	2.80	0.00	11.50
CH2	4.17	0.83	4.50	6.67	16.17
CH3	0.83	1.67	0.00	0.00	2.50
CH4	1.33	4.83	1.08	30.83	38.08
CH5	1.67	4.00	14.00	30.00	49.67
CH6	3.33	0.67	0.00	0.00	4.00
Ti1	6.04	5.88	8.80	11.80	32.52
Ti2	3.00	3.50	9.25	0.00	15.75
HE1	3.27	1.67	0.87	4.40	10.20
HU1	0.82	2.65	2.94		6.41
HU2		0.00		1.67	1.67
HU3		1.20	1.00		2.20
HU4	0.57	3.14	2.14		5.86
HU5		10.00	25.00		35.00
HU6		0.67			0.67
HU7		10.00	30.00		40.00
HU8	3.14	2.57	10.29	0.29	16.29
HU9		3.00	5.00		8.00
HU10	1.60	1.80	26.00	4.00	33.40
HU11	1.00	3.00	3.50		7.50
HU12	4.46	4.23	5.92		14.62
HU13	2.70	3.66	11.18	2.91	20.45

7.3 Summary and discussion

The purpose of this chapter was to characterise the soil structure and to identify trends in ped type, size, abundance or development and to assess to what extent the variation relates to site conditions caused by either burial practice or site context. To achieve this, the nature and distribution of peds and voids between sites, grave, control samples and samples from the burial plane was assessed. The three elements detailed in this chapter (peds, total void abundance and void type) are highly interrelated, due to this, only patterns that appear to relate to the presence of the grave or other relevant environmental factors will be highlighted.

7.3.1 Distinguishing different sites (inter site variation).

Apedal soils, sub-angular blocky peds and platy peds were present at all sites, as were packing voids, channels, vughs and planes. The extent, distribution and abundance of the types of peds and voids as well as the overall void abundance, however, differed between sites, perhaps due to the influence of the environmental contexts of sites, as well as burial practice and decomposition rates, on the formation and stabilisation of voids and peds.

Çatalhöyük contained a high diversity of ped types, with apedal sediments, sub-angular, angular, platy, crumb and granular peds. In addition, Çatalhöyük had a low overall void abundance, which was dominated by packing voids. This would be consistent with the thin section observations at Çatalhöyük which contained well-developed, ultra fine to fine blocky and spheroidal peds, with few intrapedal voids, creating packing voids. In an open soil environment, the development of blocky and spheroidal peds, as well as apedal sediments, have been well documented. In addition to this, the development of void types and abundance in thin section can elucidate crucial information about the soils structural development, as well as the movement and storage of water. Spheroidal peds (crumbs and granules) and angular blocky peds, which have been observed at Çatalhöyük, can be caused by wetting and drying (Kovda & Mermut, 2010, Kovda *et al.*, 2008), reworking of the soil by organisms (Davidson *et al.*, 2004, Davidson & Grieve, 2006) and freeze thaw (Bockheim & Tarnocai, 1998, Van Vliet-Lanoë, 2010). Freeze thaw is unlikely at any of the sites in this study given the geographic location and a lack of other micromorphological features associated with cryoturbation (Bockheim & Tarnocai, 1998). The evidence for wetting and drying and soil organisms at Çatalhöyük was also limited, with few indicators of soil organisms present (see Pedofeatures Chapter 8.3.1), including low instances of channels and vughs (Figure 92), which have also been linked to soil organisms (Brewer, 1964, Kooistra & Pulleman, 2010). Granular structures can be formed at the surface of the soils and attributed to rapid desiccation (Hussein & Adey, 1998). The granular peds at Çatalhöyük, however, had mostly formed below the surface, suggesting other processes may be a factor. The environmental and contextual information from Çatalhöyük indicates that the floor deposits would have been sheltered from external environmental factors such as rainfall and raising groundwater (Asouti *et al.*, 1999), suggesting that, although the burial soils may have become wet, they are unlikely to have been saturated to an extent that would strongly influence soil formation. The platform areas, under which the burials were placed at Çatalhöyük, were constructed from disaggregated building material (see microfabrics Chapter 3), the aggregates of which contained few voids but had

formed as spheroidal and blocky peds with inter pedal packing voids accounting for the high abundances of both features at Çatalhöyük. It is therefore likely that the microstrucutre at Çatalhöyük has been strongly influenced by the construction of the platform with minimal post depositional soil development occurring.

Thessaloniki contained apedal sediments, sub-angular blocky peds, granules and platy peds. The site was also dominated by high abundances of total void space (mean 15.95%) and packing voids. Apedal sediments and sub-angular blocky peds were common but generally poorly developed and varied greatly in size (Table 49). Sub-angular blocky peds are typically caused by organisms reworking the soil, wetting and drying and freeze thaw (Bockheim & Tarnocai, 1998, Bullock *et al.*, 1985, FitzPatrick, 1993, Kovda & Mermut, 2010, Kovda *et al.*, 2008, Stoops, 2003). Apedal sediments, however, are the result of either the failure of peds to form (Bullock *et al*., 1985, FitzPatrick, 1993, Stoops, 2003) or their subsequent disaggregation through processes such as saturation and compaction, leading to soil collapse and loss of structure (Kooistra & Tovey, 1994). The presence of high abundances of poorly developed peds as well as apedal soils would suggest that peds have either struggled to form or that disaggregation processes were/are occurring across the site. Iron-(hydr)oxides have been shown to be instrumental in the binding of particles to aggregates (Regelink *et al*., 2015). Therefore the disaggregation of soil particles can occur though the mobilisation of chemicals in the soil (Barbiero *et al.*, 2010, Brinkman, 1970, Brinkman *et al.*, 1973, Lindbo *et al.*, 2010), releasing chemical bonds between soil particles and allowing their subsequent movement and infilling or collapse of void space. For Fe and Mn this is achieved through seasonally alternating reduction and oxidation of Fe and Mn that causes the displacement of base cations (Ca, Mg, K and Na), which can then be leached, coinciding with the destruction of part of the clay lattice (Brinkman, 1970, Brinkman *et al*., 1973). These processes can be further intensified by the addition of organic matter (Lindbo et al., 2010, Schlesinger, 1991). Barbiero *et al*(2010) also argues that environments that promote the weathering of clay minerals may favour $CaCO_3$ pedofeature formation. The occurrence of saturation at Thessaloniki is unknown. There is, however, evidence of iron and manganese pedofeature formation (see Pedofeatures section 8.1.3) and thick laminated coatings (see Pedofeatures 8.2.3), which would suggest that there was some wetting and drying occurring. In addition, the internal collapse of the soil may also have occurred due to decomposition of the body creating a void into which the soil overburden may have collapsed (Dent, 2002): the likelihood is that a combination of these processes occurred. Thessaloniki also had a high overall total void space composed of high abundances of packing voids, both features that have been linked to cyclic wetting and drying

(Hussein & Adey, 1998, Kovda & Mermut, 2010). High abundances of void space would also have created a high surface area to volume ratio in which cation exchange could have occurred.

Heslington East had the highest total void abundance at 17.82%, although each of the void classes were present only at low abundances. Ped formation was also restricted and composed of ultra fine to coarse primary sub-angular blocky peds and moderately to well developed secondary coarse to very coarse platy peds. Infrequent apedal sediments were also present. The causes of sub-angular blocky peds are explored above. Platy peds are caused by wetting and drying (Hussein & Adey, 1998), compaction (Kooistra & Tovey, 1994), frost action (Van Vliet-Lanoë, 2010), or the presence of pre-existing layers, such as the formation of banded sediments by multiple depositional phases resulting in planes of weakness on the deposition boundary (Bullock *et al*., 1985, FitzPatrick, 1993, Stoops, 2003). Platy peds caused by compaction are generally confined to the upper surface horizons (Kooistra & Tovey, 1994). At Heslington East platy peds were present in the grave fill and burial plane and not in the C1 samples, suggesting that compaction from heavy farm equipment was minimal. Wetting and drying may also be a factor in ped formation and disaggregation at Heslington East, as the site is located on an active spring line (National Soil Resources Institute, 2011a, O'Connor *et al.*, 2011), although the spring line was positioned away from the burial (Roskams pers. coms.). Alternative causes of platy peds specific to grave environments, must be considered. Platy peds may be due to the collapse and compaction of the soil around decomposing bodies and associated grave goods as well as the collapse of the soil overburden. There may also have been layering occurring when the grave was backfilled. If this is the case, platy peds would be expected to be preferentially located around soft tissue or voids in the grave such as the pelvic area and the middle/upper grave fill where soil has collapsed into the grave (see conceptual model in Introduction 1.6). At Heslington East platy peds are located in the grave fill and the hand sample (which was over the pelvis), suggesting that compaction may be a factor in the formation of platy peds. Like Thessaloniki, Heslington East contains some apedal soils with poorly to moderately developed sub-angular blocky peds. Similar processes may therefore be occurring at Heslington East and Thessaloniki in terms of the disaggregation of soil particles due to high redox potentials and collapse creating a weakly developed ped structures. Again this may have been exacerbated by high overall abundances of total void space creating a high surface area for cation exchange. High total void abundance also suggests a well-aerated soil and, although all void classes were present at low abundances, channels and vughs, both of which are proxy indicators for soil organisms (Bottinelli *et al.*, 2010, Brewer, 1964, VandenBygaart *et al.*, 2000), where frequent, suggests that there was some biological activity occurring at Heslington

East. This would also be consistent with the pedofeature evidence described in Chapter 8 and the organic coarse material evidence for roots at Heslington East (see section 6.4.3). Biological activity may be related to the presence of the body or could be more recent and due to the use of the area as farm land. It would however be difficult to distinguish between these two causes without a much larger sampling strategy.

Hungate contained a high diversity of peds with apedal sediments, angular, sub-angular, crumb, granule and platy peds. It was, however, fairly low in total void space at a mean of 12.63%, which was dominated by vughs. As with Thessaloniki, there was a predominance of apedal soils and weakly to moderately developed sub-angular blocky peds with sporadic well developed crumbs, granules and platy peds (Table 51). As with Thessaloniki and Heslington East, it is possible that high redox potentials caused by abundant organic matter and periodic saturation from the River Foss (Evans, 2007b) may have contributed to the weakening of the ped structure and collapse of the soil leading to the formation of vughs, which can be caused by the dissolution of components, aggregation, flocculation and soil fauna (Brewer, 1964, Kooistra & Pulleman, 2010, Ringrose-Voase & Bullock, 1984, Stoops, 2003). Soil fauna and bioturbation may have been occurring at Hungate, as there are low levels of packing voids and channels present as well as vughs which can be produced through the action of soil organisms (Davidson & Grieve, 2006, Kooistra & Pulleman, 2010, Pagliai *et al.*, 2003, Ringrose-Voase & Bullock, 1984, Russell, 1971). The presence of soil fauna would also be supported by the pedofeature evidence (see section 8.3.4).

The number of ped types (platy, blocky, angular etc) and the types themselves varied between the sites, although this may have been influenced by sample size or number of microfabrics. The number of ped types at sites varied (Hungate n=6, Çatalhöyük n=6, Thessaloniki n=4 and Heslington East n=3) and loosely correlates with the number of samples analysed at each site (Hungate n=68, Thessaloniki n=26, Çatalhöyük n=13 and Heslington East n=10). Çatalhöyük, however, does not fit well within the sequence. A better correlation exists between microfabric types and ped types present (Hungate n=13, Çatalhöyük n=6, Thessaloniki n=2 and Heslington East n=1). As the number of ped types correlated better with the number of microfabric types this would suggest that differences in the number of ped types between sites is not entirely due to the number of samples taken at each site but that the number of microfabric types is also important, suggesting that soils that have a high diversity of soil processes occurring tend to create high numbers of microfabrics tend to have more diversity in ped types.

7.3.2 Distinguishing C1 samples and different graves (intra site variation).

7.3.2.1 Distinguishing the C1 samples

C1 samples were obtained from Çatalhöyük, Heslington East and Hungate. In terms of the ped types, sizes total void abundance and void types, there were some differences between the C1 samples and the samples from the graves. The expression of these differences, however, varied between sites.

At Çatalhöyük, the difference between the C1 sample and those from the graves consisted of high abundances of packing voids in the C1 and a lack of vughs compared to the grave samples, as well as smaller crumb and to some extent smaller sub-angular blocky peds present in the grave than in the C1 sample. Packing voids are caused by the loose packing of soil materials, faunal excreta and shrinking and swelling processes (Brewer, 1964, Kooistra & Pulleman, 2010, Ringrose-Voase & Bullock, 1984, Stoops, 2003). As discussed above, shrinking and swelling, as well at faunal evidence, is limited at Çatalhöyük, suggesting that the high abundance of vughs in the burial plane is caused by a higher degree of coalesce than in the C1 samples. This implies that the material used to build the platform in which the graves were placed was more densely packed than the C1 sample, thus creating a closed void structure with a predominance of vughs as opposed to packing voids.

At Heslington East and Hungate, the C1 samples were distinguishable by a narrower range of total void abundance and lower total void abundance means compared to the samples from the graves. In addition at Heslington East, the C1 samples had a lack of platy peds and an increase in apedal sediments with depth, as well as a high abundance of packing voids and high ped sizes compared to the grave. At Hungate the C1 samples were completely apedal, whereas the majority of grave samples had some ped development. Previous studies assessing the microstrucutre of soil in relation to cyclic wetting and drying have noted that such cycles produce an increase in total void space (Hussein & Adey, 1998, Pires *et al.*, 2008) including instances where soil was wetted through capillary action (Hussein & Adey, 1998), suggesting that the grave samples experienced more wetting and drying than the C1 sample, possibly due to the grave samples being lower in the soil profile and therefore closer to the water table. The narrow range of total void abundance in the C1 samples from both sites is likely to be an artefact of samples size. The absence of peds in the C1 samples at Heslington East and Hungate is possibly due to either the

destruction of peds by saturation, or at Heslington East by cultivation or compaction (Birkeland, 1984, Bullock *et al.*, 1985, FitzPatrick, 1993, Kooistra & Tovey, 1994, Stoops, 2003).

7.3.2.2 Distinguishing different graves

There was mixed success in distinguishing different graves based on their soil structure as expressed in the ped type, sizes, total void abundance and void type abundance. Systematic changes that related to specific environmental conditions or burial taphonomy were sporadic. There were, however, some noteworthy trends which were apparent in the total void abundance at all sites and in the abundance of different void classes at Hungate.

At Çatalhöyük grave 18666 was distinguished from the C1 sample and grave 19295 due to low mean abundances of total void space at 5.19% of total slide area compared to 10.74% in the C1 and 12.51% in grave 19295. This also correlated well with higher abundances of packing voids in the C1 and 19295 compared to 18666, meaning that either the void space has been reduced in 18666 compared to the C1 or increased in 19295 to the same abundances as the C1 samples. As there is a correlation between total void space and an abundance of packing voids, this may be due to similar processes as described above for the C1 sample, where there has been a higher level of aggregation in 18666. 18666 contained sub-angular blocky and granular primary peds where as in 19295 sub-angular blocky peds had formed as secondary structures and granular peds as primary ped formations, suggesting that there may have been different ped developmental processes occurring in each grave.

Graves from Thessaloniki may be grouped according to their total void abundance with the oldest graves (TF157, TF182 and TF177) forming a group with low, but variable, total void abundance and the younger graves (TF178 and TF162) formed a second group with high total void space and low variability. In the first group, all graves contained a mixture of channels, packing voids and planes that varied in abundance, but were all low level with the exception of TF177 that had slightly elevated levels of packing voids and planes. In the latter group high total void abundance was caused by high abundance of channels and planes in TF178 and packing voids in TF162, suggesting that different processes may be responsible for the high abundance of total void space. The possibility of a number of different processes being responsible for high total void abundance would account for the unsystematic nature of the groups that do not relate to either burial practice or grave position. Channels are caused by soil organisms either through the presence of roots or soil faunal activities (Brewer, 1964, Kooistra & Pulleman, 2010). The causes

of planes, however, are more varied and include mechanisms which causes stress on the soil including, compaction, freeze thaw and wetting and drying (Brewer, 1964, FitzPatrick, 1993, Hussein & Adey, 1998, Kooistra & Tovey, 1994). TF177 also contained high abundances of sub-angular blocky peds (linked to high levels of planes). Like planes and channels sub-angular blocky peds have also been linked to faunal activity as well as wetting and drying. Packing voids which were abundant in TF178 can be caused by loose packing of soil materials, fauna excreta and shrinking and swelling processes (Davidson & Grieve, 2006, Hussein & Adey, 1998, Kovda & Mermut, 2010), suggesting that these process were more influential in the formation of grave TF178 than the other graves at Thessaloniki due to the high abundances of packing voids in TF178 compared to the other graves.

At Hungate there were distinct patterns in total void abundance, with two groups of graves. Firstly SK54898, SK51326, SK51387, SK51351, SK54341, SK54342 and SK54908 that had low porosity (low mean void abundances and low upper quartiles). The second group consisted of SK54090, SK54085 and SK51350 with high porosity (higher median void abundances and high upper quartile ranges). These groupings, however, did not appear to be systematic or relate to burial practice, age of the individual buried or location within the cemetery (Figure 89). In addition SK54898 was atypical, as it contained high abundances of planes and low abundances of vughs, as well as a high abundance of fine to very fine sub-angular blocky peds. The context of SK54898 was very different from the other graves at Hungate, it being a lead coffin that contained layers of sediment (see method and microfabrics chapter section 3.5). The high plane abundance had probably been influenced by the presence of layered material and also reflected in the sporadic presence of platy peds in SK54898. The nature of the lead coffin sediments, being generally layered inwash (see Microfabrics Chapter 3.5), may not have been conducive to vugh formation, which form through the dissolution of components, aggregation and soil fauna (Brewer, 1964, Kooistra & Pulleman, 2010, Ringrose-Voase & Bullock, 1984, Stoops, 2003). In other graves aggregation, as well as soil fauna, may have been a key vugh formation factor through the collapse of the soil overburden, creating small aggregates and the ingress of soil fauna into the graves. The size of the peds was also interesting in SK51350 where coarse to very coarse platy peds had formed as well as SK54342 and SK54908 where ultra fine to medium crumbs had formed.

7.3.3 C2 and C3 vs burial plane samples and systematic variations in the burial plane (intra grave variation).

7.3.3.1 C2 and C3 vs samples from the burial plane

Inter grave variation was considered for ped development, presence and diversity, total void space and the nature of void space. On the intra grave level there were no systematic differences in the C2 and C3 samples and those from the burial plane. This may be partly due to the wide level of variation in the soil that has developed independently of the grave deposits and partly due to the positioning of C3 samples in the burial plane as the ped types in the C3 samples were particularly similar to the grave samples.

7.3.3.2 Systematic variations in the burial plane

There was no single pattern of lateral changes to void space and types that could be applied universally to all graves. Instead the distribution and abundance varied between graves. There was, however, a general trend, of reduced levels of total void space in the pelvic area. The type of voids also varied laterally in the burial plane and tended to consist of low levels of channels and vughs in the skull, and high levels of vughs and planes coinciding with low levels of packing voids in the pelvic area. The low levels of channels and vughs in the skull area suggests that there has been a general lack of bioturbation from either root penetration and / or soil faunal activity, compared to other areas of the grave, the reason for this is however unknown (Brewer, 1964, Kooistra & Pulleman, 2010, Ringrose-Voase & Bullock, 1984, Stoops, 2003). Reduced levels of packing voids and total void space, as well as elevated levels of planes, in the pelvis area is consistent with the process that results in stress on the soil such as compaction and wetting and drying (Brewer, 1964, Kooistra & Pulleman, 2010, Kourkoutidou-Nicolaidou, 1997, Ringrose-Voase & Bullock, 1984, Stoops, 2003). Compaction would create a greater degree of aggregation, reducing the levels of packing voids, whereas saturating the soil would result in the loss of shear resistance resulting in the collapse of the soil and loss of void space (Kooistra & Tovey, 1994), whereas wetting and drying cycles may have contributed to the formation of planes (Kovda & Mermut, 2010). This pattern, however, is not consistent for every grave, meaning that there are grave specific factors that are strongly influencing the distribution and nature of void space around the skeleton such as localised wetting and drying, compaction and bioturbation.

At Çatalhöyük, slide orientation affected the abundance of peds with the perpendicular samples from 18666 and 19295 showing high levels of apedal material. The understanding of the

processes responsible for this pattern may have important implications for sampling strategy, depending on whether it is a real effect caused by taphonomic processes or an artefact of low sample numbers and high local variability.

7.3.4 The influence of microfabric types.

The ped distribution, ped size, total void abundance and void type abundance was assessed across the 22 microfabrics identified in this study (see Microfabrics Chapter 3). Although the abundance and distribution of peds, total voids and void types varied between microfabrics, the variation was not systematic and not linked to concentrations of ped and void types or overall void abundance in the graves or samples. Concentrations or systematic variation in ped and void types as well as total void abundance was therefore likely to be caused by grave taphonomic processes and was not the product of concentrations of or the occurrence of microfabrics.

7.4 Conclusions

It is clear that both site environmental factors as well as post depositional taphonomic processes specific to inhumations have a strong influence on the development of the soil structure within the grave. At an inter site level, the contexts of the sites are strongly influencing the soil structure, particularly at Çatalhöyük where soil formation processes are limited due to the nature and location of the burials within built structures. At Thessaloniki, Heslington East and Hungate, however, a more extensive suite of formation processes appear to be active and processes such as collapse and disaggregation appear to be more common, producing graves with high levels of apedal soils and quite weakly to moderately developed ped profiles. It is also difficult but not impossible to discern C1 samples from those from the burials. However, again, site influences complicate this process, as each site needs to be evaluated on a case by case basis. When the C2 and C3 samples are also considered, these tend to reflect the soil structures that are present in the graves, which may be either the effect of the grave extending into the burial fill or an artefact due to samples, particularly the C3, being taken from the burial plane. Having established this, however, it is possible to identify a limited number of graves, namely SK54898 due to its soil structure, which is probably due to the unusual context of the grave. What is interesting, however, is that when the lateral variation in total void abundance and void types is considered, the ‘grave signal’ begins to assert itself providing some ‘grave markers’ in the form of low levels of total void space in the pelvic area, low levels of channels and vughs in the skull area, and high

levels of vughs and planes coinciding with low levels of packing voids in the pelvic area, that are apparent in most graves in the study.

8 Pedofeatures

Pedofeatures are fabric units in soil that are distinguishable from the surrounding material by differences in the internal fabric or the concentration and arrangement of soil components (Brewer, 1964 p. 142, Stoops, 2003 p. 101). Pedofeatures are produced through a number of pedogenic processes and can be inherited from the parent material as well as formed in situ (Brewer, 1964). The identification of the composition, morphology and location of pedofeatures can, therefore, be diagnostic of soil conditions, making them important in recognising and establishing past pedogenic processes. In reference to inhumations, pedofeatures could provide evidence for the presence of large amounts of organic material resulting in high levels of bioturbation. Evidence of soil settling or the collapse of the burial void may be expressed by the presence of coatings from particle translocation and the fragmentation of existing pedofeatures. Movement or concentrations of inorganic chemicals from the body may also be apparent and expressed as Mn/Fe concentrations in the soil. Coffined burials in particular present a unique set of microenvironmental conditions. The 'bucket effect' (Dent, 2002) may result in the pooling of water within the burial and increase the formation of pedofeatures associated with waterlogged environments, such as Mn/Fe concentrations, as well as promote anoxic conditions (Lindbo *et al*., 2010). Pedofeatures were analysed under the following categories: Mn/Fe pedofeatures, clay, silt and sand typic coatings, excremental and bioturbation features and $CaCO_3$ related features. Where possible and appropriate, the pedofeature presence, abundance and distribution will be assessed on three levels:

- Inter site (Çatalhöyük, Thessaloniki, Heslington East and Hungate).
- Intra site (Çatalhöyük, Thessaloniki and Hungate).
- Intra grave (Çatalhöyük, Thessaloniki, Heslington East and Hungate).

8.1 Iron and manganese pedofeatures

The nature of iron and manages pedofeatures within burials is important as their formation processes may lead to a fuller understanding of the burial environment and the distribution of bodily fluids. Iron and manganese pedofeatures are formed though oxidation and reduction which are highly influenced by the soil ph and redox potential (Lindbo *et al.,* 2010). The ph and redox potential can in turn be affected by soil temperature, chemical species, microbes, addition of organic matter and saturation level (Lindbo *et al*., 2010), aspects that can be influenced by the presence of a burial (Dent, 2000, Bethell & Carver, 2002, Janaway, 2003), therefore changes in the distribution and frequency of iron and manganese could be used as proxy indicators for these processes.

8.1.1 Inter site variation

Features containing manganese and iron were identified in thin section and, where possible, their chemical composition was confirmed using SEM-EDX analysis (Table 54). Fe and Mn/Fe pedofeatures were present at all sites (Table 54). Mn pedofeatures however were more sporadic and only present at Çatalhöyük and Hungate. Anorthic nodules, typic coatings and intercalations were common at all sites and present as Fe and Mn/Fe pedofeatures. Orthic and disorthic nodules, as well as hypocoatings, were also fairly common, although their composition was more restricted. Aggregated nodules, pendant coatings, quasicoatings, infillings and depletions were more sporadic, as were pedofeatures composed of Mn with no evidence of Fe. There was no systematic variation in the composition of iron and manganese pedofeatures, as determined by optical techniques or SEM-EDX and their distribution between sites.

Table 54: The presence of manganese and iron pedofeatures by site. Mn and Fe features were confirmed where possible using SEM-EDX analysis at Çatalhöyük, Thessaloniki and Hungate.

Pedofeature		Mn	Fe	Mn/Fe	Mn	Fe	Mn/Fe	Mn	Fe	Mn/Fe	Mn	Fe	Mn/Fe
		Çatalhöyük			Thessaloniki			Heslington East			Hungate		
Nodules	Anorthic	✓	✓	✓		✓	✓		✓	✓		✓	✓
	Orthic		✓	✓			✓				✓	✓	✓
	Disorthic		✓	✓		✓			✓			✓	✓
	Aggregated		✓			✓						✓	✓
Coatings	Typic	✓	✓	✓		✓	✓		✓	✓	✓	✓	✓
	Pendant											✓	✓
	Hypocoatings		✓	✓		✓	✓					✓	✓
	Quasicoatings											✓	✓
Impregnations			✓	✓		✓	✓		✓	✓		✓	✓
Infillings											✓	✓	
Intercalations			✓	✓		✓						✓	✓
Depletions												✓	

8.1.2 Çatalhöyük

8.1.2.1 Inter grave iron and manganese pedofeature variation at Çatalhöyük

Iron and manganese pedofeatures were present in the C1 and graves 18666 and 19295 (Table 55). Compared to the grave contexts, the C1 contained a limited range of iron and manganese pedofeatures, which included anorthic and orthic Fe nodules, typic Fe coatings, Mn/Fe hypocoatings, Fe impregnations as well as Fe intercalations. The burial contexts were more diverse with the addition of aggregated and disorthic nodules, and a wider range of chemical compositions for each pedofeature class, the implications of which will be discussed in section 8.5.2. There was however no systematic variation in the composition of iron and manganese features and their distribution between the graves and C1 samples.

8.1.2.2 Intra grave iron and manganese pedofeature variation at Çatalhöyük

The C1 sample was primarily composed of Fe pedofeatures with Mn/Fe pedofeatures only present as hypocoatings (Table 55). The graves samples however contained pedofeatures that were composed of Mn, Fe and Mn/Fe. Mn pedofeatures were rare, however they were present as anorthic nodules in the C3 and typic coatings in the parallel skull area sample from grave 18666. Iron and manganese pedofeatures were generally present at low abundances (<1% of total slide area), however there were some cases of elevated levels (≥3%) of Mn/Fe anorthic nodules in the

parallel pelvic area sample from 18666 and Mn/Fe impregnations in the parallel skull area sample from 18666. Anorthic nodules were ubiquitous and tended to be composed of Fe or Mn/Fe. More sporadic pedofeatures included orthic, disorthic and aggregated nodules, as well as intercalations. The abundance of impregnations was calculated for the skull, pelvic and foot sample from each grave (Figure 102). The distribution of the impregnations showed that, in the complete grave from Çatalhöyük, impregnations were concentrated in the skulls samples compared to those from the pelvic and foot areas.

Table 55: Abundance of manganese and iron pedofeatures identified at Çatalhöyük in the C1 and graves 18666 and 19295. Those not confirmed by SEM-EDX are identified by '*'.

Grave			C1	18666						19295				
										C3	19500		19501	
Position				C3	Skull		Pelvis		Foot		Skull		Skull	
Orientation			-	-	Perp	Para	Perp	Para	Perp	*	Perp *	Para *	Perp *	Para *
Nodules	Anorthic	Mn		1.6										
		Fe	2.68	1.75	0.84	1.8		0.1		0.25	2.66	0.95	0.25	1.05
		Mn/Fe			0.3	0.35	2.58	7.7	3		0.83	1.9		0.95
	Orthic	Mn												
		Fe	0.05										1	
		Mn/Fe				0.85								
	Disorthic	Mn												
		Fe						0.75						
		Mn/Fe			0.04	0.05								
	Aggregated	Mn												
		Fe									0.15			
		Mn/Fe												
Coating	Typic	Mn				1.7								
		Fe	0.96								0.02	0.95		
		Mn/Fe				0.85	0.86		2			0.95		
	Hypocoating	Mn												
		Fe			1.09			0.7					0.45	
		Mn/Fe	0.86		0.84				3	0.85				0.85

Table 55 cont.

Grave		C1	18666							19295				
										C3	19500		19501	
Position			C3	Skull		Pelvis		Foot			Skull		Skull	
Orientation		-	-	Perp	Para	Perp	Para	Perp		*	Perp *	Para *	Perp *	Para *
Impregnation	Mn													
	Fe	1.41	3.1	1.5			1.3				0.87		0.95	0.85
	Mn/Fe				3.15		0.25						1.3	0.1
Intercalations	Mn													
	Fe	0.05								0.85				
	Mn/Fe			1.68			0.05							

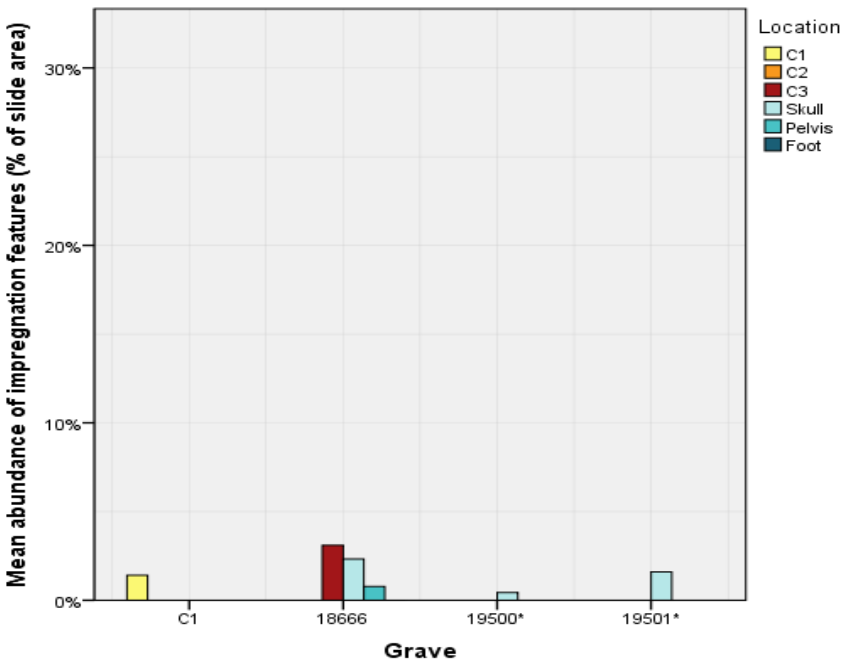

Figure 102: Abundance of impregnations in the skull, pelvic and foot samples shown in percent for all Çatalhöyük graves. Those graves that do not have all three sample points (skull, pelvis and foot) are identified by '*'. Where there is more than one sample available for sample location the average impregnation percent is given

8.1.2.3 Investigation into the distribution of P:Fe mean ratio in the fine material and impregnations at Çatalhöyük.

To investigate the movement of degradation products in the soil surrounding the burial and the controls the mean ratio of P to Fe was calculated for the fine material and the Mn/Fe impregnative pedofeatures in grave 18666 at Çatalhöyük (Figure 103). The levels of P:Fe were generally low in the fine material and impregnative Mn/Fe pedofeatures in the C1 and skull samples. The foot and C3 samples however had higher levels of P:Fe in the fine material and none in the impregnations suggesting that P had remained in the fine material or that the impregnations were inherited soil features formed prior to decomposition. There was a large peak in the relative concentration of P in the impregnations in the pelvic sample suggesting that the available P had precipitated into the impregnations with Fe. As 18666 was a crouched burial the pelvic sample was positioned below the feet the high levels of P in the impregnations in the pelvic area compared to the fine material would suggest that there has been a concentration of P in the pelvic area. The results of the P:Fe ratio do not correlate well with the micromorphological observations that showed high

levels of redoximorphic impregnations in the skull samples and high levels of redoximorphic nodules in the pelvic samples.

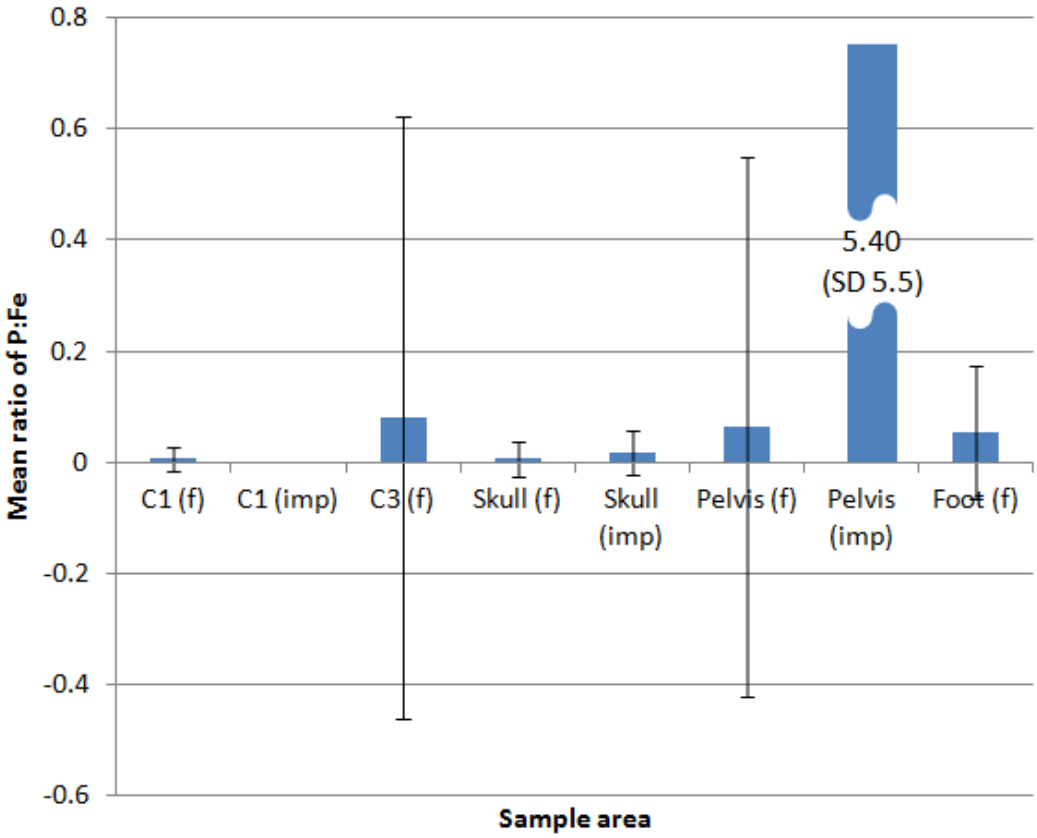

Figure 103: The mean ratio of P:Fe in the fine material (f) and the impregnations (imp) in the samples from grave 18666 at Çatalhöyük. Error bars show standard deviation

8.1.3 Thessaloniki

8.1.3.1 Inter grave Mn/Fe pedofeature variation at Thessaloniki

There was no systematic variation in the distribution and composition of iron and manganese pedofeatures between the graves (Table 56), however there were some noteworthy trends. Anorthic nodules were present in all of the graves as Fe and Mn/Fe pedofeatures. Hypocoatings and impregnations were also present in all graves as Fe pedofeatures and as Mn/Fe pedofeatures in TF182 and TF177 (hypocoatings) and TF157, TF182 and TF177 (impregnations). Orthic and disorthic nodules as well as aggregated nodules and intercalations were sporadic. Mn pedofeatures were absent from Thessaloniki. The implications of these trends will be further discussed in section 8.5.2

Table 56: The abundance of iron and manganese pedofeatures by site. Mn and Fe features were confirmed using SEM-EDX analysis. Where possible Mn/Fe features were also confirmed by SEM-EDX analysis

Grave			TF157				TF182							
Position			Skull	Pelvis	Foot	Hand	C2	C3	Skull	Pelvis		Foot	Hand	
Orientation			Para	Para	Para	Perp	-	-	Para	Perp	Para	Para	Perp	Para
Nodules	Anorthic	Mn												
		Fe	2			2	4	4	2.3	0.5	6	1.4	2	4
		Mn/Fe		2	2					5.4			2	2
	Orthic	Mn												
		Fe												
		Mn/Fe	2											
	Disorthic	Mn												
		Fe							0.5					
		Mn/Fe												
	Aggregated	Mn												
		Fe			2									
		Mn/Fe												
Coating	Typic	Mn												
		Fe							1.8	0.2	9	2.8		2
		Mn/Fe												
	Hypocoating	Mn												
		Fe				2					2	0.6		
		Mn/Fe									2			
Impregnation		Mn												
		Fe	4	4	2	6			1.8	1		2.9		
		Mn/Fe			2					1.8			5	2
Intercalations		Mn												
		Fe										1.4		
		Mn/Fe												

Table 56 continued

Grave			TF177								TF178		TF162		
Position			C3	Skull		Pelvis		Foot		Hand	Skull	Pelvis	Skull	Pelvis	Foot
Orientation			-	Perp	Para	Perp	Para	Perp	Para	Para	Para	Para	Para	Para	Para
Nodules	Anorthic	Mn													
		Fe	2		2	2				4	4	9	2		4
		Mn/Fe	2				2	1.8	2	2			2	2	
	Disorthic	Mn													
		Fe							2						
		Mn/Fe													
	Aggregated	Mn													
		Fe								2				2	
		Mn/Fe													
Coating	Typic	Mn													
		Fe		5							5				2
		Mn/Fe						1.8							
	Hypocoating	Mn													
		Fe	2	2					2			2		6	
		Mn/Fe				2	2	1.8							
Impregnation		Mn													
		Fe	4		9	7	2	10.8	4		4	2	2	4	7
		Mn/Fe		2						5					

8.1.3.2 Intra grave iron and manganese pedofeature variation at Thessaloniki

The control samples in TF182 contained few iron and manganese pedofeatures, with only Fe anorthic nodules present (Table 56). The samples from the burial plane, however, contained both Fe and Mn/Fe pedofeatures and, in addition to anorthic nodules, had disorthic nodules, typic coatings, hypocoatings, impregnations and intercalations. The C3 sample from TF177 contained a higher frequency of iron and manganese pedofeatures and more closely resembled samples from the burial plane in terms of the presence, abundance and pedofeature composition. Anorthic nodules, impregnations and hypocoatings were common and present in almost all slides studied. The majority of iron and manganese pedofeatures were present at low abundances (≤4%). Interestingly, however, almost all of

the iron and manganese pedofeatures that were present at above 4% abundance were composed of Fe. The abundance of impregnations was calculated for the skull, pelvic and foot area samples (Figure 104). The abundance of impregnations was elevated in the pelvic samples in three of the five graves from Thessaloniki, with another grave showing equal abundances of impregnations in all three locations. Interestingly the graves that showed an elevation in Fe/Mn impregnations were all located within buildings (Figure 105). The implications of this trend will be discussed further in section 8.5.4

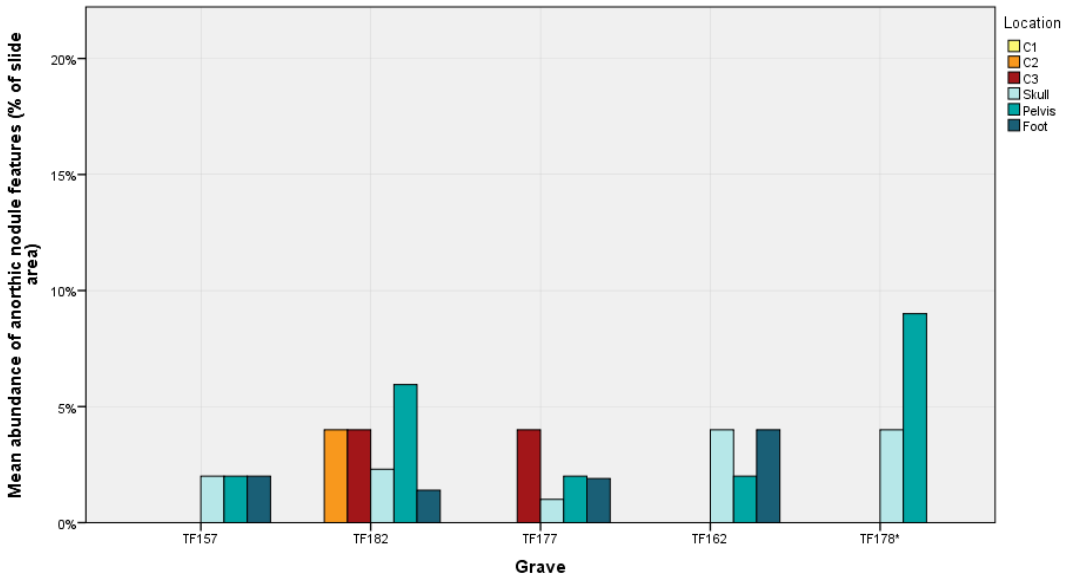

Figure 104: Abundance of impregnations in the skull, pelvic and foot samples shown in percent for all Thessaloniki graves. Those graves that do not have all three sample points (skull, pelvis and foot) are identified by '*'. Where there is more than one sample available for a sample location the average impregnation abundance is given.

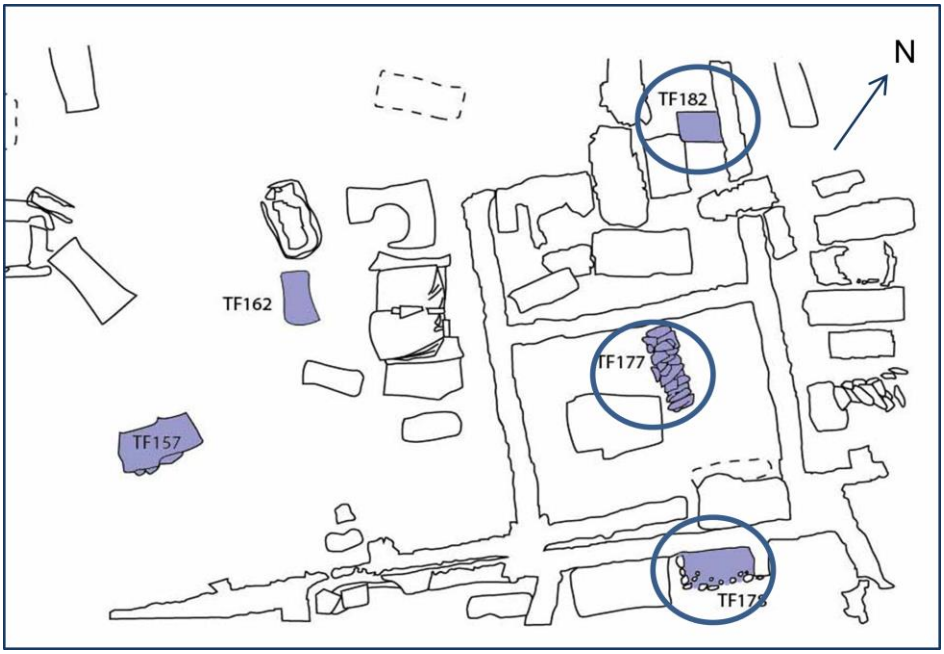

Figure 105: Location of the three graves showing elevations of Fe/Mn impregnations in the pelvic area (circled).

8.1.3.3 Investigation into the distribution of P:Fe mean ratio in the fine material and impregnations at Thessaloniki.

To investigate the movement of degradation products in the soil surrounding the burial and the controls the mean ratio of P to Fe was calculated for the fine material and the Mn/Fe impregnative pedofeatures in grave TF177 at Thessaloniki (Figure 106). P:Fe is either very low or absent in the C3, pelvis and foot fine material and impregnations in TF177. There are high levels of P:Fe in the skull impregnations and some P:Fe in the fine material in the skull sample. This would suggest that there is higher levels of available P in the skull compared to the other areas of the grave and that the available P has been co-precipitated with Fe to form impregnations in the skull. This does correlate well with the micromorphological evidence where there are high abundances of impregnations in the skull area. However there are higher abundances of impregnations in the pelvic and foot regions, suggesting that in these areas the impregnative features may be inherited.

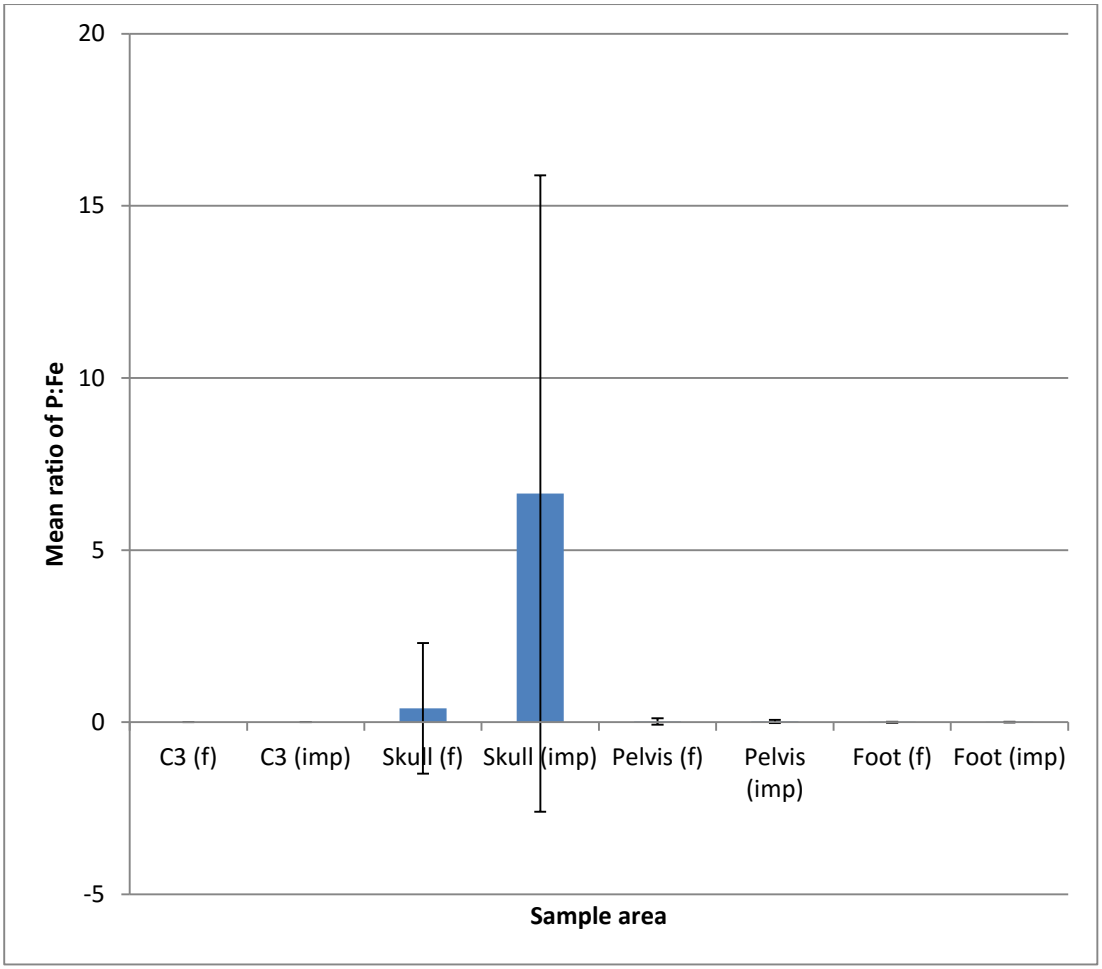

Figure 106: The mean ratio of P:Fe in the fine material (f) and the impregnations (imp) in the samples from grave TF177 Thessaloniki. Error bars show standard deviation

8.1.4 Heslington East

8.1.4.1 Intra grave iron and manganese pedofeature variation at Heslington East

All samples from Heslington East contained iron and manganese pedofeatures (Table 57). There was no systematic variation in iron and manganese pedofeatures that related to sample location however there were some interesting trends. The C1 samples contained both Fe and Mn/Fe pedofeatures, although the anorthic nodules were only present in the C1 samples as Mn/Fe pedofeatures. Typic coatings were absent from the grave samples and disorthic nodules were not present in the C1 samples. Almost all iron and manganese pedofeatures were present at low abundances (≤4%). There were, however, elevated levels of Mn/Fe anorthic nodules in the top C1 sample (9%) and in the hand area sample (10%). In addition to this, the C2 and hand area sample contained elevated Fe anorthic nodule

abundances, both at 7%. There were also high abundances of Fe impregnations in the C3 and skull area samples.

Table 57: Abundance of Mn/Fe pedofeatures features identified at Heslington East.

Grave			C1			713				
Position						C2	C3	Skull	Foot	Hand
Orientation			-	-	-	-	-	Perp	Perp	Perp
Nodules	Anorthic	Mn								
		Fe				7			2	7
		Mn/Fe	9	4	2	1		2	2	10
	Disorthic	Mn								
		Fe					2		2	
		Mn/Fe								
Coating	Typic	Mn								
		Fe		2						
		Mn/Fe			2					
Impregnation		Mn								
		Fe	2	4	4	2	5	5	2	5
		Mn/Fe	2			1	1			2

The abundance of impregnations was calculated for the skull and foot area samples for Heslington East. Grave 713 showed elevated abundances of impregnations in the skull area sample.

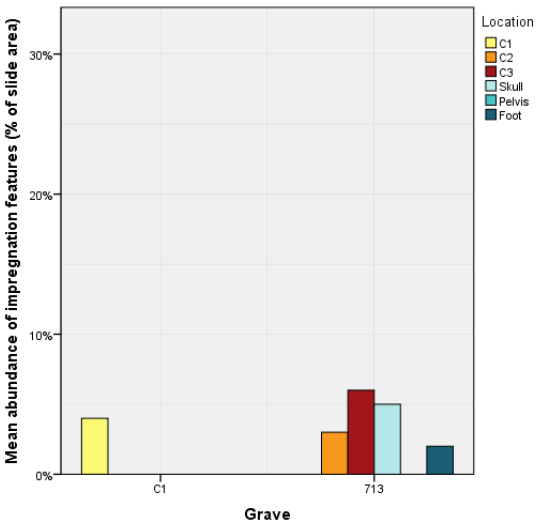

Figure 107: Abundance of impregnations in the control, skull and foot samples, shown in percentage of slide area at Heslington East graves.

8.1.5 Hungate

8.1.5.1 Inter grave iron and manganese pedofeature variation at Hungate

Hungate contained Mn, Fe and Mn/Fe pedofeatures. Anorthic nodules and impregnations were present in all graves and the C1 samples as Fe and Mn/Fe pedofeatures. Typic coatings and infillings were also present in all graves and the C1 samples, but only as Fe and Mn/Fe features in the majority of the graves analysed. Orthic, disorthic and aggregated nodules were more sporadic, as were pendant and hypocoatings, intercalations and depletions. The intra grave iron and manganese pedofeatures variation will now be explored.

8.1.5.2 Intra grave iron and manganese pedofeature variation at Hungate

All samples from Hungate contained iron and manganese pedofeatures (see Appendix 4.1). The C1 samples contained both Fe and Mn/Fe pedofeatures consisting of low abundances (1%) of Fe anorthic nodules, disorthic nodules, coating, infillings and impregnations as well as Mn/Fe impregnations (5%) and intercalations (1%). Fe and Mn/Fe impregnations, and Fe infillings increased in the middle C1 sample to 2%, 7% and 1% respectively but Fe impregnations were absent from the lower C1 and Mn/Fe impregnations had dropped to 1%. Mn/Fe anorthic nodules were present in the middle C1 at 1% however all other pedofeatures were absent. The lower C1 sample contained a peak of Mn/Fe hypocoatings at 9% in addition to Fe and Mn/Fe disorthic nodules and Fe coatings as low levels. Nearly all of the Mn/Fe pedofeatures at Hungate were present in low abundances (≤4%). However there were peaks in Mn/Fe abundance within graves mainly focused in the anorthic nodules and impregnation pedofeatures (5-20%). These two pedofeature types were, therefore, investigated further in terms of their relationship to location within the grave. There is no systematic variation in the impregnation or anorthic nodule abundance between the C1, C2, C3 and samples from the burial plane, and no systematic variation in the abundance of iron and manganese anorthic nodules in the burial plane. A comparison was also made between the impregnation abundance in the skull, pelvis and foot area samples for all the Hungate graves (Figure 109). Of the complete graves that were sampled at Hungate, all except SK54342 (six graves) have elevated levels of iron and manganese impregnations in the foot area samples compared to the pelvis and skull area samples

(86%) (Figure 109 and Figure 108). These graves are located throughout the cemetery indicating that grave location is not a contributory factor.

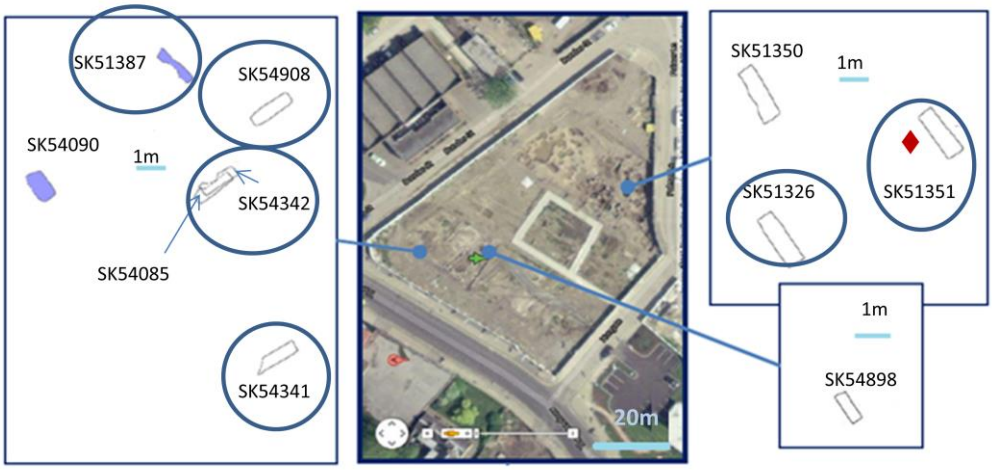

Figure 108: Location of graves with elevated concentrations of impregnations in the foot area.

8.1.5.3 Investigation into the distribution of P:Fe mean ratio in the fine material and impregnations at.

To investigate the movement of degradation products in the soil surrounding the burial and the controls the mean ratio of P to Fe was calculated for the fine material and the Mn/Fe impregnative pedofeatures in graves SK54898, SK51326, SK54908, SK54085, SK54341, SK51387, SK51351 and SK54090. When all eight graves that were sampled for SEM-EDX analysis are considered together there are higher levels of P:Fe in the fine material in the grave samples compared to the C1 samples. Grave SK54898, the lead coffin grave, also contains higher levels of P:Fe in the burial plane fine material than the other graves sampled at Hungate. When the levels of P:Fe in the impregnations are considered across Hungate most graves are similar to the abundances in the C1 samples. SK54898, SK54341 and SK54090 are the exception to this and the impregnations in these graves were high in P:Fe compared to the other graves and the C1 samples. There was no correlation between high levels of P:Fe in the impregnations and location of the grave in the cemetery.

In SK54898, the lead coffined grave, the samples that were taken inside the coffin are all high in P:Fe compared to those taken outside of the coffin (C1 and C2). There is also a higher concentration of P:Fe in the impregnations in the C3, skull and pelvic samples compared to the fine material, whereas this is reversed in the shoulder ('other' sample).

This would suggest that there was a large amount of available P inside the lead coffin that subsequently precipitated out into the impregnations. This correlates reasonably well with the micromorphological observations of impregnation formation with high levels in the pelvis, other and skull samples.

In SK51326 the C2 sample is similar to the C1 samples with higher levels of P:Fe in the impregnations than found in the fine material. The samples from the grave however have higher levels of P:Fe in the fine material compared to the C2 and are all reasonably similar at between 0.1-0.2 and just above 0.2. The ratio of P:Fe that has precipitated into the impregnations is more variable with higher levels in the C3 sample and skull compared to the fine material and slightly lower levels compared to the fine material in the pelvis and foot samples. In this instance the C3 sample was taken in the burial plane and through the coffin stain which in this instance maybe influencing the high levels of P:Fe in the C3 sample.

SK54908 contains high levels of P:Fe in the pelvis and foot samples in the impregnations compared to the fine material, suggesting that the available P in these areas has precipitated into impregnations. However in the skull sample there is a much higher concentration of P:Fe in the fine material and no impregnations present. When compared to the micromorphological evidence there are generally fewer Mn/Fe pedofeatures in the skull sample than in the rest of the grave suggesting that rather than precipitating into pedofeatures the P and Fe is remaining in the fine material.

In SK54085 the levels of P:Fe in the grave are slightly raised in the fine material and impregnations compared to the C1 and C3, although the levels of P:Fe in the pelvic impregnations are similar to the C3 sample. In all instances there is more P:Fe in the impregnations than in the fine material with particularly high levels in the skull. This correlates well with the micromorphological examination where the C3 contains less impregnations than the burial plane, however the grave samples contain similar abundances of Mn/Fe pedofeatures.

P:Fe is elevated in all samples from SK54341 in the impregnations compared to the fine material. In terms of the level of P:Fe in the fine material the samples in close proximity to the body, skull, pelvic and foot samples were higher than those from the C3 and A1 sample. This would suggest that the presence of the body has increased the available P in the

surrounding soil. When the levels of P:Fe in the impregnations are considered the burial plane samples are higher in concentration than the C3 with the pelvic sample being more elevated than the rest of the burial.

The concentrations of P:Fe is similar across grave SK51387. The C1 and skull samples both have higher levels of P:Fe in the fine material compared to the impregnations and have similar values. This would suggest that the available P is remaining in the soil or that the impregnations were inherited features formed before body decomposition. In the pelvic sample however the P:Fe ratio in the fine material is reduced compared to the impregnations meaning that there has been a greater degree of precipitation of P into redoximorphic pedofeatures than in the skull or C3 sample. The foot sample is interesting as the P:Fe values are similar in both the fine material and impregnations suggesting that an equilibrium has been reached.

SK51351 contained the lowest relative P:Fe ratios at Hungate and have an unusual distribution of P:Fe across the grave. There was a peak in P:Fe in the fine material of the foot sample whereas the P:Fe in the impregnations was higher in the skull sample and absent from the pelvic samples, which contained no impregnations. This pattern would suggest that in the skull and Al sample the available P was precipitating into Mn/Fe pedofeatures whereas in the foot and pelvic samples P has remained in the soil or that the impregnations were inherited features.

In SK54090 there are elevated levels of P:Fe in the impregnations in the C3 and the pelvic samples, this correlates well with the micromorphological investigation that showed elevated levels of impregnations in the C3 and pelvic sample from the same grave. In all the samples from SK54090 there are elevated concentrations of P:Fe in the impregnations compared to the fine material suggesting that the available P has precipitated into Mn/Fe pedofeatures. The C3 sample in this instance was taken from the burial plane opposite the pelvis which may be why the pelvic and C3 sample from this grave are chemically similar.

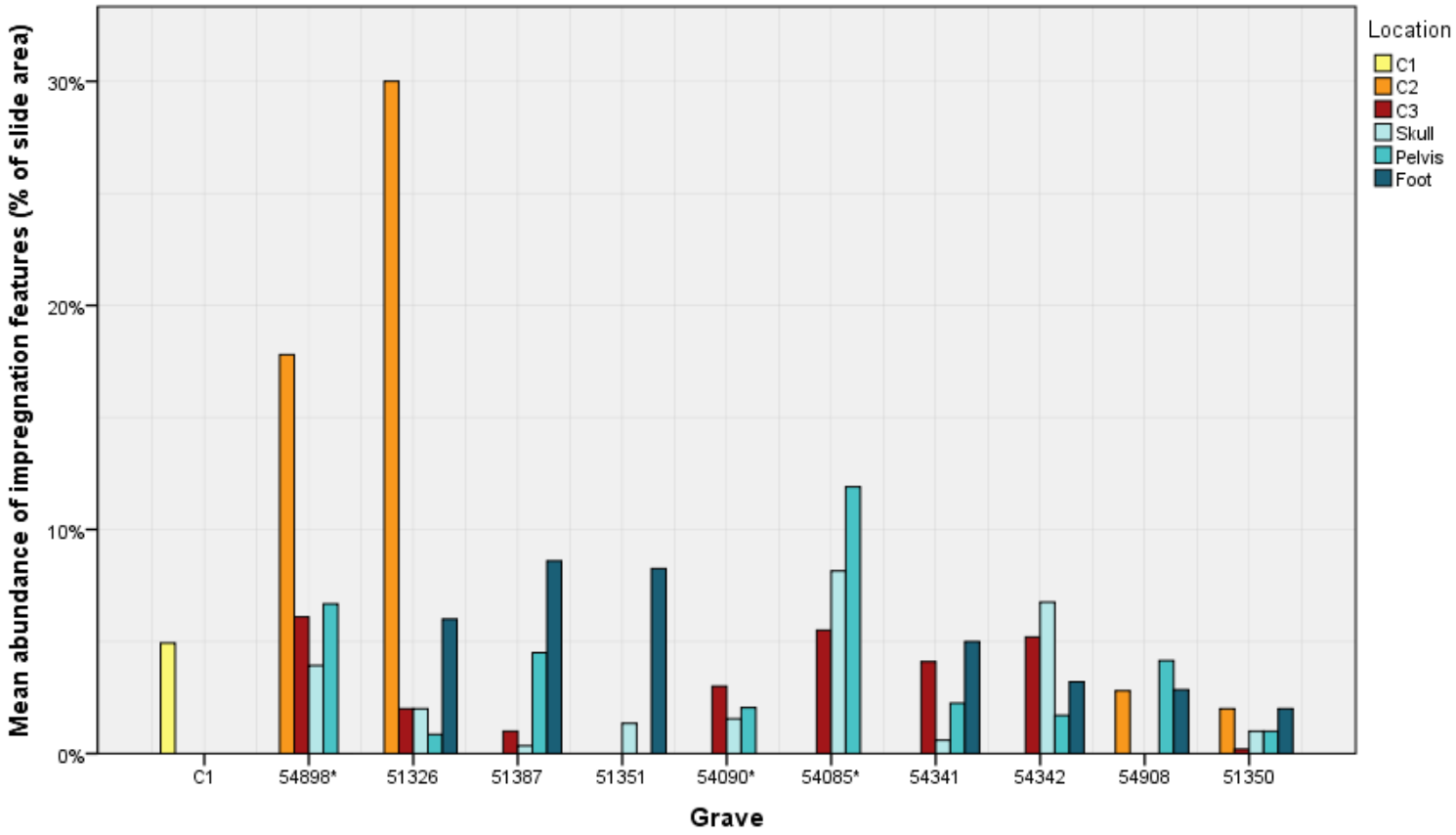

Figure 109: Abundance of impregnations in the skull, pelvic and foot samples shown in percent for all Hungate graves. Those graves that do not have all three sample points (skull, pelvis and foot) are identified by '*'. Where there is more than one sample available for a sample location the average impregnation percent is given.

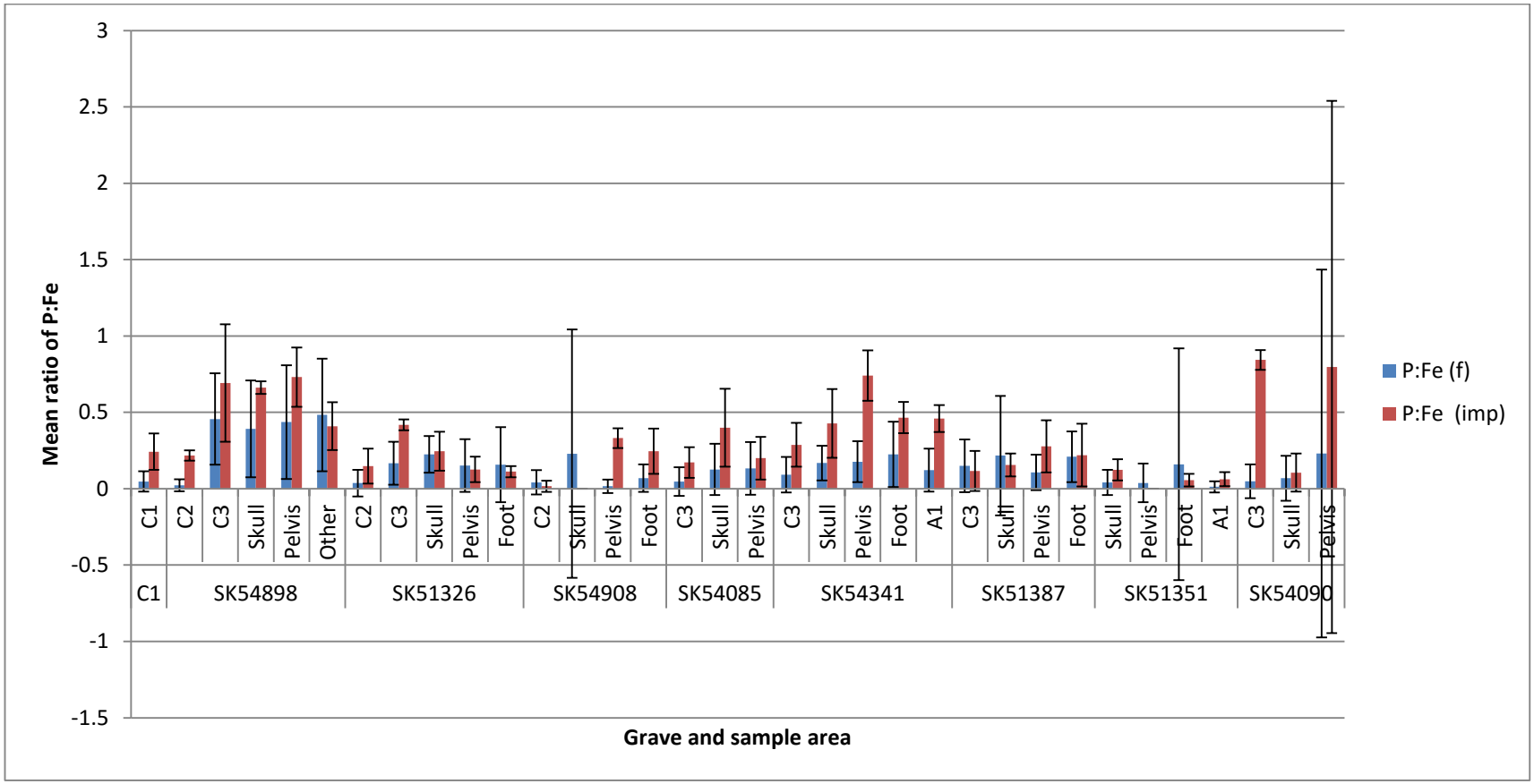

Figure 110: The mean ratio of P:Fe in the fine material (f) and the impregnations (imp) in the samples from graves SK54898, SK51326, SK54908, SK54085, SK54341, SK51387, SK51351 and SK54090 at Hungate. Error bars show standard deviation

Other iron and manganese features of note were the strong Fe intercalations which were observed in parallel skull area sample from SK54898, the perpendicular pelvic area sample from SK54090, parallel skull area sample from SK54341 and the C2 sample from SK54908.

8.1.6 Variation in iron and manganese pedofeatures by microfabric type

The distribution of iron and manganese pedofeatures between microfabric types was assessed (see Appendix 4.1.1). At Çatalhöyük, CH1, CH2, CH3 and CH4 contained multiple iron and manganese pedofeatures composed of Mn, Fe and Mn/Fe, and were all present at low abundances (<1%). Iron and manganese pedofeatures were, however, absent from CH5 and CH6. Both microfabrics at Thessaloniki contained iron and manganese pedofeatures at ≤3% abundance. Orthic and aggregated nodules, coatings (all types) and intercalations were only present in Ti1, with Ti2 containing Mn and Fe anorthic nodules as well as Fe disorthic nodules and impregnations. There was only one microfabric present at Heslington East (HE1) which contained low abundance of iron and manganese pedofeatures (<4%). At Hungate the iron and manganese pedofeatures were present in all of the microfabrics except HU2. Iron and manganese pedofeatures were present at low abundances in the majority of microfabrics (≤1%). However there were peaks in iron and manganese pedofeature abundance the most notable of which were high abundances of Fe impregnations in HU1, HU8, HU10 and HU13 although the abundances were still generally low at ≤3%.

8.2 Clay, Silt and Sand Typic Coatings

Typic clay coatings are an important marker of particle translocation (Macphail *et al*., 1990, Thompson *et al*., 1990, Usai, 2001), and could provide a means of identifying soil collapse or the dissolution of chemical bonds between soil particles caused by changing environmental conditions within the burial (Kühn *et al*., 2010). To that end it was important to both identify the type of coatings and their composition. This section focuses on typic coatings that contain clay, silt and sand; iron and manganese and $CaCO_3$ coatings are dealt with in iron and manganese pedofeatures and $CaCO_3$ pedofeatures (sections 8.1 and 8.4, this chapter).

8.2.1 Inter site clay, silt and sand typic coating distribution.

All sites contained dusty typic and impure clay coatings. Sandy coatings were limited to Heslington East and silt coatings were only present at Thessaloniki. Limpid clay coatings were present at all

sites except Çatalhöyük. Overall there was no systematic correlation between the presence of coatings and site. The implications of this are discussed in section 8.5.1

8.2.2 Çatalhöyük

8.2.2.1 Intra site and intra grave clay, silt and sand typic coating variation at Çatalhöyük.

Typic coatings were sporadic at Çatalhöyük and present at low quantities (<1% of total slide area). All coatings were located in the control samples and consisted of limpid clay in the C1 and dusty clay in the C3 from grave 19295. Both coating types were located on ped surfaces.

8.2.3 Thessaloniki

8.2.3.1 Intra site clay, silt and sand typic coating variation at Thessaloniki.

Limpid clay, dusty clay, impure clay and silt coatings were present at Thessaloniki and were unevenly distributed between graves (Table 58). All graves contained impure clay coatings. Limpid clay and silt coatings were the most sporadic and present in TF182 and TF162 and TF177 and TF162 respectively. Dusty clay coatings were present in TF157, TF177 and TF178. There was no systematic pattern in coating types between the graves at Thessaloniki

8.2.3.2 Intra grave clay, silt and sand typic coatings variation at Thessaloniki.

All typic coatings were present at between ≤12% of total slide area, and were unevenly distributed within the graves (Table 58). There was no systematic distribution of typic coatings at Thessaloniki, however there were some noteworthy trends. Impure clay coatings (Figure 112 g and h) were abundant and widespread at Thessaloniki. Their abundance peaked at 10-12% and coincided with a peak in the silt coatings (5-12%) in the pelvic area samples of TF177 (Figure 111). In TF177 the hands were placed over the pelvis, and both areas contained impure clay and silt coatings. There was also a slight peak in impure clay coatings in the pelvic sample from TF182. The control samples were not distinct from those of the burial plane in terms of the abundance, distribution or types of coatings. Fragments of coatings were observed in the C3 sample from TF182 and the parallel hand sample from TF177 (Figure 112 c and d).

Table 58: Distribution of typic coatings and their composition at Thessaloniki by grave and slide location. '*' indicate areas where coating fragments were observed.

Grave	Position	Orientation	Limpid yellow	Dusty clay	Impure clay	Silt
TF157	Skull	Para		4		
	Pelvis	Para		2		
	Foot	Para		2		
	Hand	Perp			2	
TF182	C2	-				
	C3	-	4		2*	
	Skull	Para			3	
	Pelvis	Perp			3	
		Para			5	
	Foot	Para			3	
	Hand	Perp			2	
		Para			2	

Grave	Position	Orientation	Limpid yellow	Dusty clay	Impure clay	Silt
TF177	C3	-			2	
	Skull	Perp		5	3	
		Para			2	
	Pelvis	Perp			10	12
		Para			12	5
	Foot	Perp		0.2	2	
		Para		5	4	
	Hand	Perp				
		Para			4*	2*
TF178	Skull	Para		2		
	Pelvis	Para			2	
TF162	Skull	Para			4	4
	Pelvis	Para			4	
	Foot	Para	2		2	

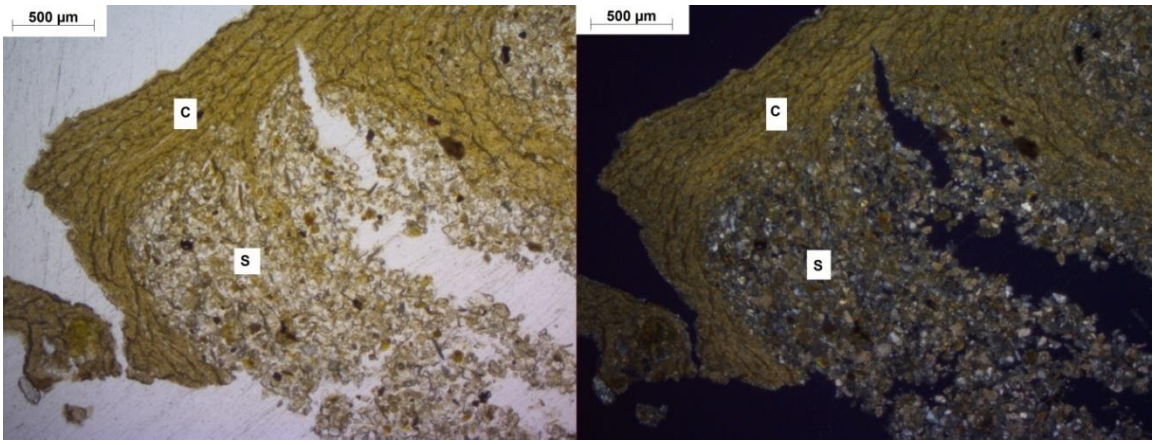

Figure 111: Microlaminated clay coatings (C) and silt coatings (S) in the pelvic sample of TF177. Note there is some fragmention of the coating occuring.

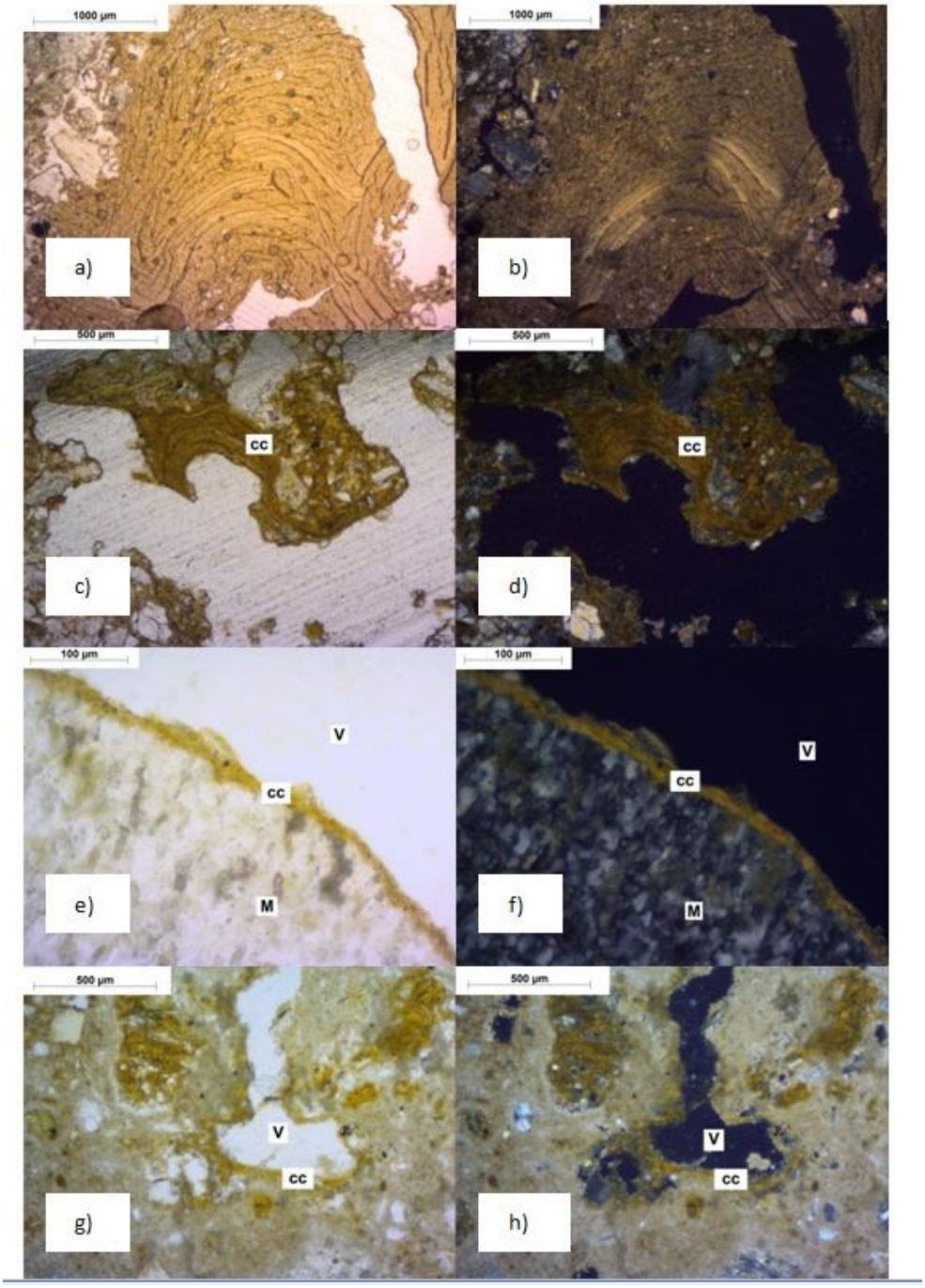

Figure 112: a) Limpid clay coating from the C3 sample from TF177in PPL b) in XPL c) Relict dusty clay coating (CC) from the foot sample TF177 in PPL d) in XPL e) Dusty clay coating (CC) from the pelvic sample of TF178 in PPL mineral (M) and void (V) f) in XPL g) Impure clay coating (CC) on void (V) wall from the skull sample of TF182 in PPL h) in XPL

Typic coatings at Thessaloniki were located on void and aggregate surfaces (Figure 112 e, f, g and h), and some had been fragmented (Figure 112 c and d). The clay orientations in the coatings at Thessaloniki varied from continuous clay coatings (seen in the thick episodic clay and silt coatings that were present in the skull area sample from TF162 and the pelvic and hand area samples in

TF177; Figure 111 and Figure 112 a and b), to discontinuous clay coatings. Coatings that showed little or no clay orientation were most common at the site, the implications of which are discussed in section 8.5.1. The clay and silt coatings within TF177 had formed immediately adjacent to a large bone fragment.

8.2.4 Heslington East

8.2.4.1 Inter and intra grave clay, silt and sand typic coatings at Heslington East.

Typic coatings were present at Heslington East at between 2-5% of slide area (Table 59). Coating types were unevenly distributed between sample locations, and dusty clay coatings were only located in the samples from the burial plane. Typic clay coatings at Heslington East also had strong continuously orientated clay (Figure 113) and were located on void surfaces.

Table 59: Abundances in percentage of slide area of clay, silt and sand coatings at Heslington East by sample location in grave 713

Sample location			Limpid yellow	Dusty clay	Impure clay	Sand
C1		-				
		-	2		2	
		-	5			2
713	C2	-			5	
	C3	-	5			
	Skull	Perp		2	2	
	Foot	Perp		2	5	
	Hand	Perp	5		2	

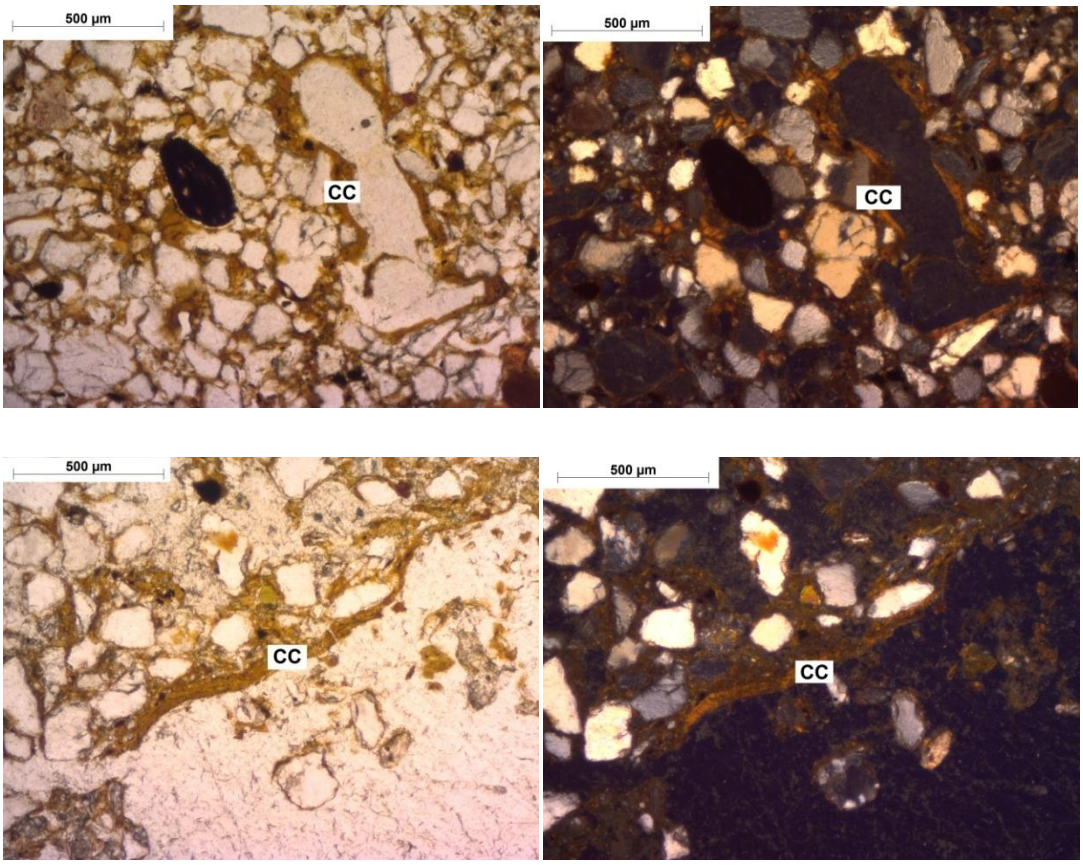

Figure 113: Clay coatings (CC) showing strongly oriented clay domains in PPL (left) and XPL (right).

8.2.5 Hungate

8.2.5.1 Intra site clay, silt and sand typic coating variation at Hungate

Limpid, dusty and impure clay coatings were widely distributed at Hungate. The C1 samples contained only impure clay coatings. Limpid clay coatings were present in all graves whereas dusty clay and impure clay were present in all graves apart from SK54090 and SK51326 respectively.

8.2.5.2 Intra grave variation in clay, silt and sand typic coatings at Hungate.

Typic coatings at Hungate were present at ≤10% of total slide area (Table 60) with the majority of coatings at <4%. There was no systematic variation in the location and abundance of coating types within graves, although some important trends were observed. Coatings were generally unevenly distributed throughout the graves, but few were present in the C1 sample. In the majority of graves coatings were common, with samples from the burial plane routinely containing two or more coating types. The implications of which are discussed in section 8.5.2

Table 60: Abundances (as a percentage of slide area) of clay, silt and sand coatings at Hungate by sample location in the C1 samples and all Hungate graves. * indicates the presence of HU6 a microfabric type composed of limpid clay coatings.

Grave	Position	Orientation	Limpid yellow	Dusty clay	Impure clay
C1	C1	-			
		-			
		-			1.1
SK54898	C2	-	9.9		
	C3	-		0.4	
	Skull	Perp			1.6
		Para			0.4
	Pelvis	Perp			
		Para			
	Foot	Perp			
		Para			
	Hand	Perp			
		Para			
	Other	Perp	*		
SK51326	C2	-			
	C3	-			
	Skull	Perp			
	Pelvis	Perp	0.9		
		Para	1	3	
	Foot	Perp		1	
		Para		2	
SK51387	C3	-		0.1	0.2
	Skull	Perp	0.2		
		Para	0.7	0.7	
	Pelvis	Perp		1	
		Para	1		
	Foot	Perp		0.9	
		Para	1	1	

Grave	Position	Orientation	Limpid yellow	Dusty clay	Impure clay
SK51350	C2	-			2
	C3	-			
	Skull	Para			
	Pelvis	Perp	2		
	Foot	Perp		7.4	1.5
SK54341	C3	-	0.7		
	Skull	Perp			2.5
		Para	3.5		1.1
	Pelvis	Perp	0.7		1.4
		Para	1.4		
	Foot	Perp	1	1	
		Para	1	1	
	Hand	Perp			
		Para			
	Other	Perp	0.4		0.2
		Para	2		
SK54342	C3	-	3.8	3.2	
	Skull	Perp	5.4		1.4
		Para	3.2		1.6
	Pelvis	Perp			
		Para			
	Foot	Perp			
		Para			0.6
SK54908	C2	-	4.9		
	C3	-			
	Skull	Perp	5		
		Para			
	Pelvis	Perp			
		Para			1.5
	Foot	Perp		4.5	0.9
		Para		7	

Table 60: cont.

Grave	Position	Orientation	Limpid yellow	Dusty clay	Impure clay	Grave	Position	Orientation	Limpid yellow	Dusty clay	Impure clay
SK51351	Skull	Perp	1								
		Para	0.3	0.7							
	Pelvis	Para	1								
	Foot	Perp				SK54085	C3	-	1.4		
		Para			1		Skull	Perp	1	1	2
	Other	Perp	1.5					Para			0.9
		Para	0.8		1.6		Pelvis	Perp	1	1	
SK54090	C3	-			3			Para		0.2	
	Skull	Perp	1		1						
		Para	0.9								
	Pelvis	Perp	2.7								
		Para			1.8						

Typic coatings at Hungate were formed on the surface of voids and peds (Figure 114 a-h and Figure 115 a-h). As with previous sites there was evidence of both continuous (Figure 114 c and d) and discontinuous (Figure 115 a and b) coatings. SK54341 contained microlaminated coatings in the skull area sample (Figure 115 e and f). Similar, less dramatic, examples of microlaminated coatings were also observed in the skull area sample from SK54342 (Figure 114 a and f) and the pelvic area sample from SK51387 (Figure 114 g and h).

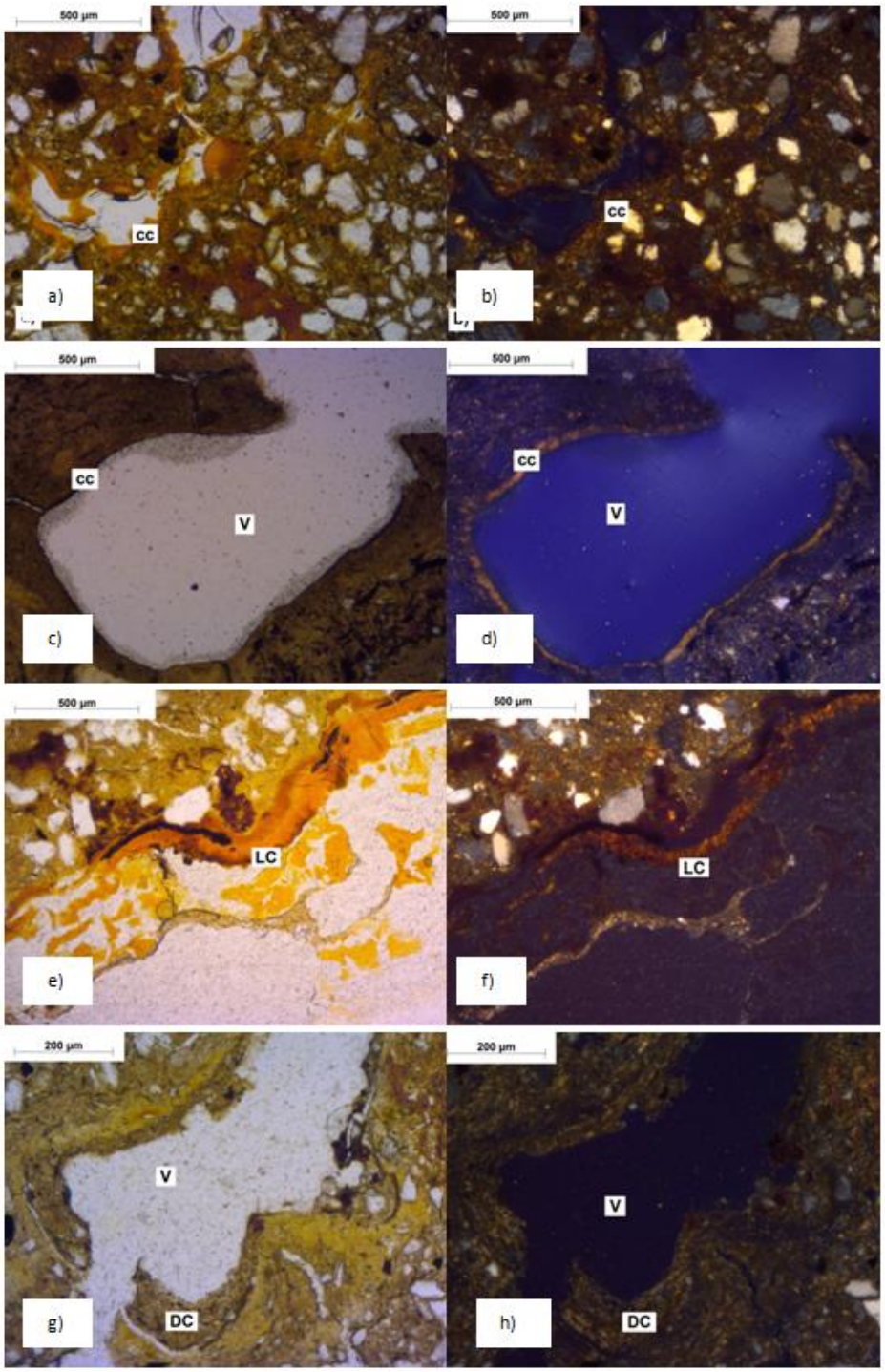

Figure 114: a) Limpid clay coating (CC) in the C2 sample of SK54898 in PPL b) and in XPL c) continuous limpid clay coating (CC), on a void (V) wall, from the skull sample of SK54898 in PPL d) and in XPL e) limpid clay (LC) coating from the skull sample of SK54342 in PPL f) and in XPL g) dusty clay coating (DC) from the pelvic sample of SK51387 in PPL h) and in XPL

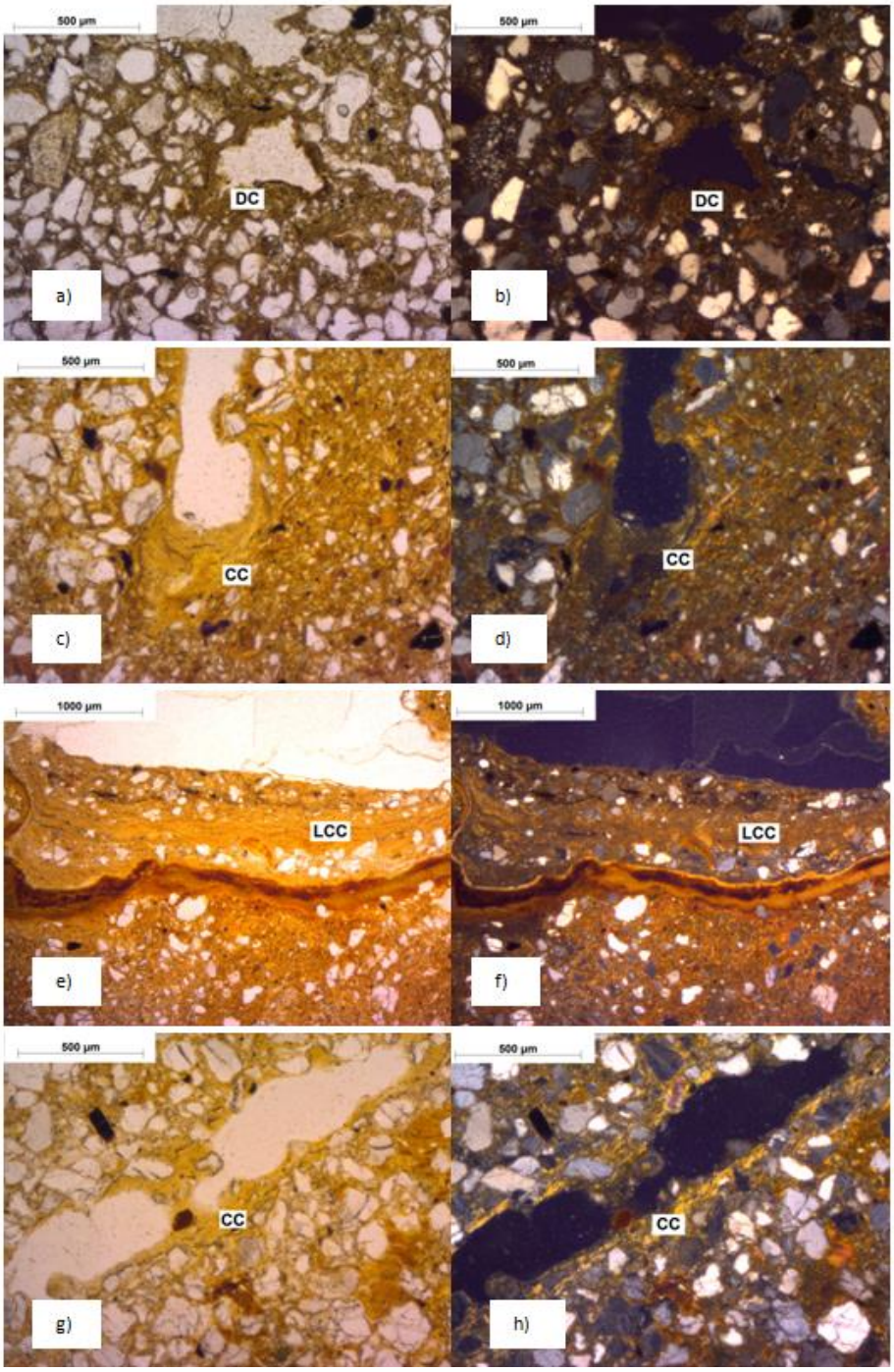

Figure 115: a) dusty clay (DC) coating from the skull sample of SK51351 in PPL b) and in XPL c) impure clay coating (CC) from the skull sample of SK54341 in PPL and d) and in XPL e) laminated clay coating (LCC) in the skull sample of SK54341 in PPL f) and in XPL g) impure coating (CC) in the skull sample from SK54341 in PPL h) and in XPL.

8.2.6 The distribution of clay, silt and sand typic coatings between microfabrics.

The distribution of coating types between microfabrics was calculated (Table 61). At Çatalhöyük the coatings were sporadic and only present in CH4 and CH5 and then only in trace amounts. At

Thessaloniki the majority of coatings were present in Ti1 with limpid, dusty and impure clay as well as silt coatings present. Only impure clay coatings were present in Ti2. At Hungate coatings were sporadic between microfabrics but were most common in HU4, HU7 (with a large peak of dusty clay coatings at 6%), HU8 (with another large peak of dusty clay coatings at 4.24%), HU10 and HU13. Coatings were also present as trace amounts in HU1, HU11 and HU12. HU7 was a microfabric mostly composed of bone with coatings positioned on the inside of the bone, whereas HU8 was composed of bioturbated soils with quartz clusters surrounded by dusty and impure clay coatings.

Table 61: Distribution of clay, silt and sand typic coatings shown as a percentage of the microfabric area.

	Limpid yellow	Dusty clay	Impure clay	Silt	Sand
CH1					
CH2					
CH3					
CH4			0.07		
CH5		0.03			
CH6					
Ti1	0.32	0.80	2.59	0.84	
Ti2			1.00		
HE1	2.13	0.50	2.00		0.25
HU1			0.15		
HU2					
HU3	0.10				
HU4	0.11	0.29	0.03		
HU5	0.07				
HU6					
HU7		6.00	1.50		
HU8	0.56	4.24	0.14		
HU9					
HU10	1.24	0.14	0.32		
HU11			0.90		
HU12	0.09	0.01	0.05		
HU13	0.73	0.31	0.44		

8.3 Excremental pedofeatures

Excremental pedofeatures are important as they could be used as a proxy indicator for the degree of bioturbation occurring in a burial and as a means to detect the inclusion of organic matter into the deposit by identifying if bioturbators and decomposers where in high abundances compared to control areas. The distribution of excremental pedofeatures across the four sites was varied. Çatalhöyük and Heslington East had restricted excremental types, with only coprolites present at Çatalhöyük and excremental pedofeatures at Heslington East. Coprolites were identified by the pale yellowish colour in PPL and amorphous fine fabric (Shillito *et al.*, 2011a). Thessaloniki and Hungate appear to have been more biologically active with excremental pedofeatures and $CaCO_3$ granules and infillings present. $CaCO_3$ granules were identified as worm granules by their size (between 0+5-2mm), the ovoid shape as well as their crystal formation, being roughly radial, with elongated wedge shaped crystals pointing outward (Canti, 1998a).

8.3.1 Çatalhöyük

8.3.1.1 Intra site and grave excremental pedofeature variation at Çatalhöyük

Coprolites were present at Çatalhöyük in the C1 sample and in the foot sample from 18666 (Figure 116) and the skull sample from 19295.

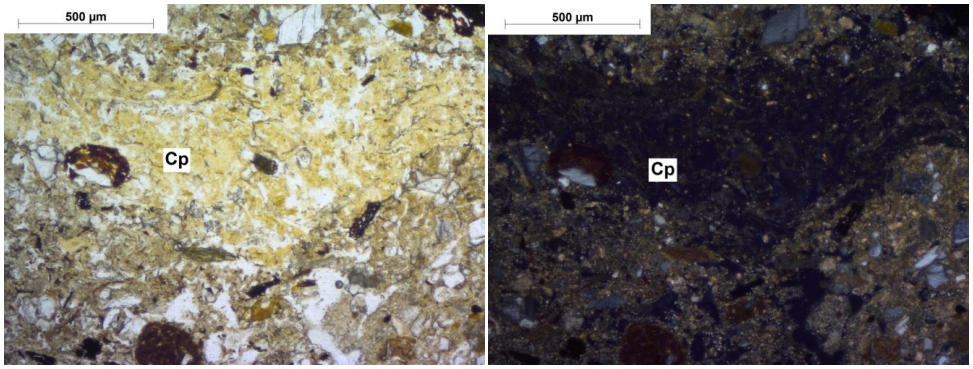

Figure 116: Coprolite (Cp) from the foot sample from Çatalhöyük 18666. Left in PPL and right in XPL.

8.3.2 Thessaloniki

8.3.2.1 Intra site and grave excremental pedofeature variation at Thessaloniki

Three graves at Thessaloniki contained sporadic excremental pedofeatures present at 1-5% of total slide area. Infillings, which were possibly due to burrows (Figure 117 a and b), were present in the parallel foot area sample from TF177 in addition to worm granules from the parallel pelvic

area sample in TF178. Excremental pedofeatures (Figure 117 c and d) were present in the perpendicular hand area sample from TF157 as well as the parallel hand area sample from TF177. There was no systematic variation in the location of excremental features and sample location or orientation.

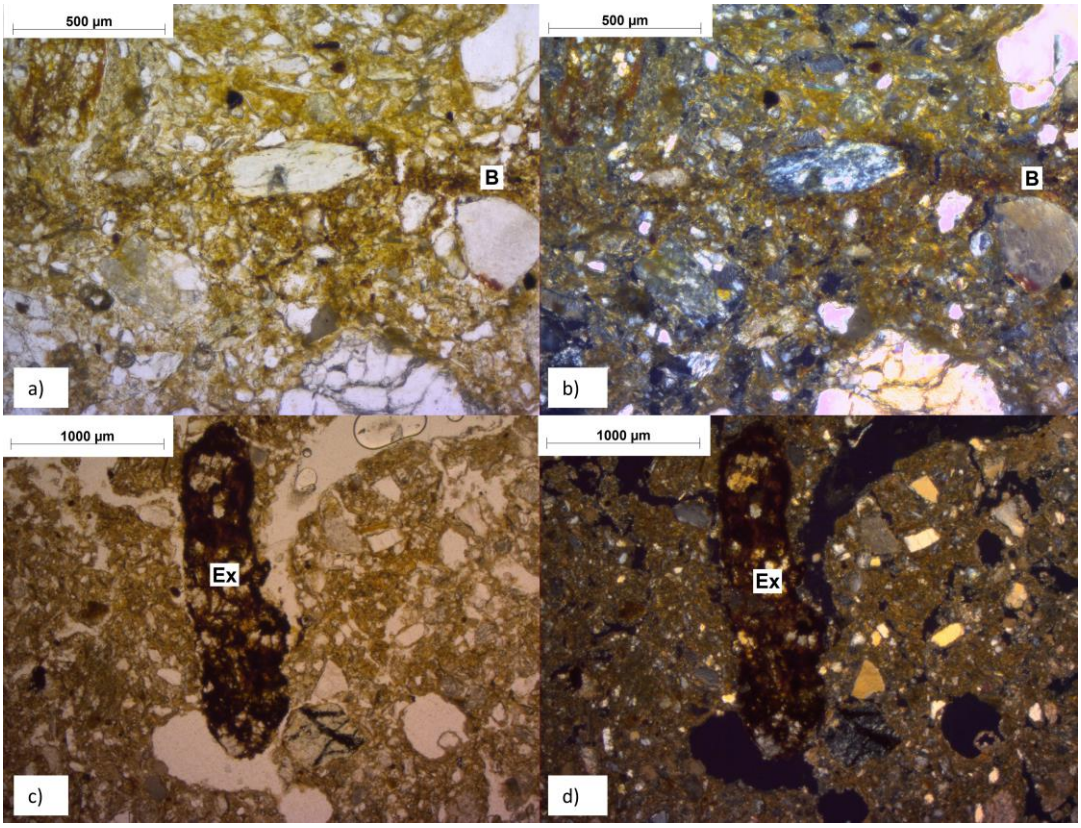

Figure 117: a) Burrow (B) from the foot sample in TF177 in PPL b) and in XPL c) Sample from the hand in TF157 showing excremental pedofeature (Ex) in the void space in PPL d) and in XPL.

8.3.3 Heslington East

8.3.3.1 Intra site and grave excremental pedofeature variation at Heslington East

Heslington East contained excremental pedofeatures in the C1, C3, skull and hand area samples. All excremental pedofeatures were sporadic and present at low abundances (1-7% of sample area).

8.3.4 Hungate

All graves from Hungate contained excremental pedofeatures (Table 62 and Figure 118 a-d), except SK54085 and SK51350. Generally the excremental pedofeatures and $CaCO_3$ worm granules

(Figure 118 e and f) were sporadic and present at 1-10% of total sample area. There was no systematic correlation between the location of excremental features and sample location or orientation. Infillings were present at higher quantities (up to a total of 100% of sample area).

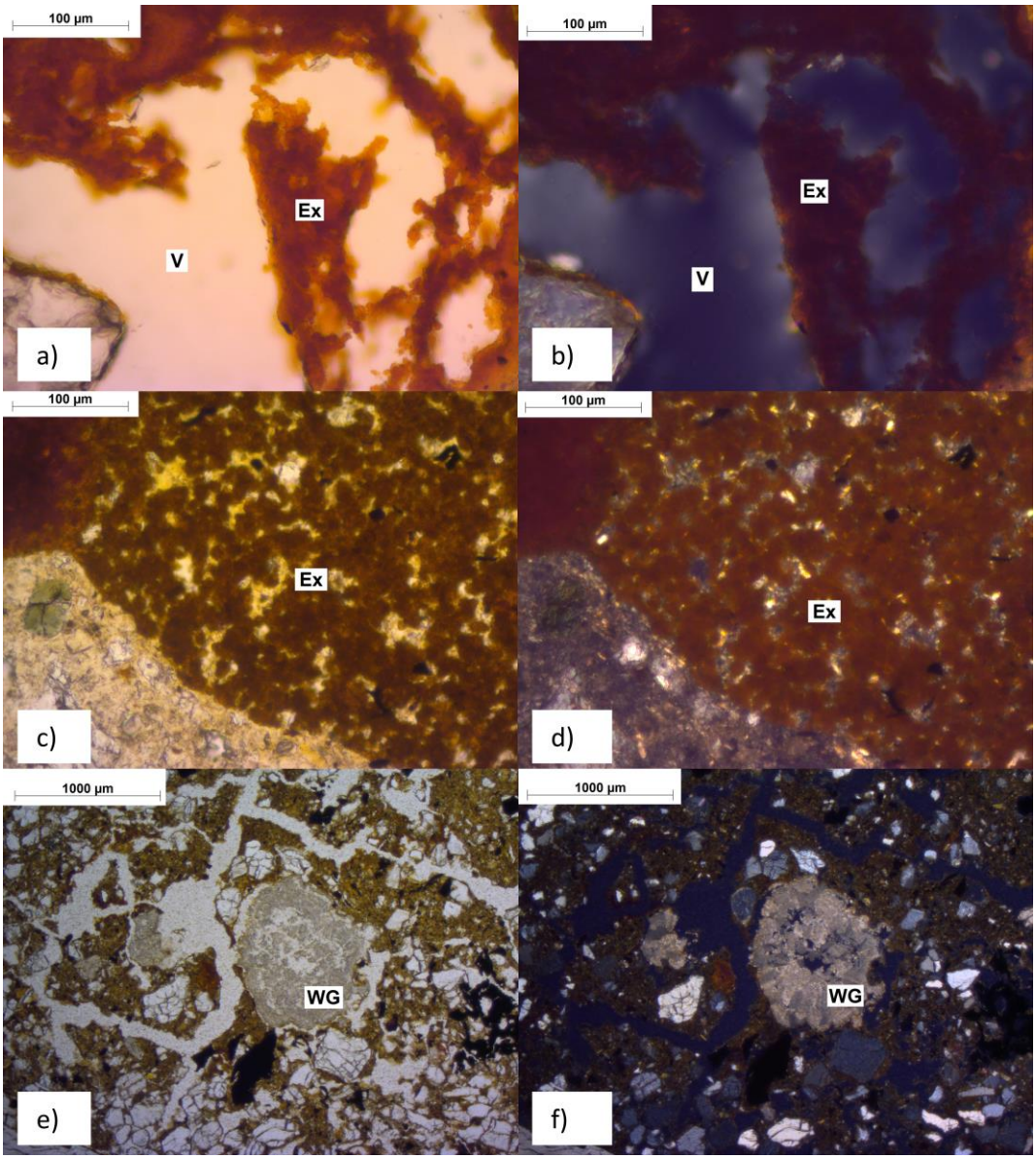

Figure 118: a) Excrement (Ex) inside a void (V) from the foot sample from SK54342 in PPL b) and in XPL c) excrement (Ex) from the pelvic sample in SK54341 PPL d) and in XPL e) worm granule (WG) in the C3 sample from SK51387 in PPL and f) and in XPL.

Table 62: Location and abundance of excremental and biological pedofeatures at Hungate.

Location		Orientation	Excrement	Infilling	$CaCO_3$ granule	Coprolite
C1		-				
		-		90		
		-				
SK54898	C2	-	1.1			
	C3	-				
	Skull	Perp		80		
		Para				
	Pelvis	Perp		0.5		
		Para	0.81			
	Other	Perp				
SK51326	C2	-				
	C3	-	3	2		
	Skull	Perp				
	Pelvis	Perp				
		Para				
	Foot	Perp				
		Para				
SK51387	C3	-			0.4	
	Skull	Perp			0.7	
	Pelvis	Perp				
		Para				
	Foot	Perp		9		
		Para				
SK51351	Skull	Perp				
		Para				
	Pelvis	Para		10		
	Foot	Perp				
		Para	1			
	Other	Perp	0.2			
		Para		1		
SK54090	C3	-				
	Skull	Perp				
		Para	0.9			
	Pelvis	Perp				
		Para				
SK51350	C2	-				
	C3	-				
	Skull	Para				
	Pelvis	Perp				
	Foot	Perp				
SK54341	C3	-		0.6		
	Skull	Perp				
		Para		3.9		
	Pelvis	Perp	1.4			
		Para				
	Foot	Perp				
		Para				
	Other	Perp	0.4	1		
		Para				
SK54342	C3	-		60		
	Skull	Perp	0.7			
		Para				
	Pelvis	Perp	1			
		Para	0.8			
	Foot	Perp	0.4			
		Para	0.4			
SK54908	C2	-				
	Skull	Perp		100		
	Pelvis	Perp		90		
		Para		50		
	Foot	Perp		90		
		Para		40		
SK54085	C3	-				
	Skull	Perp				
		Para				
	Pelvis	Perp				
		Para				

8.3.5 Excremental pedofeatures by microfabric type

The distribution and abundance of excremental pedofeatures in each microfabric type was calculated. Excremental pedofeatures were sporadic at Çatalhöyük and were only present in CH4. Excremental pedofeatures were also limited to one microfabric at Thessaloniki (Ti1). At Hungate excremental pedofeatures where more common than at Çatalhöyük and Thessaloniki and were present in HU1, HU4, HU5, HU8, HU12 and HU13.

Table 63: Distribution of excremental pedofeatures shown as a percentage of the microfabric area.

	Excrement	Infilling	CaCO3 granule	Coprolite
CH1				
CH2				
CH3				
CH4				0.64
CH5				
CH6				
Ti1	0.24		0.04	
Ti2				
HE1	4.00			
HU1	0.05			
HU2				
HU3				
HU4	0.14			
HU5	0.13			
HU6				
HU7				
HU8		100.00		
HU9				
HU10				
HU11				
HU12	0.01	0.13		
HU13	0.18	0.26	0.01	

8.4 $CaCO_3$ pedofeatures.

$CaCO_3$ pedofeatures were present at Çatalhöyük, Thessaloniki and Hungate. Anorthic nodules, typic coatings, and intercalations were present at all three sites. Disorthic nodules, hypocoatings and quasicoatings were present at Çatalhöyük and Thessaloniki, infillings at Çatalhöyük and Hungate, and intercalations at Hungate. In this instance the distribution and nature of $CaCO_3$ pedofeatures is important as at sites such as Thessaloniki and Hungate $CaCO_3$ may have been included as part of the burial practice, however the morphology and frequency of the $CaCO_3$ pedofeatures must be used to ascertain if they were formed due to the use of certain burial practice (such as the plastering or graves (Norman, 2002)) or due to naturally high levels of $CaCO_3$ in the surrounding geology.

8.4.1.1 Intra site calcium carbonate variation at Çatalhöyük

$CaCO_3$ pedofeatures at Çatalhöyük were absent from the C1 sample, but were present in the C3 samples as well as the graves (Table 64). Both graves 18666 and 19295 contained anorthic nodules, impregnations and hypocoatings. They differed, however, in the presence of other pedofeature types with infillings present in 18666 and quasicoatings, disorthic nodules and typic coatings present in 19295.

Table 64: The abundance of CaCO3 pedofeatures at Çatalhöyük by sample location and grave. Abundances are shown as overall percentage of slide covered by the $CaCO_3$ pedofeature type.

Grave		Position	Orientation	Anorthic nodule	Disorthic nodules	Typic coatings	Hypocoating	Quasicoating	Impregnation	Infillings
C1		C1	-							
18666		C3	-				1.65		0.7	1.72
		Skull	Perp							
			Para							
		Pelvis	Perp	0.3			0.45			
			Para	4.75						
		Foot	Perp	2			0.25		2.5	
19295	C3		-	0.8					1	
	19500	Skull	Perp	5						
			Para	1.66						
	19501	Skull	Perp		9.25		6.5			
			Para			1.9	0.85	1		

8.4.1.2 Inter grave calcium carbonate variation at Çatalhöyük

$CaCO_3$ pedofeatures were present at Çatalhöyük at high abundances (maximum 9.2%) with sporadic peaks in anorthic nodules in the parallel pelvic area sample from 18666 and parallel skull area sample from 19500. High abundances of disorthic nodules and hypocoatings in the perpendicular skull sample from 19501. There was, however, no systematic variation in the type or abundance of $CaCO_3$ pedofeatures at Çatalhöyük by sample location or orientation.

The origins of the most common $CaCO_3$ pedofeature types were investigated. The hypocoatings and impregnations (Figure 119 a and c) appear to have developed in the soil due to their diffuse boundaries and the location of hypocoatings around pores. The internal fabric of the nodules being different to the groundmass and their sharp boundaries would suggest that they had been inherited from parent material or external sources (Figure 119 b and d). However, there does appear to have been some further development on the nodule surfaces producing depletion hypocoatings (Figure 119 b) and thin coatings (Figure 119 d).

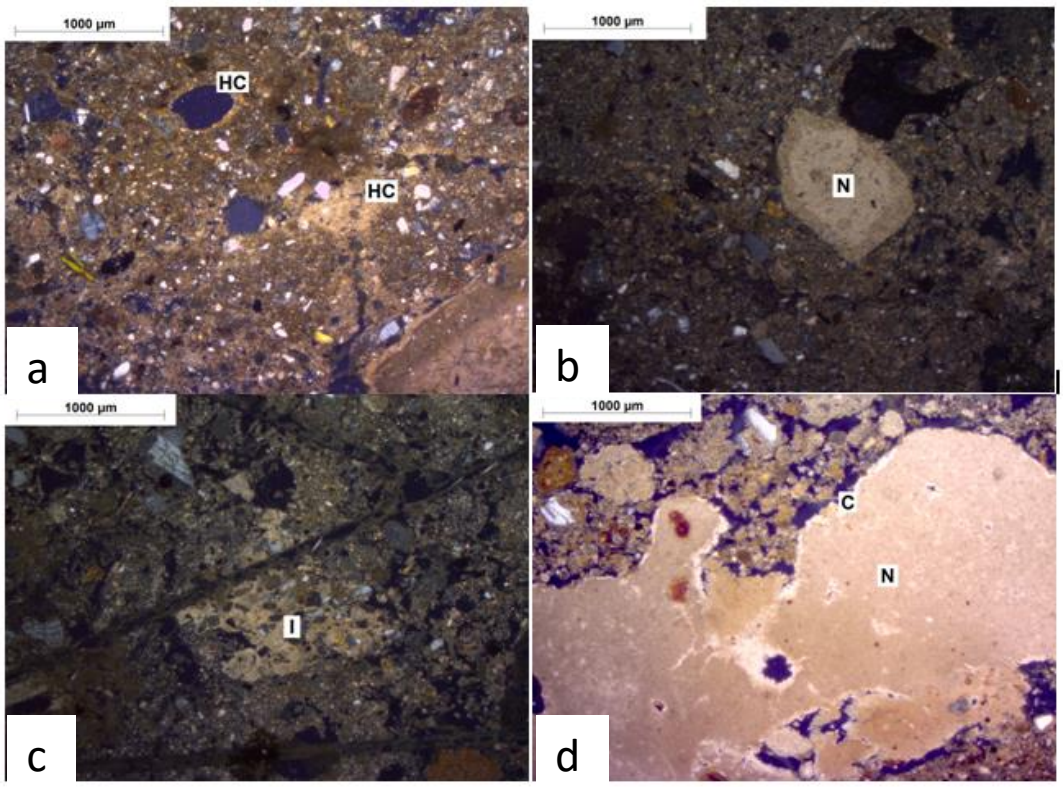

Figure 119: $CaCO_3$ pedofeatures at Çatalhöyük all shown in XPL; a) hypocoatings (HC) from the C3 sample in 18666, b) nodule (N) from the foot area sample of 18666, c) impregnation (I) from the foot sample of 18666, d) nodule (N) from the skull sample of 19500.

8.4.2 Thessaloniki

8.4.2.1 Intra site calcium carbonate variation at Thessaloniki

All graves at Thessaloniki contained $CaCO_3$ pedofeatures which ranged in abundance from 2-20%. Disorthic nodules, typic coatings and hypocoatings were present in all five graves. Crystal $CaCO_3$ pedofeatures were only present in TF177, although abundant at 10%, whilst quasicoatings were also abundant at 10%, but were only present in TF178. Anorthic nodules were uncommon and present in TF182, TF177 and TF162. There was however no systematic variation that was consistent between graves in the type or abundance of $CaCO_3$ pedofeatures at Thessaloniki by sample location or orientation.

8.4.2.2 Inter grave calcium carbonate variation at Thessaloniki

$CaCO_3$ impregnations were particularly abundant in the parallel pelvic area sample from TF182 (Table 65). There were also peaks in the abundance of anorthic nodules in the parallel foot area sample from TF177 and the parallel skull area sample from TF162. Disorthic nodule abundance was high in the parallel pelvic area sample from TF182, the perpendicular foot area sample and parallel hand area sample from TF177. In addition hypocoatings were high in the foot area sample from TF182. There was, however, no systematic variation in the location of $CaCO_3$ pedofeatures and sample location or orientation in any of the Thessaloniki graves.

The presence of $CaCO_3$ pedofeatures at Thessaloniki may have occurred through either features being inherited from the parent material or their development in the soil itself. The origin of pedofeatures can, therefore, be determined through consideration of the morphology (Brewer, 1964). Due to their location in and around pores and their diffuse boundaries, hypocoatings, quasicoatings and impregnations all appear to have developed in the soil through the percolation of calcium carbonate rich water (Figure 120 a, c, d, e and f). The nature of the anorthic nodules (Figure 120 g and h), with sharp boundaries and internal fabrics that are significantly different to the general groundmass, would, however, suggest that they had been inherited from either the parent material or some other source. This would suggest that there are multiple formation pathways for the inclusion of $CaCO_3$ in the graves at Thessaloniki, the significance of which will be discussed further in section 8.5.

Table 65: The abundance of $CaCO_3$ pedofeatures at Thessaloniki by sample location and grave. Abundances are shown as overall percentage of slide covered by the $CaCO_3$ pedofeature type

			Anorthic nodule	Disorthic nodules	Typic coatings	Hypocoating	Quasicoating	Impregnation	Crystals	Infillings
TF182	C2	-	4.5			1.4				
	C3	-						1.8		
	Skull	Para			2.5					
	Pelvis	Perp			15			9		
		Para		10		1.4		20		
	Foot	Para		5	1.8	10				
	hand	Perp				1.4				
		Para				2				
TF177	C3	-		5	2	1.8				
	Skull	Perp	2					0.5		
		Para		2		2				
	Pelvis	Perp	2					2		
		Para	1.8					2		
	Foot	Perp		10	7			4.5	10	
		Para	10			2				
	Hand	Perp								
		Para		10		2				
TF178	Skull	Para		2	2	5	10			
	Pelvis	Para			5	2				
TF162	Skull	Para	10		2	2				
	Pelvis	Para		5	5	5				
	Foot	Para		2		2				
TF157	Skull	Para		2						
	Pelvis	Para				5				
	Foot	Para				5				
	Hand	Perp								

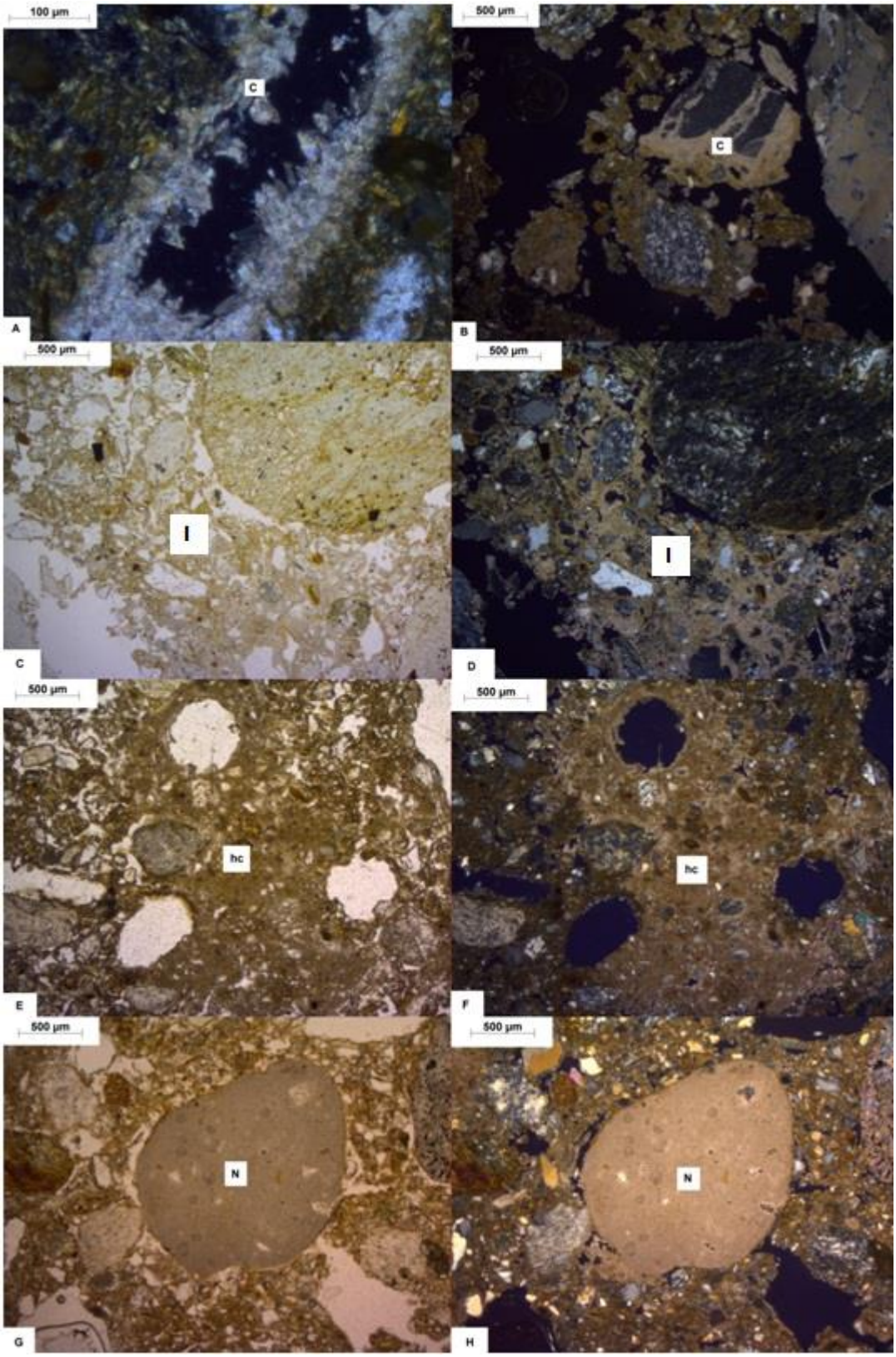

Figure 120: $CaCO_3$ pedofeatures. a) crystalline $CaCO_3$ coating (C) in XPL, b) $CaCO_3$ (C) in XPL, c) $CaCO_3$ impregnation (I) in PPL, d) $CaCO_3$ impregnation (I) in XPL, e) $CaCO_3$ hypocoating (hc) in PPL, f) $CaCO_3$ hypocoating (hc) in XPL, g) $CaCO_3$ nodule (N) in PPL, h) $CaCO_3$ nodule (N) in XPL.

8.4.3 Hungate

8.4.3.1 Intra site calcium carbonate variation at Hungate

$CaCO_3$ pedofeatures were sporadic at Hungate and only present in graves SK54090, SK54341 and SK54342.

8.4.3.2 Inter grave calcium carbonate variation at Hungate

$CaCO_3$ pedofeatures were present in low abundances at Hungate (<3% of total slide area). $CaCO_3$ anorthic nodules were present at low abundances (<1%) in the perpendicular pelvic sample and parallel pelvic sample from SK54090 and SK54341 respectively. Typic coatings were slightly more common (<3%), but still sporadic and present in the perpendicular other sample from SK54341 and the perpendicular skull and pelvic area samples from SK54342. Impregnations were present in the perpendicular other sample from SK54341 and infillings in the perpendicular pelvic area sample from SK54342. There was no systematic distribution of $CaCO_3$ pedofeatures that was related to either feature type or abundance and sample location or orientation.

8.4.4 Calcium carbonate variation in microfabrics

The abundance of $CaCO_3$ pedofeatures in each microfabric type was calculated (Table 66) to ascertain if there were particular microfabrics with high levels of $CaCO_3$ pedofeatures. $CaCO_3$ pedofeatures were absent from CH3, an orange monic microfabric, CH5, the possible oven rake out layer and CH6, a microfabric composed of burnt material. At Thessaloniki $CaCO_3$ pedofeatures were more common in Ti1 than Ti2. At Hungate $CaCO_3$ pedofeatures were present in HU12 and HU13 in trace amounts.

Table 66: Abundance (as a percentage of slide area) of CaCO3 pedofeatures by microfabric type. '*'= trace amount

Microfabrics	Anorthic nodule	Disorthic nodules	Typic coatings	Hypocoating	Quasicoating	Impregnation	Crystals	Infillings	Intercalation
CH1				0.68	0.02	0.03		0.03	
CH2		0.42	0.04	0.04					
CH3									
CH4	1.74	0.54	0.00	0.22	0.00	0.15			
CH5									
CH6									
Ti1	0.80	1.41	0.97	4.42	0.08	1.94			
Ti2			0.25				0.50		
HE									
HU1									
HU2									
HU3									
HU4									
HU5									
HU6									
HU7									
HU8									
HU9									
HU10									
HU11									
HU12			*			*			*
HU13	*		*					*	

8.5 Summary and discussion

The aim of the pedofeature analysis was to identify patterns in the occurrence and abundance of pedofeatures which relate to either burial practice, the presence of a body or to the post depositional environment. Four pedofeature types were analysed in depth; iron and manganese pedofeatures; clay, silt and sandy coatings; excremental pedofeatures; and $CaCO_3$ pedofeatures. The variation was assessed at three levels; inter site, intra site and intra grave.

8.5.1 Distinguishing between sites (inter site variation)

Pedofeatures were not evenly distributed between sites, with the abundance and presence of pedofeature classes varying greatly for excremental features and $CaCO_3$ pedofeatures. Iron and manganese pedofeatures and clay, silt and sandy coatings were more widespread and consistent between sites, suggesting that distinctions between sites is more easily expressed in pedofeatures that relate to site specific environmental conditions or specific burial practices rather than those that relate more generally to burial taphonomy.

Iron and manganese pedofeatures can be formed by reduction and oxidation reactions that are influenced by the soil pH and redox potential (Eh) (Lindbo *et al*., 2010). Any factors which influence the pH or Eh of the soil, such as temperature, organic matter, saturation, chemical species and microbes, will affect the oxidation and reduction of Mn and Fe (Lindbo *et al.*, 2010). The introduction of large quantities of organic matter into the soil, such as through inhumation and/or saturation of the soil, can change the Eh, encouraging the reduction of Mn and then the reduction of Fe (Favre *et al.*, 2002, Schlesinger, 1991 p. 231). Bacteria and micro-organisms, feeding on the organic matter induce anoxic conditions and the release of acids from the degrading body, which in turn increases the soil acidity (Dent *et al.*, 2004) and causes the oxidation of reduced organic compounds to form CO_2 (Schlesinger, 1991 p. 226). As the Eh of the soil decreases, reduction reactions become more likely (Favre *et al.*, 2002, Lindbo *et al.*, 2010) and highly soluble Fe^{+2} as well as Mn^{2+}, become part of the soil solution (Lindbo *et al.*, 2010, Schlesinger, 1991, Ye *et al.* 2013). When locally oxidised conditions are encountered Fe and then Mn hydr(oxides) will precipitate into the soil (McGowan & Prangnell, 2006, Ransom *et al.*, 1987). It is possible to use the type, composition and depth of redoximorphic pedofeatures to reconstruct the degree of water saturation, as the precipitation of Mn and Fe occurs in a highly predictable and ordered sequence that depends on the duration of water saturation and the presence of organic matter (Lindbo *et al.*, 2010). Previous studies have shown that the presence of a coffin can act as a 'bucket' retaining bodily fluids and soil water (Dent, 2002), whereas bodies placed in contact with the soil form a 'leachate' plume where decomposition fluids have saturated the surrounding soils (Pringle *et al.*, 2012). Further to this, experimental work has demonstrated that the soil can become an effective barrier to the release of gasses from the burial causing anoxic conditions around the body (Janaway *et al.*, 2003). These two processes would have been universal to all burials which is perhaps why iron and manganese pedofeatures are common at all sites. The presence of iron and manganese pedofeatures is therefore linked to alternating aerobic

and anaerobic conditions and the occurrence of organic matter, processes which would have occurred in all of the graves in this study.

Clay, silt and sandy typic coatings were identified at all sites although the types of coatings varied, with only dusty clay coatings being universal. Dusty clay coatings were the only coating type identified at Çatalhöyük and were particularly sporadic. Coatings are formed due to the dispersion, illuviation and deposition of soil particles (Kühn *et al*., 2010). Illuviation occurs when soil particles are disaggregated and translocated downward through the profile with the movement of water (Courty *et al*., 1989, Macphail *et al*., 1990, White, 1997). Disaggregation may occur due to chemical changes in the soil (Barbiero *et al*., 2010, Brinkman, 1970, Brinkman *et al.*, 1973), changes in soil hydrology, disturbance, bioturbation and rain splash through lack of ground cover on the soil surface (Bresson & Boiffin, 1990, Courty *et al.*, 1989, Lindbo *et al.*, 2010, Macphail *et al.*, 1990). The occurrence and characteristics of clay coatings have been linked to different phases of illuviation. Typic clay coatings can be caused by the translocation and subsequent accumulation of fine clay particles through slaking and illuviation (Courty *et al.*, 1989, Gunal & Ransom, 2006, Macphail *et al.*, 1990) or the *in situ* weathering of clay rich minerals such as mica, biotite and feldspar (Gunal & Ransom, 2006, Mermut & Pape, 1971). These processes are generally distinguished from one another by the degree of orientation of the clay particles as well as the location and morphology of the feature. Illuvial clay pedofeatures may be identified through the presence of strong continuous orientations of the clay particles (Gunal & Ransom, 2006). However, it is important to note that shrinking and swelling of the soil may also contribute to the alignment of clay (Dalrymple & Jim, 1984) and that particle orientation maybe lost through ageing and hydromorphism (Kühn *et al.*, 2010). Dusty clay coatings were present at all sites in this study and have been linked to soil disturbance, either through surface clearance/deforestation (Thompson *et al.*, 1990), anthropogenic changes (Slager & van de Wetering, 1977) and agriculture (Macphail *et al.*, 1990, Usai, 2001), with their 'dusty' appearance caused by the presence of organic material (Kühn *et al.*, 2010). Illuviation and disturbed surfaces are common features of soils and cemetery environments with constant soil disturbance during inhumation, subsequent inhumations and reuse of the cemetery. This process may, however, have been less prominent at Çatalhöyük where the two graves analysed were the last to be interred and there would have been little ground disturbance occurring until excavation or water percolating through the surface. This might explain why the samples from Çatalhöyük have limited numbers of coatings.

The distribution of excremental pedofeatures was similar to that seen for the coatings, with Çatalhöyük having very few examples and excremental pedofeatures being more common at Thessaloniki, Heslington East and Hungate, although at Heslington East this was limited to one feature type. The excremental pedofeatures at Çatalhöyük consisted of coprolitic material and the site actually contained no evidence of bioturbation, which would suggest that either soil organisms were scarce or that pedofeatures that were caused by them were subsequently destroyed. Thessaloniki and Hungate were more biologically, active, with a greater degree of feature types present indicating that there was either more varied biological activity occurring at Thessaloniki and Hungate or that features of biological activity were subsequently destroyed at Çatalhöyük and Heslington East.

$CaCO_3$ pedofeatures were more restricted in distribution, being widespread at Thessaloniki but rare at Çatalhöyük and Hungate and absent from Heslington East. The nature of the $CaCO_3$ pedofeatures differed between sites. At Çatalhöyük the majority of $CaCO_3$ pedofeatures consisted of nodules which had sharp boundaries and internal fabrics that differed from the groundmass, indicating that they had been inherited from the parent material. At Thessaloniki, however, pedofeatures which had formed *in situ* such as hypocoatings, quasicoating and impregnations were more common meaning that there had been a greater degree of *in situ* $CaCO_3$ pedofeature formation at Thessaloniki than at other sites. There were also greater abundances of clay coatings in some of the Thessaloniki graves suggesting that coating formation may have been more prevalent at Thessaloniki in general. Thessaloniki also contained a microfabric that was composed almost entirely from $CaCO_3$ (see microfabric 3.3 and SEM-EDX chapter 4). Thessaloniki is located in an area where the geology is rich in $CaCO_3$ (Ghilardi *et al.*, 2008b). There was also evidence of burial practices that included the plastering of graves and inclusion of plaster in contact with the body (see grave descriptions in method 2.2.3.4), which may be responsible for the introduction of $CaCO_3$ rich material in the grave which in turn was a catalyst for the formation of in situ $CaCO_3$ pedofeatures.

There were four categories of pedofeatures described in detail: Fe/Mn pedofeatures, typic coatings, excrements and $CaCO_3$ pedofeatures. Of the four, typic coatings and iron and manganese pedofeatures were more widespread and tended to relate to grave formation processes. One reason for this is the composition and presence of coatings and the formation of iron and manganese pedofeatures driven by taphonomic processes that relate directly to grave formation, such as the presence of uncovered surface soils creating dusty clay coatings and the

retention of water by grave soils and coffins creating anaerobic environments. Excrements and $CaCO_3$ pedofeatures, in contrast, are dependent on other environmental circumstances. For example, for $CaCO_3$ pedofeatures to form $CaCO_3$ needs to be present in the environment, for excrements to be deposited soil organisms need to be able to gain access to the site. The limited abundance of typic coatings at Çatalhöyük reinforces that, although coatings are often formed in graves, they are not a universal feature of them and human agency has clearly influenced their formation at Çatalhöyük.

8.5.2 Distinguishing between graves (intra site variation)

Clay, silt and sandy coatings as well as excrements were distinctive between graves, whereas iron and manganese pedofeatures and $CaCO_3$, when present at a site, were reasonably consistent. The levels of P:Fe did vary with graves and may be related to burial practice. However, there were no systematic variations in the distribution of pedofeatures between graves which were related to burial practice, meaning that the distinctions in pedofeatures that were observed were grave specific.

The ratio of P:Fe was calculated and analysed for the eight Hungate graves included in the SEM-EDX study and the C1 sample. SK54898, the lead coffin burial, was interesting as the samples from the burial plane were consistently high in the P:Fe ratios in the fine material and impregnations compared to other graves and the C1 and C2 samples. The C3 sample was taken from inside the lead coffin as were all the burial samples. The high P:Fe radios from inside the lead coffin suggests that there was a high amount of available P precipitating into the soil and pedofeatures. This may be due to the presence of the lead coffin creating an enclosed environment in which P rich body degradation products were able to pool, limiting the leaching of degradation products into the soil outside of the coffin.

At Hungate the variation in clay, silt and sandy coatings was expressed in two ways: firstly through a lack of impure and dusty clay coatings in graves SK54090 and SK51326; and secondly in the presence of micro laminated coatings in graves SK54341, SK54342 and SK51387. The variations in coatings between graves was much less pronounced at Thessaloniki with only TF177 being distinct due to the presence of elevated abundances of impure clay and silt coatings compared to the other four graves at Thessaloniki. In addition both TF177 and TF162 contained thick micro laminated coatings. Microlaminated coatings composed of multiple clay types and the interleaving of clay and silt layers present in selected graves at Thessaloniki and Hungate suggests

that formation was episodic, involving multiple types of material and different depositional energies and pathways. The coatings in this instance may have formed due to the disaggregation of soil particles or due to chemical changes in the soil such as the mobilisation of Fe and Mn (see 8.5.1) caused by changes in the soil hydrology. At Thessaloniki the graves which contained microlaminated coatings were not located close to one another in the cemetery and there were no unifying characteristics which were exclusive to these graves (Figure 121).

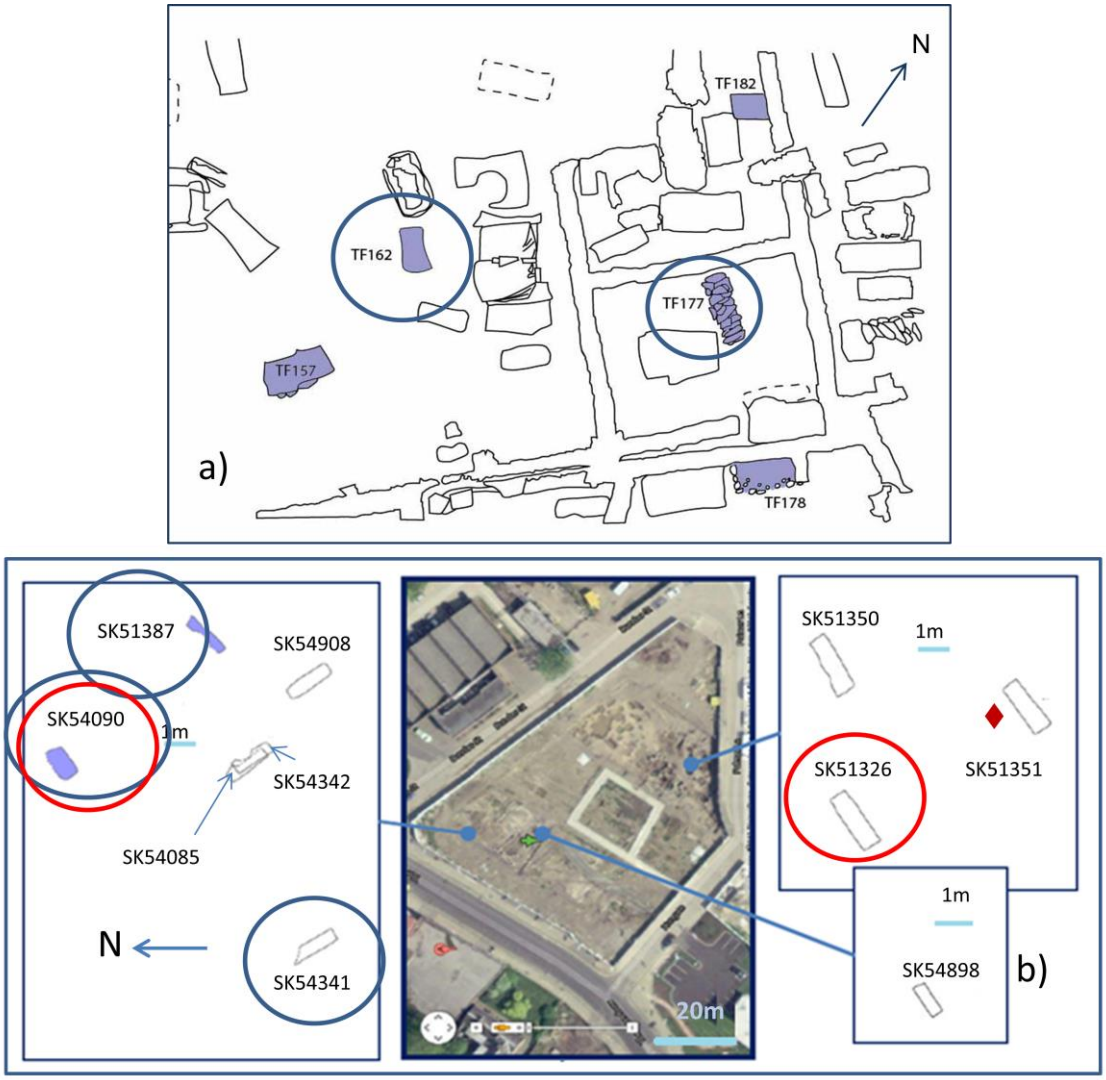

Figure 121: Position of graves with microlaminated coatings at a) Thessaloniki and B) Hungate (circled blue) and without dusty clay coatings (circled red)

At Hungate, the three graves containing microlaminated coatings, SK54090, SK54341 and SK51387 (Figure 121) were all located in the northern part of the cemetery. All were adult burials, however, this seems to have been the only common burial practice, with the mode of burial and

frequency of grave goods differing. The coatings, however, may relate to major periods of soil disturbance and disaggregation due to the placement of burials or excavation of material directly above them. Variation in dusty clay coatings occurred at Hungate with an absence of dusty clay coatings in graves SK54090 and SK51326 (Figure 121). SK54090 and SK51326 were located in different areas of the cemetery and had differences in burial practice, with SK54090 being a juvenile burial placed in a Roman ditch and SK51326 a supine adult coffined burial richly furnished with grave goods (see grave descriptions in method 2.2.6.4). Dusty clay coatings are an indicator of surface disturbance or internal soil disturbance (Macphail *et al.*, 1990, Slager & van de Wetering, 1977, Thompson *et al.*, 1990, Usai, 2001). However, a lack of dusty clay coatings suggests that there was either little or no surface disturbance occurring, a lack of water from rain or groundwater to facilitate the translocation of soil particles, that the soils themselves were not susceptible to disturbance/destruction (Courty *et al.*, 1989) or that evidence of dusty clay coatings was removed by subsequent pedogenic processes at Hungate.

At Thessaloniki and Hungate excremental pedofeatures were generally present at low abundances and were sporadic. It is therefore unsurprising that some graves do not contain evidence for biological activity (Hungate SK54085 and SK51350). This may be due to a genuine lack of activity in these graves or possibly an artefact of sampling bias because of the low level of biological and excremental pedofeatures and the comparatively small area covered by micromorphological sampling and analysis. Grave SK54908 however did contain unusually high levels of biological activity compared to the other graves at Hungate. This came in the form of microfabric HU8 (see microfabric chapter 3.5.4) which was present in the skull, pelvis and foot areas. The presence of HU8 signifies that a large area in the slide was composed of what has been interpreted as soil organism passage features. HU8 is not present in the C2 sample from SK54908 which would suggest that this activity was restricted to those areas that were in contact with the body, which had been heavy reworked by soil bioturbators. It is also interesting to note that, despite the extensive passage feature evidence, excremental features are not present. At Thessaloniki TF157, TF178 and TF177 contained evidence for biological activity which consisted of sporadic examples of infillings, worm granules and excremental pedofeatures. The distribution of the evidence for biological activity is not systematic or abundant, suggesting that there were low levels of biological activity throughout the site.

$CaCO_3$ pedofeatures were found in abundance at Thessaloniki. At the inter grave level there was no systematic variation in the presence of $CaCO_3$ feature types and sample location or

orientation. There was a predominance of $CaCO_3$ impregnations and hypocoatings, which suggests that there was percolation of $CaCO_3$ rich solutions through the soil fabric (Brewer, 1964, Courty & Fédoroff, 1985, Kemp, 1998, Sehgal & Stoops, 1972). The deposition of $CaCO_3$ can also be increased with increasing pH levels (Brady, 1969). In some cases Ca deposition can be accelerated by the presence of roots, which can cause calcium to be rapidly deposited due to high levels of CO_2 encouraging the dissolution of carbonates around plant roots and their subsequent crystallisation (Wieder & Yaalon, 1982). However there was no evidence of root activity at Thessaloniki.

8.5.3 Control vs burial plane samples and variation in the burial plane (intra grave variation)

8.5.3.1 Control vs burial plane

Of the four pedofeature types that were analysed in detail, variation between the control samples and the samples from the burial plane was observed in the iron and manganese pedofeatures and the clay, silt and sandy coatings. Differences between control samples and those from the burial plane, however, were not universal and varied between sites.

In terms of iron and manganese pedofeatures there were clear differences between the C1 and the burial plane samples at Çatalhöyük and the C2 and C3 samples and the burial plane at Thessaloniki. At Çatalhöyük this was expressed as a wider range of pedofeature types and chemical compositions in the burial plane compared to the C1. At Thessaloniki there was no C1 sample taken however the C2 and C3 samples from TF182 and the C3 sample from TF177 were again limited in both pedofeature type and composition compared to the samples from the burial plane. In both instances the control samples tended to contain Fe pedofeatures compared to the burial plane which contained Fe and Fe/Mn pedofeatures. In TF177 the P:Fe ratio in the C3 fine material was also low compared to some of the burial plane samples. The differences between the control samples and burial plane samples maybe partly down to sample size, particularly the differences in the variety of iron and manganese pedofeature types observed between samples. The differences in chemical composition between the controls and burial plane samples, however, could relate to differences in soil environment. As stated above, the burial plane may have a lower redox potential compared to the control sample due to the addition of large amounts of organic matter and the saturation of the soil by the 'bucket effect' and the formation of 'Leachate' plumes (Dent, 2002, Lindbo et al., 2010, Pringle et al., 2012, Schlesinger, 1991). In

anaerobic soil environments Mn^{4+} is reduced to Mn^{2+} first, followed by Fe^{3+} to Fe^{2+} (Schlesinger, 1991), both of which are highly soluble (Lindbo et al., 2010). In some instances, the solubility of the reduced forms of Mn and Fe cause the destabilisation of clay particles (Barbiero et al., 2010, Brinkman, 1970, Brinkman et al., 1973). When oxidising conditions are again encountered, Fe will oxidise and precipitate before Mn forming Mn and Fe oxides (Lindbo et al., 2010). In the soils from the control samples in Thessaloniki and Çatalhöyük there is a predominance of Fe, indicating that there was either a lack of Mn in its reduced state to be oxidised or that the pH or Eh reached a level that was conducive to Fe precipitation but not Mn. The same cannot be said for the burial samples, as the redoximorphic environment reached a state that was conducive to the precipitation of both elements either concurrently or at different times producing subtly changing conditions over time and space, suggesting that the presence of the burial was influencing the soil chemical composition. The same pattern is also not present in Hungate and Heslington East as both the control samples and those from the burial plane have similar iron and manganese feature compositions. The micromorphological evidence there suggests that redoximorphic conditions in the graves and in the C1 samples were similar in this instance. However when the P:Fe ratios for the Hungate graves are considered C1 and C2 samples are often lower in P:Fe compared to the samples from the burial plane and generally have a lower amount of P in the fine material compared to the impregnations, suggesting that there was less available P in the control samples compared to the burial plane, and that what was available was precipitating into the iron and manganese pedofeatures. The higher level of available P in the burial plane is probably due to the presence of the body and associated degradation products. There is also some suggestion that where C3 samples have been taken from the burial plane they are similar to the samples from the body, this can be seen particularly in the results from SK54898 and SK54090.

The control samples contained distinctive concentrations of clay, silt and sandy coatings. As with the iron and manganese pedofeatures, however, the nature of the variation between control samples and those from the burial plane changed between sites. Overall the burial environment at Çatalhöyük appears to have been physically quite stable, with little evidence for the movement and mobilisation of soil particles and inorganic geochemicals. Coatings were sporadic and those that had formed were confined to the C1 and the C3 samples. The lack of coatings further down into the grave deposits may indicate that the graves had been well sealed by plastering the surface of the grave fill, in effect restricting surface disturbance, the translocation of soil particles and the ingress of water. At Heslington East the control samples do not contain dusty clay coatings, whereas at Hungate the C1 samples were almost devoid of any coatings. This would be

consistent with the controls being situated in a zone of eluviation whilst the soil around the grave would be the area of clay accumulation (Schaetzl & Anderson, 2005 p.353).

8.5.4 Variation in the burial plane

Of the four pedofeatures analysed in detail in this study, there were clear systematic trends in the abundance and distribution of iron and manganese pedofeatures as well as the occurrence of interesting iron and manganese pedofeatures at Çatalhöyük, Thessaloniki and Hungate. Clay, silt and sand coatings. excremental pedofeatures and $CaCO_3$ pedofeatures did not demonstrate systematic trends in relation to sample location in the burial plane. Further interpretation is key to understanding what wider site formation processes were occurring, however.

Impregnations and anorthic nodules were the most abundant and common iron and manganese pedofeature across the sites. When their total abundance as a percentage of slide area was calculated for the skull, pelvic and foot area samples, there were elevated abundances of impregnations in the foot in six out of seven complete graves at Hungate. At Thessaloniki however high levels of Fe/Mn impregnations occur in the pelvis in three out of five graves. As impregnations are recognised by their higher concentrations of components, in this case Fe or Mn (hydr)oxides, differences in the abundances of impregnations between sample locations would suggest localised variations in the abundances of one or more of the iron and manganese forming factors. As this variation appears to be somewhat consistent between graves for the formation of impregnations this would suggest that the iron and manganese forming factors were also consistent between graves and more active in the foot area at Hungate and pelvic area at Thessaloniki. Reasons for this can only be speculatory at this point but may be due to pooling of bodily fluids in this area caused by a tilt in the coffin or by the narrowing of the coffin at the feet, or by higher concentrations of soft tissue in the pelvic region. However there does also seem to be a link between elevated abundances of Mn/Fe impregnations in the pelvic area and the location of burials in buildings at Thessaloniki. Further to this the P:Fe mean ratios for the fine material and impregnations were calculated for 18666 (Çatalhöyük), TF177 (Thessaloniki) SK54898, SK54908, SK54085, SK54341, SK51387, SK51351 and SK54090 (Hungate). At Çatalhöyük this showed elevated concentrations of P:Fe in the impregnations in pelvic sample which would suggest that there were elevated abundances of P in the pelvic area which were precipitated into redoximorphic features. 18666 was a crouched burial with the individual laid on their back and feet over the pelvis. The head was resting propped against the grave cut with the chin resting on their chest. The high levels of P:Fe found in the pelvis is suggestive of higher levels of pooling of

bodily fluids in this area, which may have been due to the large mass of soft material from the pelvis and feet. A lack of P:Fe in the skull may be due to the position of the head being almost upright and any fluids may not have had the right conditions for pooling to take place. The micromorphological results however would support large levels of redoximorphic activity in the skull compared to the pelvis with high abundances of iron and manganese impregnations. These features may therefore actually be formed prior to the deposition of the body and therefore not influenced by degradation products. The presence of impregnations that have either been inherited or formed before burial may also be adding to the large standard deviations present in some of the results. At Thessaloniki TF177 there are high P:Fe ratios in the skull fine material and impregnations, which suggest that there was pooling in the skull area of the grave. Again this is contradictory to the micromorphological evidence where there are peaks in the impregnations in the foot area. At Hungate there were some graves that showed interesting patterns that may be related to burial practice. In SK54898, the lead coffin grave, the C3, skull and pelvis sample, that were all taken from inside the coffin were reasonably consistent in their P:Fe ratios and all showed higher levels of P:Fe in the impregnations compared to the fine material indicating that the available P had remained in the grave and precipitated into the impregnations. SK54090 was an uncoffined infant found crouched on its side in a Roman ditch feature. The ratio of P:Fe in the fine material and impregnations was similar in the C3 and pelvic samples which were both taken in the burial plane. The C3 was taken opposite the pelvis suggesting that pooling of bodily fluids occurred in the space in front of and in the area of the pelvis. The skull sample however was quite low in P:Fe in comparison suggesting that pooling was not occurring to as high a degree.

The clay, silt and sand coatings showed no systematic variation based on sample location. It was, however, possible to ascertain important information about the development of the burial environment by the assessment of the morphology and composition of the coatings. At Thessaloniki, Heslington East and Hungate typic coatings were located on void and aggregate surfaces and were composed of continuous clay at Thessaloniki, Heslington East and Hungate. In addition to this Thessaloniki and Hungate also contained discontinuous typic coatings. The clay coatings at Thessaloniki, Heslington East and Hungate have strong continuous clay orientations, which would suggest that they have been formed by illuvuation of clay into the area around the grave and the upper grave fill (Gunal & Ransom, 2006, Kemp *et al.*, 1998). It is also possible that the alignment of the clay may have been caused by the shrinking and swelling of the soil (Dalrymple & Jim, 1984). The location of the coatings around the inside of channel voids would suggest, however, that they are associated with the translocation of clay (Kühn *et al.*, 2010). It is

not clear at what stage in soil development the illuviation took place. Heslington East has the additional complication of being located on agricultural land. It is therefore possible that clay coatings in the controls and burial plane at Heslington East have developed in response to the disturbance caused by agriculture (Carter & Davidson, 1998, Thompson *et al.*, 1990, Wilson *et al.*, 2002).

Excremental pedofeatures did not show any systematic variation between sample locations in the burial plane, but were diagnostic of some of the biological activity occurring at Thessaloniki, Heslington East and Hungate. The bioturbation and excrement at Thessaloniki consists of excrements, worm granules and burrows. The bacillo-cylindrical shape of the excrement in the hand sample from TF157 suggests that it has originated from either enchytraeids, orbatid mites or lumbricidae (Bullock *et al.*, 1985). There is also evidence from the $CaCO_3$ granules in TF178 to suggest that earthworms or slugs were active at the site (Canti, 1998a). Excremental pedofeatures were common at Heslington East but, as only one grave was sampled, this may be a sampling bias rather than a true reflection of bioturbation. Excremental pedofeatures were found in the C1 and C3 sample as well as the skull and hand area indicating biological activity in both contexts. The bioturbation and excrement at Hungate consisted of excrement, infillings, and $CaCO_3$ granules. Hungate was the most extensively sampled site and had the most wide-ranging evidence of excremental features and bioturbation. The presence of excremental features at Hungate was not systematic and there was no relationship between features and sample location or orientation. However there were some interesting distributions of bioturbation features in grave SK51326 from Hungate, which contained excremental features and burrows/infillings in the C3 sample. The remainder of the grave contained no excremental or bioturbation features. The C3 sample from SK51326 was taken in the burial plane and incorporated the coffin stain (see 2.2.6.4). Coffin wood may have attracted soil organisms and have aided future preservation due to the coffin wood providing some structural stability to the soil. The coffin may also have acted as a physical barrier to soil micro-organisms movement whereby, when the coffin was intact, organisms moving through the soil would encounter it as a physical barrier and be deflected away therefore concentrating activity around the coffin, similar to the effect seen in worms and roots around stones (Canti, 2003).

$CaCO_3$ pedofeatures were found in abundance at Thessaloniki. At the inter grave level, there was no systematic variation in the presence of $CaCO_3$ feature types and sample location or orientation. There was however a predominance of $CaCO_3$ impregnations and hypocoatings which

suggests that there was percolation of $CaCO_3$ rich solutions through the soil fabric (Brewer, 1964, Courty & Fédoroff, 1985, Kemp, 1998, Sehgal & Stoops, 1972), the deposition of $CaCO_3$ can also be increased with increasing pH levels (Brady, 1969). In some cases Ca deposition can be accelerated by the presence of roots, which can cause calcium to be rapidly deposited due to high levels of CO_2 encouraging the dissolution of carbonates around plant roots and their subsequent crystallisation (Wieder & Yaalon, 1982). However there was no evidence of root activity at Thessaloniki.

8.6 The influence of microfabric types

The abundance of iron and manganese pedofeatures, clay, silt and sandy coatings, excrements and $CaCO_3$ pedofeatures were calculated for each microfabric type (see microfabrics chapter 3 and appendix 2.1 for microfabric descriptions).

At Çatalhöyük, all pedofeature types are unevenly distributed between the six Çatalhöyük microfabrics. CH4 is the only case of a microfabric that contains all four pedofeature classes and is also the most abundant microfabric type at Çatalhöyük. The presence of all pedofeature types in CH4 could therefore be a product of sample size as CH4 is much larger in area than the other microfabrics at Çatalhöyük, meaning that sample size may be a contributory factor in pedofeature identification. Iron and manganese pedofeatures were absent from CH5 (oven rake out) and CH6 (burnt microfabric), both of which were sporadic at the site. Trace amounts of coatings were present in CH4 and CH5, in addition to excrement in CH4 and $CaCO_3$ pedofeatures were present in CH1, CH2 and CH4. High abundance of microfabrics in the graves however does not correlate well with high abundance of pedofeature types in the graves, meaning that there is not a strong causal relationship between microfabric type and the presence of the different classes of pedofeatures.

At Thessaloniki all four pedofeature types were more predominate in Ti1 compared to Ti2. Ti1 was ubiquitous at Thessaloniki and was derived from the local burial soils, whereas Ti2 was likely to have derived from either the *in situ* percolation of $CaCO_3$ or from materials high in $CaCO_3$ being incorporated in the burial fill. Ti2 was present in the parallel skull and foot area samples and perpendicular pelvic sample of TF182 and the perpendicular foot sample of TF177. As the groundmass of Ti2 was highly calcareous, this may have restricted the subsequent formation of pedofeatures. The groundmass in Ti2 may have obscured any $CaCO_3$ pedofeatures that formed in Ti2. The presence of Ti2 may relate to generally high abundances of $CaCO_3$ pedofeatures, as there are high abundances of them in the perpendicular pelvic area sample from TF182 and

perpendicular foot area sample from TF177 (however there is nothing conclusive). The formation of iron and manganese pedofeatures can be influenced by soil pH and the presence of high levels of $CaCO_3$ in Ti2 would have increased the pH of the soil, possibly influencing the likelihood of the formation of redoximorphic features (Lindbo *et al*., 2010, Schlesinger, 1991). The higher abundances of coatings and excremental features in Ti1 at Thessaloniki has however probably been influenced by Ti1 being found in a much greater abundance to Ti2. This is likely to be an artefact more of sample size that a true reflection of a lack to pedofeature formation in Ti2.

All four pedofeatures types were present at Hungate. Iron and Manganese pedofeatures were present at low abundances (<3%) throughout the site but absent from HU2. Fe impregnations at Hungate peak in HU1, HU8, HU10 and HU13. High abundances of iron and manganese pedofeatures in the graves, however, do not correlate well with high abundances of microfabric types, meaning that there is not a strong causal relationship between microfabric type and the presence of the different classes of pedofeatures. Coatings were sporadic in the Hungate microfabrics and clustered in HU1, HU7, HU8, HU11 and HU12. HU7 was composed of a large piece of bone that had coatings present on the internal bone surfaces, whereas HU8 was a heavily bioturbated microfabric composed of clusters of quartz surrounded by coatings. HU7 was only present in the foot sample of SK51350 where as HU8 was located in the C1, C3 sample from SK54342 and skull, pelvic and foot area sample from SK54908. The foot area sample from SK51350 did contain a peak in coatings which had probably been caused by the presence of HU7, however the presence of HU8 does not seem to have coincided with peaks in coating abundance. Excremental pedofeatures were sporadic at Hungate but did cluster in several microfabrics most notably HU8 which did coincide with an increase in bioturbation features in SK54908.

8.7 Conclusions

Studying the nature of pedofeatures, their frequency and composition can give an understanding of grave formation processes, as well as being a useful tool for establishing past pedogenic processes. The aim of this analysis was to ascertain if the interpretation of the presence and abundance of pedofeatures could facilitate the reconstruction of past burial practices, post depositional environments and determine the presence of a body. The above analysis has yielded a range of micromorphological features which can be related not only to the presence of a body but also to the associated burial practises and taphonomic environments.

Of the four pedofeatures that have been studied, the presence and location of $CaCO_3$ pedofeatures, the occurrence and morphology of coatings and the P:Fe ratio in the fine material and redoximorphic impregnations could be linked to burial practice. Thessaloniki had a wide distribution of $CaCO_3$ pedofeature types, particularly those that had formed *in situ.* The analysis of the location of pedofeatures and the occurrence of Ti2, a microfabric high in $CaCO_3$, indicated that there was a weak correlation between the two. Further to this, the presence of episodic layering in coatings at Thessaloniki and Hungate may relate to large scale disturbance at both sites, either external to the grave due to the excavation of further interments or due to the internal collapse of grave soils. Çatalhöyük was a site where the influence of burial practice had been particularly strong and created a rather inert burial environment. This was expressed through the lack of coatings in the burial plane and the low abundances of excremental pedofeatures. It is also noteworthy that there had been a higher frequency of intrusive pedofeatures with only small amounts of evidence for post depositional changes. The ratios of P:Fe in the fine material and impregnations can also be used as a diagnostic tool in the case of SK54898 where their consistency and high level in the burial plane in suggestive of an enclosed environment such as a well-sealed coffin.

When ascertaining if there was a body present iron and manganese pedofeatures appeared to be the most diagnostic and showed variation between the controls and grave soils as well as along the burial plane. The localised retention of fluids or the differential build up of organic matter in the grave is likely to be responsible for localised fluctuations in redoximorphic features. The graves also had higher levels of P:Fe than the controls especially at Hungate suggesting that this may be diagnostic of a body being present. Interestingly, excremental or bioturbation pedofeatures where not good indicators of the presence of a body, presumably this is due to features diagnostic of soil organisms being rapidly destroyed by continuing pedological processes (Canti, 2003).

Lastly the reconstruction of the post depositional environment and the formation of the grave was expressed in a limited number of pedofeatures most notably in redoximorphic iron and manganese pedofeatures as well as P:Fe ratios and dusty clay coatings.

9 Discussion

The aim of this research was to establish if it is possible to identify body degradation products, burial practices, grave goods and preservation conditions in Prehistoric, Hellenistic and Roman burials using soil micromorphology and inorganic geochemistry. This aim was further broken down into four objectives. The first was to establish if there was systematic variation in the micromorphological and inorganic geochemical results at three levels (inter site and inter and intra grave), that could be related to body degradation, burial practices, grave goods or preservation conditions. This objective was investigated in the results chapters. The remaining three objectives, (to identify micromorphological and/or inorganic geochemical evidence for 1) body decomposition, 2) burial practice and 3) preservation conditions), will be fully explored here. Prior to this, site narratives will be presented taking into account both cultural and environmental influences, establishing the drivers and processes at each site, which determine the broader trends that will be discussed as part of the research questions. This will be followed by an appraisal of the InterArChive protocol to provide recommendations for future sampling strategies and make suggestions for further research and development.

9.1 Site narratives

9.1.1 Çatalhöyük

Çatalhöyük, a Neolithic Tell site in Central Turkey, was situated on a seasonal alluvial fan composed of organic clay, lake marl, dark grey back-swamp clay and a reddish brown upper alluvium (Boyer *et al.*, 2006). The alluvial material surrounding Çatalhöyük, as well as that from further away, were used in the manufacture of the buildings that formed the Tell site (Doherty, 2013, Matthews *et al.*, 2013, Tung, 2005). It was into these anthropogically created sediment floors that an articulated, crouched, adult burial, 18666 was placed under the north west platform of building 97, space 365, whilst two decapitated, yet fleshed, skulls were buried under the north east platform of building 77, space 336. The micromorphological and inorganic geochemical interpretation summaries for each grave and the C1 (control) at Çatalhöyük are given in Table 67 at the end of the site narrative section.

9.1.1.1 Nature of the Çatalhöyük burial soil and burial environment

The sediment used to backfill the graves had not been significantly modified by the presence of the body or by burial practice, but was identified as building rubble (microfabrics section 3.2) consistent with the 'packing material' and 'building material' identified at Çatalhöyük (Matthews, 2005, Matthews, 2006, Shillito *et al.*, 2011b). In total six microfabrics were identified, the majority of which had been deposited as heterogeneous material and were evenly distributed between the grave and control samples, showing that microfabrics had been mixed during grave excavation and 'dumped' back into the grave with no reference to the microfabric type or body position, nor was there a contextual preference for microfabric placement. The inorganic geochemical signatures from 18666 also tentatively reflected this, with the inorganic geochemical signatures for all sample locations at Çatalhöyük being more tightly clustered than when the results where coded by microfabric type (see section 4.3.1). The aggregates of CH1, CH2, CH3, CH5 and CH6 had formed as dense spheroidal and blocky peds, embedded in CH4 with sharp boundaries, creating high abundances of interpedal packing voids. This means that there was limited post depositional chemical or physical interaction occurring, although there had been sporadic formation of coatings on some nodule surfaces (see Pedofeatures section 8.4.2).

The physical burial environment at Çatalhöyük was stable, with limited evidence for the movement and mobilisation of soil particles or bioturbation. The graves had been sealed by plaster floors, thus the movement of soil particles was limited to the surface deposits meaning coatings were only visible in the C1 and C3 samples and had not formed in the graves. The presence of low abundances of coatings in the C3 samples, however, indicated there had been sporadic translocation and deposition of soil particles. The location of the burials, in a well-sealed environment, would have limited the escape of deposition gasses (Janaway *et al.*, 2003) whilst preventing water movement, so restricting the percolation or translocation of soil particles. There was sparse evidence of bioturbation, with low abundances of vughs and a slightly elevated abundances of channels in the skull of 18666 (see 7.2.2.2.1). Excremental pedofeatures were infrequent and consisted of coprolites in the grave and C1 sample. The accessibility of the burials to the effects of bioturbation may have been restricted, due to the burial location in the large mound structure surrounded by brick built walls and plaster floors from earlier buildings.

9.1.1.2 Evidence of grave goods retained in the soil

Of the wide range of grave goods that were identified from the literature as being micromorphologically visible and potentially present in burials at Çatalhöyük (see method Table 1) (During, 2003, Hamilton, 1997, Jenkins, 2012, Rosen, 2005, Ryan, 2011, Wendrich, 1995, Wright, 2010) bone, charcoal, shell fragments, phytoliths and faecal material were observed. Of these, only phytoliths could be linked to burial practices. Phytoliths were present in the foot sample of 18666 with clusters and linear forms observed, suggesting they had been included as either matting, basketry or binding (Matthews, 1996, Nakamura & Maskell, 2005). Further phytolith analysis would be recommended to identify if there were phytoliths present in any of the other sample locations, however this was beyond the scope of this thesis. Bone, charcoal, shell and coprolites were present in both control and burial contexts meaning they may not have been incorporated as part of the burial process.

9.1.1.3 Evidence of the body degradation products retained in the soil at Çatalhöyük

Evidence of body degradation products retained by the soil were found in the iron and manganese pedofeatures that had formed in the burials. These features indicated conditions were sufficiently anoxic for Fe and Mn to become reduced and subsequently precipitate into nodules, coatings and impregnations (Chapter 8) (Lindbo *et al.*, 2010). This process was more prevalent in the burial samples than the C1 or C3 samples, suggesting organic matter, from the inclusion of the body, contributed to the reducing environment within the burial plane (Janaway *et al.*, 2003, Schlesinger, 1991). The P:Fe ratios from 18666 also supported this interpretation with higher levels of P:Fe detected, particularly in the pelvis, compared to the control samples. Further to this P was precipitating into the iron and manganese impregnations in the pelvic area suggesting that degradation materials and redoximorphic conditions were concentrated.

Fragmented bone was widespread in the Çatalhöyük samples, with similar abundances in the C1 and perpendicular pelvic area sample from 18666. Bone fragments in the burial plane were unevenly distributed and produced a 'peak' of bone fragment abundance in the pelvic area sample, which would be consistent with broader burial trends relating to the weathering and fragmentation of the pelvic bone (Chapter 6). When analysed on a site level, however, the bone fragments in the pelvic area in 18666 were found at similar concentrations in the C1 sample suggesting that other non-burial factors may have contributed to the abundance of bone in the pelvic area. Although the peaks in bone fragment abundance in the pelvic area sample from

18666 are ambiguous at best, bone fragments also formed a linear feature in the perpendicular skull sample from 19295. This would suggest that there may have been some flaking of the skull bone in the grave giving rise to the possibility that at least some of the bone fragments may be evidence of body degradation.

9.1.1.4 Summary

Grave signatures that were retained in the soil at Çatalhöyük included increased concentrations of iron and manganese pedofeatures in the burial plane and the distribution of bone fragments in the burial plane, may be significant. In addition, it was possible to reconstruct the burial environment and the taphonomic processes that had occurred in the grave. Çatalhöyük was unique, as burials were placed under floors in what was an anthropogenically produced substrate. The remains of building materials strongly affected the inorganic geochemical results so too did the nature of peds and voids. The physical stability of the sealed soil prevented particle translocation, whilst the burial position within the mound may have restricted bioturbation from flora and soil fauna.

9.1.2 Thessaloniki

Thessaloniki is situated on the mainland coast of North Eastern Greece and dates to the Early Hellenistic and Roman periods (Kourkoutidou-Nicolaidou, 1997). Many of the graves contained grave goods and there was evidence that plaster material had been used to backfill graves as part of the burial rites (Acheilara, 2010, Kourkoutidou-Nicolaidou, 1997). Five graves at Thessaloniki were sampled and investigated as part of this project (Method section 2.2.3). A summary of the onsite contextual information will now be given to support the interpretations given in sections 9.1.2.1 to 9.1.2.4. Two graves where dated to the Hellenistic period: TF157 and TF182. TF177 was buried in the Roman period at the centre of a walled structure, whilst TF178 was a chambered burial of an adult and child, lined with tiles, located in the corner of a building. A tiled 'pillow' was created in TF178 on which the adult skull rested with the child placed by their right shoulder. This burial appears to have been backfilled with calcium rich material which had adhered to the bones of the child. A fifth burial thought to be Roman in date, TF162, was located in the centre of the cemetery away from structures but close to other burials. The grave cut was disproportionately large compared to the skeleton of this individual and had been reinforced with plaster and a ceramic vessel had been included in the burial. The micromorphological and inorganic

geochemical interpretation summaries for each grave at Thessaloniki are given in Table 67 at the end of the site narrative section.

9.1.2.1 Nature of the soil and burial environment at Thessaloniki

Thessaloniki was a dynamic burial environment with evidence for soil collapse, chemical mobilisation, inundation by calcium carbonate rich waters and bioturbation. The burial plane at Thessaloniki contained $CaCO_3$ and iron and manganese pedofeatures. Impregnative $CaCO_3$ pedofeatures, particularly those that had formed in relation to void surfaces (coatings and hypocoatings) were common, suggesting that $CaCO_3$ pedofeatures were formed by percolation of $CaCO_3$ rich solutions through the soil fabric (Brewer, 1964, Courty & Fédoroff, 1985, Sehgal & Stoops, 1972). $CaCO_3$ also featured heavily in microfabric Ti2 which was chemically and micromorphologically distinct from microfabric Ti1, being highly birefringent and rich in calcium and phosphorus pointing to it being a potential contributory factor to the concentration of $CaCO_3$ rich water in the burials. Snail shells recovered from the grave bulk samples from Thessaloniki were tentatively identified by Eva Laurie, University of York, as *Pomatias elegans*, a species of snail which prefers loose, damp soils that are high in calcium (Evans 1972 and Kerney, 1999). Their presence is generally taken to indicate some form of soil disturbance. It is possible that it became part of the archaeological record in this case by burrowing into the soil post-burial. This would support the presence of loose highly calcareous soils at Thessaloniki.

9.1.2.2 Evidence for grave goods retained in the soil at Thessaloniki

Of the wide range of grave goods that were identified from the literature as micromorphologically visible and potentially present in burials at Thessaloniki (see Method Table 2) (Acheilara, 2010, Pemberton, 1985, Rife *et al.*, 2007), bone, charcoal, shell fragments and gastropod shells were observed, as were traces of calcium carbonate. The distribution of bone and charcoal varied systematically and their distribution pattern was probably due to the presence of the body (see section 9.1.2.3 this chapter). Ti2 is a potential proxy indicator for burial practices at Thessaloniki, such as adding plaster and lime mortar to the grave (Norman, 2002). However, there were several possible origins proposed for Ti2 which were not mutually exclusive; 1) accidental inclusion of building rubble or calcareous sediments, 2) intentional incorporation due to burial practice (mentioned above) and 3) percolation of calcium carbonate rich water causing calcium carbonate precipitation. TF177 and TF182 both contained Ti2 and were both located close to structural features in the cemetery (Figure 7), indicating the inclusion of construction material into the grave

could have been possible. No samples of building material were taken by the onsite team meaning that a micromorphological or chemical comparison with Ti2 was not possible. Ti2 may have been incorporated into the grave intentionally as part of the burial practice, but this did not correlate well with macro scale observations of plaster material found in all graves except TF177. $CaCO_3$ was percolating within Ti1, large areas of $CaCO_3$ percolation could therefore have occurred to create Ti2. Some examples of Ti2, however, contained sharp boundaries (Figure 12) suggesting that they were not formed by *in situ* percolation. For Ti2 to be a successful proxy indicator for burial practices there would need to be a convincing link between Ti2 and known burial practices at Thessaloniki, which is currently unfounded. Future work should, therefore include further sampling of the building and burial plaster material so micromorphological and inorganic geochemical comparisons can be drawn.

9.1.2.3 Evidence of the body degradation products retained in the soil at Thessaloniki

Evidence of the body degradation products retained in the soil were visible through the distribution and abundance of bone and charcoal fragments, iron and manganese pedofeatures in the burial plane, ped structure and morphology and the soil and composition and abundance of coatings.

Peaks in fragmented bone were present in the pelvic samples of TF182 (Hellenistic) and TF177 (Roman), which was consistent with more widespread trends in fragmented bone (Figure 63). Fragmented bone was, however, more evenly distributed in those graves positioned in open areas (Figure 64 TF157 and TF162), suggesting spatial factors were a secondary influence on the distribution of fragmented bone. TF157, TF182 and TF162 contained elevated charcoal abundances in the skull, consistent with more widespread trends of charcoal. However, the mechanism responsible for charcoal distribution is not yet understood. Ideally future work would include a comprehensive survey of burial soils to establish if there was, indeed, patterns to the abundances of bone fragments in the pelvis and charcoal in the skull. This could potentially be done using wet sieving and grab samples from specific parts of the burial plane. The bone fragments could then also be studied further to identify species using techniques such as amino acid racemisation.

All five of the graves at Thessaloniki contained iron and manganese impregnated pedofeatures in the fine material, suggesting that they had formed *in situ*. Iron and manganese pedofeatures were more concentrated in the burial plane compared to the control samples at Thessaloniki, and

particularly concentrated in the pelvic area, making them possible indicators of the previous presence of a body. The P:Fe ratio for the fine material in TF177 also supported higher levels of P:Fe in the burial compared to the C3 sample and further to this showed that there are concentrations of P:Fe in the fine material and impregnation in the skull indicating that the available P has precipitated into the impregnations. This has occurred due to decay products providing increased organic matter and soil water, thus acting as a catalyst to decrease the redox potential of the burial plane, which in the case of TF177 seems to have been particularly active in the skull area (Janaway *et al.*, 2003, Lindbo *et al.*, 2010, Schlesinger, 1991). The reduction of iron and manganese may also have had a role in destabilising the soil, contributing to partial movement and collapse within the grave (Barbiero *et al*., 2010, Brinkman, 1970, Brinkman *et al.*, 1973).

The soil structure at Thessaloniki contained high abundances of poorly developed peds and apedal soils. This suggests there was both soil disaggregation and collapse occurring or that the peds themselves failed to form. The presence of platy peds in the C3 and skull area sample from TF177, however, supports the occurrence of soil compaction in the graves (Kooistra & Tovey, 1994). There was also extensive evidence for soil translocation, with dusty clay coatings and widespread impure clay coatings on the void and ped surfaces in the burial plane. Coatings form on void and ped surfaces due to the disaggregation and translocation of soil particles through internal or external soil disturbance (Courty *et al.*, 1989, Macphail *et al.*, 1990, White, 1997). Some form of collapse and soil disturbance had occurred at Thessaloniki, as evidenced by the elevated abundances of fine material (section 5.1.3) in the burial plane suggesting depositional sorting. Future research may include grain-size analysis to further investigate this trend. However the samples were not available for this thesis. There was a high abundance of laminated clay and silt coatings in the burial plane (see section 8.2.3), particularly in the pelvic areas of TF177 and TF182, when compared to the controls suggesting periodic depositional events occurring, possibly due to a higher level of soil collapse in the pelvic area. Dramatic shifts in the soils structure in TF177, particularly in the hand area sample, are also apparent from coating fragments. Channels were widespread at Thessaloniki, yet excrements, worm granules and infillings were infrequent, suggesting bioturbation had not occurred in all areas but was concentrated in TF157 and TF178 (section 8.3). The remaining three graves all have some form of barrier between the grave fill and the soil, such as tiles or plaster that may have limited the ingress of soil organisms.

9.1.2.4 Summary

Thessaloniki has a complex history of anthropogenic influence and multiple taphonomic pathways, contributing to an intricate micromorphological and inorganic geochemical narrative. Grave backfill consisted of the local soil (Ti1) with the incorporation of calcium carbonate (Ti2). There also appears to be incidental incorporation of other organic coarse material such as bone which is more frequent in graves located away from structures. Despite this, spatial differences in fragmented bone (peaks in the pelvis) and charcoal (peaks in the skull), are consistent with patterns at other sites. The soil environment was dynamic with evidence of water movement, bioturbation and soil collapse, some of which had been modified by human agency with barriers to bioturbation and water flow in the form of plastered and tiled graves. There had also been a high degree of soil particle movement resulting in micro laminated coatings, whilst there had been inorganic chemical interaction through the development of redoximorphic features and $CaCO_3$ precipitation. The micromorphological and inorganic geochemical interpretation summaries for each grave at Thessaloniki is given in Table 67 at the end of the site narrative section.

9.1.3 Heslington East

Heslington East is a Bronze Age to Roman period site located on the outskirts of York (O'Connor *et al.,* 2011), on a natural spring line. The site is positioned on agricultural land (O'Connor *et al*., 2011) with a deep, free draining soil, that is highly permeable, but with a high water storage capacity (National Soil Resources Institute, 2011a). During the Roman period, an uncoffined mature adult female was buried in a supine position in a north south orientation. The micromorphological interpretation summaries of the grave and the C1 at Heslington East are given in Table 67 at the end of the site narrative section.

9.1.3.1 Nature of the soil and burial environment at Heslington East

There was only one microfabric at Heslington East (HE1) that had originated from the local parent material (Chapter 5 and Chapter 3). Fine material abundance and C:F related distribution diversity increased from the C2 to the C3 sample and then again in the burial plane, suggesting a greater number of soil forming factors had occurred in the burial plane (Stoops & Jongerius, 1975, Stoops *et al.*, 2010). Platy peds also increased from the C2 and C3 samples into the burial plane indicating compaction (Kooistra & Tovey, 1994), collapse or cyclic wetting and drying (Hussein & Adey, 1998) had occurred in the grave. There was an active hydrological regime at Heslington East expressed

in widely distributed iron and manganese pedofeatures, the formation of sub-angular blocky and platy peds, and also apedal soils (sections 7.3 and 8.5). Iron and manganese impregnative pedofeatures had formed in the fine material of the burial plane and C1 samples, indicating anoxic conditions were present in both (Vepraskas, 2001). High levels of saturation and inputs of organic matter may have contributed to the development of reducing conditions. Periods of soil saturation may have been common due to the proximity of natural springs, as would high levels of organic matter from the burial and later farming practices (Carter & Davidson, 1998, Meharg *et al.*, 2006). Saturation and drying could also have contributed to the formation of sub-angular blocky and platy peds at Heslington East (Hussein & Adey, 1998, Kovda *et al.*, 2008). Coatings were distributed in the burial plane, fill and soil profile, but were absent from the 22-28cm control profile sample, which would be consistent with the upper soil profile being the zone of eluviation whilst the grave was an area of clay accumulation (Schlesinger, 1991). Most coatings were composed of clay with strong continuous particle orientation and preferentially located on void surfaces, supporting an illuviation origin (Gunal & Ransom, 2006, Kemp *et al.*, 1998). It is not clear at what stage in soil development the illuviation took place as the site has been disturbed by agricultural practice, which may have contributed to the formation of the well oriented clay coatings (Carter & Davidson, 1998, Thompson *et al.*, 1990, Wilson *et al.*, 2002). Dusty clay coatings, however, only occurred around the body, indicating either, soil disturbance, the collapse of soils or other disaggregation mechanisms within the burial plane.

9.1.3.2 Evidence of grave goods retained in the soil at Heslington East

There were no grave goods with the body at Heslington East but bone and charcoal were visible in the control and burial samples. Bone fragments were found in low abundances in the skull area samples as well as the control samples. Charcoal, however, was more widespread, with fragments present in the C2, C3 and skull samples. Heslington East was an area of ritual deposition in prehistory and was later used as agricultural land. It is, therefore, likely that fragments of bone and charcoal were incorporated into the grave fill from other contexts particularly in the case of bone. Bone may have been added to the soil as part of manuring practices and subsequently been integrated into the burial (Meharg *et al.*, 2006, Scott & Damblon, 2010).

9.1.3.3 Evidence of the body degradation products retained in the soil at Heslington East

Evidence of the body degradation products retained in the soil at Heslington East was infrequent compared to other sites. Similar to other sites, redoximorphic processes were occurring at Heslington East but there was no distinction between iron and manganese pedofeatures in the control samples and those from the burial plane (section 8.1.4). However concentrations of iron and manganese impregnations in the skull sample, do correlate with wider trends at other sites.

9.1.3.4 Summary

Heslington East was a changing burial environment, with movement of soil particles through bioturbation, eluviation and illuviation occurring. Inorganic soil elements had also been mobilised, precipitating out into Iron and Manganese impregnations due to the periodic wetting and drying of the soil together with high inputs of organic matter. There is no evidence from the micromorphology of the inclusion of grave goods in the grave studied from Heslington East or for specific 'grave markers'. The lack of evidence for the products of body degradation in the grave is interesting. Heslington East was not fully sampled, therefore a pelvic area sample was not collected, thus 'grave markers' such as high concentrations of bone fragments in the pelvic area could not be observed. Furthermore, there is no macro evidence for a coffin or grave goods implying that the burial was not sheltered from external soil forming factors. Additionally, the site had been reused as agricultural land, which seems to have strongly influenced the pedofeatures that are present (Carter & Davidson, 1998).

9.1.4 Hungate

Hungate is a Roman cemetery located close to the River Foss in York, which has resulted in the periodic inundation of the site (Evans, 2007b) (section 3.5.4). The soil is a slowly permeable loam with a high clay content, and is susceptible to seasonal waterlogging (National Soil Resources Institute, 2011b). Ten burials were investigated from the extensive multi-period grave yard. A lead coffined infant burial was excavated from the centre of the cemetery (SK54898) whilst three coffined supine adults where investigated from the southern side of the site (SK51326, SK51350 and SK51351) one of which, SK51350, was truncated by a cess pit. From the northern side of the cemetery, a shrouded adult burial (SK51387), an uncoffined infant placed within a ditch feature (SK54090), a coffined infant (SK54908) and three supine coffined adults (SK54085, SK54341, SK54342) were investigated.

9.1.4.1 Nature of the soil and burial environment at Hungate

The soils used to backfill the graves were consistent with the Hungate parent material (section 5.3.2). There were, however, microfabrics that originated from periods of inundation by the River Foss (HU4 water laid sediments) and that had been modified by the burial environment (HU6) (Chapter 3.5.4). On a site level, the soil was weakly structured, with a predominance of apedal soils and weakly to moderately developed peds. The lack of soil structure would be consistent with a low redox potential caused by saturation and the incorporation of large amounts of organic matter. The formation of the reduced forms of Fe and Mn can cause the breakdown of chemical bonds between soil particles, decreasing the structural strength of the soil (Barbiero *et al*., 2010, Brinkman, 1970, Brinkman *et al.*, 1973). Subsequently, when soil becomes saturated with excess water, it can reduce the interparticle forces causing soil deformations. This, combined with a heavy overburden, can cause the subsequent collapse of the soil structure (Kooistra & Tovey, 1994) resulting in apedal sediments and weakly developed peds.

9.1.4.2 Evidence of grave goods retained in the soil at Hungate

Direct and proxy evidence of grave goods was retained in the soil at Hungate in the form of high Pb levels in the fine material and nodules, layering of microfabrics, and the presence of iron rich spherulites.

SK54898 was a lead coffined infant burial, the presence of the lead coffin being expressed in the chemical composition of the fine material and nodule inclusions, as well as in the laying and composition of microfabrics inside the coffin. In terms of inorganic geochemical composition, it was distinct from the other graves, with an elevated abundance of Pb in the fine material and fragments of Pb visible in the thin section. There had also been a higher retention of P:Fe inside the coffin. The sheltered coffin environment had also affected the composition and arrangement of microfabrics by restricting the ingress of coarse components and bioturbation creating a high proportion of fine material which had become stratified, something particularly visible in microfabric HU6 (Chapter 5, Chapter 3 and Chapter 8). The development of laminations should be further investigated by comparing the microstratigraphy of the lead coffined burial to those identified in the wider InterArChive project.

Fe spherulites were observed in SK51351, SK51350, SK51326, SK54342 and SK54341 and may be attributed to the presence of coffined burials, together with high levels of Fe either from coffin furniture, from the inclusion of Fe objects with the burials or naturally high concentrations of Fe in

the soil (Chapter 4), which would not have shown up in the C1 samples because the C1 was taken above the level of the burials and localised to one area of the cemetery. Fe spherulites were only found in the burial plane of coffined burials, a lack of Fe spherulites in the upper back fill and C1 samples (Leguédois *et al.*, 2004, Lund & Fobian, 1991), therefore suggests Fe spherulites were formed in the burial plane and may be related to high concentrations of Fe in the coffins.

9.1.4.3 Evidence of the body degradation products retained in the soil at Hungate

Direct and proxy evidence for the presence of a body had been retained in the soil at Hungate. The former comprised of the spatial distribution of bone fragments in the burial plane and the inorganic geochemical results. Proxy evidence was more abundant and consisted of the distribution of charcoal, voids, void types, coatings and pedofeatures. Proxy indicators of body degradation also provided support for taphonomic processes occurring in the burial environment including wetting and drying, collapse/soil disturbance, and bioturbation.

Direct evidence of the body was visible in the distribution of bone fragments in the burial plane, where 28% of complete graves at Hungate had elevated levels of bone fragments in the pelvis: although not a strong correlation in itself, it does conform to wider trends observed at other sites. There may be a secondary spatial effect on the abundance of bone fragments at Hungate, with graves that show high abundances of bone fragments in the pelvic area concentrated in the southern part of the cemetery (see Figure 59). Three of the graves at Hungate had a clear inorganic geochemical burial signature, with concentrations of P and Ca in the burial plane compared to the control samples (Chapter 4). These three graves subsequently underwent SEM-EDX analysis to identify concentrations of Al, Mg, K and Fe in the burial plane. The high level of Al probably relates to the higher concentration of clay particles in the fine fraction of the graves compared to the controls, whereas K and Fe are elements commonly found in the body (Abdel-Wahab *et al.*, 1992, Birkeland, 1984, He *et al.*, 2015, Lindbo *et al.*, 2010).

Charcoal fragments were unevenly distributed, with 60% of complete graves at Hungate containing elevated charcoal levels in the skull area sample, although the mechanism that has influenced charcoal distribution in the burial plane is not understood. It is possible to speculate that the cause of charcoal concentrations in the skull may be related to the tendency of charcoal to float and the pooling of bodily fluids in the gave mobilising the charcoal which then settles in the skull area due to the morphology of the head, thus trapping the charcoal around the skull. Other proxy indicators had a direct relationship to the burial environment and taphonomic

processes. Evidence for periodic saturation and the inclusion of large amounts of organic matter were apparent in the morphology, distribution and abundance of iron and manganese pedofeatures present in the control and grave samples, meaning that the redox potential across the site had been conducive to iron and manganese feature formation (Lindbo *et al.*, 2010). In the grave environment, the inclusion of abundant organic matter is likely to be a contributory factor for the development of iron and manganese pedofeatures, but the periodic inundation from the River Foss and seasonally high water table may have been a catalyst for their formation throughout Hungate (Evans, 2007b, Schlesinger, 1991). Although no work has to date been carried out on the redox potential at Hungate, evidence of the degradation products retained in the soil was apparent in the lateral distribution of iron and manganese impregnative pedofeatures. These had formed *in situ*, and concentrated in the foot samples (86% of complete graves), meaning that the soil environment at the foot of the coffin was particularly favourable to the formation of redoximorphic features possibly due to the concentration of degradation products in the foot of the burial. Extensive chemical movement in the soil may also have contributed to disaggregation and collapse (Barbiero *et al.*, 2010, Brinkman, 1970, Brinkman *et al.*, 1973). Moreover, the P:Fe ratio that was calculated for the fine material and impregnations showed that there was more available P in the burial plane, presumably from body decomposition products and that the available P was precipitating into the impregnations and not remaining in the fine material, further evidence of redoximorphic processes occurring.

There was evidence for soil particle translocation, disturbance and collapse at Hungate with a predominance of dusty clay coatings, which are indicative of disturbance (Thompson *et al*1990, Slager & van de Wetering, 1977, Macphail *et al*, Usai, 2001). Episodic depositional events occurred at Hungate and where apparent from the presence of complex coatings, which indicated there may also have been a series of disturbances. As at Thessaloniki, there was a predominance of weakly developed peds apedality suggesting a combination of the reduction of Fe and Mn, as well as periodic waterlogging combined with the weight of soil overburden, may have led to the deformation and collapse of the soil structure (Kooistra & Tovey, 1994, Barbiero, 1970, Brinkman *et al,* 1973). Platy peds were infrequent and unevenly distributed at Hungate, but this may relate to compaction (Kooistra & Tovey, 1994) and/or cyclic wetting and drying (Hussein & Adey, 1998). Platy peds would also support the theory that lateral movement of soil water was occurring.

Void space varied systematically and laterally in the burial plane and was probably related to collapse, bioturbation, and wetting and drying. The pelvic area had a decreased overall void

abundance which was composed primarily of increased abundances of vughs and planes compared to the rest of the burial plane, meaning that there was a smaller surface area to volume ratio in the pelvis for chemical reactions to take place as well as increased levels of aggregation through collapse or bioturbation creating vughs (Brewer, 1964, Kooistra & Pulleman, 2010, Ringrose-Voase & Bullock, 1984). There was also an increase in packing voids in the skull area, meaning there were loose soil materials in the skull area from either faunal excrement or shrinking and swelling (Hussein & Adey, 1998, Kovda & Mermut, 2010, Davidson & Grieve, 2006, Koosistra & Pulleman, 2010, Pagliai *et al*2003). The presence of excrements and bioturbation features at Hungate was not systematic and there was no overall relationship between features and sample location. Some patterns in the bioturbation, however, related to the presence of the body or coffin. This was particularly apparent in SK51326, where bioturbation was observed in the C3 sample taken over the coffin stain.

9.1.4.4 Summary

Hungate is the largest site in the study it, therefore, has the potential to provide the best evidence of systematic changes in the soil micromorphology and inorganic geochemistry. It had a changing soil and burial environment, with soil particle movement occurring due to bioturbation, eluviation and illuviation. Inorganic soil materials have also been mobilised with the formation of iron and manganese pedofeatures that relate to redoximorphic conditions caused by the fluctuation in soil water levels and the presence of increased levels of organic matter derived from decomposing bodies, as well as Fe spherulite formation. In general the material used to backfill the graves was consistent with having originated from the site, although there were instances where the back fill was more diagnostic of the infilling of the grave (SK54898 lead coffin) or taphonomic events (microfabrics HU4, inundation by the River Foss and HU6, clay laminations in SK54898 see 3.5.4). Hungate conformed to wider trends for elevated levels of charcoal in the skull area as well as, less convincingly, elevated levels of bone in the pelvic area. Overall what is strongly suggested by the evidence is that each grave needs individual interpretation, as soil formation processes are very grave specific (Table 67). This is due to small changes in burial practice, body position, soil structure and composition, as well as less obvious influences such as seasonality of burial that may have affected soil conditions such as amount of water logging occurring etc.

Table 67: Micromorphology and SEM-EDX interpretation summary table for all graves and C1 samples. Supporting summary evidence is given in appendix 4.2

Context		Micromorphological/SEM-EDX interpretation	Çatal			Thessaloniki					Hes East		Hungate										
			C1	18666	19295	TF157	TF182	TF177	TF178	TF162	C1	713	C1	SK54898	SK51326	SK51387	SK51351	SK54090	SK54085	SK54341	SK54342	SK54908	SK51350
Micromorphological summary interpretation	Evidence of the body	Peaks of bone fragments in the pelvic sample due to the large surface area of the pelvic bone and susceptibility to physical weathering		✓			✓	✓									✓				✓		
		Fragments of charcoal in the skull cause unknown				✓	✓		✓	✓				✓	✓	✓	✓	✓			✓	✓	✓
		Concentrations body decomposition products (P and Ca) in the burial plane												✓		✓				✓			
		Modification of the chemical composition of the burial compared to the control samples												✓	✓	✓	✓	✓	✓	✓		✓	
	Evidence of artefacts	Evidence for matting, baskets or binding		✓																			
		High concentrations of iron forming Fe spherulites													✓		✓			✓	✓		✓
		Coffin												✓									
		Plaster burials					✓	✓															
		Lead coffin												✓									
	Burial environment	Sufficient redox potential for iron and manganese pedofeatures to form	✓	✓	✓	✓	✓	✓	✓	✓	✓	✓	✓	✓	✓	✓	✓	✓	✓	✓	✓	✓	✓
		Percolation of $CaCO^3$ rich water forming impregnative pedofeatures.				✓	✓	✓	✓	✓													
		Disturbance and collapse				✓	✓	✓	✓	✓	✓	✓	✓	✓	✓	✓	✓	✓	✓	✓	✓	✓	✓
		Bioturbation				✓	✓	✓			✓	✓	✓	✓	✓	✓	✓	✓		✓	✓	✓	
		Compaction (platy peds)						✓				✓		✓	✓			✓		✓		✓	✓

9.2 Is it possible to identify body degradation products, burial practices, grave goods and preservation conditions in Roman and Prehistoric burials using soil micromorphology and inorganic geochemistry?

The identification of systematic variations in the micromorphological and inorganic geochemical results and its potential links to burial practice and decomposition has been explored in the results chapters. The links between the results and evidence for the decomposition products derived from human inhumation, grave goods and the burial environment will now be explored with reference to the hypothesis raised in the conceptual models highlighted in the introduction.

9.2.1 Is there micromorphological and/or inorganic geochemical evidence of a body degradation products retained in the soil?

There was direct and indirect micromorphological and inorganic geochemical evidence of the body degradation products retained in the soil at Çatalhöyük, Thessaloniki and Hungate. Some trends were widespread, such as peaks in the bone fragment abundance in the pelvic area, concentrations of Al, K and Fe in the grave (Hungate) and iron and manganese pedofeatures as well as increased P:Fe ratios in the burial. Others were more site or grave specific, such as concentrations of P and Ca at Hungate (graves SK54898, SK51387 and SK54085).

There was evidence of chemical movement and retention in the grave soil that is likely to have been caused by the presence of degradation products from the body. Degradation markers consisted of concentrations of Al, K and Fe in graves and P and Ca in a small number of grave soils, as well as the *in situ* precipitation of iron and manganese pedofeatures and high P:Fe ratios. SEM-EXD analysis of the Hungate burials indicated that concentrations of Al, K, Fe, Mg, P and Ca were higher than in the control sample. K and Fe are possibly direct signatures of body decay, whereas Al probably relates to the clay component as many graves had higher concentrations of fine material compared to control samples (Abdel-Wahab *et al*1992, Birkeland, 1984, He *et al,*,2015, Lindbo *et al.* 2010). However, it was not possible to detect small scale changes in soil chemistry moving away from the skeleton. Elevated concentrations of Fe in the burial plane also correlate with the abundances of impregnative iron and manganese pedofeatures, caused by low redox potentials (section 8.5), to which organic matter and waterlogging could be contributory factors (Ransom *et al.* 1987, Lindbo *et al.* 2010, Schlesinger, 1991). Interestingly, there was no detectable micromorphological difference in the abundance of iron and manganese pedofeatures between

the control samples and the samples from the graves at Hungate. Elevated concentrations of P, Fe and Ca in burial soils would be consistent with previous studies that investigated body pseudomorphs and burial soils (Bethell & Carver, 2002, Keeley *et al.*, 1977, Macphail *et al.*, 2013). The P:Fe ratio, calculated for the graves using the results of the SEM-EDX study, showed that there were higher concentrations of available P in the burial plane, consistent with the PCA analysis results for some graves. Additionally P:Fe ratios showed that in most graves the available P was higher in the iron and manganese impregnations than in the fine material, indicating that it was precipitating into the pedofeatures and providing further evidence of redoximorphic conditions. At Thessaloniki TF177, Çatalhöyük 18666 and Hungate SK54090 it was also possible to observe high levels of P:Fe in specific areas of the burial plane which have been interpreted as evidence for the pooling of degradation products (Janaway 1987).

As previously hypothesised, the soil in the pelvic area retained evidence of degradation products derived from the body. Although indicators such as intestinal parasites and seeds, though to make up gut content, were not detected, as they have been using other techniques (Berg, 2002, Reinhard *et al*., 1992). Of the complete graves studied, 42% contained elevated concentrations of bone fragments in the soils around the pelvic area, this result cannot at present be linked to gut contents as it was not possible to establish if the bone was human or not. At Thessaloniki and Hungate the pattern of bone fragments also appeared to be influenced by external soil preservation conditions due to the position of the burials in the cemetery, with the southern and central areas of Hungate particularly adverse for bone preservation due to localised properties of the soil (section 6.6). At Thessaloniki, in contrast, it was suggested that bone fragments from other on-site activities, such as feasting and trample, had affected bone distribution in the burial plane, with those burials in open areas having an even distribution of bone compared to those within structures which contained bone fragment peaks in the pelvis. As stated in section 9.1.2.4 further investigation into the extent of bone fragment peaks in the pelvic area should be conducted to ascertain if these are real patterns or circumstantial.

9.2.2 Is there micromorphological and/or inorganic geochemical evidence of grave goods or burial practice retained in the soil?

Differences in burial practice, as well as soil conditions, are both contributory factors in the preservation of grave goods and their proxy indicators. The evidence for grave goods in this study was sporadic, and in most cases, indirect. The site conditions appeared to be highly influential in the retention rates of grave goods and their proxy indicators, making identification of grave goods

extremely site specific. Although the detection of organic coarse components such as bone, shell and charcoal was straightforward, linking micromorpholoigal and inorganic geochemical features to actual grave goods or burial practice was more complicated. However, links could be made between burial practice and concentrations of phytoliths (matting/cording), Pb (lead coffin), P:Fe ratio, the arrangements and types of microfabric, to the identification of plaster in grave deposits.

There were several different types of burial examined in this study, which included under floor burials as Çatalhöyük, chambered and plastered/tiled burials at Thessaloniki, as well as shrouded and coffined burials at Hungate, with a lead coffined burial also included from Hungate. The presence of the lead coffin was expressed geochemically by high concentrations of Pb in the fine material and pedofeatures as well as a high P:Fe ratio in the burial samples compared to the C1, C2 and other graves at Hungate. The presence of a lead coffin was expressed micromorphically through the development of a fine grained laminated microfabrics, as described in Chapter 3. However, the micromorphological and inorganic geochemical expression of the other types of burial was more subtle. Coffin debris was not detected, even when samples were taken directly through coffin stains (C3 sample from Hungate SK51326), there was also generally a lack of wood preserved at all sites. There was some suggestion that coffins, plastered surfaces and tiles may have been acting as barriers to the ingress of soil bioturbators at Hungate, Çatalhöyük and Thessaloniki, with sparse evidence for soil organisms in the majority of graves (section 8.5). This was supported by grave SK51326, where bioturbation was only found in the C3 sample taken over the coffin stain, indicating that bioturbation occurred outside of the coffin but was not present within the coffin. This evidence indicates that either the coffin acted as a barrier to bioturbators or that evidence of bioturbation was removed by other soil forming processes within the coffin and not in the area of the coffin stain. However, extensive evidence of bioturbation was found in SK54908, a coffined infant burial, suggesting the coffin may not act as a universal barrier and that events such as coffin collapse or decomposition may have allowed soil ingress and bioturbation. Furthermore SK54908 may also be an example of a coffined burial where no subsequent soil development processes had occurred to erase evidence of bioturbation. A second possible proxy indicator of coffined burials at Hungate were iron spherulites present in the burial planes attributed to the presence of coffined burials, together with high levels of Fe (section 4.5). However, these were not universal indicators and, like the distribution of bone fragments at Hungate, their presences appeared to be modified depending on the location of the burial in the cemetery. Evidence of plaster burials at Thessaloniki was also problematic as, although there were microfabrics (Ti2) which were clearly related to high concentrations of calcium carbonate

and could have originated from plaster incorporated into the backfill. However, a direct link could not be made because the location of graves containing microfabric Ti2 did not correlate well with macro scale evidence for plaster used as part of the burial process.

The detection of grave goods (as opposed to modes of burial) was infrequent. The neoformed iron spherulites observed in coffined burials in Hungate could relate to iron objects or coffin furniture placed in the graves, although this link has yet to be proven. The evidence for grave goods at Çatalhöyük however was more persuasive, with phytoliths found in the foot samples which are thought to relate to the inclusion of matting or binding of the body (Nakamura *et al.* 2005, Matthews, 2006).

9.2.3 Is there micromorphological and/or inorganic geochemical evidence of the soil development related to the presence of the burial?

The conceptual models (section 1.6) highlighted three possible signatures of the body that may be expressed in the soil development. These were 1) Evidence of collapse or disturbance of soils due to their infilling voids left by the coffin and the body; 2) Compaction from the soil over burden; and 3) Soil water becoming trapped in the burial due to the 'bucket' effect, as well as the effect of macro-pores in the backfill limiting the movement of water into the surrounding soils. These aspects of the burial soils will be discussed first followed by any unexpected evidence which has led to interpretations about the burial environment.

There was substantial evidence for the translocation of soil particles, soil disturbance and collapse at Thessaloniki, Heslington East and Hungate, which consisted of extensive coatings, aggregated soil features and platy peds. These sites all contained continuously-orientated clay coatings on void and ped surfaces, indicating that illuviation was prevalent (Gunal & Ransom, 2006). Thessaloniki and Hungate also contained microlaminated clay and the interleaving clay and silt coatings, meaning that their formation was episodic. There was also a tendency for dusty clay coatings, which are caused by the translocation of soil particles and organic matter (Thompson *et al.* 1990, Slager & van de Wetering, 1977, Macphail *et al.* 1990, Usai, 2001), to concentrate in the burial plane at Heslington East, Thessaloniki and some of the Hungate graves. This would be consistent with soil particle disaggregation occurring, which can take place due to soil chemical changes (Barbiero *et al.* 2010), changes in the soil hydrology (Kooistra & Tovey, 1994), bioturbation, or a lack of ground cover (Bresson & Boiffin, 1990, Courty *et al.*, 1989, Lindbo *et al.*, 2010, Macphail *et al.*, 1990). In addition, fragmented coatings were observed in the hand area

sample from TF177 and the C3 sample from TF182, suggesting that soil disturbance in these areas was active enough to cause the displacement of coating pedofeatures (Kuhn *et al.* 2010). The soil development at Thessaloniki and Hungate was also weak, with high abundances of apedality and weakly to moderately developed peds, suggesting a combination of Fe and Mn reduction together with periodic saturation weakening the bonds between soil particles and increasing the likelihood of soil deformation and collapse within the burials (Barbiero *et al.* 2010, Kooistra & Tovey, 1994). There were, however, several examples of well developed platy ped features in the graves at Thessaloniki (TF177) Heslington East (713) and Hungate (SK54898, SK51326, SK54090, SK54341, SK54090 and SK51350). Although their location in the burial plane was not systematic, they may be an indicator of local compaction of the soil (Kooistra & Tovey, 1994) or alternatively cyclic wetting and drying (Hussein & Adey, 1998).

Active hydrological regimes were present at Thessaloniki, Heslington East and Hungate, yet, there was evidence of redoximorphic pedofeatures in the burial planes of graves at all sites, including those with little active hydrology. Further to this, in the majority of cases, the inorganic geochemical signatures of the samples in the burial plane of each grave were similar to one another, suggesting that any inorganic geochemical changes caused, by the burial were evenly distributed in the burial plane. This may be due to the pooling of degradation products around the body (Dent, 2002, Janaway, 1987, Janaway *et al.* 2009), especially in an enclosed coffin environment, or equally because there is minimal differences in the distribution of inorganic geochemicals in the human body (Heymsfield, 2005). Pooling of bodily fluids in the burial plane, causing redoxamorphic features may be particularly relevant at Çatalhöyük where there was no active hydrology (Dent, 2002, Janaway, 1987). Bioturbation may also be a factor and contributed to the even distribution of inorganic soil elements (Canti, 2003). However, the pattern is consistent with what would be expected in burials if there was a retention of water by the burial soils, as suggested by previous studies on cemeteries (Dent, 2002) as well as clandestine burials (Hansen *et al.*, 2014, Pringle *et al.*, 2012, Schultz *et al.*, 2006).

In addition to the predicted effects of burials on soil development, there were also patterns identified that were unexpected, consisting of concentrations of charcoal in the skull area, systematic variation in the distribution of void space around the burial plane, the distribution of pedofeatures types between sample locations in the burial plane, graves and sites and the preservation of bone and shell and its relationship to soil pH.

There were systematic spatial differences in the burial plane that related to the distribution of charcoal, iron and manganese pedofeatures as well as void space. 66% of complete graves had concentrations of charcoal fragments in the skull area samples. The mechanism for this concentration is not understood but it may be due to a combination of the pooling of bodily fluids in the burial plane as well as the tendency of charcoal to float. There was also a general trend for total void space abundance to be reduced in the pelvic area, as well as low levels of channels and vughs in the skull and high levels of vughs and planes coinciding with low levels of packing voids in the pelvic area. High porosity has been linked to wetting and drying cycles (Pires *et al.*, 2008), whereas low porosity may be due to compaction (Kooistra & Tovey, 1994) suggesting that low levels of porosity in the pelvic area may be caused by compaction, although this would mean that it had been a very localised process. The low abundance of total void space in the pelvic area was composed of vughs and planes. Vughs can be an indication of soil faunal activity and the aggregation of soil (Ringrose-Voase & Bullock, 1984, Brewer, 1964, Kooistra & Pulleman, 2010), which would be consistent with aggregation associated with collapse occurring around the pelvis. Iron and manganese pedofeatures also varied in the burial plane, with concentrations of impregnations in the foot area samples at Hungate and in the pelvic area at Thessaloniki, possibly caused by differentials in the Eh laterally across the burial plane (Vepraskas, 2001). Therefore several general trends in void space, charcoal abundance and the distribution of iron and manganese impregnations that varied systematically in the burial plane, could be used as 'grave markers'. However these patterns must be used with caution as these trends do not exist in every grave. They were missing from Heslington East, for example, and can, therefore only serve as a guide to burial identification, whilst assessing how processes were localised around the body. Future work looking at the variation in charcoal, void space and impregnations should begin by comparisons with other graves analysed by the InterArChive project. There should also be further work undertaken on the concentrations of charcoal in the skull area of the burials, similar to bone fragments this could take the form of residue flotation techniques for the soil surrounding burials, with charcoal fragments being analysed and identified to species ascertaining if there are any common species, furthermore, helping to identify any species bias.

Four categories of pedofeatures were described in detail: iron and manganese pedofeatures, typic coatings, bioturbation features and $CaCO_3$ pedofeatures. Of the four pedofeature groups, typic coatings and iron and manganese pedofeatures were most universal and tended to relate to grave formation processes (Chapter 8). One reason for this is that the composition and presence of coatings is driven by taphonomic processes which relate directly to grave formation. For example,

dusty clay coatings can be formed by processes that may be common in all graves; presence of loose soil caused by surface and internal soil disturbance (bioturbation) (Brewer, 1964, Brinkman, 1970, Macphail *et al.*, 1990, Usai, 2001). There may also have been soil collapse as the body degraded. Unlike iron and manganese pedofeatures, coatings were not found in the burial plane at Çatalhöyük, showing that the formation of common grave pedofeatures can be influenced by human agency. However, bioturbation features and $CaCO_3$ pedofeatures are dependent not only on the presence of a grave but also on other environmental circumstances. For example, $CaCO_3$ needs to be present in the environment for such pedofeatures to form, and for excrement to be deposited, soil organisms must have access to the site/grave.

At a site level the local soil conditions do seem to have affected the preservation rates of bone and shell fragments. The survival of shell at Çatalhöyük and Thessaloniki would indicate that the site pH has not dropped below 7 (Weiner, 2010). The absence of shell at Hungate and Heslington East may relate to either site conditions or lack of their inclusion during burial. Chicken egg shell, which is composed of calcite, was found extensively from the Viking age period at Hungate (Stewart *et al.*, 2013), indicating that it is possible for calcite based shells to survive at the site. However, calcite is more stable than aragonite (snail shell) (Weiner, 2010). The presence and abundance of shell and bone may be a proxy indicator for overall site pH and preservation levels at the time of burial.

9.3 Evaluation of the InterArChive sampling strategy

When evaluating the InterArChive sampling strategy there are five main questions to be addressed; 1) Were control samples really controls? 2) Were enough control samples being collected? 3) Were sufficient samples being taken in the burial plane? 4) What are the recommendations for future sampling strategies? 5) How could the InterArChive sampling strategy be applied in the future? These questions will now be assessed.

9.3.1 Are controls really controls?

The aim of the C1 sample(s) was to establish the nature of soil conditions on site where inhumations were absent. In practice obtaining C1 sample(s) could be problematic due to the character of the sites: extensive modern urbanisation such as at Thessaloniki, made C1 sample retrieval difficult. The acquisition of C1 samples would have been more successful if they had been collected in a more systematic way. Samples were taken by ‘a member of the InterArChive

project' and often a site would be visited my multiple team members on different occasions. This meant that different team members were required to know exactly what had been sampled prior to their site visit. This could and did become confusing, leading to situations where at larger sites such as Hungate only one C1 sample profile was taken, when multiple profiles would have been more reliable. Something that may have been identified if there had been a consistent project member present for all of the sampling. It also led to mistakes at Heslington East where the pelvic sample was missed, presumably because communication between InterArChive project members was poor. Sites were also at times sampled by project members with a limited knowledge of archaeology or soils meaning that mistakes were made such as omitting information from sampling sheets etc.

When analysing the C1 samples, it is critical to understand what exactly they represent. Initially one would assume that the C1 sample represents the soil if no burial had occurred, but this is not always the case. After the point of burial, grave soil development is influenced by the presence and decomposition of the body and its associated grave goods. The location of the C1 sample has, in theory, not been influenced by a burial. However, there may have been localised influences on the C1 sample such as proximity to cess pits and structures which may not have influenced the soil development in the area of the burial.

The C2 samples and C3 samples were meant to be taken from the upper (C2) and lower (C3) grave fill (Figure 122a). In practice, however, this proved difficult because InterArChive team members were not permanently on site. Thus, C2 samples were often taken from the grave section after the skeleton had been excavated. This means the samples were of the soil adjacent to the grave cut rather than being of the grave fill (Figure 122 b). Also, the placement of the C3 samples, in some instances, was in the burial plane (Figure 122 b). This was reflected in the results, especially in the geochemical analysis and ped distributions where some of the 'C3' samples have a 'burial plane' signature.

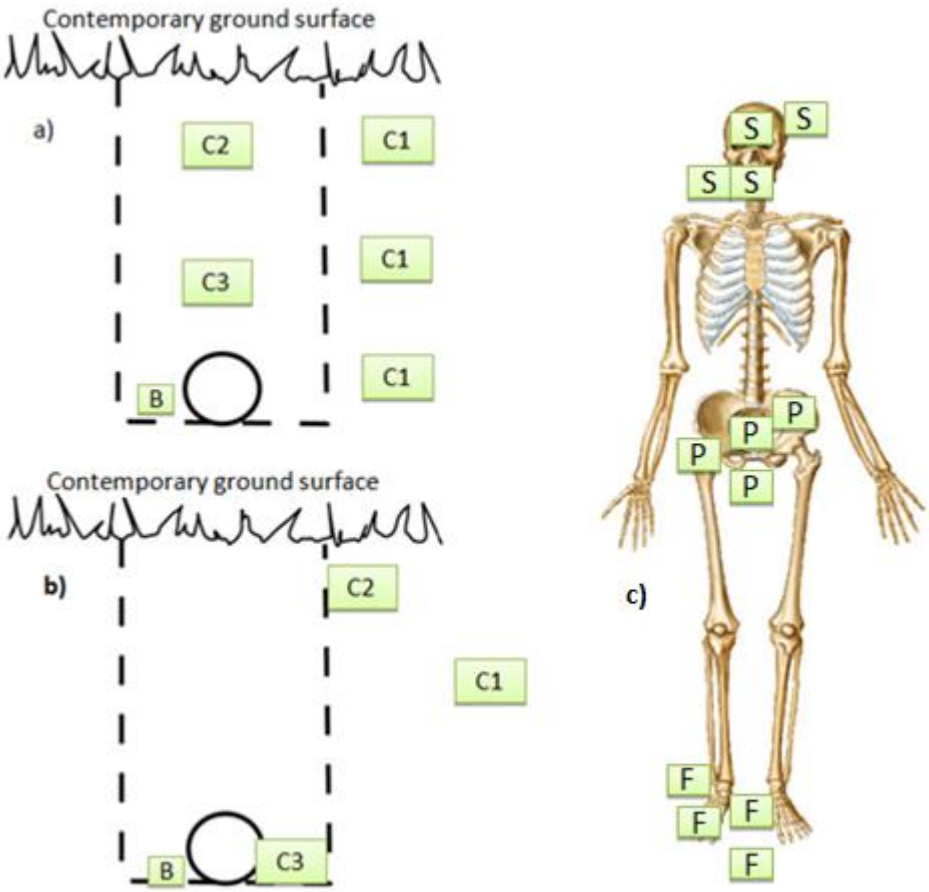

Figure 122: Illustration of a) idealised InterArChive sampling strategy, b) where samples were often taken from due to the constraints of the site dynamic. (B) = burial samples c) Examples of the different sample location possibilities in the skull (s), pelvis (p) and foot (f) areas

9.3.2 Are enough control samples being taken?

Ideally each grave should have two control samples from the fill (C2 and C3) and one sample from non-burial soils (C1). In practice the C1 samples were more effective when a set of samples were taken down a complete soil profile, from the A to the C horizon (Figure 122 a), as this gave a better assessment of how the soil changed with depth. In bigger sites, such as Hungate, multiple C1 profiles would have been advantageous as soil properties can change over relatively short distances. Multiple C1 soil profile samples would also reduce the effect of differences in sample size, making comparisons between the control and burial plane more reliable. The C1 soil profile at Hungate was taken in the southern part of the cemetery close to the southernmost grave in this study (SK51351). The applicability of the C1 sample to the central and northern parts of the cemetery may, therefore be questioned. That said, there was no correlation between grave location and differences to the C1 samples here, suggesting that localised soil changes did not

have a huge effect on interpretations. It would, however still be advantageous to have better C1 coverage particularly at larger cemeteries as this would give a better understanding of the 'non grave' soil conditions across the site making comparisons between the C1 soil profiles and the graves more accurate.

9.3.3 Are enough samples being taken in the burial plane?

In practice, the position of burial plane samples varied (Figure 122), with samples taken above, adjacent to, and below the body, as well as in several locations around the skull, pelvis and foot areas (Figure 122). The extent to which this has affected the micromorphological and inorganic geochemical results has not been investigated, and as yet there are no plans to do so. The variation in the sample locations occurred because burials, especially prehistoric burials, can vary significantly in the position of the body and inclusion of grave goods necessitating the movement of sampling locations. For example, at Hungate and Çatalhöyük samples were moved so grave goods were not damaged. A lack of standardisation in sample position may have contributed to a lack of continuity in the micromorphological characteristics of sample locations between graves. Again this was further exacerbated by a lack of continuity with regards to project members on site and a lack of analysts taking their own samples. The need for standardisation was not appreciated until the micromorphological analysts had time to feedback to the wider group. It was also then difficult to action standardisation as each project member had their own personal preferences for sample orientation.

9.3.4 Recommendations for future sampling strategies and limitations of methodological approaches

The evaluation of the microscale remains within burials was somewhat constrained by the remit of the InterArChive project, meaning that complimentary techniques, such as ICP, particle size, pollen or phytolith studies could not be introduced. The limitation on methodological approaches and resistance to amendments of the sampling strategy also meant that there were avenues of investigation that could not be followed up, due to lack of funds and samples. For example, as bulk samples were, in practice, not routinely collected, for the micromorphology side of the project, some sites had missing macro soil descriptions. It also meant that when significant findings were made, such as the presence of phytoliths in the Çatalhöyük burials, these could not be followed up as no samples were available. C1 samples, and on one occasion the pelvic samples from Heslington East, were also omitted from sampling by members of the project, meaning that

full analysis could not be conducted on all sites. However, in some cases the collection of micromorphological samples with particular sampling positions was not feasible due to the position of the burial and the lack of soil at the particular sampling location.

That being said, overall the InterArChive sampling strategy was carefully planned and provides a good framework for future research. Recommendations for future priorities when deploying the InterArChive sampling strategy would be to focus on the placement and number of samples taken. Firstly the C1 samples should be taken as a soil profile of three or more samples. On larger sites multiple C1 profiles should be taken to account for changes in soil over short distances. It is also recommended that, upon identification of a grave cut, a soil column should be left *in situ* to allow the sampling and placement of the C2 and C3 samples (as recommended by Goldberg and Macphail (2006)). In addition, the effect of slight location changes on the positioning of samples in the burial plane should be investigated by taking multiple samples in the skull, pelvic and foot areas of several graves. It would then be possible to quantify the need for standardisation of sample locations. Additional bulk samples should also be taken in conjunction with micromorphological analysis so that macro scale soil observations can be made as well as providing material for further soil analysis should it be deemed necessary. To establish the abundance of bone and charcoal fragments in a grave the remaining basal fill should be sampled at the skull, pelvis and foot areas for flotation. The micromorphological analysis should then be tailored to any specific questions being asked by the archaeologists for example where bulk chemical analysis will also be used to establish the level of soil translocation which may have occurred. When distinguishing between cenotaphs and robbed/disturbed graves establishing the presence of a body is important. This can be achieved by analysing the abundance and distribution of Mn/Fe pedofeatures and establishing redox conditions caused by high levels of organic matter; the former derived from the placement of a body. Being very specific as to what micromorphological features are relevant will mean that the cost of micromorphological analysis will be reduced.

9.3.5 How and where should the InterArChive protocol be used

There are some conclusions that we have reached using the micromorphological and inorganic geochemical analysis that could have been obtained from 'traditional' archaeological and soil analytical methods. For example, it was not necessary to use micromorphology to establish that SK54898 contained a lead coffin, this was obvious upon excavation. However in cases such as the prehistoric cemetery of Tiszapolgar-Basatanya (Whittle, 1996) (section 1.7.1), where coffined

burials were suspected, but never confirmed, micromorphological analysis may be able to resolve the presence of a coffin. It is, therefore crucial to establish what micromorphological techniques can contribute to burial archaeology that others techniques cannot. The inorganic geochemical results were interesting in that there did appear to be a 'grave' signal, which would suggest that it could be possible to identify where graves were present by assessing the inorganic geochemical signatures of the soil. Whether this would necessarily need to be conducted on micromorphological slides or whether analysis of bulk samples would be sufficient is yet to be established. If the inorganic geochemical signature of the grave was the only element being investigated, the use of bulk samples rather than micromorphological slides would bring down the cost significantly (cost of micromorphological examination of a grave is approx £1720). Concentrations of bone fragments in the pelvic area and charcoal fragments in the skull could also be ascertained on site, using grab samples and flotation. It is also unclear if a grave could be distinguished from other contexts such as rubbish pits, although the excavation processes would go a long way to identifying possible grave sites. One issue that will need to be considered is if this technique is used in future archaeological excavations is its applicability to none supine burials. The sampling strategy was developed for supine burials in cemeteries. Prehistoric burials are often in none standard positions and environments (Parker-Pearson, 2003) and it could also be argued that prehistoric burials, where there are no written or contemporary records of burial practice or belief, have the greatest potential for adding to our knowledge. If further investigations can establish that some of the hypothesis in this research can be used to identify the presence of coffins, metal objects, the inclusion of plaster and the inundation of charcoal into the grave, perhaps it is prehistoric burials which should be focused on in future. Despite the aforementioned difficulties, micromorphological examinations of graves can be both useful and cost effective. Firstly, this thesis has gone some way to identify a suite of possible 'grave markers'. The markers include: concentrations of low total void space in the pelvis; identification of iron and manganese pedofeatures as well as concentrations of impregnations in the foot and pelvic areas; iron spherulites; layered microfabrics and concentrations of coating in the burial plane; and bone concentrations in the pelvis and charcoal concentrations in the skull. These aspects would be vital when trying to determine if 'empty graves' ever contained remains. Furthermore, the identification of specific 'grave markers' means that micromorphological examination could be more cost effective, with specific micromorphological features being focused on making the process more efficient. Micromorphological examination can also have a role in informing the use of other analytical techniques. For example if in-depth chemical or microfossil investigations are

to be implemented, it may also be useful to know if there had been a significant amount of sediment translocation or if large parts of the backfill were from a source other than the local environment. Micromorphology can also be a valuable technique in 'non standard' burials such as prehistoric burials like the 'mound people' (Glob, 1973) or those that are high status like the Gokstad ship burial mound (Macphail *et al.*, 2013). This would identify subtle elements of burial practice, such as how protected the burial was from external influences by the inclusions of coffins, the inclusion of grave goods such as matting or concentrations of iron and, most importantly, in examples like Sutton Hoo, if there where actually bodies present (Bethell & Smith, 1989).

9.4 Future Research Directions

Future research directions should initially focus on a detailed comparison between this work and the micromorphological work carried out by the rest of the InterArChive team. This should centre on establishing if trends such as abundance peaks of bone in the pelvis, charcoal in the skull and iron and manganese impregnations in the foot and pelvic area are present in other graves and give a reasonable indication of how widespread the trends area. Additionally there were a number of lead coffined graves analysed by the InterArChive project, these should also be used as a comparison for SK54898 and the presence of Pb in the fine material as well as microlaminated stratigraphy could be accessed to establish if these are universal features of coffined or lead coffined burials.

There are more site specific questions that would benefit from further investigation. At Thessaloniki there is a question mark over the origin of Ti2. To fully understand the formation of Ti2 further, analysis should be conducted on the possible sources of Ti2. Mortar from the building material and the plaster used to line the graves should be collected and analysed using SEM-EDX analysis to compare to Ti2 and hopefully establish if Ti2 came from the mortar or from the material used to line the graves. Hungate contained red spherulites that were identified as rich in Fe. It has been proposed in this work that the red spherulites were caused by the presence of the coffin furniture (i.e. nails and handles etc) or Fe artefacts, these two origins however are not mutually exclusive. The most expedient method of further investigation would be to confirm that they are a feature of coffined burials by analysing none coffined burials in the south of the cemetery, as this was the area with the highest incidence of Fe spherulites. The formation of spherulites and their relationship to burial conditions could be investigated further using a series of archaeological experiments, some with and some without coffins and Fe objects and coffin

furniture. This would allow the nature of spherulite and their relationship to burials to be investigated; it would also be possible to map the location of any spherulite formation in relation to the body (ie inside or outside the coffin). There is a wide scope for future work to be conducted on complementary techniques on the soils around human burials. Ideally this would involve the investigation of particle size analysis to understand how the backfill/settling processes has affected the particle size gradient, establishing if there are significant changes that are related to the process of burial. Pollen and phytolith studies would also be recommended as they may be able to identify cases were plant remains have been added to the burial and may even pinpoint the seasonality of the internment.

The distribution of charcoal, bone and Fe/Mn impregnations in the burial plane would also warrant further analysis to ascertain if the patterns observed in this thesis were widespread. Currently, concentrations of the aforementioned features are measured using the percentage estimation charts provided in Stoops (2003) and they would, therefore benefit from a more secure method of quantification that encompasses other methodologies. Bone and charcoal fragment investigation could be conducted using standard flotation methods during excavation if the burial plane was divided into distinct areas of skull, pelvis and foot. This would then allow the charcoal and bone fragments to be quantified by weight and species of origin could, depending on fragments size, be identified, using charcoal analysis and amino acid racemisation methods. Fe/Mn pedofeatures, thus would still require micromorphological analysis to be conducted, therefore either point counting or the development of image analysis techniques could be useful to more accurately quantify the volume of Mn/Fe pedofeatures establishing if higher abundance in the foot and pelvic area compared to the rest of the burial plane and whether it is a more universal phenomenon; justifying further investigation into the causes of it.

9.5 Conclusion

This study set out to evaluate if the presence of a body and its cultural artefacts can be identified using soil micromorphology and inorganic geochemistry, through the application of the InterArChive protocol. Overall, there are significant micromorphological and inorganic geochemical signatures which can be interpreted as ‘grave’ markers (Table 67). It has been possible to reconstruct from the micromorphological and inorganic geochemical data a ‘typical’ grave signature for Hellenistic and Roman graves at some sites, which would include peaks of charcoal in the skull as well as increased levels of bone fragments with large fragments of bone in the pelvis. The formation and fragmentation of illuviation coatings occurred where there had

been soil movement. The abundance of voids was also distinctive, with most graves containing a low degree of overall porosity in the pelvis area, low levels of channels relating to bioturbation in the skull, and a reduced abundance of packing voids and elevated abundance of vughs in the pelvis relating to aggregation. In terms of the inorganic geochemical signatures, the data strongly supports that, in the future, it could be possible to identify 'graves' as they contain a higher P:Fe ratio than non-grave soils. Over and above the 'typical' grave markers, there are complex soil formation and taphonomic process occurring in each grave which are heavily influenced by site, burial practice and the soil microenvironment. It is therefore crucial that each grave is interpreted individually in light of these differences in order to reconstruct a grave-specific sequence of events.

There are several lessons that can be learned from this work about the future sampling priorities and research directions. Future recommendations for sampling would include a higher level of C1 samples being taken, partially from larger sites such as Hungate. As well as the inclusion of a small sampling column so that the C2 and C3 samples can be precisely placed in relation to the burial. The position of the skull, pelvic and foot samples should include a standard orientation and position in the burial plane i.e. adjacent to or below the body. There should also be a greater level of continuity in the specialists taking the samples so that obvious mistakes, such as omitting samples from collection, aren't made. Ideally graves should be sampled in groups. This will provide greater breadth of information to reconstruct past events that occurred on a site-wide basis and relate these to burial practice and degradation, such as water logging at Hungate. This was more achievable on sites where groups of graves were considered. Sites such as Heslington East, where only one grave was analysed, meant that it was difficult to distinguish what was grave related and what may have been caused by general soil formation processes.

In terms of a contribution to burial archaeology some of the patterns and trends highlighted by this research could have further implications for the interpretation of burials and be able to expand future research objectives. For example, it may be possible to distinguish between cenotaphs and graves where the body has been removed or subsequently decayed to nothing using the methods outlined in this thesis, or slight variations thereof. For instance, in cases where an empty grave is found it may be possible to look for the 'grave markers' highlighted in this work such as charcoal peaks at one end of the grave and bone fragment peaks in the centre as well as raised abundances of Mn/Fe impregnations in the opposite end of the grave, using a combination of flotation and micromorphological analysis. This would give a reasonable indication of the

likelihood of a body being present. The high cost of the micromorphological analysis, approximately £250 a sample for processing and analysis, however would be a limiting factor, therefore the development of more streamlined protocols and sampling analysis would be required to make the method more cost effective and more universally applicable. There are also several other complementary techniques which should be developed alongside burial micromorphology to answer further questions about the burial environment. These would include the analysis of the charcoal and bone fragments within the grave to identify them to species as well as techniques such as phytolith and pollen analysis to establish if there are remains of plants which have been included as either coffin furniture (straw pillows etc) or as offerings to the deceased (flowers etc). There should also be work conducted on a sampling strategy for non supine burials such as those at Çatalhöyük. Although sampling at the skull, pelvis and foot are effective for supine burials there may be more appropriate sampling points for crouched burials.

Further to an archaeological application there may also be a modern forensic application for micromorphological burial analysis. For example it has been possible to identify several different microfabrics in the graves at Hungate, Çatalhöyük and Thessaloniki and to link those microfabrics to the surrounding soil conditions. It was possible to identify sediments that had originated from the River Foss in the Hungate burials. In a forensic setting the micromorphological analysis of the grave fill may be able to give vital information as to where a body had been taken or moved from by looking at microfabric evidence. It would also be possible to reconstruct how the grave had been in filled which could have important implications for if the body had been wrapped or covered. In relatively fresh burials it may be possible to ascertain if the grave had been left uncovered by looking for the pooling of sediments at the bottom of the grave and for rain splash markers using micromorphological analysis to show if the grave had been prepared for any length of time before burial.

As with any significant volume of work this research has thrown up as many questions as it has answers, giving a wide scope for future research. There are several avenues of research that would benefit from further scrutiny such as the development of the inorganic chemical analysis to create a model that would be able to predict if samples were from ‘grave’ deposits. There is also more work to be done by looking at the movement of water and chemicals around the body, involving the establishment of the directionality of voids, using image analysis, as a conduit for soil water, chemical and particle movement. In future it may also be possible to make inferences about the inclusion of grave goods and the presence of coffins by establishing proxy indicators for

iron materials such as Fe spherulites and microstratigraphic layering indicating sheltered areas such as coffins. These markers however, are tentative and would require further research to fully establish their validity as 'grave markers'. Overall, what is clear from this work is that it is possible to identify degradation products, burial practices and grave goods using micromorphological analysis and that there is a significant amount of information hidden in the microremains in burials. Now that this has been established further work should be conducted to make sure that this resource is appropriately utilised to aid in the interpretation of what is a rich and varied source of both cultural and personal information.

1 Appendix

1.1 Chapter 2 Appendix

1.1.1 Macroscale soil description.

Table 68: Soil macro description summary for Çatalhöyük.

Grave	Sample location	Soil description	pH
C1		Greyish yellowish brown to moderate yellowish brown (10YR4/2 Dry and 10YR2/2 Wet), silty clay, moderately strong sub-angular blocky structures, with no visible pores. Very few (<5%) small (<1mm) spherical white mineral nodules, with some ceramics (5%) and microcharcoal visible.	7.6
18666	Skull area	Brown (7.5YR4/2 Dry and 7.5YR4/2 Wet), silty clay loam, very weak to moderately strong subangular blocky structure, with no visible pores. Inclusions are very few (<5%) small (<1mm) angular red minerals and small infrequent (5%) bone fragments.	7.6
	Pelvis area	Brown to very dark brown (10YR4/3 Dry and 10YR2/2 Wet) silty clay, moderately strong subangular blocky peds, with very few (<5%) micro (<0.075mm) planes. Very few (<5%), small (<1mm) white mineral inclusions.	7.8
	Foot area	Brown (7.5YR4/3 Dry and 7.5YR4/2 wet) silty clay loam, moderate subangular blocky peds with no visible pores. Inclusions consist of very few (<5%), angular, weathered, white, gravel (2-6mm), very few, small (<1mm) irregular orange mineral nodules and fragmented bone (5%) and microcharcoal (2%).	7.9
19295	19500 Skull area	Brown to very dark brown (10YR4/3 Dry and 10YR2/2 Wet) silty clay, moderately strong subangular blocky peds with no visible pores. Inclusions consisted of very few (<5%) angular, fresh, gravel (2-6mm), very few, small (<1mm) angular, white mineral inclusions and fragmented bone (2%).	7.6
	19501 Skull area	Brown to very dark brown (10YR4/3 Dry and 10YR2/2 Wet) silty clay, moderate subangular blocky peds with no visible pores. Inclusions consisted of very few (<5%) angular, gravel (2-6mm) and very few, small (<1mm) white minerals. Fragmented bone was also present (2%).	7.2

Table 69: Soil macro description summary for Thessaloniki.

Grave	Sample location	Soil description	pH
C1		Greyish yellowish brown to moderate yellowish brown (10YR4/2 Dry and 10YR2/2 Wet), silty clay, moderately strong sub-angular blocky structures, with no visible pores. Very few (<5%) small (<1mm) spherical white mineral nodules, with some pottery (5%) and microcharcoal visible.	7.6
TF178	Skull	Dark yellowish brown (10YR4/6 Wet) slightly calcareous	
	Pelvis	Dark yellowish brown (10YR4/6 Wet) slightly calcareous	
	Foot	Dark yellowish brown (10YR4/6 Wet) slightly calcareous	

Table 70: Soil macro description summary for Helsington East.

Sample location	Soil description	pH
Skull	Very dark brown (7.5YR 2.5/3) silty clay loam, weak sub-angular structure, with few small cavities, planes and channels. Few fine roots, boulder inclusions and small infrequent black minerals.	6.9
Right hand	Very dark brown (10YR 2/2) sandy clay loam, weak sub-angular structure with few small cavities and planes. Few fine roots, boulder inclusions and small infrequent white and black mineral.	7.1
Feet	Very dark grey (10YR 3/1) loamy sand, weak sub-angular structure with small and infrequent channels. No roots and few stones and infrequent white and black minerals.	6.8
C3	Dark brown (10YR 3/3) sandy loam, with a weak granular/sub-angular blocky structure and few small channels and planes. No roots, infrequent boulders and small white and red minerals.	7.2
C2	Brown (10YR 3/2) sandy clay loam, with a sub-angular blocky very weak structure and infrequent small channels and planes. Fine roots and boulders present in low quantities. Infrequent small red and white minerals.	6.9
22-28cm Soil profile	Brown (10YR 3/2) sandy clay loam with weak sub-angular blocky structure and infrequent channels and planes. Few fine roots and some boulder sized inclusions. Infrequent small red and white minerals.	6.2
46-52cm Soil profile	Dark brown (10YR 3/3) sandy clay loam with very weak sub-angular blocky structure and small infrequent channels and planes. Some stone inclusions and infrequent small white minerals.	6.8
74-80cm soil profile	Brown (10YR 3/2) sandy loam with structreless to weak sub-angular blocks and few small planes. Some stones and infrequent, small, white and red minerals.	6.4

Table 71: Soil macro description summary for Hungate.

Grave	Sample location	Soil description	pH
SK54898	Shoulder	Dark reddish brown (5YR3/3 Wet) silty clay, apedal in structure with no visible inclusions.	7.9
SK54341	C3	Brown (10YR4/3 Wet) sandy clay with a very strong granular and subangular blocky peds present as are mico cavities (<0.075) (very few). Inclusions include very few (<5%) subangular gravel (2-6mm) and very few, small (<1mm) diffuse red mineral nodules.	7.9
	Skull	Brown (10YR4/3 Wet) clay loam with a moderate granular structure and very few (<5%), very fine (<1mm) cavities and few (5-15%) very fine planes. Inclusions consist of very few (<5%) fine roots and very few, small (<1mm) diffuse red mineral nodules.	8
	Pelvis	Brown (10YR4/3 Wet) silty clay loam with weak angular blocky peds and very few (<5%) micro (<0.075) cavities and planes visible. Inclusions consisted of very few small (<1mm) spherical, diffuse, white and yellow mineral nodules.	7.9
	Feet	Brown (10YR4/3 Wet) sandy clay loam with a moderately strong subangular blocky ped structure with no visible voids present. Inclusions consisted of few (5-15%) large (>3mm) irregular red mineral nodules and very few, small (<1mm) white mineral nodules.	7.9
SK54342	C3	Dark yellowish brown (10YR3/4 Wet) silty clay with a moderately strong subangular blocky ped structure. Visible pores were very few (<5%) micro (<1mm) random cavities and planes. Inclusions consisted of very few small (<1mm) red nodules.	7.2
	Skull	Dark brown to brown (10YR3/3 Dry and 10YR4/3 Wet) sandy clay loam with a very strong subangular blocky ped structure. Visible pores consisted of few (<5%) micro (<1mm) cavities and few (5-15%) micro continuous planes. Inclusions consisted of very few (<5%) sub-angular, weathered stones (6-20mm).	7.7
	Pelvis	Dark yellowish brown (10YR3/6 Wet) silty clay with a very strong subangular blocky peds. Voids include very few (<5%) micro (<1mm) cavities, channels and planes. Inclusions consist of very few, small (<1mm) diffuse red mineral nodules and fresh stones (6-20mm),	7.9
	Feet	Dark brown (10YR3/3 Wet) clay loam with a moderately strong subangular and a weak prismatic ped structure. Pores include very few (<5%) small (<1mm) channels. Inclusions consist of very few, medium (1-3mm) diffuse red mineral nodules.	7.7
SK54085	C2	Dark yellowish brown (10YR4/4 Wet) sandy loam with a very strong subangular blocky ped structure. Pores consist of very few (<5%) small (<1mm) random cavities. Inclusions are very	7.7

		few angular gravels (2-6mm), very few large (>3mm) diffuse red, and very few small, diffuse black mineral nodules.	
	C3	Dark yellowish brown (10YR3/4 Wet) silt with very strong subangular blocky peds. Voids consist of very few (<5%), small (<1mm) random planes and cavities. Inclusions consist of very few angular white mineral nodules and very few angular gravels (2-6mm).	7.8
	Skull	Dark brown (10YR3/3 Wet) silty loam with moderately strong subangular blocky peds structure and very few (<5%) small (<1mm) random discontinuous channels. Mineral nodules were very few, small, irregular and white. Inclusions include very few, angular gravels (2-6mm)	8.1
	Pelvis	Dark yellowish brown (10YR3/4 Dry and 10YR3/6 Wet) clay loam with very strong subangular blocky peds with very few (<5%) small (<1mm) discontinuous channels and planes. Very few fine (1-2mm) roots were visible as were very few, large (>3mm) angular red mineral nodules. Charcoal was also visible (5%).	7.6
SK54090	C3	Dark brown to very dark grayish brown (10YR3/3 Dry and 10YR3/2 Wet) sandy clay with moderately strong subangular blocky and crumb peds. Pores include very few (<5%) small (<1mm) cavities and planes. Mineral nodules were composed of very few, small, angular white and red.	8.2
	Skull	Dark brown to very dark grayish brown (10YR3/3 Dry and 10YR3/2 Wet) sandy clay loam with subangular blocky moderately strong peds. The pores were very few (<5%) small (<1mm) cavities. Mineral nodules were composed of red and white irregular, medium (1-3mm) very few (<5%).	8.3
	Pelvis	Dark yellowish brown (10YR3/6 Wet) silty clay. Pores were very few (<5%) small (<1mm) cavities and few (5-15%) small planes. Inclusions included angular, weathered stones (6-20mm). Mineral nodules consisted of red, white and black spherical, small and very few inclusions.	8.1

1.1.2 InterArchive sample recording sheet

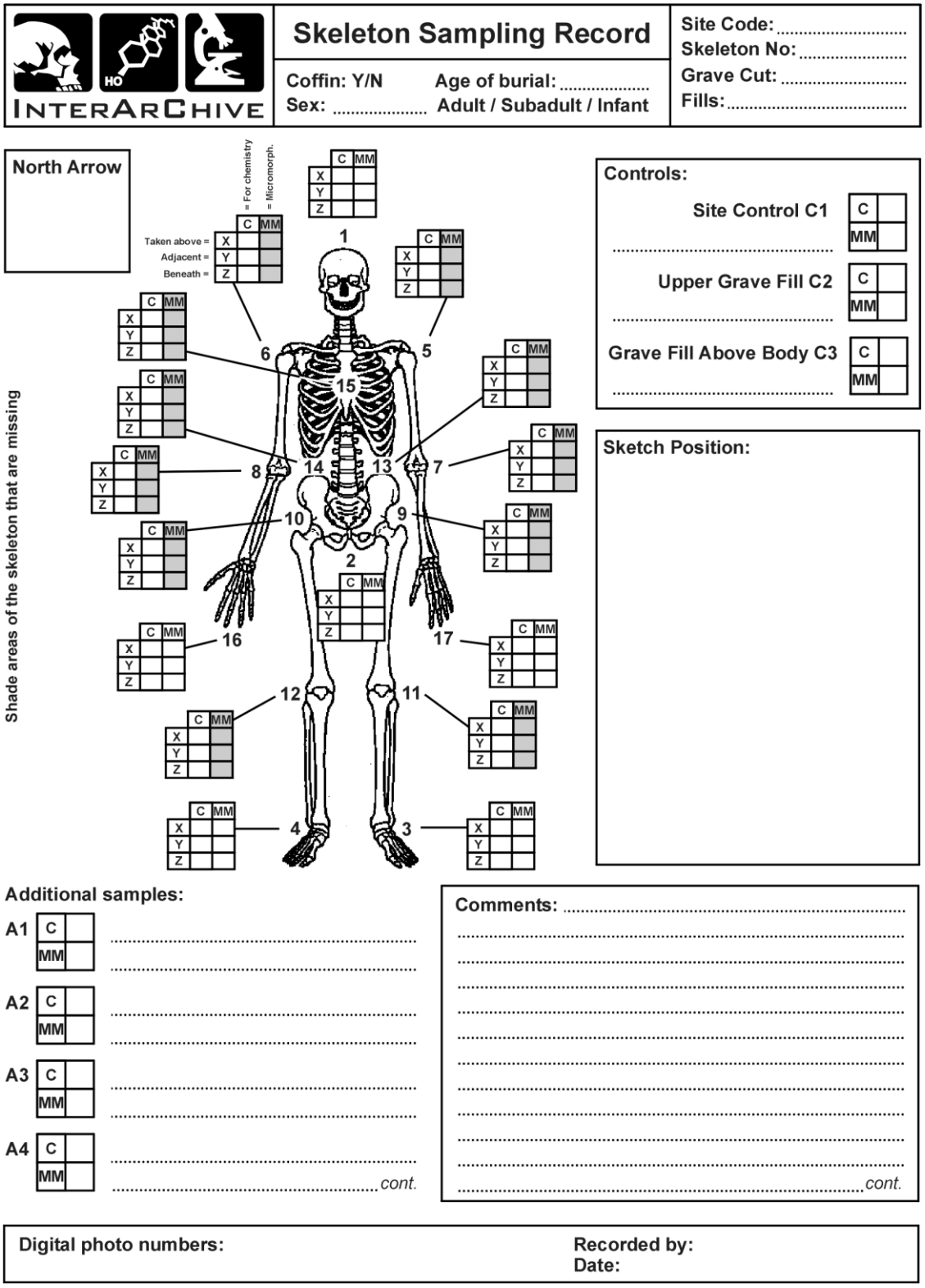

Figure 123: InterArChive sample recording sheet designed by Mat Pickering

1.1.3 Annotated slide scan.

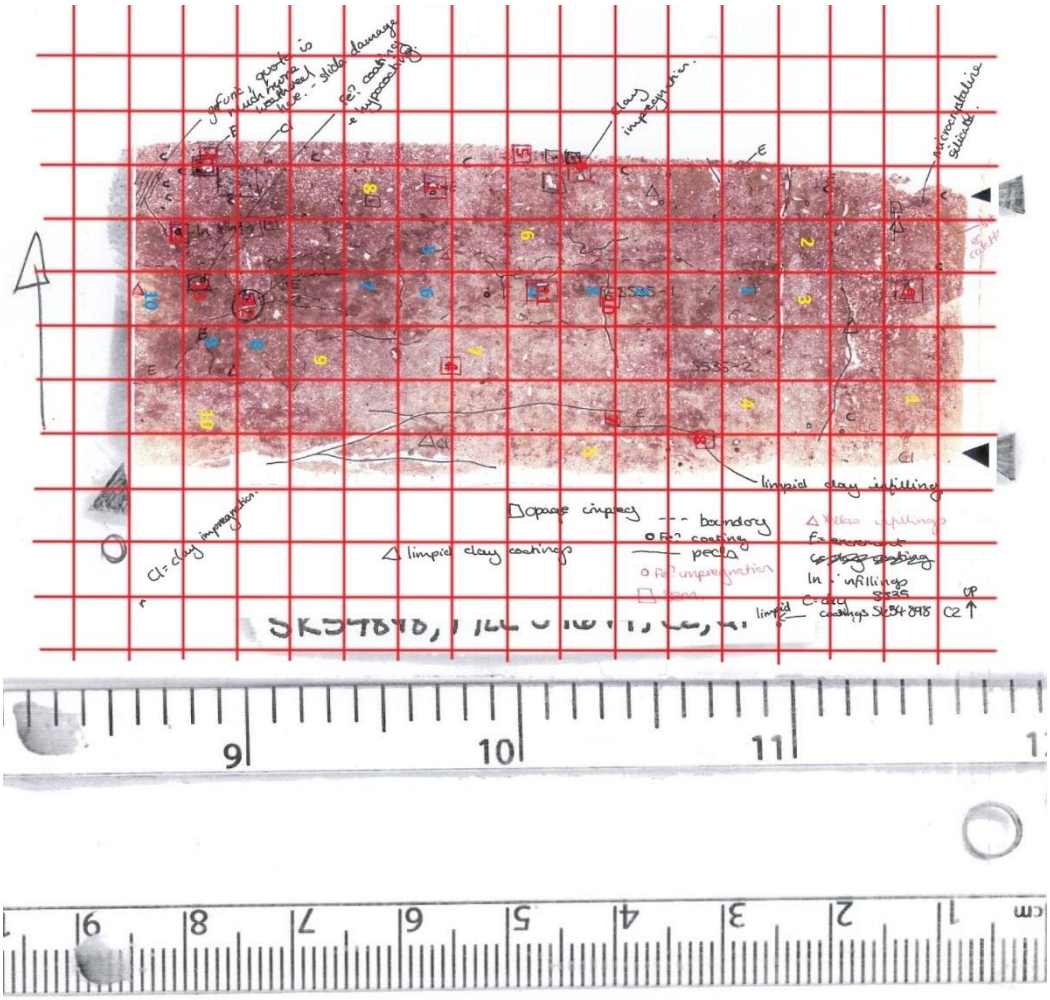

Figure 124: Annotated slide scan with overlaid grid of the C2 sample from SK54898.

1.1.4 Database Table Description

Table 72: Site table

Field name	Data type	Field description/rational
Site name	Text	The name of the site.
Site location	Text	The country in white the site is located.
Link to data file	Hyperlink	Link to where the data about it site is stored.

Table 73: Period table

Field name	Data type	Field description/rational
ID	AutoNumber	Used to generate a unique identifying number.
Site name	Text	Linked to site name field in the site table.
Period	Text	Linked to period in grave table.
Date range (YYYY-YYYY)	Text	Describes the date range given for each grave.

Table 74: Site code table

Field name	Data type	Field description/rational
Site name	Text	Name of the site which links to site table.
Site code	Text	Site code as written on the burial records.

Table 75: Grave table.

Filed name	Data type	Field description/rational
Grave ID	Text	The grave ID assigned to each grave on the site was retained and used as a unique identifier for the database. This was so that the grave information could be linked back to the onsite record and easily distinguished from other graves in the InterArChive project.
Site name	Text	Linked to site table.
Site code	Text	Linked to site code table.
Period	Text	This was used to date each grave.
Fill context number	Text	This was used to record the fill number which was the material which was being described micromorphologically.
Preservation	Text	Used to describe the degree of preservation in each grave using a drop down menu and three categories, ‘low, medium’ and ‘high’.
Link to data file	Hyperlink	Used to link the grave to the additional grave information stored on the computer.
Micromorphological interpretation	Memo	Used to add a general micromorphological interpretation of the grave if needed.

Table 76: Skeleton number

Field name	Data type	Field description/rational
ID	AutoNumber	Creates a unique identifying number for each skeleton.
Skeleton number	Text	Record of the skeleton number assigned to each skeleton as in the site record.
Grave ID	Text	Linked to Grave ID field in Grave Table, this was used to allow multiple skeletons to be linked to one grave.

Table 77: Slide information table

Field name	Data type	Field description/rational
Slide number	Number	Links each slide record with the unique identifying number given to each slide during processing. This is essential as it also links each slide to the larger InterArChive database.
Grave ID	Text	Links to Grave ID field in Grave Table.
Slide location	Drop down	Drop down menu of standard InterArChive sample locations.
Micromorphological summary	Memo	Summary of the overall micromorphological interpretation of the slide.
Micromorphological slide interpretation	Memo	Detailed micromorphological interpretation of the slide.
Link to file	Hyperlink	Link to folder on computer which holds relevant data.
PPL slide scan	Attachment	JPEG of PPL slide scan
XPL slide scan	Attachment	JPEG of XPL slide scan
Skeleton ID	Text	Link to the skeleton ID in the Skeleton number table.
Analysed	Yes/no	This was used to track slide analysis progress.
Orientation	Drop down	Drop down menu of the InterArChive slide orientations.

Table 78: Area information table

Field name	Data type	Field description/rational
Area number	Text	Each different fabric type observed within each slide was given a unique area number, that used the slide number as a prefix. This was so that each area could be described independently and easily linked back to the slide.
Soil microfabric number	Text	After micromorphological description the areas within all of the slides in a grave or site were grouped by common features, and each group was given a unique soil microfabric number. This meant that the frequency and spatial arrangement of microfabrics could be analysed on an intra grave and intra site basis.
Slide number	Number	The number that was given to each slide during processing was recorded and used a unique identifier to link slides and slide areas.
Micromorphological summary	Memo	This was used to summarise the micromorphological data obtained from each area.
Micromorphological description	Memo	A full description of each area type could be recorded here.
Attention	Yes/no	This field was used when there was features within the area which needed further study.
Notes	Memo	This field was used to write general notes or observations.
Link to file	Hyperlink	This field linked to the file on the computer which related to the area in question.
CF%	Text	Record of the CF% for each area studied.
CF limit µm	Text	The standard CF limit for the InterArChive project was agreed to be 50µm however it was also agreed that this could be modified where needed on a site by site basis, any modification to this was recorded here.
Sorting	Text	Slide sorting was recorded here according to Bullock *et al*(1985), using a drop down menu, as only one sorting type was permitted per area.
Vughy	Yes/no	The microstructure types were recorded using 'Yes/no' tick boxes. This was so that multiple microstructures could be recorded. These were bases on the microstructures as outlined in Stoops (2003). Tick boxes were used as opposed to a drop down menu so that each microstrucutre would be given its own field in the tables produced by Access which would make this data easier to search.
Spongy	Yes/no	
Channel	Yes/no	
Chamber	Yes/no	
Vesicular	Yes/no	
Crumb	Yes/no	
Granular	Yes/no	
Subangular	Yes/no	
Angular blocky	Yes/no	

Platy	Yes/no	
Lecticular	Yes/no	
Massive	Yes/no	
Complex	Yes/no	
Limpidity	Text	The limpidity was recorded using a drop down menu as only one limpidity was permitted per area. The limpidity types included all of those outlined in Stoops (2003) and an additional type 'masked' as outlined in Usai (1996)
Colour at 30µm in PPL	Text	The PPL, OIL and UV colour was recorded using a three colour system prefixed by either 'light, mid' or 'dark' followed by the secondary colour and then primary colour. The XPL inference colour was recorded using the method outlined in MacKenzie and Adams (2005)
Colour at 30µm in XPL	Text	
Colour at 30µm in OIL	Text	
Colour at 30µm in UV	Text	
Undifferentiated	Yes/no	The b-fabric was recorded using the terminology in Stoops (2003). Multiple types of b-fabric were allowed therefore 'yes/no' tick boxes were used to create easily searchable tables.
Crystalitic	Yes/no	
Stipple speckled	Yes/no	
Mosaic speckled	Yes/no	
Porostriated	Yes/no	
Granostriated	Yes/no	
Monostriated	Yes/no	
Parallel striated	Yes/no	
Cross striated	Yes/no	
Random striated	Yes/no	
Circular striated	Yes/no	
Concentric striated	Yes/no	
Crescent striated	Yes/no	
Monic	Yes/no	The coarse fine related distribution was recorded using the terminology found in Stoops (2003). Multiple types were allowed therefore 'yes/no' tick boxes were used to create easily searchable tables. The InterArChive protocol only used the main coarse fine related distribution types, porphyric, enaulic, monic, gefuric and chitonic, however this was considered too generic as the shrink swell capacity of the microfabric was not recorded by using the main types alone, therefore the subtypes were also included for the purposes of this thesis.
Fine monic	Yes/no	
Coarse monic	Yes/no	
Chitonic	Yes/no	
Gefuric	Yes/no	
Concave gefuric	Yes/no	
Convex gefuric	Yes/no	
Porphyric	Yes/no	
Close porphyric	Yes/no	
Single spaced porphyric	Yes/no	
Double spaced porphyric	Yes/no	
Open porphyric	Yes/no	
Close fine enaulic	Yes/no	
Single spaced fine enaulic	Yes/no	
Double spaced fine enaulic	Yes/no	
Single spaced fine enaulic	Yes/no	
Single spaced equal enaulic	Yes/no	
Double spaced equal enaulic	Yes/no	
Double spaced coarse enaulic	Yes/no	

Enaulic	Yes/no	

Table 79: Inorganic component table

Field name	Data type	Field description/rational
ID inorganic coarse material	AutoNumber	Used to create a unique identifying number for each inorganic component.
Area number	Text	Links each inorganic component to an area
Type	Drop down	Identifies the type of inorganic component either mineral or rock fragment, terminology which is taken from Stoops (2003).
Identification	Text	Identification of the component to mineral or rock fragment. The minerals were identified using standard techniques as outlined in MacKenzie and Adams (2005) and rock fragments were described using the recommended terminology in Stoops (2003).
2-50µm	Yes/no	Size categories were used to describe the size of the inorganic components. The categories were based on those used by Usai (1996). As multiple categories could be used 'yes/no' tick boxes were used to create easily searchable tables.
50-100µm	Yes/no	
100-200µm	Yes/no	
200-500µm	Yes/no	
500-1000µm	Yes/no	
1000-2000µm	Yes/no	
>2000µm	Yes/no	
Abundance	Drop down	The abundance was recorded using a drop down menu to create standardisation. The InterArChive project originally agreed to base the categories on size ranges, however upon initial analysis these were found to be too general and difficult to manipulate using a spreadsheet. The size ranges were therefore abandoned and absolute value categories were adopted.
Rounded	Yes/no	The angularity of inorganic components were recorded to the major subdivisions found in Stoops (2003), as this was considered to be a sufficient level of detail. These were recorded using 'yes/no' tick boxes so more than one field could be selected and so that easily searchable tables could be created.
Subrounded	Yes/no	
Subangular	Yes/no	
Angular	Yes/no	
Weathering	Drop down	Weathering categories were based on those used by Usai (1996). A drop down menu was created as only one category was used per component type.
Colour at 30µm in PPL	Text	The colour was recorded according to standard mineral and rock fragment description techniques as outlined in
Colour at 30µm in XPL	Text	
Colour at 30µm in OIL	Text	

Colour at 30µm in UV	Text	MacKenzie and Adams (2005).
Basic distribution pattern	Text	The basic and referred distribution and orientation patterns observed in the inorganic material were recorded using the terminology outlined in Stoops (2003). The referral object was also identified.
Basic orientation pattern	Text	
Referred distribution pattern	Text	
Referred orientation pattern	Text	
Referral object	Text	
Notes	Memo	This field was used for any additional notes for each inorganic component.

Table 80: organic component table

Field name	Data type	Field description/rational
ID organic coarse material	AutoNumber	Used to create a unique identifying number for each inorganic component.
Area number	Text	Links each organic component to an area
Type	Drop down	Identifies the type of organic component.
Identification	Text	Identification of the component to species if possible.
2-50µm	Yes/no	Size categories were used to describe the size of the inorganic components. The categories were based on those used by Usai (1996). As multiple categories could be used 'yes/no' tick boxes were used to create easily searchable tables.
50-100µm	Yes/no	
100-200µm	Yes/no	
200-500µm	Yes/no	
500-1000µm	Yes/no	
1000-2000µm	Yes/no	
>2000µm	Yes/no	
Abundance	Drop down	The abundance was recorded using a drop down menu to create standardisation. The InterArChive project originally agreed to base the categories on size ranges, however upon initial analysis these were found to be too general and difficult to manipulate using a spreadsheet. The size ranges were therefore abandoned and absolute value categories were adopted.
Rounded	Yes/no	The angularity of inorganic components w ere recorded to the major subdivisions found in Stoops (2003), as this was considered to be a sufficient level of detail. These were recorded using 'yes/no' tick boxes so more than one field could be selected and so that easily searchable tables could be created.
Subrounded	Yes/no	
Subangular	Yes/no	
Angular	Yes/no	
Weathering	Drop down	Weathering categories were based on those used by Usai (1996). A drop down menu was created as only one category was used per component type.
Colour at 30µm in PPL	Text	The PPL, OIL and UV colour was recorded using a three colour system prefixed by either 'light, mid' or 'dark' followed by the
Colour at 30µm in XPL	Text	
Colour at 30µm in OIL	Text	

Colour at 30µm in UV	Text	secondary colour and then primary colour. The XPL inference colour was recorded using the method outlined in MacKenzie and Adams (2005)
Basic distribution pattern	Text	The basic and referred distribution and orientation patterns observed in the inorganic material were recorded using the terminology outlined in Stoops (2003). The referral object was also identified.
Basic orientation pattern	Text	
Referred distribution pattern	Text	
Referred orientation pattern	Text	
Referral object	Text	
Notes	Memo	This field was used for any additional notes for each inorganic component.

Table 81: Ped table

Field name	Data type	Field description/rational
ID ped	AutoNumber	Used to create a unique identifying number for each ped.
Area number	Text	Used to link the peds to specific areas.
Ped type	Drop down	Used to describe peds using the types as described in Stoops (2003)
Ultrafine	Yes/no	The ped sizes were described by using the size ranges and terminology as described in Bullock *et al*(1985). This was done to create a more standard measurement that made the size ranges between peds comparable.
Very fine	Yes/no	
Fine	Yes/no	
Medium	Yes/no	
Coarse	Yes/no	
Very coarse	Yes/no	
Abundance %	Text	The abundance was recorded using a drop down menu to create standardisation. The InterArChive project originally agreed to base the categories on size ranges, however upon initial analysis these were found to be too general and difficult to manipulate using a spreadsheet. The size ranges were therefore abandoned and absolute value categories were adopted.
Accommodation	Drop down	This was used to describe the degree to which the faces of the peds can be fitted together. The three standard degree of accommodation as outlined in Stoops (2003) were used. In each case only one degree of accommodation was selected and where multiple were present the most abundant was used.
Development	Drop down	Development was used to describe how well separated the peds were or had been (in the case were voids has subsequently been infilled). The three standard degree of development as outlined in Stoops (2003) were used. In each case only one degree of accommodation was selected and where multiple were present the most abundant was used.
Referred orientation	Text	The referred orientation of the peds was recorded according to the terminology in Stoops (2003).
Referred object	Drop down	The referral object was recorded using a drop down menu as either the ground surface or the body.
Notes	Memo	This field was used for any additional notes relating to the ped that had been described.

Table 82: Pedofeature table

Field name	Data type	Field description/rational
ID pedofeatures	AutoNumber	Creates a unique identifying number for each pedofeature.
Area number	Text	Links the pedofeature to the area.
Type	Drop down	Identifies the type of pedofeature using the standard terminology in Stoops (2003)
Subtype	Text	Identifies the subtype of pedofeature using the standard terminology in Stoops (2003)
Composition	Text	Identifies what the pedofeature is composed of where possible. This may also be added after SEM analysis has been conducted.
Attribute	Text	Used to describe any additional attributes which were not covered in the type or subtype categories.
Colour at 30µm in PPL	Text	The PPL, OIL and UV colour was recorded using a three colour system prefixed by either 'light, mid' or 'dark' followed by the secondary colour and then primary colour. The XPL inference colour was recorded using the method outlined in MacKenzie and Adams (2005)
Colour at 30µm in XPL	Text	
Colour at 30µm in OIL	Text	
Colour at 30µm in UV	Text	
Abundance %	Drop down	The abundance was recorded using a drop down menu to create standardisation. The InterArChive project originally agreed to base the categories on size ranges, however upon initial analysis these were found to be too general and difficult to manipulate using a spreadsheet. The size ranges were therefore abandoned and absolute value categories were adopted.
<10µm	Yes/no	Three standardised size ranges were used to describe the size of pedofeatures. These size ranges were adopted from Usai (1996).
10-150µm	Yes/no	
>150µm	Yes/no	
Basic distribution pattern	Text	The basic and referred distribution and orientation patterns observed in the pedofeatures were recorded using the terminology outlined in Stoops (2003). The referral object was also identified.
Basic orientation pattern	Text	
Referred distribution pattern	Text	
Referred orientation pattern	Text	
Referral object	Text	
Notes	Memo	This field was used to store any additional notes related to the pedofeature.

Table 83: Void table

Field name	Data type	Field description/rational
ID voids	AutoNumber	Generates a unique number for each void type by area.
Void type	Drop down	Used to identify voids, using the terminology in Stoops (2003)
Area number	Text	Linked each void to its area within the slide.
<40µm	Yes/no	Size categories were used to describe the size of voids. The categories were based on those used by Usai (1996). As multiple categories could be used 'yes/no' tick boxes were used to create easily searchable tables.
40-300µm	Yes/no	
300-500µm	Yes/no	
500-1000µm	Yes/no	
1000-2000µm	Yes/no	
2000-5000µm	Yes/no	
5000-10000µm	Yes/no	
Abundance %	Drop down	The abundance was recorded using a drop down menu to create standardisation. The InterArChive project originally agreed to base the categories on size ranges, however upon initial analysis these were found to be too general and difficult to manipulate using a spreadsheet. The size ranges were therefore abandoned and absolute value categories were adopted.
Basic distribution pattern	Text	The basic and referred distribution and orientation patterns observed in the voids were recorded using the terminology outlined in Stoops (2003). The referral object was also identified.
Referred distribution pattern	Text	
Basic orientation pattern	Text	
Referred orientation pattern	Text	
Referral object	Text	
Notes	Memo	This field was used to store any additional information that related to the void populations that has been described.

1.1.5 Image analysis

Previous studies have used image analysis to describe the macro pore structure of soils (Moran *et al.*, 1988, Murphy *et al.*, 1977, Ringrose-Voase & Bullock, 1984) and more recently link micromorphological and field colour descriptions (Adderley et al., 2002). However a universal methodology has yet to be developed, for either technique, due to rapid technological advancement and the need for specialist technology. In this thesis image analysis was used to produce quantitative data void space.

The use of image analysis to describe the pore structure relies on isolating the pore space from all other soil elements. Two methods were suggested for motorised, none rotary stage microscopes (Figure 125 and Figure 126). Both methods were run on a small area mosaic from the C1 sample from Çatalhöyük the results of which are shown in Table 84.

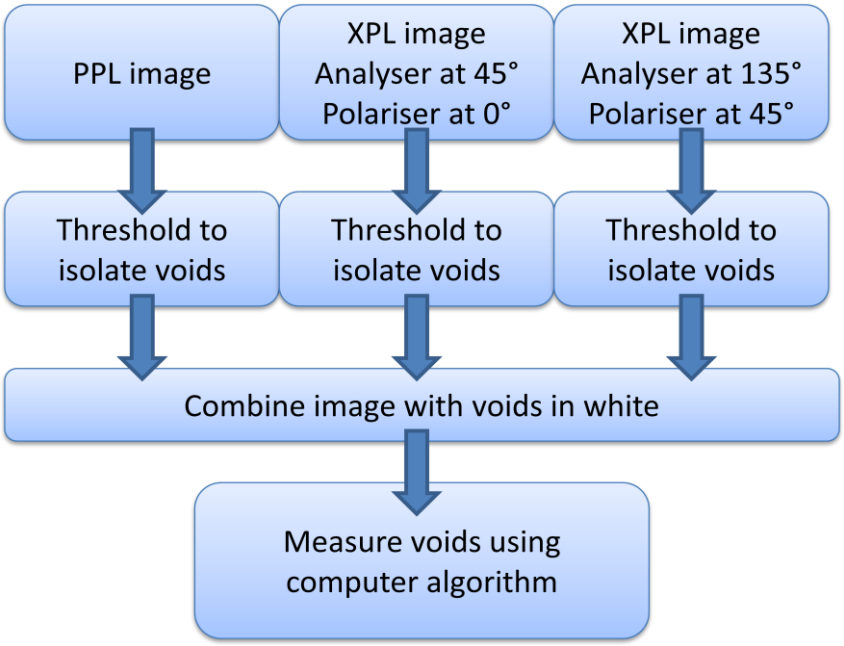

Figure 125: Image analysis method developed by Williams at York University.

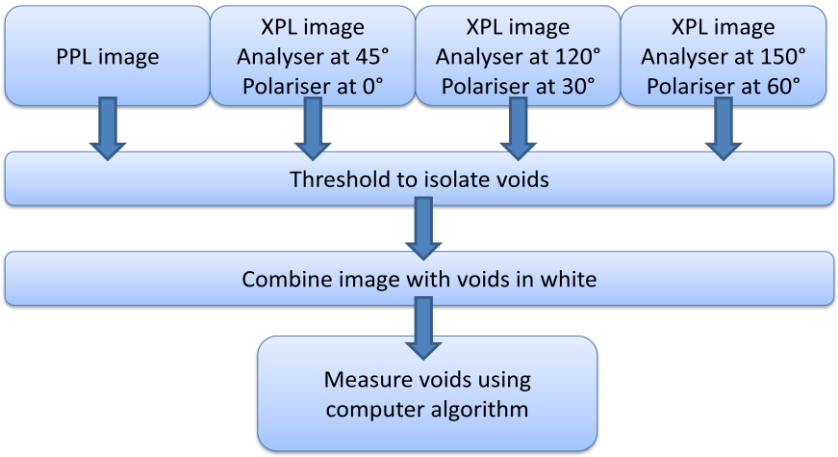

Figure 126: Image analysis method developed by Wilson at Stirling University.

Table 84: Image analysis of voids using the Williams and Wilson methodologies

Method	Number of regions	Area percent	Area in μm^2
York (fig 1)	1164	12.9	12454860.55
Stirling (fig 2)	1133	12.71	12262720.33

There are slight differences in void area percent between the methods which equate to 0.19%. This difference is marginal and therefore, as the method in Figure 125 requires fewer images to be captured, this method will be applied.

1.1.6 SEM-EDX validation

The SEM-EDX data was utilised to;

- Characterise the inorganic geochemical signature of the fine material for each microfabric and slide.
- Map inorganic geochemical change in the fine material of the slide moving away from the body.
- Identify the inorganic geochemical composition of soil features.

For points one and two a methodology needed to be developed and tested to establish the optimum number of sample points to characterise the fine material (excluding pedofeatures and coarse material). As soil is highly variable it was crucial to establish the level of variability across the slide and minimise its effect on the results. To this end a 5x5 mm grid was laid across the slide and five observations were taken in 10 grid squares selected by a random number generator. Wide variation was present in the inorganic geochemical composition of micromorphologically similar fine material (Figure 127 and Figure 128), indicating that to obtain a representative signature several observation points across the slide should be utilised. To establish the optimum number of sampling points per grid square the average of 1, 2, 3, 4 and 5 points per square (n = 10, 20, 30, 40 and 50 respectively) were calculated (Figure 129 and Figure 130). As expected most elements had a wide standard error, probably caused by the high variability in the soil (Figure 127 and Figure 128), that narrowed slightly as more samples were obtained. The wide variability in the data would suggest that presenting gross average values would build in large margins of error therefore alternative analytical methods were explored. Principle Component Analysis (PCA) was selected as the most appropriate method as PCA was designed to evaluate variation in large data sets and group variables together. In the case of the inorganic geochemical data, PCA identified which elements were varying and grouped elements into components according to the nature of their variation. When the components were plotted along the x and y axis this gave a visual representation of the variation in the form of a data cloud, maintaining the integrity of the data by omitting gross averages. Data clouds could then be compared and variation, as described by the components, used to infer inorganic geochemical differences between samples.

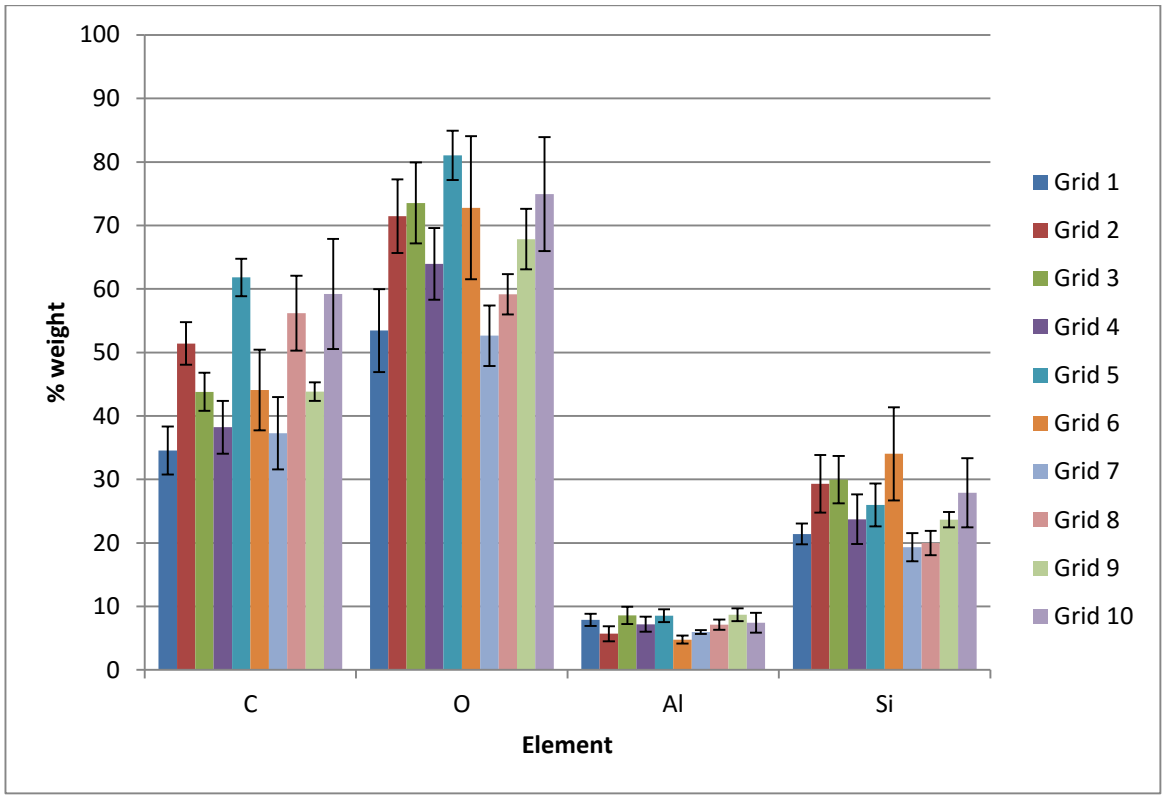

Figure 127: Means and standard error for C, O, Al and Si from Hungate SK51387 foot sample taken from the fine material.

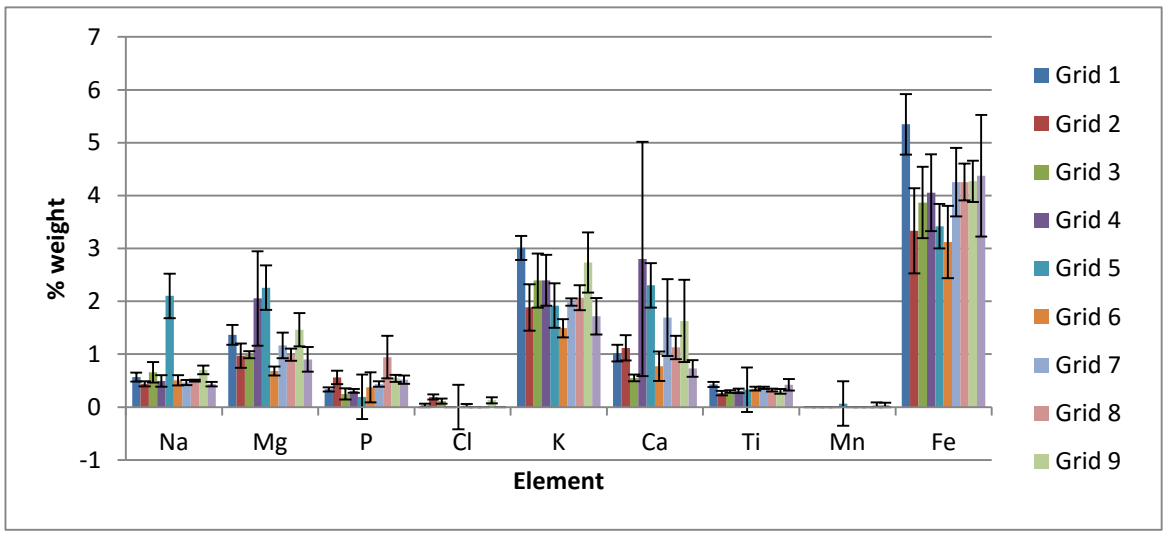

Figure 128: Means and standard error for Na, P, S, Cl, K, Ca, Ti, Mn and Fe from Hungate SK51387 foot sample taken from the fine material.

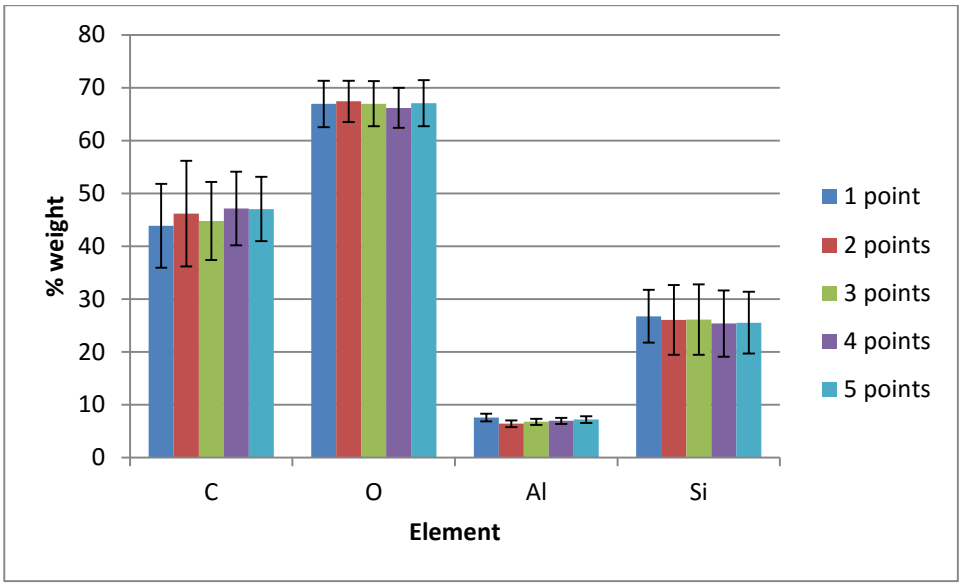

Figure 129: Means and standard error for C, O, Al and Si from Hungate SK51387 foot sample taken from the fine material.

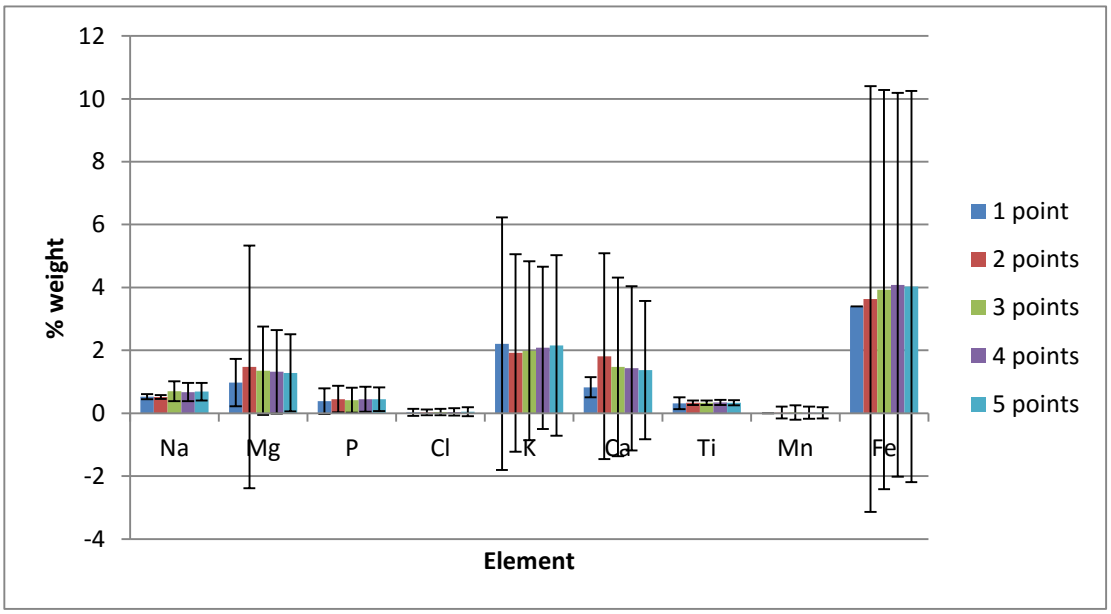

Figure 130: Means and standard error for Na, Mg, P, S, Cl, K, Ca, Ti, Mn and Fe from Hungate SK51387 foot sample taken from the fine material.

2 Chapter 3 Appendix: Soil Microfabrics

2.1 Soil microfabric description summaries

2.1.1 Çatalhöyük microfabric description summaries

2.1.1.1 CH1 White monic material

Soil micromorphology: Well to perfectly sorted homogeneous material, with sporadic examples of micro laminations.

Structure and voids*:* Angular, sub-angular blocky peds and granules were present. Ped development ranges from high to weakly developed. The microfabric was present as embedded aggregates. Voids included small (<300µm) planes and channels at between 5-10% abundance.

C:F ratio*:* 10:90% or less coarse material

Fine material*:* Pale grey white to pale yellow grey in PPL with a crystalitic to undifferentiated b-fabric in XPL. C:F related distribution was monic with some porphyric and enaulic areas present.

Coarse material*:* The coarse fraction ranged from partly to unweathered with sporadic instances of weathered grains. Grains were mostly angular to sub-angular. Quartz abundance ranged from <1-5% and varied in size between 2-500µm. Other minerals, present at low abundances (<1-2%), included carbonates, phyllosilicates, inosilica based rock fragments, tectosillicates and sulphates. Minor coarse material ranged from 2-1000µm.

Pedofeatures**:** high percentages of typic coatings (=/<40%) and impregnations (=/<10%). Other pedofeatures included typic nodules (5%), internal quasicoatings (2%) and internal and typic hypocoatings, excrements (2%) and impregnations (2%).

Organic coarse components*:* Organic coarse components were sporadic (<1-2%) and consisted of bone and shell fragments, charcoal and some plant material.

Inorganic geochemistry given in weight % using SEM:EDX*:* C=42%, O=58%, Mg=1%, Al=5%, Si=13%, K=1%, Ca=14%, Mn=2%, Fe=3%.

2.1.1.2 CH2 White material with plant voids

Soil micromorphology*:* Moderately sorted homogeneous material.

Structure and voids*:* Apedal with abundant (40%) compound packing voids and lower levels (2-5%) planes, channels and vughs.

C:F ratio*:* 10:90% or less coarse material.

Fine material*:* Pale white grey in colour in PPL with stipple speckled to crystalitic b-fabric in XPL and a porphyric C:F related distribution.

***Coarse material**:* The coarse fraction ranges from weathered to not weathered. Grains were mostly angular to sub-angular with sporadic instances of rounded and sub-rounded grains. Coarse grain size ranged from 2-500µm. Quartz was present at the highest abundance at between 1-5% with lower levels (<1-2%) of phyllosilicates, carbonates, tectosilicates and sulphates.

***Pedofeatures*:** Pedofeatures were sporadic with infillings (10%), impregnations (2%) and nodules (2%) present.

***Organic coarse components**:* Organic coarse material was rare with low levels of fragmented bone (2%) and charcoal (<1-5%). All fragments of organic coarse components ranged between 100-500µm and were angular to sub-angular. The organic coarse component fraction was also weathered.

Inorganic geochemistry given in weight % using SEM:EDX: C=48%, O=58%, Mg=1%, Al=5%, Si=15%, K=1%, Ca=10%, Mn=2% and Fe=3%.

2.1.1.3 CH3 Orange monic material

***Soil micromorphology**:* Perfectly sorted homogeneous material.

Structure and voids: Highly to weakly developed angular blocky, sub-angular blocky and granular peds with low levels of voids consisting of planes (<1-2%) and channels (5%) present.

C:F ratio: 1:99.

Fine material: Mid yellow in PPL with a stipple speckled, undifferentiated or mosaic speckled b-fabric in XPL and a monic C:F related distribution.

***Coarse material**:* The coarse fraction ranges from partly weathered to unweathered with a grain size from 2-200µm. There were few minerals present with quartz being the most abundant at <1-5% and sulphates present at low quantities (2%).

***Pedofeatures*:** There were few pedofeatures with strong opaque impregnations (2-10%), sporadic coatings (<1%), and opaque nodules, which were sometimes clustered present (<1-2%).

Organic coarse components: Organic coarse components were rare and ranged in size from 2-200µm. They consisted of charcoal and plant material (2%).

Inorganic geochemistry given in weight % using SEM:EDX: C=43%, O=61%, Na=1%, Mg=1%, Al=7%, Si=19%, K=2%, Ca=6%, Ti=1%, Mn=1%, Fe=4%.

2.1.1.4 CH4 Heterogeneous white/yellow material

Soil micromorphology: Heterogeneous material that ranges from perfectly sorted to unsorted.

Structure and voids: Highly variable structure with apedal soils, moderately developed crumbs, strong to weakly developed granules and sub-angular blocky peds. The nature of the void space

ranged from channels (<1-5%), packing voids (10-80%), planes (2-20%) and low abundances of vughs (2-5%).

C:F ratio: Variable C:F ratio between 10:90 and 30:70.

Fine material: Mid brown grey to pale grey yellow colour in PPL with b-fabrics which included undifferentiated, crystalitic, stipple speckled and mosaic speckled. C:F related distributions were mainly porphyric with some enaulic and chitonic material in places.

Coarse material: The coarse material was composed of weathered to fresh grains between 2-2000µm in size with sporadic instances of grains above 2000µm. Grains were mainly angular with some instances of sub-angular and rounded grains. Quartz was most abundant and ranged from <1-20%. Other coarse material were present at low quantities (<5%) and included phyllosilicates, carbonates, tectosilicates, sulphates and inosilica based rock fragments.

***Pedofeatures*:** Pedofeatures consist of typic/external hypocoatings (<1) typic and crystalitic coatings (2-1%). strong opaque, red and orange impregnations and nodules (<1-10%) and sporadic intercalations (2%). Coprolitic material is also present sporadically and at low quantities (<1-5%), as well as sporadic interactions (<1-2%) and infillings (<1-2%).

Organic coarse components*:* Coarse organic components were varied and sporadic and varied in size from 2-2000µm. The majority of organic components were weathered or partly weathered. They consisted of low abundances (<1-2%) of fragmented bone and shell with slightly raised levels (<1-10%) charcoal. Plant material (<1-10%) and phytoliths (2-5%) were also present but sporadic.

Inorganic geochemistry given in weight % using SEM:EDX: C=58%, O=60%, Na=1%, Mg=1%, Al=5%, Si=16%, P=1%, K=1%, Ca=7% and Fe=3%.

2.1.1.5 CH5 White plaster with large amounts of plane material

Soil micromorphology*:* Moderately to poorly sorted heterogeneous material.

Structure and voids: Variable structure with apedal soils and strongly developed sub-angular blocky and granular peds. Void space was variable with high levels of compound packing voids (90%), vughs (40%) and low abundances (2-5%) of channels, planes and vughs.

C:F ratio: C:F ratios range from 10:90% to 30:70%

Fine material: The fine material is mid yellow brown in colour in PPL with a stipple speckled b-fabric in XPL. C:F related distributions were mainly porphyric with some enaulic areas.

Coarse material: The coarse material ranges from weathered to not weathered, the majority of which was angular to sub-angular with sporadic instances of rounded grains present. The coarse material was mainly quartz grains (<1-30%) which ranged from 2-1000µm with low abundances (2%) of carbonates with ranges from 50-100µm.

***Pedofeatures*:** Pedofeatures were rare and consisted of sporadic dusty clay coatings (<1%) with higher levels (10%) of typic opaque to brown nodules.

Organic coarse components: Organic coarse components were weathered and generally angular. The organic coarse components ranged from plant material (10%) that are 100-200µm in size and charcoal (10-30%) that are between 2-500µm in size.

***Inorganic geochemistry given in weight % using SEM:EDX**:* C=70%, O=63%, Na=1%, Mg=1%, Al=5%, Si=18%, P=2%, K=2%, Ca=6%, Fe=2% and F=3%.

2.1.1.6 CH6 Burnt material

***Soil micromorphology**:* Moderately sorted homogeneous material

***Structure and voids**:* The structure showed little variation with the microfabric containing apedal material and the fragments of microfabric composed of strongly developed granules. Voids were sporadic and consisted of low levels (<1%) or planes and channels.

C:F ratio: 10:90

Fine material: The fine material was opaque to dark brown black in PPL and isotropic in XPL with a porphyric C:F related distribution.

Coarse material: The coarse material ranges from weathered to not weathered and the grains are generally angular with some sub-angular and sub-rounded grains present. Grain size varied from 2-200µm. Coarse material was dominated by quartz (<1-40%) and carbonates at 2%.

***Pedofeatures*:** There are no pedofeatures present.

***Organic coarse components**:* Organic components consisted of weathered angular charcoal fragments (20%)

***Inorganic geochemistry given in weight % using SEM:EDX**:* C=44%, O=61%, Na=1%, Mg=1%, Al=6%, Si=19%, K=2%, Ca=9%, Mn=3% and Fe=3%.

2.1.2 Thessaloniki microfabric summaries

2.1.2.1 Ti1

Soil micromorphology: Unsorted to poorly sorted heterogeneous material.

***Structure and voids**:* The structure of the microfabric is variable with areas of apedal soils, strongly to moderately developed crumbs, moderately developed plates and weakly to strongly developed sub-angular blocky peds. Void space varied from channels (<2-20%), complex packing voids (2-30%), planes (<2-20%) and vughs (<2-20%).

C:F ratio: C:F ratio varied from 10:90% to 40:60%.

***Fine material**:* The fine material is dark yellow brown to pale orange brown in PPL and 1st order brown, yellow and orange in XPL with a crystalitic, stipple/mosaic speckled, grano/mono/parallel and cross striated b-fabric in XPL. The C:F related distribution present in this microfabric was mainly porphyric with chitonic, gefuric and enaulic areas.

***Coarse material**:* The coarse fraction ranged from weathered to not weathered and is composed of rounded to angular grains. The size of grains ranges from 2-2000µm with sporadic grains over 2000µm. The coarse material was mainly composed of quartz (2-20%), with small amounts (<2-5%) of carbonates, tectosilicates, nesosilicas, phyllosilicates and unidentified rock and mineral grains.

***Pedofeatures*:** Pedofeatures consisted of a wide range of coatings (<2-10%) which varied from being composed of carbonates, iron, silt and clay. Fabric pedofeatures composed of clay and impure clay at between <2-5% abundance. Hypocoatings are also widespread at between <2-10% and composed of a wide variety of material including carbonates, iron and manganese. Weak to strong impregnations are present at between <2-10% again they were composed of a wide range of material including carbonates, iron and manganese, and organic material. Continuous dense and loose infillings are present at low abundances (<2-5%) as are intercalations. There are a wide variety of anorthic, disorthic and typic nodules, which range from opaque to carbonate based and are present at <2-10%. Quasicoatings and intercalations were also present but were sporadic in nature.

Organic coarse components: Organic coarse components were fragmented and ranged from 2-2000µm and between not weathered and weathered. The organic coarse components were generally angular but also included sub-angular, sub-rounded and rounded examples. Bone fragments were present at between <2-20%, shell and charcoal were both present at low abundances (<2%).

***Inorganic geochemistry given in weight % using SEM:EDX**:* C=58%, O=58%, Na=1%, Mg=2%, Al=5%, Si=18%, K=1%, Ca=3% and Fe=4%.

2.1.2.2 Ti2 Calcareous material

Soil micromorphology: The soil micromorphology varies from unsorted to moderately sorted and was generally heterogeneous.

Structure and voids: The structure of the microfabric contained apedal soils with strongly developed sub-angular blocky peds. The void space is mostly composed of vughs (<2-20%) with smaller more consistent abundances (<2-5%) of channels and planes.

C:F ratio: There is some variation in the C:F ratio from 10:90% to 30:70%.

***Fine material**:* The fine material is pale grey white in PPL and low order in XPL with a crystalitic b-fabric. C:F related distribution is composed of porphyric material.

Coarse material: The coarse fraction ranges from weathered to not weathered with the majority of grains being angular with sporadic instances of rounded, sub-rounded and sub-angular grains. The size of grains ranges from 2-500µm. Quartz is the most abundant coarse component at between 2-10%. Other coarse components are present at low abundances (<2-5%) and include carbonates, phyllosilicates and tectosilicates.

***Pedofeatures*:** Typic coatings are present (<2-10%) and composed of carbonates, iron, dusty and impure clay. Anorthic and disorthic nodules are present at low abundances (2-5%) and were opaque composed of iron and manganese. Infillings, impregnations and hypocoatings were also present but were sporadic.

***Organic coarse components**:* Organic coarse components were sporadic and consisted only of fragmented, weathered and partly weathered bone. These were at low abundances (2-5%), rounded to sub-rounded and ranges in size from 100-500µm.

***Inorganic geochemistry given in weight % using SEM:EDX**:* C=25%, O=60%, Na=1%, Mg=1%, Al=2%, Si=10%, Ca=27% and Fe=2%.

2.1.3 Heslington East microfabric summaries

2.1.3.1 HE1

***Soil micromorphology**:* Heterogeneous microfabric which is moderately sorted.

Structure and voids: There is some variation in the structure of the microfabric with apedal soils present as well as moderately to strongly developed plates and weakly to strongly developed sub-angular blocks. Void space ranged in nature from channels (<2-10%), complex packing voids (2-10%), planes (<2-5%), simple packing voids (2-5%) and vughs (<2-30%)

***C:F ratio**:* There was a high level of coarse material present in this microfabric and the C:F ratio ranged from 60:40% to 80:20%.

***Fine material**:* The fine material was dark orange brown to mid yellow orange in PPL. In XPL the fine material is 1st order orange to yellow with a b-fabric that includes undifferentiated, stipple/mosaic speckled and poro/grano striated areas. The C:F related distribution pattern was dominated by porphyric material with chitonic, gefuric and enaulic patterns also present.

Coarse material: The coarse fraction ranges from weathered to not weathered and is generally composed of angular grains with some instances of rounded to sub-angular grains. The size of the coarse fraction ranges from 2-500µm and is mostly composed of quartz grains (2-10%). Other

coarse material was present in small quantities (2-5%) and consisted of carbonates, and phyllosilicates.

***Pedofeatures*:** Pedofeatures consisted of typic coatings which were composed of limpid clay, dusty clay and iron some of which were micolaminated (<2-5%). Strong to moderate opaque impregnations were also present at between <1-20% abundance. Anorthic and disorthic nodules (<2-10%) were opaque to mid red and orange in colour. Impregnations, hypocoatings, fabric pedofeatures and excrement were also present but sporadic.

Organic coarse components: Organic components were fragmented and ranged from partly weathered to weathered. The majority of organic coarse components were angular with some instances of rounded and sub-angular examples. The size of organic coarse components ranges from 2-2000µm. Organic components were composed of fragmented bone and wood as well as roots.

2.1.4 Hungate microfabric summaries

2.1.4.1 HU1

***Soil micromorphology**:* This microfabric is composed of perfectly to poorly sorted homogenous material.

***Structure and voids**:* The structure of the microfabric shows some variation with apedal soils, strongly to weakly developed sub-angular blocks and strongly developed crumbs present. Void space is generally low and variable in nature. Voids include channels (<1-5%), planes (<1-10%) and vughs at between 2-10%.

***C:F ratio**:* The coarse fine ratio varied slightly from 0:100% to 20:80%.

Fine material: The fine material has a slight variation in colour from mid orange brown to pale yellow orange in PPL, although slide thickness may account for some of this variation. The fine material was clouded in appearance. In XPL the colour varied from 1st order brown to 1st order orange and yellow, with small areas of undifferentiated soil. The fabric was mostly undifferentiated in XPL with some stipple speckled, cross, grano and random striated b-fabrics apparent. The C:F related distribution pattern is porphyric with some monic material.

Coarse material: The coarse fraction ranges from weathered to not weathered, rounded to angular grains. The size of grains also varies with the majority of grains between 2-2000µn. Coarse material abundance is low and is dominated by quartz at between 2-30% with sporadic examples of silica based rock fragments (2%) and lead (5-20).

***Pedofeatures*:** Pedofeatures consisted of typic clay, impure clay and unsorted coatings (<1-2%), weak to strong opaque to mid yellow red impregnations (<1-10%), simple and serrated intercalations (2-5%), opaque anorthic and typic nodules (<1-10%) and sporadic infillings (5%), hypocoatings (1-10%), fabric (20%) and depletion pedofeatures (2-30%).

***Organic coarse components**:* Organic coarse components are rare and composed of not weathered to weathered charcoal (<1-10%). The charcoal is fragmented and ranges in size from 2-1000µm.

Inorganic geochemistry given in weight % using SEM:EDX: C=64%, O=42%, Na=<1%, Mg=1%, Al=5%, Si=11%, P=1%, K=1%, Ca=<1%, Fe=3%, Pb=3%, Ti=<1%.

2.1.4.2 HU2

***Soil micromorphology**:* HU2 appeared as a linear arrangement of moderately to well sorted heterogeneous coarse material.

***Structure and voids**:* Structurally the microfabric was apedal throughout with complex packing voids at around 5% abundance.

***C:F ratio**:* 70:30% to 95:5%

***Fine material**:* The fine material was pale orange yellow to pale white yellow in PPL and 1st order orange in XPL with a dotted to clouded limpidity. The b-fabric ranged from stipple speckled to mosaic and granostriated. The C:F related distribution is porphyric.

Coarse material: The coarse material consists of partly weathered, sub-rounded to angular quartz grains between 2-200µm in size. The abundance of quartz grains ranges from 70-100%.

***Pedofeatures*:** There are no pedofeatures present.

Organic coarse components: Organic coarse components are fragmented and consist of weathered angular charcoal ranging from 50-100µm at 10% abundance.

***Inorganic geochemistry given in weight % using SEM:EDX**:* C=56%, O=54%, Mg=1%, Al=5%, Si=20%, K=1%, Fe=2%

2.1.4.3 HU3

***Soil micromorphology**:* This fabric as a heterogeneous and well sorted.

***Structure and voids**:* There is some variation in the structure of the microfabric with apedal material present as well as strongly developed angular to sub-angular blocky and platy peds all of which are strongly developed. These are internal to the microfabric. The microfabric itself is present as moderately developed crumbs embedded in the groundmass of other more abundant fabric types. Voids are sparse and consist of planes (<1-2%) and vughs (5%).

***C:F ratio**:* 2:98%

***Fine material**:* The fine material ranges in colour in PPL from mid orange brown to pale white yellow. It has a limpid to clouded and dotted appearance. In XPL the fine material ranges in colour from undifferentiated red, perhaps due to variations in iron staining, to 1st order yellow. The b-fabric varies from areas of stipple speckled, monostriated, parallel striated and cross striated. The C:F related distribution pattern ranged from porphyric to monic.

***Coarse material**:* The coarse material ranges from weathered to not weathered sub-rounded and angular grains of quartz (<1-2%) with the occasional phyllosilicate grain (2%). The size of the coarse fraction ranges from 2-200µm.

***Pedofeatures*:** Impregnations are present at between 2-5% ranging from weak to strong and in colour from opaque to mid orange red suggesting an iron component to them. Dark orthic and anorthic nodules are also present (5-10%), as are sporadic quasicoatings (5%), limpid clay typic coatings (5%), fabric pedofeatures (5%) and intercalations (5%).

Organic coarse components: Organic coarse components are fragmented and weathered. They are present as angular inclusions of plant material and charcoal ranging from 2- 500µm.

***Inorganic geochemistry given in weight % using SEM:EDX**:* C=59%, O=47%, Mg=2%, Al=6%, Si=13%, K=2%, Ca=1%, Fe=3%, Pb=1%

2.1.5 HU4 (water laid clay)

***Soil micromorphology**:* Heterogeneous microfabric which is perfectly to well sorted in most context but has some areas which are poorly sorted.

***Structure and voids**:* There is variation in the structure of this microfabric with areas of apedal soils and ped formation. The peds consist of strongly developed angular blocky and sub-angular blocky peds, plates and crumbs as well as moderately developed sub-angular blocky peds. Void space is low (<1-2%) and consists of channels, planes and vughs, although in some areas the abundance of vughs and planes reaches 10%.

***C:F ratio**:* The C:F ratio ranges from 1:99% to 20:80%.

***Fine material**:* The fine material colour ranges from dark orange red to mid yellow brown in PPL with an opaque, clouded or limpid limpidity. In XPL the birefengence colour varies from 1st order red and orange to 1st order yellow with areas of undifferentiated, stipple speckled, mosaic speckled, cross and ransom striated b-fabric. The C:F related distribution pattern is porphyric with areas of monic material.

Coarse material: The coarse material present ranges from not weathered to weathered and rounded to angular. The size of coarse components varies between 2-500µm. The coarse material itself is composed of quartz grains (<1-60%) as well as silicate based rock fragments (<1-2%), mica (<1%) and carbonates (2%).

***Pedofeatures*:** There are several different coatings present in the microfabric which consist of typic dusty, impure and limpid clay, as well as dusty clay pendant coatings (>1-5%). Dark red to red brown quasicoatings are also present (<1-5%). Anorthic and orthic nodules and present (2-10%) and composed of mid brown red to mid yellow material. There are sporadic examples of excrements (<1%) and limpid clay infillings (2%). Fabric pedofeatures are widespread and consist of mid orange brown material which could be Fe as well as quartz grains (10-40%) as are intercalations (5-40%).

***Organic coarse components**:* Organic components consist of unweathered fragmented charcoal that is rounded to angular in appearance. The charcoal ranges in size from 2-500µm and is present at <1%.

Inorganic geochemistry given in weight % using SEM:EDX: C=57%, O=67%, Mg=1%, Al=10%, Si=26%, K=3%, Fe=5%

2.1.6 HU5

***Soil micromorphology**:* A heterogeneous microfabric which is unsorted to poorly sorted.

***Structure and voids**:* The structure of this microfabric is composed of strongly developed crumbs and moderately to strongly developed sub-angular blocky peds. Void space consists of planes (10-20%) and vughs (5-60%).

***C:F ratio**:* Varies between 20:80% and 60:40%

***Fine material**:* The fine material is dark orange to opaque in PPL with a limpid, opaque or clouded limpidity. The birefringence colour of the fine material was undifferentiated brown/orange in places to 1st order yellow/orange and brown and isotropic. The b-fabric ranged from undifferentiated with some stipple speckling and porostriations The C:F related distribution pattern is mainly porphyric with some enaulic.

***Coarse material**:* The coarse fraction ranges from weathered to unweathered grains of rounded to angular material. There was also a wide variation in grain size from 2-2000µm and some examples over 2000µm. The coarse material consists of high levels of quartz (10-50%) and lower levels of carbonates (<1%) and silica based rock fragments (2%).

***Pedofeatures*:** Pedofeatures consisted of mid orange to opaque orthic and anorthic nodules (<1%), typic limpid clay coatings (2%), instances of quartz and infillings (2%), simple intercalations

(<1) as well as sporadic fabric pedofeatures (40%) and calcite worm granules (<1%). Strong impregnations are present (<1%) and consist of dark red material.

***Organic coarse components**:* Organic components are fragmented and ranged from weathered to not weathered. There were mainly angular in shape with some rounded to sub-angular examples. There is also a wide variation in size from between 2-2000µm. The organic coarse components consist of bone (<1%), charcoal (10%) and shell (<1%).

***Inorganic geochemistry given in weight % using SEM:EDX**:* C=51%, O=60%, Na=1%, Mg=1%, Al=7%, Si=22%, K=2%, Ca=1%, Fe=4%

2.1.7 HU6

***Soil micromorphology**:* This microfabric is homogenous and perfectly sorted.

***Structure and voids**:* The microfabric structure consists of apedal soils and strongly developed platy peds. The void space has a low abundance at 2% and consist of interpedal planes.

***C:F ratio**:* 0:100%

***Fine material**:* The fine material is mid orange to mid yellow brown in PPL. In XPL the fine material is 1st order yellow with some random striations and undifferentiated areas. The C:F related distribution in monic throughout.

***Coarse material**:* There is no coarse material present.

***Pedofeatures*:** Intercalations are wide spread in some areas of the microfabric (70%) where as fabric pedofeatures and hypocoatings were more sporadic (2-5%).

***Organic coarse components**:* None present.

Inorganic geochemistry given in weight % using SEM:EDX: C=63%, O=43%, Mg=1%, Al=6%, Si=10%, K=1%, Ca=1%, Fe=3%

2.1.8 HU7 (Bone)

***Soil micromorphology**:* Heterogeneous microfabric that is moderately sorted.

***Structure and voids**:* The microfabric has an apedal structure with high levels of planes (10%) and vughs (30%)

***C:F ratio**:* 60:40%

***Fine material**:* The colour of the fine material is mid orange brown in PPL with a clouded limpidity. In XPL the fine material has a 1st order yellow birefringence colour with a stipple speckled b-fabric.

***Coarse material**:* The coarse material ranges from weathered to not weathered and consists of sub-angular to angular grains of quartz (10%) and tectosilicates (<1%). The size of coarse material ranges from 50-200µm.

***Pedofeatures*:** Coatings are the dominate pedofeature and consist of pendant/fragmented impure clay (5%), typic dusty clay (20%) and typic opaque coatings (2%). Infillings are also common and composed of dusty clay (20%). Impregnations are strong and composed of opaque material possibly iron with some spheralitic features (2%).

***Organic coarse components**:* Organic components are overwhelmingly composed of weathered bone (40%) with some weathered, angular fragments of charcoal (2%) that range is size from 100-200µm.

2.1.9 HU8 (Bioturbation)

***Soil micromorphology**:* Heterogeneous microfabric that is poorly sorted.

***Structure and voids**:* The structure of this microfabric is composed of areas of apedal soils along with weakly developed crumbs and sub-angular blocky peds. Void spaces shows some diversity with channels (2-5%), planes (<1-5%) and vughs (<1-20%) present.

***C:F ratio**:* There is a high degree of variation in the C:F ratio that ranges from 20:80% to 60:40%.

***Fine material**:* The colour of the fine material in PPL ranged from light brown grey to mid orange brown with a clouded limpidity. In XPL the birefringence colour is 1st order yellow with stipple speckled, grano-, cross- and random striations. The C:F related distribution patter is mainly porphyric with sporadic areas of monic material.

***Coarse material**:* The coarse material ranges from not weathered to weathered, rounded to angular grains of quartz (20-60%), silicate rock fragments (<1-5%), tectosilicates (<1%), phyllosilicas (<1%) and vivianite (<1%). The size of the coarse fraction ranges from 2-500µm.

Pedofeatures: Typic coatings that are composed of limpid and dusty clay as well as dark coloured material are present at between <1-20% abundance. Hypocoatings of opaque material as well as dark brown red in colour are present at between <1-5% abundance. Strong opaque to mid yellow impregnations are visible (<1-10%) as are simple impure clay intercalations (2%), and anorthic and disorthic nodules (<1-5%). Loose discontinuous and continuous infillings composed of quartz grains and dusty clay are very common at between <1-80%.

***Organic coarse components**:* Organic coarse components are primarily fragmented charcoal (<1-5%) with sporadic fungal schlorocha (<1%). The charcoal ranges between weathered and unweathered and is angular. The size of organic coarse components ranges from 2-500µm.

***Inorganic geochemistry given in weight % using SEM:EDX**:* C=58%, O=68%, Mg=1%, Al=8%, Si=26%, K=2%, Fe=4%

2.1.10 HU9

***Soil micromorphology**:* This is a poorly sorted heterogeneous microfabric.

***Structure and voids**:* The structure of the microfabric consists of weakly to strongly developed sub-angular blocky peds with low abundances of planes (<1-5%) and vughs (10%).

***C:F ratio**:* Varies slightly from 70:60% to 60:40%.

***Fine material**:* The fine material is mid red orange to mid yellow orange in PPL with a clouded limpidity

***Coarse material**:* The course material consists of weathered to unweathered grains of rounded to angular quartz (ranging in size from 2-200µm).

***Pedofeatures*:** There are few pedofeatures in this microfabric and those that are present consist of dark orange brown to mid brown yellow impure and dusty coatings (2%), mid orange red impregnations (1%), mid yellow intercalations (1%) and mid black grey to mid orange red nodules (1-5%).

***Organic coarse components**:* Organic components consist of weathered and fragmented angular charcoal that ranges in size from 2-1000µm and in abundance from 10-40%.

Inorganic geochemistry given in weight % using SEM:EDX: C=72%, O=51%, Mg=2%, Al=6%, Si=14%, K=2%, Ca=1%, Fe=3%

2.1.11 HU10

***Soil micromorphology**:* This microfabric is heterogeneous and poorly to well sorted in appearance.

***Structure and voids**:* The structure of this microfabric is generally apedal with some areas of moderate crumbs and weakly to strongly developed sub-angular blocky peds. Void space consists of low abundances (<1-5%) of channels and planes and high abundances (10-40%) of simple packing voids and vughs.

***C:F ratio**:* There is some variation in the C:F ratio from 40:60% to 70:30%.

***Fine material**:* In PPL the fine material is dark brown orange to mid orange brown with a clouded limpidity. In XPL the fine material is first order orange to yellow with some areas that are undifferentiated. The b-fabric also shows some variation with undifferentiated material, stipple speckling, mosaic speckling, porostriations, granostriations and random striations visible. The C:F related distribution includes chitonic, gefuric and porphyric areas.

***Coarse material**:* The coarse material varies from weathered to not weathered and is generally angular in shape with some examples of sounded, sub-rounded and sub-angular grains. The size

of coarse material ranges from 2-1000µm and is composed of quartz (40-70%), silica based rock fragments (<1-2%), tectosilicas (<1%), and secondary phosphate minerals (2%).

Pedofeatures: Typic, pendant and fragmented coatings are present and composed of limpid, impure and dusty clay as well as amorphous dark material. Coatings are present at between <1-5% abundance. Hypocoatings are also present in HU10 at between <1-5% abundance. They are composed of similar materials to the coatings. Fabric pedofeatures are uncommon and not present in all examples of HU10 but can be seen in the form of passage features at between 2-10%. Strong impregnations are present (<1-10%), as well as anorthic nodules (<1-2%) and are composed of opaque material as well as limpid clay. Simple intercalations were also observed (10%).

Organic coarse components*:* Organic components are generally fragmented and vary in condition between weathered and not weathered. The fragments are generally angular with some rounded, sub-rounded and sub-angular examples. Organic component size varies from 2-500µm and consist of bone (<1-2%), spherulites (<1-5%) and charcoal (<1-10%).

Inorganic geochemistry given in weight % using SEM:EDX*:* C=75%, O=68%, Na=1%, Al=6%, Si=27%, K=2%, Fe=3%

2.1.12 HU11

Soil micromorphology*:* This is a heterogeneous poorly to moderately sorted microfabric.

Structure and voids*:* The structure of the microfabric is composed of strongly developed plates as well as areas of apedal soils. Voids range from channels (2%), planes (<1-5%) and vughs (2-5%).

C:F ratio*:* There is some variation in the C:F ratio between 10:90% and 30:70%.

Fine material*:* The colour of the fine material is mid orange brown to yellow in PPL with a clouded limpidity. In XPL the fine material is 1st order orange to yellow with a stipple speckled, granostiated or random striated b-fabric. The C:F related distribution pattern is porphyric throughout.

Coarse material*:* The coarse material ranges from weathered to not weathered sub-rounded to angular grains of quartz (10-30%) and silica based rock fragments (<1%). Grain size ranges from 2-500µm.

Pedofeatures**:** Pedofeatures consist of impure clay typic coatings (<1-5%), impure clay and dark typic hypocoatings (<1-5%), strong clay impregnations (10%), dense continuous limpid clay impregnations (20%) as well as dark disorthic nodules (10%).

Organic coarse components*:* The coarse organic material varies in condition between weathered and not weathered angular to sub-angular fragments of charcoal (<1%). The size of the organic coarse components range from 2-50µm.

Inorganic geochemistry given in weight % using SEM:EDX: C=49%, O=60%, Mg=1%, Al=8%, Si=23%, K=2%, Ti=1%, Fe=5%

2.1.13 HU12

Soil micromorphology*:* Heterogeneous microfabric which is poorly to well sorted.

Structure and voids*:* The structure ranges from weakly to strongly developed sub-angular blocky peds, strongly developed granules/crumbs, and moderately developed plates to apedal soils. Voids consist of channels (<1-10%), planes (1-10%) and vughs (<1-20%).

C:F ratio*:* 2:98% to 50:50%

Fine material*:* The fine material is dark brown orange to mid yellow orange in PPL with an opaque to clouded limpidity. In XPL the fine material is 1st order yellow and orange to undifferentiated red with an undifferentiated, stipple speckled, poro-, grano-, parallel and cross-striated b-fabric. The C:F related distribution pattern is mainly porphyric with sporadic chitonic, monic and gefuric areas.

Coarse material: The coarse fraction varies from not weathered to partly weathered and is mainly sub-angular to angler in nature. There are however some sporadic rounded and sub-rounded grains. The size of coarse material ranges from 2-1000µm, with the majority of quartz grains below 200µm. Coarse material consists of quartz (10-50%) and silica based rock fragments (2%) as well as secondary phosphate minerals (2%), phyllosilicas (<1%) and tectosilicas (<1%).

Pedofeatures**:** Weak to strong impregnations are present at varying quantities (<1-50%). These are dark brown black/opaque to limpid yellow in PPL. There are sporadic opaque anorthic nodules (<1-2%) as well as typic clay, and dark brown red/typic coatings (<1-5%), some coatings are also composed of spherulites. Porous microaggregated excrements are present at <1% as well as small amounts of quasicoatings (<1-20%). Limpid yellow/dusty clay and quartz infillings are present (<1-10%) as well as dusty and dark amorphous material clay hypocoatings (<1-20%). Simple intercalations consist of limpid clay, carbonates, dark amorphous material and spherulites (<1-5%)

Organic coarse components*:* Weathered to unweathered fragments of charcoal are present in HU12. These range from 2-500µm in size and <1-5% in abundance, with one example of very high concentrations of charcoal at 40%. The shape of the fragments are mostly angular with some rounded to sub-rounded examples.

Inorganic geochemistry given in weight % using SEM:EDX: C=49%, O=63%, Na=1%, Mg=1%, Al=8%, Si=24%, K=2%, Fe=4%

2.1.14 HU13

Soil micromorphology*:* Heterogeneous microfabric that ranges from unsorted to well sorted in appearance.

Structure and voids*:* The microfabric has a large amount of variation within it and the structure of the microfabric varies from areas of apedal soils to strongly developed crumb peds, strongly to moderatly developed granules, weakly to strongly developed platy peds and weakly to strongly developed sub-angular blocky peds. The void structure is composed of channels (<1-10%), sporadic compound, simple and complex packing voids that range from 2-20% when they are present and one instance of compound packing voids present at 80%, planes (1-20%) and vughs that generally range from <1-40%.

C:F ratio*:* C:F ratio is high but shows a high degree of variation from 30:70% to 90:10%

Fine material*:* The fine material ranges in colour from dark brown orange to pale yellow brown in PPL with an opaque, limpid or clouded limpidity. In XPL the birefringence colour is first order orange to sporadic areas of undifferentiated material. The b-fabric is mainly stipple speckled with areas of undifferentiated material, mosaic speckling, porostriations, granostriations, cross striation, random striations and one instance of circular striations. The C:F related distribution is mainly porphyric with areas of gefuric, chitonic and monic material.

Coarse material*:* The coarse fraction ranges from not weathered to weathered in appearance with rounded to angular grains present. Grain size ranges from 2-2000µm with sporadic examples above 2000µm and the majority of quartz grains below 500µm. The coarse fraction in HU13 is dominated by quartz (10-90%) with silica based rock fragments (<1-20%), tectosilicates (<1%), phyllosilicas (<1%), nesosilicas (<1%) and secondary phosphate minerals (<1-2%).

Pedofeatures**:** Coating present in the microfabric included both typic and pendant coatings that are composed of limpid, impure and dusty clay, excrement, spherulites, carbonates and both dark coloured and light yellow material. Coatings range in abundance from <1-10%. Hypocoatings are generally typic or external in nature and are composed of similar material to the coating described above. They are present at low levels between <1-10%. Excremental pedofeatures are present but are generally uncommon and not observed in all examples of the microfabric (<1-2%). Fabric pedofeatures are composed of both sand grains and impure clay and are present mostly in low quantities (<1-5%) with sporadic examples of them being present at between 10-20% abundance. Weak to strong dark coloured and limpid to impure clay impregnations are common

and present at between <1-5% with levels as high at 20% in some microfabrics. There are several different types of infillings present from dense incomplete and complete examples which are composed of clays and loose discontinuous examples composed of quartz grains. There are also rare examples of passage features. Infillings are present at between <1-20%. With one exceptional case at 60%. Intercalations are also present although not in all examples of HU13. They range in abundance from <1-30% although those at the lower abundances are more common. They tend to be composed of different impure, limpid or dusty clay and at times dark red amorphous material. Anorthic, orthic and disorthic nodules are widespread and present in most examples of HU13. They are generally composed of dark amorphous material or carbonates. They range in abundance from <1-10%. Quasicoatings are present sporadically and composed of dark amorphous material at <1-2% abundance.

Organic coarse components*:* Organic coarse components are fragmented and are generally angular in shape however there are examples of rounded to sub-angular organic coarse components. The size of the organic coarse components range from 2-2000µm. The organic coarse components include weathered, partly weathered and unweathered examples. Bone is present between <1-5%, fungal schlarocha at <1%, spherulites at <1-2%, charcoal is the most common organic coarse component and ranges in abundance from at <1-10%.

Inorganic geochemistry given in weight % using SEM:EDX*:* C=56%, O=63%, Mg=1%, Si=25%, K=2%, Fe=3%

3 Chapter 5 Appendix:

3.1 Abundance of inorganic coarse material at Hungate

Table 85: The percentage of sample area composed of different mineral and rock fragments by sample location and overall coarse material abundance at Hungate, as well as the C:F related distributions present in each slide. Percentages are rounded to whole numbers. '*' indicate trace abundances (<0.5%).

Grave	Location	Orientation	Quartz	Silicate	Phyllosilicate	Tectosilicates	Nesosilicates	Carbonates	Unknown	Spherulites	Secondary phosphate mineral	Lead	Total	C:F Related Distribution	Enaulic	Monic	Chitonic	Gefuric	Porphyric
C1	C1	NA	70	10	1	0	0	0	0	0	0	0	81						✓
		NA	66	1	0	1	0	0	1	0	0	0	69						✓
		NA	64	10	0	0	0	0	0	0	*	0	74						✓
SK54898	C2	NA	64	2	1	0	0	0	0	0	0	0	67					✓	✓
	C3	NA	23	1	0	0	0	0	12	0	*	4	40			✓			✓
	Skull	Para	3	1	*	0	0	0	0	0	0	0	4			✓			✓
		Perp	12	0	0	0	0	0	0	0	0	0	12			✓			✓
	Pelvis	Para	2	0	0	0	0	0	1	0	*	9	12			✓			✓
		Perp	2	10	0	0	0	0	0	0	0	8	20			✓			✓
	Other	Perp	21	0	0	0	0	0	0	0	0	0	21			✓			✓

Table 85: Continued

Grave	Location	Orientation	Quartz	Silicate	Phyllosilicate	Tectosilicates	Nesosilicates	Carbonates	Unknown	Spherulites	Secondary phosphate mineral	Lead	Total	C:F Related Distribution	Enaulic	Monic	Chitonic	Gefuric	Porphyric
SK51326	C2	NA	70	1	0	0	0	0	0	0	0	0	71					✓	✓
	C3	NA	70	0	1	0	0	0	0	*	0	0	71						✓
		NA	90	2	1	1	0	0	0	0	0	0	94						✓
	Skull	Perp	70	11	1	1	0	0	1	0	*	0	84						✓
	Pelvis	Para	70	1	2	1	0	1	0	0	0	0	75				✓		✓
		Perp	89	1	8	1	0	0	0	*	0	0	99					✓	✓
	Feet	Para	90	2	1	0	0	0	3	0	0	0	96						✓
		Perp	90	1	0	1	0	0	0	*	0	0	92						✓
SK51387	C3	NA	41	4	0	0	0	1	1	0	0	0	47		✓				✓
	Skull	Perp	24	2	0	0	0	1	0	0	0	0	27						✓
	Pelvis	Para	40	11	0	0	0	1	2	0	0	0	54						✓
		Perp	1	1	0	0	0	0	1	0	0	0	3						✓
	Feet	Para	1	3	0	1	0	2	0	0	0	0	7						✓
		Perp	41	9	0	0	0	2	2	0	0	0	54						✓

Table 85: Continued

Grave	Location	Orientation	Quartz	Silicate	Phyllosilicate	Tectosilicate	Nesosilicate	Carbonates	Unknown	Spherulites	Secondary phosphate mineral	Lead	Total	C:F Related Distribution	Enaulic	Monic	Chitonic	Gefuric	Porphyric
SK51351	Skull	Para	60	1	0	1	0	0	0	*	0	0	62					✓	✓
		Perp	70	1	1	0	0	0	0	*	0	0	72					✓	
	Pelvis	NA	70	3	1	0	0	0	0	*	*	0	74				✓	✓	
	Feet	Para	70	2	1	2	0	0	0	*	*	0	75					✓	✓
		Perp	73	1	1	2	0	0	0	*	*	0	77						✓
	Other	Para	60	2	0	0	0	0	0	*	*	0	62					✓	✓
		Perp	65	1	*	0	0	0	0	0	0	0	66				✓	✓	✓
SK54090	C3	NA	6	3	0	1	0	0	0	0	0	0	10				✓		✓
	Skull	Para	45	5	0	0	0	0	0	0	0	0	50			✓			✓
		Perp	50	10	1	0	0	0	0	0	0	0	61				✓		✓
	Pelvis	Para	54	5	0	0	0	0	0	0	0	0	59			✓	✓		✓
		Perp	36	20	1	0	0	0	0	0	0	0	57			✓			✓
SK54085	C3	NA	46	3	0	1	1	0	0	0	0	0	51				✓		✓
	Skull	Para	1	1	1	1	0	0	0	0	0	0	4				✓		✓
		Perp	30	50	1	2	0	0	0	0	0	0	83						✓
	Pelvis	Para	35	1	1	8	0	0	0	0	0	0	45						✓
		Perp	60	2	0	0	0	0	0	0	0	0	62			✓			✓

Table 85: Continued

Grave	Location	Orientation	Quartz	Silicate	Phyllosilicate	Tectosilicates	Nesosilicates	Carbonates	Unknown	Spherulites	Secondary phosphate mineral	Lead	Total	C:F Related Distribution	Enaulic	Monic	Chitonic	Gefuric	Porphyric
SK54341	C3	NA	37	0	1	1	0	0	1	*	*	0	40						✓
	Skull	Para	52	0	1	1	0	0	0	0	0	0	54						✓
		Perp	51	0	0	0	0	0	0	0	0	0	51						✓
	Pelvis	Para	64	2	1	0	0	0	0	0	0	0	67						✓
		Perp	45	1	0	1	0	0	0	0	0	0	47						✓
	Feet	Para	60	5	3	1	0	0	0	0	0	0	69			✓			✓
		Perp	60	0	0	0	0	0	0	0	0	0	60			✓			✓
	Other	Para	53	0	0	0	0	0	0	0	0	0	53						✓
		Perp	33	0	*	0	0	0	0	0	0	0	33						✓
SK54342	C3	NA	32	1	1	1	0	0	0	0	0	0	35			✓			✓
	Skull	Para	56	2	0	1	0	0	0	0	0	0	59			✓	✓	✓	✓
		Perp	37	2	1	0	0	0	0	0	0	0	40			✓			✓
	Pelvis	Para	41	1	0	0	0	0	2	*	0	0	45			✓			✓
		Perp	25	0	0	0	0	2	0	*	0	0	27			✓			✓
	Feet	Para	25	0	0	0	0	0	0	0	0	0	25			✓			✓
		Perp	30	0	0	0	0	0	0	0	0	0	30						✓

Table 85: Continued

Grave	Location	Orientation	Quartz	Silicate	Phyllosilicate	Tectosilicates	Nesosilicates	Carbonates	Unknown	Spherulites	Secondary phosphate mineral	Lead	Total	C:F Related Distribution	Enaulic	Monic	Chitonic	Gefuric	Porphyric
SK54908	C2	NA	56	0	0	0	0	0	0	0	0	0	56				✓	✓	✓
	Skull	Perp	60	1	1	0	0	0	0	0	0	0	62						✓
	Pelvis	Para	35	1	1	1	0	0	0	0	0	0	38						✓
		Perp	56	1	1	1	0	0	0	0	*	0	59						✓
	Feet	Para	44	1	0	0	0	0	0	0	0	0	45						✓
		Perp	55	5	1	0	0	0	0	0	0	0	61						✓
SK51350	C2	NA	40	10	1	1	0	0	0	0	0	0	52					✓	✓
	C3	NA	50	0	1	1	0	0	0	*	0	0	52				✓	✓	✓
	Skull	Para	70	2	1	0	0	0	0	0	0	0	73				✓	✓	✓
	Pelvis	NA	50	2	1	2	0	0	0	*	0	0	55				✓	✓	✓
	Feet	NA	52	1	0	*	0	0	0	*	0	0	53						✓

4 Chapter 8 Appendix

4.1 Hungate Iron and Manganese Pedofeatures

Table 86: The presence of manganese and iron pedofeatures at Hungate.

Grave			C1	C1	C1	SK54898						
Position			Upper	Middle	Lower	C2	C3	Skull		Pelvis		Other
Orientation			-	-	-	-	-	Perp	Para	Perp	Para	Perp
Nodules	Anorthic	Mn										
		Fe	0.8			0.2	14.5		1.15		0.4	1
		Mn/Fe		1			0.9	0.3			0.2	
	Orthic	Mn										
		Fe								0.9		
		Mn/Fe										
	Disorthic	Mn										
		Fe	0.6		0.2				4.5			
		Mn/Fe			5.6							1.8
	Aggregated	Mn										
		Fe					1.3					
		Mn/Fe										
Coating	Coating	Mn										
		Fe	3		0.6	0.9	1				1.7	1.8
		Mn/Fe				0.8						
	Pendant	Mn										
		Fe										
		Mn/Fe										
	Hypocoating	Mn										
		Fe					1.7			4.05	0.9	1
		Mn/Fe			0.6		0.3				2	3
	Quasicoating	Mn										
		Fe						1.5				
		Mn/Fe				2.5						
Impregnation		Mn										
		Fe	0.8	0.5		6.1	2	3.7	17.4	5.35	9.8	10.7
		Mn/Fe	2	2.5	0.5	1	1.2				0.8	3.6
Infillings		Mn										
		Fe	4	0.4		1.5						
		Mn/Fe										
Intercaltions		Mn										
		Fe						1.5		8.15		
		Mn/Fe	1									
Depleations		Mn										
		Fe						2				0.5
		Mn/Fe										

Table 86 cont.

Grave			SK51326						
Position			C2	C3	Skull	Pelvis		Foot	
Orientation			-	-	Perp	Perp	Para	Perp	Para
Nodules	Anorthic	Mn							
		Fe	6			0.2	1.95	4	1.65
		Mn/Fe	0.6	2.5	1	0.3			
	Orthic	Mn							
		Fe							
		Mn/Fe						2.75	
	Disorthic	Mn							
		Fe							1.1
		Mn/Fe		0.8					
	Aggregated	Mn							
		Fe							
		Mn/Fe							
Coating	Coating	Mn							
		Fe			1	0.1	0.6	0.5	
		Mn/Fe	1.2	4.8	5		1.1	3.6	1
	Pendant	Mn							
		Fe							
		Mn/Fe			0.5				
	Hypocoating	Mn							
		Fe				0.2			
		Mn/Fe				0.15			
	Quasicoating	Mn							
		Fe							
		Mn/Fe							
Impregnation		Mn							
		Fe	1.2			0.15	1		0.8
		Mn/Fe	0.1	4.1	6	0.2		0.3	
Infillings		Mn							
		Fe						0.2	
		Mn/Fe							
Intercaltions		Mn							
		Fe				0.1			
		Mn/Fe							
Depleations		Mn							
		Fe							
		Mn/Fe							

Table 86 cont.

Grave			SK51387					
Position			C3	Skull	Pelvis		Foot	
Orientation			-	Perp	Perp	Para	Perp	Para
Nodules	Anorthic	Mn						
		Fe	2.9	1.4	1.4	2	1	1
		Mn/Fe		2		2		1
	Orthic	Mn						
		Fe	11					
		Mn/Fe						
	Disorthic	Mn						
		Fe						
		Mn/Fe						
	Aggregated	Mn						
		Fe						
		Mn/Fe						
Coating	Coating	Mn						
		Fe						
		Mn/Fe			1.9			
	Pendant	Mn						
		Fe	1					
		Mn/Fe						
	Hypocoating	Mn						
		Fe	2	1.9	1.8			0.8
		Mn/Fe					0.7	1
	Quasicoating	Mn						
		Fe				9		
		Mn/Fe	2					
Impregnation		Mn						
		Fe	3.4		5.3		1.8	2.25
		Mn/Fe	20	1.7		0.7	0.85	
Infillings		Mn						
		Fe		0.8		1.8		
		Mn/Fe						
Intercaltions		Mn						
		Fe	2	0.8				
		Mn/Fe						
Depleations		Mn						
		Fe						
		Mn/Fe						

Table 86 cont.

Grave			SK51351						
Position			Skull		Pelvis	Foot		Other	
Orientation			Perp	Para	Para	Perp	Para	Perp	Para
Nodules	Anorthic	Mn							
		Fe	1	1		0.9	4	0.7	1.6
		Mn/Fe	0.4	1.8	3			0.9	
	Orthic	Mn							
		Fe							1.6
		Mn/Fe							
	Disorthic	Mn							
		Fe				1			1
		Mn/Fe						1	
	Aggregated	Mn							
		Fe							
		Mn/Fe							
Coating	Coating	Mn							
		Fe	0.4	1	0.8				2
		Mn/Fe							
	Pendant	Mn							
		Fe							
		Mn/Fe							
	Hypocoating	Mn							
		Fe				0.9			
		Mn/Fe							
	Quasicoating	Mn							
		Fe							
		Mn/Fe							
Impregnation		Mn							
		Fe	0.4	1		2	2	9.9	1
		Mn/Fe					1	1.8	
Infillings		Mn							
		Fe		1	1.8				1.8
		Mn/Fe							
Intercaltions		Mn							
		Fe							
		Mn/Fe							
Depleations		Mn							
		Fe							
		Mn/Fe							

Table 86 cont

Grave			SK54090					SK51350				
Position			C3	Skull		Pelvis		C2	C3	Skull	Pelvis	Foot
Orientation			-	Perp	Para	Perp	Para	-	-	Para	Perp	Perp
Nodules	Anorthic	Mn										
		Fe	5	0.9					0.1	1		
		Mn/Fe		5		0.7	3	1				
	Orthic	Mn										
		Fe					1.8					
		Mn/Fe			0.7							
	Disorthic	Mn										
		Fe			1.8							
		Mn/Fe										
	Aggregated	Mn										
		Fe										
		Mn/Fe										
Coating	Coating	Mn				1.6						
		Fe	5	6.3		10	7.5	0.2				0.1
		Mn/Fe			21.4							
	Pendant	Mn										
		Fe										0.1
		Mn/Fe										
	Hypocoating	Mn										
		Fe	5.5	3.5		2.3	1	0.2				
		Mn/Fe			2		8.5					
	Quasicoating	Mn										
		Fe				2				2		
		Mn/Fe										
Impregnation		Mn										
		Fe	1		0.7	10	1.2	1	0.2	1	3.5	1.6
		Mn/Fe	4.5	0.9	1	14.5	1					
Infillings		Mn										
		Fe			2		2	0.4		0.9		
		Mn/Fe										
Intercaltions		Mn										
		Fe				1	0.9		0.3			
		Mn/Fe										
Depleations		Mn										
		Fe			2							
		Mn/Fe										

Table 86 cont

Grave			54341								
Position			C3	Skull		Pelvis		Foot		Other	
Orientation			-	Perp	Para	Perp	Para	Perp	Para	Perp	Para
Nodules	Anorthic	Mn									
		Fe				1			1		2.5
		Mn/Fe	3.5				3.1				
	Orthic	Mn									
		Fe	4.25				1	0.75			
		Mn/Fe	5.4		0.5						
	Disorthic	Mn									
		Fe				0.3					
		Mn/Fe									
	Aggregated	Mn									
		Fe									
		Mn/Fe			0.8						
Coating	Coating	Mn									
		Fe		2.15			1.8		1		1
		Mn/Fe	0.9							1	2
	Pendant	Mn									
		Fe		1	0.2						
		Mn/Fe	6	0.7							
	Hypocoating	Mn		1							
		Fe		6.9	0.8			1	1.8	4	3.4
		Mn/Fe	29.4		2.6	2	1.9				
	Quasicoating	Mn									
		Fe									1.2
		Mn/Fe									2
Impregnation		Mn									
		Fe	9.2		0.8		1.4				2
		Mn/Fe	1.6		1				0.2		
Infillings		Mn			2						
		Fe	0.8		2.4					2	
		Mn/Fe									
Intercaltions		Mn									
		Fe			1.8		0.9				2
		Mn/Fe									0.9
Depleations		Mn									
		Fe									
		Mn/Fe									

Table 86 cont

Grave			SK54342							
Position			C2	C3	Skull		Pelvis		Foot	
Orientation			-	-	Perp	Para	Perp	Para	Perp	Para
Nodules	Anorthic	Mn								
		Fe					3			1
		Mn/Fe			0.6			1.8	0.9	4.6
	Orthic	Mn								
		Fe		0.9					1.4	
		Mn/Fe		1.8	2			1.3		
	Disorthic	Mn								
		Fe								
		Mn/Fe								
	Aggregated	Mn								
		Fe								
		Mn/Fe								
Coating	Coating	Mn								
		Fe		0.9		1				
		Mn/Fe								
	Pendant	Mn								
		Fe								
		Mn/Fe								
	Hypocoating	Mn								
		Fe		0.4		0.8	0.5		0.7	3.7
		Mn/Fe							10	
	Quasicoating	Mn								
		Fe					1			
		Mn/Fe			2		0.9			
Impregnation		Mn								
		Fe		2.8		4		0.8		1.8
		Mn/Fe		1	12	1		6.6	10.8	2.15
Infillings		Mn								
		Fe		1.8				1.6		
		Mn/Fe								
Intercaltions		Mn								
		Fe		1.8						
		Mn/Fe								
Depleations		Mn								
		Fe								0.9
		Mn/Fe								

Table 86 cont

Grave			SK54908						SK54085				
Position			C2	Skull	Pelvis		Foot		C3	Skull		Pelvis	
Orientation			-	Perp	Perp	Para	Perp	Para	-	Perp	Para	Perp	Para
Nodules	Anorthic	Mn											
		Fe	0.1	0.4	1.25	2		0.3	9		2.9	2	
		Mn/Fe	3.5								0.9		1
	Orthic	Mn						0.4					
		Fe			0.8					2		2	0.9
		Mn/Fe				0.9			0.8				
	Disorthic	Mn											
		Fe							2.8		4.5		
		Mn/Fe			0.8								
	Aggregated	Mn											
		Fe											
		Mn/Fe											
Coating	Coating	Mn											
		Fe		0.4			0.6				2.7	2.3	
		Mn/Fe	3.3										
	Pendant	Mn											
		Fe							0.1				
		Mn/Fe	0.3										
	Hypocoating	Mn											
		Fe	1.8		2	2.2	1.4		1.9	9.2			2.6
		Mn/Fe										5	
	Quasicoating	Mn											
		Fe				0.9							
		Mn/Fe											
Impregnation		Mn											
		Fe			2.65	0.9	0.6	1	1	10		0.9	7.6
		Mn/Fe	1		0.4	2.9			1.8		5		1.7
Infillings		Mn											
		Fe	0.76		2.25	0.4	0.6		0.9		5	5	
		Mn/Fe											
Intercaltions		Mn											
		Fe					0.3						
		Mn/Fe	0.6										0.5
Depleations		Mn											
		Fe											
		Mn/Fe											

4.1.1 Iron and manganese pedofeatures by microfabric type

Table 87: Distribution of iron and manganese pedofeatures shown as a percentage of the microfabric area

Microfabrics			HU1	HU2	HU3	HU4	HU5	HU6
Nodules	Anorthic	Mn						
		Fe	0.12			0.14		
		Mn/Fe	0.18					
	Orthic	Mn						
		Fe				0.09	0.13	
		Mn/Fe			0.10	0.11		
	Disorthic	Mn						
		Fe						
		Mn/Fe						
	Aggregated	Mn						
		Fe	0.12					
		Mn/Fe						
Coating	Coating	Mn						
		Fe	0.12			0.1		
		Mn/Fe						
	Pendant	Mn						
		Fe				0.01		
		Mn/Fe						
	Hypocoating	Mn						
		Fe	0.24			1.71		0.03
		Mn/Fe	0.06					
	Quasicoating	Mn						
		Fe			0.08	0.07		
		Mn/Fe			0.10	0.09		
Impregnation		Mn						
		Fe	1.88		0.31	0.71	0.13	
		Mn/Fe	0.24		0.10	0.43		
Infillings		Mn						
		Fe				0.11		
		Mn/Fe						
Intercaltions		Mn						
		Fe				0.86		
		Mn/Fe						
Depleations		Mn						
		Fe	1.53					
		Mn/Fe						

Table 87 cont

Microfabrics			HU7	HU8	HU9	HU10	HU11	HU12	HU13
Nodules	Anorthic	Mn							
		Fe		0.60	0.67	0.54		0.05	0.91
		Mn/Fe		0.13	0.33	0.83			0.54
	Orthic	Mn							
		Fe		1.07				0.05	0.25
		Mn/Fe						0.05	0.32
	Disorthic	Mn							
		Fe					1.50		0.21
		Mn/Fe		0.26					0.20
	Aggregated	Mn							
		Fe							
		Mn/Fe							
Coating	Coating	Mn							0.03
		Fe	0.60	0.91		0.86	0.90	0.01	0.61
		Mn/Fe				0.09		0.03	0.25
	Pendant	Mn							
		Fe	1.50						0.10
		Mn/Fe						0.05	0.07
	Hypocoating	Mn							
		Fe		0.64	0.03	1.43	0.90	0.23	0.54
		Mn/Fe		0.26				0.09	0.52
	Quasicoating	Mn							
		Fe						0.50	0.06
		Mn/Fe						0.07	
Impregnation		Mn							
		Fe	0.60	1.09	0.17	2.14			0.73
		Mn/Fe		1.36		0.98			0.41
Infillings		Mn							
		Fe		0.26		0.54			0.23
		Mn/Fe							
Intercaltions		Mn							
		Fe				0.90			0.05
		Mn/Fe							
Depleations		Mn							
		Fe							0.23
		Mn/Fe							

4.2 Micromorphology summary descriptions

Table 88: Çatalhöyük micromorphology summary description

Context	Date and type of burial	Microfabrics	Micromorphological summary		
			Coarse material	Soil structure	Post depositional Pedofeatures
C1		Composed of building materials used as packing to support platforms. Obtained from the surrounding alluvial sediments. Microfabrics evenly distributed in all contexts	Quartz, silicates, phyllosilicates, tectosilicates and sulphates (≤4%). Bone, shell and charcoal (≤2%)	Apedal, Sub-angular blocky and granular peds with 10.75% total void space. High abundances of packing voids	Iron and manganese pedofeatures Limpid clay coatings (<1%). Coprolite present
18666	Neolithic crouched, articulated adult		Quartz, silicates, phyllosilicates, tectosilicates, Inosilica based rock fragments and sulphates (≤20%). Bone (<2%) and charcoal peak (6%) in pelvis, shell (≤3%) and phytoliths in foot area sample (1%)	Apedal, blocky and granular peds. High total void space in the skull. High abundances of packing voids	Iron and manganese pedofeatures with impregnation peaks in skull Dusty clay coatings in controls (<1%). Coprolite in foot area. $CaCO^3$ pedofeatures in grave and controls
19295	Two Neolithic fleshed skulls		Quartz, silicates, phyllosilicates, tectosilicates, carbonates and sulphates (≤15%). Bone (<3%), charcoal (<5%) and shell (1%)	Apedal, blocky, spheroidal peds and plates High total void space in the skull. High abundances of packing voids	Iron and manganese pedofeatures. $CaCO^3$ pedofeatures in grave and controls

Table 89: Thessaloniki micromorphological summary description

Context	Date and type of burial	Micromorphological summary			
		Microfabrics	Coarse material	Soil structure	Post depositional Pedofeatures
TF157	Early Hellenistic supine adult burial	Ti1	Quartz, silicates, phyllosilicates, tectosilicates and carbonates (≤20%). Shell, bone (2%) and charcoal (1% in skull)	Apedal and sub-angular blocky peds. High total void space in the skull.	Iron and manganese pedofeatures. Dusty and impure clay coatings (≤4%). Excremental pedofeatures in hand area. $CaCO^3$ pedofeatures
TF182	Late Hellenistic supine adult burial in a plastered grave	Ti1 with Ti2 in skull, pelvic and foot area samples (≤30%)	Quartz, silicates, phyllosilicates, tectosilicates Nesosilicates and carbonates (≤20%). Shell (2%), charcoal peak in skull (1%), bone peak in pelvis (≤10%)	Apedal, sub-angular blocky and crumb peds. High total void space in the foot	Iron pedofeatures in controls and iron and manganese pedofeatures in the burial plane with impregnation peak in foot area Impure clay coatings in controls and grave with relict and limpid coating in C3 (≤4%). Worm granules in pelvic area. $CaCO^3$ pedofeatures in grave and controls
TF177	Roman supine adult burial in partially tiled grave	Ti1 with Ti2 in foot area sample (10%)	Quartz, silicates, phyllosilicates, tectosilicates, Nesosilicates and carbonates (≤20%). Bone (≤5%) and charcoal (≤2%) peak in pelvis and shell (2%)	Apedal, sub-angular blocky, crumb peds and planes High total void space in the foot. High abundances of packing voids and vughs.	Iron and manganese pedofeatures with impregnation peak in foot area. Impure clay and silt coating peaks in pelvic area (≤12%) with dusty clay coating sin the burial (≤5%) and relict coatings in the hand area. Excremental pedofeature in hand area and burrows in foot area. $CaCO^3$ pedofeatures in grave and controls

Table 89 cont

Context	Date and type of burial	Micromorphological summary			
		Microfabrics	Coarse material	Soil structure	Post depositional Pedofeatures
TF178	Roman supine adult burial in an open chamber tomb buried with a child	Ti1	Quartz, silicates, phyllosilicates, tectosilicates Nesosilicates and carbonates (≤24%). Shell (≤5%) and charcoal (1%).	Apedal, sub-angular blocky and crumb peds High total void space in the pelvis. High abundances of channels and planes	Iron and manganese pedofeatures. Dusty and impure clay coatings (2%). $CaCO^3$ pedofeatures
TF162	Roman (?) supine adult burial in a plastered grave	Ti1	Quartz, silicates, phyllosilicates, tectosilicates and carbonates (≤20%). Shell, bone (2%) and charcoal (1%).	Angular blocky and crumb peds High total void space in the skull. High abundances of packing voids	Iron and manganese pedofeatures with impregnation peak in foot area. Limpid, impure clay and silt coatings (≤4%). $CaCO^3$ pedofeatures

Table 90: Heslington East micromorphology summary descriptions

Context	Date and type of burial	Soil type	Micromorphological summary		
			Coarse material	Soil structure	Post depositional Pedofeatures
C1	C1	Agricultural land, with deep free draining soils.	Quartz, silicates, phyllosilicates, tectosilicates (≤70%). Charcoal (≤5%) and roots (2%)	Apedal and sub-angular blocky peds with 12.79% total void space. High abundances of packing voids and vughs	Iron and manganese pedofeatures. Limpid, impure clay and sand coatings in lower samples (≤5%). Excremental pedofeatures.
713	Late Roman (1704 ± 30BP) supine adult burial		Quartz, silicates, phyllosilicates, tectosilicates, carbonates and vivianite (≤70%). Bone (2%), charcoal (≤5%) and roots (2%)	Apedal, sub-angular blocky peds and plates. High total void space in the foot. High abundances of packing voids and vughs	Iron and manganese pedofeatures with impregnation peak in skull area. Limpid, dusty and impure clay coatings (≤5%). Excremental pedofeatures in controls and grave

Table 91: Hungate micromorphology summary description

Context	Date and type of burial	Micromorphological summary			
		Significant microfabrics	Coarse material	Soil structure	Post depositional Pedofeatures
C1		HU8 (bioturbation)	Quartz, silicates, phyllosilicates and tectosilicates (≤70%). Shell (7%), charcoal (≤5%) and fungal sclerotia (1%)	Apedal with 5.08% total void space. High abundance of vughs	Iron and manganese pedofeatures. impure clay coatings (<2%). Bioturbation infillings.
SK54898	3rd C Roman supine infant lead coffin burial	HU6 (monic clay laminations). Microstratigraphic microfabric assemblages	Quartz, silicates phyllosilicates and lead (≤64%). Charcoal (≤9%)	Apedal, blocky, prisms and platy peds. High total void space in the pelvis. High abundances of planes	Iron and manganese pedofeatures with impregnation peak in pelvic area. Limpid and dusty clay coatings in control and burial with impure clay in the skull areas (≤2%). Excrement in controls (<2%) and excrement and infillings in grave.
SK51326	Roman supine adult coffined burial	-	Quartz, silicates, phyllosilicates, tectosilicates and carbonates (≤90%). Bone (≤5%), charcoal (peak in skull ≤10%) and fungal sclerotia (1%), Fe spherulites	Apedal in controls with apedal, sub-angular blocky and platy peds in burial. High total void space in the feet. High abundances of vughs	Iron and manganese pedofeatures with impregnation peak in foot area. Dusty and limpid clay coatings in the burial plane (≤3%). Excrement and infillings in C3 (≤3%).

Table 91. Cont

Context	Date and type of burial	Micromorphological summary			
		Significant microfabrics	Coarse material	Soil structure	Post depositional Pedofeatures
SK51387	Roman supine adult shrouded burial	HU4 (water laid deposits)	Quartz, silicates, tectosilicates and carbonates (≤50%). Bone (≤2%) and charcoal (peak in skull ≤5%)	Apedal, sub-angular blocky and crumb peds. High total void space in the skull.	Iron and manganese pedofeatures with impregnation peak in foot area. Limpid clay coatings in the burial plane with impure clay in C3 and dusty clay coatings throughout (≤1%). Worm granules in controls and grave with infillings in grave (≤9%)
SK51351	Roman adult supine burial	-	Quartz, silicates, phyllosilicates and tectosilicates (≤73%). Bone (1%) and charcoal (peak in skull ≤10%), Fe spherulites	Sub-angular blocky and apedal soils. High total void space in the skull. High abundances of vughs	Iron and manganese pedofeatures with impregnation peak in foot area. Limpid, dusty and impure clay coatings (≤1%). Excrement and infilling in grave (≤10%).
SK54090	Roman child/juvenile burial located in a ditch	HU4 (water laid deposits)	Quartz, silicates, phyllosilicates and tectosilicates (≤60%). Bone (≤1%), charcoal (2%) and fungal sclerotia (1%)	Apedal soils plates and crumbs in C3 with apedal, blocky, crumbs and platy ped in the grave. High total void space in the pelvis. High abundances of vughs	Iron and manganese pedofeatures with impregnation peak in pelvic area. Impure coatings in C3 and burial plane and limpid coatings in the burial (≤3%). Excrement in grave (<1%). $CaCO^3$ pedofeatures

Table 91 cont

Context	Date and type of burial	Micromorphological summary			
		Significant microfabrics	Coarse material	Soil structure	Post depositional Pedofeatures
SK54085	Roman supine adult coffined burial	-	Quartz, silicates, phyllosilicates, tectosilicates and nesosilicates (≤60%). Charcoal peak in pelvis (≤5%)	Sub-angular blocky C3 with apedal, sub-angular blocky and crumbs in the grave. High total void space in the pelvis. High abundances of planes	Iron and manganese pedofeatures with impregnation peak in pelvic area. Limpid coatings in C3 and burial with dusty and impure coatings in the burial (<2%).
SK54341	Roman supine adult coffined burial	-	Quartz, silicates, phyllosilicates and tectosilicates (≤64%). Bone (≤1%), charcoal (5%) and fungal sclerotia (1%), Fe spherulites	Apedal, sub-angular blocky and granules in the C3 with apedal, sub-angular blocky, platy and spheroidal peds. High total void space in the foot.	Iron and manganese pedofeatures with impregnation peak in foot area. Limpid coatings in the C3 and burial plane with dusty and impure clay coatings in the burial (<4%). Infillings in C3 and grave and excrement in grave (<4%). $CaCO^3$ pedofeatures
SK54342	Roman supine adult coffined burial	HU4 (water laid deposits) and HU8 (bioturbation)	Quartz, silicates, phyllosilicates and tectosilicates (<57%). Bone (peak in pelvis ≤2%), charcoal (peak in skull ≤3%) and fungal sclerotia (1%), Fe spherulites	Apedal, sub-angular blocky and crumb peds in C3 and grave in addition to angular blocky in the grave. High total void space in the skull. High abundances of vughs	Iron and manganese pedofeatures with impregnation peak in skull area. Dusty and impure clay coatings in the control with limpid and impure clay in the burial (<6%). Infilling in C3 (60%) and excrement in grave (≤1%). $CaCO^3$ pedofeatures

Table 91 cont

Context	Date and type of burial	Micromorphological summary			
		Significant microfabrics	Coarse material	Soil structure	Post depositional Pedofeatures
SK54908	Roman supine infant coffined burial	HU8 (bioturbation)	Quartz, silicates, phyllosilicates and tectosilicates (≤56%). Bone (<1%), charcoal (peak in skull ≤7%) and fungal sclerotia (1%)	Apedal, sub-angular blocky and crumb peds in C3 and grave in addition to platy peds in the grave. High total void space in the skull. High abundances of vughs	Iron and manganese pedofeatures with impregnation peak in pelvic area. Limpid clay coatings in the C2 and burial plane with dusty and impure coatings in the burial (≤5%). Infilling in grave (≤100%).
SK51350	Roman supine adult coffined burial truncated by cess pit	HU7 (bone)	Quartz, silicates, phyllosilicates and tectosilicates (≤70%). Bone (<2%), charcoal (peak in skull ≤3%) and fungal sclerotia (<1%), Fe spherulites	Apedal, sub-angular blocky and platy peds in controls and grave. High total void space in the foot. High abundances of vughs	Iron and manganese pedofeatures with impregnation peak in foot area. Impure clay coatings in the C2 and grave with limpid and dusty coatings in the grave.

Glossary

The definition for all terms are given using those found in Stoops (2003) or those developed for the protocol used in this report.

Term	Definition
Angular blocky peds	More or less equal sided peds which have flat surfaces.
Anorthic nodule	Inherited nodules.
Apedal	Structureless, absence of peds.
B-fabric	The arrangement in the micromass of streaks of inference colours, caused by the movement or pressure in the soil aligning clay particles producing patterns visible in XPL.
C:F related distribution	The relationship between the coarse fabric units and the fine fabric unites.
Channels	Smooth, tubular voids which are generally uniform with an arched or cylindrical cross section.
Chitonic	Larger fabric units are coated in smaller fabric units.
Circular striated b-fabric	Streaks of interference colours which are more or less circular.
Clay	All that material below 2 µm
Coarse fraction	All that material above 50 µm.
Coating	Pedofeatures which are intrusive, but not occupy more than 90% of the void and coat a natural surface.
Crumb peds	More or less equal sided, porous peds which have rounded surfaces.
Crystals	Crystals embedded within the fabric.
Disorthic nodule	Nodules which have been formed in situ but subsequently translocated.
Dusty clay coatings	Fine to coarse clay coatings which contain microparticles $\leq$ 3 µm
Enaulic	Aggregates of smaller units which are between larger units.
Fabric pedofeatures	Recognisable from the groundmass only by differences in fabric.
Fanlike crystals	Crystals ranged in a fan like pattern.
Gefuric	Bridges of smaller fabric units link larger fabric units.

Term	Definition
Granostriated b-fabric	Striations of interference colours are arranged parallel to larger fabric units (i.e. mineral grains).
Hypocoating	Pedofeatures which have formed within the matrix which both adjoin and refer to a natural surface.
Impregnation	Situated in the micromass impregnations are recognisable by their high concentrations of components.
Impure clay coatings	Clay coatings which contain many particles of silt.
Infilling	Filled or partly filled voids with soil material, not including packing voids.
Intercalations	Undulating, elongated pedofeatures which are not referred to natural surfaces.
Limpid clay coatings	Clay without inclusions which is uniform in appearance.
Microlaminated	Alternating speckled or limpid clay in thin (<30 μm) layers.
Monic	Fabric only contains one unit.
Monostriated b-fabric	Parallel streaks of interference colours.
Nodule	Natural features which do not contain crystals and are unrelated to surfaces or voids.
Packing voids	Composed of loose soil components which are generally unaccommodated.
Ped	Relatively permanent natural aggregates which are separated by voids.
Ped development	The degree of separation between peds by voids, coatings or infillings.
Pedofeature	Features which are distinguished from the adjacent soil material due to differences in concentration, components or internal fabric.
Planes	Flat, planar voids, with may or may not be accommodated with at least one sharp terminus.
Platy peds	Elongate horizontal peds which are more or less straight.
Porostriated b-fabric	Striations of interference colours are arranged parallel to voids.
Porphyric	A dense fabric of smaller unites, which contains larger fabric unites
Quasicoatings	Pedofeature within the matrix which is related to a natural surface but not adjoining it.
Rock fragments	Minerals which are formed of multiple grains which can be identified to genesis.
Sand	All that material above 50 μm
Silt	All that material between 2 – 50 μm
Sorting	The degree of particle diameter variation within a given sample at x2.5 magnification.
Stipple speckled b-fabric	Isolated specks of randomly orientated interference colours.
Sub-angular blocky	More or less equal sided peds which have rounded and flat surfaces.
Typic	Coatings, hypocoatings and quasicoatings which do not fall into any of the conventional coating categories.
Undifferentiated	Lack of interference colours in the groundmass.
Vughs	Smooth or rough, equidimensional, irregular voids that may or may not be interconnected.

References

Abdel-Wahab, M. S., Youssef, S. K., Aly, A. M., El-Fiki, S. A., El-Enany, N. & Abbas, M. T. (1992). A simple calibration of a whole-body counter for the measurement of total body potassium in humans. *International Journal of Radiation Applications and Instrumentation. Part A. Applied Radiation and Isotopes* **43**, 1285-1289.

Acheilara, L. (2010). Μετρό Θεσσαλονίκης 2007 Το αρχαιολογικό έργο της ιστ' επκα. *Το Αρχαιολογικο Εργο Στη Μακεδονια Καιστη Θρακη 21, 2007*: Υπουργειο Πολιτισμου Και Τουρισμου, 215-222.

Adderley, W. P., Simpson, I. A. & Davidson, D. A. (2002). Colour description and quantification in mosaic images of soil thin sections. *Geoderma* **108**, 181-195.

Adderley, W. P., Wilson, C. A., Simpson, I. A. & Davidson, D. A. (2010). Anthropogenic Features. In: Stoops, G., Marcelino, V. & Mees, F. (eds.) *Interpretation of Micromorphological Features of Soils and Regoliths*. Oxford: Elsevier Science Ltd, 569-588.

Allaire-Leung, S. E., Gupta, S. C. & Moncrief, J. F. (2000). Water and solute movement in soil as influenced by macropore characteristics: 2. Macropore tortuosity. *Journal of Contaminant Hydrology* **41**, 303-315.

Alvarez, R., Evans, L. A., Milham, P. J. & Wilson, M. A. (2004). Effects of humic material on the precipitation of calcium phosphate. *Geoderma* **118**, 245-260.

Amendas, G., McConnachie, G. & Pournou, A. (2012). Selective reburial: A potential approach for the in situ preservation of waterlogged archaeological wood in wetland excavations. *Journal of Archaeological Science* **1**, 99-108.

Arnold, B. (2002). Chapter 8. A Landscape of Ancestors: The Space and Place of Death in Iron Age West-Central Europe. *Archeological Papers of the American Anthropological Association* **11**, 129-143.

Asouti, E., Erkal, A., Fairbairn, A., Hastrof, C., Kennedy, A., Near, J. & Rosen, A. M. (1999). *Catalhoyuk 1999 Archive Report Archaeobotany and Related Plant Studies*. Catalhoyuk Research Team.

Baldock, J. A. & Smernik, R. J. (2002). Chemical composition and bioavailability of thermally altered Pinus resinosa (Red pine) wood. *Organic Geochemistry* **33**, 1093-1109.

Banerjea, R., Bell, M., Matthews, W. & Brown, A. (2015). Applications of micromorphology to understanding activity areas and site formation processes in experimental hut floors. *Archaeological and Anthropological Sciences* **7**, 89-112.

Barbiero, L., Kumar, M. S. M., Violette, A., Oliva, P., Braun, J. J., Kumar, C., Furian, S., Babic, M., Riotte, J. & Valles, V. (2010). Ferrolysis induced soil transformation by natural drainage in Vertisols of sub-humid South India. *Geoderma* **156**, 173-188.

Behrensmeyer, A. K. (1978). Taphonomic and Ecologic Information from Bone Weathering. *Paleobiology* **4**, 150-162.

Bell, M., Fowler, P. J. & Hillson, S. W. (eds.) (1996). *The Experimental Earthwork Project 1960-1992*. York: Council for British Archaeology

Berg, G. E. (2002). Last Meals: Recovering Abdominal Contents From Skeletonized Remains. *Journal of Archaeological Science* **29**, 1349-1365.

Bethell, P. H. & Carver, M. O. H. (2002). Detection and enhancement of decayed inhumations at Dutton Hoo. In: Haglund, W. D. & Sorg, M. H. (eds.) *Advances in Forensic Taphonomy: Method, Theory and Archaeological Perspective*. London: CRC, 10-21.

Bethell, P. H. & Smith, J. U. (1989). Trace-element Analysis of an Inhumation from Sutton Hoo, Using Inductively Coupled Plasma Emission Spectrometry: An Evaluation of the Technique Applied to Analysis of Organic Residues. *Journal of Archaeological Science* **16**, 47-55.

Birkeland, P. (1984). *Soils and Geomorphology*. Oxford: Oxford University Press.

Bobrowsky, P. T. (1984). The History and Science of Gastropods in Archaeology. *American Antiquity* **49**, 77-93.

Bockheim, J. G. & Tarnocai, C. (1998). Recognition of cryoturbation for classifying permafrost-affected soils. *Geoderma* **81**, 281-293.

Bottinelli, N., Henry-des-Tureaux, T., Hallaire, V., Mathieu, J., Benard, Y., Duc Tran, T. & Jouquet, P. (2010). Earthworms accelerate soil porosity turnover under watering conditions. *Geoderma* **156**, 43-47.

Boyer, P., Roberts, N. & Baird, D. (2006). Holocene Environment and Settlement on the Casamba Alluvial Ran, South-Central Turkey: Intergrating Geoarchaeology and Archaeological Field Survey. *Geoarchaeology* **21**, 675-698.

Boylston, A., Knüsel, C. J., Roberts, C. A. & Dawson, M. (2000). Investigation of a Romano-British Rural Ritual in Bedford, England. *Journal of Archaeological Science* **27**, 241-254.

Brady, N. C. (1969). *The Nature and Properties of Soils*. London: Collier Macmillan Publishers.

Bresson, L. M. & Boiffin, J. (1990). Morphological characterization of soil crust development stages on an experimental field. *Geoderma* **47**, 301-325.

Breuning-Madsen, H. & Holst, M. K. (1998). Recent Studies on the Formation of Iron Pans around the Oaken Log Coffins of the Bronze Age Burial Mounds of Denmark. *Journal of Archaeological Science* **25**, 1103-1110.

Brewer, R. (1964). *Fabric and mineral analysis of soils*. New York: John Wiley & Sons.

Brinkman, R. (1970). Ferrolysis, a hydromorphic soil forming process. *Geoderma* **3**, 199-206.

Brinkman, R., Jongmans, A. G., Miedema, R. & Maaskant, P. (1973). Clay decomposition in seasonally wet, acid soils: Micromorphological, chemical and mineralogical evidence from individual argillans. *Geoderma* **10**, 259-270.

Brown, A. B. (1997). *Alluvial Geoarchaeology*. Cambridge: Cambridge University Press.

Buckman, H. O. & Brady, N. C. (1969). *The Nature and Properties of soils*. USA: The Macmillan Company.

Bullock, P., Fedoroff, N., Jongerius, A., Stoops, G., Tursina, T. & Babel, U. (1985). *Handbook for Soil Thin Section Description*. Wolverhampton: Waine Research.

Bundt, M., Widmer, F., Pesaro, M., Zeyer, J. & Blaser, P. (2001). Preferential flow paths: biological 'hot spots' in soils. *Soil Biology and Biochemistry* **33**, 729-738.

Cameron, E. (1991). Identification of skin and leather preserved by iron corrosion products. *Journal of Archaeological Science* **18**, 25-33.

Canti, M. (1998a). Origin of Calcium carbonate granules found in buried soils and Quaternary deposits. *Boreas* **27**, 275-288.

Canti, M. (2003). Earthworm Activity and Archaeological Stratigraphy: A Review of Products and Processes. *Journal of Archaeological Science* **30**, 135-148.

Canti, M. G. (1997). An Investigation of Microscopic Calcareous Spherulites from Herbivore Dungs. *Journal of Archaeological Science* **24**, 219-231.

Canti, M. G. (1998b). The Micromorphological Identification of Faecal Spherulites from Archaeological and Modern Materials. *Journal of Archaeological Science* **25**, 435-444.

Canti, M. G. (1999). The Production and Preservation of Faecal Spherulites: Animals, Environment and Taphonomy. *Journal of Archaeological Science* **26**, 251-258.

Carter, S. P. & Davidson, D. A. (1998). An evaluation of the contribution of soil micromorphology to the study of ancient arable agriculture. *Geoarchaeology* **13**, 535-547.

Cessford, C. (2001). A new dating sequence for Çatalhöyük. *Antiquity* **75**, 717-725.

Claassen, C. (1998). *Shells*: Cambridge University Press.

Cole, G. (2013). Human Burials. In: Matthews, R., Matthews, W. & Mohammadifar, Y. (eds.) *The Earliest Neolithic of Iran 2008 Excavations at Sheikh-e Abad and Jani*. Oxford: Oxbow Books, 163-174.

Courty, M. A. & Fédoroff, N. (1985). Micromorphlogy of recent and buried soils in a semi-arid region of northwestern India. *Geoderma* **35**, 287-332.

Courty, M. A., Goldberg, P. & Macphail, R. (1989). *Soils and Micromorphology in Archaeology*. Cambridge: Cambridge University Press.

Crowther, J. (2002). The Experimental Earthwork at Wareham, Dorset after 33 Years: Retention and Leaching of Phosphate Released in the Decomposition of Buried Bone. *Journal of Archaeological Science* **29**, 405-411.

Cunliffe, B. (1991). *Iron age communities in Britain. Settlement and Settlement Pattern in the South and East*: Routledge.

Czimczik, C. I., Preston, C. M., Schmidt, M. W. I. & Schulze, E.-D. (2003). How surface fire in Siberian Scots pine forests affects soil organic carbon in the forest floor: Stocks, molecular structure, and conversion to black carbon (charcoal). *Global Biogeochemical Cycles* **17**, 1020.

Dalrymple, J. B. & Jim, C. Y. (1984). Experimental study of soil microfabrics induced by isotropic stresses of wetting and drying. *Geoderma* **34**, 43-68.

Davidson, D. A., Bruneau, P. M. C., Grieve, I. C. & Wilson, C. A. (2004). Micromorphological assessment of the effect of liming on faunal excrement in an upland grassland soil *Applied Soil Ecology* **26**, 169-177.

Davidson, D. A. & Carter, S. P. (1998). Micromorphological Evidence of Past Agricultural Practices in Cultivated Soils: The Impact of a Traditional Agricultural System on Soils in Papa Stour, Shetland. *Journal of Archaeological Science* **25**, 827-838.

Davidson, D. A. & Grieve, I. C. (2006). Relationships between biodiversity and soil structure and function: Evidence from laboratory and field experiments. *Applied Soil Ecology* **33**, 176-185.

Dent, B. B. (2002). *The hydrogeological context of cemetery operations and planning in Australia*. Sydney: University of Technology.

Dent, B. B., Forbes, S. L. & Stuart, B. H. (2004). Review of human decomposition processes in soil *Environmental Geology* **45**, 576-585.

Devreker, J., Thoen, H. & Vermeulen, F. (2003). *Excavations in Pessinus: the so-called Acropolis: from Hellenistic and Roman cemetery to Byzantine castle*: Academia Press.

Doherty, C. (2013). Sourcing Catalhoyuk's Clays. In: Hodder, I. (ed.) *Substantive technologies at Çatalhöyük: reports from the 2000-2008 seasons*. Ankara: The British Institute at Ankara, 115-136.

During, B. S. (2003). Burials in context: The 1960s inhumations of Catalhoyuk East. *Anatolian Studies* **53**, 1-15.

Evans, D. (2007a). *Areas A, B and C Hungate Development York: A Report on an Archaeological Watching Brief*. York York Archaeological Trust, 30.

Evans, D. (2007b). *Block A, B, C Pre-Piling Probes: Hungate Development York: A Report on an Archaeological Watching Brierf*. York: York Archaeological Trust, 18.

Evans, J. E. (1972). *Land Snails in Archaeology, with special reference to the British Isles*. London: Seminar Press Inc LTD.

Favre, F., Tessier, D., Abdelmoula, M., Génin, J. M., Gates, W. P. & Boivin, P. (2002). Iron reduction and changes in cation exchange capacity in intermittently waterlogged soil. *European Journal of Soil Science* **53**, 175-183.

Fiedler, S. & Graw, M. (2003). Decomposition of buried corpses, with special reference to the formation of adipocere *Naturwissenschaften* **90**, 291-300.

FitzPatrick, E. A. (1993). *Soil Microscopy and Micromorphology*. Chichester: John Wiley & Sons.

Fontijn, D. (1996). Socializing landscape. *Archaeological dialogues* **3**, 77-87.

Forbes, M. S., Raison, R. J. & Skjemstad, J. O. (2006). Formation, transformation and transport of black carbon (charcoal) in terrestrial and aquatic ecosystems. *Science of The Total Environment* **370**, 190-206.

Fortun, A., Benayas, J. & Fortun, C. (1990). The effects of fulvic and humic acids on soil aggregation: a micromorphological study. *Journal of Soil Science* **41**, 563-572.

Garland, R. (1971). *The Greek way of death*: Cornell University Press.

Ghilardi, M., Fouache, E., Queyrel, F., Syrides, G., Vouvalidis, K., Kunesch, S., Styllas, M. & Stiros, S. (2008a). Human occupation and geomorphological evolution of the Thessaloniki Plain (Greece) since mid Holocene. *Journal of Archaeological Science* **35**, 111-125.

Ghilardi, M., Kunesch, S., Styllas, M. & Fouache, E. (2008b). Reconstruction of Mid-Holocene sedimentary environments in the central part of the Thessaloniki Plain (Greece), based on microfaunal identification, magnetic susceptibility and grain-size analyses. *Geomorphology* **97**, 617-630.

Glob, P. V. (1973). *The Mound People: Danish Bronze-Age Man Preserved*. London: Book Club Associates.

Going, C. J., Green, M., Duhig, C. & Alison, T. (1997). A Roman Child Burial with Animal Figurines and Pottery, from Godmanchester, Cambridgeshire. *Britannia* **28**, 386-393.

Goldberg, P. & Macphail, R. (2006). *Practical and Theoretical Geoarchaeology* Oxford, UK: Blackwell Publishing.

Goldberg, P., Weiner, S., Bar-Yosef, O., Xu, Q. & Liu, J. (2001). Site formation processes at Zhoukoudian, China. *Journal of Human Evolution* **41**, 483-530.

Gordon, C. C. & Buikstra, J. E. (1981). Soil pH, Bone Preservation, and Sampling Bias at Mortuary Sites. *American Antiquity* **46**, 566-571.

Gunal, H. & Ransom, M. D. (2006). Clay illuviation and calcium carbonate accumulation along a precipitation gradient in Kansas. *CATENA* **68**, 59-69.

Hald, M. (1980). *Ancient Danish textiles from bogs and burials: a comparative study of costume and Iron Age textiles*: National museum of Denmark.

Hamilton, N. (1997). Figurines, clay balls, small finds and burials. *On the surface: Çatalhöyük 1993-95*, 215-263.

Hansen, J. D., Pringle, J. K. & Goodwin, J. (2014). GPR and bulk ground resistivity surveys in graveyards: Locating unmarked burials in contrasting soil types. *Forensic Science International* **237**, e14-e29.

Hanson, M. & Cain, C. R. (2007). Examining histology to identify burned bone. *Journal of Archaeological Science* **34**, 1902-1913.

He, P., Yang, L., Xu, X., Zhao, S., Chen, F., Li, S., Tu, S., Jin, J. & Johnston, A. M. (2015). Temporal and spatial variation of soil available potassium in China (1990–2012). *Field Crops Research* **173**, 49-56.

Henderson, J. (1987). Factors determining the state of preservation of human remains. In: Boddington A, & Garland A. N. (eds.) *Death, Decay, and Reconstruction*. Manchester: Manchester University Press, 43-54.

Heymsfield, S. (2005). *Human body composition*: Human kinetics.

Hodder, I. (2005). Introduction. In: Hodder, I. (ed.) *Catalhoyuk Perspectives: Reports from the 1995-99 Seasons.* . Cambridge: McDonald Institute for Archaeological Research and British Institute of Archaeology at Ankara, 1-14.

Hodder, I. (2006). *Catalhoyuk, The Leopard's tale: Revealing the mysteries of Turkey's ancient "town'.* London: Thames and Hudson Ltd.

Holliday, V. T. & Gartner, W. G. (2007). Methods of soil P analysis in archaeology. *Journal of Archaeological Science* **34**, 301-333.

Holst, M. (2010). *Osteological Analysis, Heslington East, York.* York: York Osteoarchaeology Ltd.

Hope, V. M. (2007). *Death in Ancient Rome*. Oxon: Routledge.

House, M. (2010). Building 77, Space 336 & Space 337. In: Farid, S. (ed.) *Catalhoyuk 2010 Archive Report; Catalhoyuk Research Project*: Catalhoyuk Research Project, 31-43.

Hseu, Z.-Y. & Chen, Z.-S. (2001). Quantifying Soil Hydromorphology of a Rice-Growing Ultisol Toposequence in Taiwan. *Soil Sci. Soc. Am. J.* **65**, 270-278.

Huisman, D. J. & Klaassen, R. K. W. M. (2009). Wood. In: Huisman, D. J. (ed.) *Degradation of Archaeological Remains*. Den Haag: Sdu Uitgevers 17-32.

Huisman, D. J., Manders, M. R., Kretschmar, E. I., Klaassen, R. K. W. M. & Lamersdorf, N. (2008). Burial conditions and wood degradation at archaeological sites in the Netherlands. *International Biodeterioration & Biodegradation* **61**, 33-44.

Hunter, J. & Ralston, I. (1999). *The archaeology of Britain. An introduction from the Upper Palaeolithic to the Industrial Revolution.* Psychology Press.

Hussein, J. & Adey, M. A. (1998). Changes in microstructure, voids and b-fabric of surface samples of a Vertisol caused by wet/dry cycles. *Geoderma* **85**, 63-82.

Hutchenson, G. & Sofroniou, N. (1999). *The Multivariate Social Scientist*. London: Sage.

InterArChive. (Unpublished). *Interred with their bones - linking soil micromorphology and chemistry to unlock the hidden archive of archaeological human burials*. European Research Council Proposal.

Janaway, R. C. (1987). The Preservation of Organic Materials in Association with Metal Artefacts Deposited in Inhumation Graves. In: Boddington, A., Garland, A. N. & Janaway, R. C. (eds.) *Death, decay and Reconstruction; Approaches to Archaeology and Forensic Science*. UK: Manchester University Press, 127-148.

Janaway, R. C. (2002). Degradation of clothing and other dress materials associated with buried bodies of archaeological and forensic interest. In: Haglund, W. D. & Sorg, M. H. (eds.) *Advances in Forensic Taphonomy: Method, Theory and Archaeological Perspective*. London: CRC, 379-402.

Janaway, R. C., Wilson, A. S., Díaz, G. C. & Guillen, S. (2009). Taphonomic Changes to the Buried Body in Arid Environments: An Experimental Case Study in Peru. In: Ritz, K., Dawson, L. & Miller, D. (eds.) *Criminal and Environmental Soil Forensics*: Springer Netherlands, 341-356.

Janaway, R. C., Wilson, A. S., Holland, A. D. & Baran, E. N. (2003). Taphonomic changes to the buried body and associated materials in an upland peat environment: Experiments using pig carcasses as human body analogues. In: Lynnerup, N., Andreasen, C. & Berglund, J. (eds.) *Mummies in a new millenium: Proceedings of the 4th World Congress on Mummy Studies, 4th to 10th September 2003 Nuuk, Greenland.* Copenhagen: Greenland National Museum and Archives and Danish polar centre, 56-59.

Jenkins, E. (2012). Mice, scats and burials: Unusual concentrations of microfauna found in human burials at the Neolithic site of Çatalhöyük, Central Anatolia *Journal of Social Archaeology* **12**, 380-403.

Jongmans, A. G., Pulleman, M. M. & Marinissen, J. C. Y. (2001). Soil structure and earthworm activity in a marine silt loam under pasture versus arable land. *Biology and Fertility of Soils* **33**, 279-285.

Keeley, H. M. C., Hudson, G. E. & Evans, J. (1977). Trace element contents of human bones in various states of preservation. 1. The soil silhouette. *Journal of Archaeological Science* **4**, 19-24.

Kelly, A. T., Rusakova, I., Ould-Ely, T., Hofmann, C., Lüttge, A. & Whitmire, K. H. (2007). Iron Phosphide Nanostructures Produced from a Single-Source Organometallic Precursor: Nanorods, Bundles, Crosses, and Spherulites. *Nano Letters* **7**, 2920-2925.

Kemp, R. A. (1998). Role of micromorphology in paleopedological research. *Quaternary International* **51–52**, 133-141.

Kemp, R. A., McDaniel, P. A. & Busacca, A. J. (1998). Genesis and relationship of macromorphology and micromorphology to contemporary hydrological conditions of a welded Argixeroll from the Palouse in Idaho. *Geoderma* **83**, 309-329.

Kerney, M. (1999). *Atlas of the Land and Freshwater Molluscs of Britain and Ireland*. Essex: Harley Books.

Klaassen, R. K. W. M. (2008a). Bacterial decay in wooden foundation piles—Patterns and causes: A study of historical pile foundations in the Netherlands. *International Biodeterioration & Biodegradation* **61**, 45-60.

Klaassen, R. K. W. M. (2008b). Water flow through wooden foundation piles: A preliminary study. *International Biodeterioration & Biodegradation* **61**, 61-68.

Kooistra, M. J. & Pulleman, M. M. (2010). Features related to faunal activity. In: Stoops, G., Marcelino, V. & Mees, F. (eds.) *Interpretation of Micromorphological Features of Soils and Regoliths*. London: Elsevier, 397-418.

Kooistra, M. J. & Tovey, N. (1994). Effects of compaction on soil microstructure. *Soil compaction in crop production* **11**, Elsevier Amsterdam, 91-111.

Kourkoutidou-Nicolaidou, E. (1997). From the Elysian Fields to the Christian paradise. In: Webster, L. & Brown, M. (eds.) *The Transformation of the Roman World AD 400-900*. London: Trustees of the British Museum, 128-142.

Kovda, I. & Mermut, A. R. (2010). Vertic Features. In: Stoops, G., Marcelino, V. & Mees, F. (eds.) *Interpretation of Micromorphological Features of Soils and Regoliths*. Amsterdam: Elsevier, 109-127.

Kovda, I., Mora, C. I. & Wilding, L. P. (2008). PaleoVertisols of the northwest Caucasus: (Micro)morphological, physical, chemical, and isotopic constraints on early to late Pleistocene climate. *Journal of Plant Nutrition and Soil Science* **171**, 498-508.

Kühn, P., Aguilar, J. & Miedema, R. (2010). Textural pedofeatures and related horizons. *Interpretation of Micromorphological Features of Soils and Regoliths*, In: Stoops, G., Marcelino, V. & Mees, F. (eds.) *Interpretation of Micromorphological Features of soils and Regoliths*. Amsterdam: Elsevier, 217-250.

Kutschera, W. & Rom, W. (2000). Ötzi, the prehistoric Iceman. *Nuclear Instruments and Methods in Physics Research Section B: Beam Interactions with Materials and Atoms* **164–165**, 12-22.

Lang, C. (2014) *The Hidden Archive of Historical Human Inhumations Locked within Burial Soils.* York: York University.

Leguédois, S., van Oort, F., Jongmans, T. & Chevallier, P. (2004). Morphology, chemistry and distribution of neoformed spherulites in agricultural land affected by metallurgical point-source pollution. *Environmental Pollution* **130**, 135-148.

Lindbo, D. L., Stolt, M. H. & Vepraskas, M. J. (2010). Redoximorphic Features. In: Stoops, G., Marcelino, V. & Mees, F. (eds.) *Interpretation of Micromorphological Features of Soils and Regoliths*. London: Elsevier, 129-147.

Loveluck, C. P. (1998). A high-status Anglo-Saxon settlement at Flixborough, Lincolnshire. *Antiquity* **72**, 146-161.

Lund, U. & Fobian, A. (1991). Pollution of two soils by arsenic, chromium and copper, Denmark. *Geoderma* **49**, 83-103.

MacKenzie, W. S. & Adams, A. E. (2005). *A colour atlas of Roacks and Minerals in Thin Section*. London: Manson Publishing.

Macphail, R., Bill, J., Cannell, R., Linderholm, J. & Rødsrud, C. L. (2013). Integrated microstratigraphic investigations of coastal archaeological soils and sediments in Norway: The Gokstad ship burial mound and its environs including the Viking harbour settlement of Heimdaljordet, Vestfold. *Quaternary International* **315**, 131-146.

Macphail, R. I. (1998). A reply to Carter and Davidson's “An evaluation of the contribution of soil micromorphology to the study of ancient arable agriculture”. *Geoarchaeology* **13**, 549-564.

Macphail, R. I., Courty, M. A. & Gebhardt, A. (1990). Soil micromorphological evidence of early agriculture in north-west Europe. *World Archaeology* **22**, 53-69.

Macphail, R. I., Cruise, G., Allen, M. J., Linderholm, J. & Reynolds, P. (2004). Archaeological soil and pollen analysis of experimental floor deposits; with special reference to Butser Ancient Farm, Hampshire, UK. *Journal of Archaeological Science* **31**, 175-191.

Macphail, R. I. & Goldberg, P. (2010). Archaeological Materials. In: Stoops, G., Marcelino, V. & Mees, F. (eds.) *Interpretation of Micromorphological Features of Soils and Regoliths*. Amsterdam: Elsevier, 589-622.

Mathison, G. E. (1964). The microbiological decomposition of keratin. *Annales de la Societe Belge de Medecine Tropicale* **44**, 767-792.

Matthews, W. (1996). Exploring the 1960s surface: The Stratigraphy of Catalhoyuk. In: Hodder, I. (ed.) *On The Surface: Catalhoyuk 1993-95.* London: McDonald Institute for Archaeological Research, 179-189.

Matthews, W. (2005). Micromorphological and Microstratigraphic Traces of Uses and Concepts of Space. In: Hodder, I. (ed.) *Inhabiting Catalhoyuk reports from the 1995-99 seasons*. Oxford: McDonald institute for archaeological research 355-398.

Matthews, W. (2006). Life-cycle and life-course of buildings. In: Hodder, I. (ed.) *Çatalhöyük Perspectives. Themes from the 1995-99 Seasons.* . Cambridge: McDonald Institute for Archaeological Research and British Institute of Archaeology at Ankara, 125-149.

Matthews, W., Almond, M. J., Anderson, E., Wiles, J., Williams, H. & Rowe, J. (2013). Biographies of architectural materials and buildings: integrating high-resolution micro-analysis and geochemistry. In: Hodder, I. (ed.) *Substantive technologies at Çatalhöyük: reports from the 2000-2008 seasons*. Ankara: The British Institute at Ankara, 115-136.

Matthews, W., French, C., Lawrence, T. & Cutler, D. (1996). Multiple Surfaces: the Micromorphology. In: Hodder, I. (ed.) *On the Surface: Catalhoyuk 1993-95*. Cambridge: MacDonald Institute for Archaeological Research.

Mays, S., Vincent, S. & Campbell, G. (2012). The value of sieving of grave soil in the recovery of human remains: an experimental study of poorly preserved archaeological inhumations. *Journal of Archaeological Science* **39**, 3248-3254.

McGowan, G. & Prangnell, J. (2006). The significance of vivianite in archaeological settings. *Geoarchaeology* **21**, 93-111.

McGowan, G. & Prangnell, J. (2015). A method for calculating soil pressure overlying human burials. *Journal of Archaeological Science* **53**, 12-18.

Mee, C. (2011). *Greek archaeology: a thematic approach*: Wiley-Blackwell.

Meharg, A. A., Deacon, C., Edwards, K. J., Donaldson, M., Davidson, D. A., Spring, C., Scrimgeour, C. M., Feldmann, J. & Rabb, A. (2006). Ancient manuring practices pollute arable soils at the St Kilda World Heritage Site, Scottish North Atlantic. *Chemosphere* **64**, 1818-1828.

Mermut, A. & Pape, T. (1971). Micromorphology of two soils from Turkey, with special reference to in-situ formation of clay cutans. *Geoderma* **5**, 271-281.

Moran, C. J., Koppi, A. J., Murphy, B. W. & McBratney, A. B. (1988). Comparison of the macropore structure of a sandy loam surface soil horizon subjected to two tillage treatments. *Soil Use and Management* **4**, 96-102.

Morris, M. (1986). A Lead-lined Coffin Burial from Winchester. *Britannia* **17**, 343-346.

Müldner, G. & Richards, M. P. (2007). Stable isotope evidence for 1500 years of human diet at the city of York, UK. *American Journal of Physical Anthropology* **133**, 682-697.

Murphy, C. P., Bullock, P. & Turner, R. H. (1977). The Measurement and Characterisation of Voids in Soil Thin Sections by Image Analysis. Part I. Principles and Techniques. *Journal of Soil Science* **28**, 498-508.

Nakamura, C. & Maskell, L. (2005). The Catalhoyuk Burial Assemblage. In: Hodder, I. (ed.) *Human Landscapes of Catalhoyuk: Reports from the 200-2008 seasons*. Cambridge: British Institute at Ankara, 441-466.

National Soil Resources Institute. (2011a). *Soils Site Report*. Undergraduate Student Report. Heslington East. Cranfield: Cranfield University.

National Soil Resources Institute. (2011b). *Soils Site Report*. Undergraduate Student Report. Hungate. Cranfield: Cranfield University.

Nielsen-Marsh, C. M., Smith, C. I., Jans, M. M. E., Nord, A., Kars, H. & Collins, M. J. (2007). Bone diagenesis in the European Holocene II: taphonomic and environmental considerations. *Journal of Archaeological Science* **34**, 1523-1531.

Nilsson, L. (1998). Dynamic Cadavers: A Field-Anthrological Analysis of the Skateholm II Burials. Lund. *Archaeological Review* **4**, 5-17.

Norman, N. J. (2002). Death and burial of Roman children: The case of the Yasmina Cemetery at Carthage—Part I, setting the stage. *Mortality* **7**, 302-323.

Notman, D. N., Anderson, L., Beattie, O. & Amy, R. (1987). Arctic paleoradiology: portable radiographic examination of two frozen sailors from the Franklin expedition (1845-1848). *American Journal of Roentgenology* **149**, 347-350.

Nunan, N., Ritz, K., Crabb, D., Harris, K., Wu, K., Crawford, J. W. & Young, I. M. (2001a). Quantification of the in situ distribution of soil bacteria by large-scale imaging of thin sections of undisturbed soil. *FEMS Microbiology Ecology* **36**, 67-77.

Nunan, N., Ritz, K., Crabb, D., Harris, K., Wu, K., Crawford, J. W. & Young, I. M. (2001b). Quantification of the in situ distribution of soil bacteria by large-scale imaging of thin sections of undisturbed soil. *FEMS Microbiology Ecology* **37**, 67-77.

O'Connor, S., Ali, E., Al-Sabah, S., Anwar, D., Bergström, E., Brown, K. A., Buckberry, J., Buckley, S., Collins, M., Denton, J., Dorling, K. M., Dowle, A., Duffey, P., Edwards, H. G. M., Faria, E. C., Gardner, P., Gledhill, A., Heaton, K., Heron, C., Janaway, R., Keely, B. J., King, D., Masinton, A., Penkman, K., Petzold, A., Pickering, M. D., Rumsby, M., Schutkowski, H., Shackleton, K. A., Thomas, J., Thomas-Oates, J., Usai, M.-R., Wilson,

A. S. & O'Connor, T. (2011). Exceptional preservation of a prehistoric human brain from Heslington, Yorkshire, UK. *Journal of Archaeological Science* **38**, 1641-1654.

Oeggl, K., Kofler, W., Schmidl, A., Dickson, J. H., Egarter-Vigl, E. & Gaber, O. (2007). The reconstruction of the last itinerary of "Ötzi", the Neolithic Iceman, by pollen analyses from sequentially sampled gut extracts. *Quaternary Science Reviews* **26**, 853-861.

Pagliai, M. & De Nobili, M. (1993). Relationships between soil porosity, root development and soil enzyme activity in cultivated soils. *Geoderma* **56**, 243-256.

Pagliai, M. & Kutilek, M. (2008a). Soil Micromorphology and Soil Hydraulics. In: Kapur, S., Mermut, A. & Stoops, G. (eds.) *New Trends in Soil Micromorphology*. Berlin: Springer.

Pagliai, M. & Kutilek, M. (2008b). Soil Micromorphology and Soil Hydraulics. In: Kapur, S., Mermut, A. & Stoops, G. (eds.) *New Trends in Soil Micromorphology*. Berlin: Springer, 5-18.

Pagliai, M., Marsili, A., Servadio, P., Vignozzi, N. & Pellegrini, S. (2003). Changes in some physical properties of a clay soil in Central Italy following the passage of rubber tracked and wheeled tractors of medium power. *Soil and Tillage Research* **73**, 119-129.

Pagliai, M., Vignozzi, N. & Pellegrini, S. (2004). Soil structure and the effect of management practicies. *Soil and Tillage Research* **79**, 131-143.

Parker-Pearson, M. (2003). *The Archaeology of Death and Burial*. Stroud: Sutton Publishing.

Payton, R. W. (1993). Fragipan formation in argillic brown earths (Fragiudalfs) of the Milfield Plain, north-east England. II. Post Devensian developmental processes and the origin of fragipan consistence. *Journal of Soil Science* **44**, 703-723.

Pearson, M. P., Chamberlain, A., Craig, O., Marshall, P., Mulville, J., Smith, H., Chenery, C., Collins, M., Cook, G. & Craig, G. (2005). Evidence for mummification in Bronze Age Britain. *Antiquity* **79**, 529-546.

Pemberton, E. G. (1985). Ten Hellenistic Graves in Ancient Corinth. *Hesperia: The Journal of the American School of Classical Studies at Athens* **54**, 271-307.

Philpott, R. A. (1991). *Burial practices in Roman Britain: a survey of grave treatment and furnishing AD 43-410*: BAR British Series 219. Oxford.

Piepenbrink, H. (1986). Two examples of biogenous dead bone decomposition and their consequences for taphonomic interpretation. *Journal of Archaeological Science* **13**, 417-430.

Piperno, D. R. (2006). *Phytoliths; a comprehensive guide for archaeologists and paleoecologists*. Oxford: Altamira Press.

Pires, L. F., Cooper, M., Cássaro, F. A. M., Reichardt, K., Bacchi, O. O. S. & Dias, N. M. P. (2008). Micromorphological analysis to characterize structure modifications of soil samples submitted to wetting and drying cycles. *Catena* **72**, 297-304.

Pringle, J. K., Jervis, J. R., Hansen, J. D., Jones, G. M., Cassidy, N. J. & Cassella, J. P. (2012). Geophysical Monitoring of Simulated Clandestine Graves Using Electrical and

Ground-Penetrating Radar Methods: 0–3 Years After Burial. *Journal of Forensic Sciences* **57**, 1467-1486.

Ransom, M. D., Smeck, N. E. & Bigham, J. M. (1987). Micromorphology of seasonally wet soils on the Illinoian Till Plain, U.S.A. *Geoderma* **40**, 83-99.

Regelink, I. C., Stoof, C. R., Rousseva, S., Weng, L., Lair, G. J., Kram, P., Nikolaidis, N. P., Kercheva, M., Banwart, S. & Comans, R. N. J. (2015). Linkages between aggregate formation, porosity and soil chemical properties. *Geoderma* **247–248**, 24-37.

Reinhard, K. J., Geib, P. R., Callahan, M. M. & Hevly, R. H. (1992). Discovery of colon contents in a skeletonized burial: Soil sampling for dietary remains. *Journal of Archaeological Science* **19**, 697-705.

Richards, M. P., Pearson, J. A., Molleson, T. I., Russell, N. & Martin, L. (2003). Stable Isotope Evidence of Diet at Neolithic Çatalhöyük, Turkey. *Journal of Archaeological Science* **30**, 67-76.

Rife, J. L., Morison, M. M., Barbet, A., Dunn, R. K., Ubelaker, D. H. & Monier, F. (2007). Life and Death at a Port in Roman Greece: The Kenchreai Cemetery Project, 2002-2006. *Hesperia: The Journal of the American School of Classical Studies at Athens* **76**, 143-181.

Ringrose-Voase, A. J. & Bullock, P. (1984). The automatic recognition and measurement of soil pore types by image analysis and computer programs. *Journal of Soil Science* **35**, 673-684.

Roberts, C. A. (2009). *Human Remains in Archaeology: A Handbook*. York: Antiquity Publications Ltd.

Roberts, N., Boyer, P. & Parish, R. (1996). Preliminary Results of Geoarchaeological Investigations at Catalhoyuk. In: Hodder, I. (ed.) *On the surface: Catalhoyuk 1993-95*. Cambridge: McDonald Institute of Arvhaeological Research, 19-40.

Rosen, A. & Roberts, N. (2005). The nature of Catalhoyuk: people and their changing environments on the Konya Plain, with a note on modelling field location by Donovan, P. In: Hodder, I. (ed.) *Catalhoyuk Perspectives: reports from the 1995-99 seasons.* Cambridge: McDonald Institute for Archaeological Research and British Institute of Archaeology at Ankara, 39-53.

Rosen, A. M. (2005). Phytolith indicators of plant and land use at Çatalhöyük. In: Hodder, I. (ed.) *Inhabiting Catalhoyuk: Reports from the 1995-99 Seasons,* Cambridge: McDonald Institute for Archaeological Research and British Institute of Archaeology at Ankara, 203-212.

Russell, E. W. (1971). Soil strucutre: Its maintenance and improvement. *Journal of Soil Science* **22**, 137-151.

Ryan, P. (2011). Plants as material culture in the Near Eastern Neolithic: Perspectives from the silica skeleton artifactual remains at Çatalhöyük. *Journal of Anthropological Archaeology* **30**, 292-305.

Schaetzl, R. & Anderson, S. (2005). *Soils: Genesis and Geomorphology*. Cambridge: Cambridge University Press.

Schlesinger, W. H. (1991). *Biochemistry An Analysis of Global Change*. London: Accademic Press.

Schultz, J. J., Collins, M. E. & Falsetti, A. B. (2006). Sequential Monitoring of Burials Containing Large Pig Cadavers Using Ground-Penetrating Radar. *Journal of Forensic Sciences* **51**, 607-616.

Scott, A. C. & Damblon, F. (2010). Charcoal: Taphonomy and significance in geology, botany and archaeology. *Palaeogeography, Palaeoclimatology, Palaeoecology* **291**, 1-10.

Scott, C. D., Strandberg, G. W. & Lewis, S. N. (1986). Microbial Solubilization of Coal. *Biotechnology Progress* **2**, 131-139.

Sehgal, J. L. & Stoops, G. (1972). Pedogenic calcite accumulation in arid and semi-arid regions of the indo-gangetic alluvial plain of erstwhile Punjab (India) — Their morphology and origin. *Geoderma* **8**, 59-72.

Shillito, L.-M., Almond, M. J., Nicholson, J., Pantos, M. & Matthews, W. (2009). Rapid characterisation of archaeological midden components using FT-IR spectroscopy, SEM–EDX and micro-XRD. *Spectrochimica Acta Part A: Molecular and Biomolecular Spectroscopy* **73**, 133-139.

Shillito, L.-M., Bull, I. D., Matthews, W., Almond, M. J., Williams, J. M. & Evershed, R. P. (2011a). Biomolecular and micromorphological analysis of suspected faecal deposits at Neolithic Çatalhöyük, Turkey. *Journal of Archaeological Science* **38**, 1869-1877.

Shillito, L.-M., Matthews, W., Almond, M. J. & Bull, I. D. (2011b). The microstratigraphy of middens: capturing daily routine in rubbish at Neolithic Çatalhöyük, Turkey *Antiquity* **85**, 1024-1038.

Slager, S. & van de Wetering, H. T. J. (1977). Soil formation in archaeological pits and adjacent loess soils in Southern Germany. *Journal of Archaeological Science* **4**, 259-267.

Smith, C. I., Nielsen-Marsh, C. M., Jans, M. M. E. & Collins, M. J. (2007). Bone diagenesis in the European Holocene I: patterns and mechanisms. *Journal of Archaeological Science* **34**, 1485-1493.

Smith, G. S. & Zimmerman, M. R. (1975). Tattooing Found on a 1600 Year Old Frozen, Mummified Body from St. Lawrence island, Alaska. *American Antiquity* **40**, 433-437.

Sofaer, J. R. (2006). *The Body as Material Culture; A Theoretical Osteoarchaeology*. Cambridge: Cambridge University Press.

Sparey-Green, C. & Struck, M. (1993). The rite of plaster burial in the context of the Romano-British cemetery at Poundbury, Dorset (England). *Romerzeitlicher Graber als Quellen zur Religion, Bevólkerungsstruktur und Sozialgeschichte*, 421-432.

Stewart, J. R. M., Allen, R. B., Jones, A. K. G., Penkman, K. E. H. & Collins, M. J. (2013). ZooMS: making eggshell visible in the archaeological record. *Journal of Archaeological Science* **40**, 1797-1804.

Stokes, H. R. (Unpublished BSc Dissertation). *Investigation of Mineralogical and Micromorphological Evidence for Spatial and Environmental Change from Level Five, the Later Occupation of Catalhoyuk*. Reading: Reading University.

Stoops, G. (2003). *Guidelines for Analysis and Description of Soil and Regolith Thin Sections*. Madison, Wisconsin: Soil Science Society of America, Inc.

Stoops, G. & Jongerius, A. (1975). Proposal for a micromorphological classification of soil materials. I. A classification of the related distributions of fine and coarse particles. *Geoderma* **13**, 189-199.

Stoops, G., Marcelino, V. & Mees, F. (2010). Micromorphological Features and Their Relation to Processes and Classidication: General Guidelines and Keys. In: Stoops, G., Marcelino, V. & Mees, F. (eds.) *Interpretation of Micromorphological Features of Soils and Regoliths*. London: Elsevier.

Stutz, L. N. (2003). *Embodied Rituals and Ritualized Bodies*. Lund: Wallin and Dahlholm Boktryckeri AB.

Thompson, M. L., Fedoroff, N. & Fournier, B. (1990). Morphological features related to agriculture and faunal activity in three loess-derived soils in France. *Geoderma* **46**, 329-349.

Tung, B. (2005). A preliminary investigation of mudbrick in Çatalhöyük. In: Hodder, I. (ed.) *Changing materialities at Çatalhöyük: Reports from the 1995–99 seasons.* Cambridge: McDonald Institute for Archaeological Research, 215-219

Tung, B. (2013). Building with mud: as analysis of architectural materials at Catalhoyuk. In: Hodder, I. (ed.) *Substantive Technologies at Catalhoyuk: Reposrts from the 2000-2008 Seasons*. London: British Institute at Ankara, 67-80.

Usai, M. R. (1996). *Paleosol Interpretation Micromorphological and Pedological Studies*. York: The Ebor Press.

Usai, M. (2001). Textural Pedofeatures and Pre-Hadrian's Wall Ploughed Paleosols at Stanwix, Carlisle, Cumbria, U.K. . *Journal of Archaeological Science* **28**, 541-553.

Usai, M., Brothwell, D., Buckley, S., Al-Thour, K. & Canti, M. (2010). Micromorphology of two prehistoric ritual burials from Yemen, and considerations on methodological aspects of sampling the burial matrix, work in progress. *EGU General Assembly 2010*. Vienna.

Usai, M., Pickering, M. D., Wilson, C. A., Keely, B. J. & Brothwell, D. R. (2014). 'Interred with their bones': soil micromorphology and chemistry in the study of human remains. *Antiquity* **88**.

Van der Sanden, W. (1996). *Through nature to eternity: the bog bodies of northwest Europe*: Batavian Lion International.

Van Veen, J. A. & Kuikman, P. J. (1990). Soil structural aspects of decomposition of organic matter by micro-organisms. *Biogeochemistry* **11**, 213-233.

Van Vliet-Lanoë, B. (2010). Frost action. In: Stoops, G., Marcelino, V. & Mees, F. (eds.) *Interpretation of Micromorphological Features of soils and Regolithis*. Amsterdam: Elsevier, 81-108.

Van Vliet-Lanoë, B. (1998). Frost and soils: implications for paleosols, paleoclimates and stratigraphy. *CATENA* **34**, 157-183.

VandenBygaart, A. J., Fox, C. A., Fallow, D. J. & Protz, R. (2000). Estimating Earthworm-Influenced Soil Structure by Morphometric Image Analysis. *Soil Sci. Soc. Am. J.* **64**, 982-988.

Vass, A. (2001). Beyond the grave – understanding human decomposition. *Microbiology Today* **28**, 190-192.

Veneman, P. L. M., Vepraskas, M. J. & Bouma, J. (1976). The physical significance of soil mottling in a Wisconsin toposequence. *Geoderma* **15**, 103-118.

Vepraskas, M. (2001). Morphological features of seasonally reduced soils. *Wetland soils: Genesis, hydrology, landscapes, and classification*, 163-182.

Weiner, S. (2010). *Microarchaeology, Beyond the visible archaeological record*. Cambridge: Cambridge University Press.

Wendrich, W. (1995). Çatalhöyük Basketry. *Changing Materialities at Çatalhöyük, Reports from the* **1999**, 15-25.

White, E. M. & Hannus, L. A. (1983). Chemical Weathering of Bone in Archaeological Soils. *American Antiquity* **48**, 316-322.

White, R. E. (1997). *Principles and Practice of Soil Science: soil as a natural resorce*. Oxford: Blackwell Science.

Whittle, A. W. (1996). *Europe in the Neolithic: the creation of new worlds*: Cambridge University Press.

Wieder, M. & Yaalon, D. H. (1982). Micromorphological fabrics and developmental stages of carbonate nobular forms related to soil characteristics. *Geoderma* **28**, 203-220.

Williams, A. C., Edwards, H. G. M. & Barry, B. W. (1995). The 'Iceman': molecular structure of 5200-year-old skin characterised by raman spectroscopy and electron microscopy. *Biochimica et Biophysica Acta (BBA) - Protein Structure and Molecular Enzymology* **1246**, 98-105.

Willis, A. & Tayles, N. (2009). Field anthropology: application to burial contexts in prehistoric Southeast Asia. *Journal of Archaeological Science* **36**, 547-554.

Wilson, A. S., Janaway, R. C., Holland, A. D., Dodson, H. I., Baran, E., Pollard, A. M. & Tobin, D. J. (2007). Modelling the buried human body environment in upland climes using three contrasting field sites. *Forensic Science International* **169**, 6-18.

Wilson, C., Simpson, I. A. & Currie, E. J. (2002). Soil management in pre-Hispanic raised field systems: Micromorphological evidence from Hacienda Zuleta, Ecuador. *Geoarchaeology* **17**, 261-283.

Wright, K. I. (2010). Beads and the body: Ornament technologies of the BACH area buildings at Catalhoyuk. In: Tringham, R. & Stevanovic, M. (eds.) *House lives: Building, Inhabiting, Excavating a House at Catalhoyuk, Turkey*. Los Angeles: Cotsen Institute of Archaeology Publications, 331-363

Ye, S., Laws, E. A. & Gambrell, R. (2013) Trace element remobilization following the resuspension of sediments under controlled redox conditions: City Park Lake, Baton Rouge, LA. *Applied Geochemistry*, 91-99

Dighungate.com, (2015). *Roman Hungate*. Online. 2015. Available at: http://www.dighungate.com/content.asp?ID=106. Accessed: 10 November 2015.